Alan G. Davenport Wind Engineering Group

A STUDY OF WIND EFFECTS FOR THE

MESSINA STRAIT BRIDGE, ITALY

Section Model - Sub-Tests D3, D5 and D6

J.P.C. King / L. Kong / B. Bakht

BLWT-SS42-2010 / DRAFT 3 / January 2011

The Boundary Layer Wind Tunnel Laboratory
The University of Western Ontario, Faculty of Engineering
London, Ontario, Canada N6A 5B9; Tel: (519) 661-3338; Fax: (519) 661-3339
Internet: www.blwtl.uwo.ca; E-mail: info@blwtl.uwo.ca

TABLE OF CONTENTS

APPENDIX A THE SECTION MODEL APPROACH FOR THE STUDY OF WIND ACTION ON LONG SPAN BRIDGES

APPENDIX B FLUTTER INSTABILITY CRITERIA

APPENDIX C RESULTS OF STATIC SECTION MODEL TESTS

APPENDIX D FORMULATION OF AERODYNAMIC DERIVATIVES FROM FREE OSCILLATION TESTS

APPENDIX E AERODYNAMIC DERIVATIVES IN SDM NOTATION

APPENDIX F WIND PROFILES IN TRAFFIC LANES

APPENDIX G RESULTS OF DYNAMIC SECTION MODEL TESTS, IN-SERVICE

LIST OF TABLES

LIST OF FIGURES

ACKNOWLEDGEMENTS

The section model study of wind effects for the deck section of the Messina Straits Crossing between Sicily and Reggio Calabria, Italy was initiated by Dr. Allan Larsen of COWI A/S, Denmark. The co-operation and support of Dr. Larsen throughout the study is greatly appreciated. Acknowledgement is also made of the support of Mr. Sandro Ordanini of Eurolink S.C.p.A.

Acknowledgment is made of the contributions by various members of the engineering and technical staff of the Laboratory, particularly: Mr. Gerry Dafoe and Mr. Anthony Burggraaf who carried out the experimental phases of the study. The section model was constructed by members of the University Machine Shop under the direction of Mr. Kevin Barker.

DETAILS OF THE STUDY

Project Name:	Messina Strait Bridge
Project Location:	Straits of Messina – between Sicily and Reggio Calabria Italy
Project Description:	The proposed suspension bridge across the Straits of Messina is situated over a narrow section of water between the eastern tip of Sicily and Reggio Calabria on the mainland of Italy. With a length of 3.3km and a width of 60m, the bridge will be supported by two 382 m high towers. There will be three motorway lanes and one emergency lane in each direction and a two-track railway.
Test Dates:	Steady State Wind Load Coefficients – September 2010 Stability and Buffeting – October 2010 Aerodynamic Derivatives – October 2010 Aerodynamic Admittance – November 2010 Steady State Wind Load Coefficients in Skew Winds – November 2010
Preliminary Reporting:	Steady State Wind Load Coefficients – October 2010 Aerodynamic Stability and Buffeting – November 2010 Aerodynamic Derivatives and Aerodynamic Damping – December 2010 Aerodynamic Admittance – December 2010 Steady State Wind Load Coefficients in Skew Winds – December 2010 Velocity Profiles over In-Service Deck – December 2010
Report Scope and Format:	The report is organized as follows: Section 1 – Introduction Section 2 – Section Model Design and Scope of Testing Section 3 – Sub Test D3 Section 4 – Sub Test D5 Section 5 – Sub Test D6
General Reference:	Discussion and details of the general methodology used by the Alan G Davenport Wind Engineering Group can be found in “Wind Tunnel Testing – A General Outline” (Reference 1).

1 INTRODUCTION

1.1 General

This report describes the section model study for the Messina Strait Bridge in Italy. The proposed bridge is located between the island of Sicily and Reggio Calabria on the mainland. The bridge will feature a six-lane highway, two service lanes and a double-track railway. It is a steel suspension bridge with a central span of 3,300 m between the two towers and two side spans of different lengths and arrangements, for an additional 960 m to the Sicily anchorage and 810 m to the Reggio Calabria anchorage. The steel towers, standing at a height of 382 m, each consist of two vertical legs linked by three cross beams. The deck has a total width of about 60 m and comprises a central double-track railway deck flanked on either side by a 3-lane road deck. The suspension system consists of two pair of steel cables, each with a diameter of 120 cm. The deck is suspended from the cables by a system of vertical steel hangers at 30 m intervals.

The site of the bridge is shown in Figure 1.1. The overall dimensions of the prototype bridge are given in Figure 1.2. Figures 1.3 through 1.7 provide general details of the bridge deck upon which the design of the section model was based.

The section models were studied at the inlet to the high speed section of BLWT II, located at the University of Western Ontario.

1.2 Scope of Report

This report includes results from the static and dynamic tests of the section model. The series of tests follows as closely as possible, the outline test specification documents referenced in [1] and [2], provided by COWI A/S. The wind tunnel tests addressed Sub-tests D3, D5 and D6 as defined by Eurolink s.c.p.a "Overall Aerodynamic Design Methodology and Plan for Aerodynamic Testing [3]. The section model tests included:

Sub-Test D3:

a) the measurement of steady state wind load coefficients for the deck while under construction and in-service
b) the measurement of Aerodynamic Derivatives
c) the measurement of Aerodynamic Admittance Functions

Sub-Test D5:

a) the measurement of steady state wind load coefficients at skew angles and for various traffic conditions
b) the measurement of wind profiles over the deck for various traffic conditions

Sub-Test D6:

a) the assessment of aerodynamic stability
b) the measurement of the response to turbulence

A section model was designed and constructed at a geometric scale of 1 to 80. The section model was ballasted to the scaled mass and mass moment of inertia properties and mounted on the BLWTL section model test rig. The static test rig was adapted to measure the steady state wind load coefficients at skew winds. The dynamic test rig was modified to include drag degrees of freedom such that the fundamental vertical, lateral and torsional modal frequencies were simulated.

The methodology and test results for Sub Test D3 are detailed in Section 3, those for Sub Test D5 are in Section 4 and those for Sub Test D6 are in Section 6 of this report.

2 SECTION MODEL STUDY

2.1 General

The behaviour of the deck for the Messina Strait Bridge using the section model technique was studied at the inlet to the High Speed Test Section of the Boundary Layer Wind Tunnel II, located at the University of Western Ontario. Tests of the section model were conducted under the action of both grid-generated turbulence and in smooth, uniform flow conditions.

2.2 Model Design

The 2.286m long section model corresponds to a 182.9 m long section of the full scale deck and was constructed at a scale of 1 to 80. The full scale deck section has a deck width of 60.36 m (or 0.755m in model scale) and a depth of 4.68m (or 0.059m in model scale). The overall length of the section model was 2.299m resulting in an aspect ratio of 2.299 / 0.755 = 3.05 to 1, which is a satisfactory length to width ratio in order to develop the correct correlation of the forces in the span-wise coordinate. The overall height of the wind tunnel test section is 1.77m, which results in a minimum blockage of 3.3% at 0 degrees angle of attack for the under construction deck section. At the maximum angle of incidence of 10 degrees, the in-service bridge deck (from the middle airfoil on the outside windscreen to the lower deck of the adjacent girder) is approximately 13.8m deep which corresponds to a maximum blockage of 9.8%. These satisfy the Eurolink general specifications for the section model [3].

A summary of the similitude requirements for the design of the basic section model is given in Table 2.1. Further details concerning the design of a section model and the approach to testing can be found in Appendix A and in Reference [4].

The design of the section model was complicated by the requirement that the model be utilized to develop the Aerodynamic Admittance Functions in the vertical, lateral and torsional degrees of freedom. Two common techniques for measuring some form of the aerodynamic admittance functions involve the measurement of surface pressures around the deck section or to instrument an isolated portion of the model with a multi-component force transducer. The former technique could not be used due to the difficulty in measuring the surface pressure over the porous surfaces and numerous discrete components (such as the railings and airfoils) each of which contribute to the overall forces on the deck. Therefore, it was decided to isolate the central portion of the model from the model skeleton and to measure the wind-induced forces on this portion of the model. The stiffness of the model, was therefore controlled by the available space within the model in which structural members could be located. Consequently the model skeleton was constructed using five commercially available carbon fibre tubes as longitudinal structural members with cross-tubes glued to the longitudinal members to form a “ladder-shaped” structure. Carbon-fibre sheets were glued to the upper surface of the tubes to add stiffness to the model and to replicate the road and rail decks. Aluminum sheets were rolled to form the curved soffit of the road girders and then glued to the carbon fibre deck sheets. The rail girder soffit was formed using bent, thin gauge aluminum sheet and the cross boxes were clad with machined structural foam. Two aluminum end plates were machined with the cross-box profile, glued to the longitudinal carbon fibre tubes and provided additional torsional rigidity to the model by restraining the ends of the model.

Since the model was to be used to simulate the under construction as well as the in-service condition, all deck furniture such as the lamp standards and rail catenary masts were removable. In addition, the service lane cantilevers, wind screens, outer crash barrier and triangular nosing for the in-service condition were replaced by a similar component consisting of the nosing and service lane cantilever alone. Similarly, the inner safety screen and rail girder platform were also removable.

Drawings of the Section Model are provided in Figures 2.1 to 2.3.

2.2.1 Modifications to Model Design for Aerodynamic Admittance and Skew Wind Tests

The central 0.375m portion of the model (centred about one cross-box) was fabricated as a shell, isolated from the longitudinal carbon fibre tubes and mounted to a 6-component load cell, which was in turn, fixed to the central longitudinal member in the model structural skeleton. As an added measure to stiffen this portion of the model, four aluminum links were machined and inserted between the instrumented central portion of the model and the neighbouring non-instrumented portions. These links, which were relatively stiff for vertical motion, while very flexible for lateral motion, were located within the triangular nosing of the model. The links had the effect of reducing the sensitivity of the centrally-located 6-component load cell, while stiffening the instrumented portion of the model in the torsional degree of freedom. The effect of the links was considered through in-situ calibrations of the central portion of the model for lift, drag and torsional forces.

The model was modified for use in the measurement of steady state wind load coefficients for skew winds through the manufacture of additional triangular end pieces for the 10, 20, 30 and 45 degree cases. Attachment to the model was accomplished through a sliding structural member within the main carbon fibre structural tube which was bolted to each end of the basic 2.3m long model at the correct position for the yaw angle. As the yaw angle increased through 45 degrees, the model was 42% longer than in the non-yawed case, with the inescapable corresponding reduction in stiffness of the model.

The compromise of including the central portion of the model as an isolated and separate component, meant that the model structure was less stiff than would typically be the case if the entire skin were structural, rather than simply used as cladding to the skeletal model structure. The model bending and torsional frequencies were considerably less than desirable as a result of the use of this technique to measure the admittance function. The model properties as realised in the 1 to 80 scale model are given in Table 2.2.

2.2.2 Screening Design and Verification of Loss Coefficient

An important component of the model design was the proper simulation of the aerodynamic effect of the wind screens located at the outer edge of the service lanes as well as the inner and outer safety screens on the roadway. The prototype wind screen and safety screen is constructed out of an expanded metal mesh with a porosity of 55% (i.e. open void ratio). The desired porosity of 55% and effective loss coefficient of 2.7 was specified by COWI and SdM to be within an error margin of +/- 5% [1,3]. Model screening material containing holes of appropriate diameter and spacing was constructed using a rapid prototyping process known as the “Fused Deposition Method” or FDM. Several sample sheets of the ABS material with various arrangements of hole diameter and spacing were designed, fabricated and tested in the pilot study wind tunnel at the Boundary Layer Wind Tunnel Laboratory to verify that the loss coefficient was within the desired tolerance.

The pilot study wind tunnel has a test section of 0.46m x 0.46m and a working length of 1.3m. A test piece of the model screen was located about 0.5m from the tunnel inlet and completely spanned the working section. Pitot static tubes were placed upstream and downstream of the test piece in order to measure the pressure drop across the screen. A photograph of the test setup is provided in Figure 2.4a.

Differential pressure transducers were used to measure: a) the mean wind speed in the test section of the wind tunnel (V) and b) the difference between the upstream and downstream static pressures (Δp). The ratio of the static pressure drop across the screen to the velocity pressure is a measure of the mean loss coefficient (ξ). The velocity pressure, q, is equal to $0.5\rho V^2$, where ρ is the density of air.

$$\xi = \frac{(p_1 - p_2)}{\frac{1}{2}\rho V^2} = \frac{\Delta P}{q} \tag{2.1}$$

Figure 2.4b shows the variation of mean loss coefficient of the prototype screen with wind speed. It can be seen that the loss coefficient across the screen increases with the test wind speed. The variation in the loss coefficient tends to become stable at a value of near 2.7 once the test wind speed reaches 6 to 6.5 m/s. Therefore, it can be considered that the prototype screen is independent of wind velocity (i.e. independent of the Reynolds Number) for wind speeds critical to defining the instability regime in the section model study.

The final model screening had an open ratio of 55% with a hole diameter of 5.736mm and was selected based on the mean loss coefficient of 2.7.

2.2.3 Test Set-up in the Wind Tunnel

Photos of the section model test setup are shown in Figure 2.5. The turbulence generating grid which was located at the inlet of the wind tunnel can be seen in the background for the turbulent flow test. Figure 2.6 presents the static section model test rig with the load cells and the automated angle of incidence apparatus visible on the photograph. The dynamic section model test rig is shown in Figure 2.7, where the elliptical aluminum end plates used in the static tests were replaced by acrylic end plates to enhance visibility of model behaviour. The test wind speed was measured continuously throughout all tests as indicated throughout the output from two pitot-static tubes mounted to the roof of the wind tunnel above the model centre-line and midpoint.

3 Sub-Test D3

3.1 Steady State Wind Load Coefficients

3.1.1 Definition

Two configurations of the Messina Bridge deck section were studied in the static section model test. These were: 1) the in-service bridge deck and 2) an under construction stage, where all deck furniture was removed from the upper surface of the bridge deck (i.e. wind screens, inner and outer safety screens, crash barriers, light masts, catenary masts as well as rail platforms). Figure 3.1 shows the two configurations used in the static section model test.

The section model was mounted on the BLWTL Bridge 3-component balance, which is capable of measuring the total forces on the section (X and Z body forces as well as the torque). Tests were performed

adjusting the model inclination relative to the mean wind flow. Lift and Drag were calculated from the measured X and Z body force components. The sign conventions for the definition of the force coefficients for the deck section are given in Figures 3.2 and 3.3 for the in-service bridge and under construction stage respectively.

A typical force coefficient is defined as follows:

$$C_{x,z,l,d} = \frac{F_{x,z,l,d}}{qB} \qquad (3.1)$$

in which C is an aerodynamic coefficient, F is the mean aerodynamic force per unit span length, $q = \frac{1}{2}\rho V^2$ is the mean wind velocity pressure at deck level, ρ is the density of air (1.225 kg/m^3), V is the mean wind velocity at deck level in m/s, and B is the bridge deck width. The subscripts x,z,l,d refer to the X and Z body force components and lift and drag respectively. It is important to note that C_x, C_z and C_m are “Body-Force Coefficients” and not aligned with the axis of the wind (i.e. as a “drag” coefficient) nor perpendicular to the wind (i.e. as a “lift” coefficient).

The torque coefficient is defined:

$$C_m = \frac{F_t}{qB^2} \qquad (3.2)$$

Tests were carried out for both bridge deck configurations in smooth flow and grid generated turbulent flow for angles of mean vertical inclination between -10 to +10 degrees, in increments of 0.5 degrees. The tests in smooth flow were performed for wind speeds corresponding to Reynolds numbers (based on an overall model deck width dimension of 0.755m) of 9.0×10^5 and 1.0×10^6 for the in-service bridge and the under construction stage. The corresponding Reynolds numbers are 5.9×10^5 and 7.7×10^5 respectively for the two deck configurations for the turbulent flow tests, due to slightly lower wind speeds achieved in the tests. Two additional tests were conducted at the wind angle of 0 degrees in smooth flow for different wind speeds to investigate a potential for Reynolds Number effects on the aerodynamic force coefficients.

The resulting static aerodynamic coefficients for the in-service section model are summarised in Tables 3.1 and 3.2 for smooth and turbulent flow tests, respectively. The static force coefficients for the under construction stage are presented in Tables 3.3 and 3.4 for the two flow conditions. The corresponding summary curves of the force coefficient vs. angle of attack are also shown in Figures 3.4 and 3.5 for the in-service deck section and in Figures 3.7 to 3.8 for the under construction stage. In addition, Figures 3.6 and 3.9 present the static force coefficients vs. Reynolds number at 0 degrees in smooth flow for the two deck configurations. All results from the static section model tests are also given in Appendix C.

The coefficients are normalized by deck width to make comparisons with other structures more meaningful. Should the results be desired on a projected area to the wind basis, as is sometimes the case, the $C_{x,z,l,d}$ coefficients should be multiplied by the ratio of deck width to the section height (for example, 60.36/4.68=12.9), and for C_m by the square of this value ($(60.36/4.68)^2$=166.3). The centre of measurement of the forces is at the centreline of the deck section and 3.5m above the bottom surface of the cross-box.

3.1.2 In-Service Deck Condition

General comments on the static test results of the in-service deck section are given below.

- Noticeable differences are observed between the smooth flow and turbulent flow test results, especially at large angles of attack in the torsional force coefficient.
- The drag coefficients are generally higher in smooth flow than those obtained from the turbulent flow test.
- No apparent negative slope is observed in the lift and torsional force coefficients. However, the slope of the torsional force coefficient reduces at large positive angles of attack. The torsional force coefficient also shows a mild negative slope between -6^o and -3^o. The lift coefficient is observed to be insensitive to angle of attack in smooth flow for angles between -3^o and $+4^o$.
- The turbulent flow test results for the in-service deck section does not exhibit any tendency for negative slopes in the lift and torsional force coefficients.
- Force coefficient vs. Reynolds number plots for 0^o angle of attack in smooth flow (see Figure 3.6) shows Reynolds number dependency of the lift coefficient up to about Re = 6.5×10^5. This dependency diminishes for Reynolds numbers above this value. Force coefficient dependency on Reynolds number is less significant in turbulent flow.

3.1.3 Under Construction Stage Deck Condition

General comments on the static test results of the under construction stage deck section are given below.

- In general, the drag and lift force coefficients obtained from the under construction stage test show a similar trend as those from the in-service deck section test.
- The drag coefficients are consistently higher in smooth flow than those from the turbulent flow test. As expected, the drag coefficients are relatively small compared to the results from the in-service deck section.
- No negative slope was observed in the lift force coefficient for either the smooth or turbulent flow condition. The only noticeable difference found was at large negative angles of attack. The magnitude of the lift force coefficients for the under construction stage section was found to be larger than that of the in-service deck section.
- The torsional force coefficient indicates a larger dependence on the flow conditions. The turbulent flow test result does not show a negative slope. The smooth flow test result does not indicate a negative slope, however it has ranges of angles of attack in which the torsional force coefficient is insensitive to angle of attack; for example between -7^o and -5^o as well as above $+3^o$. The magnitude of the torsional force coefficient is consistently higher than that for the in-service deck section.

- The result of the force coefficient vs. Reynolds number at 0^o in smooth flow in Figure 3.9 indicates a Reynolds number dependency for the lift and torque coefficients up to about Re = 4.5×10^5.

3.2 Aerodynamic Derivatives

3.2.1 General

This section of the report includes the results for the aerodynamic derivative test (i.e. Sub Test D3 – Item 3.2). Results for the aerodynamic damping test (Sub Test D6 – Item 6.1) is presented in Section 5.1.5. The experimental set-up for both types of tests was nearly identical with the only difference being in the stiffness of the drag springs used in the test. Relatively stiff drag springs were utilized in the aerodynamic damping tests in order to reduce the overall drag amplitudes as the aerodynamic damping measurements concentrated on the vertical and torsional degrees of freedom. Further details on this test and the results are presented in Section 5.1.5.

A photo of the section model test setup for these studies is shown in Figure 3.10. The general set-up of the aerodynamic derivative and damping tests is similar to the dynamic section model test described in Section 5.1, however, with the addition of a pneumatic "displace and release" system to provide consistent initial displacements of the section model in the three degrees of freedom throughout the tests.

3.2.2 Theoretical Model

Aerodynamic Derivatives are aeroelastic parameters and have been widely used to study catastrophic flutter phenomena in bridge structures since first introduced by Scanlan and summarised in Simiu and Scanlan [5]. They are defined as a function of reduced frequency and assuming purely sinusoidal motion, the unsteady aerodynamic forces are expressed as follows:

$$L=\frac{1}{2}\rho U^2B\left[KH_1^*\dot{h}/U+KH_2^*B\dot{\alpha}/U+K^2H_3^*\alpha+K^2H_4^*h/B+KH_5^*\dot{p}/U+K^2H_6^*p/B\right] \qquad (3.3)$$

$$M=\frac{1}{2}\rho U^2B^2\left[KA_1^*\dot{h}/U+KA_2^*B\dot{\alpha}/U+K^2A_3^*\alpha+K^2A_4^*h/B+KA_5^*\dot{p}/U+K^2A_6^*p/B\right] \qquad (3.4)$$

$$D=\frac{1}{2}\rho U^2B\left[KP_1^*\dot{p}/U+KP_2^*B\dot{\alpha}/U+K^2P_3^*\alpha+K^2P_4^*p/B+KP_5^*\dot{h}/U+K^2P_6^*h/B\right] \qquad (3.5)$$

where:

L, M and D are the Lift, Moment and Drag forces produced by the moving deck.

ρ is the density of air

B is the characteristic width of the Bridge Deck

K is a reduced frequency, $B\omega/U$

U is the wind speed at deck height

ω is the circular natural frequency, and

H^*_{1-6}, A^*_{1-6} and P^*_{1-6} are the Lift, Torsion and Drag Aerodynamic Derivatives

In the analysis, different frequencies are used for each of the derivatives, depending on the specific coupling term in question, rather than the same frequency for all reduced *K* terms in the same equation. The normalizing frequencies used in the analysis are provided in Table 3.5 for the aerodynamic derivative test.

3.2.3 Experimental Methodology

The section model was mounted on soft springs permitting the simulation of the lateral, vertical and torsional frequencies of vibration in the 3-D test. Although not a critical component of the technique, the sprung model was ballasted with additional mass to represent the dynamically scaled mass and mass moment of inertia. The aerodynamic derivatives are characteristics of the deck shape and are therefore independent of the mass properties of the deck. During each test, twenty-one three-degree-of-freedom impacts were given to the model at each wind speed. A pneumatic "displace and release" system was used for this study to provide consistent initial displacements in all three directions. The response after release from the initial displacement was digitized and stored for later analysis. Two of the pneumatic cylinders used to provide the initial displacement can be seen in Figure 3.10.

A sketch showing the 3-D displacement of the section model and the sign convention is given in Figure 3.11 for the in-service deck section and in Figure 3.12 for the under construction stage deck section.

The "displace and release" pneumatic system consisted of 2 pairs of air cylinders located at each end of the section model, in the plane of the vertical springing and inclined relative to the vertical axis. One cylinder in each pair was located below the torsional arm of the model springing while the other cylinder was located above the arm, each aimed at an inclined target situated on the torsional arm. The system was able to capture the model and hold it at the desired initial vertical, lateral and rotational displacement as shown in Figure 1.1. The system was controlled through an automated "on-off" step-function by the data acquisition and control computer to initiate a 3-D displacement of the model, hold it in position for approximately 10 seconds and then release it such that the model would be free to oscillate for ten to fifteen cycles. This process was repeated 21 times and the time history of the model displacement recorded. The simultaneous initial displacements were within the limits specified by COWI and SdM of: rotation 0.5 to 1.5 degrees, vertical & lateral initial displacements between 2.5 & 7.5mm [1,3].

Parameter Estimation Techniques were used to fit the response of the section model to linearized equations of motion, with the resulting estimates of the aerodynamic derivatives. A detailed description of the methodology used in the analysis is given in Appendix D.

3.2.4 Estimates of Aerodynamic Derivatives

Note that all results of the aerodynamic derivatives in the report follow the notation in given in Equations (3.3) to (3.5).

Tests were performed to evaluate the aerodynamic derivatives for the in-service and under construction configurations of the deck, at angles of attack, 0^o, $\pm 2^o$, $\pm 4^o$ and $\pm 6^o$. All tests conducted in the smooth flow condition. A summary of the aerodynamic derivative tests performed is given in Table 3.6.

The results of the aerodynamic derivatives for the in-service condition are presented in Tables 3.7 to 3.13, while the results for the under construction condition are given in Tables 3.14 to 3.20. These results are also plotted in Figure 3.13 for the in-service condition and Figure 3.14 for the under construction condition respectively. Some observations of these results are given below,

- All results for the in-service condition in Tables 3.7 to 3.13 show negative H_1^* and A_2^* values, implying that no negative aerodynamic damping for these test conditions. No instability is expected within the range of wind speeds tested for these conditions. At an angle of attack of +6°, both H_1^* and A_2^* become comparatively small at the final test speed examined (corresponding to a full scale wind speed about 100 m/s). This is possibly an indication that negative aerodynamic damping may exist at a slightly higher wind speed. However, the dynamic section model test indicated an instability at +4° at about 85 m/s.

- Table 3.14 (angle of attack of 0°), Table 3.15 (angle of attack of -2°) and Table 3.18 (angle of attack of +2°) show that in the under construction stage, the aerodynamic derivative parameters H_1^* and A_2^* are negative, thus the deck section does not exhibit negative aerodynamic damping in either of the vertical or torsional degrees of freedom up to the reduced wind speeds given in the tables. However, at larger angles of attack ±4° and ±6°, since A_2^* becomes positive at higher reduced velocities, the under construction condition would experience negative aerodynamic damping.

3.2.5 Conversion of Aerodynamic Derivatives to Scanlan (1971) Notation

The Scanlan notation for the presentation of Aerodynamic derivatives has evolved since the first description in 1971, perhaps owing to the roots of the concept in Airfoil Flutter rather than in Bridge Aerodynamics [9]. The definition adopted by the BLWTL described in Section 3.2.2 and in Appendix D differs from Scanlan's original definition in two areas. The first is that Scanlan's Flutter Derivatives are based on a notation for vertical motion where the positive direction is downwards, whereas the BLWTL definition for vertical motion is positive upwards. While this change in orientation for positive response and force does not have any influence on the diagonal terms such as $H_1{}^*$ The second, and more subtle difference is that originally, the notation was based on "2b", where "b" was identified as the half-chord of an airfoil or the half-width of the bridge deck. At some point in Scanlan's numerous writings on the subject, the notation was switched to "B", or the deck width, however still retaining the factor "2", thereby resulting in some confusion. The BLWTL has adopted the notation based on "B" alone as noted in Section 3.2.2.

It is understood that COWI uses a definition similar to that of the original Scanlan definition of the aerodynamic derivatives with a vertical axis h, and thus L, positive *downwards*. K is the reduced frequency, K = ωB/V and B is the bridge deck width, not the half-deck width.

The equations are given in reference [1] as follows:

$$D = \tfrac{1}{2}\rho V^2(2B)\left(KP_1^*\frac{\dot{y}}{V} + KP_2^*\frac{B\dot{\theta}}{V} + K^2P_3^*\theta + K^2P_4^*\frac{y}{B} + KP_5^*\frac{\dot{h}}{V} + K^2P_6^*\frac{h}{B}\right) \quad (3.6)$$

$$L = \tfrac{1}{2}\rho V^2(2B)\left(KH_1^*\frac{\dot{h}}{V} + KH_2^*\frac{B\dot{\theta}}{V} + K^2H_3^*\theta + K^2H_4^*\frac{h}{B} + KH_5^*\frac{\dot{y}}{V} + K^2H_6^*\frac{y}{B}\right) \quad (3.7)$$

$$M = \tfrac{1}{2}\rho V^2(2B^2)\left(KA_1^*\frac{\dot{h}}{V} + KA_2^*\frac{B\dot{\theta}}{V} + K^2A_3^*\theta + K^2A_4^*\frac{h}{B} + KA_5^*\frac{\dot{y}}{V} + K^2A_6^*\frac{y}{B}\right) \quad (3.8)$$

The conversion between the BLWTL derivatives (the results of which are presented in Section 3.2.4) should be modified as follows to develop the derivatives in the COWI-preferred notation:

$P_{1\,COWI}^* = P_{1\,BLWTL}^*$	$P_{2\,COWI}^* = P_{2\,BLWTL}^*$	$P_{3\,COWI}^* = P_{3\,BLWTL}^*$	$P_{4\,COWI}^* = P_{4\,BLWTL}^*$	$P_{5\,COWI}^* = -P_{5\,BLWTL}^*$	$P_{6\,COWI}^* = -P_{6\,BLWTL}^*$
$H_{1COWI}^* = H_{1BLWTL}^*$	$H_{2COWI}^* = -H_{2BLWTL}^*$	$H_{3COWI}^* = -H_{3BLWTL}^*$	$H_{4COWI}^* = H_{4BLWTL}^*$	$H_{5COWI}^* = -H_{5BLWTL}^*$	$H_{6COWI}^* = -H_{6BLWTL}^*$
$A_{1COWI}^* = -A_{1\,BLWTL}^*$	$A_{2COWI}^* = A_{2BLWTL}^*$	$A_{3COWI}^* = A_{3BLWTL}^*$	$A_{4COWI}^* = -A_{4BLWTL}^*$	$A_{5COWI}^* = A_{5BLWTL}^*$	$A_{6COWI}^* = A_{6BLWTL}^*$

3.2.6 Presentation of Aerodynamic Derivatives in SdM Notation

Reference [1,3] defines the preferred SdM notation for the aerodynamic derivatives $p^*_{1\text{-}6}$, $h^*_{1\text{-}6}$, $a^*_{1\text{-}6}$ as follows:

$$D = \tfrac{1}{2}\rho V^2 B\left(-p_1^* \frac{i\omega z}{V} - p_4^* \frac{\pi}{2V^{*2}}\frac{z}{B} - p_2^* \frac{i\omega B\theta}{V} + p_3^*\theta - p_5^* \frac{i\omega y}{V} - p_6^* \frac{\pi}{2V^{*2}}\frac{y}{B}\right) \quad (3.9)$$

$$L = \tfrac{1}{2}\rho V^2 B\left(-h_1^* \frac{i\omega z}{V} - h_4^* \frac{\pi}{2V^{*2}}\frac{z}{B} - h_2^* \frac{i\omega B\theta}{V} + h_3^*\theta - h_5^* \frac{i\omega y}{V} - h_6^* \frac{\pi}{2V^{*2}}\frac{y}{B}\right) \quad (3.10)$$

$$M = \tfrac{1}{2}\rho V^2 B^2\left(-a_1^* \frac{i\omega z}{V} - a_4^* \frac{\pi}{2V^{*2}}\frac{z}{B} - a_2^* \frac{i\omega B\theta}{V} + a_3^*\theta - a_5^* \frac{i\omega y}{V} - a_6^* \frac{\pi}{2V^{*2}}\frac{y}{B}\right) \quad (3.11)$$

Assuming harmonic motion, $h = h_0 e^{i\omega t}$, $y = y_0 e^{i\omega t}$, $\theta = \theta_0 e^{i\omega t}$ and inserting h = $-z$ into the Scanlan expressions yields the following relationships between the SdM form ($p^*_{1\text{-}6}$, $h^*_{1\text{-}6}$, $a^*_{1\text{-}6}$) and the COWI (Scanlan) form ($P^*_{1\text{-}6}$, $H^*_{1\text{-}6}$, $a^*_{1\text{-}6}$) of aerodynamic derivatives:

$P_1^* = -\frac{1}{2}\frac{V}{\omega B}p_5^*$	$P_2^* = -\frac{1}{2}\frac{V}{\omega B}p_2^*$	$P_3^* = \frac{1}{2}\left(\frac{V}{\omega B}\right)^2 p_3^*$	$P_4^* = -\frac{1}{2}\frac{\pi}{2}p_6^*$	$P_5^* = \frac{1}{2}\frac{V}{\omega B}p_1^*$	$P_6^* = \frac{1}{2}\frac{\pi}{2}p_4^*$
$H_1^* = -\frac{1}{2}\frac{V}{\omega B}h_1^*$	$H_2^* = \frac{1}{2}\frac{V}{\omega B}h_2^*$	$H_3^* = -\frac{1}{2}\left(\frac{V}{\omega B}\right)^2 h_3^*$	$H_4^* = -\frac{1}{2}\frac{\pi}{2}h_4^*$	$H_5^* = \frac{1}{2}\frac{V}{\omega B}h_5^*$	$H_6^* = \frac{1}{2}\frac{\pi}{2}h_6^*$
$A_1^* = \frac{1}{2}\frac{V}{\omega B}a_1^*$	$A_2^* = -\frac{1}{2}\frac{V}{\omega B}a_2^*$	$A_3^* = \frac{1}{2}\left(\frac{V}{\omega B}\right)^2 a_3^*$	$A_4^* = \frac{1}{2}\frac{\pi}{2}a_4^*$	$A_5^* = -\frac{1}{2}\frac{V}{\omega B}a_5^*$	$A_6^* = -\frac{1}{2}\frac{\pi}{2}a_6^*$

The conversion from the BLWTL notation, to that of the SdM form has been performed and is presented for the in-service and under construction condition in Figures 3.15 and 3.16, respectively. The results are also provided in Tabular form in Tables E-1 to E-7 of Appendix E, while the results for the under construction condition are given in Tables E-8 to E-14.

3.3 Aerodynamic Admittance

3.3.1 General

The aerodynamic admittance function (AAF) represents the degree to which the bridge response departs from that which would be obtained using the quasi-steady aerodynamics assumption for describing the impact of turbulence. Davenport [8] has utilised this concept in the formulation of the modal forces due to the buffeting action of the wind on a bridge deck. The AAF also reflects both the efficiency of the section as a lift and torsion generator as well as the correlation of the flow in the vicinity of the deck. At very low reduced frequencies ($f^* = fB/V$), the efficiency should approach the quasi-steady flow value and $|A(f^*)|^2 = 1$. At high reduced frequency, the deck is less efficient and the vertical and torsional forces usually fall off. The quasi-steady aerodynamics assumption implies that over the chord of the deck the wind forces are perfectly correlated assuming that the scale of the turbulence is much larger than the width of the deck. This assumption is accurate for low frequencies but deteriorates with increased frequencies.

The aerodynamic admittance function is determined in the frequency domain as the transfer function between the input turbulence and the output turbulence-induced forces. The aerodynamic admittance function can be obtained experimentally by simultaneous measurements of the time histories of the wind turbulence and the buffeting forces on a stationary model in the wind tunnel [9,10,11,12,13]. Postprocessing is then used to develop the appropriate transfer functions and hence the AAF for each component of wind and wind-induced force.

The pressure measurement approach [9], whereby the sectional lift, drag and torsional forces are computed as a summation of surface pressures isolates the aerodynamic admittance from any span-wise correlation effects of the aerodynamic forces. However, due to the discrete elements on the Messina Bridge deck section (i.e. the airfoils, screening, railing, porous plates, etc.) this approach could not be utilized, since it would not be possible to measure the surface pressures on these aerodynamically significant components. Instead, the central portion of the section model (centred on one cross-girder and 0.375m in length) was supported by a small, 6-component load cell (details of which are shown in Figure 2.2c and in Figure 3.17). To stiffen this central section of the model, 4 machined links were inserted in the triangular nosing between the end of the model and the central instrumented portion (shown in Figure 3.17a). This had the effect of stiffening the central portion (primarily in the torsional degree of freedom), while at the same time, reducing the overall sensitivity of the 6-component load cell to wind-induced forces. Some attenuation of the wind-induced forces can be expected due to the span-wise correlation effects over the 0.375m length of the instrumented portion of the model, however this effect is expected to be small for the frequency range of interest. The effect of span-wise correlation can be investigated through a theoretical examination of the Joint Acceptance Function (related to the length of the model and the scale of the turbulence).

The vertical, lateral and longitudinal components of the turbulence were measured using two “Cobra” probe anemometers placed at a distance B/2 upwind of the leading edge of the model at a separation distance of B , where B is the chord dimension of the section model. Figure 3.18 shows the experimental set up. Background discussion on the “Cobra” probe and its operation can be found in Section 4.2 as the same instruments were utilised in the measurement of the vertical profiles above the road and rail girders.

A complete form of the AAF related to this approach is defined as follows for the influence of the vertical (w) and longitudinal (u) components of turbulence on the fluctuating lift (L) forces (see reference [9]) which is termed the “COMPLETE” Method:

$$\left|A_{Lu}(f^*)\right|^2 = \frac{U}{C_L 0.5\rho U^2 B}\left[\frac{S_{Lu}(f^*)S_w(f^*) - S_{Lw}(f^*)S_{wu}(f^*)}{S_u(f^*)S_w(f^*) - S_{uw}(f^*)S_{wu}(f^*)}\right] \quad (3.12)$$

$$\left|A_{Lw}(f^*)\right|^2 = \frac{U}{\frac{dC_L}{d\alpha} 0.5\rho U^2 B}\left[\frac{S_{Lw}(f^*)S_u(f^*) - S_{Lu}(f^*)S_{uw}(f^*)}{S_u(f^*)S_w(f^*) - S_{uw}(f^*)S_{wu}(f^*)}\right] \quad (3.13)$$

Similarly the aerodynamic admittance functions between the torsional (T) force and the w and u components of the wind are:

$$\left|A_{Tu}(f^*)\right|^2 = \frac{U}{C_T 0.5\rho U^2 B^2}\left[\frac{S_{Tu}(f^*)S_w(f^*) - S_{Tw}(f^*)S_{wu}(f^*)}{S_u(f^*)S_w(f^*) - S_{uw}(f^*)S_{wu}(f^*)}\right] \quad (3.14)$$

$$\left|A_{Tw}(f^*)\right|^2 = \frac{U}{\frac{dC_T}{d\alpha} 0.5\rho U^2 B^2}\left[\frac{S_{Tw}(f^*)S_u(f^*) - S_{Tu}(f^*)S_{uw}(f^*)}{S_u(f^*)S_w(f^*) - S_{uw}(f^*)S_{wu}(f^*)}\right] \quad (3.15)$$

Equations (3.12) and (3.13) are the lift aerodynamic admittance functions resulting from the longitudinal and vertical components of the turbulence of oncoming wind, while equations (3.14) and (3.15) are the torsional aerodynamic admittance functions resulting from the longitudinal and vertical components of the turbulence. In the equations, S_{xy} is the cross-spectrum between x and y, and S_x is the auto-spectrum of x. C_L and $dC_L/d\alpha$ are the lift force coefficient and lift slope at the appropriate angle of attack, while C_T and $dC_T/d\alpha$ are the torque coefficient and torque slope (also at the mean angle of attack).

In many cases of practical analyses, some terms in the above equations are small and negligible. The aerodynamic admittances for the lift can be simplified as follows, termed the "SIMPLIFIED" Method:

$$\left|A_{Lu}(f^*)\right|^2 = \frac{1}{C_L^2\rho^2U^2B^2}\left[\frac{S_L(f^*)}{S_u(f^*)}\right] \tag{3.16}$$

$$\left|A_{Lw}(f^*)\right|^2 = \frac{1}{\frac{1}{4}(\frac{dC_L}{d\alpha})^2\rho^2U^2B^2}\left[\frac{S_L(f^*)}{S_w(f^*)}\right] \tag{3.17}$$

Similarly the aerodynamic admittance for the torsional forces can be written as:

$$\left|A_{Tu}(f^*)\right|^2 = \frac{1}{C_T^2\rho^2U^2B^4}\left[\frac{S_T(f^*)}{S_u(f^*)}\right] \tag{3.18}$$

$$\left|A_{Tw}(f^*)\right|^2 = \frac{1}{\frac{1}{4}(\frac{dC_T}{d\alpha})^2\rho^2U^2B^4}\left[\frac{S_T(f^*)}{S_w(f^*)}\right] \tag{3.19}$$

These simplified equations indicate that the main frequency-dependent terms in the aerodynamic admittance can be determined by dividing the spectra of the forces (S_L and S_T) by the spectrum of the wind velocity fluctuations (S_u and S_w). The individual components of this form of aerodynamic admittance $\left|A_{Lu}(f^*)\right|^2$, $\left|A_{Lw}(f^*)\right|^2$, $\left|A_{Tu}(f^*)\right|^2$ and $\left|A_{Tw}(f^*)\right|^2$ can also be combined for the u and w components of turbulence. The AAF in this case is obtained by a quotient of a combination of the spectral functions as follows, termed the "COMBINED" Method:

$$\left|A_L(f^*)\right|^2 = \frac{S_L(f^*)}{C_L^2\rho^2U^2B^2S_u(f^*) + \frac{1}{4}(\frac{dC_L}{d\alpha})^2\rho^2U^2B^2S_w(f^*)} \tag{3.20}$$

$$\left|A_T(f^*)\right|^2 = \frac{S_T(f^*)}{C_T^2\rho^2U^2B^4S_u(f^*) + \frac{1}{4}(\frac{dC_T}{d\alpha})^2\rho^2U^2B^4S_w(f^*)} \quad (3.21)$$

The drag aerodynamic admittance in this combined form is formulated as follows:

$$\left|A_D(f^*)\right|^2 = \frac{S_D(f^*)}{C_D^2\rho^2U^2B^2S_u(f^*) + \frac{1}{4}(\frac{dC_D}{d\alpha})^2\rho^2U^2B^2S_w(f^*)} \quad (3.22)$$

The pressure integration approach relates the integrated lift and torque on a cross-sectional strip of the model to the fluctuation of the wind, which does not account for the contribution of the correlation of the wind-induced forces along the span. Therefore, equations (3.12) to (3.22) in calculating the AAF do not include the span-wise correlation of the aerodynamic forces. However in the situation as for the Messina Bridge, where a span-wise portion of the model was instrumented, the total lift and torque on the instrumented section of the model are obtained using a force balance. The aerodynamic admittance evaluated using the total lift and torque on the section of the model therefore includes a combination of the cross-sectional admittance given in equations (3.12) to (3.22) and the span-wise distribution of the forces, which has been referred to as the segmental admittance. As discussed previously, the segmental aerodynamic admittance has a 3-D character when compared to the cross-sectional admittance of a strip. Mathematically, the major difference of these two admittance functions is the extra parameter in these equations, termed by Davenport as the joint acceptance function $\left|J(f^*)\right|^2$.

Equations (3.20) to (3.22) can be re-written as follows for the segmental admittance function,

$$\left|A_L(f^*)\right|^2 = \frac{S_L(f^*)}{[C_L^2\rho^2U^2B^2S_u(f^*) + \frac{1}{4}(\frac{dC_L}{d\alpha})^2\rho^2U^2B^2S_w(f^*)]\left|J_L(f^*)\right|^2} \quad (3.23)$$

$$\left|A_T(f^*)\right|^2 = \frac{S_T(f^*)}{[C_T^2\rho^2U^2B^4S_u(f^*) + \frac{1}{4}(\frac{dC_T}{d\alpha})^2\rho^2U^2B^4S_w(f^*)]\left|J_T(f^*)\right|^2} \quad (3.24)$$

$$\left|A_D(f^*)\right|^2 = \frac{S_D(f^*)}{[C_D^2\rho^2U^2B^2S_u(f^*) + \frac{1}{4}(\frac{dC_D}{d\alpha})^2\rho^2U^2B^2S_w(f^*)]\left|J_D(f^*)\right|^2} \quad (3.25)$$

The study has used equations (3.12) to (3.22) to estimate the cross-sectional aerodynamic admittances, which can be used to compare to other benchmark studies.

3.3.2 Results and Discussion

Power spectra of the vertical, lateral and longitudinal wind turbulence component for the grid-generated turbulence are presented in Figure 3.19 and typical power spectrum of the lift, drag and torque forces are given in Figure 3.20. This constitutes the basis for the evaluation of the aerodynamic admittance, since this parameter is essentially a transfer function of the aerodynamic force (output) and wind turbulence spectra (input). These figures indicate that the peaks of the spectra do not necessarily coincide and that the deck appears to be able to extract more energy from the lower frequency components of the flow. The parameters used in the normalization process (e.g. static force coefficients, slopes of the coefficients, deck dimensions etc.) are presented in Table 3.21.

The observed form of the aerodynamic admittance of the bridge deck is shown in Figures 3.21 through 3.23 for the three methods described above “Simplified”, “Combined” and “Complete”. These measurements cover the critical values of f^* at resonance for the design wind speed range and were determined from the transfer function between the local fluctuating lift (and torque) forces on the "segment" of the bridge cross-section with the vertical, w , and longitudinal, u , components of turbulence as required. The aerodynamic admittance functions are presented for five test wind speeds, where the resonant peaks due to the natural frequency of the instrumented portion of the model are clearly identified and appear at different values of fB/U , as the wind speed, U , changes for each test.

Also shown on these figures is the "Sears" function, a functional form of the aerodynamic admittance introduced in the theoretical treatment of flat plate airfoils (with a lift slope of 2π) [14]. Liepmann’s approximation to the Sears function is the commonly used form of the lift aerodynamic admittance of a thin airfoil in fully correlated gusts [15]:

$$\left|\phi_Z\left(f^*\right)\right|^2 = \frac{1}{1+2\pi^2 f^*} \qquad (3.26)$$

Vickery’s approximation for the drag admittance for flat plates normal to a turbulent wind is used as a comparison to the measured admittance functions in the drag direction [15]:

$$\left|A_D(f^*)\right|^2 = \frac{1}{1+\left[2f\sqrt{DL}/U\right]^{4/3}} \qquad (3.27)$$

The Sears function appears to over estimate the aerodynamic admittance at low reduced frequencies while underestimating at somewhat higher frequencies. Given that the lift slope of the Messina Bridge section is less than 1/3 of that of the airfoil, any agreement with the Sears function would seem to be fortuitous.

Figures 3.24 through 3.26 present an averaged form of the measured aerodynamic admittance function which is developed from an arithmetic average of the functions over the wind speeds used in the tests.

4 Sub Test D5

Sub-test D5 measures steady state wind load coefficients with and without traffic and at skew wind directions relative to the bridge centre line. The sub-test also measures the mean wind and turbulence profiles at selected positions on the road deck traffic lanes and railways with various traffic conditions present on the road girders and railway girder.

4.1 Steady State Wind Load Coefficients

Steady state lift, drag and moment coefficients were measured for wind directions perpendicular to the bridge centre line and at skew wind directions of $\psi = 10°, 20°, 30°$ and $45°$, at angles of attack with respect to the horizontal in the range $-10^0 < \alpha < +10^0$ in increments of 0.5°. Measurements for $\psi = 0°$ were carried out for the three different traffic conditions and the measurements at skew angles of $\psi = 10°, 20°, 30°$ and $45°$ were carried out for the three different traffic set-ups as well as the no traffic case. The steady state wind load coefficient tests were carried out in both smooth and turbulent flow conditions.

Definitions of the model skew angle with respect to the mean wind is presented in Figures 4.1 and 4.2. The model was lengthened through the addition of custom triangular deck modules for each skew angle to be examined, which included elliptical aluminum end plates parallel to the mean wind direction. Fixity to the load cells within the static test rig was through a “universal joint” located between the model end and each load cell. The “universal joint” permitted free yawing and rolling motion, while transmitting torsion (i.e. pitching moment) and all shear forces to the load cells. In this manner, the BLWTL automated static test rig could be utilized, stepping through the 41 angles of attack in an automated manner, requiring manual intervention only for changes to traffic and skew angle.

As with the steady state wind load coefficient tests for Sub-test D3 and reported in Section 3.1, the force coefficients are defined in the same manner and repeated for convenience below:

$$C_{x,z,l,d} = \frac{F_{x,z,l,d}}{qB} \qquad (4.1)$$

in which C is an aerodynamic coefficient, F is the mean aerodynamic force per unit length of the model, L is the extended model length (including triangular insert pieces), $q = \frac{1}{2}\rho V^2$ and is the mean wind velocity pressure at deck level, ρ is the density of air (1.25 kg/m^3), V is the mean wind velocity at deck level in m/s, and B is the bridge deck width. The subscripts x,z,l,d refer to the X and Z body force components and lift and drag respectively. It is important to note that C_x , C_z and C_m are “Body-Force Coefficients”, however are relative to the longitudinal axis of the wind tunnel and not aligned perpendicular to the axis of the model.

The torque coefficient is defined:

$$C_m = \frac{F_t}{qB^2} \qquad (4.2)$$

Figure 4.3 presents the sign convention for the steady state wind load coefficient tests under skew wind azimuth. Photographs of the triangular model inserts are shown in Figure 4.4, while photographs of the model under skew wind are presented in Figure 4.5. The full scale truck traffic convoy is given in Figure 4.6, while the dimensions of the train traffic is given in Figure 4.7. Truck and rail traffic convoys were represented by scaled geometric shapes cut from Styrofoam blocks and fixed to strips of brass in the appropriate traffic pattern given in Figure 4.6. Dimensions of the model traffic are presented in Figure 4.8. The brass strip was mass-scaled to represent the lane loading which would be required for the stability and buffeting tests (discussed in Section 5) as well as to provide a convenient and repeatable manner of removing and re-installing the traffic as required during the tests.

Photographs of the traffic conditions are given in Figure 4.9. The traffic conditions examined in the steady state wind load coefficient tests were as follows:

1) Traffic 1 - road traffic on outward lane of upwind girder plus train on upwind track;
2) Traffic 2 - road traffic on outward lane of downwind girder plus train on upwind track;
3) Traffic 3 - train on upwind track only.

A fourth traffic condition is shown in Figure 9, termed "Traffic 2*", which was comprised of road traffic on outward lane of upwind girder only. This condition was utilized in the dynamic tests only and not the static tests and is discussed further in Section 5.1.

The results of the load tests are presented in graphs giving the left, drag and moment coefficients in a deck (C_L, C_D and C_m) and fixed (C_x, C_z and C_m) frame of reference relative to the mean wind. Graphical and tabular results for all tests are presented in Appendix C.

4.2 Wind Profiles

Vertical profiles of the mean wind and turbulence intensity ranging from deck level to 8-7 m (full-scale) above the deck were be measured by means of "Cobra" probes situated at 8 stations across the deck, corresponding to the centre of the roadway and railway lanes. The profile measurements were made for wind perpendicular to the bridge, $\psi = 0°$, and at an angle of attack $\alpha = 0°$. The wind profile measurements were made without traffic and in selected positions with the 3 traffic configurations present. Wind profile measurements were carried out in turbulent flow only.

The Cobra Probe is a multi-hole pressure probe able to resolve 3-components of velocity within a range of ±45° and local static pressure in real time. A frequency response in excess of 2000 Hz means the Cobra Probe is especially suited to the measurement of turbulent flows. Accuracy of measurements is somewhat dependent on turbulence levels but is generally within ±0.5 m/s and ±1° pitch and yaw up to about 30% turbulence intensity. The Cobra Probe remains relatively accurate to greater than 30% turbulence intensity. The set-up for the velocity profile measurement is shown in Figure 4.10. Further details concerning the probe technology are available in references [16, 17].

The results of the wind profile measurements are presented in graphs giving the mean wind normalized by the free stream wind speed and turbulence intensity as function of height above roadway / railway surface for the various stations across the bridge deck. The heights above the roadway and rail girder used for the measurements are (in full scale units): 0.8, 1.6, 2.4, 3.2, 4.0, 4.8, 5.6, 6.4, 8.0, 16.0 and 24.0m.

The results of the tests are given in summary form in Figures 4.11 through 4.14 for the bare deck and Traffic Conditions 1 through 3, respectively. A full set of data is presented in Tables 4.1 through 4.4. Plots for each position and traffic condition are given in Appendix F.

5 Sub-test D6

Sub-test D6 provides experimental data for the verification of aerodynamic calculations of aerodynamic stability and buffeting responses using the three degree of freedom spring suspended section model.

5.1 Aerodynamic Stability and Buffeting

5.1.1 General

Full scale dynamic properties of the in-service deck section as well as the corresponding scaled properties for the dynamic section model are given in Table 5.1. Three-dimensional motion of the bridge section was modelled in the test. The fundamental lateral, vertical and torsional modal frequencies of vibration were selected as the frequencies to be simulated in the dynamic section model tests. During the test, the section model properties were matched to the scaled mass and mass moment of inertia of the prototype, as well as the frequency ratio between the torsional and vertical modes of vibration.

The section model was mounted on soft springs and was ballasted with additional mass to represent the dynamically scaled mass and mass moment of inertia of the prototype. The drag wire and spring selected for simulating the horizontal motion of the model is shown in Figure 5.1. A bearing system was designed to connect the drag wires and spring system to the ends of the section model, to minimise the damping in the torsional degree of freedom as well as the cross-talk between torque and drag which would be present if a fixed drag wire to model connection were used. The lift, drag and torsional damping were all less than 0.5% of critical, as specified by COWI and SdM [1,3].

The dynamic section model test was performed for three angles of attack at -4^o, 0^o and +4^o, and for the following test configurations: 1) the in-service deck section; 2) the in-service deck section with both road vehicles and train (Traffic Condition 1); 3) the in-service deck section with road vehicles only (Traffic Condition 2*); and 4) the in-service deck section with train only (Traffic Condition 3). Figure 5.2 presents the four test configurations for the dynamic section model study.

5.1.2 Generation of Turbulence

Turbulence in the wind tunnel for the section model test was generated by a grid placed upstream of the model. The grid used in the test has a mesh size of 140mm and 600mm centre to centre spacing, which can be seen in Figure 2.5. The vertical (I_w) and horizontal (I_u) turbulence intensities generated using this grid were 5.9% and 11.7% respectively. The turbulence intensity in the smooth flow test was less than 0.5%. The flow properties, including the spectral estimates, integral length scales, coherences and turbulence intensities are documented further in Section 5.2.

5.1.3 Dynamic Response

Tables 5.2 to 5.4 summarize all tests performed in Sub-Test D6. The test conditions, their corresponding full scale parameters and maximum wind speeds, indication of deck performance as well as the corresponding test number and figure number in the report are also presented in summary form in these tables.

All results from the dynamic section model tests are plotted in Appendix G. Selected test results are also given in Figures 5.3 to 5.7. Rotations and full scale displacements in drag and lift directions in these plots have been plotted against the full scale mean wind speed at deck height in m/s. In each of the plots, the mean and root-mean-square (RMS) responses are presented. The total response of the section is equal to the mean, plus or minus the RMS value multiplied by an appropriate peak factor, as shown in Equation (5.1),

$$y_{\max} = \bar{y} \pm g \cdot y_{RMS} \qquad (5.1)$$

where g is the peak factor and $y_{\max}, \bar{y}$ and y_{RMS} are the maximum, mean and root mean square (RMS) response.

It should be noted that a nominal peak factor of 3.5 can be used in estimating the total response. However, the peak factor in Equation (5.1) should be modified to the measured value whenever the Peak Factor computed from the time history approaches a value indicative of either an instability or vortex shedding. The peak factor during instability decreases to a value approaching 1.4 or $\sqrt{2}$, (i.e. 1/(RMS) of a sinusoidal signal with amplitude of 1.0). Thus, for the range of wind speeds where the model has shown either a large vortex shedding peak or experiences any other instability, the “Measured Peak Factor” determined from the test for the corresponding wind speed should be used to obtain the peak response. This is necessary since the use of a constant peak factor of 3.5 would tend to overestimate the peak response in regions of sinusoidal motion.

Full scale displacements for drag and lift were obtained from the measured model displacements and converted using the geometric length scaling of 1:80. Rotations need no such scaling. The full scale and model frequencies have been used to determine the conversion factors from model scale velocity to full scale wind speed through the following relationship:

$$V_{\text{full scale}} = V_{\text{model}} \cdot \left(\frac{f_{\text{full scale}}}{f_{\text{model}}} \right) \cdot \left(\frac{1}{\lambda_L} \right) \qquad (5.2)$$

where $(1/\lambda_L) = 80$, the geometric scale of the model and f is the natural frequency of either the lateral, vertical or torsional mode of vibration.

In section model testing, the onset of an “instability” can be defined as when the character of the response changes from a random type motion to that of a regular, sinusoidal motion, involving either pure torsional or a coupled vertical-torsional vibration. This can be clearly identified through an examination of the “peak factor” as discussed above. For the purpose of this investigation, a peak factor of less than 2 was selected as the governing criteria for the onset of aerodynamic instability. Further discussion on this can be found in Appendix B.

5.1.4 Results of Dynamic Tests

Selected test results are presented in Figures 5.3 to 5.7. All results from the dynamic section model tests are presented in Appendix G.

Some general comments on the dynamic response of the section model tests of the bridge deck are given below.

- The damping ratios in the current set-up are 0.15% of critical in drag, 0.34% in lift and 0.49% in torque, all of which are less than the requirement of 0.5% as specified by COWI and SdM [1,3].
- The velocity scaling is nearly identical for lift and torque with the torque being approximately 3% higher. The velocity scaling for the drag direction is about 78% of the lift velocity scaling, due to the limitations in the test rig and spring availability.
- In all plots, the wind speed shown corresponds to the mean hourly wind speed at deck height taking into account the different velocity scaling for drag, lift and torsional degrees of freedom.
- No vortex shedding induced instability was observed in any of the tests.
- No instability was observed in any of the tests at -4^{o} angle of attack in smooth flow, and all tests reached over 100 m/s.

- All tests at +4° angle of attack in smooth flow experienced a vertical / torsional instability, and all tests were halted to avoid damage to the model or test rig. Instability occurred at about 83 m/s for the two configurations with no traffic and with train only, while the tests were stopped at about 93 m/s for the configurations with road vehicles only and with both road vehicles and train.

- Only the test with the Traffic Condition 1 (both road vehicles and train) shows an instability at about 50 m/s at 0° in smooth flow. The remaining tests at 0° in smooth flow do not show any instability up to 100 m/s.

- No instability was observed in any of the turbulent flow tests at 0°, and all tests reached a mean wind speed of 100 m/s.

- The dynamic response of the bridge deck under turbulent flow conditions was characterized by turbulent buffeting. The mean components of the responses were comparable to those found in the smooth flow tests.

- The tests at 0° angle of attack without traffic present (Figure 5.3) and -4° (Figure 5.7) reached about 120 m/s in lift and torque without any instability observed. Instability was not seen up to about 100 m/s in the turbulent flow test (Figure 5.4) at 0°. At an angle of attack of +4°, an instability was observed at 84 m/s, as shown in Figure 5.6. Figure 5.5 shows the test result for 0° angle of attack in smooth flow with both road vehicles and train present, in which an instability was observed at about 50 m/s.

5.1.5 Estimates of Aerodynamic Damping

All tests were conducted in smooth flow conditions. The normalizing frequencies used in the analysis are provided in Table 5.5 for the aerodynamic damping tests and a summary of the tests performed is given in Table 5.6.

The following configurations, wind speeds and angles of attack were examined for the in-service bridge deck:

a) Traffic Condition:
   i. No Traffic
   ii. Traffic 1 - Road traffic in outward (slow) lane on windward girder, train on upwind track
   iii. Traffic 2 - Road traffic in outward lane (slow) on downwind girder, train on upwind track
   iv. Traffic 3 - No road traffic, train on upwind track

b) Wind Speeds:
   i. full scale wind speeds of 44, 47, 54, 60 and 75 m/s

c) Angles of Attack:
   i. -4.0 degrees;
   ii. 0.0 degrees;
   iii. +4.0 degrees

Traffic Condition 2 was mistakenly performed as the “Road traffic in outward (slow) lane on windward girder” and omitted the train traffic in the dynamic section model tests. The tests for this condition are therefore referred to as Traffic Condition 2*. In order to assess the likely impact of the omission of the train traffic, the static force coefficients with each traffic condition were examined. Table 5.7 presents a summary of the static force coefficients and their slopes for Traffic 2 and Traffic 3. The static force coefficients and their slopes at -4°, 0° and +4° are essentially the same for Traffic Conditions 2 and 3. Therefore, the results from Traffic Condition 3 can be applied to Traffic Condition 2 directly with reasonable confidence.

The two most important aerodynamic derivatives in an evaluation of aerodynamic damping are the H_1^* and A_2^* derivatives, which govern the equivalent aerodynamic damping values in the vertical and torsional directions respectively. The conversion of the aerodynamic derivative to an equivalent structural damping as a ratio to critical, is through the following relationships;

$$\zeta_{aZ} = -\frac{\rho B^2}{m}\frac{H_1^*}{4} \tag{5.3}$$

$$\zeta_{a\theta} = -\frac{\rho B^4}{I_o}\frac{A_2^*}{4} \tag{5.4}$$

Where:

ρ is the density of air

B is the characteristic width of the Bridge Deck

m is the deck mass per unit length, and

I_o is the deck mass moment of inertia per unit length.

The results of the aerodynamic damping test are presented in Table 5.8 for 0^o, Table 5.9 for +4^o and Table 5.10 for -4^o, respectively. Some observations of the test results are as follows,

- Table 5.8 shows that at 0^o, both Traffic Condition 1 (road vehicles upwind of train) and Traffic Condition 3 (train only) indicate negative aerodynamic damping values for vertical motions. A similar result was obtained for Traffic Condition 1 in the dynamic section model test reported in Section 5.1.4, where an instability was found at 50 m/s. Traffic Condition 3 would also result negative aerodynamic damping, while aerodynamic instability was not observed in the dynamic section model test for this traffic condition.
- The aerodynamic damping results for the +4^o test in Table 5.9 do not show negative aerodynamic damping values for any of the wind speeds examined. However, the torsional aerodynamic damping values for the no traffic condition and the Traffic Condition 3 are close to 0 at wind speeds around 80 m/s. This is consistent with the observations from the dynamic section model test in which an instability was observed at about 85 m/s.
- Table 5.10 for the -4^o test shows large positive aerodynamic damping values for all conditions, which are consistent with the findings in the dynamic section model test with no observed instabilities up to 100 m/s.

5.2 Documentation of Turbulent Flow

5.2.1 Intensity of Turbulence

Turbulence developed in the wind tunnel using the fixed grid technique is normally lacking sufficient energy in the low frequency – large scale range to match full scale, resulting in an lower overall turbulence intensity. The energy in the high frequency end of the spectrum is well modelled and is critical for the definition of resonant response and the overall behaviour of the structure to turbulent wind.

Turbulence in the wind tunnel for the section model test was generated by a grid placed upstream of the model. The large mesh size (140 mm) and bar spacing (600 mm) were selected to give a close representation of the natural wind. The “Cobra” probes discussed in Section 4.2, were used to measure three components of wind speed at deck level at the location shown in Figure 5.8. Time histories of the wind speeds were sampled at 10,000 Hz for a duration of 5 minutes. Typical time histories are shown in Figures 5.9 and 5.10 for smooth and turbulent flows respectively. The corresponding power spectral densities of the longitudinal, transverse and vertical components of turbulence were computed using standard techniques and are shown in Figure 5.11 as $fS(f)/U^2$ as a function of reduced frequency, fB/U. The spectral estimates, represented by the open circle markers, correspond to 49152 (1024 x 48) points of the Fourier Transform with 60 spectral averages. The number of spectral averages is sufficient to ensure a stable estimate of the power spectrum. The solid lines are fits to the spectral estimates and are of the form

$$\frac{fS_{u,v,w}(f)}{U^2} = \left[\frac{AB}{C}\right]_{u,v,w} \frac{\sigma^2_{u,v,w}}{U^2} \tag{5.5}$$

where:

$$A_{u,v,w} = \frac{4X_{Lu,v,w}f}{U} \tag{5.6}$$

$$B_u = 1 \text{, and } B_{v,w} = 1 + 755.2\left(\frac{X_{Lv,w}f}{U}\right)^2 \tag{5.7}$$

$$C_u = \left[1 + 70.8\left(\frac{X_{Lu}f}{U}\right)^2\right]^{5/6} \tag{5.8}$$

$$C_{v,w} = \left[1 + 283.2\left(\frac{X_{Lv,w}f}{U}\right)^2\right]^{11/6} \tag{5.9}$$

where f is frequency in Hz, U is longitudinal wind speed and $\sigma^2_{u,v,w}$ and $X_{Lu,v,w}$ are the variance and integral length scale in the longitudinal, transverse and vertical directions respectively.

The form shown in Equation (5.5) is similar to the ESDU formulation of atmospheric turbulence [7] which allows for the estimation of the integral length scales. The resulting turbulence intensities and integral length scales for the grid-generated turbulence are as follows:

I_u = 11.7 %; X_{Lu} = 0.141 m

I_v = 10.4 %; X_{Lv} = 0.062 m

I_w = 10.0 %; X_{Lw} = 0.059 m

5.2.2 Span-wise Cross-correlation of the Wind

The classical representation of the span-wise coherence of the wind velocity fluctuations is given in Figure 5.12 for the longitudinal and vertical components as a function of $f^* = f\Delta y/U$, where Δy represents the span-wise separation. The coherence function is defined as the ratio of the sums of the squares of the real and imaginary parts of the cross spectra between two points to the product of the auto-spectra of these points;

$$Coherence\,(f^*) = \frac{Co_{12}^2(f^*) + Qu_{12}^2(f^*)}{S_{11}(f^*)S_{22}(f^*)} \qquad (5.10)$$

where:

$Co_{12}^2(f^*)$ is the Co-spectrum, i.e. real (in-phase) component of the cross spectrum between points y_1 and y_2

$Qu_{12}^2(f^*)$ is the Quadrature spectrum, i.e. imaginary (out-of-phase) component of the cross spectrum between points y_1 and y_2

$S_{11}(f^*)$, $S_{22}(f^*)$ are Auto-spectra at points y_1 and y_2

The solid line on the graphs is an attempt to express the coherence function by the generally accepted exponential form expressed as

$$\sqrt{Coherence} = e^{-c(f^*)} \qquad (5.11)$$

where the value of the constant "*c*" the decay coefficient of the coherence, which is 7.4 for the longitudinal component and 4.8 for the vertical component.

REFERENCES

1. “Wind tunnel tests deck, Sub-tests D3, D5 and D6, Scope of Work”, 5 July, 2010, COWI, Denmark
2. “Traffic Configurations, wind tunnel testing”, 10 June, 2010, COWI, Denmark.
3. “Messina Strait Bridge, Tender Design - Overall Aerodynamic Design Methodology and Plan for Aerodynamic Testing”, Eurolink s.p.c.a., May 2009.
4. “Wind Tunnel Testing: A General Outline”, The University of Western Ontario, Boundary Layer Wind Tunnel Laboratory General Outline Report, May 1999.
5. Simiu, E and Scanlan, R.H., Wind Effects on Structures – Third Edition, John Wiley & Sons, Inc, New York, NY, 1996.
6. Turbulent Flow Instrumentation Pty, Limited, Victoria, Australia, http://www.turbulentflow.com.au/Products/CobraProbe/CobraProbe.html
7. Engineering Sciences Data Unit, "Characteristics of Atmospheric Turbulence Near the Ground", Data Item 74031, October, 1974.
8. Davenport, A.G., 1962, “The response of slender, line-like structures to gusty wind”, Proc. Of the Institution of Civil Engineers, Vol 23, pp 389-408.
9. Scanlan, R.H. and Tomko, J., “Airfoil and Bridge Deck Flutter Derivatives”, Journal of the Engineering Mechanics Division, ASCE, EM6, December 1971, pp 1717-1737.
10. King, J.P.C., Larose, G.L. and Davenport, A.G., 1991, "A Study of Wind Effects for the Storebælt Bridge, Tender Design, Denmark", The University of Western Ontario, Faculty of Engineering Science Research Report, BLWT-SS31-1991, The University of Western Ontario, London, Ontario, Canada.
11. Hatanaka, A. and Tanaka, H., 2002, “New estimation method of aerodynamic admittance function”, Journal of Wind Engineering and Industrial Aerodynamics, Vol. 90 (12-15), pp 2073-2086.
12. Larose, G.L., 1999, “Experimental determination of the aerodynamic admittance of a bridge deck segment”, Journal of fluids and structures (13), pp1029-1040.
13. Larose, G.L., Tanaka, H., Gimsing, N.J. and Dyrbye, C., 1998, “Direct measurements of buffeting wind forces on bridge decks”, Journal of Wind Engineering and Industrial Aerodynamics, , Vol. 74-76, 809-818.
14. Kawatani, M. and Kim, H., 1992, “Evaluation of aerodynamic admittance for buffeting analysis”. Journal of Wind Engineering and Industrial Aerodynamics, Vol. 41, pp613-624.
15. Liepmann, H.W., 1952, On the application of statistical concepts to the buffeting problem”, Journal of Aeronautical Science, V19, pp 783-810.
16. Vickery, B.J., 1965, “On the flow behind a coarse grid and its use as a model of atmospheric turbulence in studies related to wind loads on buildings”, National Physical Laboratory (U.K.), Aero Report 1143.
17. Watkins, S., Mousley, P.D. & Hooper, J.D., 2002, “Measurement of fluctuating flows using multi-hole probes”, Proceedings of the 9th International Congress of Sound and Vibration, Orlando, Florida, USA, 8-11 July, International Institute of Acoustics and Vibration (IIAV).
18. Turbulent Flow Inc., 2008, http://www.turbulentflow.com.au/Home.html

TABLES

TABLE 2.1 SECTION MODEL SCALING PARAMETERS

PARAMETER	SIMILITUDE REQUIREMENT	VALUE
Length*	$\lambda_L = \mathbf{L}_m / \mathbf{L}_p$	0.0125
Density	$\lambda\rho = \rho_m / \rho_p$	1
Velocity**	$\lambda_V = \mathbf{V}_m / \mathbf{V}_p = \lambda_L \, \mathbf{f}_m / \mathbf{f}_p$	
Mass per Unit Length	$\lambda_m = \lambda_\rho \lambda_L^2$	1.56E-04
Mass	$\lambda_M = \lambda_\rho \lambda_L^3$	1.95E-06
Mass Moment of Inertia per Unit Length	$\lambda_i = \lambda_m \lambda_L^2$	2.44E-08
Mass Moment of Inertia	$\lambda_I = \lambda_M \lambda_L^2$	3.05E-10
Time	$\lambda_T = \mathbf{T}_m / \mathbf{T}_p = \lambda_L / \lambda_V$	
Damping	$\lambda_\zeta = \zeta_m / \zeta_p$	1

* Length Scale 1: 80

TABLE 2.2 SECTION MODEL PROPERTIES

Length of Model (for non-yawed tests)	2.297 m
Deck Width (to outside of nosing on service lanes)	0.755 m
Mass per unit length (excluding springing)	6.51 kg/m
Mass Moment of Inertia per unit length (excluding springing)	0.356 kg-m²/m (approximately)
Fundamental Bending Frequency (pin-ended model)	7.13 Hz
Fundamental Torsional Frequency (fixed ended model)	13.87 Hz

TABLE 3.1 STATIC FORCE COEFFICIENTS, SMOOTH FLOW, IN-SERVICE

Reynolds Number = 9.0 × 10^5					
Angle of Attack (degrees)	C_X	C_Z	C_m	C_D	C_L
-10	0.162	-0.277	-0.017	0.208	-0.245
-9.5	0.158	-0.261	-0.016	0.199	-0.231
-9	0.154	-0.245	-0.016	0.190	-0.218
-8.5	0.150	-0.231	-0.015	0.182	-0.206
-8	0.145	-0.216	-0.014	0.174	-0.194
-7.5	0.141	-0.201	-0.013	0.166	-0.181
-7	0.136	-0.186	-0.013	0.158	-0.168
-6.5	0.131	-0.171	-0.013	0.150	-0.155
-6	0.127	-0.156	-0.013	0.142	-0.142
-5.5	0.122	-0.143	-0.013	0.135	-0.131
-5	0.117	-0.131	-0.013	0.128	-0.120
-4.5	0.112	-0.121	-0.013	0.121	-0.112
-4	0.108	-0.112	-0.013	0.115	-0.104
-3.5	0.103	-0.104	-0.013	0.110	-0.098
-3	0.099	-0.098	-0.013	0.104	-0.092
-2.5	0.096	-0.093	-0.012	0.100	-0.088
-2	0.092	-0.089	-0.011	0.095	-0.085
-1.5	0.089	-0.086	-0.010	0.092	-0.083
-1	0.087	-0.084	-0.009	0.089	-0.082
-0.5	0.086	-0.082	-0.008	0.087	-0.082
0	0.085	-0.082	-0.007	0.085	-0.082
0.5	0.086	-0.081	-0.005	0.085	-0.081
1	0.087	-0.080	-0.004	0.085	-0.081
1.5	0.089	-0.078	-0.003	0.087	-0.081
2	0.092	-0.076	-0.002	0.089	-0.080
2.5	0.096	-0.074	-0.002	0.093	-0.079
3	0.100	-0.072	-0.001	0.096	-0.077
3.5	0.104	-0.068	0.000	0.100	-0.074
4	0.109	-0.062	0.001	0.104	-0.070
4.5	0.114	-0.056	0.002	0.109	-0.064
5	0.119	-0.048	0.003	0.115	-0.059
5.5	0.125	-0.041	0.004	0.120	-0.053
6	0.130	-0.034	0.004	0.126	-0.047
6.5	0.136	-0.026	0.006	0.132	-0.041
7	0.141	-0.019	0.006	0.138	-0.036
7.5	0.147	-0.011	0.007	0.144	-0.031
8	0.153	-0.005	0.008	0.150	-0.026
8.5	0.159	0.001	0.008	0.157	-0.023
9	0.165	0.006	0.008	0.164	-0.020
9.5	0.171	0.014	0.008	0.171	-0.014
10	0.175	0.024	0.009	0.176	-0.007

TABLE 3.2 STATIC FORCE COEFFICIENTS, TURBULENT FLOW, IN-SERVICE

Reynolds Number = 5.9 × 10^5					
Angle of Attack (degrees)	C_X	C_Z	C_m	C_D	C_L
-10	0.139	-0.284	-0.021	0.186	-0.256
-9.5	0.136	-0.272	-0.020	0.179	-0.246
-9	0.132	-0.256	-0.019	0.171	-0.232
-8.5	0.128	-0.242	-0.019	0.163	-0.221
-8	0.124	-0.225	-0.018	0.154	-0.206
-7.5	0.120	-0.212	-0.017	0.147	-0.195
-7	0.117	-0.201	-0.017	0.141	-0.185
-6.5	0.114	-0.188	-0.016	0.134	-0.174
-6	0.109	-0.175	-0.016	0.127	-0.163
-5.5	0.105	-0.164	-0.015	0.121	-0.153
-5	0.102	-0.153	-0.015	0.115	-0.144
-4.5	0.099	-0.144	-0.014	0.110	-0.136
-4	0.097	-0.136	-0.014	0.106	-0.129
-3.5	0.094	-0.127	-0.013	0.102	-0.121
-3	0.092	-0.120	-0.012	0.098	-0.115
-2.5	0.090	-0.113	-0.011	0.095	-0.109
-2	0.088	-0.105	-0.010	0.092	-0.102
-1.5	0.087	-0.098	-0.009	0.090	-0.096
-1	0.087	-0.092	-0.008	0.088	-0.090
-0.5	0.086	-0.084	-0.007	0.087	-0.084
0	0.086	-0.077	-0.007	0.086	-0.077
0.5	0.087	-0.070	-0.006	0.086	-0.071
1	0.088	-0.064	-0.005	0.087	-0.065
1.5	0.090	-0.057	-0.004	0.088	-0.059
2	0.092	-0.050	-0.004	0.090	-0.053
2.5	0.094	-0.044	-0.003	0.092	-0.048
3	0.097	-0.037	-0.003	0.095	-0.042
3.5	0.100	-0.031	-0.002	0.098	-0.037
4	0.104	-0.025	-0.002	0.102	-0.032
4.5	0.107	-0.019	-0.001	0.105	-0.027
5	0.111	-0.013	0.000	0.109	-0.022
5.5	0.114	-0.007	0.000	0.113	-0.018
6	0.118	-0.001	0.001	0.117	-0.013
6.5	0.122	0.005	0.002	0.122	-0.009
7	0.126	0.010	0.003	0.126	-0.005
7.5	0.129	0.016	0.004	0.131	-0.001
8	0.133	0.023	0.005	0.135	0.004
8.5	0.137	0.029	0.006	0.140	0.009
9	0.140	0.036	0.007	0.144	0.014
9.5	0.144	0.043	0.008	0.149	0.019
10	0.147	0.050	0.009	0.154	0.024

TABLE 3.3 STATIC FORCE COEFFICIENTS, SMOOTH FLOW, UNDER CONSTRUCTION STAGE

Reynolds Number = 1.0 × 10^6					
Angle of Attack (degrees)	C_X	C_Z	C_m	C_D	C_L
-10	0.038	-0.536	-0.040	0.131	-0.522
-9.5	0.039	-0.517	-0.039	0.124	-0.504
-9	0.039	-0.497	-0.038	0.117	-0.485
-8.5	0.040	-0.477	-0.036	0.110	-0.466
-8	0.040	-0.455	-0.035	0.103	-0.445
-7.5	0.041	-0.434	-0.034	0.097	-0.424
-7	0.042	-0.413	-0.033	0.092	-0.404
-6.5	0.042	-0.392	-0.032	0.086	-0.384
-6	0.042	-0.372	-0.031	0.081	-0.366
-5.5	0.042	-0.352	-0.031	0.075	-0.347
-5	0.041	-0.331	-0.029	0.070	-0.326
-4.5	0.041	-0.306	-0.026	0.065	-0.302
-4	0.041	-0.279	-0.023	0.060	-0.276
-3.5	0.040	-0.251	-0.020	0.056	-0.248
-3	0.039	-0.224	-0.017	0.051	-0.222
-2.5	0.038	-0.199	-0.014	0.047	-0.197
-2	0.038	-0.175	-0.012	0.044	-0.174
-1.5	0.037	-0.152	-0.008	0.041	-0.151
-1	0.038	-0.131	-0.005	0.040	-0.130
-0.5	0.039	-0.110	-0.002	0.040	-0.110
0	0.041	-0.088	0.001	0.041	-0.088
0.5	0.042	-0.067	0.004	0.041	-0.067
1	0.043	-0.048	0.007	0.042	-0.048
1.5	0.045	-0.027	0.011	0.044	-0.029
2	0.047	-0.007	0.014	0.046	-0.009
2.5	0.049	0.010	0.017	0.049	0.008
3	0.052	0.025	0.019	0.053	0.022
3.5	0.055	0.036	0.020	0.057	0.033
4	0.059	0.046	0.020	0.062	0.042
4.5	0.062	0.056	0.021	0.066	0.051
5	0.065	0.067	0.021	0.071	0.061
5.5	0.068	0.078	0.022	0.076	0.071
6	0.072	0.089	0.023	0.080	0.081
6.5	0.075	0.099	0.023	0.085	0.090
7	0.078	0.109	0.023	0.090	0.099
7.5	0.080	0.119	0.023	0.095	0.107
8	0.083	0.129	0.024	0.100	0.116
8.5	0.085	0.142	0.025	0.105	0.128
9	0.087	0.156	0.027	0.110	0.140
9.5	0.089	0.168	0.028	0.115	0.151
10	0.090	0.179	0.029	0.120	0.161

TABLE 3.4 STATIC FORCE COEFFICIENTS, TURBULENT FLOW, UNDER CONSTRUCTION STAGE

Reynolds Number = 7.7 × 10^5					
Angle of Attack (degrees)	C_X	C_Z	C_m	C_D	C_L
-10	0.031	-0.444	-0.039	0.107	-0.432
-9.5	0.031	-0.423	-0.037	0.100	-0.412
-9	0.032	-0.408	-0.036	0.095	-0.398
-8.5	0.032	-0.393	-0.035	0.090	-0.384
-8	0.033	-0.373	-0.033	0.084	-0.365
-7.5	0.033	-0.353	-0.031	0.078	-0.345
-7	0.033	-0.337	-0.030	0.074	-0.331
-6.5	0.033	-0.316	-0.028	0.069	-0.311
-6	0.033	-0.301	-0.027	0.065	-0.296
-5.5	0.033	-0.283	-0.025	0.060	-0.279
-5	0.033	-0.262	-0.023	0.056	-0.258
-4.5	0.033	-0.243	-0.022	0.052	-0.240
-4	0.032	-0.223	-0.020	0.048	-0.220
-3.5	0.032	-0.202	-0.017	0.044	-0.200
-3	0.032	-0.181	-0.015	0.041	-0.179
-2.5	0.032	-0.162	-0.013	0.039	-0.160
-2	0.032	-0.143	-0.011	0.037	-0.142
-1.5	0.032	-0.126	-0.009	0.036	-0.125
-1	0.033	-0.108	-0.006	0.035	-0.108
-0.5	0.033	-0.093	-0.004	0.034	-0.092
0	0.034	-0.076	-0.002	0.034	-0.076
0.5	0.036	-0.061	0.000	0.035	-0.061
1	0.037	-0.046	0.002	0.036	-0.046
1.5	0.039	-0.031	0.004	0.038	-0.032
2	0.040	-0.017	0.006	0.040	-0.019
2.5	0.042	-0.004	0.008	0.042	-0.006
3	0.044	0.009	0.009	0.045	0.007
3.5	0.046	0.022	0.011	0.048	0.019
4	0.049	0.034	0.012	0.051	0.030
4.5	0.051	0.046	0.014	0.054	0.042
5	0.053	0.058	0.015	0.058	0.053
5.5	0.055	0.069	0.016	0.062	0.063
6	0.057	0.079	0.017	0.065	0.073
6.5	0.059	0.090	0.018	0.069	0.083
7	0.060	0.099	0.019	0.072	0.091
7.5	0.063	0.109	0.019	0.077	0.100
8	0.065	0.120	0.020	0.081	0.110
8.5	0.067	0.130	0.021	0.086	0.119
9	0.069	0.139	0.021	0.089	0.126
9.5	0.070	0.147	0.021	0.094	0.133
10	0.072	0.156	0.022	0.098	0.142

TABLE 3.5 NORMALIZING FREQUENCIES USED IN ANALYSIS OF AERODYNAMIC DERIVATIVES

AERODYNAMIC DERIVATIVE	FREQUENCY (MODEL)	MODE OF VIBRATION
$H_1^*, H_4^*, A_1^*, A_4^*, P_5^*, P_6^*$	1.127 Hz	Vertical
$H_2^*, H_3^*, A_2^*, A_3^*, P_2^*, P_3^*$	1.356 Hz	Torsional
$H_5^*, H_6^*, A_5^*, A_6^*, P_1^*, P_4^*$	1.527 Hz	Lateral

TABLE 3.6 SUMMARY OF AERODYNAMIC DERIVATIVE TESTS

TEST GROUP	CONFIGURATION	FLOW CONDITION	ANGLE OF ATTACK	NO. OF SPEEDS	FILENAME	OTHER TEST CONDITIONS
A)	In-Service	Smooth	-6	10	A1	Yaw angle: 0 degree; Amplitude range: rotation 0.5 to 1.5 degrees, vertical & lateral initial displacements between 2.5 & 7.5mm
			-4		A2	
			-2		A3	
			0		A4	
			2		A5	
			4		A6	
			6		A7	
B)	Under Construction		-6		B1	
			-4		B2	
			-2		B3	
			0		B4	
			2		B5	
			4		B6	
			6		B7	

TABLE 3.7 AERODYNAMIC DERIVATIVES, 0 DEGREES, SMOOTH FLOW, IN-SERVICE CONDITION, BLWTL FORMAT

	Vrh	Vra	Vrp	A1*	A2*	A3*	A4*	A5*	A6*
M072a4E01R008P002a.wttd	1.51	1.25	1.12	0.01555	-0.02212	-0.03610	-0.08765	-0.02106	-0.11613
M072a4E01R008P003a.wttd	4.62	3.76	3.37	-0.02672	-0.06045	-0.01028	-0.14231	-0.01389	-0.12896
M072a4E01R008P004a.wttd	7.79	6.36	5.65	-0.12248	-0.14067	0.04927	-0.15811	-0.01245	-0.13884
M072a4E01R008P005a.wttd	10.93	9.10	7.93	-0.18326	-0.19037	0.16621	-0.13510	-0.01238	-0.14482
M072a4E01R008P006a.wttd	14.08	12.07	10.18	-0.24483	-0.23709	0.31547	-0.11781	-0.00417	-0.13932
M072a4E01R008P007a.wttd	17.14	15.14	12.48	-0.30361	-0.28037	0.51771	-0.10293	0.00268	-0.12995
M072a4E01R008P008a.wttd	20.46	18.46	14.74	-0.37258	-0.35521	0.72615	-0.09360	0.01240	-0.13048
M072a4E01R008P009a.wttd	23.62	22.47	16.98	-0.39579	-0.39414	0.94952	-0.08353	0.02737	-0.13071
M072a4E01R008P010a.wttd	26.71	25.58	19.23	-0.38209	-0.47628	0.97957	-0.09859	0.03261	-0.14390
M072a4E01R008P011a.wttd	29.47	27.86	21.49	-0.29045	-0.48423	0.81642	-0.12655	0.03962	-0.17257
	Vrh	Vra	Vrp	H1*	H2*	H3*	H4*	H5*	H6*
M072a4E01R008P002a.wttd	1.51	1.25	1.12	-0.44890	0.01959	0.15624	-0.01669	0.03305	0.03833
M072a4E01R008P003a.wttd	4.62	3.76	3.37	-0.69191	0.49684	0.65164	0.86683	-0.01249	0.07019
M072a4E01R008P004a.wttd	7.79	6.36	5.65	-0.35092	1.41460	0.65435	1.00120	0.04731	0.09161
M072a4E01R008P005a.wttd	10.93	9.10	7.93	-0.26681	2.11750	0.61823	1.07780	0.02291	0.07301
M072a4E01R008P006a.wttd	14.08	12.07	10.18	-0.24989	2.84800	0.71180	1.13260	0.08421	0.03699
M072a4E01R008P007a.wttd	17.14	15.14	12.48	-0.34531	3.48650	0.87811	1.19560	0.09721	-0.01748
M072a4E01R008P008a.wttd	20.46	18.46	14.74	-0.52750	4.15000	1.25040	1.35570	0.12649	-0.09542
M072a4E01R008P009a.wttd	23.62	22.47	16.98	-0.80757	4.95460	1.98410	1.49670	0.12362	-0.14070
M072a4E01R008P010a.wttd	26.71	25.58	19.23	-1.28790	5.96410	3.45550	1.66550	0.12850	-0.20465
M072a4E01R008P011a.wttd	29.47	27.86	21.49	-2.41350	5.84070	3.29510	0.83979	0.63034	-0.57634
	Vrh	Vra	Vrp	P1*	P2*	P3*	P4*	P5*	P6*
M072a4E01R008P002a.wttd	1.51	1.25	1.12	-0.02594	-0.04326	-0.44380	0.09424	-0.05577	0.08953
M072a4E01R008P003a.wttd	4.62	3.76	3.37	-0.11679	0.03079	-0.45404	0.19050	-0.04986	0.19485
M072a4E01R008P004a.wttd	7.79	6.36	5.65	-0.15559	0.22737	-0.59160	0.20864	0.05990	0.17835
M072a4E01R008P005a.wttd	10.93	9.10	7.93	-0.24519	0.34718	-0.91204	0.22881	0.13866	0.16961
M072a4E01R008P006a.wttd	14.08	12.07	10.18	-0.29182	0.42707	-1.36420	0.23602	0.22997	0.10674
M072a4E01R008P007a.wttd	17.14	15.14	12.48	-0.40717	0.44796	-2.21390	0.33769	0.42777	0.04962
M072a4E01R008P008a.wttd	20.46	18.46	14.74	-0.46098	0.40986	-3.55160	0.47428	0.71767	-0.00092
M072a4E01R008P009a.wttd	23.62	22.47	16.98	-0.58743	-0.01650	-6.16370	0.47224	1.22180	-0.23370
M072a4E01R008P010a.wttd	26.71	25.58	19.23	-0.64059	-0.84202	-9.76650	0.70440	1.85750	-0.52293
M072a4E01R008P011a.wttd	29.47	27.86	21.49	-0.80547	-2.95780	-14.95490	0.87336	2.83960	-1.05040

Notes: $V_{rh}=V/(f_vB)$, $V_{ra}=V/(f_aB)$ and $V_{rp}=V/(f_pB)$,
B – deck width of 60.36m,
V – deck height wind speed,
f_v, f_a and f_p – vertical, torsional and lateral frequencies respectively

TABLE 3.8 AERODYNAMIC DERIVATIVES, -2 DEGREES, SMOOTH FLOW, IN-SERVICE CONDITION, BLWTL FORMAT

	Vrh	Vra	Vrp	A1*	A2*	A3*	A4*	A5*	A6*
M072a3E01R001P002a.wttd	1.51	1.24	1.11	-0.00698	-0.02525	-0.04362	-0.08172	-0.02223	-0.20255
M072a3E01R001P003a.wttd	3.62	2.97	2.65	0.00711	-0.05746	0.02365	-0.13132	0.02267	-0.20544
M072a3E01R001P004a.wttd	5.71	4.66	4.15	-0.01374	-0.07287	-0.01436	-0.12185	-0.00843	-0.21517
M072a3E01R001P005a.wttd	7.91	6.41	5.71	-0.05491	-0.13529	-0.00033	-0.13606	-0.00432	-0.21374
M072a3E01R001P006a.wttd	10.02	8.15	7.23	-0.08218	-0.19178	0.01667	-0.12475	0.00399	-0.23130
M072a3E01R001P007a.wttd	12.13	9.94	8.74	-0.13761	-0.24753	0.07563	-0.12236	0.00993	-0.23025
M072a3E01R001P008a.wttd	14.28	11.81	10.25	-0.14983	-0.27611	0.14686	-0.10311	0.01208	-0.22268
M072a3E01R001P009a.wttd	16.50	13.62	11.79	-0.19611	-0.33526	0.20676	-0.09895	0.02205	-0.22555
M072a3E01R001P010a.wttd	18.61	15.58	13.33	-0.20260	-0.38671	0.25839	-0.12377	0.01886	-0.21600
M072a3E01R001P011a.wttd	20.79	17.15	14.87	-0.20125	-0.43276	0.28743	-0.11940	0.03073	-0.22215
M072a3E01R001P012a.wttd	22.74	19.20	16.37	-0.14528	-0.43148	0.25818	-0.11808	0.02699	-0.21726
M072a3E01R001P013a.wttd	24.56	20.30	17.83	-0.06640	-0.42426	0.11706	-0.10195	0.01677	-0.22162
	Vrh	Vra	Vrp	H1*	H2*	H3*	H4*	H5*	H6*
M072a3E01R001P002a.wttd	1.51	1.24	1.11	-0.50319	-0.02227	0.19834	0.07401	0.05724	0.07882
M072a3E01R001P003a.wttd	3.62	2.97	2.65	-0.89776	0.24013	0.39362	0.65280	-0.04929	0.03474
M072a3E01R001P004a.wttd	5.71	4.66	4.15	-0.98290	0.73970	0.91052	0.93433	0.08879	0.06424
M072a3E01R001P005a.wttd	7.91	6.41	5.71	-0.80570	1.44800	1.15960	1.13830	0.10831	0.09147
M072a3E01R001P006a.wttd	10.02	8.15	7.23	-0.79421	2.10230	1.37990	1.38040	0.09402	0.04143
M072a3E01R001P007a.wttd	12.13	9.94	8.74	-0.77742	2.75140	1.58280	1.37560	0.10328	0.06739
M072a3E01R001P008a.wttd	14.28	11.81	10.25	-0.92279	3.25860	1.82500	1.38220	0.14301	0.01207
M072a3E01R001P009a.wttd	16.50	13.62	11.79	-1.01140	3.89000	2.34040	1.56410	0.11139	-0.01525
M072a3E01R001P010a.wttd	18.61	15.58	13.33	-1.19820	4.47890	2.95560	1.70690	0.13184	-0.08285
M072a3E01R001P011a.wttd	20.79	17.15	14.87	-1.55230	5.04960	3.84750	1.85880	0.15958	-0.21467
M072a3E01R001P012a.wttd	22.74	19.20	16.37	-2.05520	5.58190	5.08760	1.93560	0.27252	-0.28133
M072a3E01R001P013a.wttd	24.56	20.30	17.83	-2.38660	6.57990	5.91700	0.86562	0.02035	0.03693
	Vrh	Vra	Vrp	P1*	P2*	P3*	P4*	P5*	P6*
M072a3E01R001P002a.wttd	1.51	1.24	1.11	-0.00917	-0.02242	-0.28690	0.23750	0.00381	0.07804
M072a3E01R001P003a.wttd	3.62	2.97	2.65	-0.01672	-0.02428	-0.34193	0.30816	0.12295	0.05677
M072a3E01R001P004a.wttd	5.71	4.66	4.15	-0.12247	0.09288	-0.55194	0.26127	0.26294	0.11845
M072a3E01R001P005a.wttd	7.91	6.41	5.71	-0.14857	0.11826	-0.86834	0.25918	0.39755	0.08924
M072a3E01R001P006a.wttd	10.02	8.15	7.23	-0.19443	0.11614	-1.27550	0.26824	0.57986	0.04368
M072a3E01R001P007a.wttd	12.13	9.94	8.74	-0.25569	0.08473	-1.78670	0.29404	0.67979	-0.01006
M072a3E01R001P008a.wttd	14.28	11.81	10.25	-0.30848	0.03464	-2.34980	0.31742	0.82032	-0.02487
M072a3E01R001P009a.wttd	16.50	13.62	11.79	-0.34319	-0.03471	-3.14780	0.33585	0.97964	-0.08077
M072a3E01R001P010a.wttd	18.61	15.58	13.33	-0.43876	-0.12852	-4.05430	0.45211	1.17370	-0.13018
M072a3E01R001P011a.wttd	20.79	17.15	14.87	-0.54016	-0.26945	-5.19190	0.55148	1.39940	-0.17568
M072a3E01R001P012a.wttd	22.74	19.20	16.37	-0.69116	-0.30848	-6.6468	0.58764	1.7321	-0.23577
M072a3E01R001P013a.wttd	24.56	20.30	17.83	-0.84712	-0.54664	-9.0973	0.81094	2.1176	-0.63767

Notes: $V_{rh}=V/(f_vB)$, $V_{ra}=V/(f_aB)$ and $V_{rp}=V/(f_pB)$,
B – deck width of 60.36m,
V – deck height wind speed,
f_v, f_a and f_p – vertical, torsional and lateral frequencies respectively

TABLE 3.9 AERODYNAMIC DERIVATIVES, -4 DEGREES, SMOOTH FLOW, IN-SERVICE CONDITION, BLWTL FORMAT

	Vrh	Vra	Vrp	A1*	A2*	A3*	A4*	A5*	A6*
M072a2E01R001P002a.wttd	1.84	1.52	1.36	-0.10432	-0.09987	-0.07255	-0.11364	-0.02145	-0.22033
M072a2E01R001P003a.wttd	3.93	3.26	2.89	0.01888	-0.03732	0.03024	-0.00994	0.02345	-0.21869
M072a2E01R001P004a.wttd	6.06	4.98	4.43	0.07676	-0.01027	0.01181	-0.01976	-0.00262	-0.22651
M072a2E01R001P005a.wttd	8.20	6.61	5.94	0.07077	-0.04838	-0.04347	-0.06584	-0.00082	-0.22540
M072a2E01R001P006a.wttd	10.31	8.26	7.42	0.06344	-0.10934	-0.08992	-0.08103	0.00682	-0.23520
M072a2E01R001P007a.wttd	12.43	9.99	8.98	0.06660	-0.13285	-0.11390	-0.07934	0.01409	-0.22674
M072a2E01R001P008a.wttd	14.53	11.56	10.48	0.06609	-0.16608	-0.15057	-0.07605	0.01510	-0.22334
M072a2E01R001P009a.wttd	16.88	13.24	12.06	0.08770	-0.18493	-0.20616	-0.08851	0.01704	-0.22262
M072a2E01R001P010a.wttd	18.81	14.78	13.53	0.10457	-0.20691	-0.26153	-0.07317	0.02158	-0.22283
M072a2E01R001P011a.wttd	20.78	16.19	15.12	0.10889	-0.22809	-0.28642	-0.05396	0.00960	-0.22905
	Vrh	Vra	Vrp	H1*	H2*	H3*	H4*	H5*	H6*
M072a2E01R001P002a.wttd	1.84	1.52	1.36	-0.43336	0.15078	0.26882	0.14923	0.12719	0.03878
M072a2E01R001P003a.wttd	3.93	3.26	2.89	-1.15000	0.15098	0.53595	0.24068	0.05578	0.10720
M072a2E01R001P004a.wttd	6.06	4.98	4.43	-1.76390	0.49256	1.33360	0.75024	0.14647	0.06077
M072a2E01R001P005a.wttd	8.20	6.61	5.94	-2.03990	1.10250	2.10490	1.02130	0.17184	0.01539
M072a2E01R001P006a.wttd	10.31	8.26	7.42	-2.15420	1.91490	2.90460	1.35010	0.16538	0.00715
M072a2E01R001P007a.wttd	12.43	9.99	8.98	-2.39880	2.60810	3.73710	1.53000	0.19796	-0.06473
M072a2E01R001P008a.wttd	14.53	11.56	10.48	-2.61890	3.34900	4.74960	1.61000	0.24467	-0.06596
M072a2E01R001P009a.wttd	16.88	13.24	12.06	-3.10210	4.01360	6.09040	1.90830	0.27825	-0.11013
M072a2E01R001P010a.wttd	18.81	14.78	13.53	-3.51590	4.73530	7.51180	1.99630	0.26798	-0.16629
M072a2E01R001P011a.wttd	20.78	16.19	15.12	-4.12210	4.93350	8.80150	1.03940	0.07053	-0.15083
	Vrh	Vra	Vrp	P1*	P2*	P3*	P4*	P5*	P6*
M072a2E01R001P002a.wttd	1.84	1.52	1.36	-0.06993	-0.01870	-0.40300	0.09345	0.09891	0.01640
M072a2E01R001P003a.wttd	3.93	3.26	2.89	-0.08563	0.02374	-0.47105	0.17900	0.36091	0.12146
M072a2E01R001P004a.wttd	6.06	4.98	4.43	-0.19272	0.14276	-0.90623	0.14362	0.72633	0.06693
M072a2E01R001P005a.wttd	8.20	6.61	5.94	-0.25835	0.09995	-1.52010	0.14543	0.91663	0.01015
M072a2E01R001P006a.wttd	10.31	8.26	7.42	-0.32574	-0.05387	-2.28370	0.13679	1.14350	-0.08410
M072a2E01R001P007a.wttd	12.43	9.99	8.98	-0.38756	-0.18098	-3.14750	0.20575	1.36280	-0.16782
M072a2E01R001P008a.wttd	14.53	11.56	10.48	-0.47382	-0.36896	-4.16530	0.24025	1.53170	-0.23294
M072a2E01R001P009a.wttd	16.88	13.24	12.06	-0.57191	-0.42751	-5.38100	0.38151	1.85230	-0.29483
M072a2E01R001P010a.wttd	18.81	14.78	13.53	-0.64235	-0.63219	-6.78020	0.49705	2.09360	-0.37363
M072a2E01R001P011a.wttd	20.78	16.19	15.12	-0.86632	-0.95791	-8.21900	0.68288	2.25840	-0.59071

Notes: $V_{rh}=V/(f_v B)$, $V_{ra}=V/(f_a B)$ and $V_{rp}=V/(f_p B)$,
B – deck width of 60.36m,
V – deck height wind speed,
f_v, f_a and f_p – vertical, torsional and lateral frequencies respectively

TABLE 3.10 AERODYNAMIC DERIVATIVES, -6 DEGREES, SMOOTH FLOW, IN-SERVICE CONDITION, BLWTL FORMAT

	Vrh	Vra	Vrp	A1*	A2*	A3*	A4*	A5*	A6*
M072a1E01R001P002a.wttd	1.71	1.37	1.26	0.04474	-0.04210	-0.07496	-0.19290	-0.05236	-0.18996
M072a1E01R001P003a.wttd	3.55	2.91	2.62	-0.00462	-0.05109	0.05884	0.04197	0.02256	-0.22424
M072a1E01R001P004a.wttd	5.38	4.47	4.00	0.09860	0.00781	0.04845	0.07138	0.00002	-0.24758
M072a1E01R001P005a.wttd	7.37	5.98	5.39	0.10554	0.00459	-0.00932	0.02237	-0.02100	-0.23588
M072a1E01R001P006a.wttd	9.47	7.45	6.80	0.09705	-0.04015	-0.03431	-0.03412	-0.02464	-0.22938
M072a1E01R001P007a.wttd	11.31	8.98	8.17	0.05768	-0.12262	-0.04577	-0.07109	-0.01690	-0.23539
M072a1E01R001P008a.wttd	13.26	10.52	9.55	0.03082	-0.15742	-0.03234	-0.08628	-0.02165	-0.22796
M072a1E01R001P009a.wttd	15.21	12.38	10.96	0.01281	-0.18198	0.01094	-0.06723	-0.01226	-0.23152
M072a1E01R001P010a.wttd	17.35	13.94	12.35	-0.02682	-0.23492	0.07758	-0.08611	-0.00040	-0.22541
M072a1E01R001P011a.wttd	18.68	15.45	13.86	-0.05760	-0.23962	0.16063	-0.07460	0.00507	-0.21893
	Vrh	Vra	Vrp	H1*	H2*	H3*	H4*	H5*	H6*
M072a1E01R001P002a.wttd	1.71	1.37	1.26	-0.62196	-0.00675	0.28239	0.36233	0.17558	0.03514
M072a1E01R001P003a.wttd	3.55	2.91	2.62	-1.16430	0.06347	0.39592	-0.13574	0.01347	0.09004
M072a1E01R001P004a.wttd	5.38	4.47	4.00	-2.17410	0.07205	1.26970	0.18977	0.22189	0.16962
M072a1E01R001P005a.wttd	7.37	5.98	5.39	-2.76150	0.56134	2.46940	0.69374	0.32853	0.02630
M072a1E01R001P006a.wttd	9.47	7.45	6.80	-3.02120	1.26310	3.50580	1.08110	0.33815	-0.06440
M072a1E01R001P007a.wttd	11.31	8.98	8.17	-3.46460	2.12220	4.52720	1.44070	0.44409	-0.09778
M072a1E01R001P008a.wttd	13.26	10.52	9.55	-3.74610	2.73100	5.79160	1.58950	0.46493	-0.11268
M072a1E01R001P009a.wttd	15.21	12.38	10.96	-4.04190	3.43350	6.84920	1.68390	0.52809	-0.18395
M072a1E01R001P010a.wttd	17.35	13.94	12.35	-4.45840	4.35100	8.40350	1.87120	0.58743	-0.19350
M072a1E01R001P011a.wttd	18.68	15.45	13.86	-4.63350	4.73490	9.05890	0.92810	0.50806	0.03957
	Vrh	Vra	Vrp	P1*	P2*	P3*	P4*	P5*	P6*
M072a1E01R001P002a.wttd	1.71	1.37	1.26	-0.01025	-0.00546	-0.35901	0.15775	0.24530	0.04975
M072a1E01R001P003a.wttd	3.55	2.91	2.62	0.00239	-0.06319	-0.48886	0.23608	0.32994	0.14380
M072a1E01R001P004a.wttd	5.38	4.47	4.00	-0.11673	0.16345	-0.87362	0.10322	0.83081	0.20089
M072a1E01R001P005a.wttd	7.37	5.98	5.39	-0.24501	0.14453	-1.63530	0.14856	1.13790	0.07813
M072a1E01R001P006a.wttd	9.47	7.45	6.80	-0.33780	-0.03992	-2.40850	0.21184	1.31300	-0.06487
M072a1E01R001P007a.wttd	11.31	8.98	8.17	-0.43104	-0.39681	-3.33170	0.16063	1.55690	-0.19802
M072a1E01R001P008a.wttd	13.26	10.52	9.55	-0.52768	-0.58972	-4.28600	0.26282	1.69840	-0.28583
M072a1E01R001P009a.wttd	15.21	12.38	10.96	-0.62160	-0.85453	-5.26350	0.36871	1.86910	-0.34906
M072a1E01R001P010a.wttd	17.35	13.94	12.35	-0.72646	-1.30480	-6.63440	0.46475	2.08470	-0.48990
M072a1E01R001P011a.wttd	18.68	15.45	13.86	-1.00960	-1.78180	-8.11980	0.78493	2.29040	-0.76708

Notes: $V_{rh}=V/(f_vB)$, $V_{ra}=V/(f_aB)$ and $V_{rp}=V/(f_pB)$,
B – deck width of 60.36m,
V – deck height wind speed,
f_v, f_a and f_p – vertical, torsional and lateral frequencies respectively

TABLE 3.11 AERODYNAMIC DERIVATIVES, +2 DEGREES, SMOOTH FLOW, IN-SERVICE CONDITION, BLWTL FORMAT

	Vrh	Vra	Vrp	A1*	A2*	A3*	A4*	A5*	A6*
M072a5E01R001P002a.wttd	2.74	2.24	2.02	0.07519	-0.06342	-0.06907	-0.13061	-0.04148	-0.19147
M072a5E01R001P003a.wttd	5.68	4.57	4.14	-0.02545	-0.13534	-0.06558	-0.14341	-0.04714	-0.19395
M072a5E01R001P004a.wttd	8.72	7.05	6.31	-0.08908	-0.18636	-0.01526	-0.14318	-0.05663	-0.19879
M072a5E01R001P005a.wttd	11.69	9.60	8.48	-0.14510	-0.23148	0.09688	-0.13670	-0.05852	-0.19588
M072a5E01R001P006a.wttd	14.59	12.30	10.60	-0.21020	-0.29446	0.24222	-0.13412	-0.03895	-0.19384
M072a5E01R001P007a.wttd	17.66	15.12	12.77	-0.26189	-0.33697	0.42264	-0.12198	-0.01600	-0.19481
M072a5E01R001P008a.wttd	20.67	18.73	14.85	-0.33474	-0.36446	0.66845	-0.10651	-0.01709	-0.17099
M072a5E01R001P009a.wttd	23.59	22.63	17.10	-0.43579	-0.44085	1.01800	-0.07918	0.00722	-0.16165
M072a5E01R001P010a.wttd	26.15	28.91	19.12	-0.54776	-0.47582	1.50530	-0.04244	0.05352	-0.18670
M072a5E01R001P011a.wttd	29.08	35.43	21.25	-0.59434	-0.53322	1.81860	-0.05896	0.03897	-0.22874
	Vrh	Vra	Vrp	H1*	H2*	H3*	H4*	H5*	H6*
M072a5E01R001P002a.wttd	2.74	2.24	2.02	-0.77547	0.04997	0.33740	0.34124	0.02891	0.12879
M072a5E01R001P003a.wttd	5.68	4.57	4.14	-0.50306	0.86309	0.73098	0.94441	0.01264	0.15407
M072a5E01R001P004a.wttd	8.72	7.05	6.31	-0.24261	1.65140	0.68359	1.03710	0.03901	0.16895
M072a5E01R001P005a.wttd	11.69	9.60	8.48	-0.22212	2.22230	0.73455	1.03330	0.15257	0.09268
M072a5E01R001P006a.wttd	14.59	12.30	10.60	-0.24138	2.80690	0.77374	1.01050	0.18757	0.05783
M072a5E01R001P007a.wttd	17.66	15.12	12.77	-0.27192	3.38090	0.81917	1.05250	0.16086	0.03281
M072a5E01R001P008a.wttd	20.67	18.73	14.85	-0.33025	3.87980	0.89312	1.09810	0.25647	0.07435
M072a5E01R001P009a.wttd	23.59	22.63	17.10	-0.41593	4.39800	1.05310	1.14010	0.26364	-0.04793
M072a5E01R001P010a.wttd	26.15	28.91	19.12	-0.59641	4.75430	1.32990	1.16050	0.23532	-0.15296
M072a5E01R001P011a.wttd	29.08	35.43	21.25	-0.89113	5.32320	1.86660	1.19990	0.29333	-0.30275
	Vrh	Vra	Vrp	P1*	P2*	P3*	P4*	P5*	P6*
M072a5E01R001P002a.wttd	2.74	2.24	2.02	-0.11242	-0.05248	-0.28523	0.18704	-0.16328	0.07684
M072a5E01R001P003a.wttd	5.68	4.57	4.14	-0.20015	0.02555	-0.08729	0.23979	-0.29687	0.16473
M072a5E01R001P004a.wttd	8.72	7.05	6.31	-0.27268	0.20007	0.09508	0.24138	-0.37271	0.17891
M072a5E01R001P005a.wttd	11.69	9.60	8.48	-0.28636	0.29827	0.29541	0.24134	-0.43592	0.17161
M072a5E01R001P006a.wttd	14.59	12.30	10.60	-0.35054	0.43804	0.59298	0.20628	-0.52043	0.16182
M072a5E01R001P007a.wttd	17.66	15.12	12.77	-0.40410	0.57127	0.75115	0.12783	-0.54487	0.16778
M072a5E01R001P008a.wttd	20.67	18.73	14.85	-0.51325	0.65516	0.60265	0.27108	-0.50691	0.13937
M072a5E01R001P009a.wttd	23.59	22.63	17.10	-0.58986	0.67008	0.04448	0.43131	-0.37909	0.07535
M072a5E01R001P010a.wttd	26.15	28.91	19.12	-0.62867	0.55140	-1.40360	0.30716	-0.04624	-0.11602
M072a5E01R001P011a.wttd	29.08	35.43	21.25	-0.64883	0.49543	-3.20640	0.77374	0.35439	-0.23534

Notes: $V_{rh}=V/(f_vB)$, $V_{ra}=V/(f_aB)$ and $V_{rp}=V/(f_pB)$,
B – deck width of 60.36m,
V – deck height wind speed,
f_v, f_a and f_p – vertical, torsional and lateral frequencies respectively

TABLE 3.12 AERODYNAMIC DERIVATIVES, +4 DEGREES, SMOOTH FLOW, IN-SERVICE CONDITION, BLWTL FORMAT

	Vrh	Vra	Vrp	A1*	A2*	A3*	A4*	A5*	A6*
M072a6E01R001P002a.wttd	2.74	2.27	2.03	0.00626	-0.05063	-0.04081	-0.13108	-0.04164	-0.16652
M072a6E01R001P003a.wttd	5.67	4.68	4.20	-0.18103	-0.33461	-0.04052	-0.35237	-0.07135	-0.11310
M072a6E01R001P004a.wttd	8.75	7.13	6.37	-0.08283	-0.20395	-0.03606	-0.07861	-0.08342	-0.14143
M072a6E01R001P005a.wttd	11.74	9.57	8.55	-0.01127	-0.29289	-0.05697	-0.13844	0.16525	-0.08774
M072a6E01R001P006a.wttd	14.73	12.16	10.73	-0.07849	-0.31843	-0.00208	-0.13858	0.02674	-0.18344
M072a6E01R001P007a.wttd	17.77	14.95	12.91	-0.15374	-0.39031	0.15725	-0.16138	-0.01750	-0.18680
M072a6E01R001P008a.wttd	20.71	18.36	14.99	-0.24745	-0.48916	0.47987	-0.12332	-0.02062	-0.18109
M072a6E01R001P009a.wttd	23.72	22.10	17.28	-0.34944	-0.57282	0.80448	-0.09711	-0.02687	-0.18383
M072a6E01R001P010a.wttd	26.15	28.06	19.24	-0.48065	-0.72645	1.22580	-0.08908	-0.02569	-0.19263
M072a6E01R001P011a.wttd	29.53	28.91	21.33	-0.59479	-0.90354	1.61730	-0.08035	-0.03282	-0.17882
	Vrh	Vra	Vrp	H1*	H2*	H3*	H4*	H5*	H6*
M072a6E01R001P002a.wttd	2.74	2.27	2.03	-0.71767	0.00559	0.31616	0.08585	-0.00373	0.20517
M072a6E01R001P003a.wttd	5.67	4.68	4.20	-0.96120	0.29764	0.60365	0.05394	-0.15316	0.10523
M072a6E01R001P004a.wttd	8.75	7.13	6.37	-0.90553	1.31050	0.86279	0.76384	-0.27575	-0.12328
M072a6E01R001P005a.wttd	11.74	9.57	8.55	-0.66996	2.31890	1.26770	1.03470	-0.12111	0.15199
M072a6E01R001P006a.wttd	14.73	12.16	10.73	-0.78409	2.90110	1.74950	1.11600	0.06292	0.20109
M072a6E01R001P007a.wttd	17.77	14.95	12.91	-1.20450	3.23560	2.56170	1.09370	0.10714	0.17945
M072a6E01R001P008a.wttd	20.71	18.36	14.99	-1.61170	3.56140	3.57380	0.92497	0.12750	0.08161
M072a6E01R001P009a.wttd	23.72	22.10	17.28	-2.09770	3.59100	5.02260	0.73657	0.27446	0.08197
M072a6E01R001P010a.wttd	26.15	28.06	19.24	-2.46980	3.74720	6.66490	0.68830	0.32447	0.02626
M072a6E01R001P011a.wttd	29.53	28.91	21.33	-2.80980	4.01800	8.71740	0.62833	0.38111	-0.05410
	Vrh	Vra	Vrp	P1*	P2*	P3*	P4*	P5*	P6*
M072a6E01R001P002a.wttd	2.74	2.27	2.03	-0.15107	-0.04411	-0.11622	0.21121	-0.36815	0.10797
M072a6E01R001P003a.wttd	5.67	4.68	4.20	-0.27323	0.26338	0.33468	0.16800	-0.60591	0.28421
M072a6E01R001P004a.wttd	8.75	7.13	6.37	-0.29314	0.43078	1.01200	0.10354	-0.98424	0.27001
M072a6E01R001P005a.wttd	11.74	9.57	8.55	-0.41288	0.62207	2.07150	0.25341	-1.39970	0.35326
M072a6E01R001P006a.wttd	14.73	12.16	10.73	-0.47025	0.87629	3.13920	0.41740	-1.65120	0.42503
M072a6E01R001P007a.wttd	17.77	14.95	12.91	-0.60303	1.30130	4.24760	0.43246	-1.87070	0.42506
M072a6E01R001P008a.wttd	20.71	18.36	14.99	-0.66957	1.62140	5.45270	0.54024	-2.06090	0.38615
M072a6E01R001P009a.wttd	23.72	22.10	17.28	-0.67850	1.89140	7.06620	0.56684	-2.32600	0.35112
M072a6E01R001P010a.wttd	26.15	28.06	19.24	-0.69675	2.34140	9.35470	0.56438	-2.64040	0.39862
M072a6E01R001P011a.wttd	29.53	28.91	21.33	-0.86323	2.83620	11.89300	0.68418	-2.88460	0.38292

Notes: $V_{rh}=V/(f_vB)$, $V_{ra}=V/(f_aB)$ and $V_{rp}=V/(f_pB)$,
B – deck width of 60.36m,
V – deck height wind speed,
f_v, f_a and f_p – vertical, torsional and lateral frequencies respectively

TABLE 3.13 AERODYNAMIC DERIVATIVES, +6 DEGREES, SMOOTH FLOW, IN-SERVICE CONDITION, BLWTL FORMAT

	Vrh	Vra	Vrp	A1*	A2*	A3*	A4*	A5*	A6*
M072a7E01R001P002a.wttd	2.76	2.30	2.05	-0.03002	-0.03904	-0.01600	-0.06403	-0.07402	-0.21533
M072a7E01R001P003a.wttd	5.72	4.75	4.20	-0.14226	-0.16639	0.02323	-0.10707	-0.09267	-0.15635
M072a7E01R001P004a.wttd	8.66	7.38	6.42	-0.37900	-0.43760	0.22488	-0.13603	-0.11252	-0.09765
M072a7E01R001P005a.wttd	11.62	9.64	8.58	-0.29636	-0.29843	0.14270	-0.01506	-0.14724	-0.37670
M072a7E01R001P006a.wttd	14.70	12.32	10.73	-0.15918	-0.34547	0.18967	-0.12291	-0.00524	-0.18996
M072a7E01R001P007a.wttd	17.78	15.39	12.96	-0.22862	-0.44414	0.35206	-0.14286	-0.02978	-0.18228
M072a7E01R001P008a.wttd	20.76	18.76	15.12	-0.35096	-0.59049	0.66951	-0.13640	-0.04306	-0.18295
M072a7E01R001P009a.wttd	23.63	23.20	17.31	-0.43949	-0.64272	1.06190	-0.09038	-0.05515	-0.17677
M072a7E01R001P010a.wttd	26.11	25.64	19.31	-0.44912	-0.20735	0.65234	0.07386	-0.11316	-0.12435
M072a7E01R001P011a.wttd	Malfunction Instrumentation								
	Vrh	Vra	Vrp	H1*	H2*	H3*	H4*	H5*	H6*
M072a7E01R001P002a.wttd	2.76	2.30	2.05	-0.62079	0.01981	0.28362	0.05937	-0.00445	0.23056
M072a7E01R001P003a.wttd	5.72	4.75	4.20	-1.13850	0.41258	0.87890	0.36281	-0.23582	0.12965
M072a7E01R001P004a.wttd	8.66	7.38	6.42	-1.89530	0.44664	1.68270	0.28232	-0.35164	0.34180
M072a7E01R001P005a.wttd	11.62	9.64	8.58	-1.71980	0.88305	0.92876	-0.06277	-0.69237	-0.16004
M072a7E01R001P006a.wttd	14.70	12.32	10.73	-1.36890	2.13150	2.12200	0.74174	0.05048	0.24277
M072a7E01R001P007a.wttd	17.78	15.39	12.96	-1.63950	2.72540	2.99350	0.87637	0.02194	0.17396
M072a7E01R001P008a.wttd	20.76	18.76	15.12	-1.87660	3.47020	4.01120	0.96308	-0.00195	0.11601
M072a7E01R001P009a.wttd	23.63	23.20	17.31	-2.07130	3.98740	4.87190	0.91446	0.04720	0.08620
M072a7E01R001P010a.wttd	26.11	25.64	19.31	-0.40613	5.19470	6.53310	0.62019	-0.15166	-0.00056
M072a7E01R001P011a.wttd	Malfunction Instrumentation								
	Vrh	Vra	Vrp	P1*	P2*	P3*	P4*	P5*	P6*
M072a7E01R001P002a.wttd	2.76	2.30	2.05	-0.10234	-0.03536	-0.09496	0.30514	-0.42998	0.13256
M072a7E01R001P003a.wttd	5.72	4.75	4.20	-0.25262	0.18283	0.48755	0.20745	-0.75859	0.26380
M072a7E01R001P004a.wttd	8.66	7.38	6.42	-0.42544	0.67719	1.07120	0.18662	-0.90600	0.34122
M072a7E01R001P005a.wttd	11.62	9.64	8.58	-0.76218	0.97623	1.52560	0.17646	-1.08120	0.17185
M072a7E01R001P006a.wttd	14.70	12.32	10.73	-0.70644	1.27500	3.47090	0.30717	-1.82830	0.41784
M072a7E01R001P007a.wttd	17.78	15.39	12.96	-0.71922	1.57040	4.88900	0.50590	-2.15540	0.42959
M072a7E01R001P008a.wttd	20.76	18.76	15.12	-0.84545	2.09400	6.48760	0.59977	-2.39340	0.43534
M072a7E01R001P009a.wttd	23.63	23.20	17.31	-0.89561	2.64860	8.00230	0.68399	-2.52910	0.31758
M072a7E01R001P010a.wttd	26.11	25.64	19.31	-1.04730	4.05240	9.39240	0.88447	-1.63730	-1.33210
M072a7E01R001P011a.wttd	Malfunction Instrumentation								

Notes: $V_{rh}=V/(f_vB)$, $V_{ra}=V/(f_aB)$ and $V_{rp}=V/(f_pB)$,
B – deck width of 60.36m,
V – deck height wind speed,
f_v, f_a and f_p – vertical, torsional and lateral frequencies respectively

TABLE 3.14 AERODYNAMIC DERIVATIVES, 0 DEGREES, SMOOTH FLOW, UNDER CONSTRUCTION CONDITION, BLWTL FORMAT

	Vrh	Vra	Vrp	A1*	A2*	A3*	A4*	A5*	A6*
M072b4E01R001P002a.wtd	1.30	1.09	0.96	0.00509	-0.01989	-0.00985	-0.05033	-0.01802	-0.20945
M072b4E01R001P003a.wtd	2.76	2.32	2.05	-0.10595	-0.10021	0.00182	-0.11936	-0.04928	-0.22625
M072b4E01R001P004a.wtd	4.23	3.58	3.12	-0.23026	-0.16687	0.06845	-0.13050	-0.03965	-0.22888
M072b4E01R001P005a.wtd	5.64	4.83	4.18	-0.27674	-0.19377	0.13480	-0.12024	-0.01978	-0.24103
M072b4E01R001P006a.wtd	7.19	6.21	5.28	-0.34164	-0.22716	0.24235	-0.09910	-0.02043	-0.23330
M072b4E01R001P007a.wtd	8.59	7.60	6.37	-0.37567	-0.22732	0.36370	-0.07722	-0.02745	-0.20970
M072b4E01R001P008a.wtd	9.92	9.13	7.45	-0.45575	-0.24837	0.51320	-0.05770	-0.00971	-0.21058
M072b4E01R001P009a.wtd	11.41	10.76	8.54	-0.43274	-0.21765	0.63674	-0.04526	-0.00298	-0.27926
M072b4E01R001P010a.wtd	Malfunction Instrumentation								
M072b4E01R002P002a.wtd	14.24	13.89	10.49	-0.63892	-0.37026	1.0155	-0.06560	-0.00950	-0.21070
	Vrh	Vra	Vrp	H1*	H2*	H3*	H4*	H5*	H6*
M072b4E01R001P002a.wtd	1.30	1.09	0.96	-0.51380	0.00825	0.10724	0.00792	0.00686	0.12721
M072b4E01R001P003a.wtd	2.76	2.32	2.05	-0.88120	0.13882	0.36034	0.08987	0.00659	0.12838
M072b4E01R001P004a.wtd	4.23	3.58	3.12	-1.31390	0.26763	0.70051	0.07874	0.03253	0.12433
M072b4E01R001P005a.wtd	5.64	4.83	4.18	-1.67380	0.38564	1.13300	0.01148	0.04188	0.04692
M072b4E01R001P006a.wtd	7.19	6.21	5.28	-2.13780	0.49247	1.78850	0.00553	0.06615	0.03702
M072b4E01R001P007a.wtd	8.59	7.60	6.37	-2.54640	0.64117	2.58860	0.03773	0.01074	0.11922
M072b4E01R001P008a.wtd	9.92	9.13	7.45	-2.88850	0.83370	3.48800	0.11382	0.09420	0.06232
M072b4E01R001P009a.wtd	11.41	10.76	8.54	-2.93900	1.20690	4.45740	0.23236	0.44372	-0.22953
M072b4E01R001P010a.wtd	Malfunction Instrumentation								
M072b4E01R002P002a.wtd	14.24	13.89	10.49	-4.5313	1.0032	7.3046	-0.00762	0.22533	0.04664
	Vrh	Vra	Vrp	P1*	P2*	P3*	P4*	P5*	P6*
M072b4E01R001P002a.wtd	1.30	1.09	0.96	-0.00197	-0.00963	-0.36345	0.15618	0.00298	0.10664
M072b4E01R001P003a.wtd	2.76	2.32	2.05	-0.02946	-0.00325	-0.35979	0.14743	-0.00640	0.11493
M072b4E01R001P004a.wtd	4.23	3.58	3.12	-0.03030	-0.02157	-0.36084	0.14876	-0.03724	0.08349
M072b4E01R001P005a.wtd	5.64	4.83	4.18	-0.04953	-0.05406	-0.33684	0.14332	-0.10288	0.05638
M072b4E01R001P006a.wtd	7.19	6.21	5.28	-0.07539	-0.04928	-0.29781	0.13178	-0.12841	0.06135
M072b4E01R001P007a.wtd	8.59	7.60	6.37	-0.11254	-0.07025	-0.22973	0.15242	-0.21547	0.06073
M072b4E01R001P008a.wtd	9.92	9.13	7.45	-0.12798	-0.13112	-0.17403	0.15242	-0.29335	0.02624
M072b4E01R001P009a.wtd	11.41	10.76	8.54	-0.11945	-0.10745	-0.08194	0.12807	-0.31795	0.04956
M072b4E01R001P010a.wtd	Malfunction Instrumentation								
M072b4E01R002P002a.wtd	14.24	13.89	10.49	-0.15318	-0.37467	-0.2946	0.22033	-0.29182	-0.06114

Notes: $V_{rh}=V/(f_vB)$, $V_{ra}=V/(f_aB)$ and $V_{rp}=V/(f_pB)$,
B – deck width of 60.36m,
V – deck height wind speed,
f_v, f_a and f_p – vertical, torsional and lateral frequencies respectively

TABLE 3.15 AERODYNAMIC DERIVATIVES, -2 DEGREES, SMOOTH FLOW, UNDER CONSTRUCTION CONDITION, BLWTL FORMAT

	Vrh	Vra	Vrp	A1*	A2*	A3*	A4*	A5*	A6*
M072b3E01R001P002a.wttd	1.25	1.04	0.92	-0.00186	-0.01771	-0.01865	-0.07691	-0.02852	-0.22397
M072b3E01R001P003a.wttd	2.72	2.29	2.02	-0.07396	-0.06819	-0.00145	-0.08062	-0.04100	-0.23313
M072b3E01R001P004a.wttd	4.13	3.50	3.06	-0.14144	-0.12583	0.04085	-0.10496	-0.04600	-0.23279
M072b3E01R001P005a.wttd	5.62	4.79	4.14	-0.21187	-0.16903	0.11236	-0.11345	-0.03040	-0.23197
M072b3E01R001P006a.wttd	7.05	6.13	5.24	-0.26235	-0.19435	0.19433	-0.09841	-0.01141	-0.22492
M072b3E01R001P007a.wttd	8.53	7.51	6.32	-0.31793	-0.21363	0.30632	-0.05214	-0.02864	-0.22411
M072b3E01R001P008a.wttd	10.04	8.95	7.40	-0.39396	-0.24620	0.42436	-0.06359	-0.02405	-0.22376
M072b3E01R001P009a.wttd	11.43	10.47	8.48	-0.45911	-0.27459	0.56260	-0.07096	0.02522	-0.24545
M072b3E01R002P002a.wttd	12.74	11.65	9.44	-0.44669	-0.10283	0.69280	0.02621	0.03541	-0.23745
M072b3E01R003P002a.wttd	12.80	11.70	9.48	-0.52530	-0.32701	0.72102	-0.07384	0.01566	-0.21412
	Vrh	Vra	Vrp	H1*	H2*	H3*	H4*	H5*	H6*
M072b3E01R001P002a.wttd	1.25	1.04	0.92	-0.45601	0.01114	0.09256	-0.00366	0.03786	0.09881
M072b3E01R001P003a.wttd	2.72	2.29	2.02	-0.84883	0.09261	0.33659	-0.04313	0.04862	0.11622
M072b3E01R001P004a.wttd	4.13	3.50	3.06	-1.38720	0.14439	0.75816	-0.09979	0.07745	0.14235
M072b3E01R001P005a.wttd	5.62	4.79	4.14	-1.87900	0.24193	1.36230	-0.11839	0.12712	0.14668
M072b3E01R001P006a.wttd	7.05	6.13	5.24	-2.42240	0.37479	2.13920	-0.05730	0.12401	0.11752
M072b3E01R001P007a.wttd	8.53	7.51	6.32	-2.92190	0.46215	3.01690	-0.18182	0.14197	0.09318
M072b3E01R001P008a.wttd	10.04	8.95	7.40	-3.38120	0.63128	4.07950	-0.11567	0.09059	0.05608
M072b3E01R001P009a.wttd	11.43	10.47	8.48	-3.94630	0.94227	5.53270	0.21587	0.31738	-0.03181
M072b3E01R002P002a.wttd	12.74	11.65	9.44	-4.43180	1.59930	7.24340	0.37823	0.45611	-0.16875
M072b3E01R003P002a.wttd	12.80	11.70	9.48	-4.25580	1.15230	6.58070	0.16124	0.22783	0.04136
	Vrh	Vra	Vrp	P1*	P2*	P3*	P4*	P5*	P6*
M072b3E01R001P002a.wttd	1.25	1.04	0.92	-0.00941	-0.00620	-0.36995	0.15829	0.02193	0.08980
M072b3E01R001P003a.wttd	2.72	2.29	2.02	-0.02912	-0.00291	-0.40272	0.15794	0.07970	0.11079
M072b3E01R001P004a.wttd	4.13	3.50	3.06	-0.04438	-0.01180	-0.45889	0.14895	0.08833	0.09541
M072b3E01R001P005a.wttd	5.62	4.79	4.14	-0.06052	-0.02275	-0.52439	0.17067	0.07182	0.09134
M072b3E01R001P006a.wttd	7.05	6.13	5.24	-0.07916	-0.04595	-0.63847	0.16827	0.09249	0.06575
M072b3E01R001P007a.wttd	8.53	7.51	6.32	-0.09684	-0.01565	-0.74647	0.16674	0.12912	0.11080
M072b3E01R001P008a.wttd	10.04	8.95	7.40	-0.10285	-0.10480	-0.93880	0.20022	0.11421	0.01819
M072b3E01R001P009a.wttd	11.43	10.47	8.48	-0.11423	-0.17593	-1.19000	0.23506	0.14612	-0.03541
M072b3E01R002P002a.wttd	12.74	11.65	9.44	-0.10349	-0.21598	-2.21950	0.40602	0.32360	-0.12330
M072b3E01R003P002a.wttd	12.80	11.70	9.48	-0.16581	-0.16991	-1.38460	0.29842	0.16785	-0.00876

Notes: $V_{rh}=V/(f_vB)$, $V_{ra}=V/(f_aB)$ and $V_{rp}=V/(f_pB)$,
B – deck width of 60.36m,
V – deck height wind speed,
f_v, f_a and f_p – vertical, torsional and lateral frequencies respectively

TABLE 3.16 AERODYNAMIC DERIVATIVES, -4 DEGREES, SMOOTH FLOW, UNDER CONSTRUCTION CONDITION, BLWTL FORMAT

	Vrh	Vra	Vrp	A1*	A2*	A3*	A4*	A5*	A6*
M072b2E01R001P002a.wttd	1.11	0.94	0.83	0.00754	-0.01118	-0.01293	-0.03102	-0.02068	-0.19602
M072b2E01R001P003a.wttd	2.37	2.00	1.76	-0.08371	-0.05541	0.00278	-0.08231	-0.02243	-0.21117
M072b2E01R001P004a.wttd	3.62	3.07	2.68	-0.16202	-0.08797	0.04212	-0.08725	-0.01874	-0.21357
M072b2E01R001P005a.wttd	4.88	4.19	3.63	-0.21159	-0.10780	0.09670	-0.05656	-0.01313	-0.23028
M072b2E01R001P006a.wttd	6.17	5.34	4.60	-0.23837	-0.11514	0.16063	-0.02185	-0.00337	-0.23400
M072b2E01R001P007a.wttd	7.47	6.56	5.56	-0.27233	-0.12536	0.25795	0.05963	-0.05318	-0.22592
M072b2E01R001P008a.wttd	8.78	7.82	6.52	-0.35841	-0.16912	0.34165	-0.03124	0.00341	-0.22744
M072b2E01R001P009a.wttd	10.11	9.08	7.47	-0.40735	-0.18486	0.43603	-0.04197	0.03539	-0.23559
M072b2E01R001P010a.wttd	Malfunction Instrumentation								
M072b2E01R002P002a.wttd	12.93	11.44	9.90	-0.19960	-0.02886	0.43593	-0.01775	0.03220	-0.21887
	Vrh	Vra	Vrp	H1*	H2*	H3*	H4*	H5*	H6*
M072b2E01R001P002a.wttd	1.11	0.94	0.83	-0.31961	0.00121	0.06007	-0.11153	0.07633	0.09071
M072b2E01R001P003a.wttd	2.37	2.00	1.76	-0.70498	0.06573	0.27801	-0.12909	0.08517	0.06140
M072b2E01R001P004a.wttd	3.62	3.07	2.68	-1.18860	0.10527	0.63711	-0.24244	0.12338	0.05912
M072b2E01R001P005a.wttd	4.88	4.19	3.63	-1.76140	0.14298	1.19980	-0.26340	0.18209	0.03176
M072b2E01R001P006a.wttd	6.17	5.34	4.60	-2.26650	0.22215	1.91360	-0.28984	0.22382	0.01917
M072b2E01R001P007a.wttd	7.47	6.56	5.56	-2.84520	0.23059	2.73270	-0.42854	0.09755	0.05665
M072b2E01R001P008a.wttd	8.78	7.82	6.52	-3.37870	0.44021	3.83680	-0.19347	0.28370	-0.03136
M072b2E01R001P009a.wttd	10.11	9.08	7.47	-3.75580	0.71030	4.99010	-0.00211	0.36590	0.01268
M072b2E01R001P010a.wttd	Malfunction Instrumentation								
M072b2E01R002P002a.wttd	12.93	11.44	9.90	-4.37230	1.63560	7.61740	0.11258	0.48171	-0.10301
	Vrh	Vra	Vrp	P1*	P2*	P3*	P4*	P5*	P6*
M072b2E01R001P002a.wttd	1.11	0.94	0.83	-0.01255	0.00452	-0.35877	0.25090	0.04683	0.13688
M072b2E01R001P003a.wttd	2.37	2.00	1.76	-0.02944	-0.00214	-0.42036	0.20918	0.07229	0.06851
M072b2E01R001P004a.wttd	3.62	3.07	2.68	-0.06149	-0.01269	-0.50698	0.18200	0.09555	0.03781
M072b2E01R001P005a.wttd	4.88	4.19	3.63	-0.08161	-0.00155	-0.63480	0.19483	0.16327	0.04270
M072b2E01R001P006a.wttd	6.17	5.34	4.60	-0.09475	0.02010	-0.79003	0.21815	0.22127	0.07319
M072b2E01R001P007a.wttd	7.47	6.56	5.56	-0.08792	0.13726	-0.91353	0.24060	0.31636	0.23447
M072b2E01R001P008a.wttd	8.78	7.82	6.52	-0.15020	0.01066	-1.26010	0.29504	0.30598	0.04489
M072b2E01R001P009a.wttd	10.11	9.08	7.47	-0.16073	-0.14808	-1.60870	0.33309	0.27309	-0.08108
M072b2E01R001P010a.wttd	Malfunction Instrumentation								
M072b2E01R002P002a.wttd	12.93	11.44	9.90	-0.21993	-0.29197	-2.74130	0.51711	0.48691	-0.20597

Notes: $V_{rh}=V/(f_vB)$, $V_{ra}=V/(f_aB)$ and $V_{rp}=V/(f_pB)$,
B – deck width of 60.36m,
V – deck height wind speed,
f_v, f_a and f_p – vertical, torsional and lateral frequencies respectively

TABLE 3.17 AERODYNAMIC DERIVATIVES, -6 DEGREES, SMOOTH FLOW, UNDER CONSTRUCTION CONDITION, BLWTL FORMAT

	Vrh	Vra	Vrp	A1*	A2*	A3*	A4*	A5*	A6*
M072b1E01R001P002a.wttd	0.92	0.78	0.68	0.01000	-0.00844	-0.01117	-0.07047	-0.02073	-0.20938
M072b1E01R001P003a.wttd	2.03	1.71	1.50	-0.07922	-0.04480	0.00476	-0.10555	-0.02317	-0.20460
M072b1E01R001P004a.wttd	3.16	2.67	2.34	-0.14697	-0.07328	0.04941	-0.02418	-0.01661	-0.20642
M072b1E01R001P005a.wttd	4.23	3.61	3.14	-0.17333	-0.06388	0.09223	-0.02481	-0.00009	-0.21469
M072b1E01R001P006a.wttd	5.34	4.59	3.97	-0.17601	-0.05204	0.13334	0.03105	-0.00060	-0.21238
M072b1E01R001P007a.wttd	6.48	5.61	4.81	-0.20655	-0.04449	0.17429	0.03446	0.02456	-0.21457
M072b1E01R001P008a.wttd	7.70	6.59	5.64	-0.22142	-0.01894	0.21406	0.06282	0.03143	-0.22061
M072b1E01R001P009a.wttd	8.95	7.57	6.47	-0.22770	0.01072	0.24927	0.08450	0.04383	-0.21816
M072b1E01R001P010a.wttd	Malfunction Instrumentation								
M072b1E01R002P002a.wttd	11.53	9.94	8.43	-0.26635	0.06749	0.30199	0.10570	0.04641	-0.20837
	Vrh	Vra	Vrp	H1*	H2*	H3*	H4*	H5*	H6*
M072b1E01R001P002a.wttd	0.92	0.78	0.68	-0.35782	-0.02151	0.02294	-0.08302	0.06161	0.10703
M072b1E01R001P003a.wttd	2.03	1.71	1.50	-0.69659	0.06035	0.20867	0.00216	0.11805	0.05639
M072b1E01R001P004a.wttd	3.16	2.67	2.34	-1.10270	0.10935	0.46850	-0.03653	0.17599	0.05631
M072b1E01R001P005a.wttd	4.23	3.61	3.14	-1.54850	0.15467	0.87128	-0.04782	0.22139	0.04191
M072b1E01R001P006a.wttd	5.34	4.59	3.97	-2.01530	0.21962	1.39980	0.03072	0.23918	0.03762
M072b1E01R001P007a.wttd	6.48	5.61	4.81	-2.47560	0.32415	2.06140	0.09308	0.34019	0.08948
M072b1E01R001P008a.wttd	7.70	6.59	5.64	-2.84780	0.50351	2.79150	0.18894	0.43875	0.03202
M072b1E01R001P009a.wttd	8.95	7.57	6.47	-3.23320	0.70076	3.59620	0.26094	0.54172	0.01035
M072b1E01R001P010a.wttd	Malfunction Instrumentation								
M072b1E01R002P002a.wttd	11.53	9.94	8.43	-4.04540	1.34140	5.76880	0.55284	0.72084	-0.04701
	Vrh	Vra	Vrp	P1*	P2*	P3*	P4*	P5*	P6*
M072b1E01R001P002a.wttd	0.92	0.78	0.68	0.02293	-0.00480	-0.36647	0.13841	0.04086	0.09813
M072b1E01R001P003a.wttd	2.03	1.71	1.50	-0.01836	-0.01749	-0.42376	0.12793	0.05415	0.04054
M072b1E01R001P004a.wttd	3.16	2.67	2.34	-0.03980	0.00223	-0.49065	0.13609	0.13413	0.09795
M072b1E01R001P005a.wttd	4.23	3.61	3.14	-0.05808	-0.00848	-0.62799	0.13394	0.17509	0.00831
M072b1E01R001P006a.wttd	5.34	4.59	3.97	-0.06858	0.00309	-0.78013	0.17517	0.23764	0.03632
M072b1E01R001P007a.wttd	6.48	5.61	4.81	-0.08563	-0.02062	-0.99103	0.15476	0.27524	-0.00995
M072b1E01R001P008a.wttd	7.70	6.59	5.64	-0.13206	-0.03820	-1.22210	0.18006	0.31965	-0.02303
M072b1E01R001P009a.wttd	8.95	7.57	6.47	-0.16017	-0.06034	-1.49580	0.24550	0.36044	-0.03451
M072b1E01R001P010a.wttd	Malfunction Instrumentation								
M072b1E01R002P002a.wttd	11.53	9.94	8.43	-0.29683	-0.16299	-2.44010	0.59913	0.45983	-0.13504

Notes: $V_{rh}=V/(f_vB)$, $V_{ra}=V/(f_aB)$ and $V_{rp}=V/(f_pB)$,
B – deck width of 60.36m,
V – deck height wind speed,
f_v, f_a and f_p – vertical, torsional and lateral frequencies respectively

TABLE 3.18 AERODYNAMIC DERIVATIVES, +2 DEGREES, SMOOTH FLOW, UNDER CONSTRUCTION CONDITION, BLWTL FORMAT

	Vrh	Vra	Vrp	A1*	A2*	A3*	A4*	A5*	A6*
M072b5E01R001P002a.wtd	1.62	1.36	1.20	-0.01130	0.01586	0.00216	-0.07792	-0.03682	-0.20815
M072b5E01R001P003a.wtd	3.44	2.89	2.54	-0.13590	-0.08405	0.03500	-0.15908	-0.08515	-0.20780
M072b5E01R001P004a.wtd	5.22	4.48	3.87	-0.31965	-0.23191	0.14734	-0.25726	-0.08054	-0.19720
M072b5E01R001P005a.wtd	7.05	6.24	5.21	-0.55703	-0.40032	0.35890	-0.27654	-0.06335	-0.20555
M072b5E01R001P006a.wtd	8.87	8.02	6.58	-0.83984	-0.62238	0.65525	-0.26318	-0.07532	-0.23327
M072b5E01R001P007a.wtd	9.96	8.44	7.95	-1.31980	-1.22070	1.11190	-0.52400	0.00614	-0.16676
M072b5E01R001P008a.wtd	13.39	12.10	9.30	-0.71861	-0.66182	1.26280	-0.21921	0.08910	-0.20310
M072b5E01R001P009a.wtd	14.39	13.29	10.61	-0.71502	-0.80378	0.80581	-0.42345	0.02780	-0.20884
M072b5E01R001P010a.wtd	16.57	14.82	11.99	-0.40683	-0.42860	0.62567	-0.20019	-0.15705	-0.21955
M072b5E01R001P011a.wtd	18.69	17.10	13.35	-0.39321	-0.48633	0.73319	-0.13095	-0.05563	-0.25951
	Vrh	Vra	Vrp	H1*	H2*	H3*	H4*	H5*	H6*
M072b5E01R001P002a.wtd	1.62	1.36	1.20	-0.61266	0.04115	0.17171	0.07128	-0.01869	0.14193
M072b5E01R001P003a.wtd	3.44	2.89	2.54	-1.02810	0.24692	0.49381	0.19759	0.01873	0.16471
M072b5E01R001P004a.wtd	5.22	4.48	3.87	-1.47200	0.32117	0.91044	0.06667	-0.04898	0.15074
M072b5E01R001P005a.wtd	7.05	6.24	5.21	-2.14050	0.21003	1.59620	-0.18240	0.00497	0.19020
M072b5E01R001P006a.wtd	8.87	8.02	6.58	-3.11440	-0.16264	2.64560	-0.46391	-0.06942	0.18910
M072b5E01R001P007a.wtd	9.96	8.44	7.95	-5.07020	-1.50160	4.55090	-1.15940	0.25013	0.47986
M072b5E01R001P008a.wtd	13.39	12.10	9.30	-2.40980	0.56387	3.93690	-0.64857	0.08833	-0.20909
M072b5E01R001P009a.wtd	14.39	13.29	10.61	-3.59270	0.74179	5.15780	-0.27858	0.10045	0.11167
M072b5E01R001P010a.wtd	16.57	14.82	11.99	-3.34620	1.98720	5.76500	0.31778	-0.33574	0.11333
M072b5E01R001P011a.wtd	18.69	17.10	13.35	-2.48790	2.52410	4.93160	-0.77901	-0.12327	0.41572
	Vrh	Vra	Vrp	P1*	P2*	P3*	P4*	P5*	P6*
M072b5E01R001P002a.wtd	1.62	1.36	1.20	0.01680	-0.00883	-0.33329	0.09105	-0.08668	0.08461
M072b5E01R001P003a.wtd	3.44	2.89	2.54	-0.03205	0.01281	-0.23427	0.09653	-0.17508	0.10888
M072b5E01R001P004a.wtd	5.22	4.48	3.87	-0.08905	0.08540	-0.12251	0.11638	-0.21951	0.15773
M072b5E01R001P005a.wtd	7.05	6.24	5.21	-0.08166	0.16340	0.03073	0.12120	-0.24695	0.18724
M072b5E01R001P006a.wtd	8.87	8.02	6.58	-0.13699	0.23924	0.27292	0.08280	-0.33896	0.20419
M072b5E01R001P007a.wtd	9.96	8.44	7.95	-0.13433	0.42559	0.71300	0.07834	-0.49074	0.27398
M072b5E01R001P008a.wtd	13.39	12.10	9.30	0.01133	-0.69613	-0.60546	0.21956	0.37867	-0.20577
M072b5E01R001P009a.wtd	14.39	13.29	10.61	-0.08161	0.18266	1.46680	0.03745	-0.81097	0.01652
M072b5E01R001P010a.wtd	16.57	14.82	11.99	-0.21006	0.27918	2.69990	-0.45090	-1.18980	0.16925
M072b5E01R001P011a.wtd	18.69	17.10	13.35	-0.27535	0.31341	4.06830	-0.42532	-1.57110	0.35424

Notes: $V_{rh}=V/(f_vB)$, $V_{ra}=V/(f_aB)$ and $V_{rp}=V/(f_pB)$,
B – deck width of 60.36m,
V – deck height wind speed,
f_v, f_a and f_p – vertical, torsional and lateral frequencies respectively

TABLE 3.19 AERODYNAMIC DERIVATIVES, +4 DEGREES, SMOOTH FLOW, UNDER CONSTRUCTION CONDITION, BLWTL FORMAT

	Vrh	Vra	Vrp	A1*	A2*	A3*	A4*	A5*	A6*
M072b6E01R001P002a.wttd	1.10	0.92	0.81	0.02715	-0.00464	-0.01716	0.02753	-0.03565	-0.20929
M072b6E01R001P003a.wttd	2.47	2.06	1.82	-0.03080	-0.05728	-0.01374	-0.00743	-0.06003	-0.21067
M072b6E01R001P004a.wttd	3.78	3.19	2.80	-0.08913	-0.11240	0.02253	-0.04688	-0.09121	-0.20034
M072b6E01R001P005a.wttd	5.14	4.29	3.75	-0.20310	-0.19144	0.07204	-0.04180	-0.13584	-0.18879
M072b6E01R001P006a.wttd	6.39	5.45	4.75	-0.19170	-0.23163	0.12034	0.01176	-0.11810	-0.20715
M072b6E01R001P007a.wttd	7.75	6.66	5.75	-0.31597	-0.31770	0.23515	-0.03040	-0.14983	-0.20200
M072b6E01R001P008a.wttd	8.31	7.59	6.74	0.01259	-0.26739	0.11725	-0.34632	-0.10919	-0.21276
M072b6E01R001P009a.wttd	10.71	9.39	7.74	-0.57152	-0.46254	0.53216	0.00466	-0.16992	-0.10103
M072b6E01R001P010a.wttd	12.21	10.55	8.81	-0.40515	-0.37124	0.50967	0.00546	-0.14207	-0.15742
M072b6E01R001P011a.wttd	13.06	11.86	9.65	-0.43513	-0.45294	0.59740	-0.02008	-0.01617	0.00242
M072b6E01R002P002a.wttd	19.80	17.30	14.30	0.95347	0.41514	-0.98946	-0.37376	-0.03272	-0.04353
	Vrh	Vra	Vrp	H1*	H2*	H3*	H4*	H5*	H6*
M072b6E01R001P002a.wttd	1.10	0.92	0.81	-0.40105	0.01106	0.09381	-0.04361	0.00797	0.17038
M072b6E01R001P003a.wttd	2.47	2.06	1.82	-0.75960	0.16352	0.32658	0.12438	-0.03807	0.18935
M072b6E01R001P004a.wttd	3.78	3.19	2.80	-1.12020	0.31001	0.59701	0.17960	-0.05944	0.18699
M072b6E01R001P005a.wttd	5.14	4.29	3.75	-1.26640	0.52179	0.95963	0.31759	-0.00533	0.22205
M072b6E01R001P006a.wttd	6.39	5.45	4.75	-1.97170	0.69446	1.51760	0.72665	-0.02172	0.18094
M072b6E01R001P007a.wttd	7.75	6.66	5.75	-1.52080	1.03000	1.90200	0.31227	-0.11997	0.15881
M072b6E01R001P008a.wttd	8.31	7.59	6.74	-1.77900	1.32960	2.27320	0.16460	-0.26598	0.24691
M072b6E01R001P009a.wttd	10.71	9.39	7.74	-2.29160	1.72780	3.15090	0.67441	0.05071	-0.08881
M072b6E01R001P010a.wttd	12.21	10.55	8.81	-2.96290	2.00790	4.23950	1.00350	-0.00594	-0.26780
M072b6E01R001P011a.wttd	13.06	11.86	9.65	-2.60220	1.96580	3.59710	-0.32833	-1.08750	-0.58457
M072b6E01R002P002a.wttd	19.80	17.30	14.30	-1.47120	9.25650	13.88940	5.92570	-1.22420	0.02832
	Vrh	Vra	Vrp	P1*	P2*	P3*	P4*	P5*	P6*
M072b6E01R001P002a.wttd	1.10	0.92	0.81	0.01419	-0.01326	-0.33844	0.09589	-0.17201	0.26107
M072b6E01R001P003a.wttd	2.47	2.06	1.82	-0.04359	0.00625	-0.25142	0.13084	-0.21189	0.19441
M072b6E01R001P004a.wttd	3.78	3.19	2.80	-0.09836	0.03702	-0.13751	0.13010	-0.25548	0.17715
M072b6E01R001P005a.wttd	5.14	4.29	3.75	-0.17567	0.11949	0.01711	0.12829	-0.30317	0.28477
M072b6E01R001P006a.wttd	6.39	5.45	4.75	-0.13685	0.19971	0.23223	0.11733	-0.44756	0.28747
M072b6E01R001P007a.wttd	7.75	6.66	5.75	-0.25968	0.25993	0.45835	0.08469	-0.44429	0.27922
M072b6E01R001P008a.wttd	8.31	7.59	6.74	-0.17794	0.38046	0.63541	0.08071	-0.46316	0.11534
M072b6E01R001P009a.wttd	10.71	9.39	7.74	-0.35140	0.36613	1.42110	0.18249	-1.02320	0.36543
M072b6E01R001P010a.wttd	12.21	10.55	8.81	-0.2888	0.57749	1.72130	-0.18681	-0.88132	0.27958
M072b6E01R001P011a.wttd	13.06	11.86	9.65	-0.85249	0.81528	2.41300	-0.89442	-1.01380	0.46456
M072b6E01R002P002a.wttd	19.80	17.30	14.30	-0.99623	-0.03796	10.10840	-0.95860	-3.63170	1.05300

Notes: $V_{rh}=V/(f_vB)$, $V_{ra}=V/(f_aB)$ and $V_{rp}=V/(f_pB)$,
B – deck width of 60.36m,
V – deck height wind speed,
f_v, f_a and f_p – vertical, torsional and lateral frequencies respectively

TABLE 3.20 AERODYNAMIC DERIVATIVES, +6 DEGREES, SMOOTH FLOW, UNDER CONSTRUCTION CONDITION, BLWTL FORMAT

	Vrh	Vra	Vrp	A1*	A2*	A3*	A4*	A5*	A6*
M072b7E01R001P002a.wttd	1.29	1.08	0.95	0.01025	-0.00866	-0.01701	0.00862	-0.04966	-0.20459
M072b7E01R001P003a.wttd	2.74	2.30	2.02	-0.04360	-0.05841	0.00081	0.07243	-0.08464	-0.20629
M072b7E01R001P004a.wttd	4.23	3.57	3.12	0.00455	-0.05732	0.02005	0.12072	-0.10238	-0.20818
M072b7E01R001P005a.wttd	5.74	4.80	4.22	0.02268	-0.06954	0.01094	0.09095	-0.11461	-0.20571
M072b7E01R001P006a.wttd	7.26	6.00	5.31	-0.08053	-0.10887	0.01445	0.11956	-0.17198	-0.20182
M072b7E01R001P007a.wttd	8.79	7.37	6.43	-0.36036	-0.28602	-0.01299	-0.18311	-0.19946	-0.19684
M072b7E01R001P008a.wttd	10.34	8.43	7.59	-0.20502	-0.31638	0.04431	0.05435	-0.09940	-0.02424
M072b7E01R001P009a.wttd	12.38	9.60	8.60	-0.17564	-0.33894	0.14346	0.11273	0.00720	-0.17686
M072b7E01R001P010a.wttd	13.08	11.15	9.71	-0.25455	-0.27337	0.20273	0.16762	-0.04237	-0.16903
M072b7E01R002P002a.wttd	14.24	12.57	10.75	0.80232	0.60488	-0.23945	-0.11588	-0.19411	-0.04264
	Vrh	Vra	Vrp	H1*	H2*	H3*	H4*	H5*	H6*
M072b7E01R001P002a.wttd	1.29	1.08	0.95	-0.39251	0.01885	0.12314	0.01269	0.00026	0.16323
M072b7E01R001P003a.wttd	2.74	2.30	2.02	-0.84261	0.16572	0.36052	0.01352	-0.02501	0.17761
M072b7E01R001P004a.wttd	4.23	3.57	3.12	-1.52760	0.24406	0.79824	0.20942	-0.05113	0.20771
M072b7E01R001P005a.wttd	5.74	4.80	4.22	-1.63850	0.55316	1.42520	0.66434	-0.07818	0.27536
M072b7E01R001P006a.wttd	7.26	6.00	5.31	-1.95900	1.04520	2.14790	0.94003	-0.09031	0.19268
M072b7E01R001P007a.wttd	8.79	7.37	6.43	-1.57770	1.90120	2.88230	1.84970	-0.02528	0.05795
M072b7E01R001P008a.wttd	10.34	8.43	7.59	-2.05440	2.31160	3.46260	0.93240	-0.24150	-0.21796
M072b7E01R001P009a.wttd	12.38	9.60	8.60	-2.56350	2.73800	4.26970	0.76939	-0.83256	-0.23119
M072b7E01R001P010a.wttd	13.08	11.15	9.71	-2.53500	2.68970	4.23060	-1.29440	-0.43096	0.15321
M072b7E01R002P002a.wttd	14.24	12.57	10.75	-3.06090	2.90750	7.88330	3.71360	-0.96253	-0.04550
	Vrh	Vra	Vrp	P1*	P2*	P3*	P4*	P5*	P6*
M072b7E01R001P002a.wttd	1.29	1.08	0.95	-0.05411	-0.00996	-0.31090	0.07767	-0.16217	0.22022
M072b7E01R001P003a.wttd	2.74	2.30	2.02	-0.11780	0.03105	-0.18952	0.10462	-0.29611	0.22919
M072b7E01R001P004a.wttd	4.23	3.57	3.12	-0.17147	0.01772	0.01477	0.07008	-0.48836	0.21517
M072b7E01R001P005a.wttd	5.74	4.80	4.22	-0.23138	0.08372	0.35455	0.03964	-0.52992	0.34657
M072b7E01R001P006a.wttd	7.26	6.00	5.31	-0.35067	0.11634	0.80627	0.05134	-0.85786	0.27726
M072b7E01R001P007a.wttd	8.79	7.37	6.43	-0.36533	0.18104	1.35890	0.07155	-1.16730	0.16059
M072b7E01R001P008a.wttd	10.34	8.43	7.59	-0.22213	0.29659	2.03680	0.36375	-1.28460	0.26839
M072b7E01R001P009a.wttd	12.38	9.60	8.60	-0.24185	0.43681	2.57160	-0.16286	-1.12010	0.18709
M072b7E01R001P010a.wttd	13.08	11.15	9.71	-0.37053	0.50487	2.86290	-0.00589	-0.90961	0.42835
M072b7E01R002P002a.wttd	14.24	12.57	10.75	-1.0946	0.5635	6.02760	-0.48744	-2.34760	1.73860

Notes: $V_{rh}=V/(f_vB)$, $V_{ra}=V/(f_aB)$ and $V_{rp}=V/(f_pB)$,
B – deck width of 60.36m,
V – deck height wind speed,
f_v, f_a and f_p – vertical, torsional and lateral frequencies respectively

TABLE 3.21 PARAMETERS USED IN FORMULATION OF AERODYNAMIC ADMITTANCE

In-Service Bridge						
Angle of Attack	$dC_T / d\alpha$	$dC_D / d\alpha$	$dC_L / d\alpha$	C_T	C_D	C_L
-6^o	0.059	-0.705	1.129	-0.016	0.127	-0.163
-4^o	0.080	-0.494	0.845	-0.014	0.106	-0.129
-2^o	0.104	-0.287	0.722	-0.010	0.092	-0.102
0^o	0.096	-0.021	0.696	-0.007	0.086	-0.077
2^o	0.070	0.225	0.657	-0.004	0.090	-0.053
4^o	0.065	0.388	0.572	-0.002	0.102	-0.032
6^o	0.087	0.481	0.508	0.001	0.117	-0.013

Under Construction Bridge						
Angle of Attack	$dC_T / d\alpha$	$dC_D / d\alpha$	$dC_L / d\alpha$	C_T	C_D	C_L
-6^o	0.183	-0.508	2.017	-0.027	0.065	-0.296
-4^o	0.234	-0.414	2.259	-0.020	0.048	-0.220
-2^o	0.249	-0.193	2.046	-0.011	0.037	-0.142
0^o	0.245	0.041	1.783	-0.002	0.034	-0.076
2^o	0.209	0.233	1.530	0.006	0.040	-0.019
4^o	0.161	0.370	1.310	0.012	0.051	0.030
6^o	0.106	0.425	1.117	0.017	0.065	0.073

Deck Width, B	0.755	m
Length of Instrumented Portion of Model, L	0.375	m
Deck Depth, D	0.059	m
Number of points in FFT, $nfft$	2048	
Sample Frequency, f_s	200	Hz

TABLE 4.1 VELOCTIY PROFILES OVER BRIDGE DECK – NO TRAFFIC

Bare Bridge Deck Profiles

z (m)	Outer Downwind Vehicle Lane, U_{max}/U_{ref} = 0.968				Middle Downwind Vehicle Lane, U_{max}/U_{ref} = 0.972				Inner Downwind Vehicle Lane, U_{max}/U_{ref} = 0.967			
	$U(z)/U_{max}$	I_u	I_v	I_w	$U(z)/U_{max}$	I_u	I_v	I_w	$U(z)/U_{max}$	I_u	I_v	I_w
0.8	0.153	1.146	0.712	0.531	0.110	1.393	0.829	0.841	0.038	1.724	1.051	1.071
1.6	0.243	0.882	0.538	0.415	0.231	0.931	0.535	0.490	0.152	1.109	0.640	0.769
2.4	0.332	0.726	0.426	0.323	0.360	0.676	0.396	0.313	0.366	0.700	0.342	0.329
3.2	0.448	0.561	0.324	0.235	0.468	0.546	0.305	0.233	0.531	0.503	0.251	0.220
4	0.547	0.461	0.261	0.188	0.586	0.427	0.236	0.179	0.655	0.381	0.203	0.174
4.8	0.645	0.373	0.213	0.150	0.670	0.362	0.202	0.148	0.750	0.302	0.166	0.139
5.6	0.723	0.312	0.183	0.128	0.753	0.292	0.166	0.119	0.819	0.248	0.147	0.114
6.4	0.802	0.254	0.152	0.106	0.826	0.231	0.144	0.102	0.887	0.198	0.126	0.092
8	0.902	0.168	0.118	0.081	0.923	0.151	0.110	0.074	0.971	0.124	0.097	0.067
16	1.000	0.079	0.075	0.064	1.000	0.075	0.075	0.064	1.006	0.076	0.075	0.065
24	1.000	0.077	0.074	0.067	1.000	0.077	0.073	0.069	1.000	0.080	0.077	0.069

z (m)	Leeward Train Lane, U_{max}/U_{ref} = 0.978				Windward Train Lane, U_{max}/U_{ref} = 0.975			
	$U(z)/U_{max}$	I_u	I_v	I_w	$U(z)/U_{max}$	I_u	I_v	I_w
0.8	0.028	1.766	1.047	1.222	0.019	1.686	1.045	1.044
1.6	0.096	1.372	0.799	0.997	0.020	2.180	1.371	1.315
2.4	0.308	0.713	0.393	0.374	0.171	0.860	0.493	0.583
3.2	0.535	0.473	0.234	0.171	0.556	0.437	0.196	0.127
4	0.692	0.341	0.174	0.112	0.734	0.278	0.151	0.088
4.8	0.794	0.257	0.141	0.086	0.837	0.205	0.131	0.074
5.6	0.876	0.186	0.121	0.072	0.910	0.161	0.112	0.064
6.4	0.938	0.146	0.107	0.065	0.954	0.128	0.101	0.060
8	0.998	0.099	0.091	0.058	1.005	0.094	0.086	0.060
16	1.005	0.074	0.078	0.068	1.010	0.077	0.077	0.069
24	1.000	0.080	0.078	0.072	1.000	0.084	0.079	0.072

z (m)	Inner Upwind Vehicle Lane, U_{max}/U_{ref} = 0.949				Middle Upwind Vehicle Lane, U_{max}/U_{ref} = 0.946				Outer Upwind Vehicle Lane, U_{max}/U_{ref} = 0.935			
	$U(z)/U_{max}$	I_u	I_v	I_w	$U(z)/U_{max}$	I_u	I_v	I_w	$U(z)/U_{max}$	I_u	I_v	I_w
0.8	0.125	0.885	0.545	0.473	0.155	0.561	0.441	0.364	0.143	0.628	0.509	0.370
1.6	0.274	0.571	0.353	0.289	0.276	0.516	0.332	0.293	0.263	0.389	0.322	0.263
2.4	0.462	0.383	0.225	0.156	0.489	0.352	0.204	0.132	0.592	0.234	0.146	0.062
3.2	0.641	0.269	0.163	0.093	0.691	0.217	0.140	0.074	0.762	0.156	0.119	0.071
4	0.771	0.184	0.130	0.069	0.809	0.156	0.114	0.062	0.860	0.139	0.103	0.058
4.8	0.861	0.140	0.113	0.064	0.871	0.130	0.103	0.061	0.906	0.115	0.092	0.065
5.6	0.913	0.118	0.102	0.061	0.927	0.113	0.097	0.061	0.953	0.102	0.089	0.067
6.4	0.953	0.104	0.094	0.062	0.961	0.100	0.090	0.062	0.977	0.091	0.088	0.069
8	0.991	0.083	0.085	0.067	0.985	0.085	0.085	0.069	0.987	0.083	0.084	0.075
16	1.002	0.079	0.081	0.073	0.991	0.085	0.084	0.073	0.991	0.083	0.085	0.077
24	1.000	0.084	0.081	0.077	1.000	0.086	0.081	0.076	1.000	0.084	0.083	0.077

TABLE 4.2 VELOCTIY PROFILES OVER BRIDGE DECK – TRAFFIC CONDITION 1

Traffic 1 - Bridge Deck Profiles

z (m)	Outer Downwind Vehicle Lane, U_{max}/U_{ref} = 0.968				Middle Downwind Vehicle Lane, U_{max}/U_{ref} = 0.972				Inner Downwind Vehicle Lane, U_{max}/U_{ref} = 0.967			
	$U(z)/U_{max}$	I_u	I_v	I_w	$U(z)/U_{max}$	I_u	I_v	I_w	$U(z)/U_{max}$	I_u	I_v	I_w
0.8	0.126	1.364	0.877	0.722	0.098	1.524	0.985	0.890	0.045	1.747	1.148	1.310
1.6	0.222	0.992	0.634	0.570	0.182	1.163	0.697	0.685	0.145	1.246	0.736	0.869
2.4	0.332	0.755	0.485	0.424	0.309	0.815	0.498	0.459	0.288	0.832	0.480	0.497
3.2	0.460	0.559	0.370	0.316	0.439	0.611	0.364	0.326	0.433	0.602	0.346	0.353
4	0.571	0.439	0.289	0.246	0.554	0.480	0.280	0.252	0.577	0.439	0.252	0.265
4.8	0.665	0.364	0.234	0.201	0.661	0.371	0.222	0.194	0.690	0.353	0.200	0.211
5.6	0.772	0.281	0.184	0.156	0.780	0.276	0.169	0.150	0.800	0.264	0.160	0.161
6.4	0.839	0.228	0.155	0.130	0.849	0.227	0.146	0.126	0.867	0.214	0.133	0.131
8	0.943	0.144	0.114	0.091	0.948	0.151	0.104	0.087	0.954	0.148	0.105	0.085
16	1.011	0.075	0.071	0.065	1.013	0.077	0.074	0.065	1.013	0.076	0.072	0.067
24	1.000	0.074	0.072	0.068	1.000	0.078	0.073	0.068	1.000	0.077	0.074	0.070

z (m)	Leeward Train Lane, U_{max}/U_{ref} = 0.978				Windward Train Lane, U_{max}/U_{ref} = 0.975			
	$U(z)/U_{max}$	I_u	I_v	I_w	$U(z)/U_{max}$	I_u	I_v	I_w
0.8	0.039	1.455	0.940	0.944				
1.6	0.005	4.044	3.575	2.996				
2.4	0.022	1.775	1.478	1.229				
3.2	0.038	1.795	1.073	1.312				
4	0.360	0.626	0.312	0.344				
4.8	0.768	0.296	0.144	0.085				
5.6	0.894	0.201	0.113	0.064				
6.4	0.953	0.150	0.098	0.056				
8	1.016	0.100	0.085	0.052				
16	1.015	0.074	0.074	0.067				
24	1.000	0.077	0.076	0.071				

z (m)	Inner Upwind Vehicle Lane, U_{max}/U_{ref} = 0.949				Middle Upwind Vehicle Lane, U_{max}/U_{ref} = 0.946				Outer Upwind Vehicle Lane, U_{max}/U_{ref} = 0.935			
	$U(z)/U_{max}$	I_u	I_v	I_w	$U(z)/U_{max}$	I_u	I_v	I_w	$U(z)/U_{max}$	I_u	I_v	I_w
0.8	0.105	1.052	0.610	0.519	0.285	0.643	0.225	0.212				
1.6	0.258	0.600	0.352	0.289	0.363	0.419	0.179	0.182				
2.4	0.443	0.386	0.223	0.147	0.515	0.282	0.146	0.128				
3.2	0.626	0.254	0.160	0.082	0.706	0.196	0.120	0.073				
4	0.763	0.176	0.128	0.062	0.833	0.141	0.106	0.062				
4.8	0.846	0.136	0.109	0.058	0.897	0.119	0.098	0.061				
5.6	0.897	0.114	0.099	0.060	0.937	0.109	0.093	0.062				
6.4	0.943	0.103	0.090	0.058	0.978	0.097	0.086	0.061				
8	0.984	0.084	0.085	0.066	0.999	0.087	0.085	0.068				
16	0.992	0.081	0.080	0.072	0.988	0.084	0.084	0.076				
24	1.000	0.082	0.081	0.075	1.000	0.086	0.082	0.076				

TABLE 4.3 VELOCTIY PROFILES OVER BRIDGE DECK – TRAFFIC CONDITION 2

Traffic 2 - Bridge Deck Profiles

z (m)	Outer Downwind Vehicle Lane, U_{max}/U_{ref} = 0.968				Middle Downwind Vehicle Lane, U_{max}/U_{ref} = 0.972				Inner Downwind Vehicle Lane, U_{max}/U_{ref} = 0.967			
	$U(z)/U_{max}$	I_u	I_v	I_w	$U(z)/U_{max}$	I_u	I_v	I_w	$U(z)/U_{max}$	I_u	I_v	I_w
0.8					0.079	1.685	1.068	1.025	0.036	1.938	1.289	1.417
1.6					0.155	1.239	0.766	0.748	0.121	1.379	0.839	1.013
2.4					0.275	0.896	0.538	0.488	0.252	0.894	0.542	0.590
3.2					0.414	0.623	0.378	0.323	0.408	0.622	0.377	0.402
4					0.534	0.482	0.285	0.244	0.541	0.471	0.279	0.300
4.8					0.661	0.369	0.218	0.183	0.670	0.361	0.210	0.227
5.6					0.765	0.284	0.174	0.144	0.779	0.278	0.165	0.172
6.4					0.844	0.222	0.147	0.115	0.856	0.225	0.139	0.131
8					0.949	0.137	0.108	0.078	0.955	0.142	0.104	0.082
16					1.012	0.076	0.071	0.065	1.015	0.076	0.073	0.067
24					1.000	0.075	0.073	0.070	1.000	0.078	0.075	0.069

z (m)	Leeward Train Lane, U_{max}/U_{ref} = 0.978				Windward Train Lane, U_{max}/U_{ref} = 0.975			
	$U(z)/U_{max}$	I_u	I_v	I_w	$U(z)/U_{max}$	I_u	I_v	I_w
0.8	0.026	1.798	1.130	1.185				
1.6	0.008	2.979	2.471	2.224				
2.4	0.021	1.747	1.348	1.218				
3.2	0.044	1.790	1.001	1.320				
4	0.382	0.618	0.303	0.312				
4.8	0.764	0.295	0.150	0.086				
5.6	0.889	0.201	0.118	0.064				
6.4	0.947	0.154	0.106	0.058				
8	1.015	0.101	0.086	0.052				
16	1.009	0.076	0.074	0.068				
24	1.000	0.080	0.076	0.072				

z (m)	Inner Upwind Vehicle Lane, U_{max}/U_{ref} = 0.949				Middle Upwind Vehicle Lane, U_{max}/U_{ref} = 0.946				Outer Upwind Vehicle Lane, U_{max}/U_{ref} = 0.935			
	$U(z)/U_{max}$	I_u	I_v	I_w	$U(z)/U_{max}$	I_u	I_v	I_w	$U(z)/U_{max}$	I_u	I_v	I_w
0.8	0.107	0.941	0.574	0.466	0.137	0.617	0.478	0.370	0.137	0.611	0.526	0.367
1.6	0.228	0.643	0.380	0.317	0.245	0.558	0.365	0.332	0.269	0.425	0.322	0.274
2.4	0.409	0.432	0.250	0.176	0.468	0.362	0.212	0.143	0.583	0.233	0.154	0.070
3.2	0.581	0.300	0.178	0.103	0.669	0.226	0.148	0.079	0.751	0.161	0.122	0.075
4	0.729	0.204	0.140	0.071	0.787	0.164	0.120	0.067	0.850	0.142	0.105	0.061
4.8	0.820	0.149	0.117	0.063	0.864	0.132	0.106	0.065	0.898	0.116	0.096	0.066
5.6	0.883	0.125	0.103	0.062	0.914	0.117	0.098	0.064	0.943	0.108	0.091	0.066
6.4	0.926	0.104	0.095	0.061	0.947	0.104	0.091	0.063	0.971	0.096	0.089	0.068
8	0.968	0.085	0.087	0.066	0.978	0.088	0.087	0.071	0.977	0.087	0.087	0.074
16	0.988	0.081	0.081	0.072	0.989	0.086	0.084	0.076	0.986	0.089	0.086	0.076
24	1.000	0.082	0.082	0.075	1.000	0.087	0.084	0.075	1.000	0.090	0.085	0.077

TABLE 4.4 VELOCTIY PROFILES OVER BRIDGE DECK – TRAFFIC CONDITION 3

Traffic 3 - Bridge Deck Profiles

z (m)	Outer Downwind Vehicle Lane, U_{max}/U_{ref} = 0.968				Middle Downwind Vehicle Lane, U_{max}/U_{ref} = 0.972				Inner Downwind Vehicle Lane, U_{max}/U_{ref} = 0.967			
	$U(z)/U_{max}$	I_u	I_v	I_w	$U(z)/U_{max}$	I_u	I_v	I_w	$U(z)/U_{max}$	I_u	I_v	I_w
0.8	0.122	1.423	0.910	0.723	0.084	1.625	1.047	0.994	0.036	1.834	1.187	1.348
1.6	0.218	1.019	0.650	0.580	0.169	1.191	0.732	0.727	0.112	1.395	0.846	0.973
2.4	0.331	0.743	0.476	0.424	0.292	0.840	0.524	0.488	0.241	0.911	0.527	0.554
3.2	0.462	0.539	0.351	0.303	0.420	0.622	0.376	0.347	0.394	0.629	0.355	0.373
4	0.580	0.429	0.278	0.238	0.555	0.466	0.283	0.254	0.537	0.465	0.271	0.279
4.8	0.682	0.342	0.221	0.189	0.681	0.362	0.212	0.189	0.663	0.360	0.209	0.215
5.6	0.768	0.280	0.181	0.154	0.776	0.286	0.173	0.148	0.768	0.287	0.170	0.166
6.4	0.839	0.227	0.152	0.126	0.856	0.230	0.143	0.117	0.848	0.233	0.140	0.122
8	0.936	0.151	0.113	0.090	0.951	0.152	0.111	0.085	0.950	0.153	0.109	0.077
16	1.012	0.076	0.074	0.064	1.016	0.076	0.074	0.066	1.008	0.074	0.074	0.067
24	1.000	0.075	0.076	0.070	1.000	0.079	0.076	0.071	1.000	0.076	0.073	0.070

z (m)	Leeward Train Lane, U_{max}/U_{ref} = 0.978				Windward Train Lane, U_{max}/U_{ref} = 0.975			
	$U(z)/U_{max}$	I_u	I_v	I_w	$U(z)/U_{max}$	I_u	I_v	I_w
0.8	0.047	1.182	0.782	0.853				
1.6	0.003	5.371	5.086	2.384				
2.4	0.007	3.700	3.406	1.802				
3.2	0.030	2.202	1.372	1.496				
4	0.357	0.635	0.335	0.359				
4.8	0.765	0.294	0.155	0.091				
5.6	0.896	0.192	0.114	0.063				
6.4	0.957	0.155	0.100	0.056				
8	1.018	0.099	0.083	0.052				
16	1.010	0.076	0.074	0.067				
24	1.000	0.080	0.075	0.071				

z (m)	Inner Upwind Vehicle Lane, U_{max}/U_{ref} = 0.949				Middle Upwind Vehicle Lane, U_{max}/U_{ref} = 0.946				Outer Upwind Vehicle Lane, U_{max}/U_{ref} = 0.935			
	$U(z)/U_{max}$	I_u	I_v	I_w	$U(z)/U_{max}$	I_u	I_v	I_w	$U(z)/U_{max}$	I_u	I_v	I_w
0.8	0.110	0.953	0.570	0.507	0.144	0.590	0.453	0.359	0.141	0.620	0.509	0.362
1.6	0.251	0.611	0.370	0.310	0.247	0.556	0.364	0.325	0.256	0.400	0.322	0.268
2.4	0.422	0.425	0.239	0.169	0.448	0.376	0.217	0.149	0.569	0.244	0.156	0.065
3.2	0.606	0.285	0.171	0.100	0.651	0.240	0.148	0.079	0.741	0.159	0.127	0.075
4	0.737	0.203	0.139	0.075	0.780	0.162	0.118	0.064	0.838	0.143	0.106	0.059
4.8	0.834	0.147	0.114	0.065	0.850	0.132	0.107	0.063	0.894	0.113	0.094	0.066
5.6	0.893	0.119	0.102	0.062	0.900	0.118	0.096	0.062	0.934	0.102	0.089	0.067
6.4	0.939	0.105	0.093	0.063	0.937	0.106	0.091	0.063	0.963	0.091	0.087	0.070
8	0.974	0.083	0.084	0.067	0.973	0.085	0.083	0.070	0.976	0.082	0.085	0.075
16	0.990	0.079	0.082	0.073	0.979	0.086	0.083	0.075	0.981	0.086	0.084	0.077
24	1.000	0.083	0.081	0.075	1.000	0.085	0.082	0.075	1.000	0.085	0.083	0.077

TABLE 5.1 FULL SCALE AND MODEL SCALE PROPERTIES FOR THE BRIDGE DECK SECTION

	PROTOTYPE	TARGET (prototype scaled to model)	MEASURED MODEL
Characteristic Width of Deck, B	60.36 m	0.755 m	0.755 m
Mass Properties Mass Mass Moment of Inertia	 58100 kg/m 2.893×10^7 kg-m^2/m	 9.06 kg/m 0.706 kg-m^2/m	 9.08 kg/m 0.706 kg-m^2/m
Frequency Drag f_d Lift f_l Torque f_t f_t/f_l	 0.0549 Hz 0.0647 Hz 0.0806 Hz 1.246	Selected based on desired Velocity Scaling of ~ 1 to 5	 1.218 Hz 1.126 Hz 1.354 Hz 1.203
Stiffness Drag Lift Torque	 6.90 kN/m^2 9.59 kN/m^2 129.3 kN-m/m/degree	Consequence of Frequency and Mass	 1215.5 N/m 1038.8 N/m 2.04 N-m/degree
Damping (% of critical) Drag Lift Torque	Unknown	Less than 0.3%	 0.15% 0.34% 0.49%

Velocity Scaling:

Horizontal: $$\frac{V_m}{V_p} = \frac{(fB)_m}{(fB)_p} = \frac{1.218}{0.0549}\frac{0.755}{60.36} = \frac{1}{3.604}$$

Vertical: $$\frac{V_m}{V_p} = \frac{(fB)_m}{(fB)_p} = \frac{1.126}{0.0647}\frac{0.755}{60.36} = \frac{1}{4.594}$$

Torsional: $$\frac{V_m}{V_p} = \frac{(fB)_m}{(fB)_p} = \frac{1.354}{0.0806}\frac{0.755}{60.36} = \frac{1}{4.759}$$

TABLE 5.2 DYNAMIC SECTION MODEL TEST RESULTS (DRAG)

Horizontal Responses							
NO.	**Config.**	**Test**	**Flow**	**Maximum Wind Speeds**	**Angle**	**Damping**	**Figure No.**
				m/s	degree	% of critical	
1	No Traffic	M072m1E01R001	Smooth	94	0	0.15%	Figure 5.3 & Figure F1
2	TC-2* Road Vehicles	M072m2E01R001	Smooth	79	0	0.15%	Figure F2
3	TC-3 Train	M072m3E01R001	Smooth	83	0	0.15%	Figure F3
4	TC-1 Train & Road Vehicles	M072m4E01R001	Smooth	54	0	0.15%	Figure 5.5 & Figure F4
5	No Traffic	M072l1E01R001	Smooth	90	-4	0.15%	Figure 5.7 & Figure F5
6	TC-2* Road Vehicles	M072l2E01R001	Smooth	79	-4	0.15%	Figure F6
7	TC-3 Train	M072l3E01R001	Smooth	82	-4	0.15%	Figure F7
8	TC-1 Train & Road Vehicles	M072l4E01R001	Smooth	78	-4	0.15%	Figure F8
9	No Traffic	M072n1E01R001	Smooth	65	+4	0.15%	Figure 5.6 & Figure F9
10	TC-2* Road Vehicles	M072n2E01R001	Smooth	74	+4	0.15%	Figure F10
11	TC-3 Train	M072n3E01R001	Smooth	64	+4	0.15%	Figure F11
12	TC-1 Train & Road Vehicles	M072n4E01R001	Smooth	73	+4	0.15%	Figure F12
13	No Traffic	M072o1E02R001	Turbulent	78	0	0.15%	Figure 5.4 & Figure F13
14	TC-2* Road Vehicles	M072o2E02R001	Turbulent	78	0	0.15%	Figure F14
15	TC-3 Train	M072o3E02R001	Turbulent	76	0	0.15%	Figure F15
16	TC-1 Train & Road Vehicles	M072o4E02R001	Turbulent	78	0	0.15%	Figure F16

Note: All results of the dynamic section model tests are plotted in Appendix G.

TABLE 5.3 DYNAMIC SECTION MODEL TEST RESULTS (LIFT)

Vertical Responses								
NO.	**Config.**	**Test**	**Flow**	**Maximum Wind Speeds**	**Angle**	**Damping**	**Figure No.**	**Instability**
				m/s	degree	% of critical		
1	No Traffic	M072m1E01R001	Smooth	120	0	0.34%	Figure 5.3 & Figure F1	Not Observed
2	TC-2* Road Vehicles	M072m2E01R001	Smooth	101	0	0.34%	Figure F2	Not Observed
3	TC-3 Train	M072m3E01R001	Smooth	105	0	0.34%	Figure F3	Not Observed
4	TC-1 Train & Road Vehicles	M072m4E01R001	Smooth	69	0	0.34%	Figure 5.5 & Figure F4	at about 50m/s
5	No Traffic	M072l1E01R001	Smooth	114	-4	0.34%	Figure 5.7 & Figure F5	Not Observed
6	TC-2* Road Vehicles	M072l2E01R001	Smooth	100	-4	0.34%	Figure F6	Not Observed
7	TC-3 Train	M072l3E01R001	Smooth	105	-4	0.34%	Figure F7	Not Observed
8	TC-1 Train & Road Vehicles	M072l4E01R001	Smooth	100	-4	0.34%	Figure F8	Not Observed
9	No Traffic	M072n1E01R001	Smooth	83	+4	0.34%	Figure 5.6 & Figure F9	at about 84m/s
10	TC-2* Road Vehicles	M072n2E01R001	Smooth	94	+4	0.34%	Figure F10	at about 94m/s
11	TC-3 Train	M072n3E01R001	Smooth	81	+4	0.34%	Figure F11	at about 83m/s
12	TC-1 Train & Road Vehicles	M072n4E01R001	Smooth	93	+4	0.34%	Figure F12	at about 93m/s
13	No Traffic	M072o1E02R001	Turbulent	99	0	0.34%	Figure 5.4 & Figure F13	Not Observed
14	TC-2* Road Vehicles	M072o2E02R001	Turbulent	99	0	0.34%	Figure F14	Not Observed
15	TC-3 Train	M072o3E02R001	Turbulent	97	0	0.34%	Figure F15	Not Observed
16	TC-1 Train & Road Vehicles	M072o4E02R001	Turbulent	100	0	0.34%	Figure F16	Not Observed

Note: All results of the dynamic section model tests are plotted in Appendix G.

TABLE 5.4 DYNAMIC SECTION MODEL TEST RESULTS (TORSION)

Torsional Responses								
NO.	**Config.**	**Test**	**Flow**	**Maximum Wind Speeds**	**Angle of Attack**	**Damping**	**Figure No.**	**Instability**
				m/s	deg	% of critical		
1	No Traffic	M072m1E01R001	Smooth	124	0	0.49%	Figure 5.3 & Figure F1	Not Observed
2	TC-2* Road Vehicles	M072m2E01R001	Smooth	105	0	0.49%	Figure F2	Not Observed
3	TC-3 Train	M072m3E01R001	Smooth	109	0	0.49%	Figure F3	Not Observed
4	TC-1 Train & Road Vehicles	M072m4E01R001	Smooth	71	0	0.49%	Figure 5.5 & Figure F4	at about 50m/s
5	No Traffic	M072l1E01R001	Smooth	118	-4	0.49%	Figure 5.7 & Figure F5	Not Observed
6	TC-2* Road Vehicles	M072l2E01R001	Smooth	104	-4	0.49%	Figure F6	Not Observed
7	TC-3 Train	M072l3E01R001	Smooth	109	-4	0.49%	Figure F7	Not Observed
8	TC-1 Train & Road Vehicles	M072l4E01R001	Smooth	104	-4	0.49%	Figure F8	Not Observed
9	No Traffic	M072n1E01R001	Smooth	86	+4	0.49%	Figure 5.6 & Figure F9	at about 84m/s
10	TC-2* Road Vehicles	M072n2E01R001	Smooth	97	+4	0.49%	Figure F10	at about 94m/s
11	TC-3 Train	M072n3E01R001	Smooth	84	+4	0.49%	Figure F11	at about 83m/s
12	TC-1 Train & Road Vehicles	M072n4E01R001	Smooth	96	+4	0.49%	Figure F12	at about 93m/s
13	No Traffic	M072o1E02R001	Turbulent	103	0	0.49%	Figure 5.4 & Figure F13	Not Observed
14	TC-2* Road Vehicles	M072o2E02R001	Turbulent	103	0	0.49%	Figure F14	Not Observed
15	TC-3 Train	M072o3E02R001	Turbulent	101	0	0.49%	Figure F15	Not Observed
16	TC-1 Train & Road Vehicles	M072o4E02R001	Turbulent	103	0	0.49%	Figure F16	Not Observed

Note: All results of the dynamic section model tests are plotted in Appendix G.

TABLE 5.5 NORMALIZING FREQUENCIES USED IN ANALYSIS OF AERODYNAMIC DAMPING

AERODYNAMIC DERIVATIVE	FREQUENCY (MODEL)	MODE OF VIBRATION
$H_1^*, H_4^*, A_1^*, A_4^*, P_5^*, P_6^*$	1.126 Hz	Vertical
$H_2^*, H_3^*, A_2^*, A_3^*, P_2^*, P_3^*$	1.354 Hz	Torsional
$H_5^*, H_6^*, A_5^*, A_6^*, P_1^*, P_4^*$	1.218 Hz	Lateral

TABLE 5.6 SUMMARY OF AERODYNAMIC DAMPING TESTS

<table>
<tr><th>TEST GROUP</th><th>FLOW</th><th>TRAFFIC</th><th>ANGLE OF ATTACK</th><th>SPEEDS</th><th>FILENAME</th><th>NOMINAL FULL SCALE WIND SPEEDS (m/s)</th><th>OTHER TEST CONDITIONS</th></tr>
<tr><td rowspan="4">A)</td><td rowspan="12">Smooth</td><td>None</td><td>-4</td><td>5</td><td>P1</td><td rowspan="12">44, 47, 54, 60, 75</td><td rowspan="12">Yaw:
0 deg;

Amplitude range:
Rotation:
0.5 to 1.5 deg.
Vertical / Lateral:
2.5 to 7.5mm</td></tr>
<tr><td>Traffic 1</td><td>-4</td><td>5</td><td>P2</td></tr>
<tr><td>Traffic 2*</td><td>-4</td><td>5</td><td>P3</td></tr>
<tr><td>Traffic 3</td><td>-4</td><td>5</td><td>P4</td></tr>
<tr><td rowspan="4">B)</td><td>None</td><td>0</td><td>5</td><td>Q1</td></tr>
<tr><td>Traffic 1</td><td>0</td><td>5</td><td>Q2</td></tr>
<tr><td>Traffic 2*</td><td>0</td><td>5</td><td>Q3</td></tr>
<tr><td>Traffic 3</td><td>0</td><td>5</td><td>Q4</td></tr>
<tr><td rowspan="4">C)</td><td>None</td><td>4</td><td>5</td><td>R1</td></tr>
<tr><td>Traffic 1</td><td>4</td><td>5</td><td>R2</td></tr>
<tr><td>Traffic 2*</td><td>4</td><td>5</td><td>R3</td></tr>
<tr><td>Traffic 3</td><td>4</td><td>5</td><td>R4</td></tr>
</table>

Notes:

Traffic 1 - Road traffic on outward (slow) lane of upwind girder plus train on upwind track
Traffic 2* - Road traffic on outward (slow) lane of upwind girder
Traffic 3 - Train on upwind track only

Note that Traffic 2 was mistakenly run as Road traffic on outward (slow) lane of upwind girder with no road traffic present. The desired condition was Road traffic on outward (slow) downwind lane plus train on the upwind track.

TABLE 5.7 STATIC FORCE COEFFICENTS AND SLOPES, TRAFFIC CONDITION 2 AND TRAFFIC CONDITION 3

	Traffic 2 - Road traffic on outward downwind lane plus train on upwind track (Missed Test)								
	Angle of Attack (deg)	C_X	C_Z	C_m	C_D	C_L	$dC_m/d\alpha$	$dC_D/d\alpha$	$dC_L/d\alpha$
Smooth Flow	-4	0.116	-0.078	-0.011	0.121	-0.070	0.04	-0.64	0.58
	0	0.090	-0.064	-0.007	0.090	-0.064	0.13	-0.15	-0.15
	4	0.110	-0.063	-0.002	0.106	-0.071	0.05	0.54	0.26
	Traffic 3 - Train on upwind track only								
	Angle of Attack (deg)	C_X	C_Z	C_m	C_D	C_L	$dC_m/d\alpha$	$dC_D/d\alpha$	$dC_L/d\alpha$
	-4	0.115	-0.074	-0.012	0.120	-0.066	0.03	-0.63	0.62
	0	0.090	-0.061	-0.007	0.090	-0.061	0.15	-0.14	-0.21
	4	0.110	-0.063	-0.002	0.105	-0.071	0.05	0.53	0.25
	Traffic 2 - Road traffic on outward downwind lane plus train on upwind track (Missed Test)								
	Angle of Attack (deg)	C_X	C_Z	C_m	C_D	C_L	$dC_m/d\alpha$	$dC_D/d\alpha$	$dC_L/d\alpha$
Turbulent Flow	-4	0.108	-0.106	-0.013	0.115	-0.098	0.05	-0.53	0.56
	0	0.092	-0.065	-0.008	0.092	-0.065	0.08	-0.05	0.49
	4	0.105	-0.025	-0.003	0.103	-0.032	0.08	0.33	0.47
	Traffic 3 - Train on upwind track only								
	Angle of Attack (deg)	C_X	C_Z	C_m	C_D	C_L	$dC_m/d\alpha$	$dC_D/d\alpha$	$dC_L/d\alpha$
	-4	0.107	-0.105	-0.014	0.114	-0.097	0.03	-0.47	0.58
	0	0.093	-0.062	-0.008	0.093	-0.062	0.09	-0.06	0.48
	4	0.106	-0.024	-0.003	0.104	-0.031	0.08	0.33	0.39

TABLE 5.8 AERODYNAMIC DAMPING VALUES, 0 DEGREES, SMOOTH FLOW

Configuration	File Name	Full Scale Wind Speed	Aerodynamic Damping (%)	
		(m/s)	Vertical ζ_{aZ}	Torsional $\zeta_{a\theta}$
No Traffic	M072q1E01R001P002a.wttd	45.1	0.40	2.79
	M072q1E01R001P003a.wttd	48.6	0.41	2.85
	M072q1E01R001P004a.wttd	55.9	0.40	3.13
	M072q1E01R001P005a.wttd	62.0	0.42	3.38
	M072q1E01R001P006a.wttd	77.5	0.50	5.05
Traffic 1	M072q4E01r001P002a.wttd	46.7	-0.44	3.39
	M072q4E01r001P003a.wttd	50.2	-0.48	3.68
	M072q4E01r001P004a.wttd	56.4	-0.45	3.97
	M072q4E01r001P005a.wttd	63.3	-0.46	4.43
	M072q4E01r001P006a.wttd	78.6	-0.36	3.85
Traffic 2	M072q2E01R001P002a.wttd	45.6	0.57	3.30
	M072q2E01R001P003a.wttd	49.0	0.56	3.57
	M072q2E01R001P004a.wttd	55.0	0.60	3.85
	M072q2E01R001P005a.wttd	62.0	0.67	4.31
	M072q2E01R001P006a.wttd	76.8	0.98	4.08
Traffic 3	M072q3E01R001P002a.wttd	46.1	-0.38	2.48
	M072q3E01R001P003a.wttd	49.5	-0.41	2.52
	M072q3E01R001P004a.wttd	55.7	-0.46	2.61
	M072q3E01R001P005a.wttd	62.6	-0.62	2.85
	M072q3E01R001P006a.wttd	77.6	-0.85	4.45

Notes: $V_{rh}=V/(f_v B)$ and $V_{ra}=V/(f_a B)$,
B – deck width of 60.36m,
V – deck height wind speed,
f_v and f_a - vertical and torsional frequencies respectively
Traffic 2* is Road Traffic on outward (slow) lane on windward girder with no rail traffic

TABLE 5.9 AERODYNAMIC DAMPING VALUES, +4 DEGREES, SMOOTH FLOW

Configuration	File Name	Full Scale Wind Speed	Aerodynamic Damping (%)	
		(m/s)	Vertical ζ_{aZ}	Torsional $\zeta_{a\theta}$
No Traffic	M072r1E01r001P002a.wttd	45.3	1.79	1.98
	M072r1E01r001P003a.wttd	48.6	1.81	2.11
	M072r1E01r001P004a.wttd	54.7	2.02	2.22
	M072r1E01r001P005a.wttd	61.4	2.46	1.78
	M072r1E01r001P006a.wttd	76.4	3.80	0.09
Traffic 1	M072r4E01R003P002a.wttd	46.5	0.96	2.30
	M072r4E01R003P003a.wttd	50.1	0.96	2.51
	M072r4E01R003P004a.wttd	56.3	1.03	3.08
	M072r4E01R003P005a.wttd	63.2	1.24	3.15
	M072r4E01R003P006a.wttd	78.5	2.21	1.62
Traffic 2	M072r2E01r001P002a.wttd	45.8	1.39	2.33
	M072r2E01r001P003a.wttd	49.2	1.40	2.58
	M072r2E01r001P004a.wttd	55.3	1.52	3.05
	M072r2E01r001P005a.wttd	62.2	1.77	3.19
	M072r2E01r001P006a.wttd	77.2	2.77	1.55
Traffic 3	M072r3E01R001P002a.wttd	46.1	1.07	1.67
	M072r3E01R001P003a.wttd	49.6	1.20	1.68
	M072r3E01R001P004a.wttd	55.8	1.41	1.53
	M072r3E01R001P005a.wttd	62.6	1.93	1.04
	M072r3E01R001P006a.wttd	77.7	3.02	0.17

Notes: $V_{rh}=V/(f_vB)$ and $V_{ra}=V/(f_aB)$,
B – deck width of 60.36m,
V – deck height wind speed,
f_v and f_a - vertical and torsional frequencies respectively
Traffic 2* is Road Traffic on outward (slow) lane on windward girder with no rail traffic

TABLE 5.10 AERODYNAMIC DAMPING VALUES, -4 DEGREES, SMOOTH FLOW

Configuration	File Name	Full Scale Wind Speed	Aerodynamic Damping (%)	
		(m/s)	Vertical ζ_{aZ}	Torsional $\zeta_{a\theta}$
No Traffic	M072p1E01r001P002a.wttd	44.7	4.49	2.36
	M072p1E01r001P003a.wttd	48.0	4.69	2.45
	M072p1E01r001P004a.wttd	54.1	5.25	2.79
	M072p1E01r001P005a.wttd	60.7	5.99	2.73
	M072p1E01r001P006a.wttd	75.4	7.50	3.26
Traffic 1	M072p4E01r001P002a.wttd	46.3	2.72	2.68
	M072p4E01r001P003a.wttd	49.8	2.91	2.98
	M072p4E01r001P004a.wttd	55.9	3.19	3.62
	M072p4E01r001P005a.wttd	62.9	3.54	4.40
	M072p4E01r001P006a.wttd	77.9	4.65	5.83
Traffic 2	M072p2E01r001P002a.wttd	45.3	3.60	2.49
	M072p2E01r001P003a.wttd	48.6	3.71	2.63
	M072p2E01r001P004a.wttd	54.7	3.99	3.23
	M072p2E01r001P005a.wttd	61.3	4.36	3.85
	M072p2E01r001P006a.wttd	76.2	5.59	4.96
Traffic 3	M072p3E01r001P002a.wttd	45.7	3.33	4.32
	M072p3E01r001P003a.wttd	49.2	3.46	5.02
	M072p3E01r001P004a.wttd	55.3	3.88	6.13
	M072p3E01r001P005a.wttd	62.1	4.55	7.73
	M072p3E01r001P006a.wttd	77.1	5.65	10.17

Notes: $V_{rh}=V/(f_vB)$ and $V_{ra}=V/(f_aB)$,
B – deck width of 60.36m,
V – deck height wind speed,
f_v and f_a - vertical and torsional frequencies respectively
Traffic 2* is Road Traffic on outward (slow) lane on windward girder with no rail traffic

FIGURES

FIGURE 1.1 SITE OF THE MESSINA BRIDGE

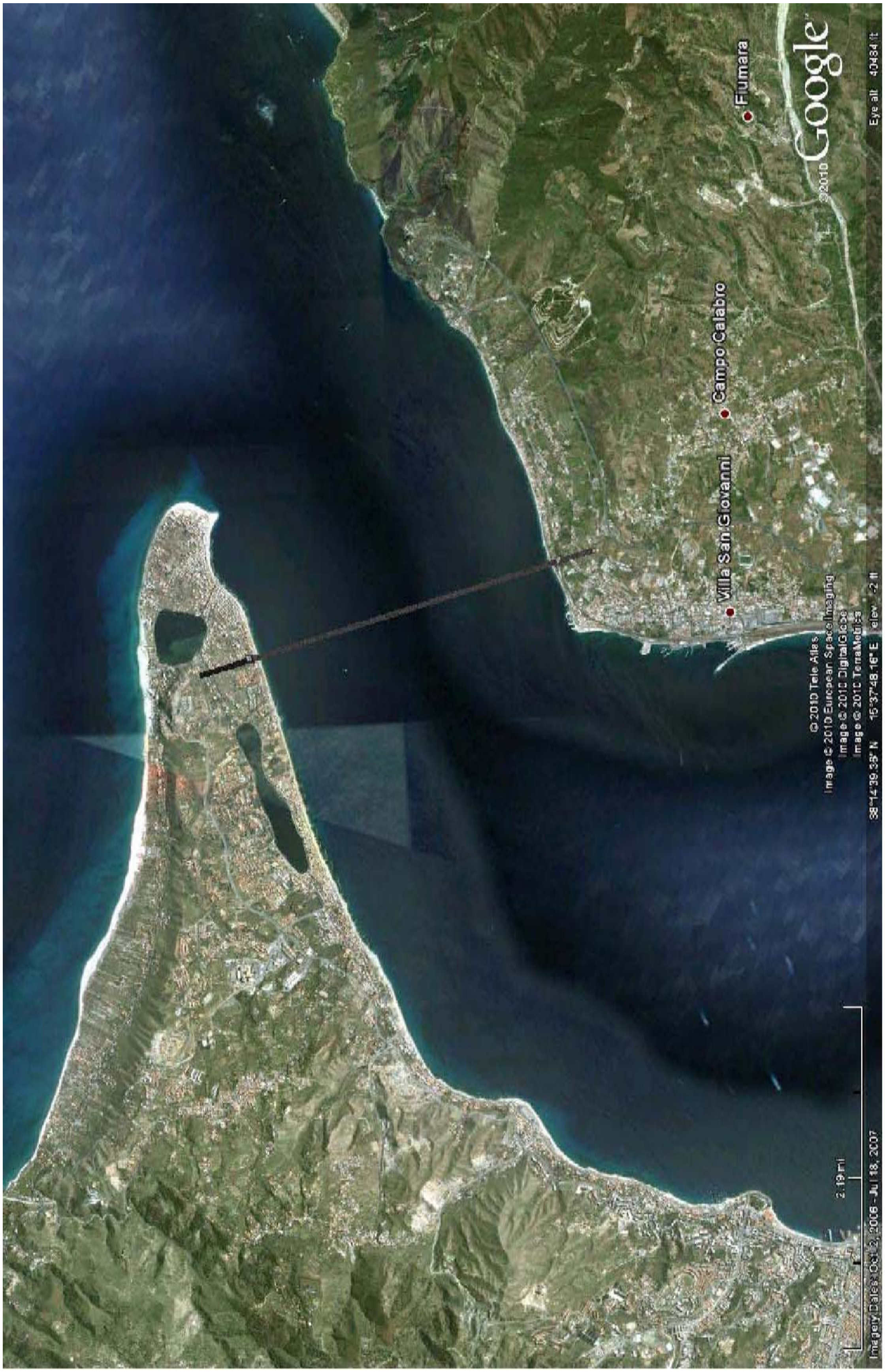

FIGURE 1.1 (CONT.) SITE OF THE MESSINA BRIDGE

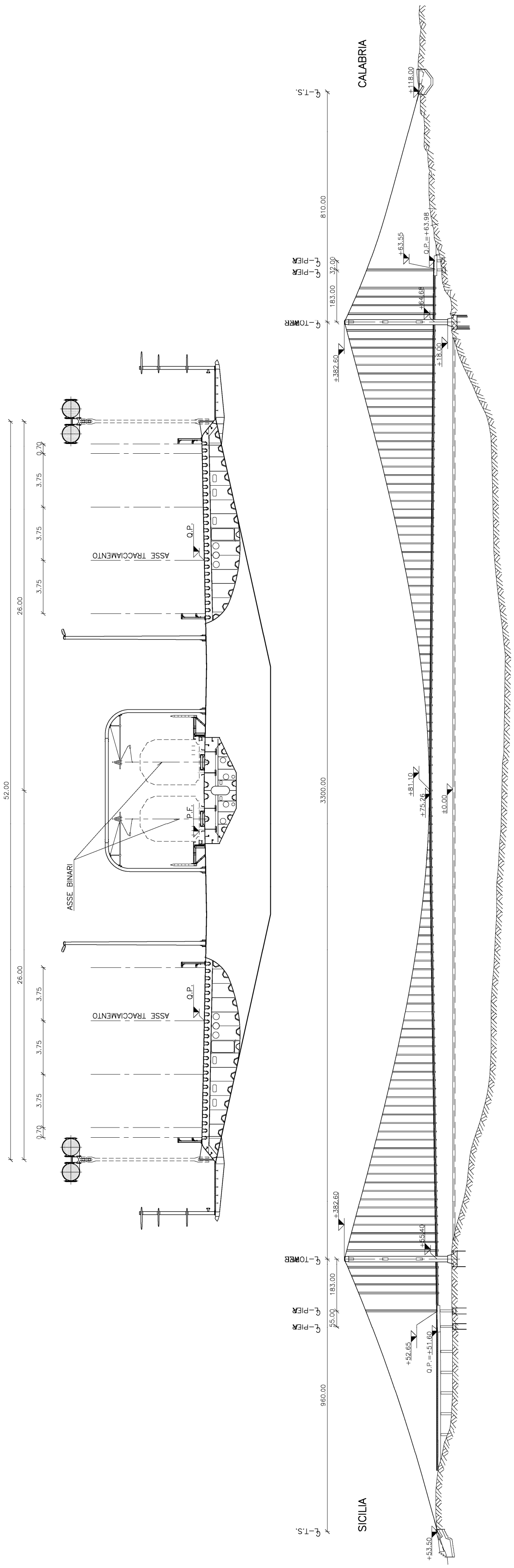

FIGURE 1.2 PROTOTYPE DIMENSIONS OF THE MESSINA BRIDGE

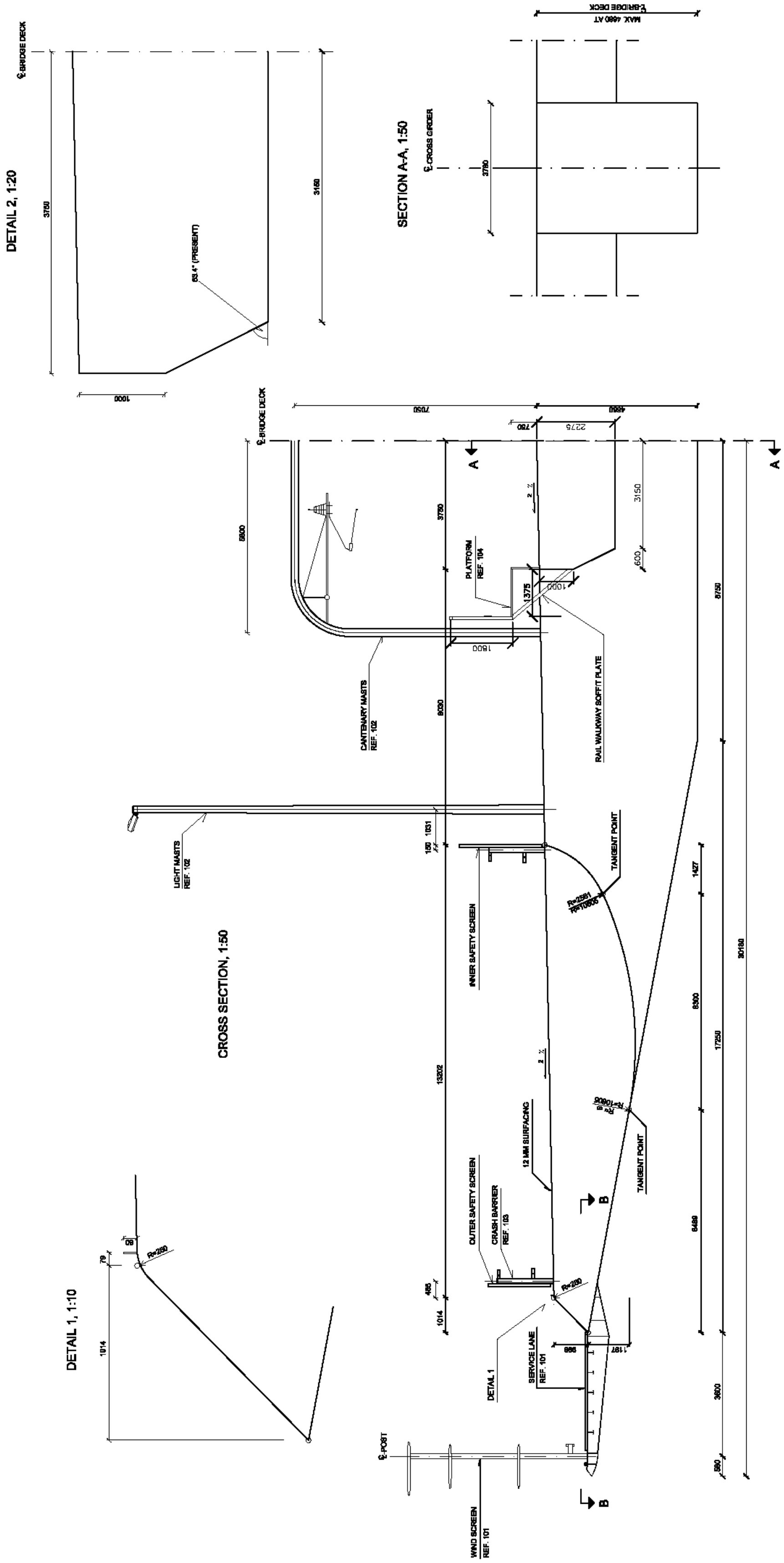

FIGURE 1.3 PROTOTYPE DIMENSIONS OF HALF DECK SECTION

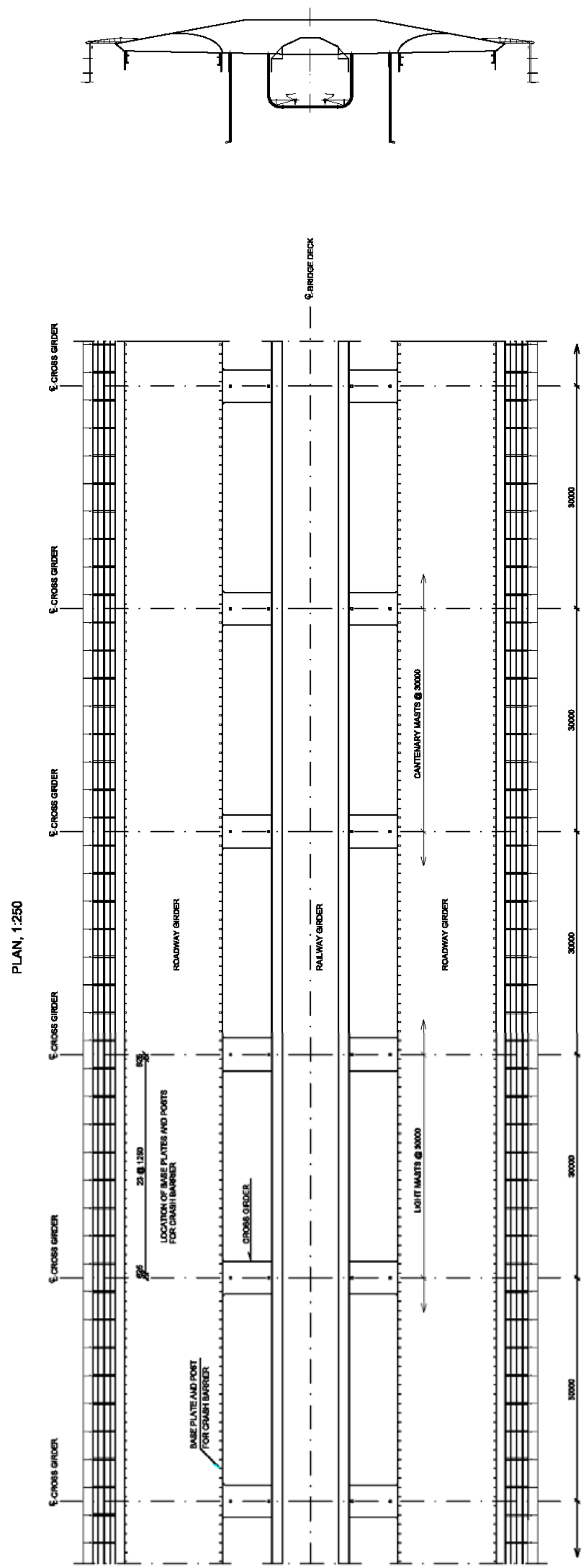

FIGURE 1.4 PROTOTYPE DIMENSIONS OF DECK PLAN

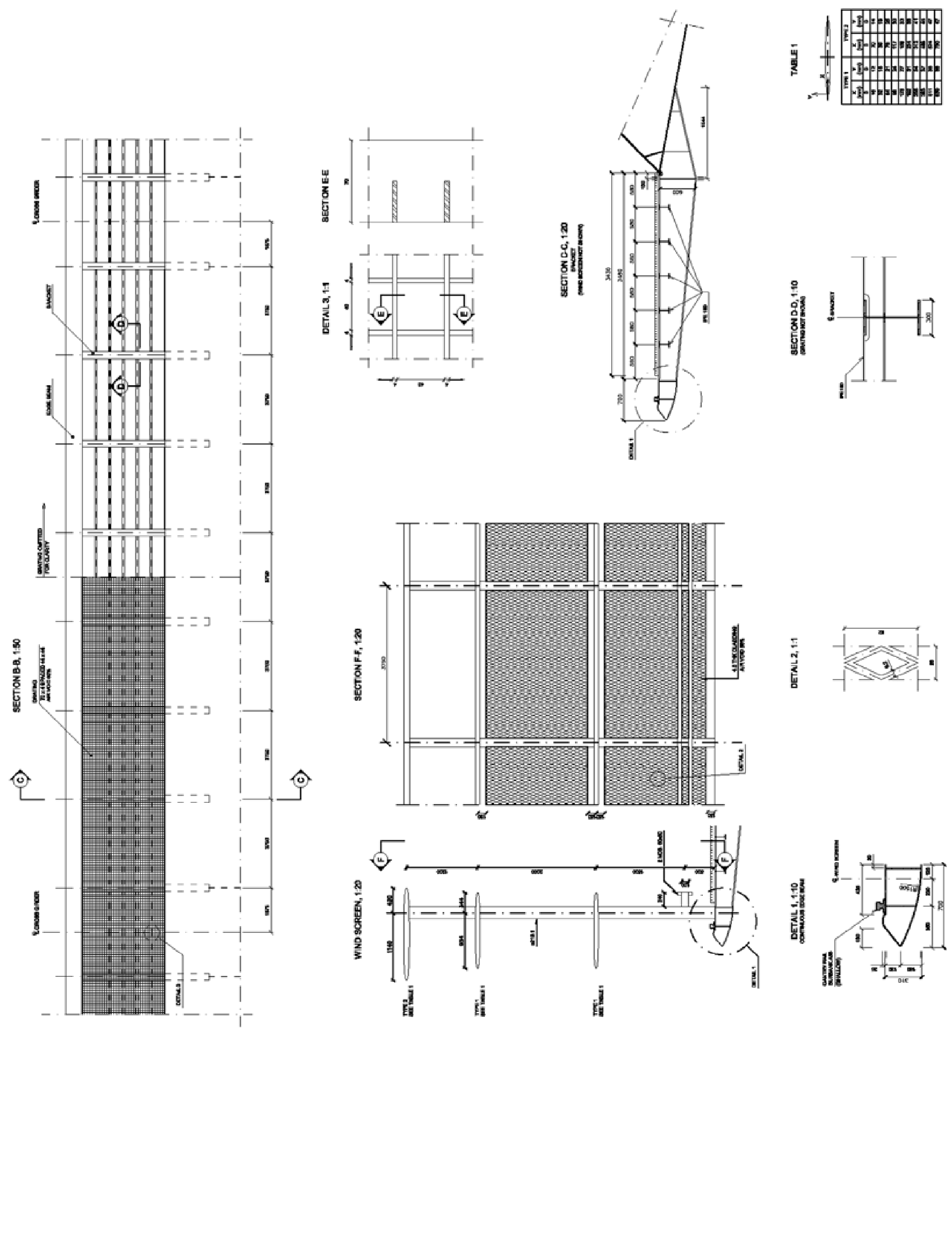

FIGURE 1.5 PROTOTYPE DIMENSIONS OF SERVICE WALKWAY

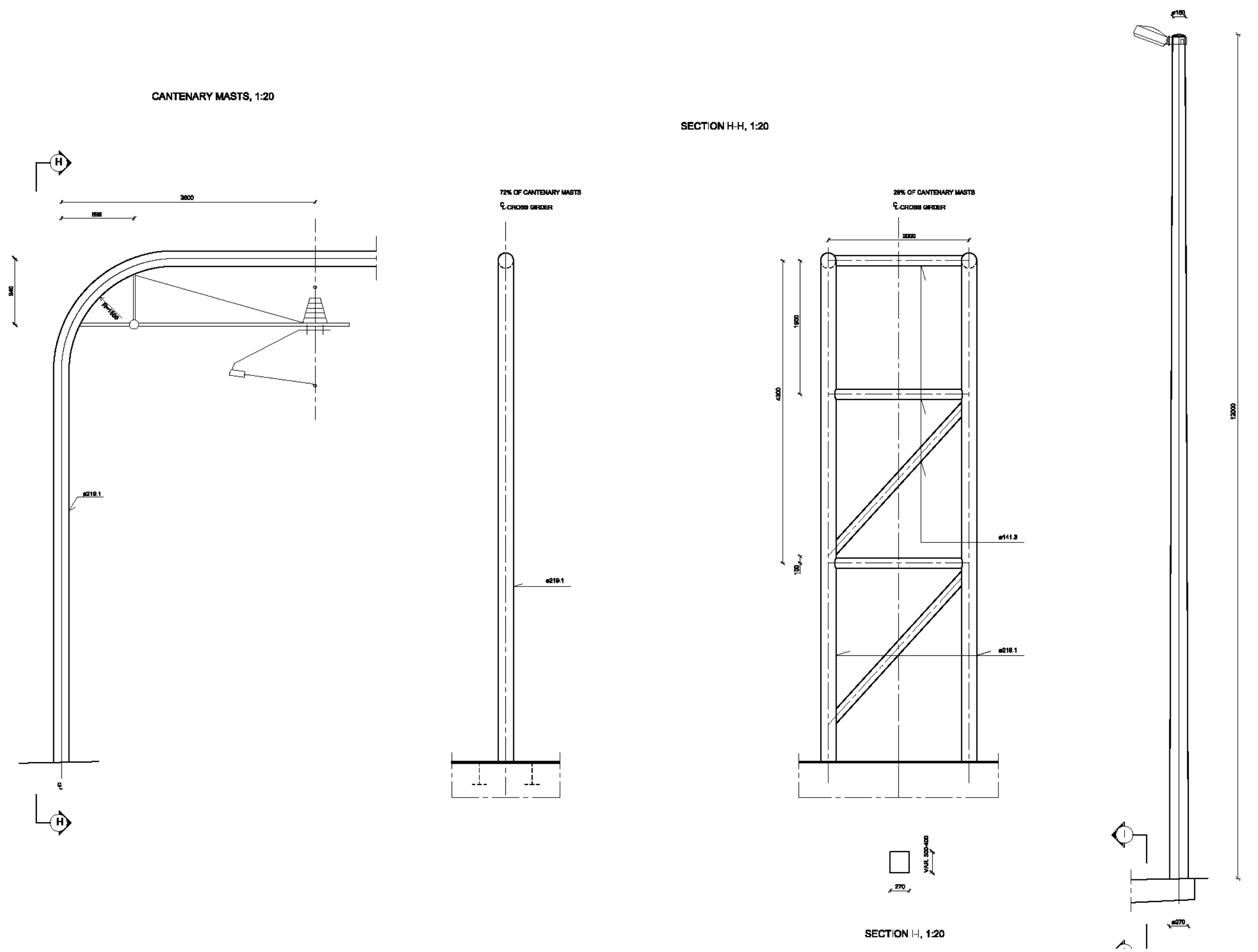

FIGURE 1.6 PROTOTYPE DIMENSIONS OF CATENARY MAST AND LIGHT STANDARD

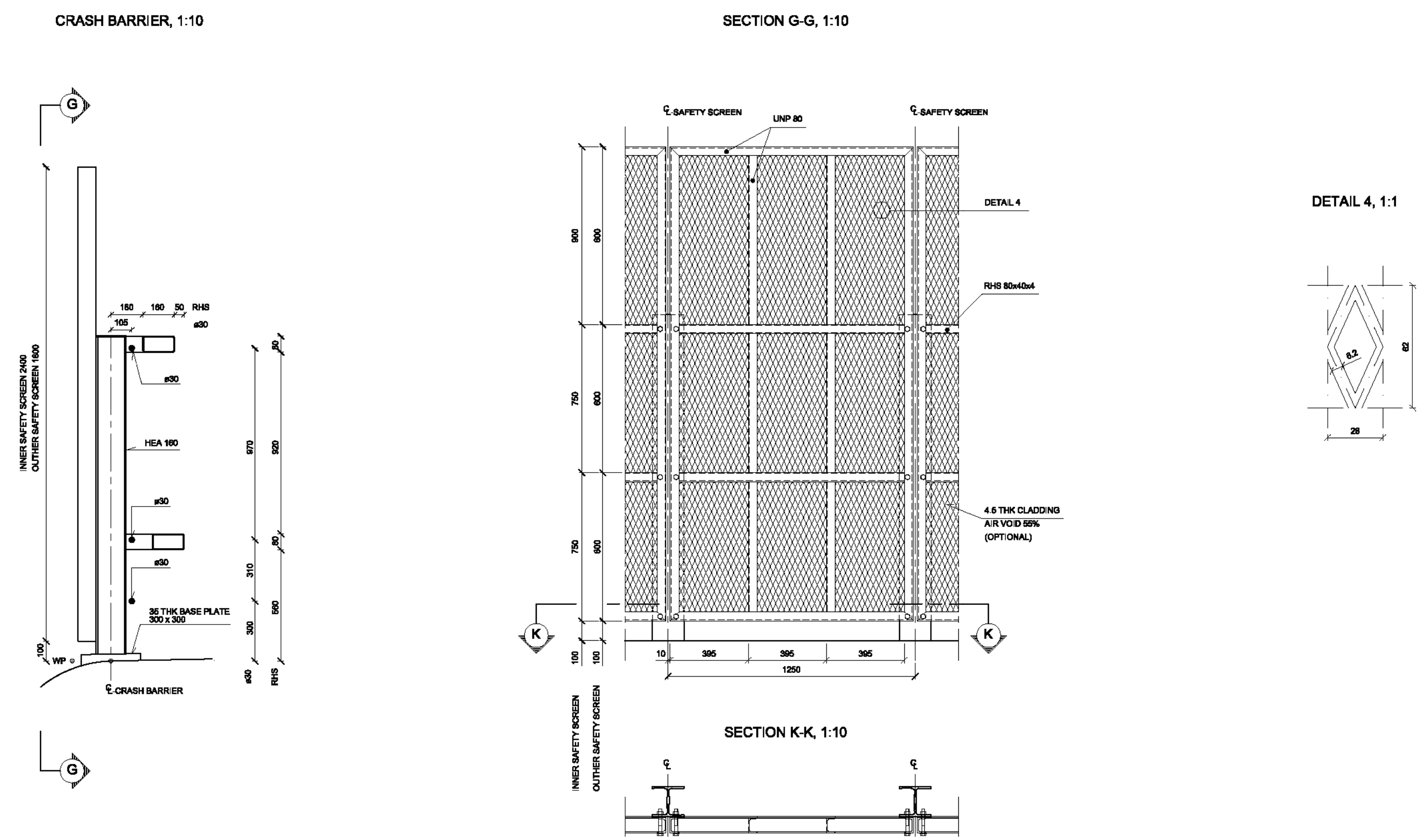

FIGURE 1.7 PROTOTYPE DIMENSIONS OF CRASH BARRIER

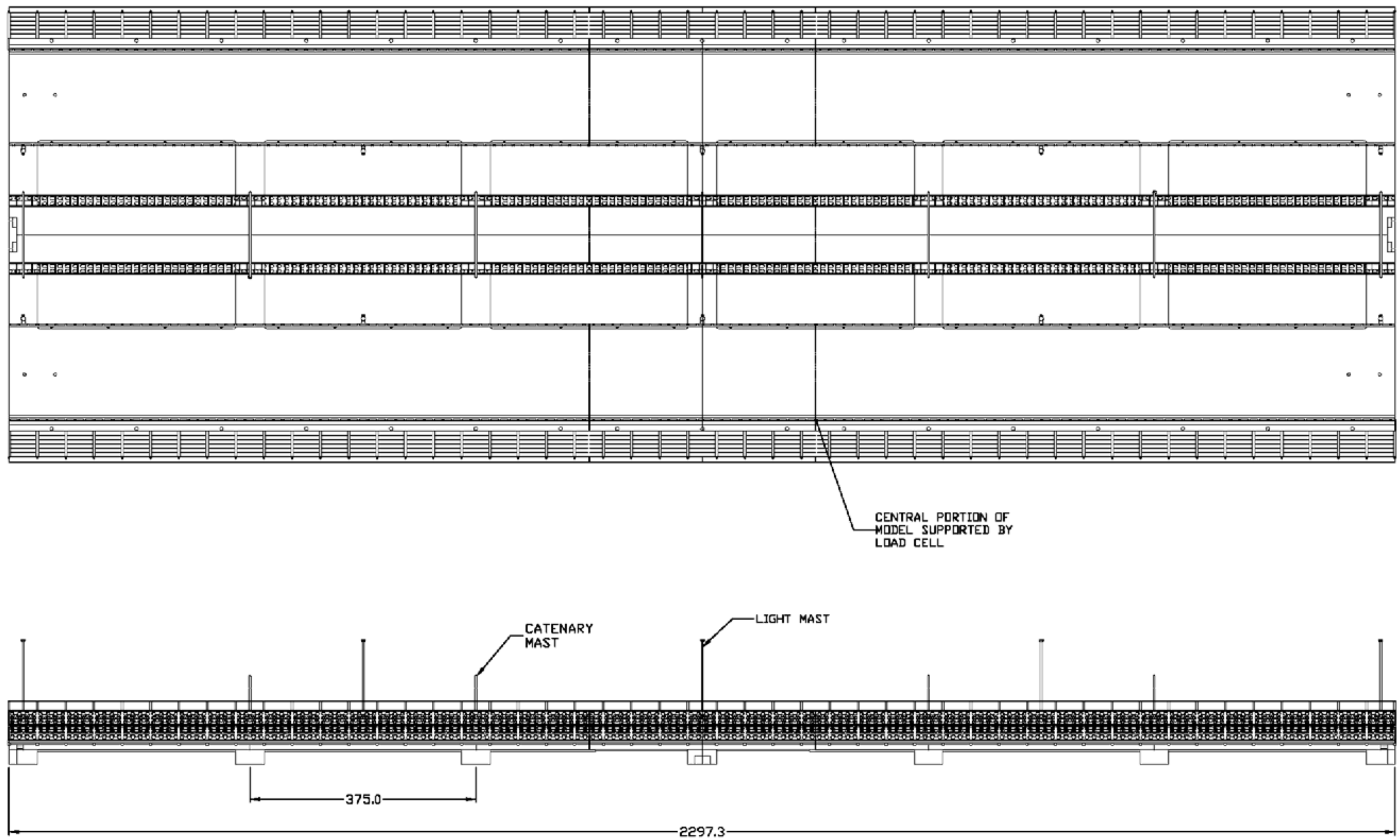

FIGURE 2.1   1 TO 80 SCALE SECTION MODEL – PLAN AND ELEVATION

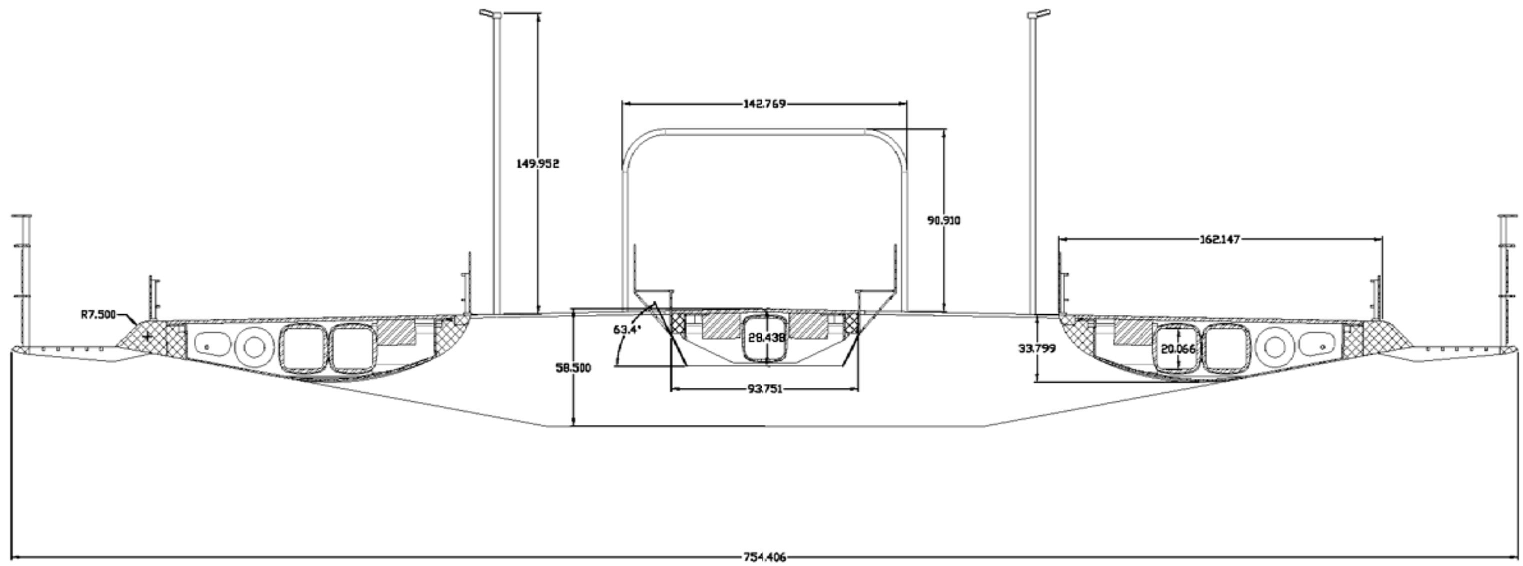

a) General Section

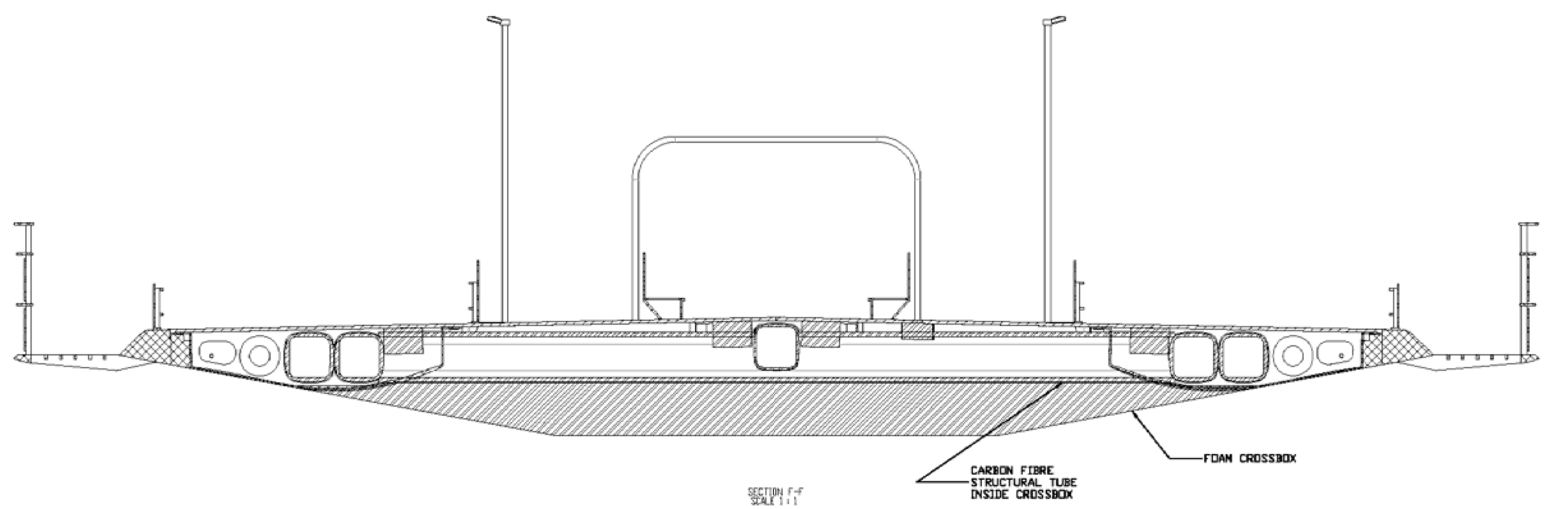

b) Section at Cross Beam

FIGURE 2.2 1 TO 80 SCALE SECTION MODEL - SECTIONS

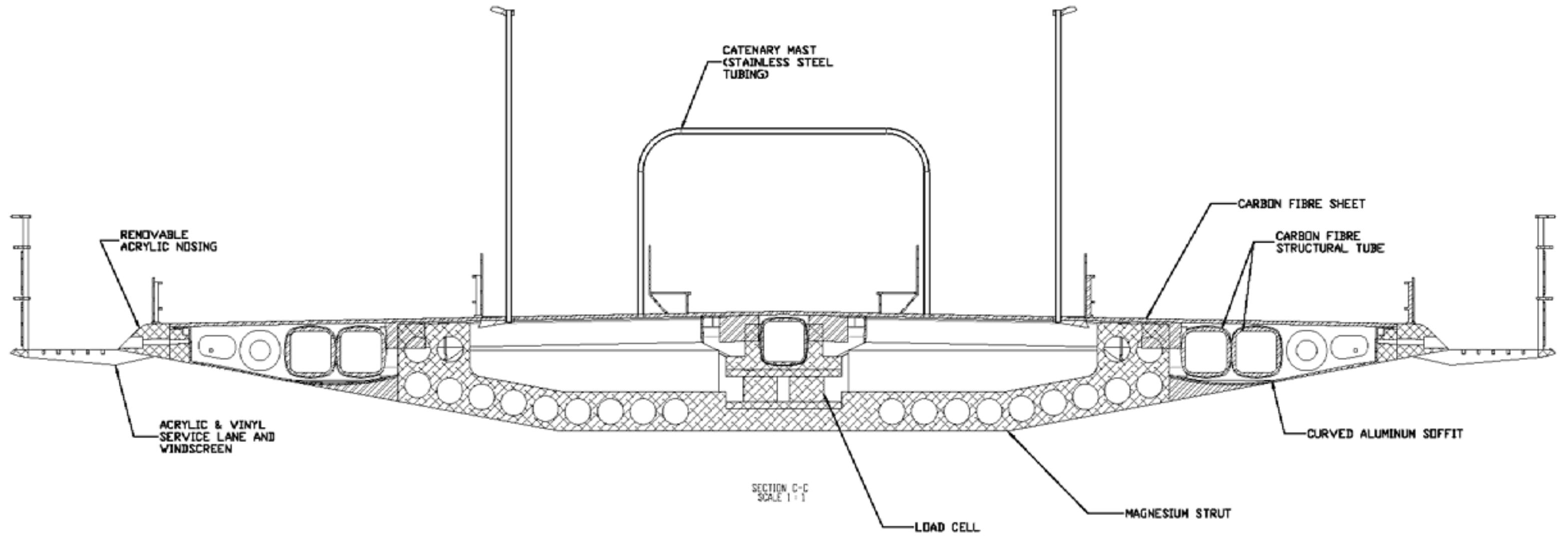

c) Section at Instrumented Panel

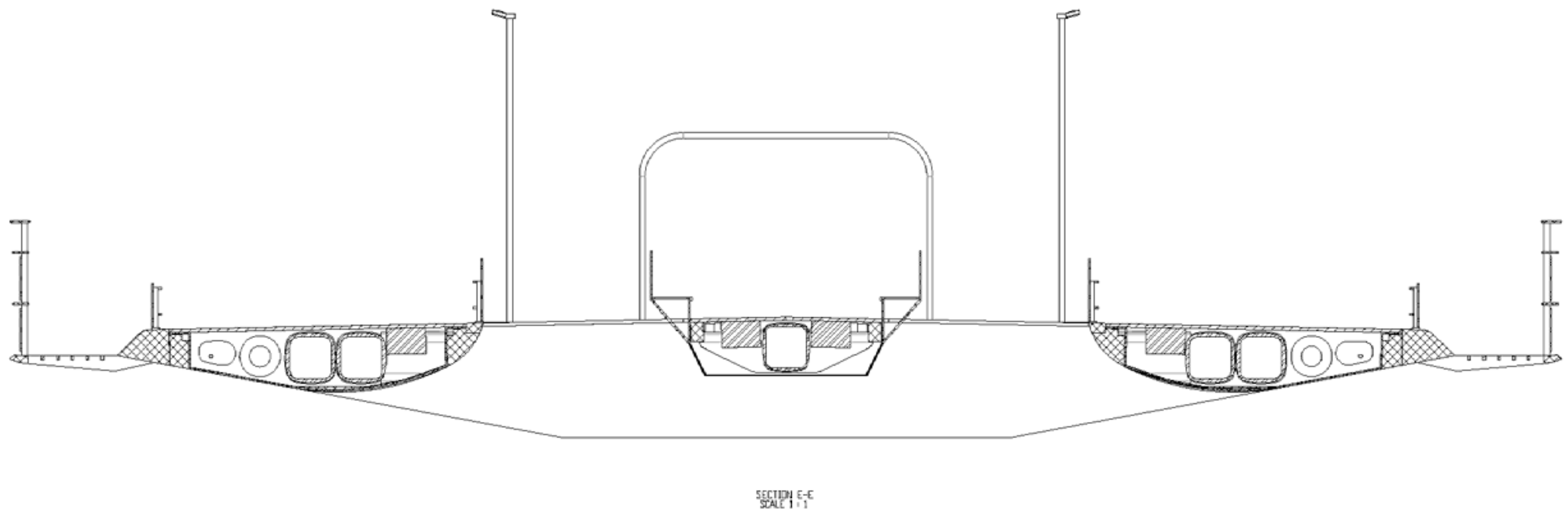

d) Section between Cross Beams

FIGURE 2.2(CONT.) 1 TO 80 SCALE SECTION MODEL - SECTIONS

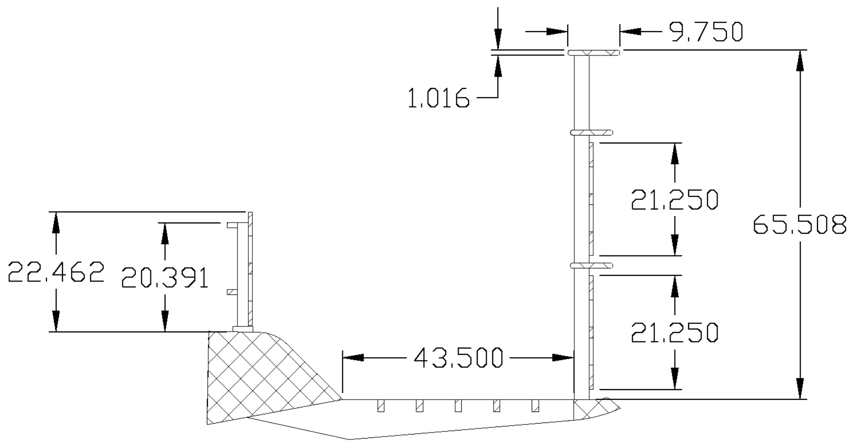

a) Section Through Service Lane Cantilever

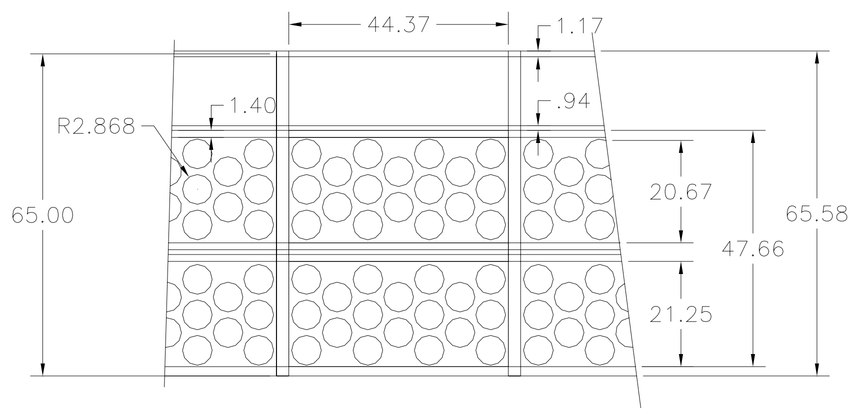

b) External Windscreen

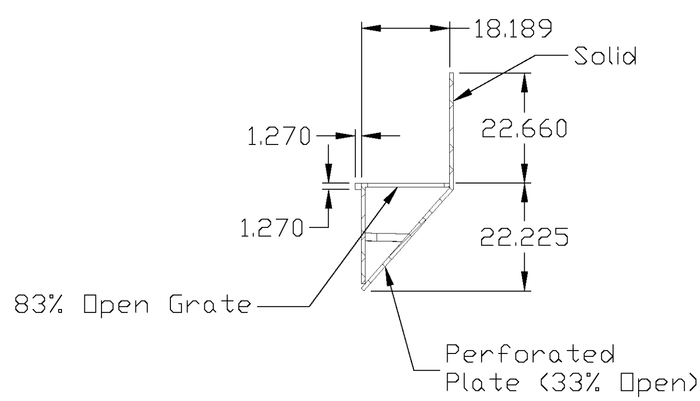

c) Rail Platform

FIGURE 2.3 1 TO 80 SCALE SECTION MODEL – WINDSCREEN, SERVICE LANE AND RAIL PLATFORM DETAILS

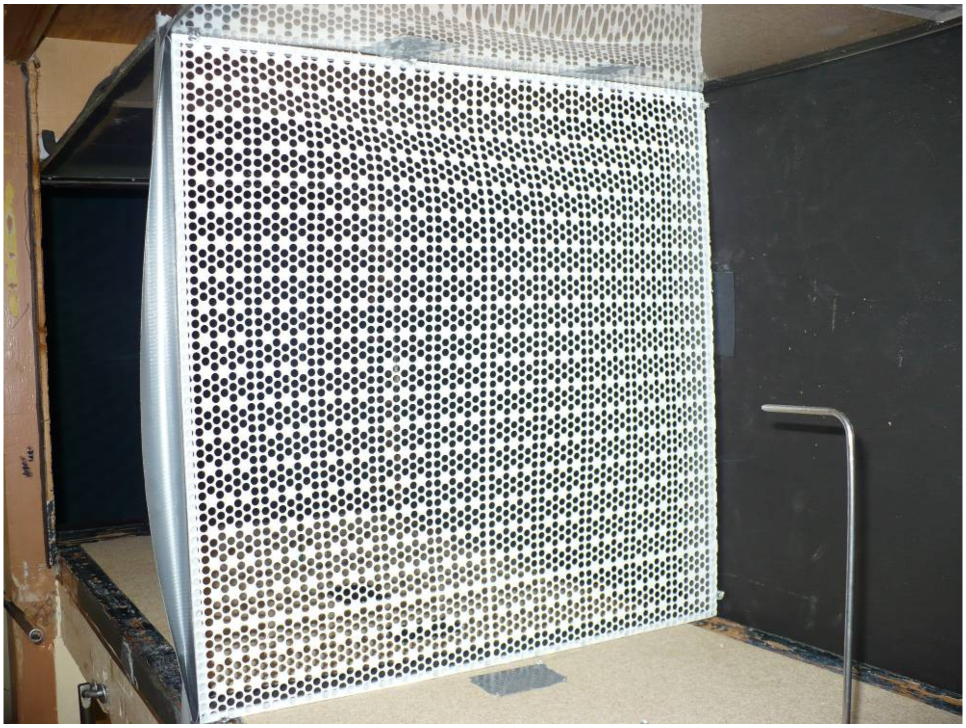

a) Windscreen test in Pilot Study Wind Tunnel

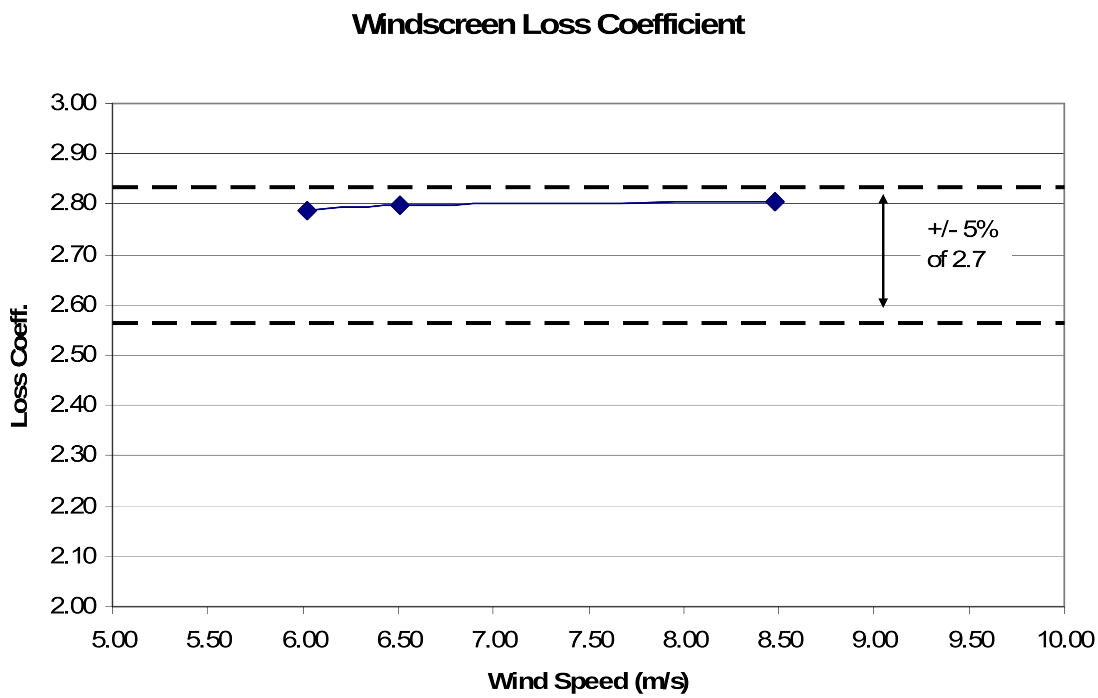

b) Windscreen Loss Coefficient

FIGURE 2.4 WINDSCREEN LOSS COEFFICIENT TEST

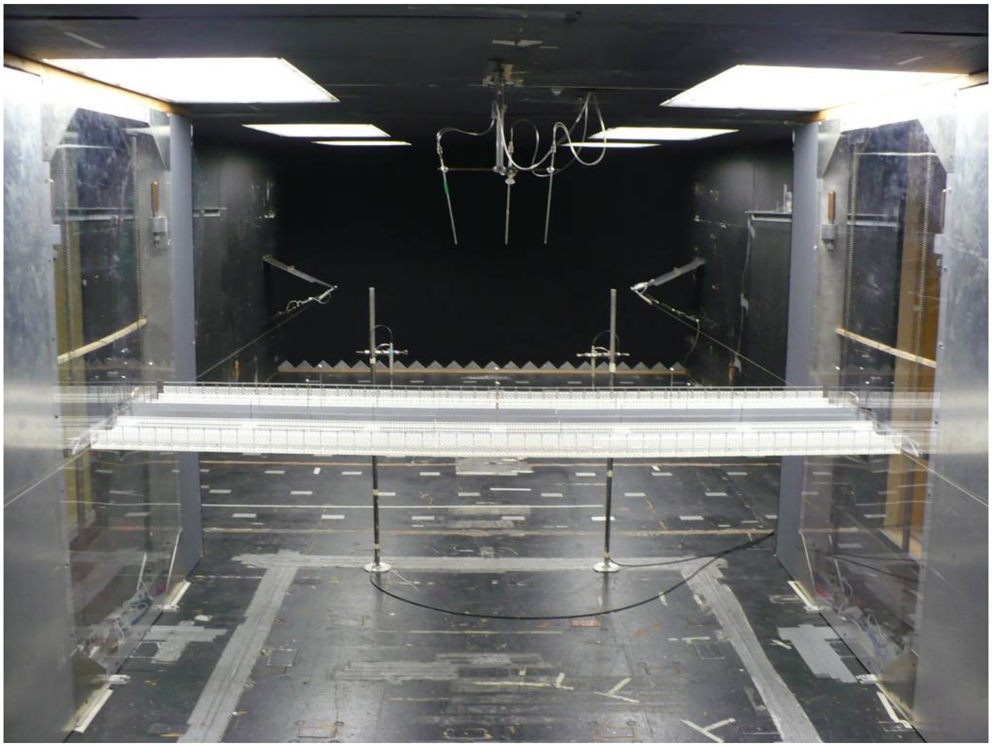

a) Smooth Flow

b) Turbulent Flow

FIGURE 2.5 SECTION MODEL TEST

FIGURE 2.6 STATIC SECTION MODEL TEST RIG

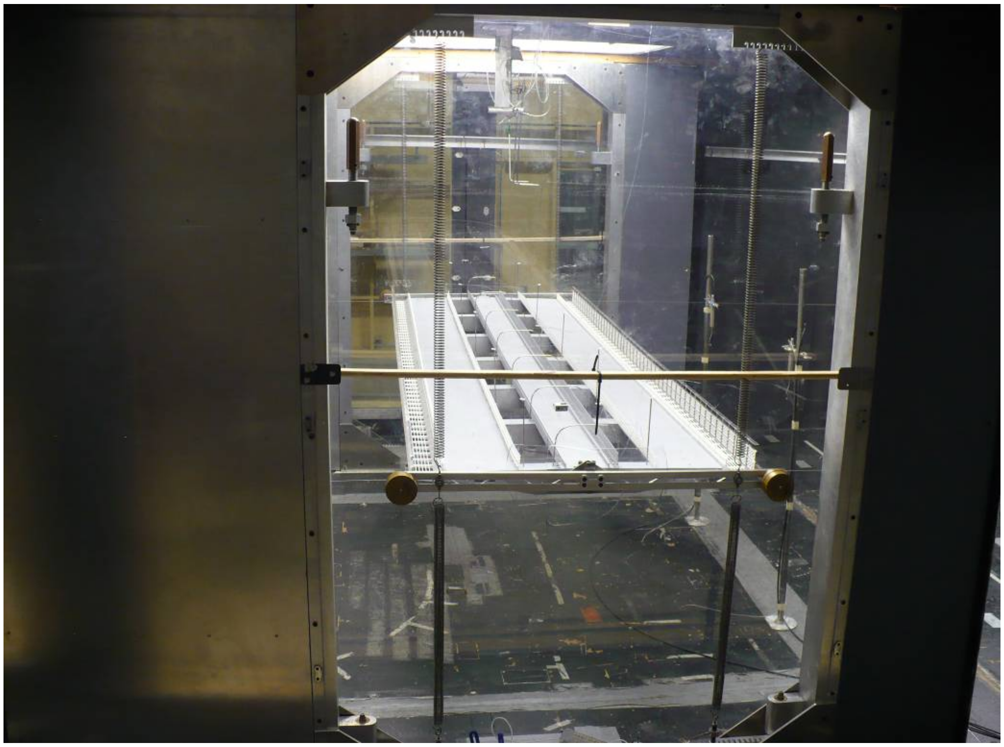

FIGURE 2.7 DYNAMIC SECTION MODEL TEST RIG

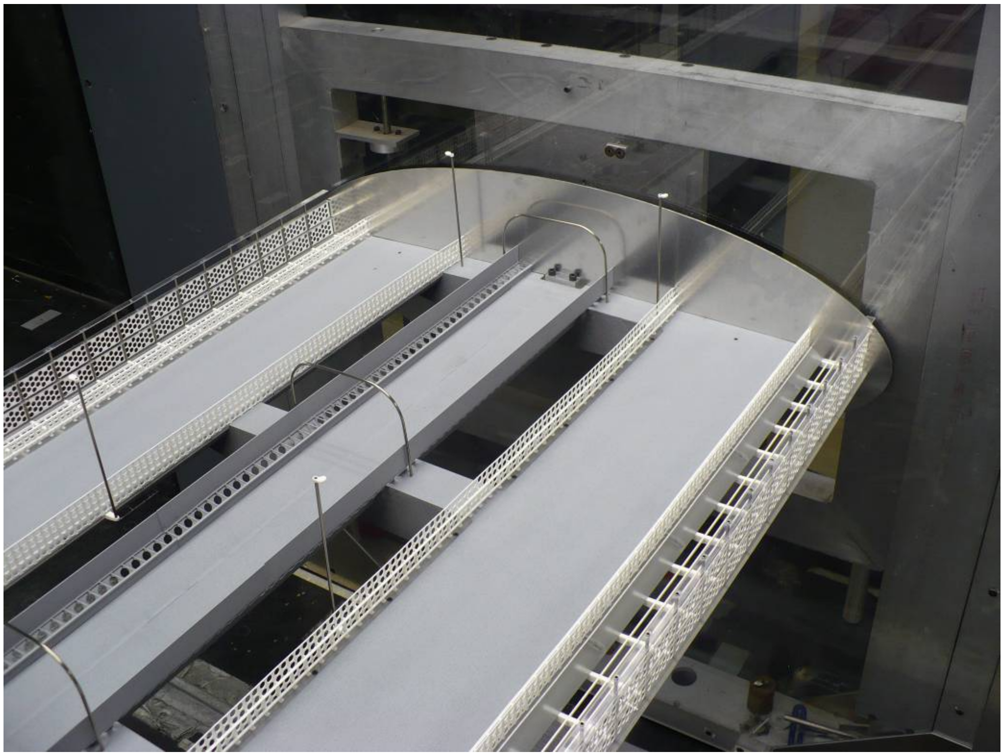

a) In-Service Deck Configuration

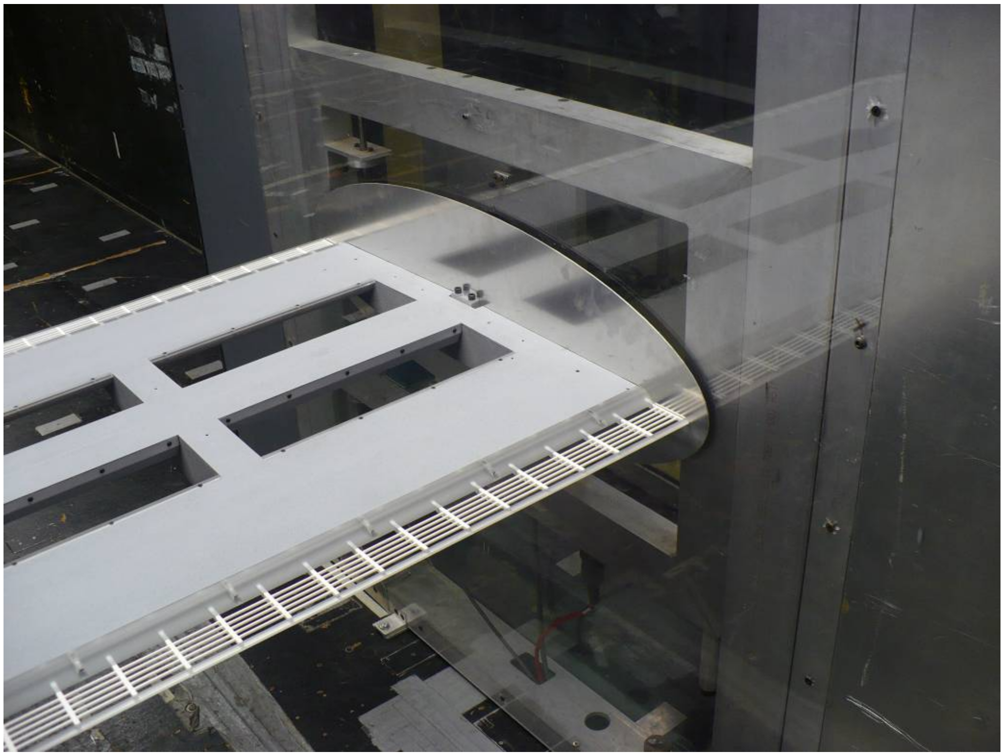

b) Under Construction Deck Configuration

FIGURE 3.1 STATIC SECTION MODEL TEST CONFIGURATION

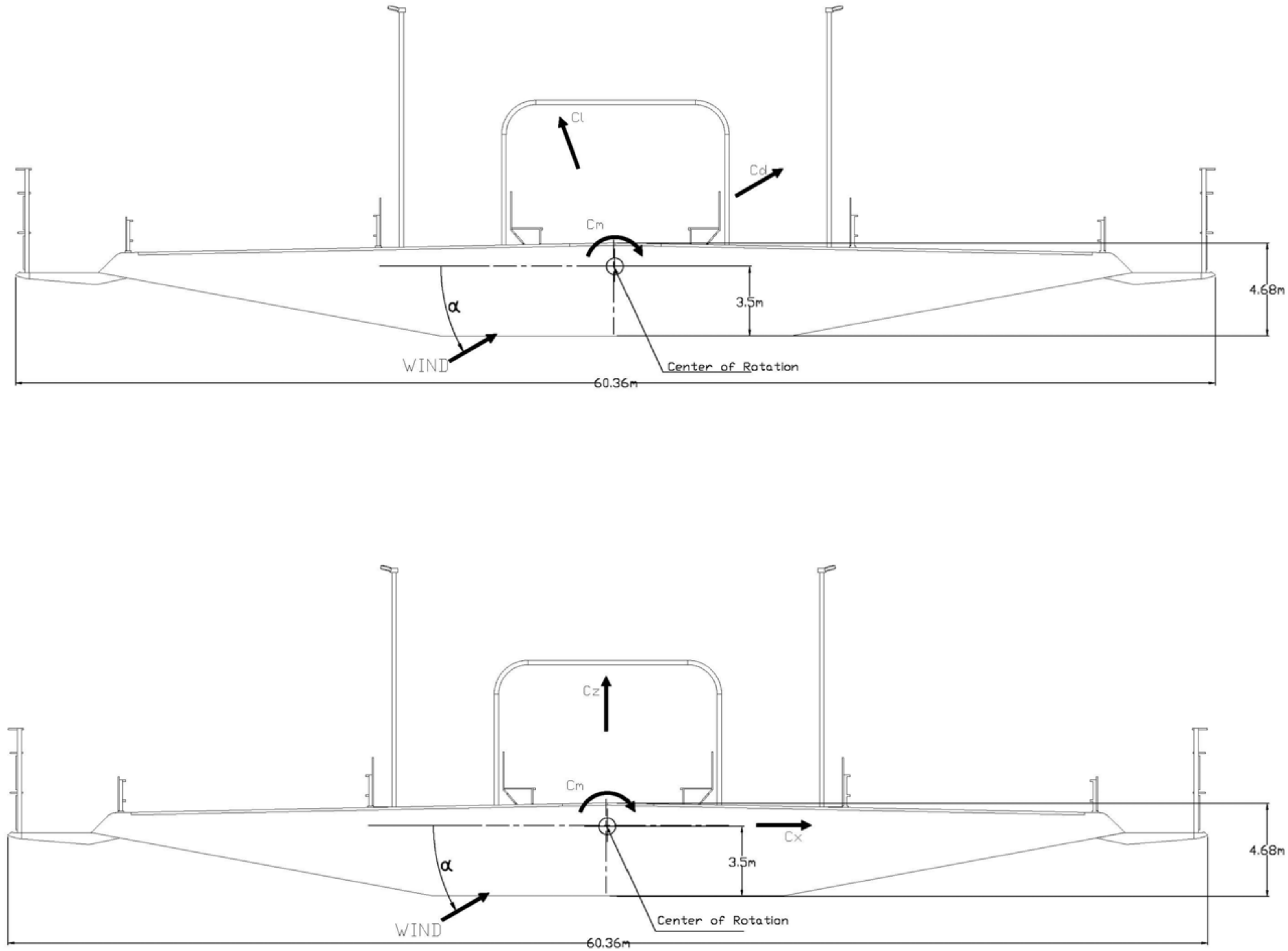

FIGURE 3.2 SIGN CONVENTION FOR STATIC TEST OF THE IN-SERVICE DECK SECTION

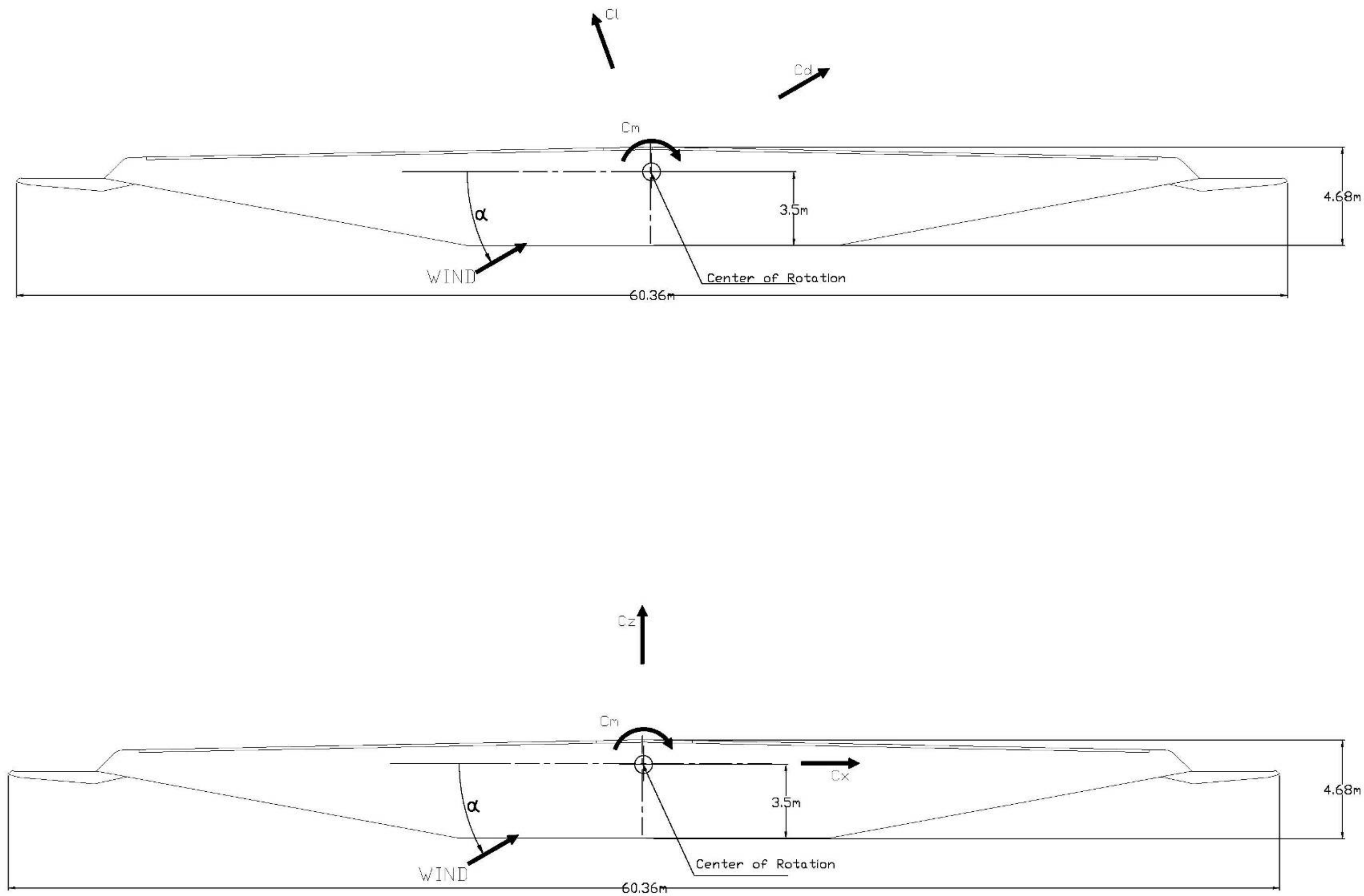

FIGURE 3.3 SIGN CONVENTION FOR STATIC TEST OF THE UNDER CONSTRUCTION STAGE DECK SECTION

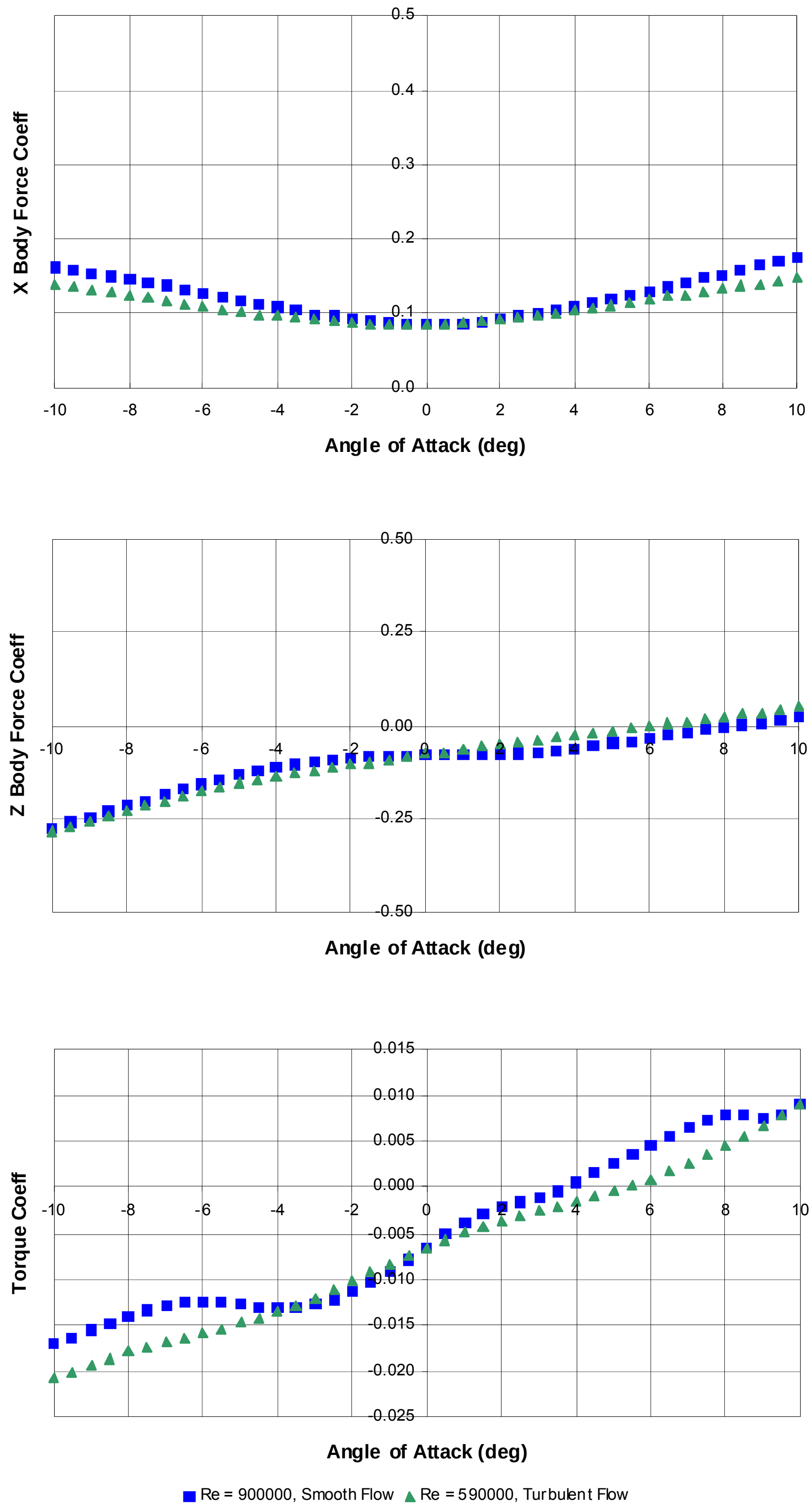

FIGURE 3.4 STATIC FORCE COEFFICIENTS (BODY FORCES), IN-SERVICE

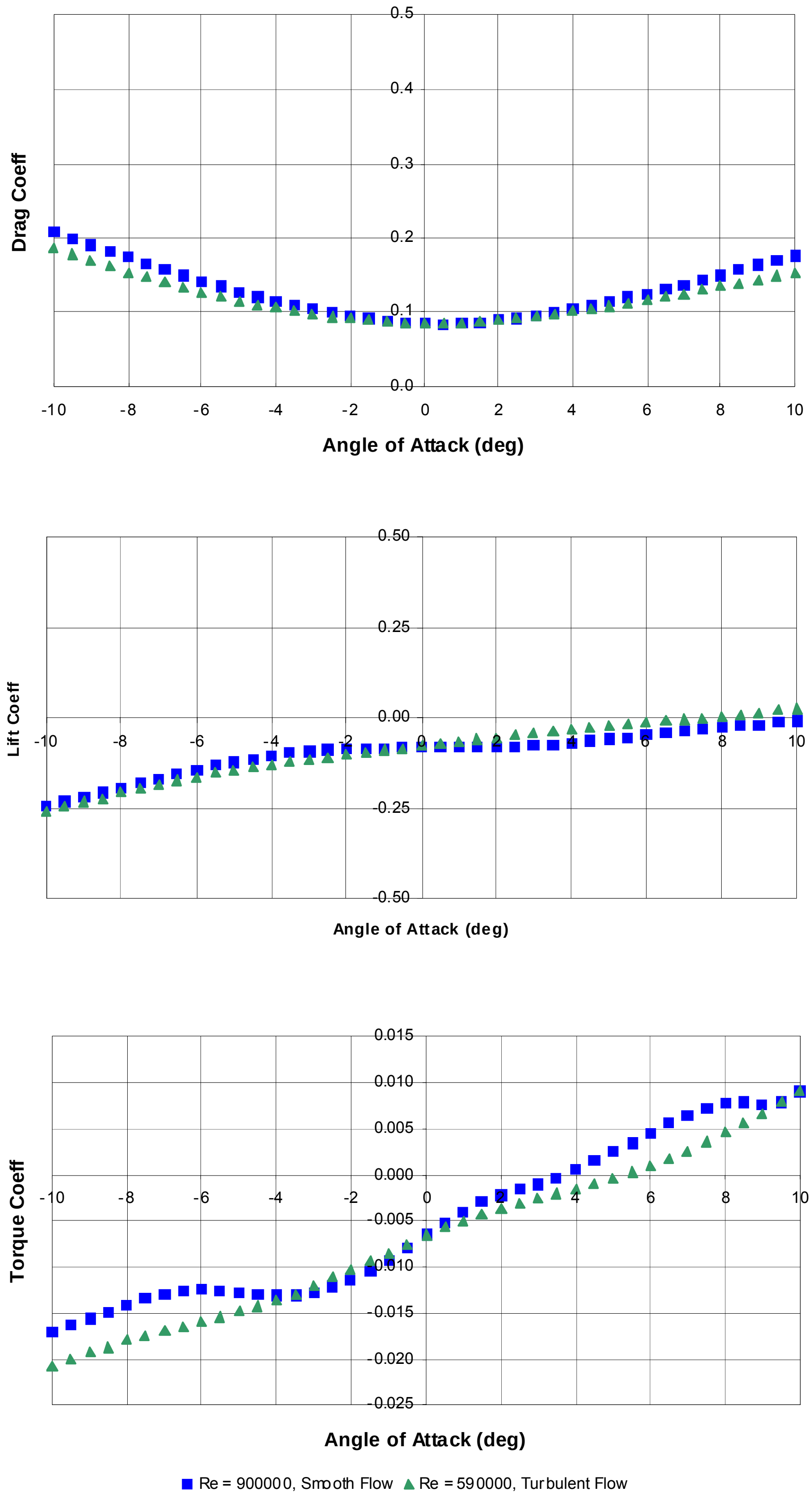

FIGURE 3.5 STATIC FORCE COEFFICIENTS (WIND AXIS FORCES), IN-SERVICE

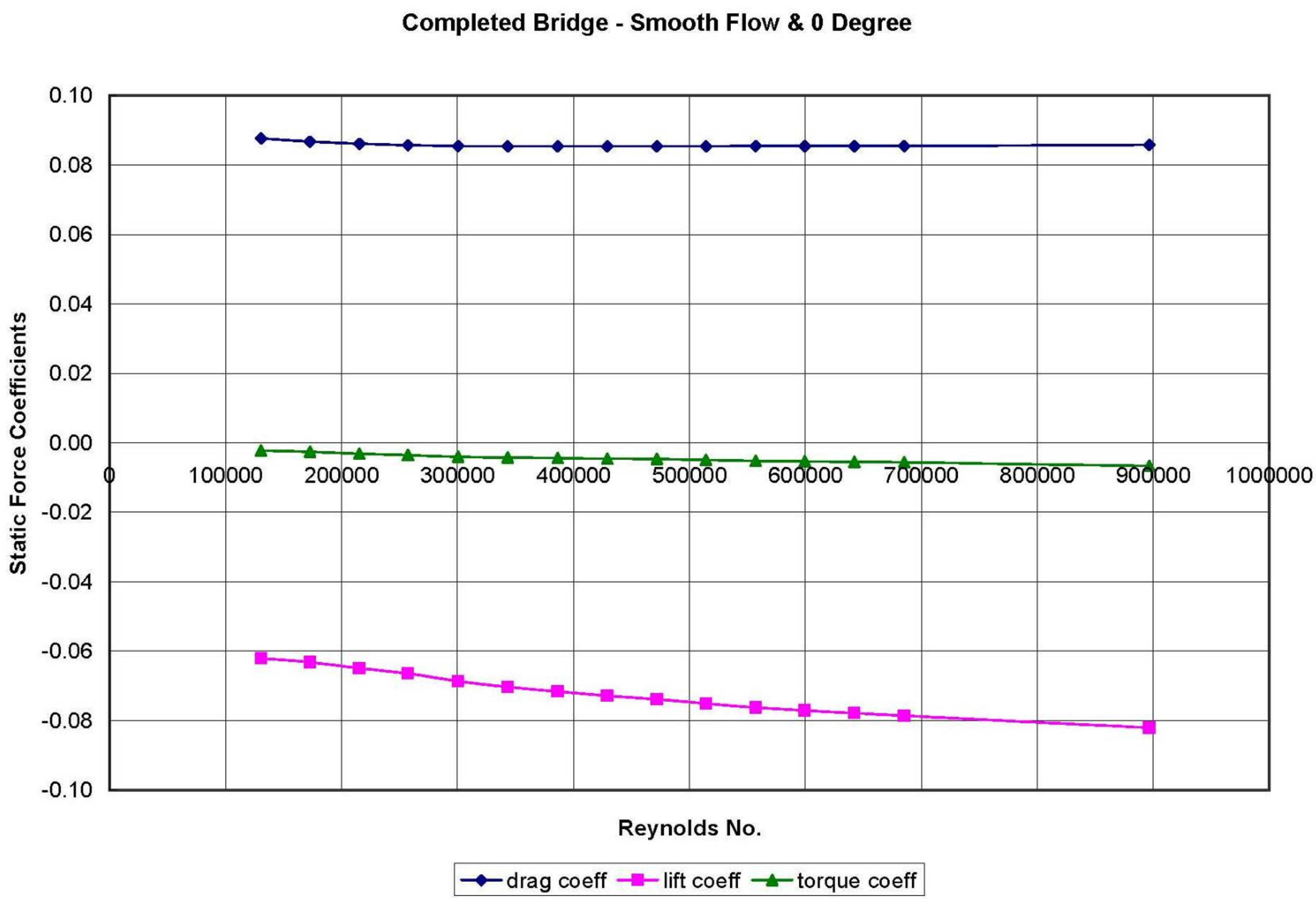

FIGURE 3.6 STATIC FORCE COEFFICIENTS VS REYNOLDS NUMBER, SMOOTH FLOW, 0 DEGREES, IN-SERVICE

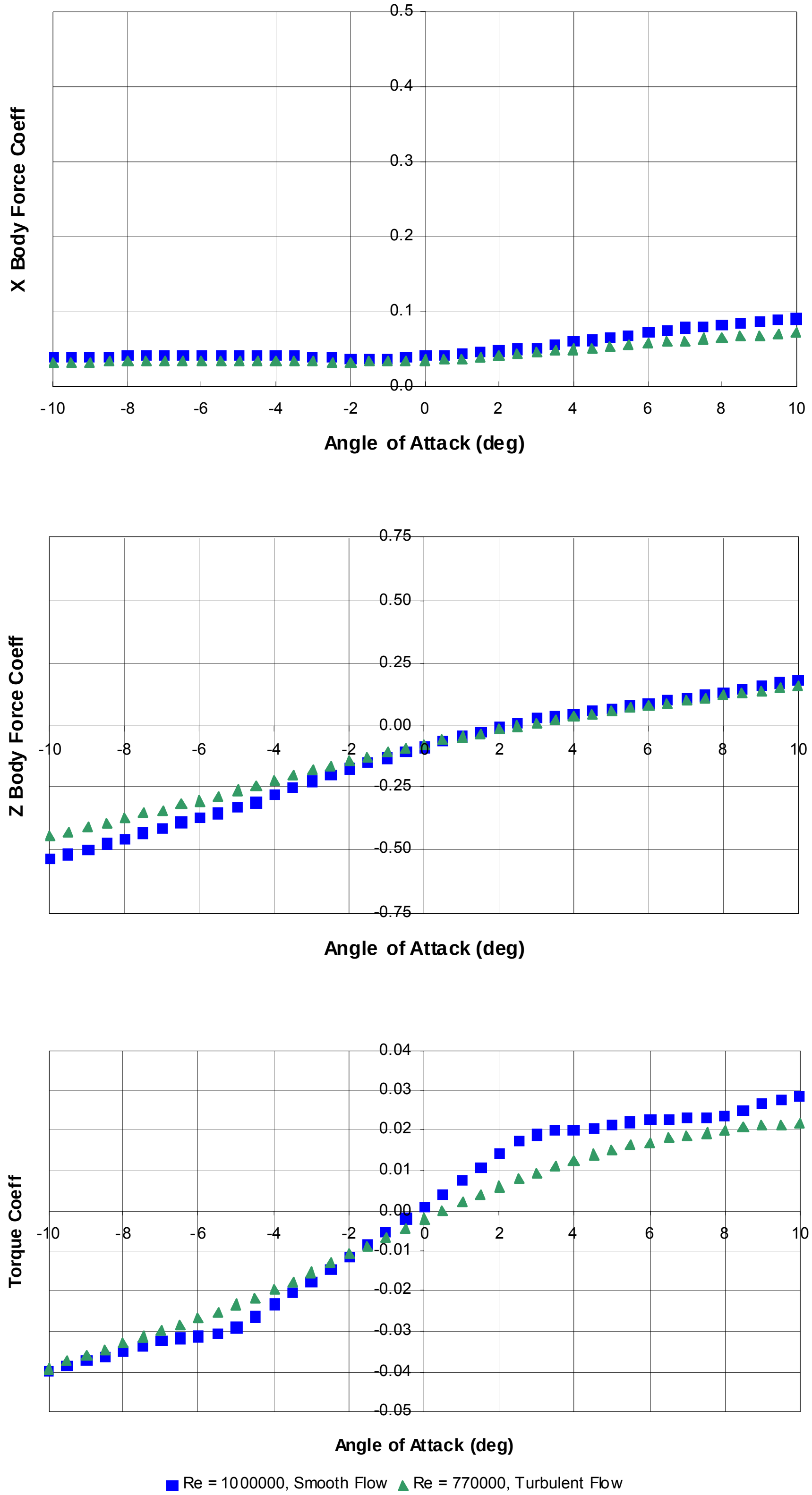

FIGURE 3.7 STATIC FORCE COEFFICIENTS (BODY FORCES), UNDER CONSTRUCTION STAGE

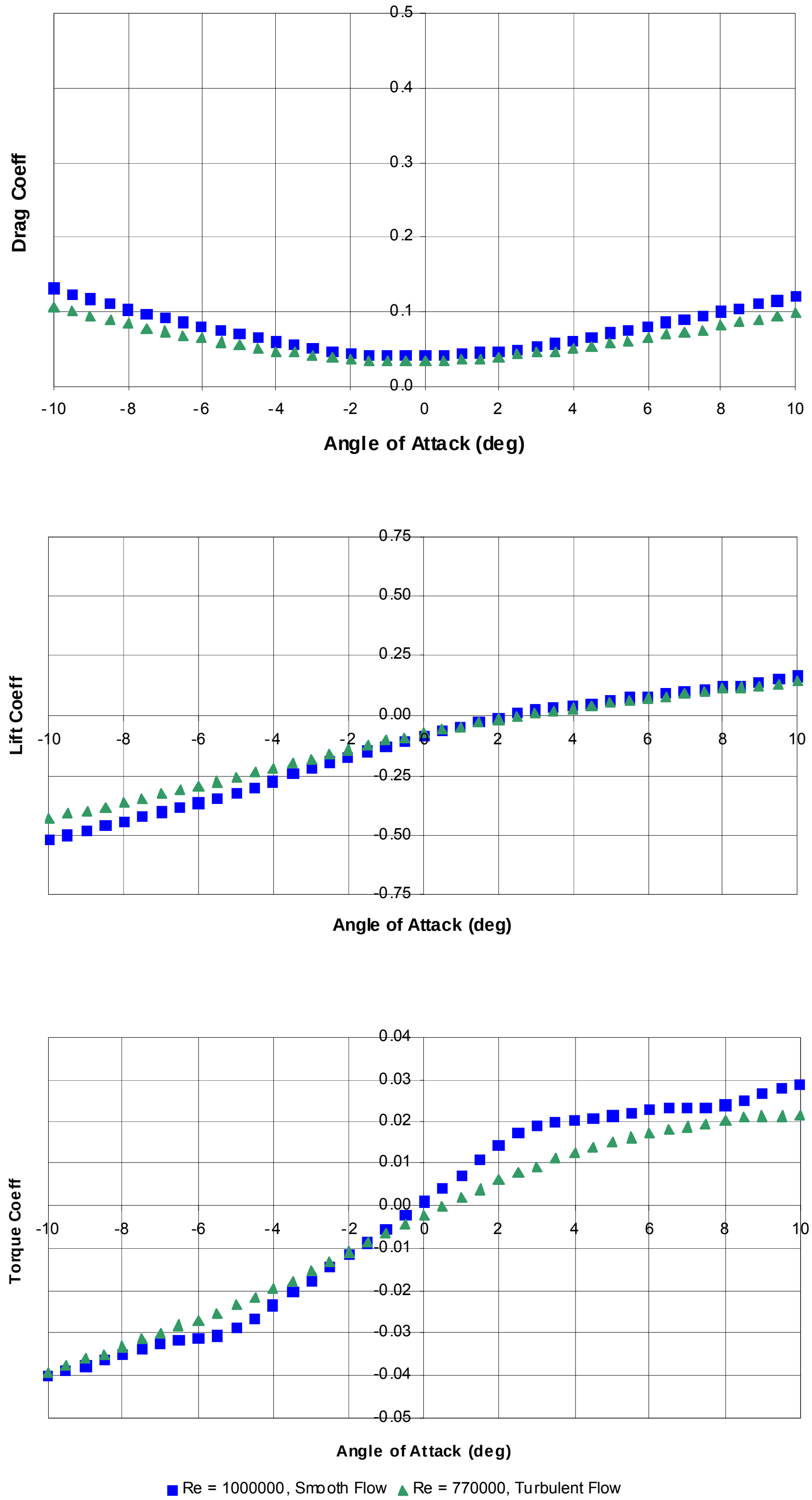

FIGURE 3.8 STATIC FORCE COEFFICIENTS (WIND AXIS FORCES), UNDER CONSTRUCTION STAGE

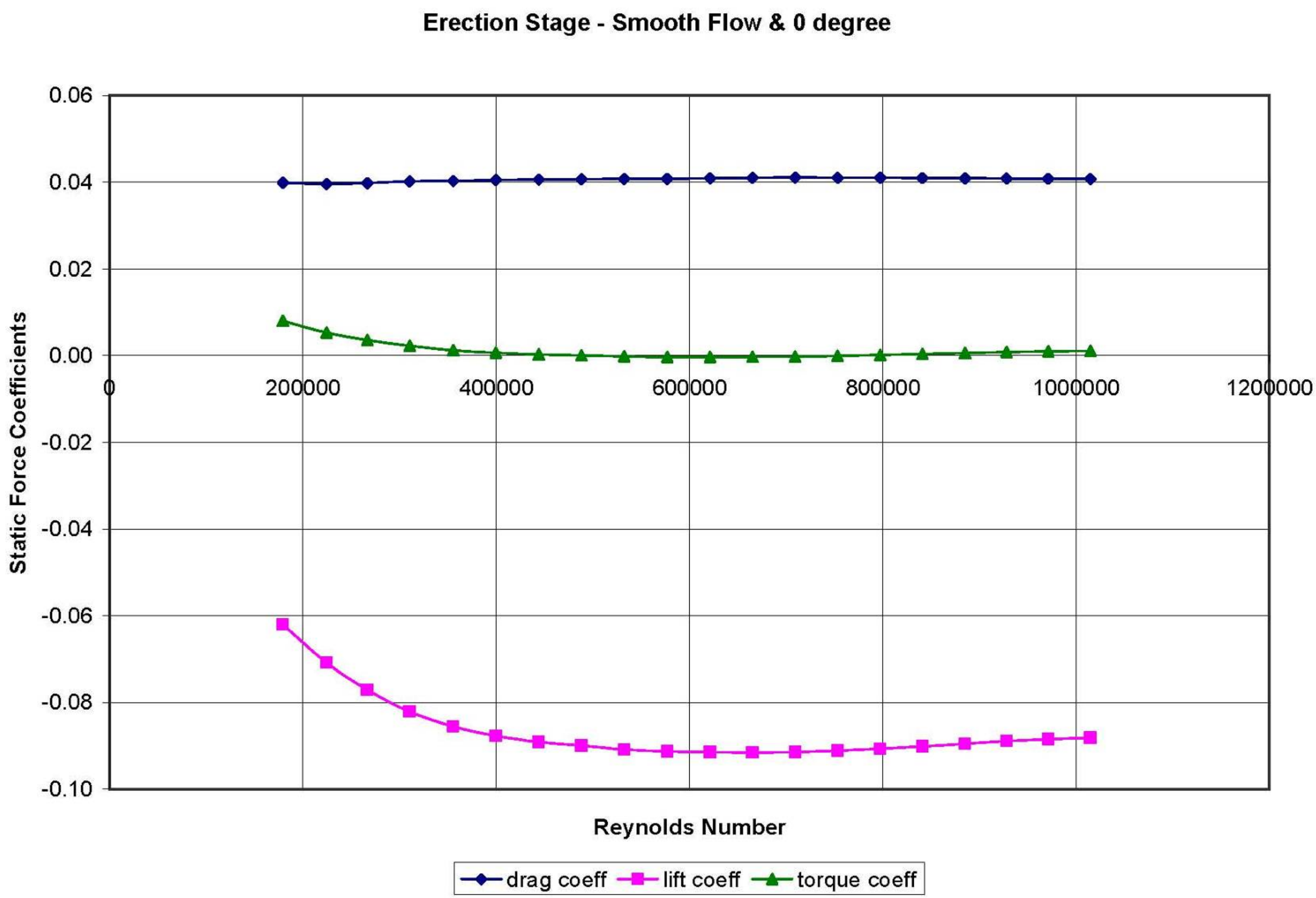

FIGURE 3.9 STATIC FORCE COEFFICIENTS VS REYNOLDS NUMBER, SMOOTH FLOW, 0 DEGREES, UNDER CONSTRUCTION CONDITION

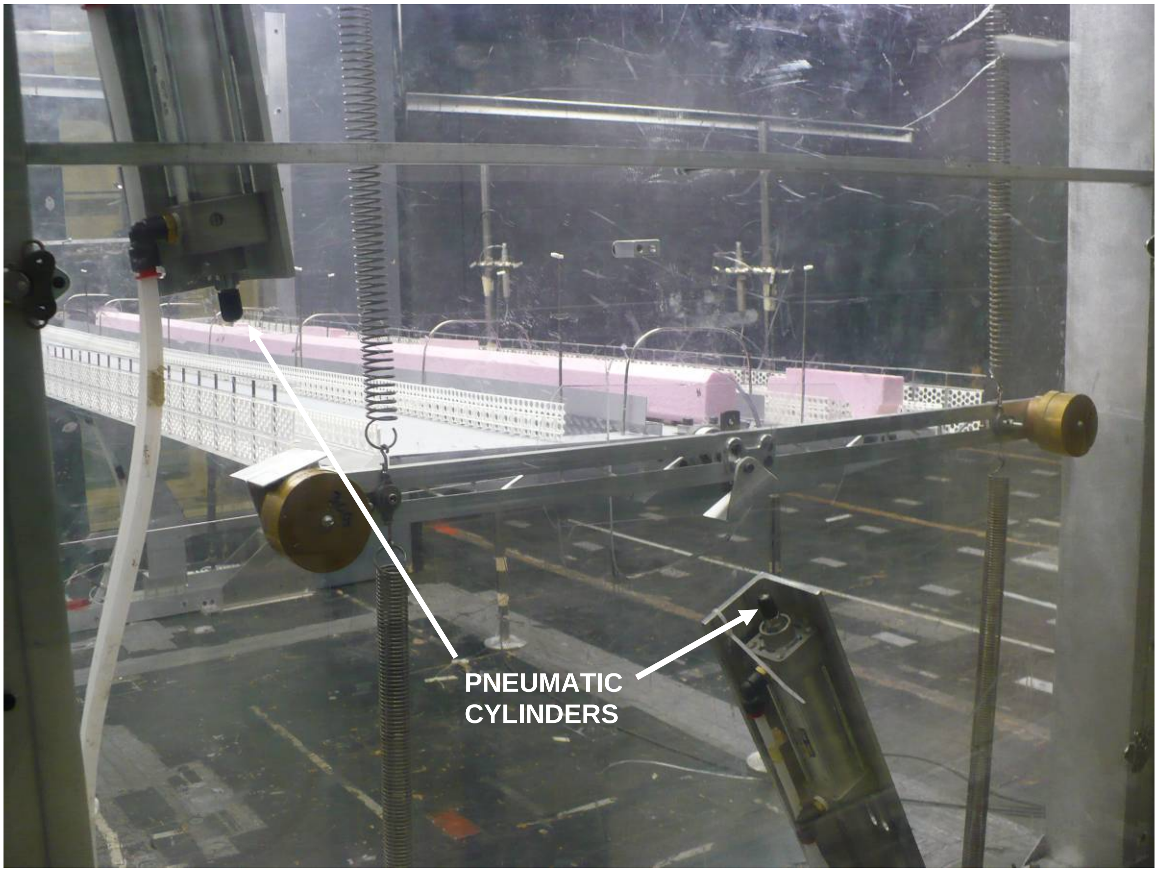

FIGURE 3.10 PNEUMATIC DISPLACE AND RELEASE SYSTEM FOR EXPERIMENTAL MEASUREMENTS OF AERODYNAMIC DERIVATIVES

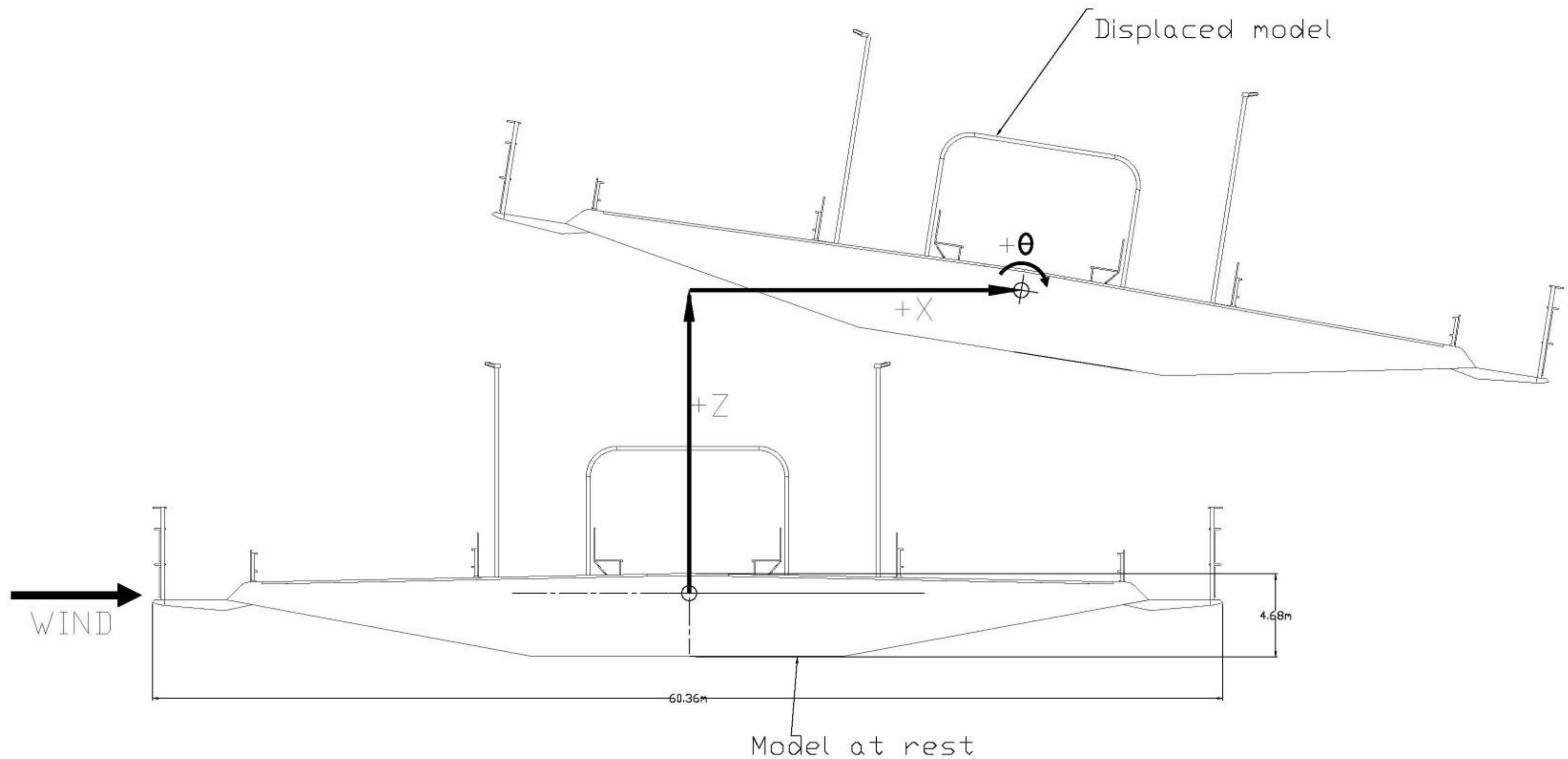

FIGURE 3.11 SIGN CONVENTION FOR AERODYNAMIC DERIVATIVE TEST OF THE IN-SERVICE CONDITION

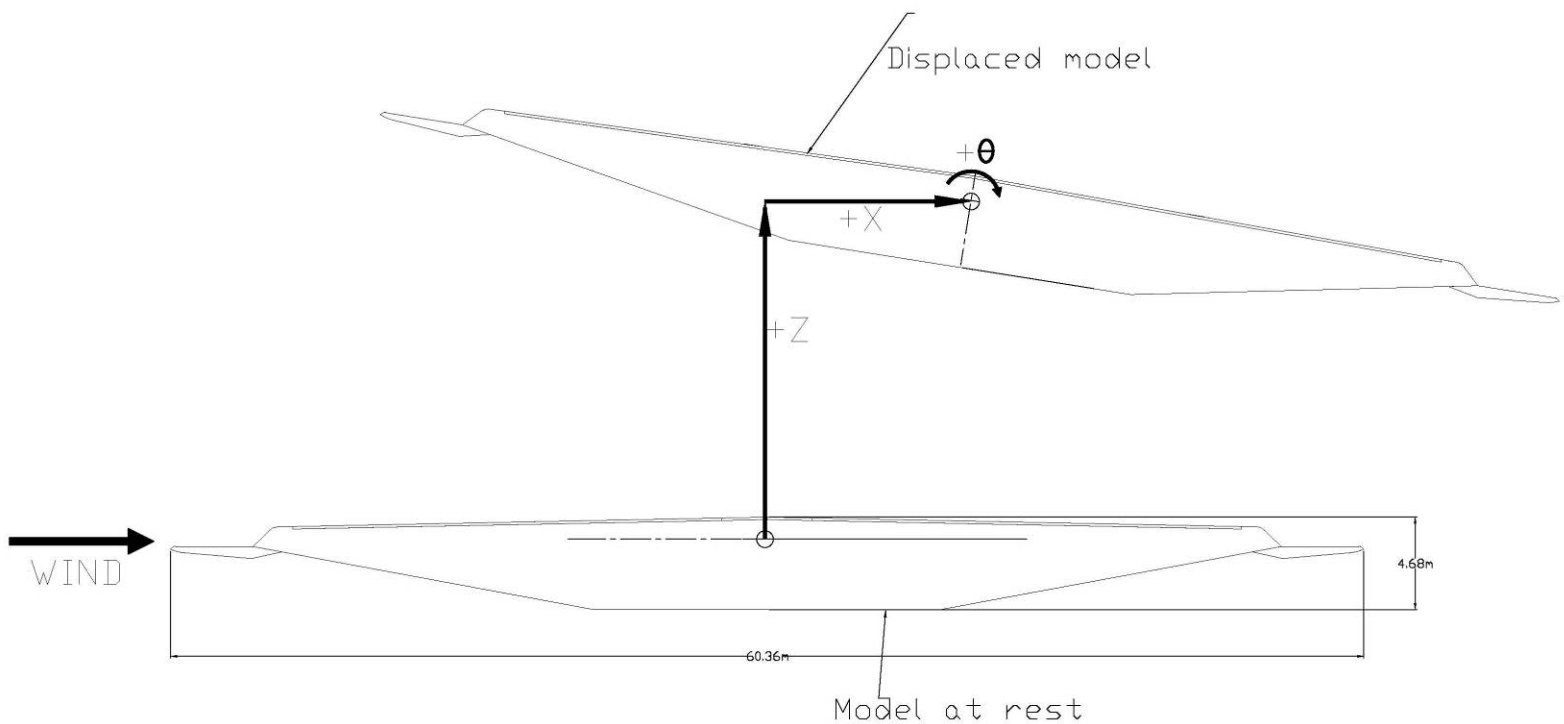

FIGURE 3.12 SIGN CONVENTION FOR AERODYNAMIC DERIVATIVE TEST OF THE UNDER CONSTRUCTION CONDITION

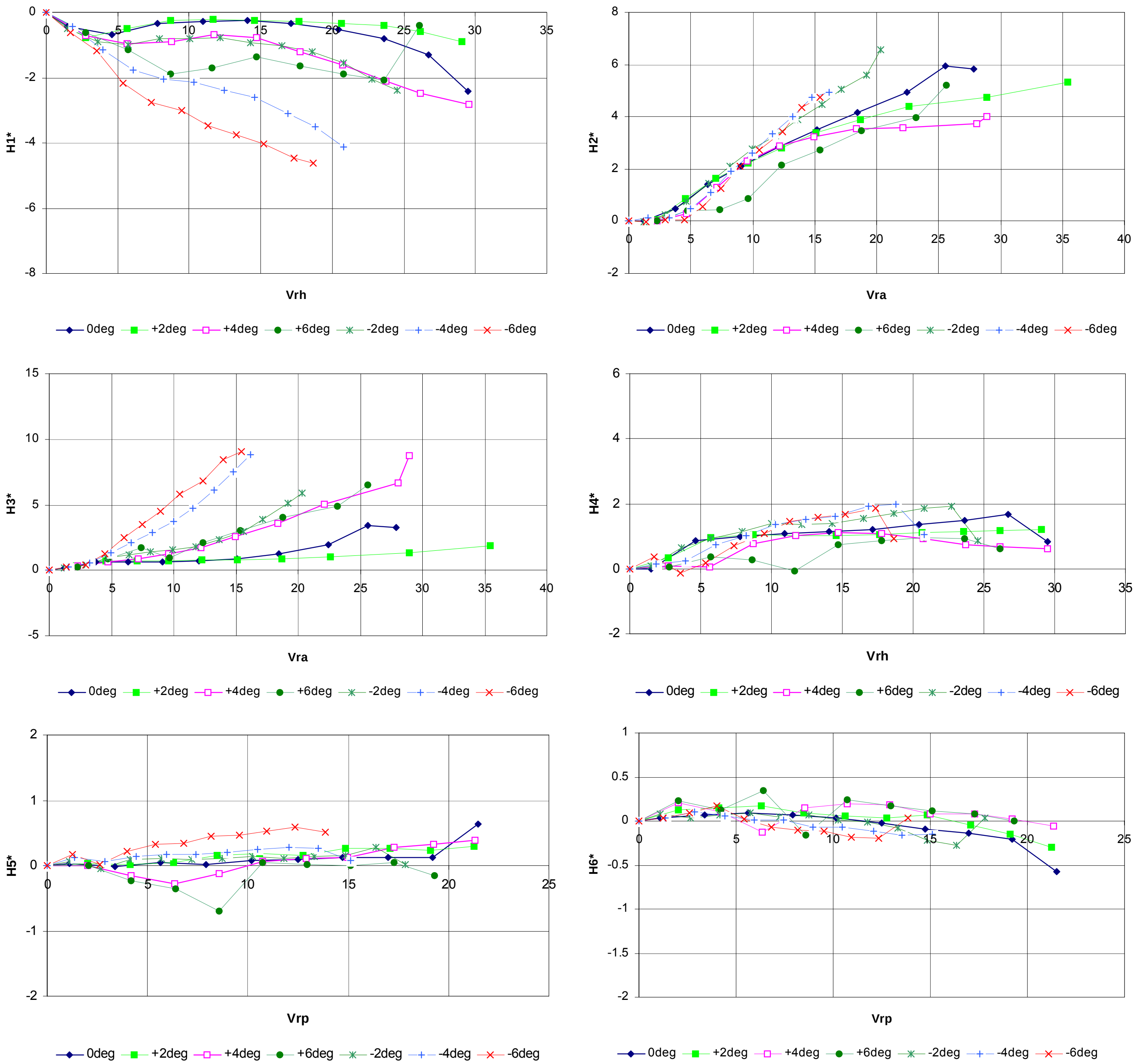

FIGURE 3.13 AERODYNAMIC DERIVATIVES IN SMOOTH FLOW, 3-D TEST OF IN-SERVICE CONDITION (BLWTL NOTATION)

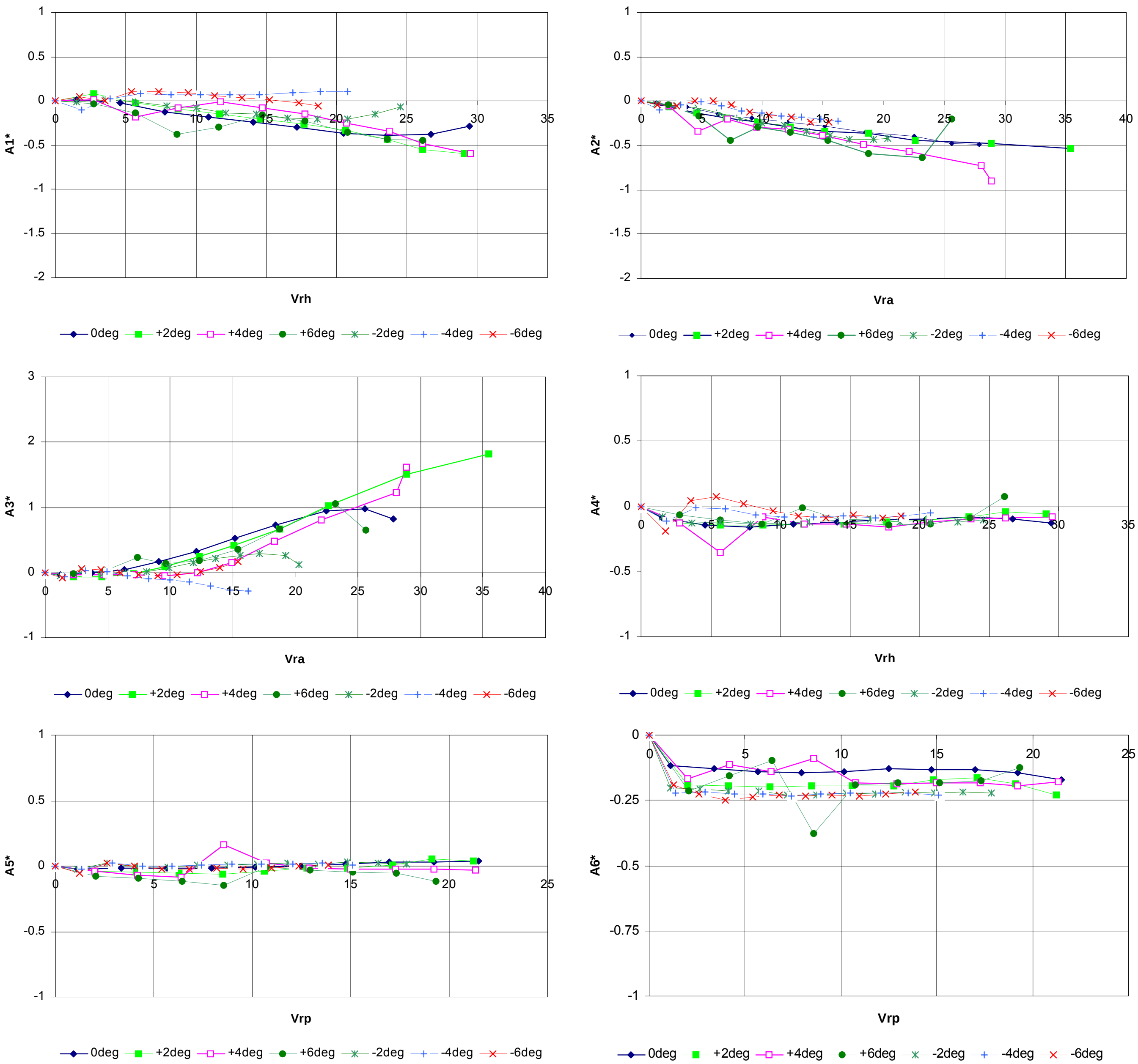

FIGURE 3.13 (CONT.) AERODYNAMIC DERIVATIVES IN SMOOTH FLOW, 3-D TEST OF IN-SERVICE CONDITION (BLWTL NOTATION)

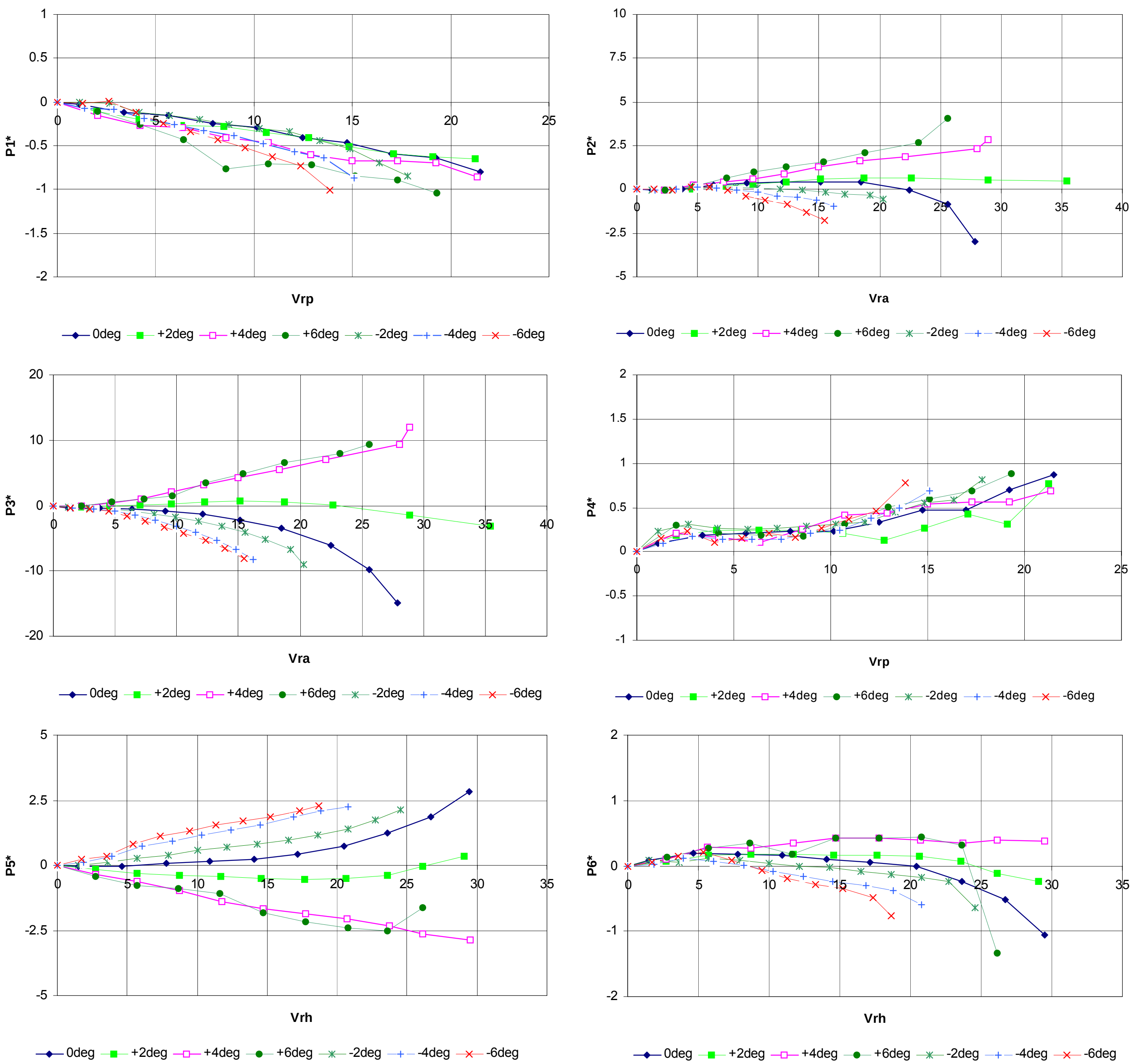

FIGURE 3.13 (CONT.) AERODYNAMIC DERIVATIVES IN SMOOTH FLOW, 3-D TEST OF IN-SERVICE CONDITION (BLWTL NOTATION)

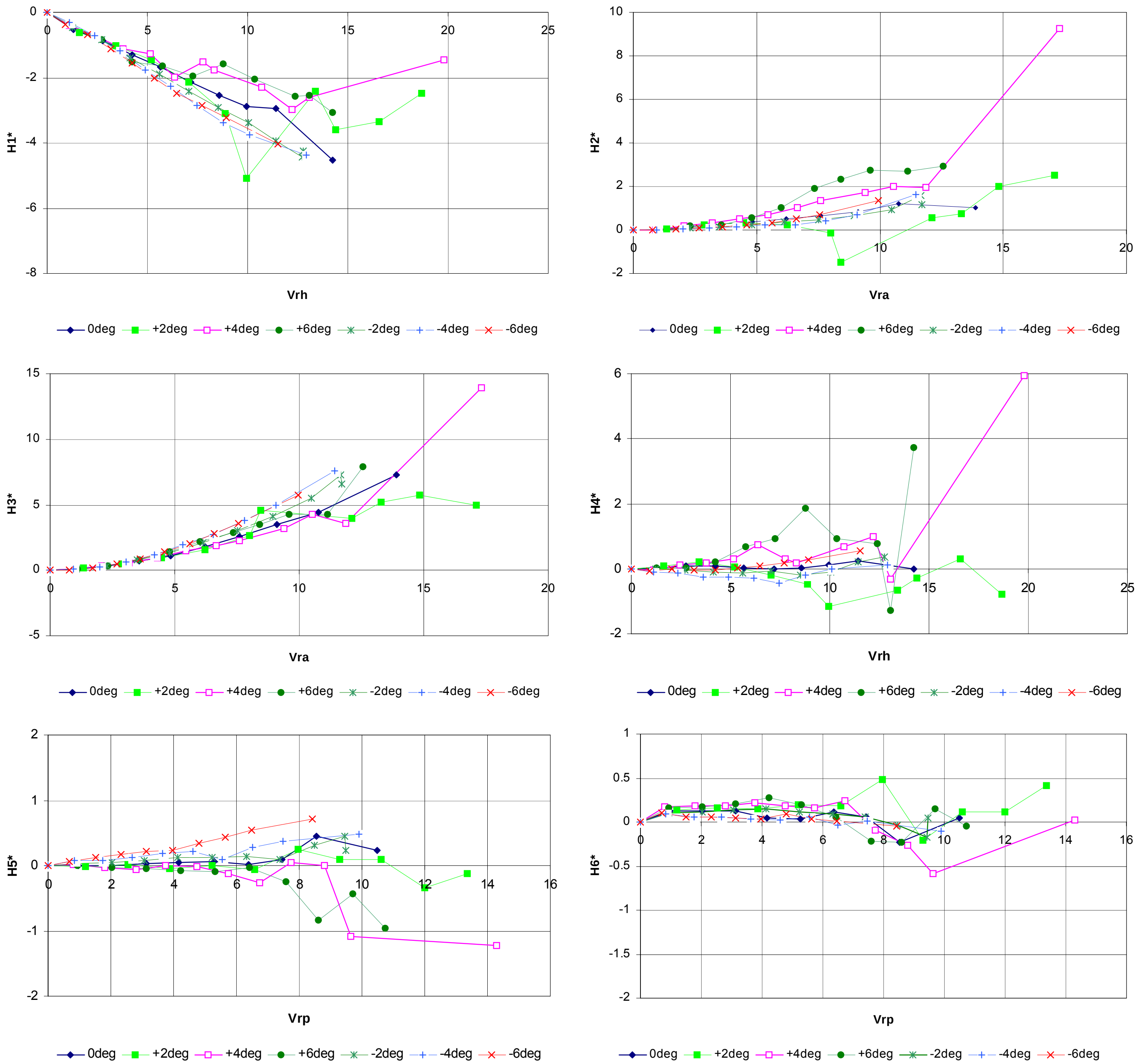

FIGURE 3.14 AERODYNAMIC DERIVATIVES IN SMOOTH FLOW, 3-D TEST OF UNDER CONSTRUCTION CONDITION (BLWTL NOTATION)

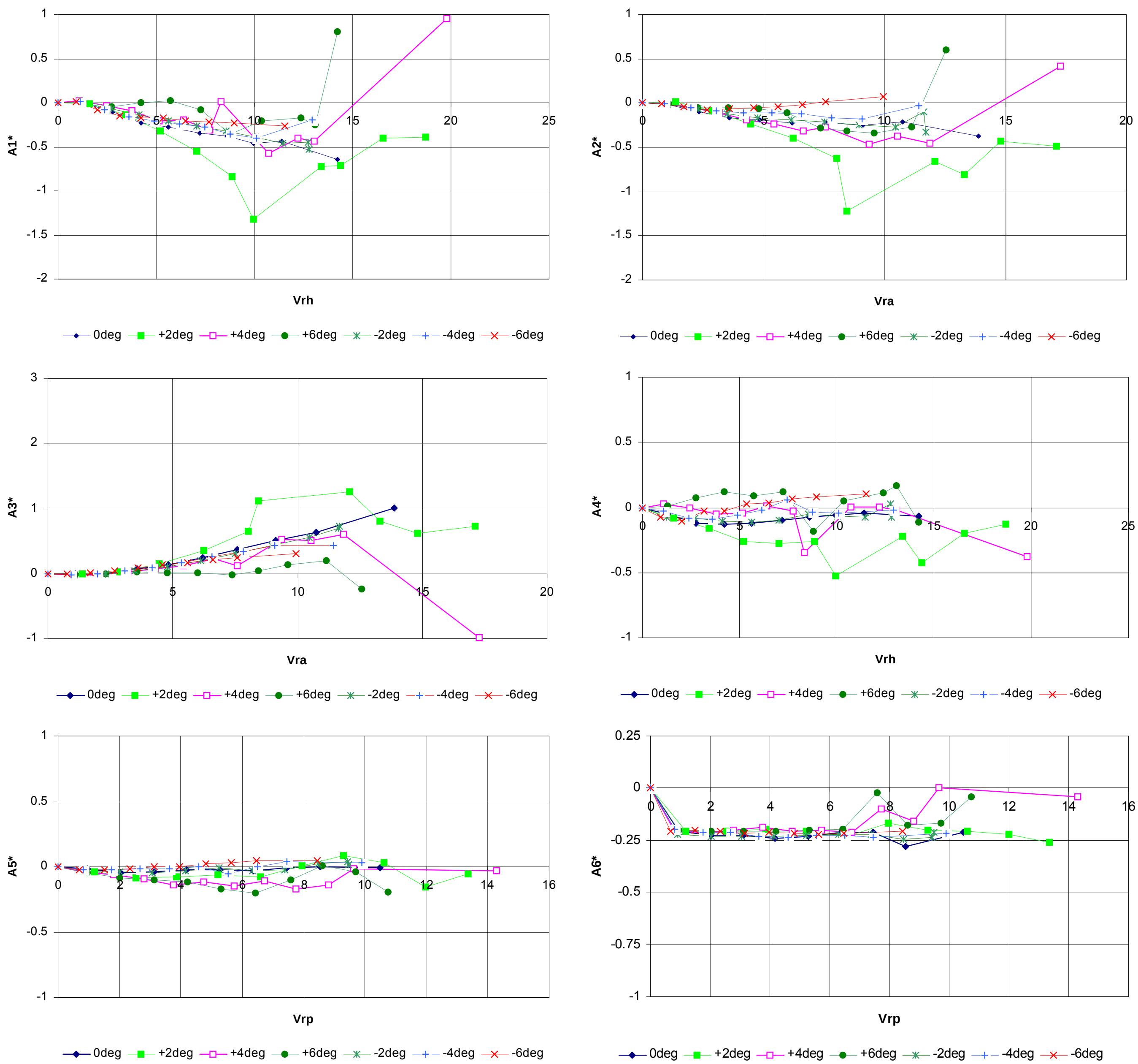

FIGURE 3.14 (CONT.) AERODYNAMIC DERIVATIVES IN SMOOTH FLOW, 3-D TEST OF UNDER CONSTRUCTION CONDITION DECK (BLWTL NOTATION)

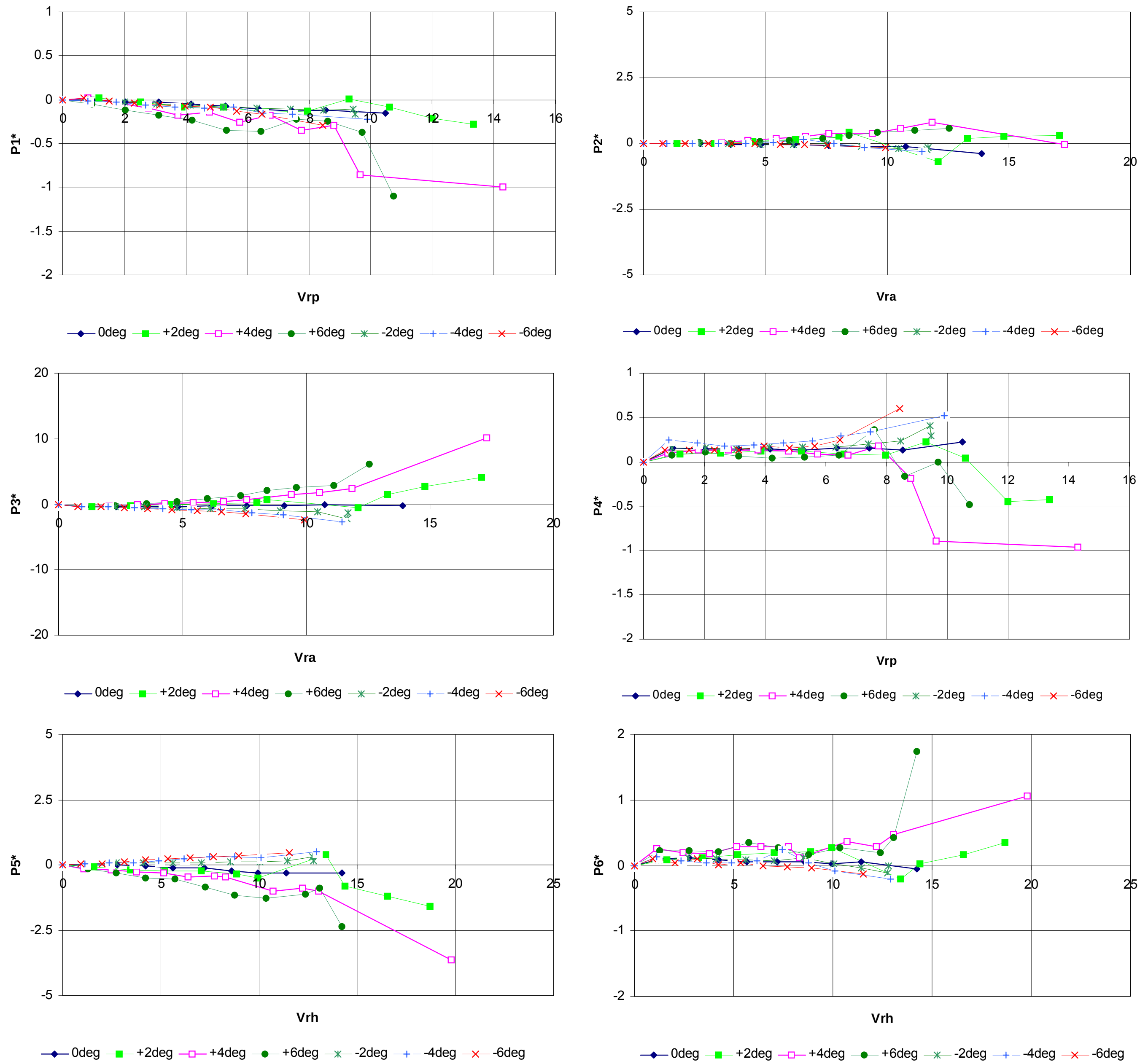

FIGURE 3.14 (CONT.) AERODYNAMIC DERIVATIVES IN SMOOTH FLOW, 3-D TEST OF UNDER CONSTRUCTION CONDITION DECK (BLWTL NOTATION)

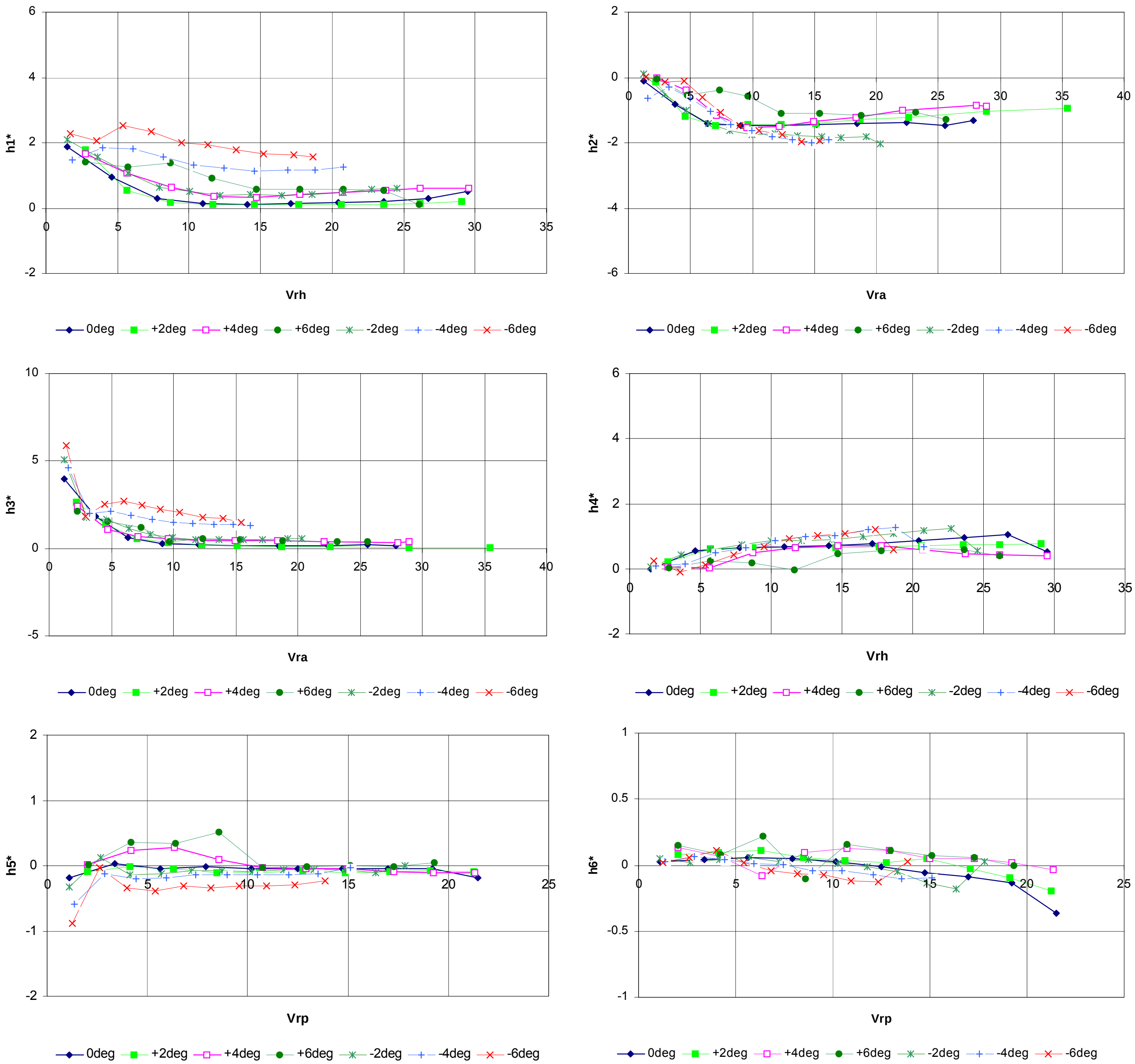

FIGURE 3.15 AERODYNAMIC DERIVATIVES IN SMOOTH FLOW, 3-D TEST OF IN-SERVICE CONDITION (SdM NOTATION)

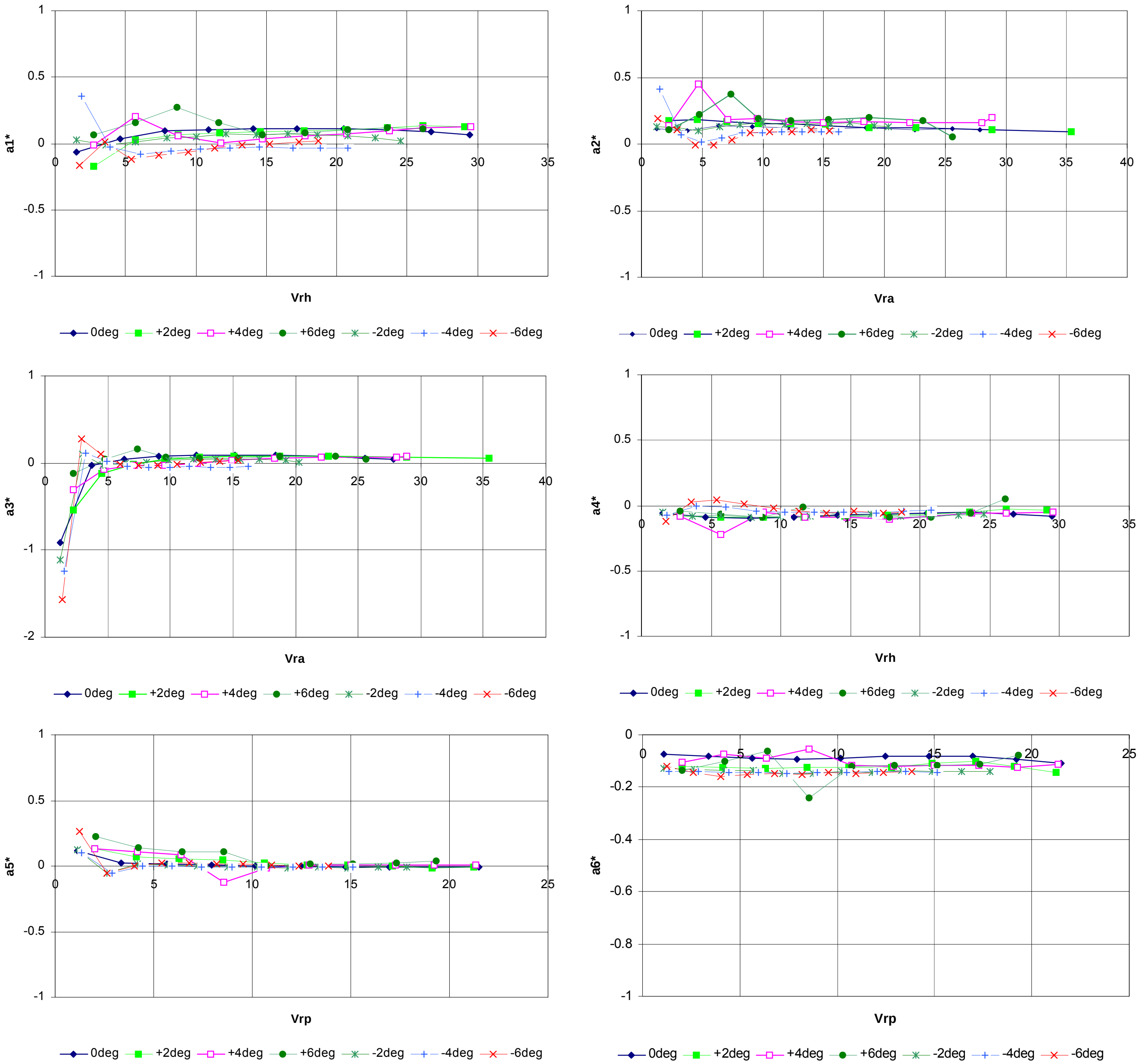

FIGURE 3.15 (CONT.) AERODYNAMIC DERIVATIVES IN SMOOTH FLOW, 3-D TEST OF IN-SERVICE CONDITION (SdM NOTATION)

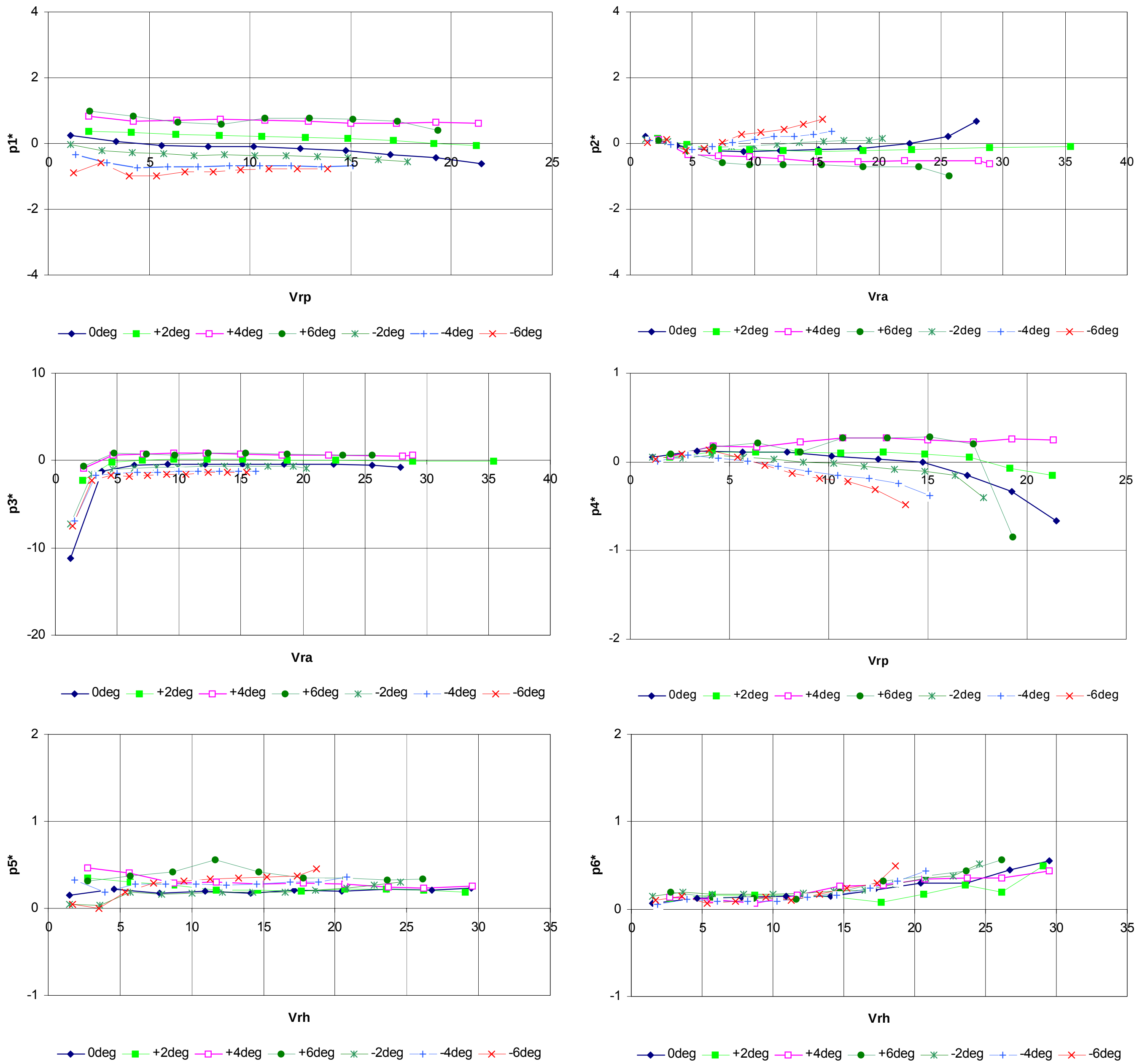

FIGURE 3.15 (CONT.) AERODYNAMIC DERIVATIVES IN SMOOTH FLOW, 3-D TEST OF IN-SERVICE CONDITION (SdM NOTATION)

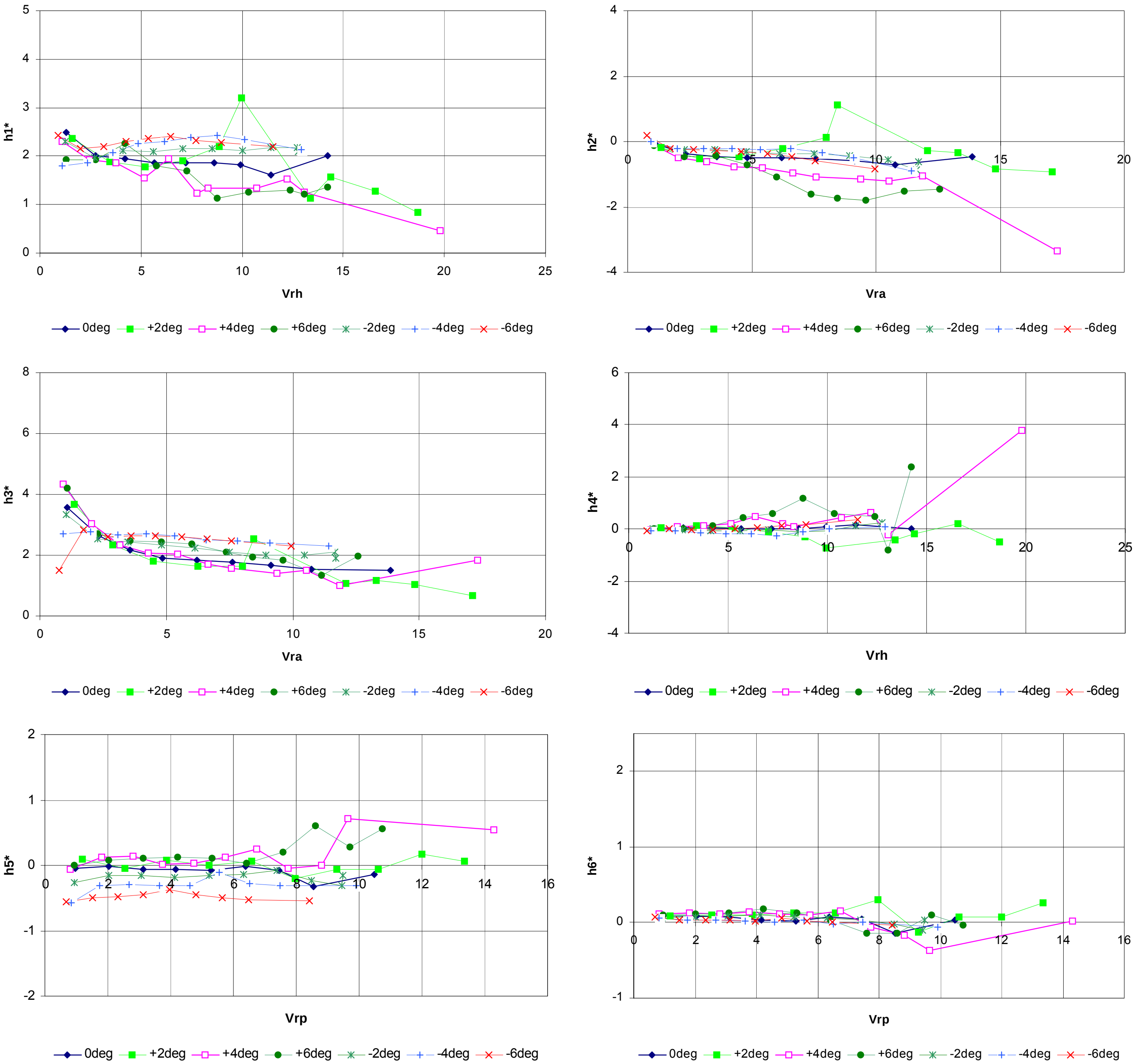

FIGURE 3.16 AERODYNAMIC DERIVATIVES IN SMOOTH FLOW, 3-D TEST OF UNDER CONSTRUCTION CONDITION (SdM NOTATION)

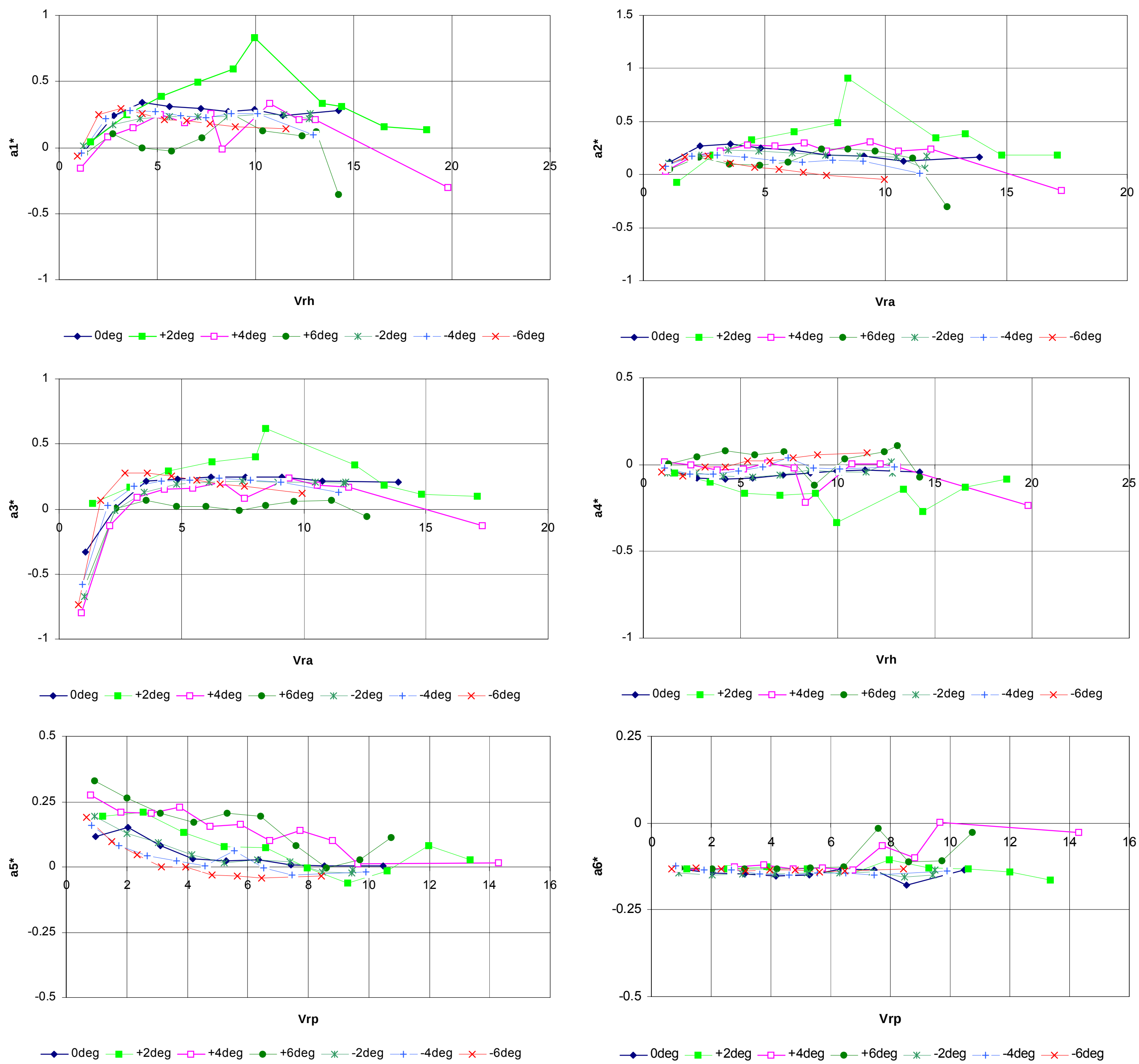

FIGURE 3.16 (CONT.) AERODYNAMIC DERIVATIVES IN SMOOTH FLOW, 3-D TEST OF UNDER CONSTRUCTION CONDITION (SdM NOTATION)

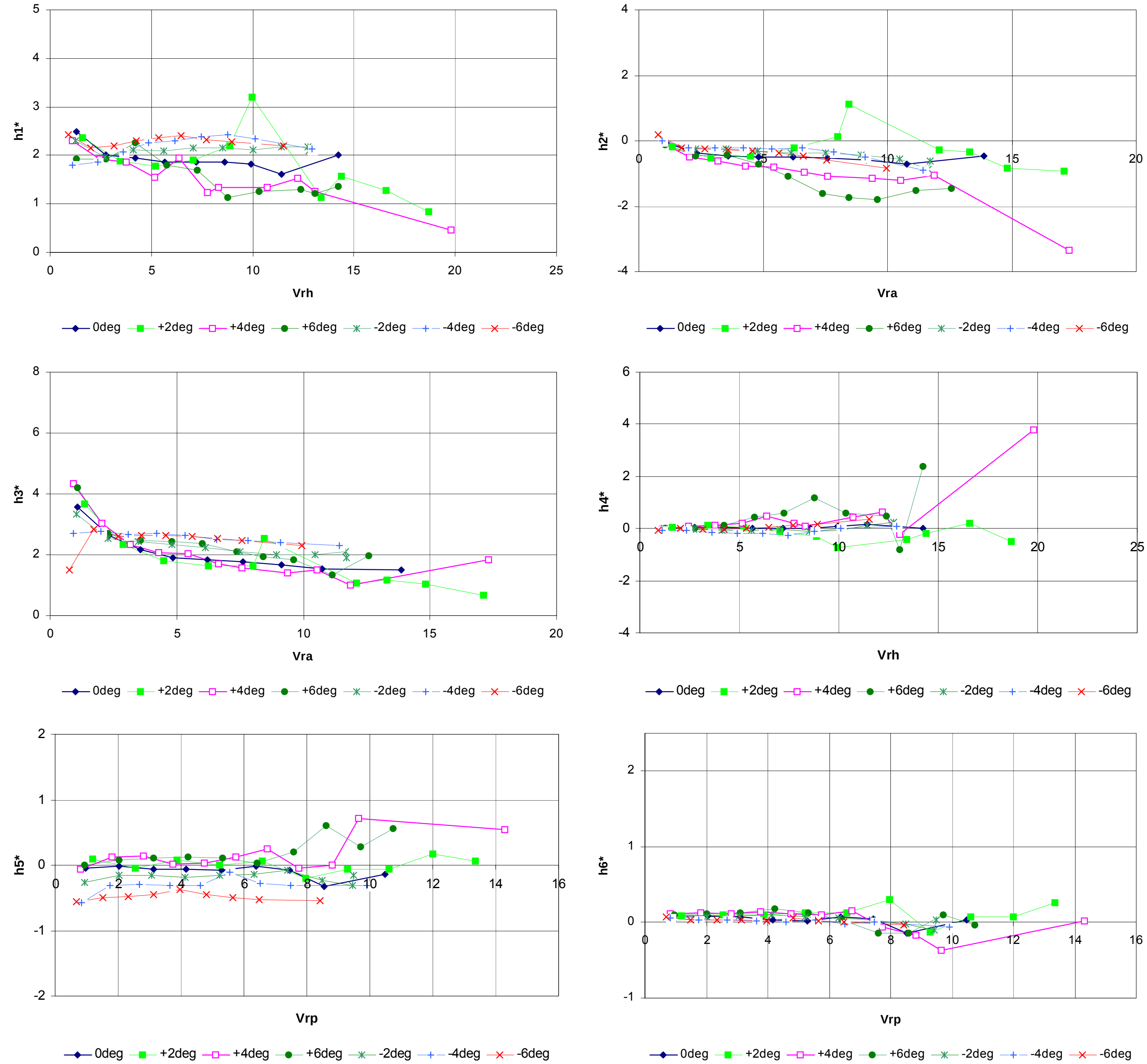

FIGURE 3.16 (CONT.) AERODYNAMIC DERIVATIVES IN SMOOTH FLOW, 3-D TEST OF UNDER CONSTRUCTION CONDITION (SdM NOTATION)

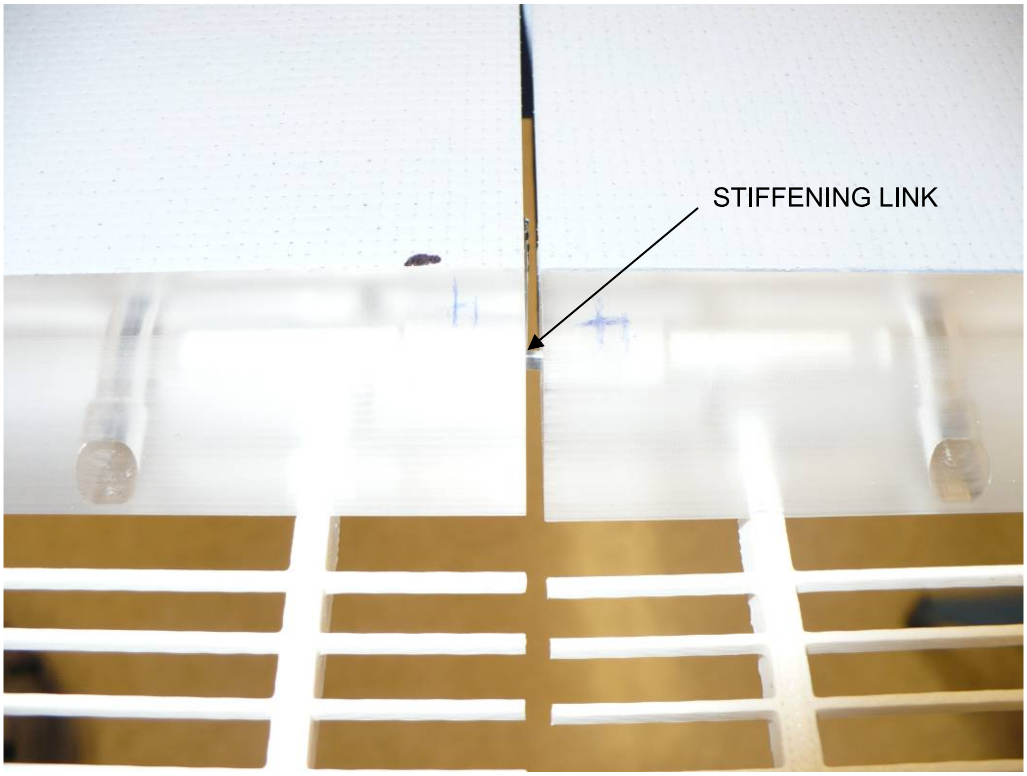

a) Stiffening Link between Instrumented Panel and Model

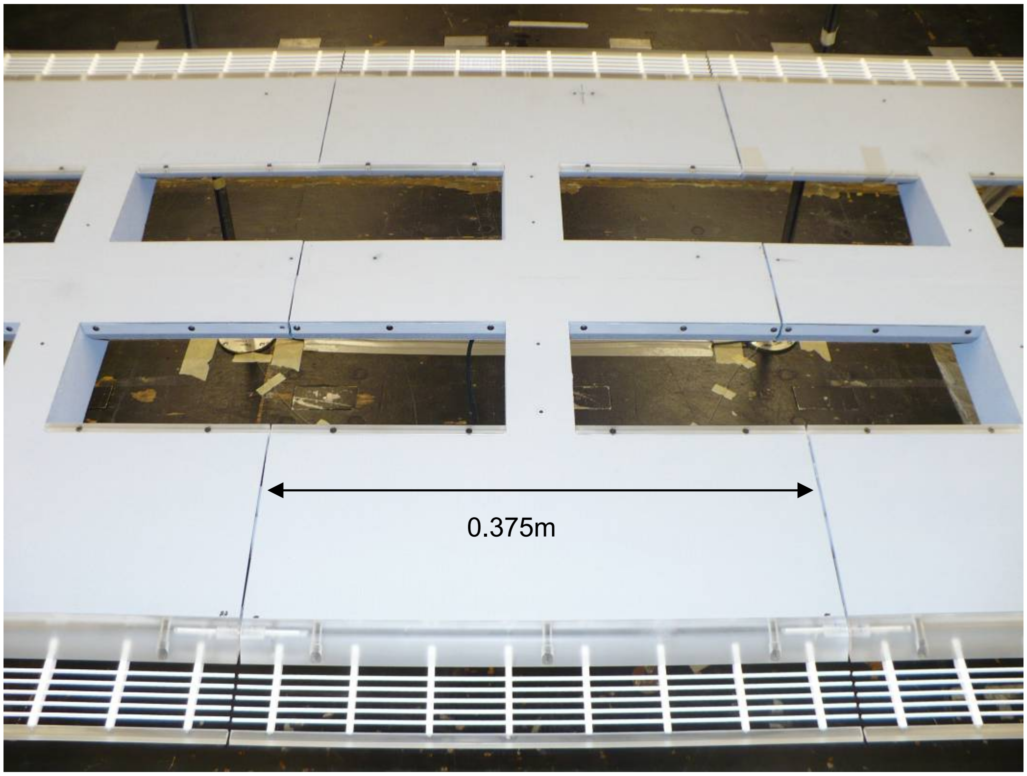

b) Instrumented Panel

FIGURE 3.17 INSTRUMENTED PANEL FOR AERODYNAMIC ADMITTANCE TESTS

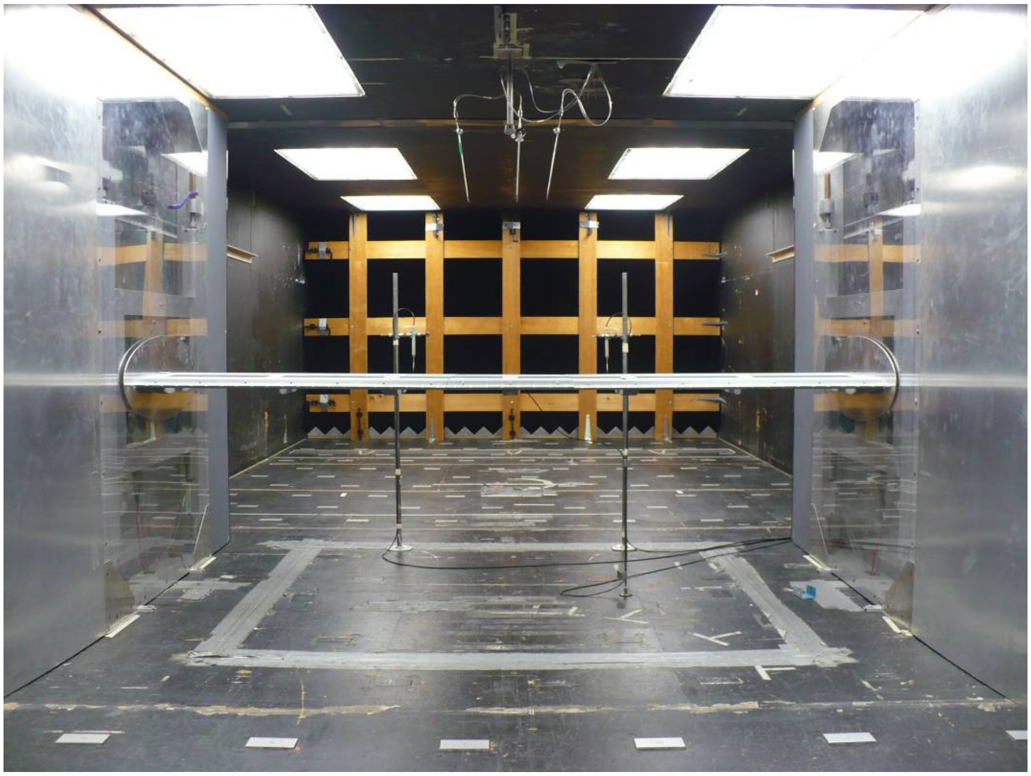

a) Aerodynamic Admittance Tests – View upwind

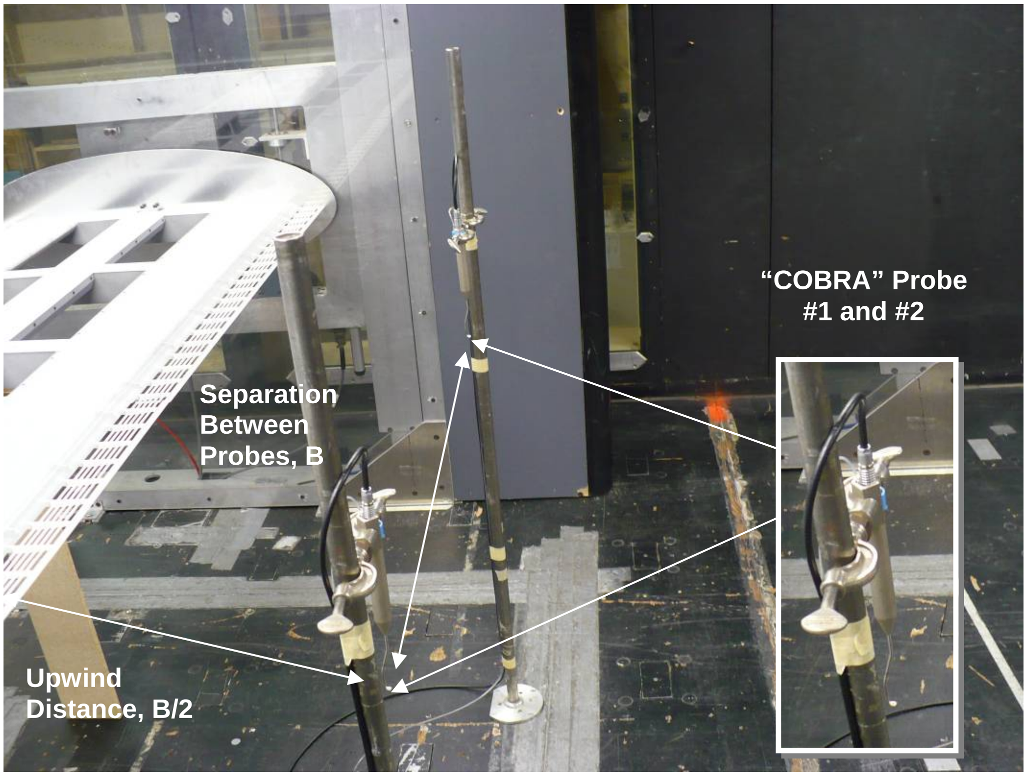

b) Cobra Probes Located Upwind of Model

FIGURE 3.18 EXPERIMENTAL SET-UP FOR AERODYNAMIC ADMITTANCE TESTS

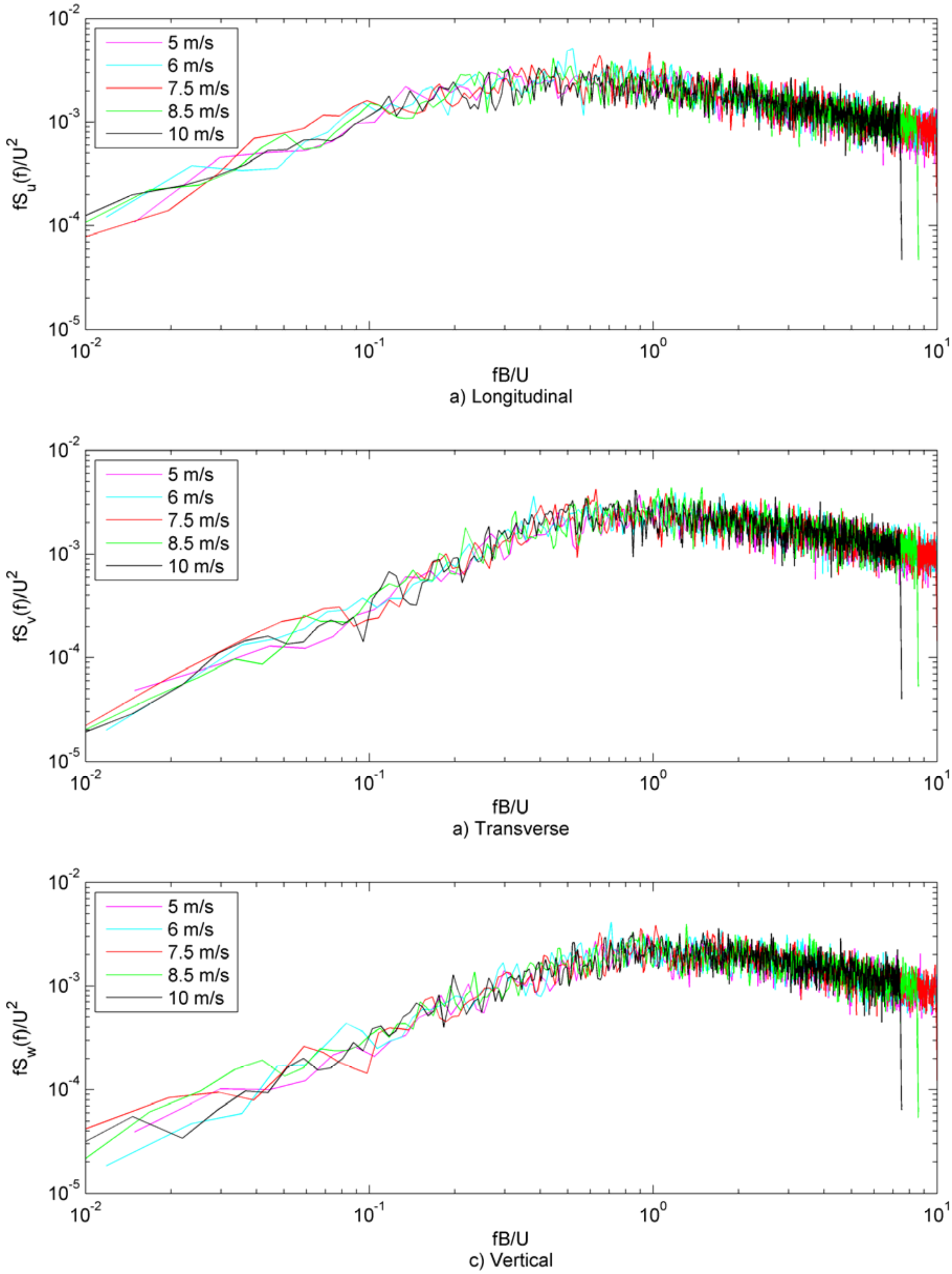

FIGURE 3.19 POWER SPECTRA OF LONGITUDINAL, LATERAL AND VERTICAL TURBULENCE

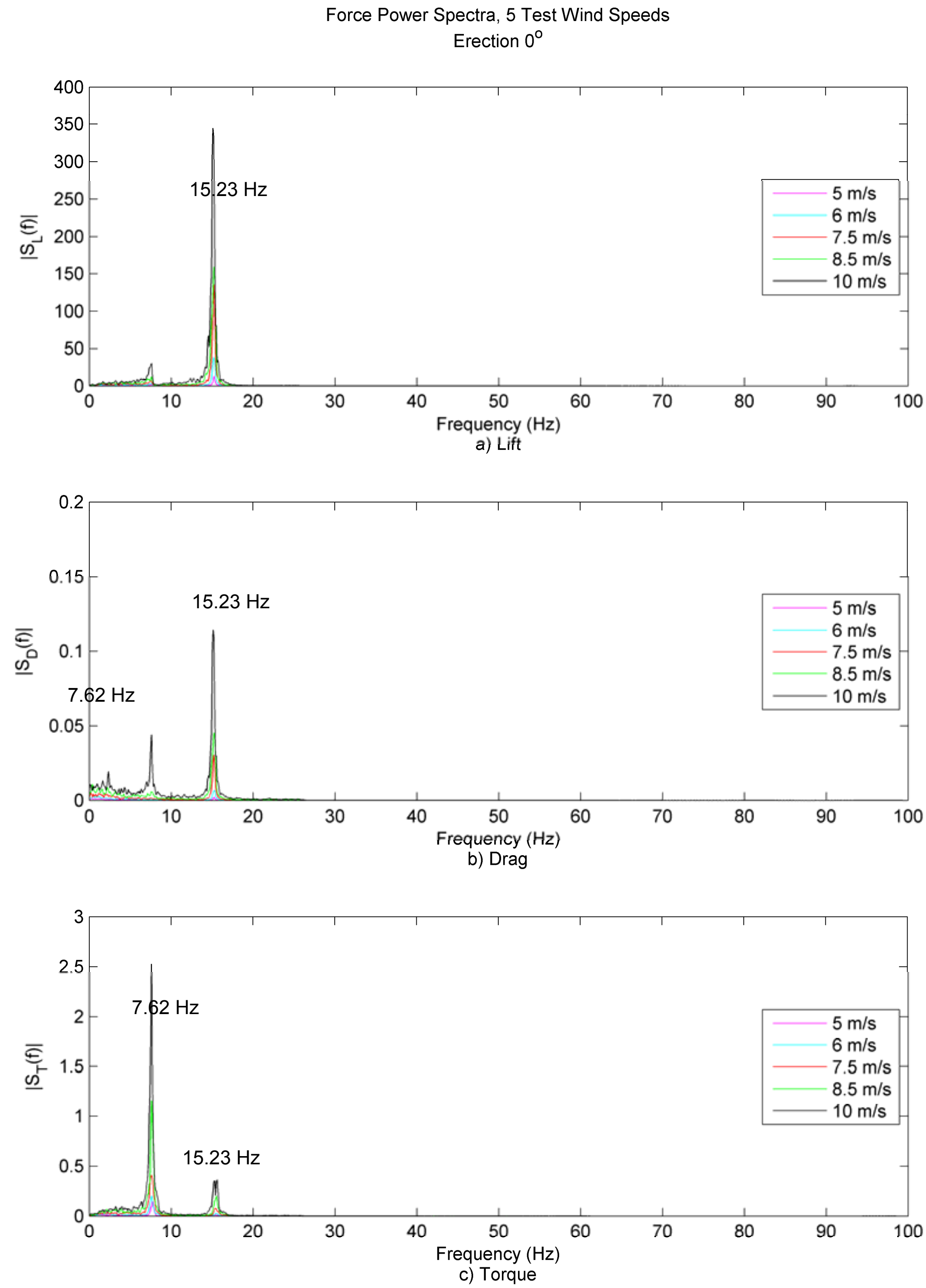

FIGURE 3.20 TYPICAL POWER SPECTRA OF INSTRUMENTED PANEL RESPONSE TO TURBULENT WIND

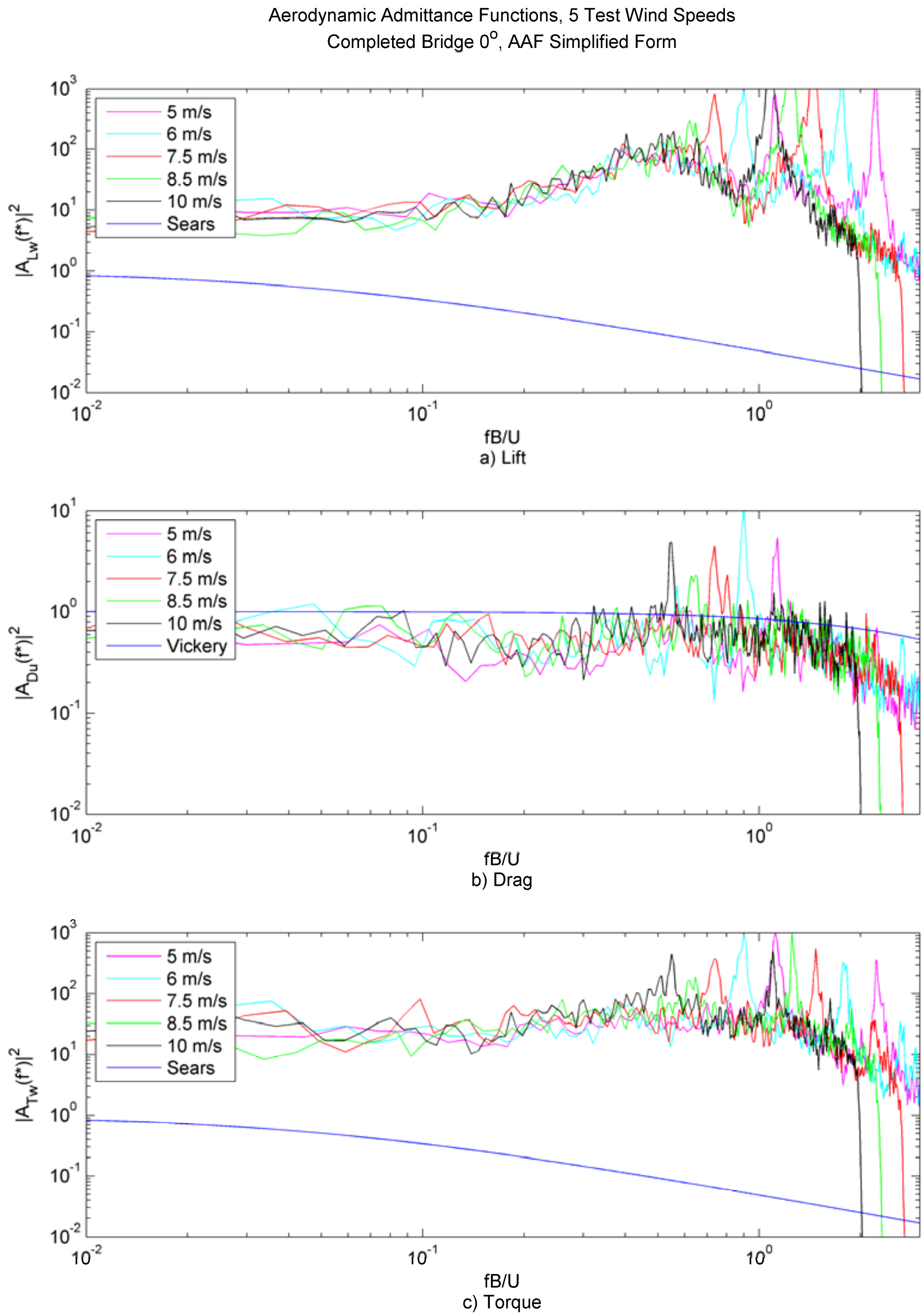

FIGURE 3.21 AERODYNAMIC ADMITTANCE FUNCTION – "SIMPLIFIED" METHOD IN-SERVICE BRIDGE, 0 DEGREE WIND INCLINATION

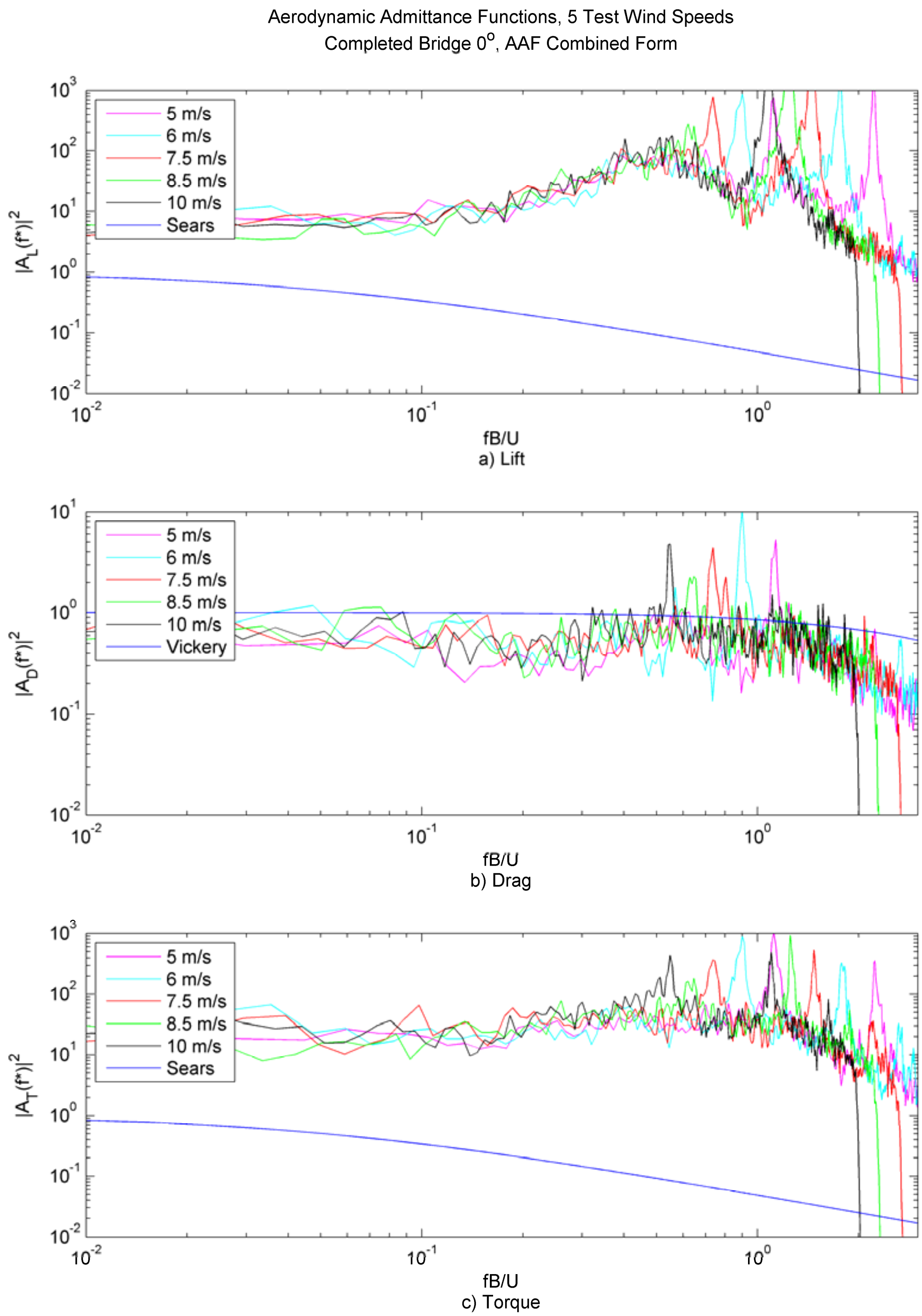

FIGURE 3.22 AERODYNAMIC ADMITTANCE FUNCTION – "COMBINED" METHOD IN-SERVICE BRIDGE, 0 DEGREE WIND INCLINATION

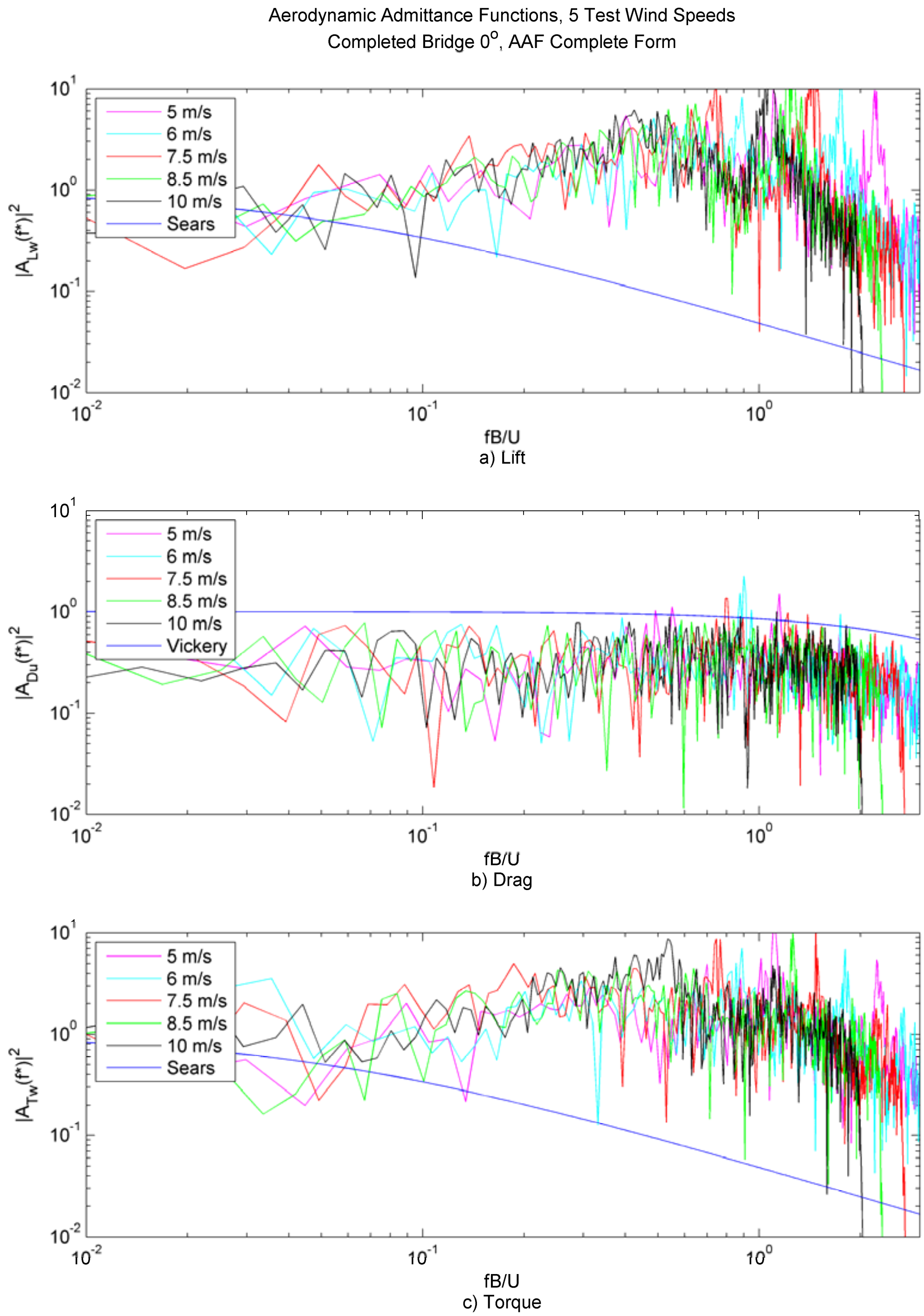

FIGURE 3.23 AERODYNAMIC ADMITTANCE FUNCTION – "COMPLETE" METHOD IN-SERVICE BRIDGE, 0 DEGREE WIND INCLINATION

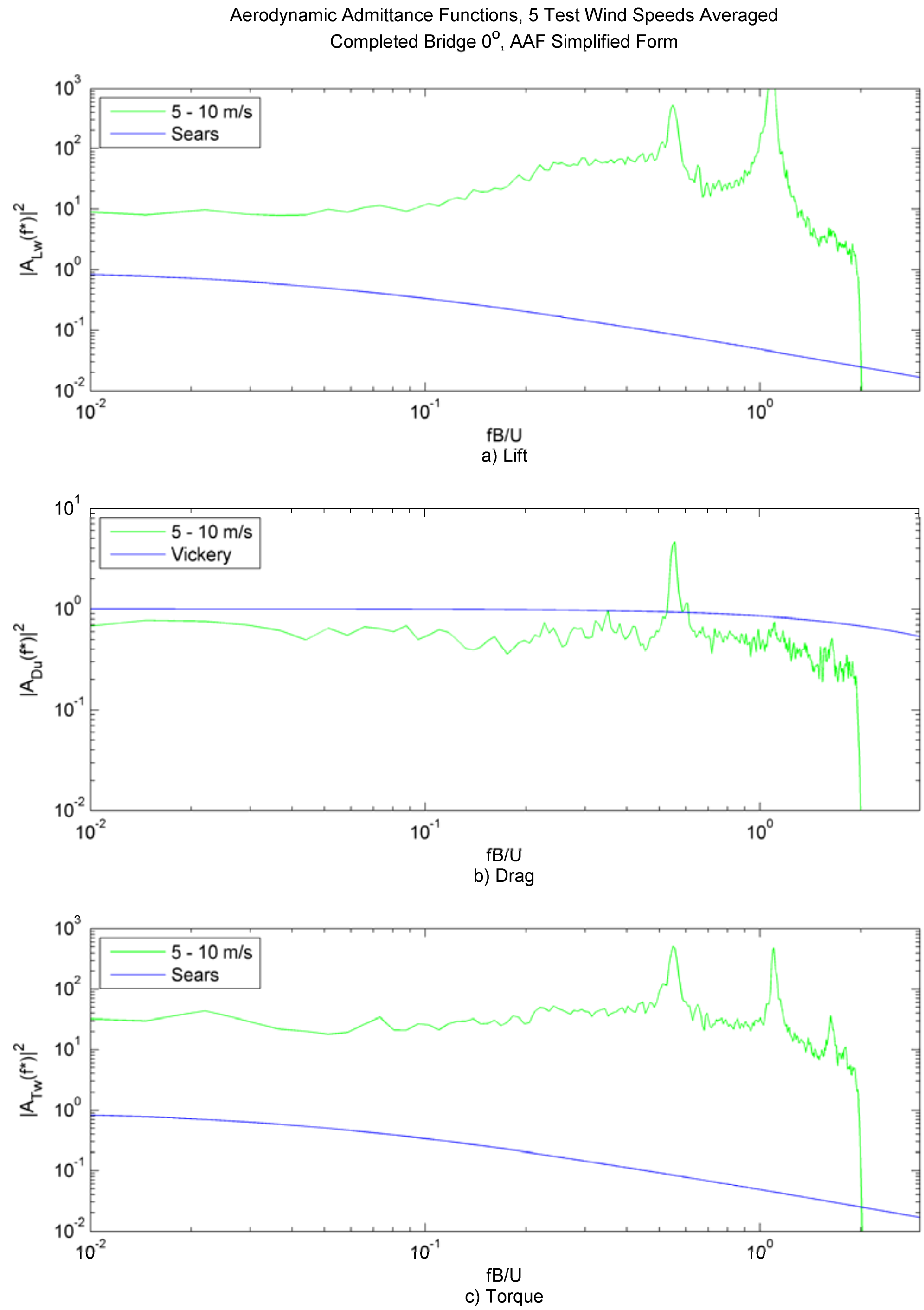

FIGURE 3.24 AERODYNAMIC ADMITTANCE FUNCTION – "SIMPLIFIED" METHOD IN-SERVICE BRIDGE, 0 DEGREE WIND INCLINATION (AVERAGED)

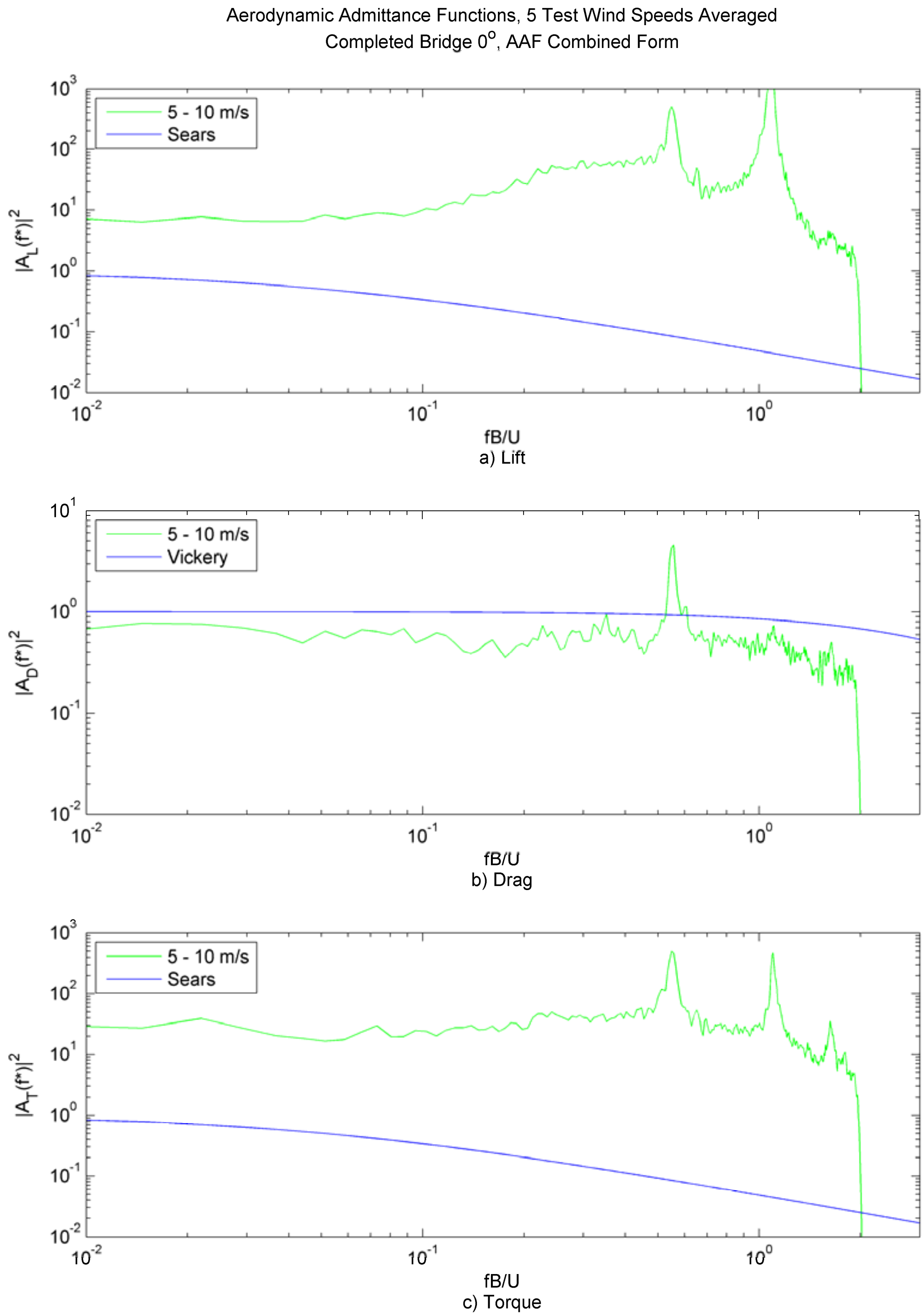

FIGURE 3.25 AERODYNAMIC ADMITTANCE FUNCTION – "COMBINED" METHOD IN-SERVICE BRIDGE, 0 DEGREE WIND INCLINATION (AVERAGED)

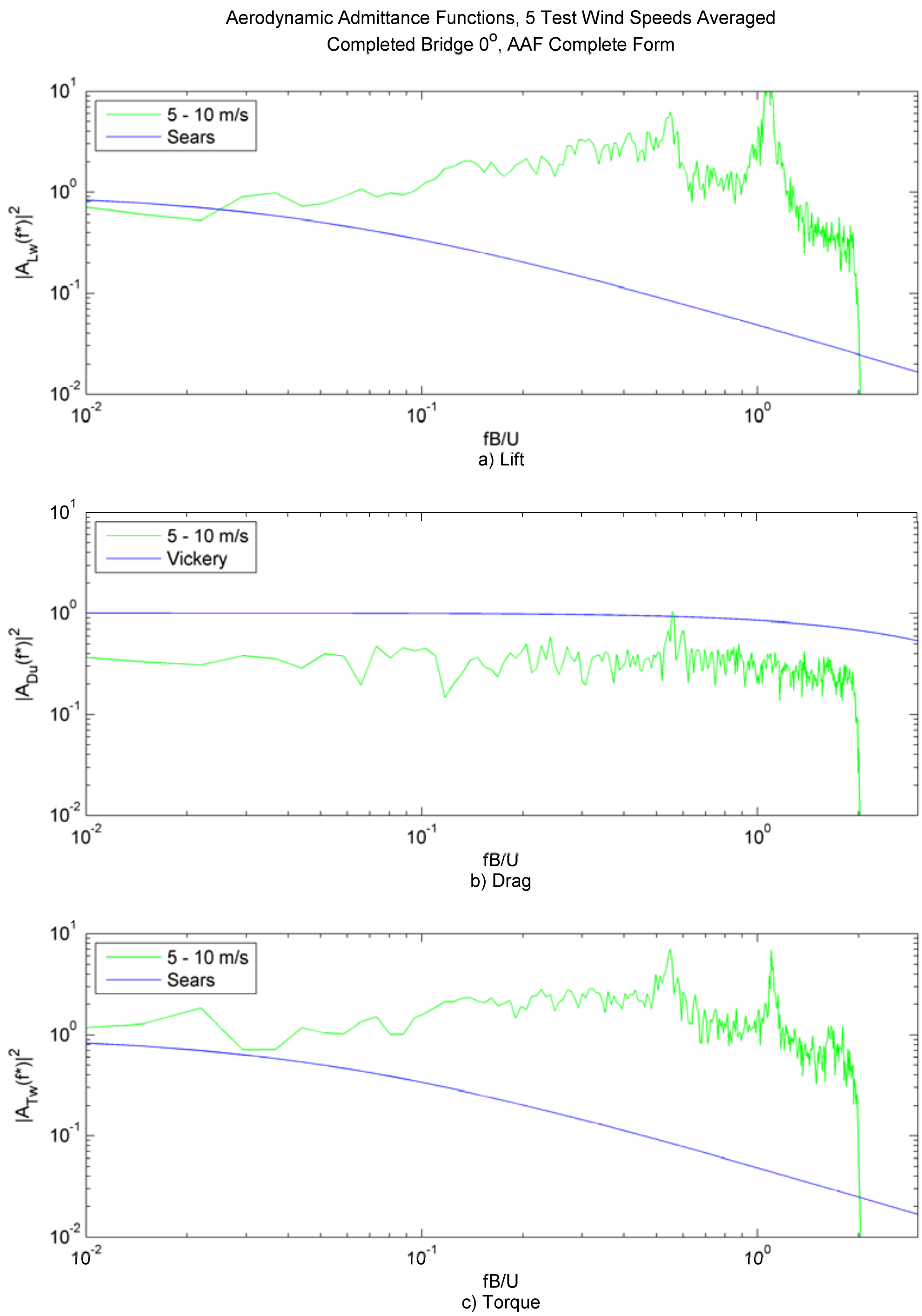

FIGURE 3.26 AERODYNAMIC ADMITTANCE FUNCTION – "COMPLETE" METHOD IN-SERVICE BRIDGE, 0 DEGREE WIND INCLINATION (AVERAGED)

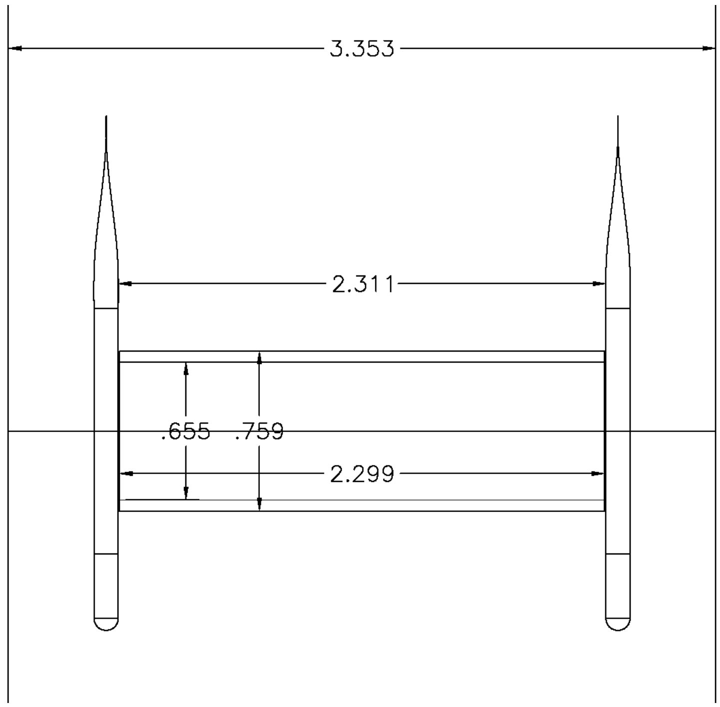

a) Model at Skew Wind Angle of 0°

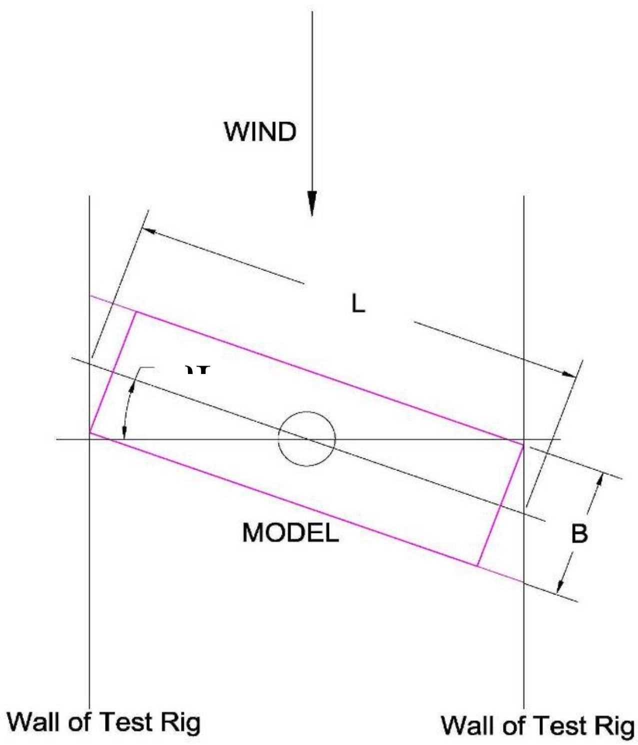

b) Model at Non-Zero Skew Wind Angle

FIGURE 4.1 DEFINITION OF SKEW WIND ANGLE TESTS

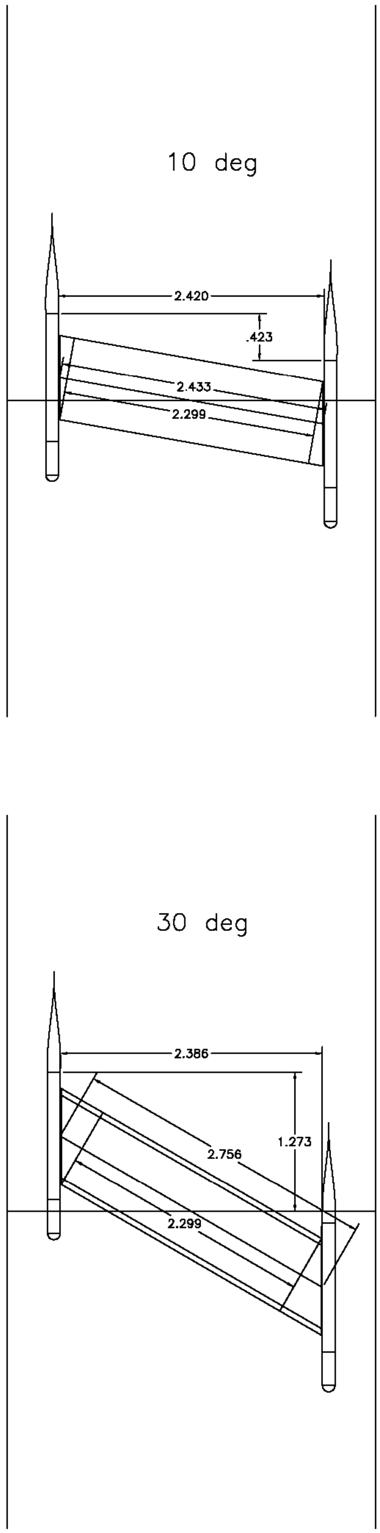

FIGURE 4.2 SKEW WIND CONFIGURATIONS

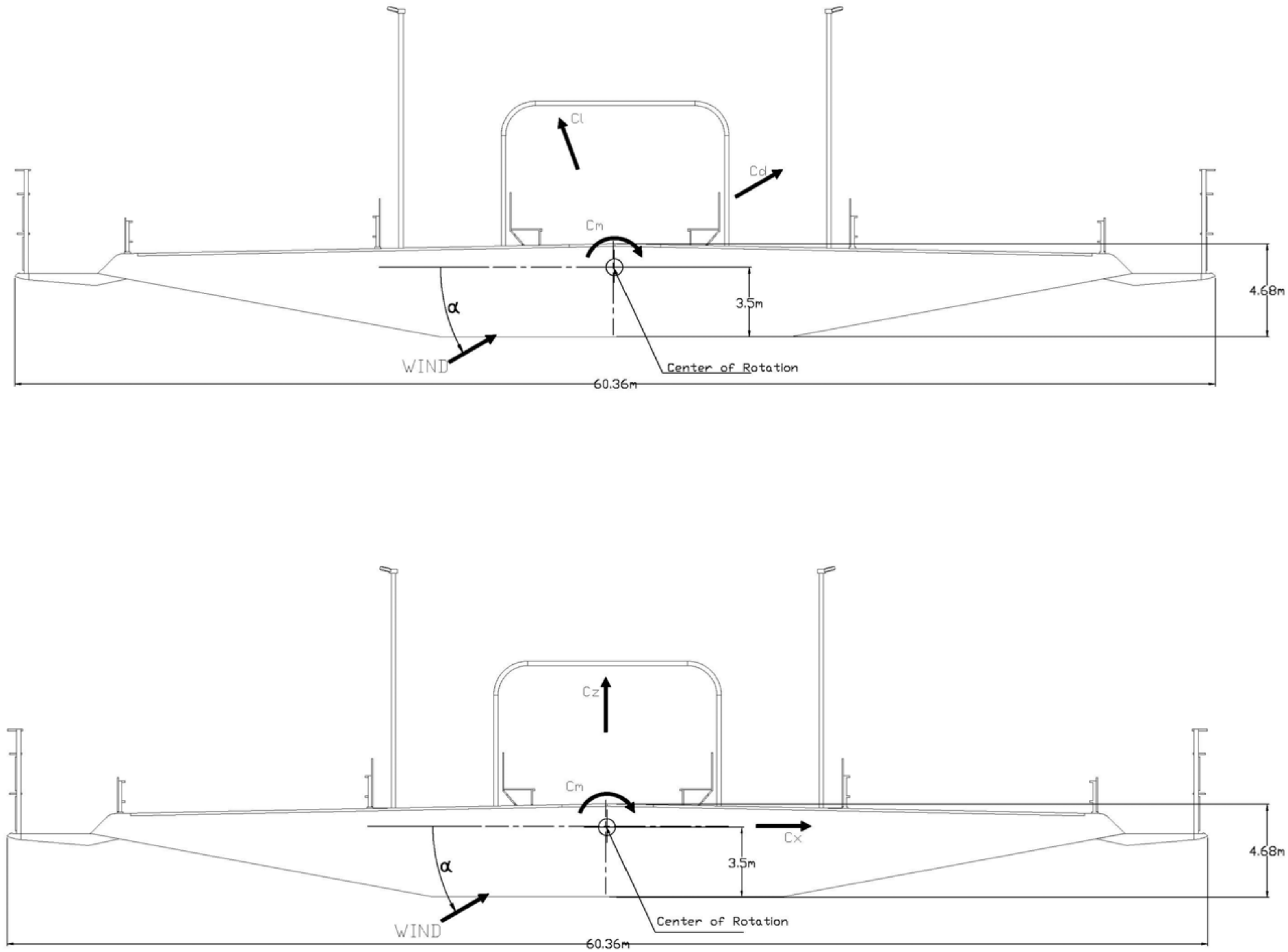

FIGURE 4.3 SIGN CONVENTION FOR STATIC TEST OF THE IN-SERVICE DECK SECTION

10 Degree Yaw	20 Degree Yaw
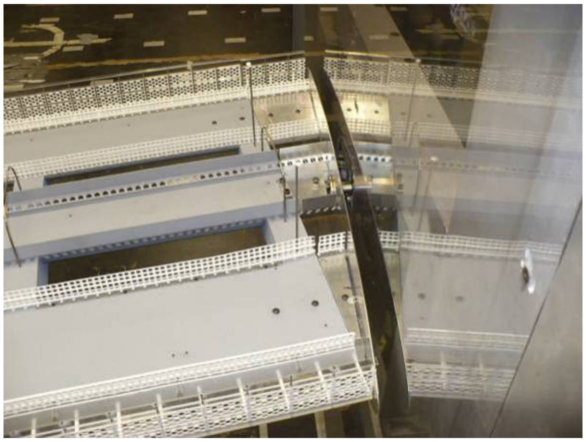	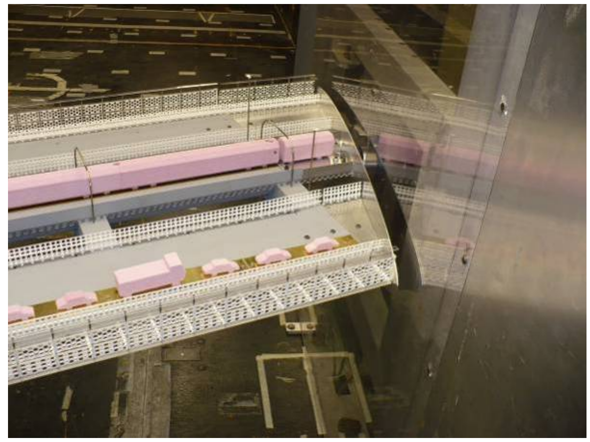
30 Degree Yaw	**45 Degree Yaw**
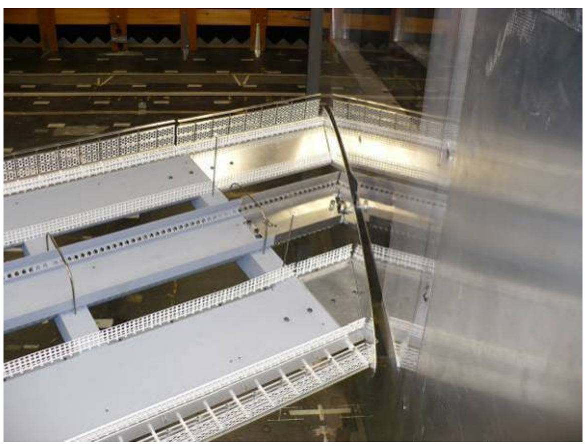	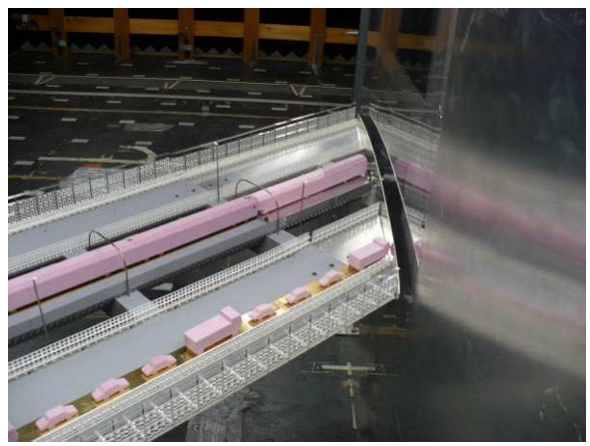

FIGURE 4.4 TRIANGULAR WEDGE ELEMENTS ADDED TO ENDS OF BASIC SECTION MODEL FOR SKEW WIND TESTS

a) 10 Degree Skew Wind

b) 20 Degree Skew Wind

FIGURE 4.5 ORIENTATIONS OF EXTENDED LENGTH SECTION MODEL FOR SKEW WIND TESTS

c) 30 Degree Skew Wind

d) 45 Degree Skew Wind

FIGURE 4.5 (CONT.) ORIENTATIONS OF EXTENDED LENGTH SECTION MODEL FOR SKEW WIND TESTS

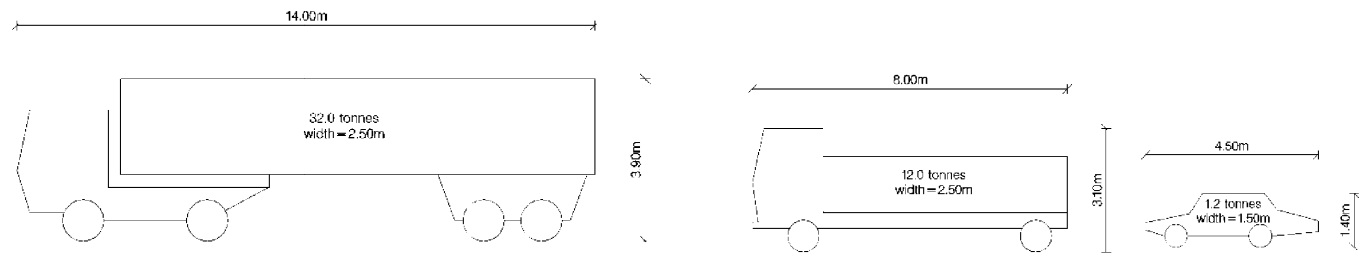

Heavy Lorry HL

Light Lorry LL

Passenger car C

Approximate spacing between vehicles: 2.0 m - 3.0 m

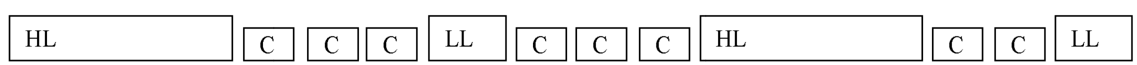

Traffic configuration occupying approximately 100 m length.

FIGURE 4.6 TRAFFIC CONFIGURATION – ROAD TRAFFIC (COWI – 10 JUNE, 2010)

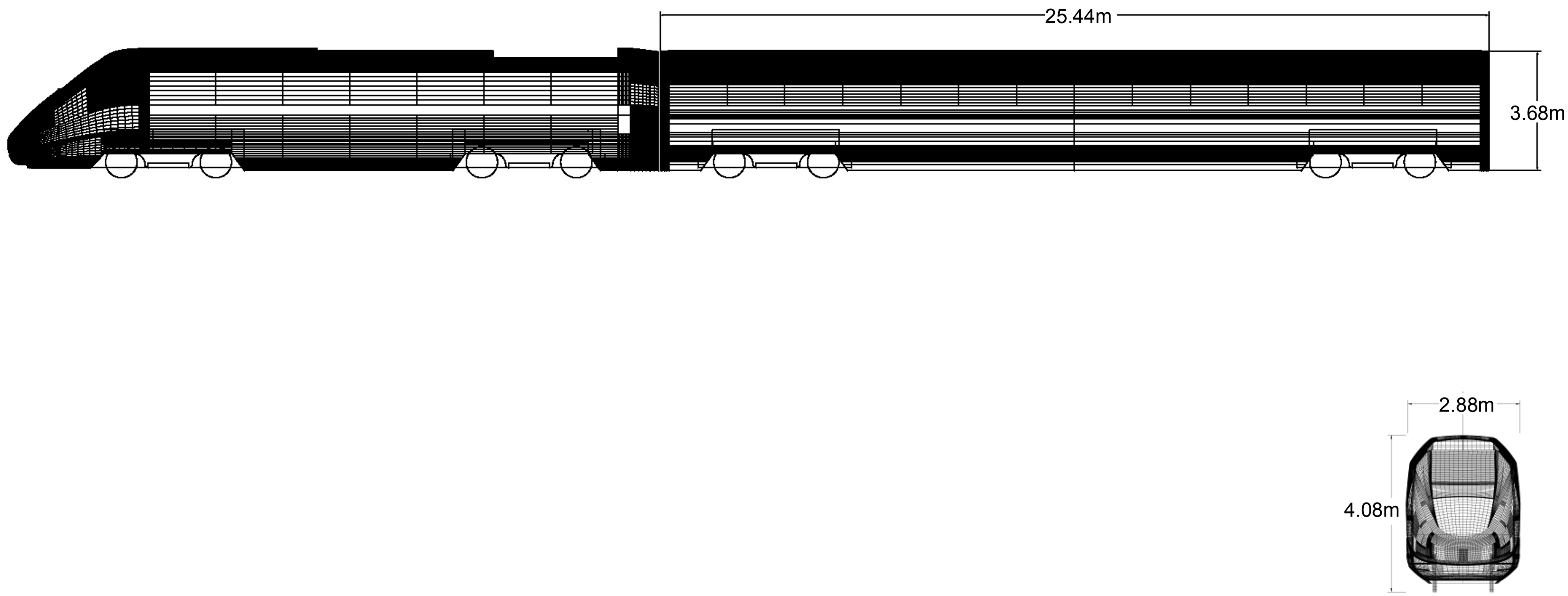

FIGURE 4.7 TRAFFIC CONFIGURATION – RAIL TRAFFIC (COWI – 18 JUNE, 2010)

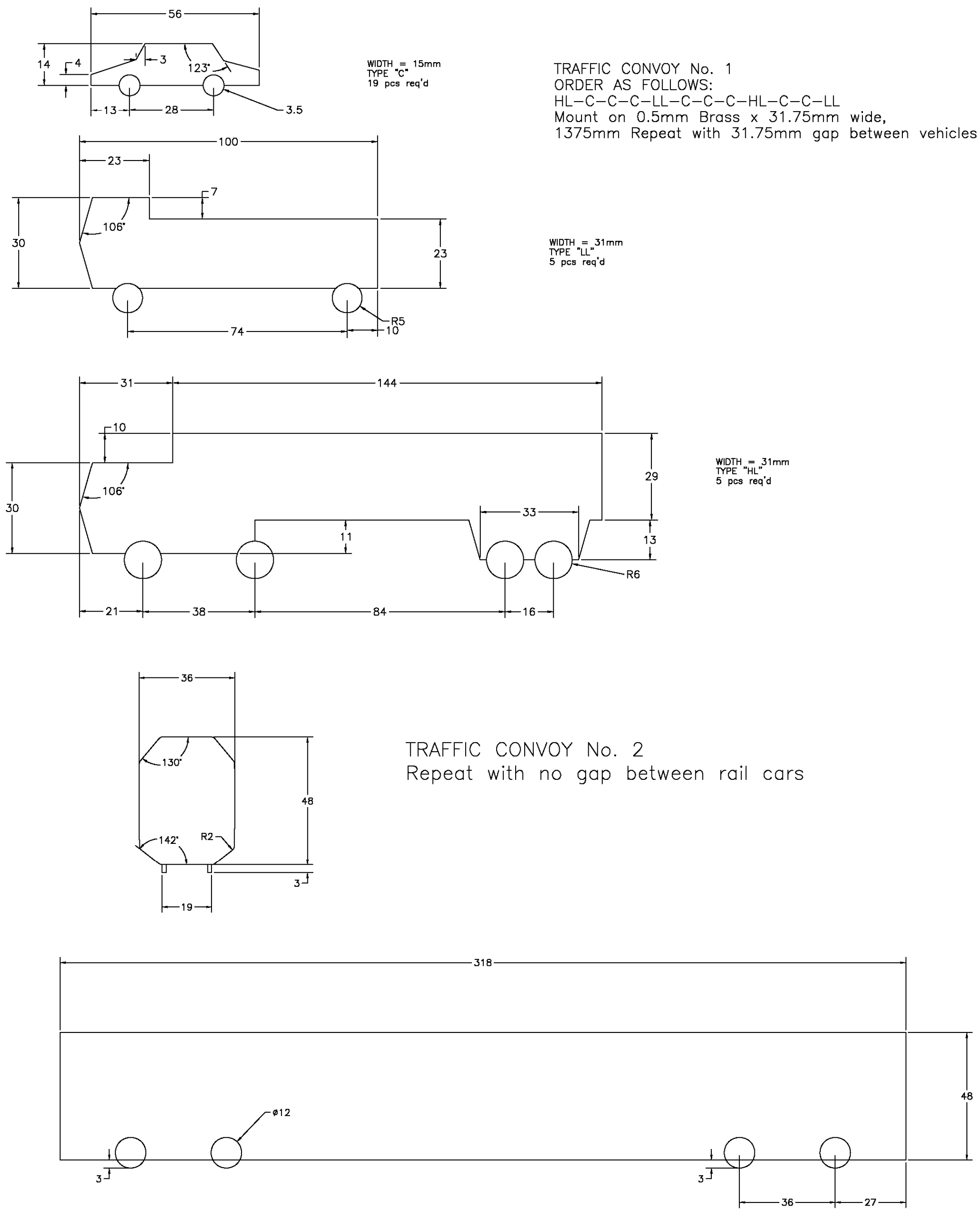

FIGURE 4.8 ROAD AND RAIL TRAFFIC - MODEL

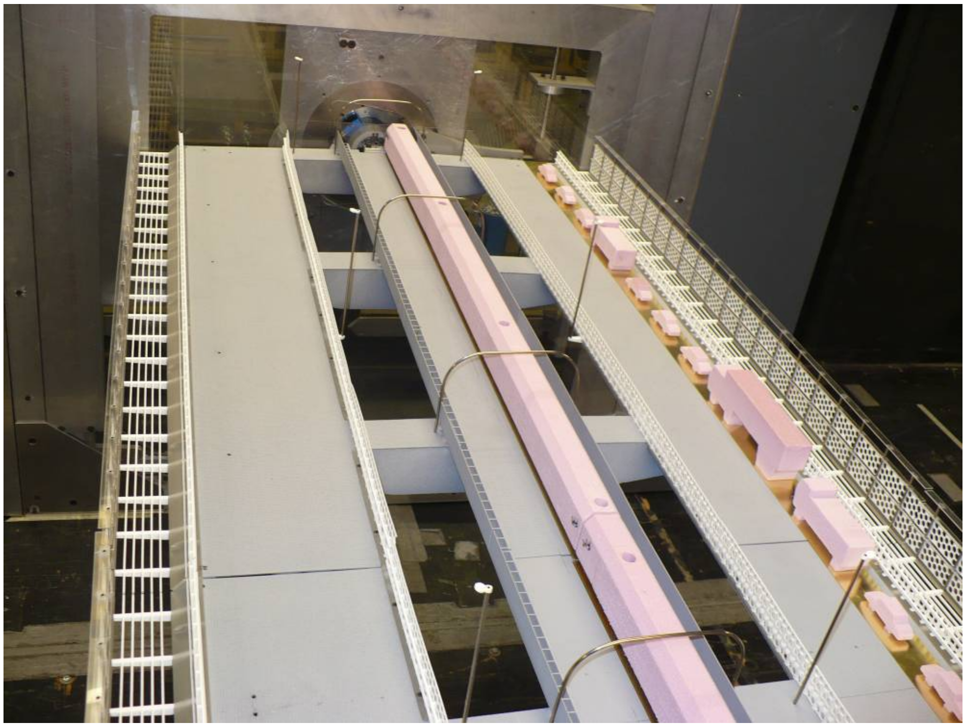

a) TRAFFIC CONDITION 1 – Road Traffic on Outward (Slow) Lane on Windward Girder, Plus Train on Upwind Track

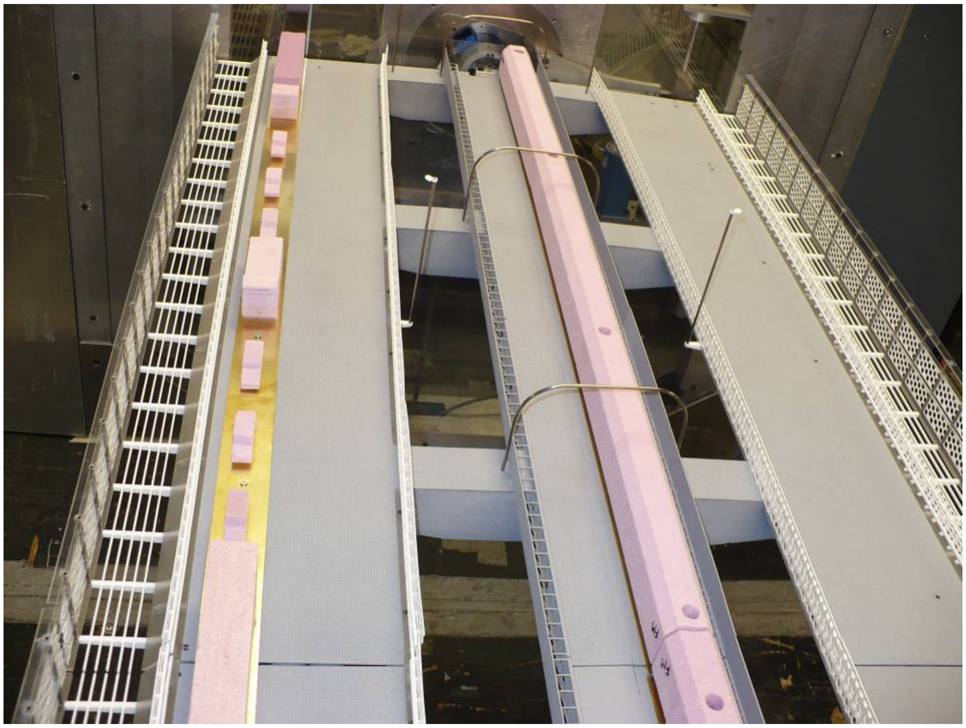

b) TRAFFIC CONDITION 2 – Road Traffic on Outward (Slow) Lane on Downwind Girder, Plus Train on Upwind Track

FIGURE 4.9 TRAFFIC CONFIGURATIONS FOR SUB-TESTS D5 AND D6

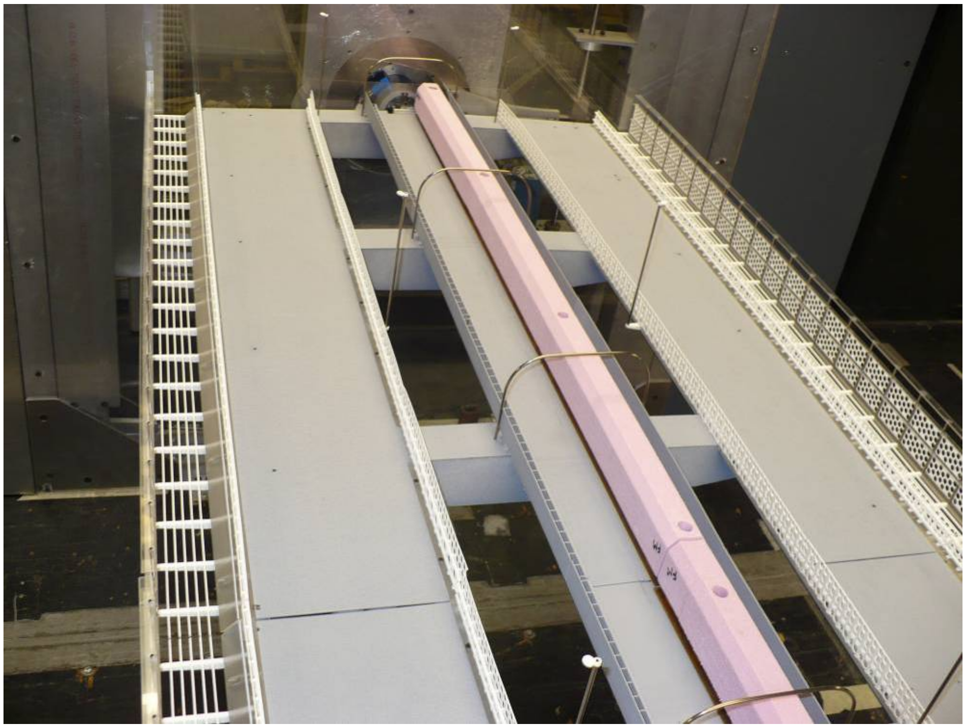

c) TRAFFIC CONDITION 3 – No Road Traffic, Train on Upwind Track

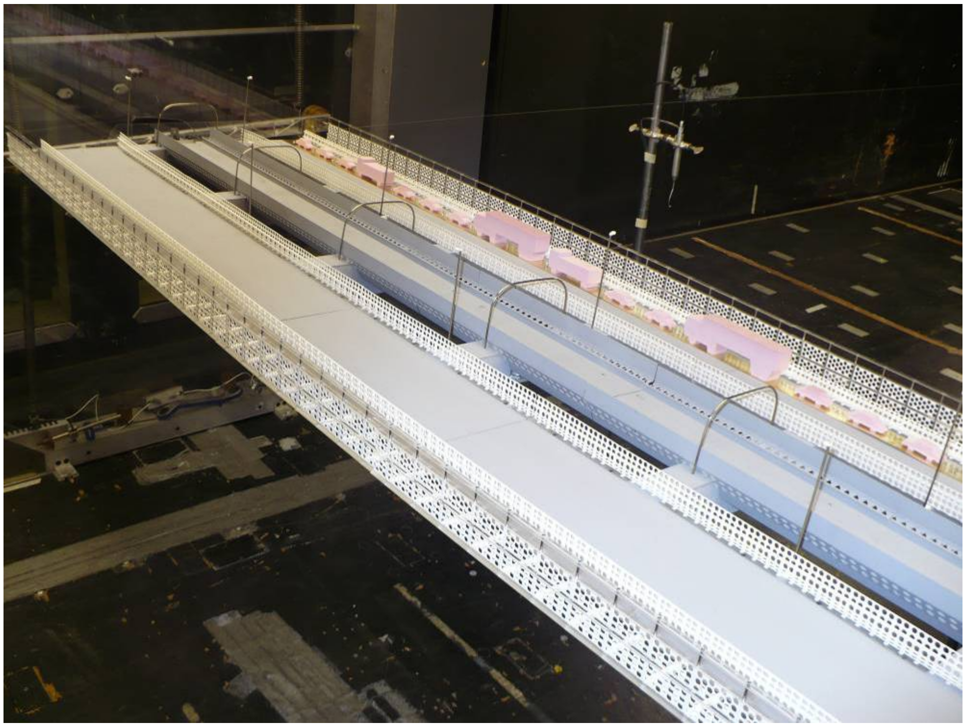

d) TRAFFIC Condition 2* – Road Traffic on Outward (Slow) Lane on Windward Girder, No Train Traffic

FIGURE 4.9 (CONT.) TRAFFIC CONFIGURATIONS FOR SUB-TESTS D5 AND D6

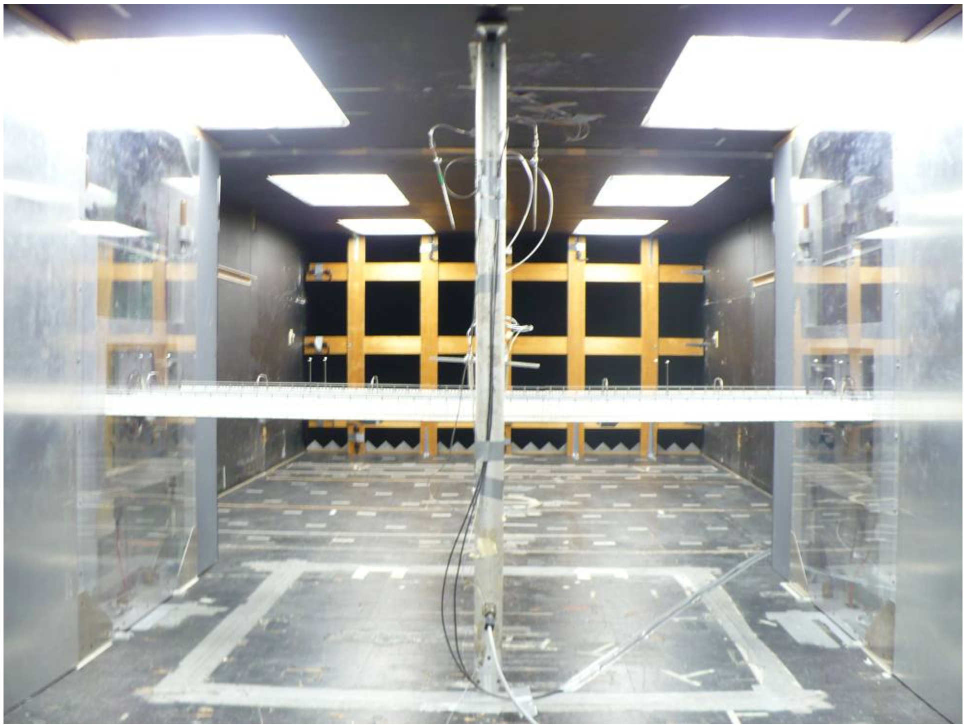

a) Vertical Traversing Rig located behind model (view looking upwind)

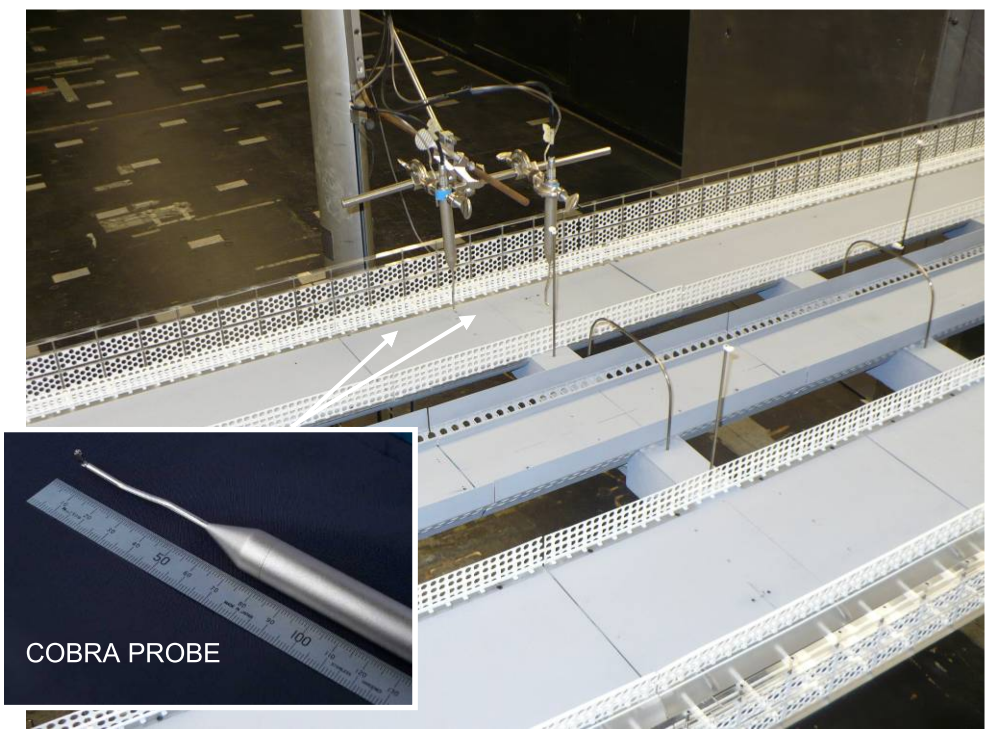

b) Twin Cobra Probe vertical profile set-up

FIGURE 4.10 VERTICAL PROFILES IN TRAFFIC LANES

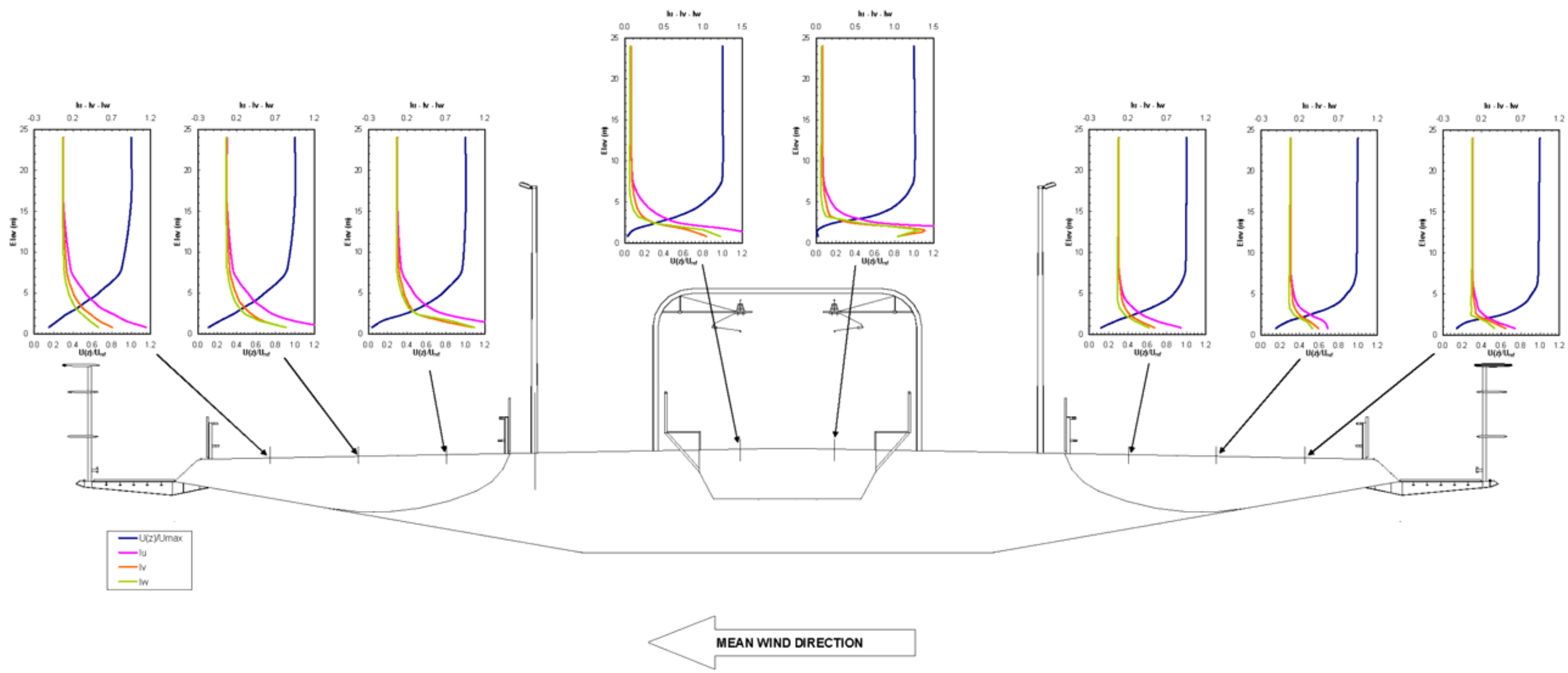

FIGURE 4.11 VELOCITY PROFILES OVER DECK – SUMMARY – NO TRAFFIC

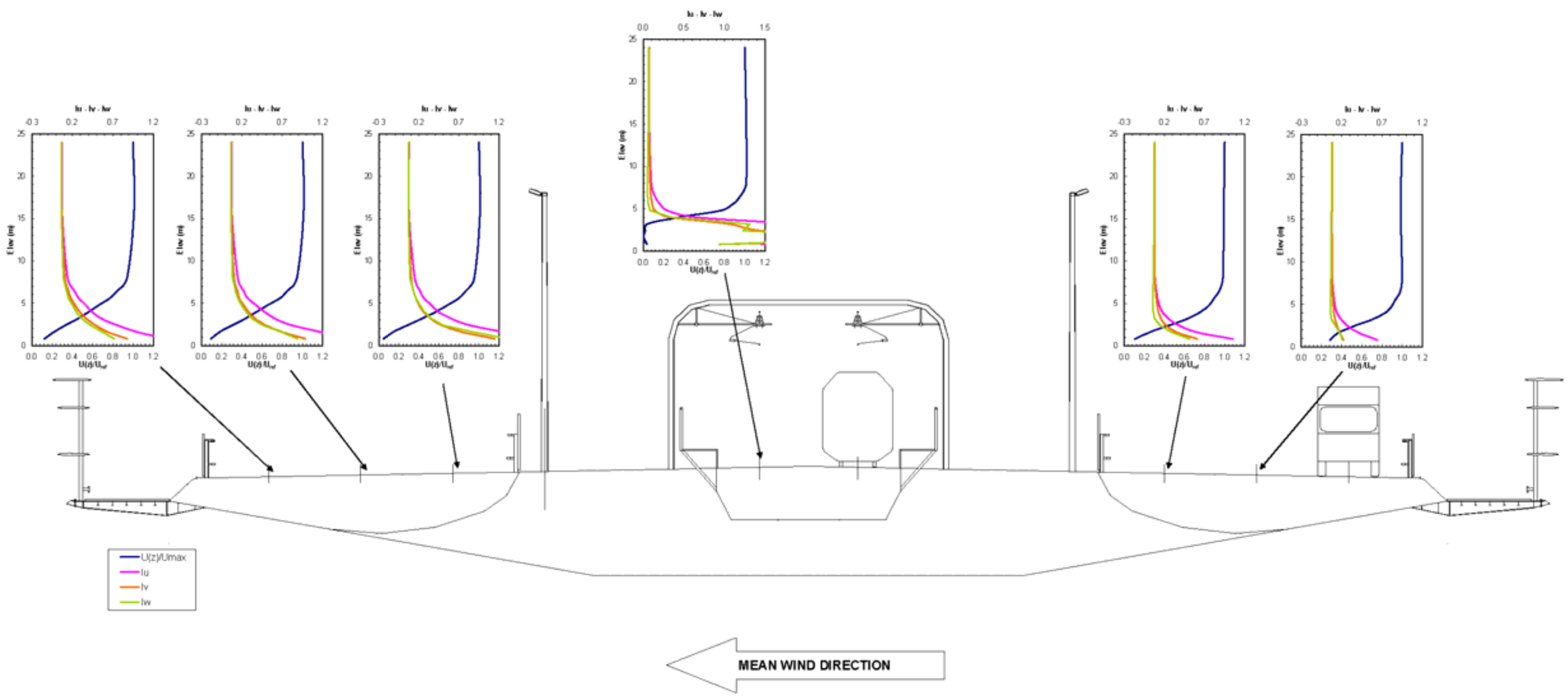

FIGURE 4.12 VELOCITY PROFILES OVER DECK – SUMMARY – TRAFFIC CONDITION 1

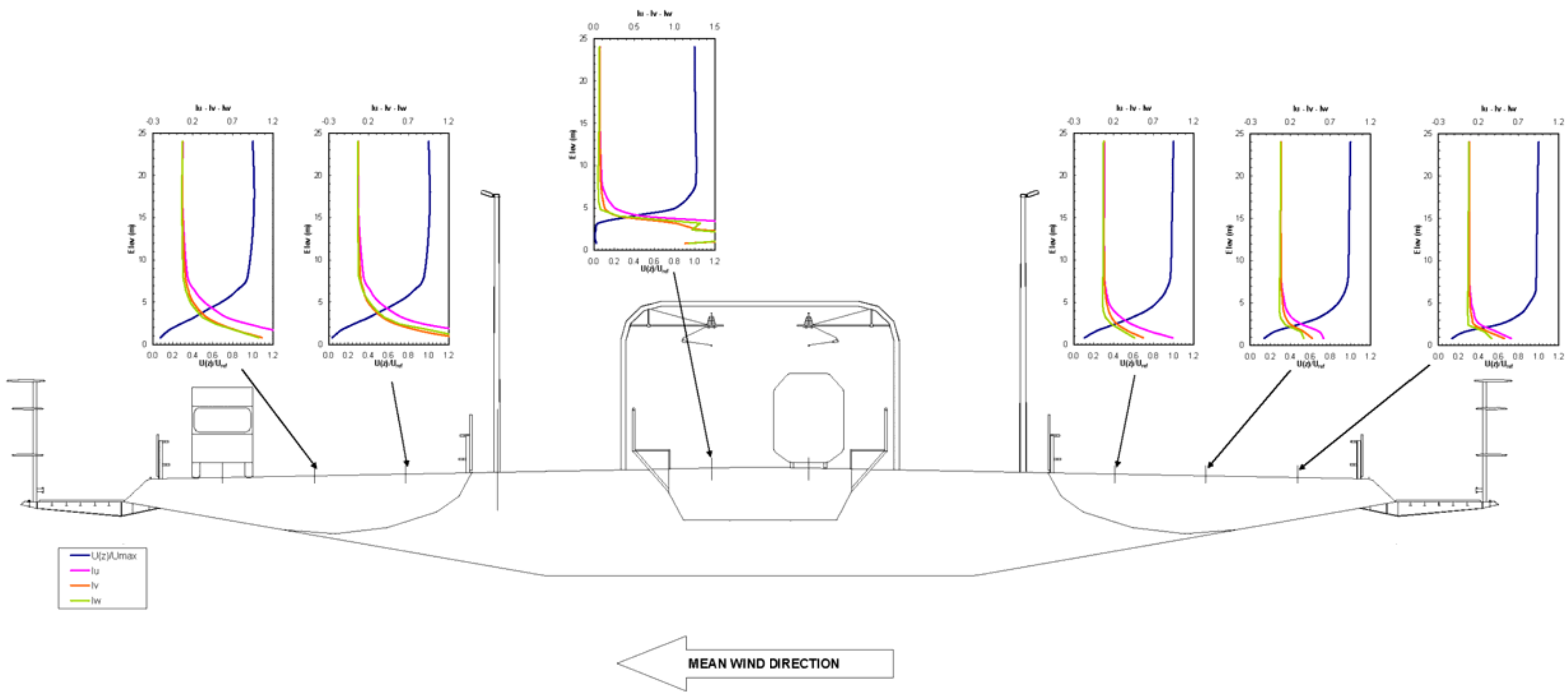

FIGURE 4.13 VELOCITY PROFILES OVER DECK – SUMMARY – TRAFFIC CONDITION 2

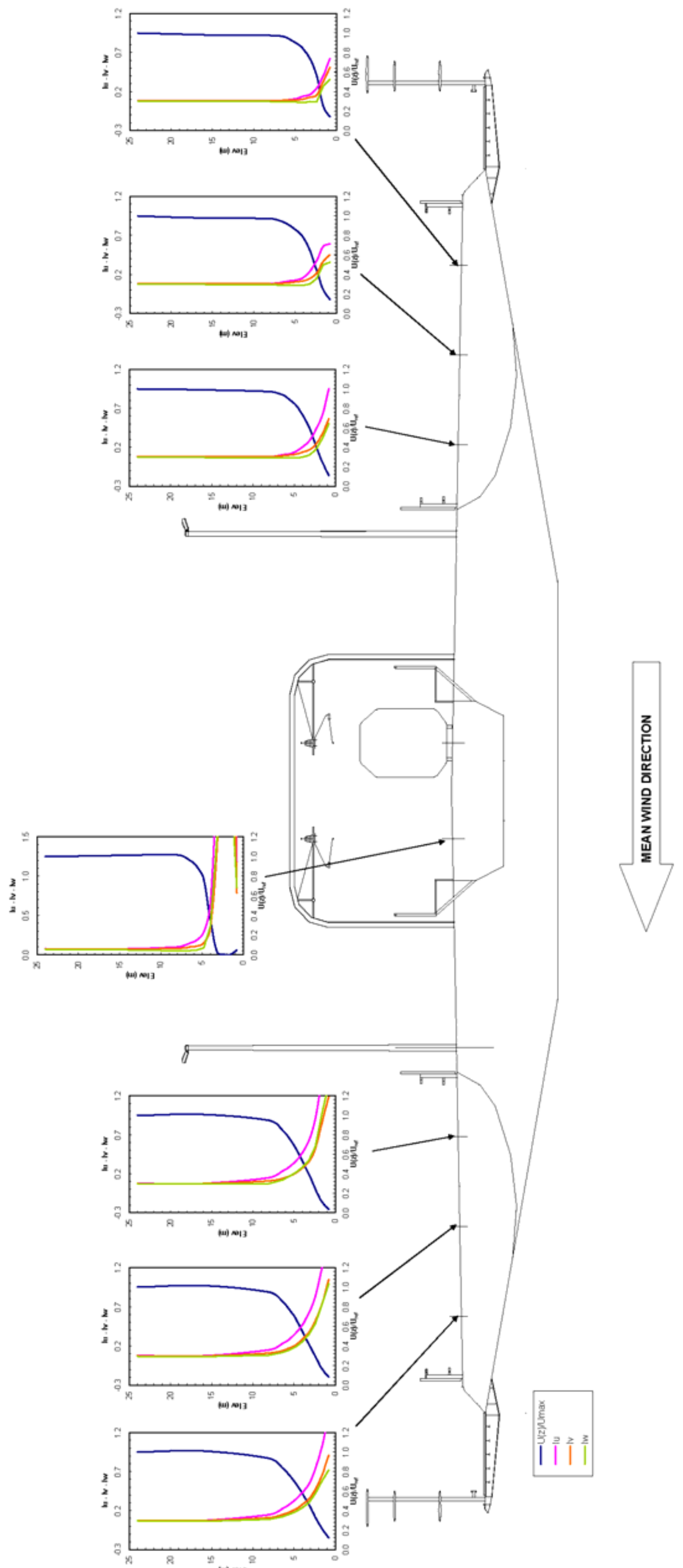

FIGURE 4.14 VELOCITY PROFILES OVER DECK – SUMMARY – TRAFFIC CONDITION 3

a) Drag Wire and Spring (Looking Upstream)

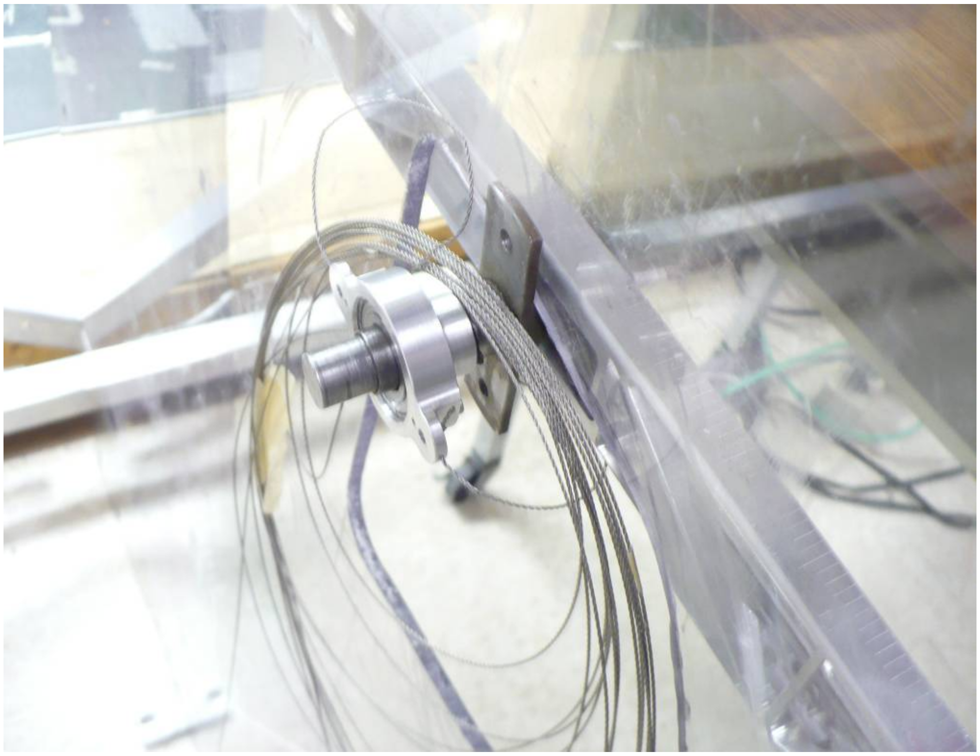

b) Bearing System and Drag Wire Attachment (Model removed for clarity)

FIGURE 5.1 DRAG MOTION SIMULATION AND BEARING SYSTEM

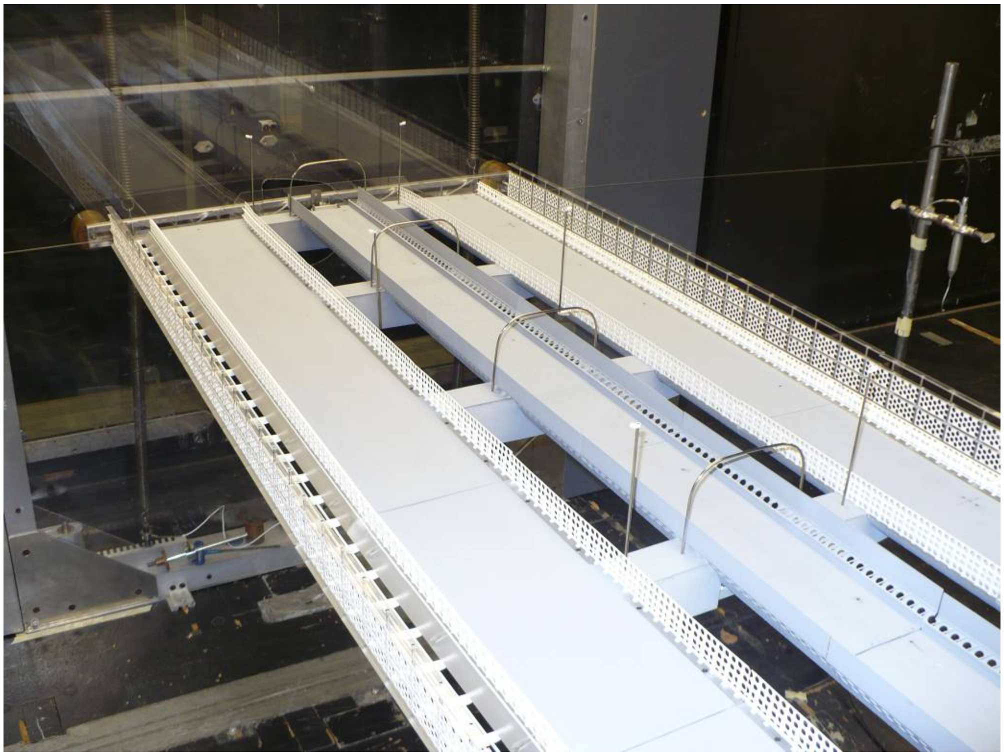

a) No Traffic

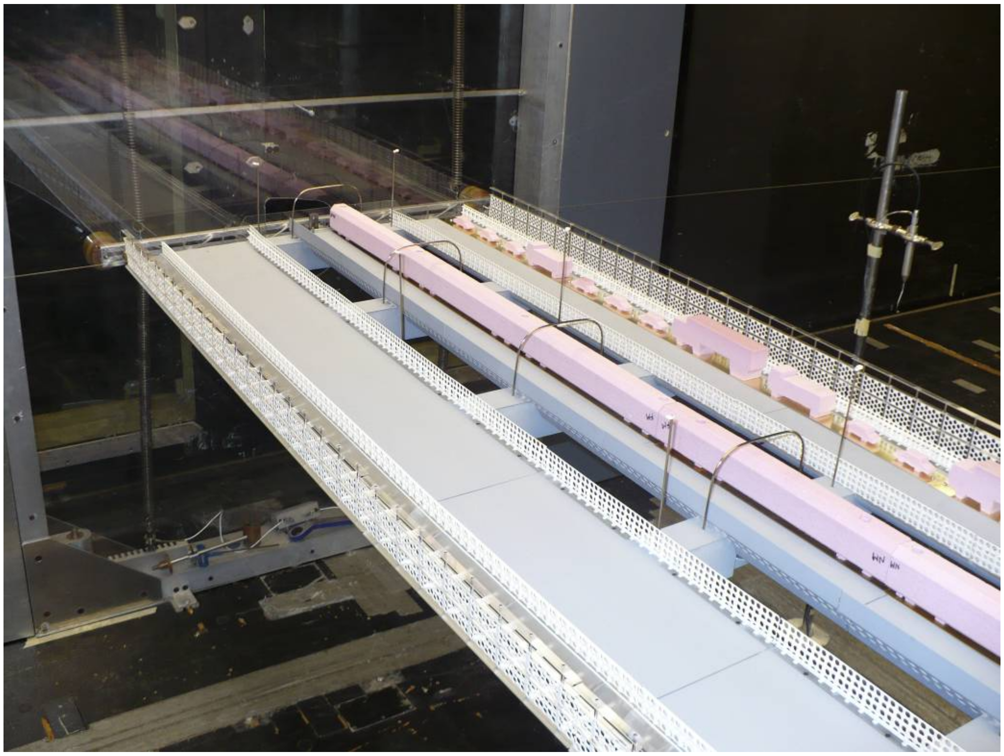

b) Traffic Condition 1

FIGURE 5.2 DYNAMIC SECTION MODEL TEST CONFIGURATIONS

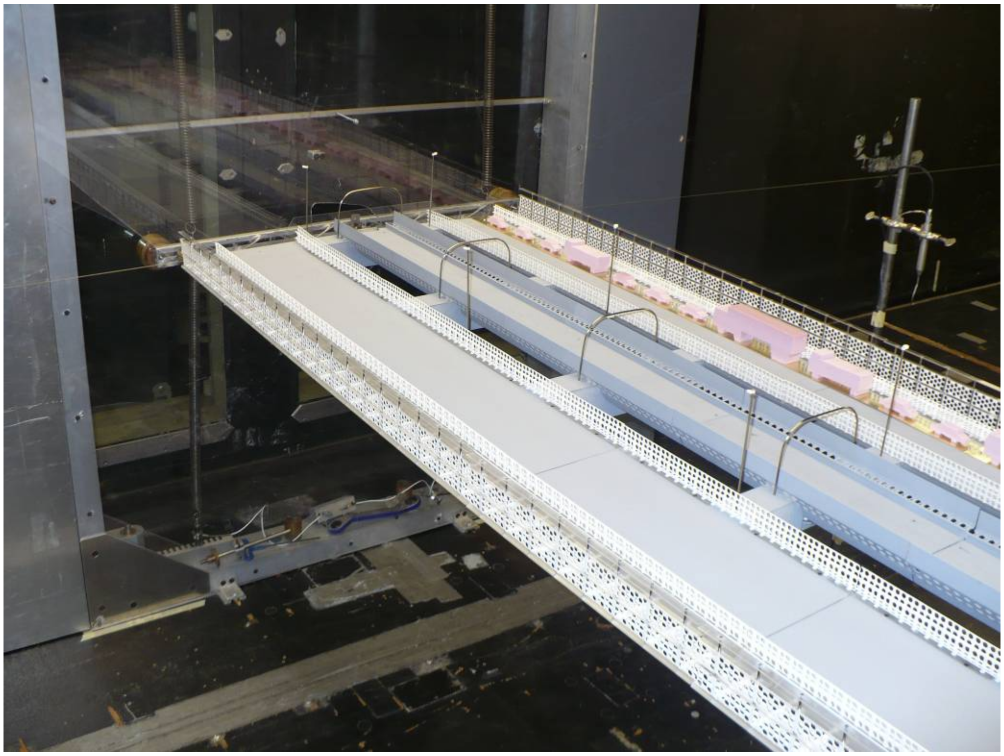

c) Traffic Condition 2*

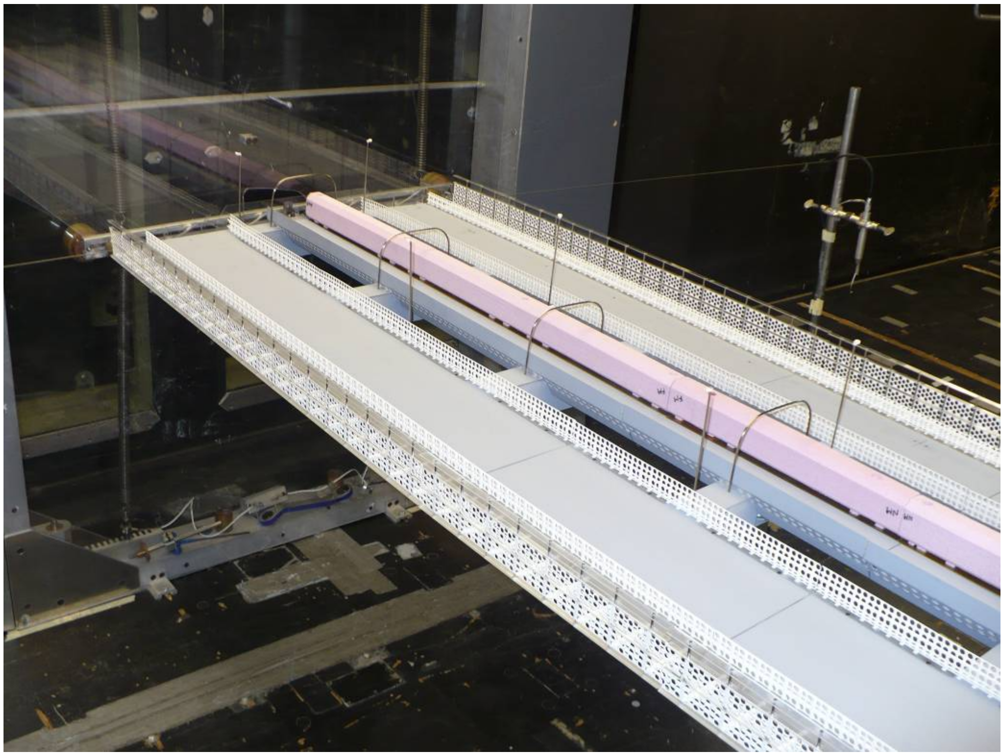

d) Traffic Condition 3

FIGURE 5.2 (CONT.) DYNAMIC SECTION MODEL TEST CONFIGURATIONS

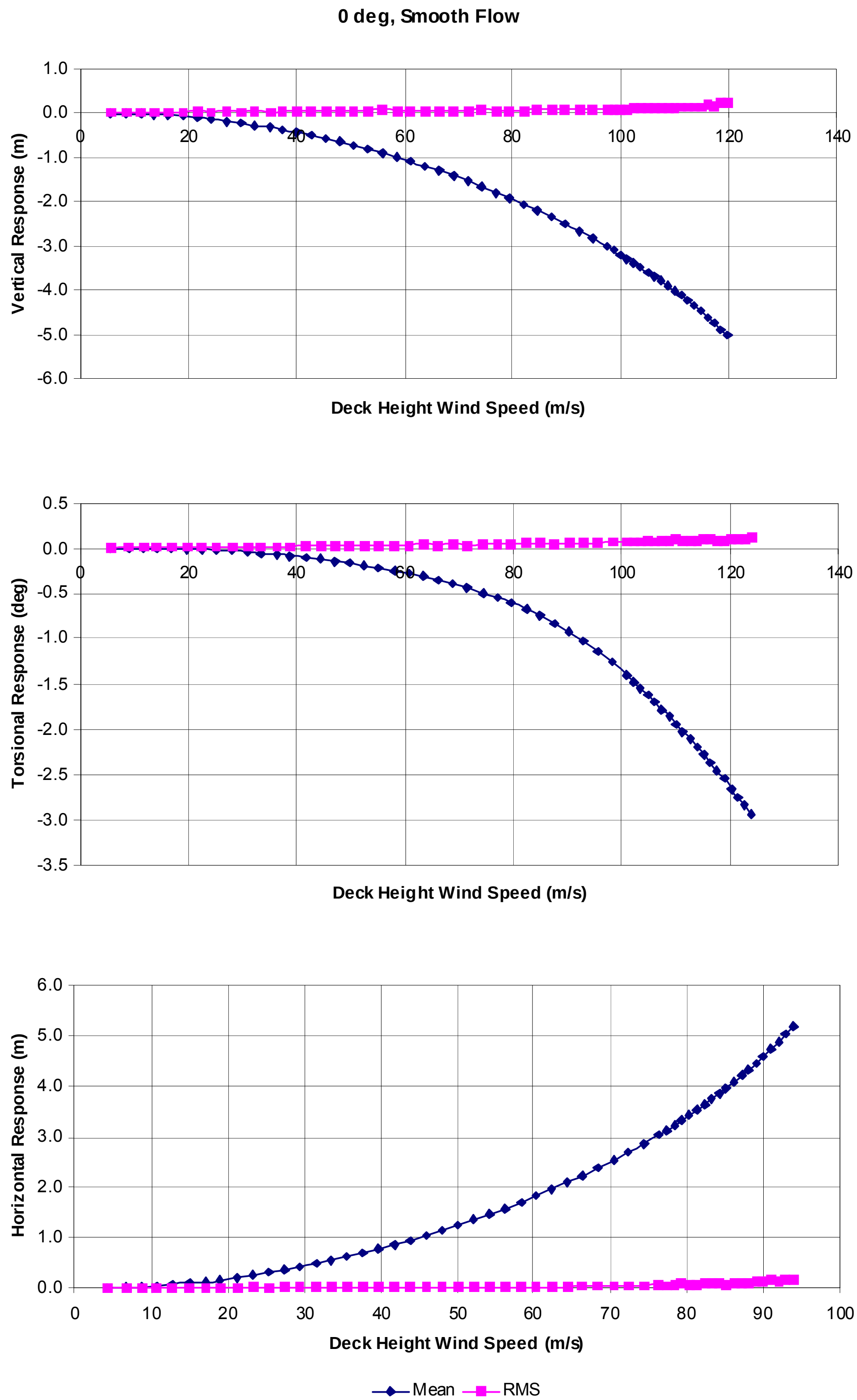

FIGURE 5.3 DYNAMIC TEST AT 0°, SMOOTH FLOW, IN-SERVICE

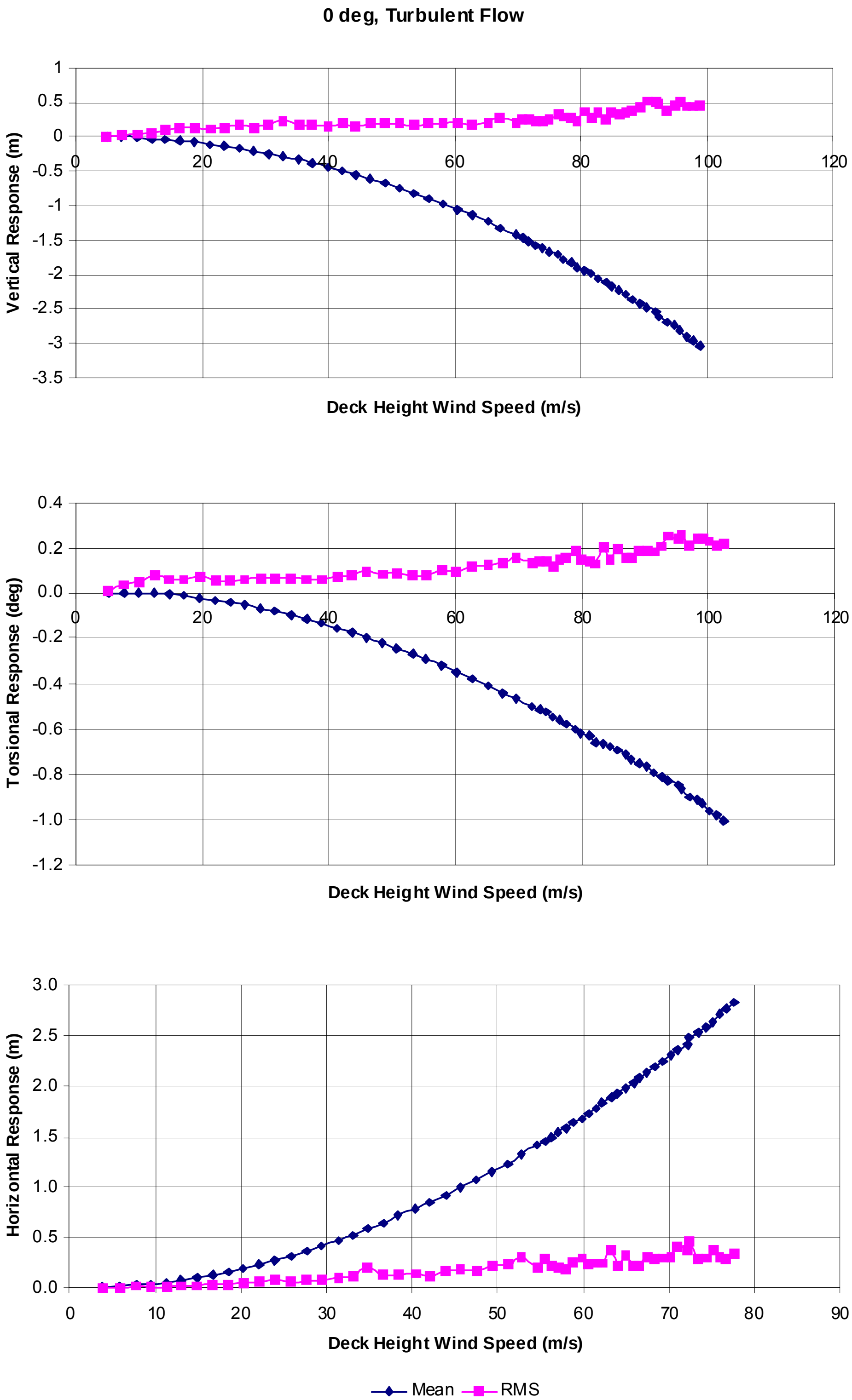

FIGURE 5.4 DYNAMIC TEST AT 0°, TURBULENT FLOW, IN-SERVICE

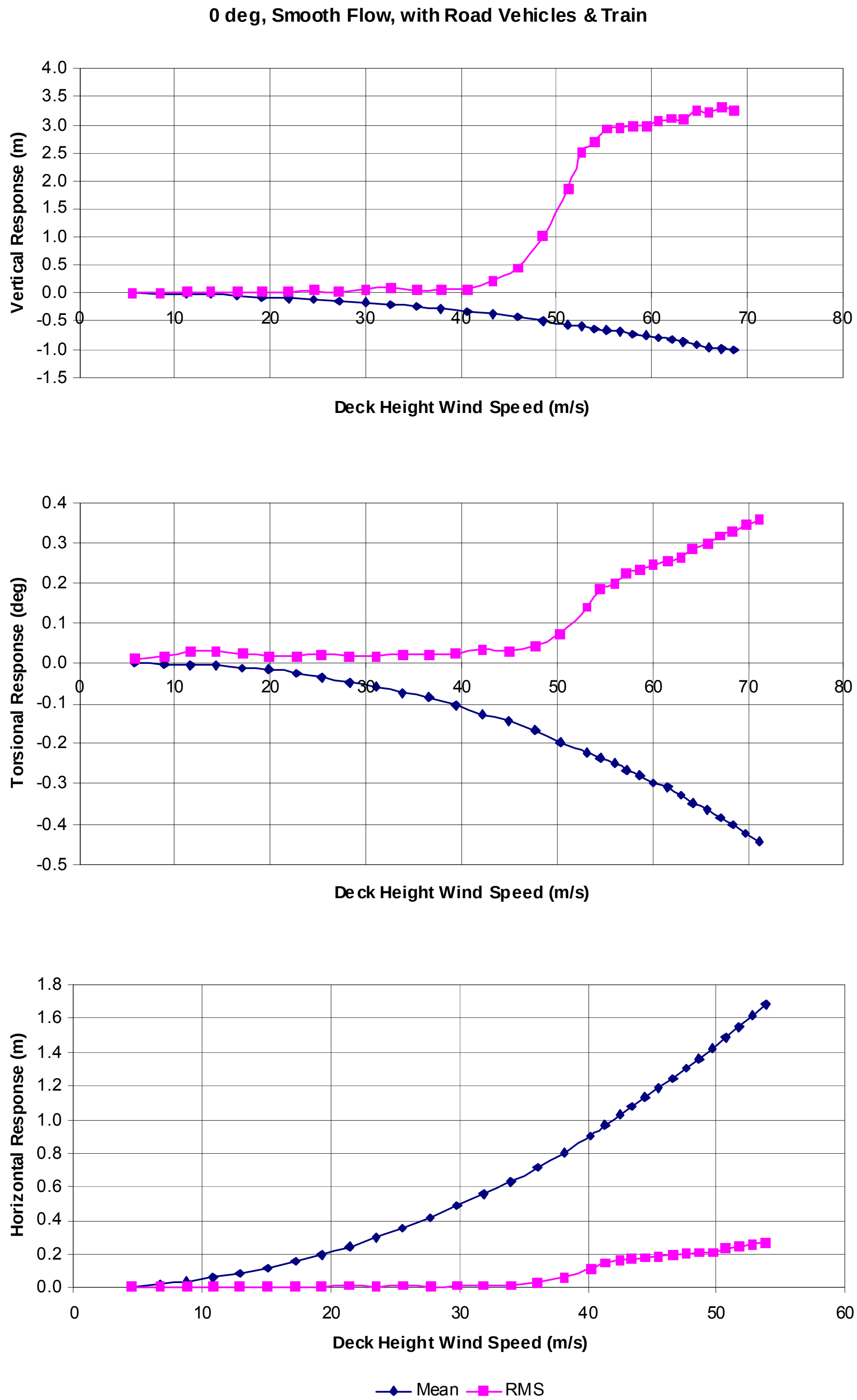

FIGURE 5.5 DYNAMIC TEST AT 0°, SMOOTH FLOW, WITH ROAD VEHICLES AND TRAIN

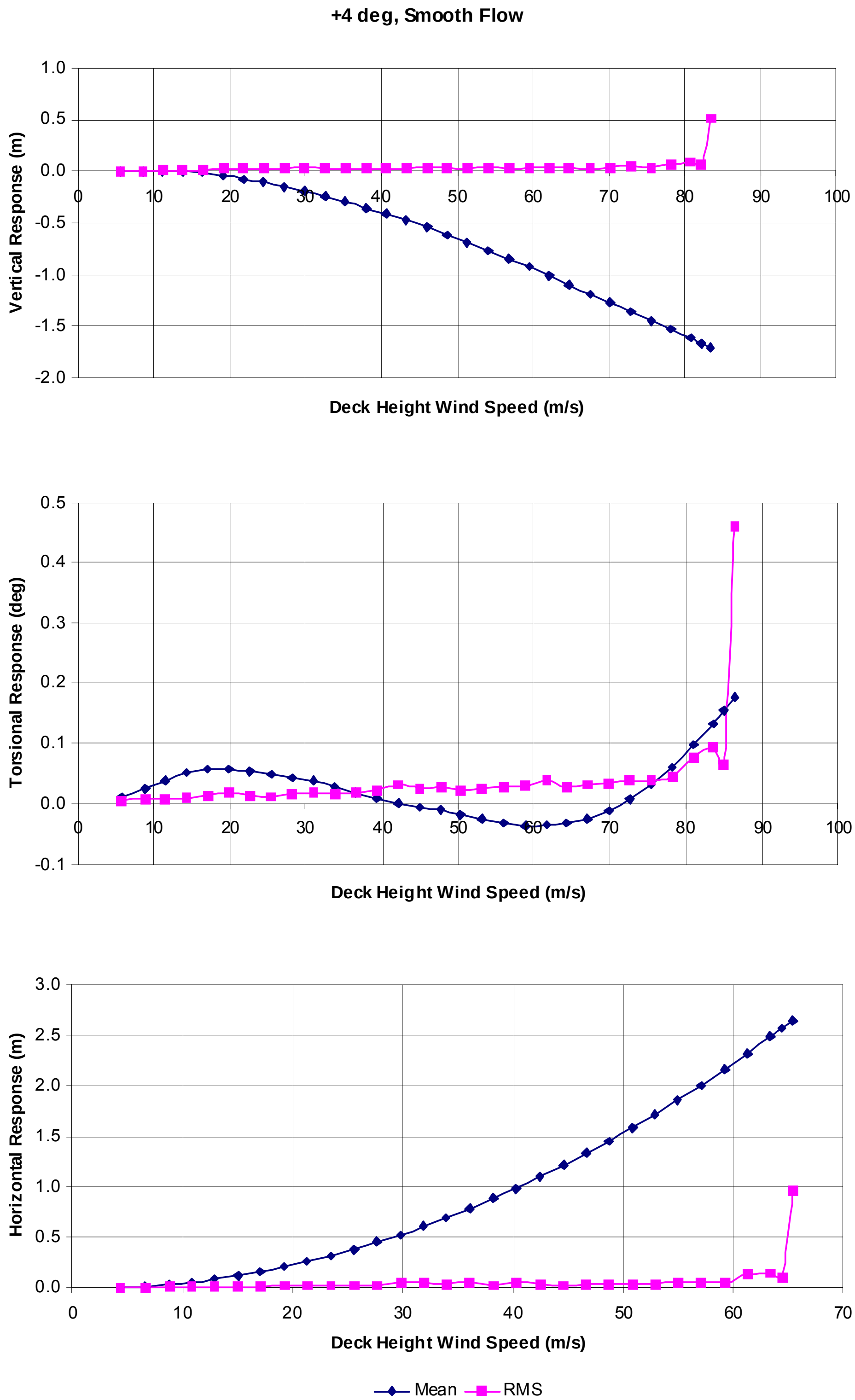

FIGURE 5.6 DYNAMIC TEST AT +4°, SMOOTH FLOW, IN-SERVICE

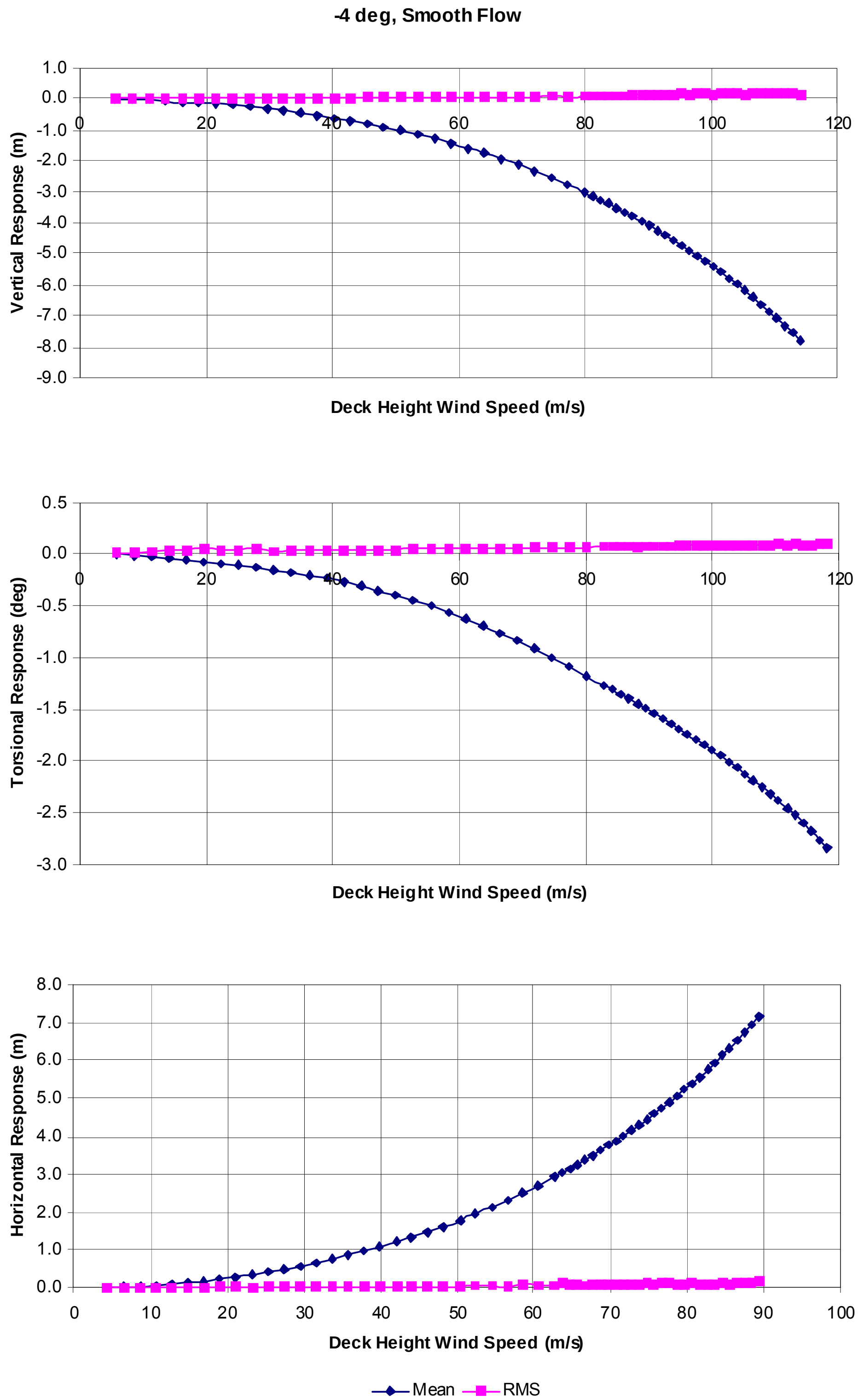

FIGURE 5.7 DYNAMIC TEST AT -4°, SMOOTH FLOW, IN-SERVICE

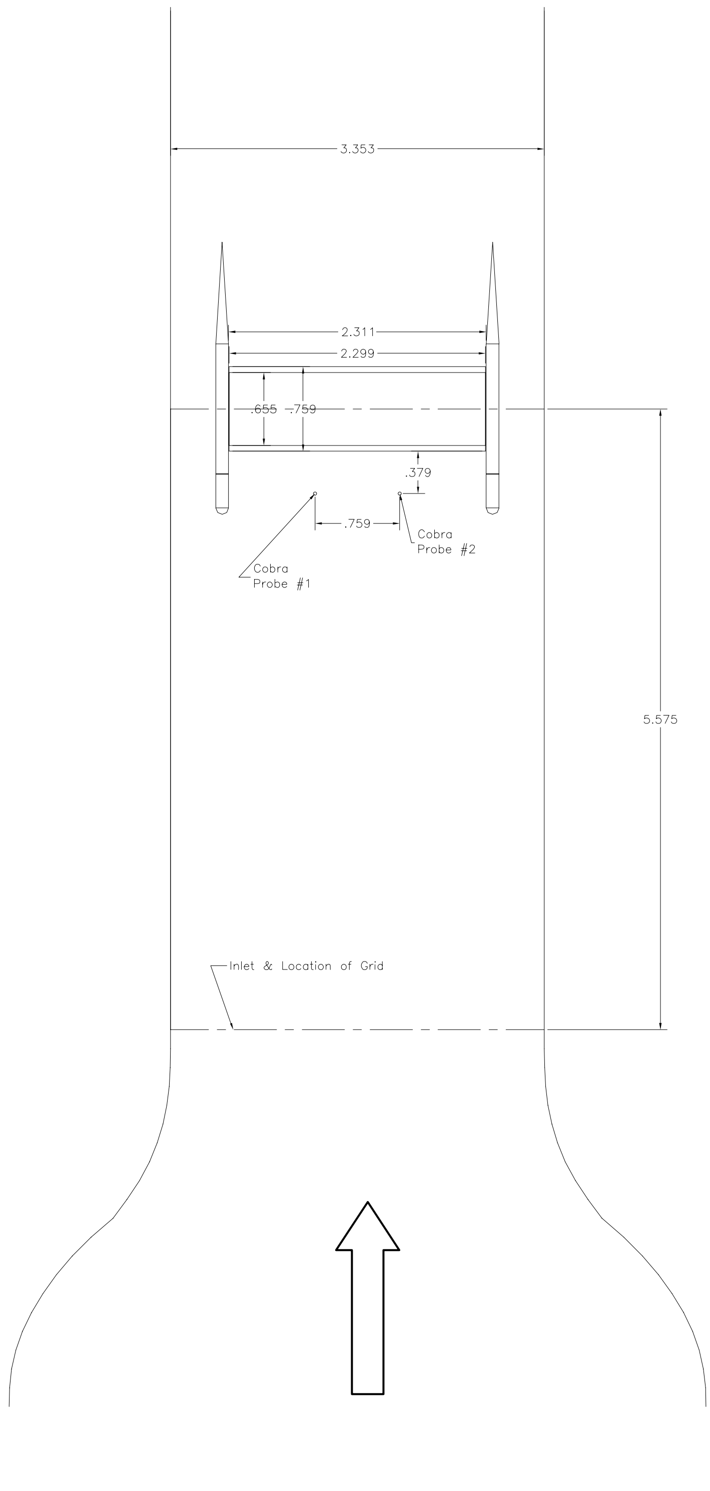

FIGURE 5.8 LOCATION OF COBRA PROBES FOR TURBULENCE MEASUREMENTS

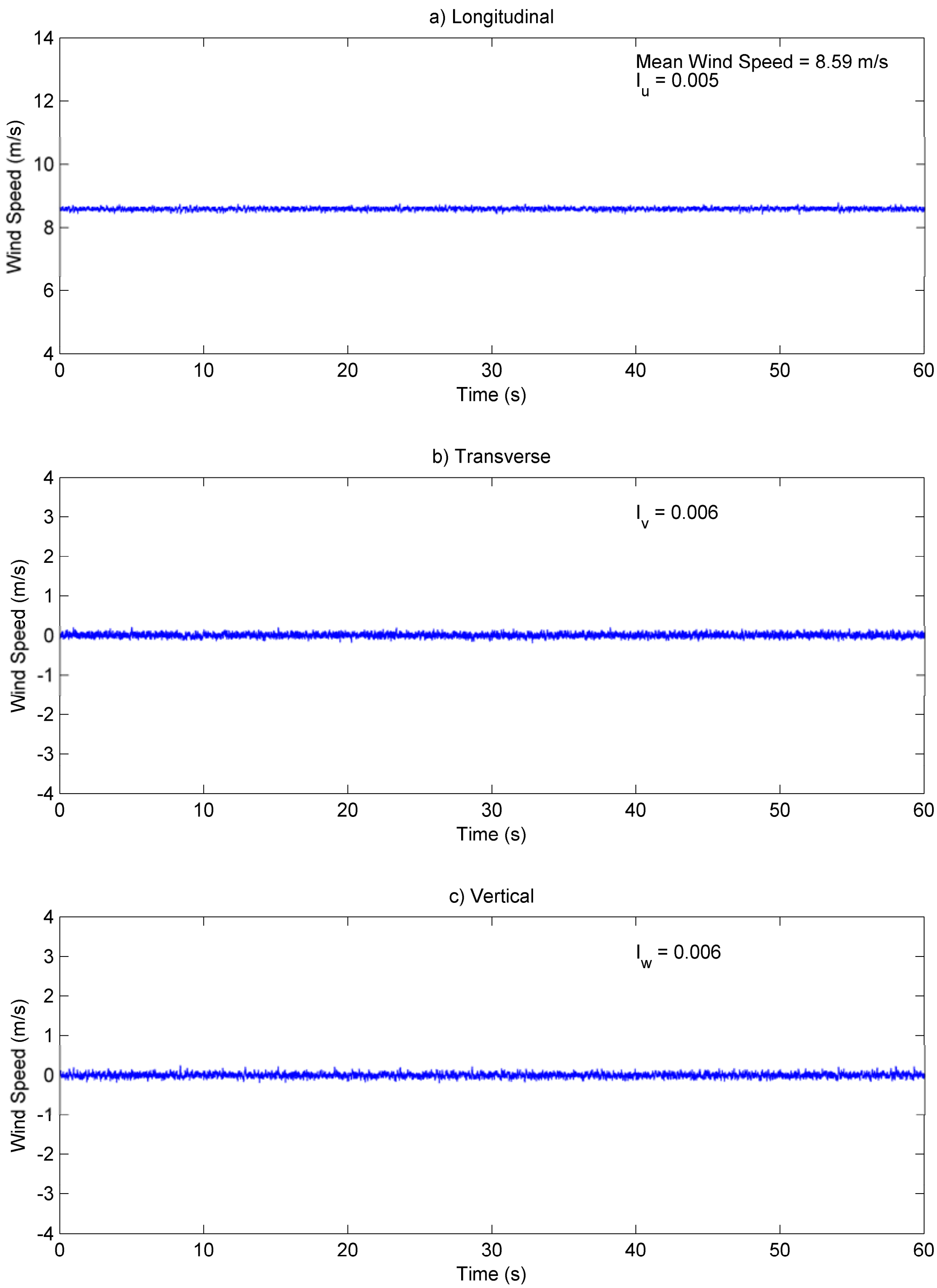

FIGURE 5.9 SMOOTH FLOW TIME HISTORY OF WIND SPEED COMPONENTS (TYPICAL)

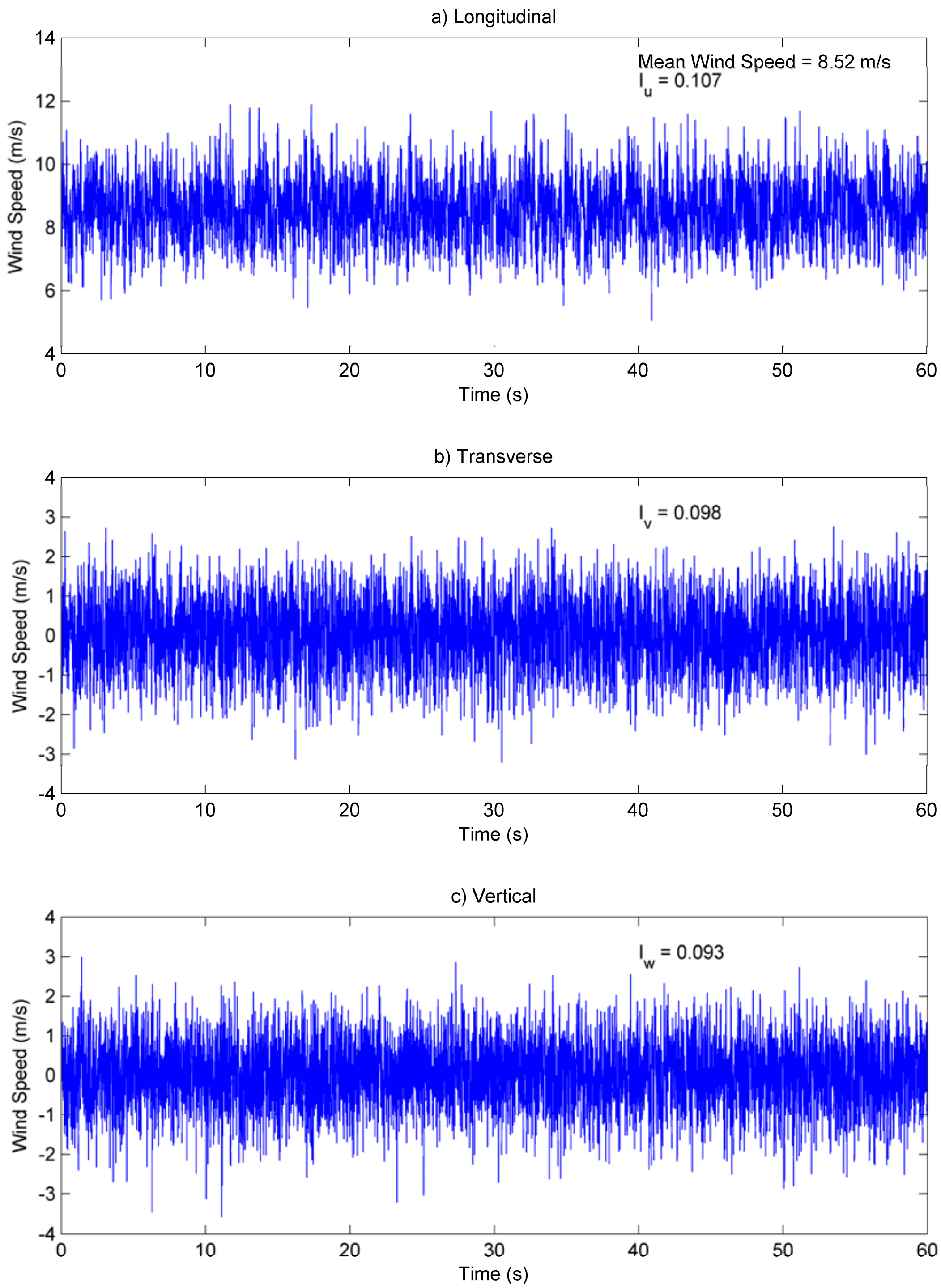

FIGURE 5.10 TURBULENT FLOW TIME HISTORY OF WIND SPEED COMPONENTS (TYPICAL)

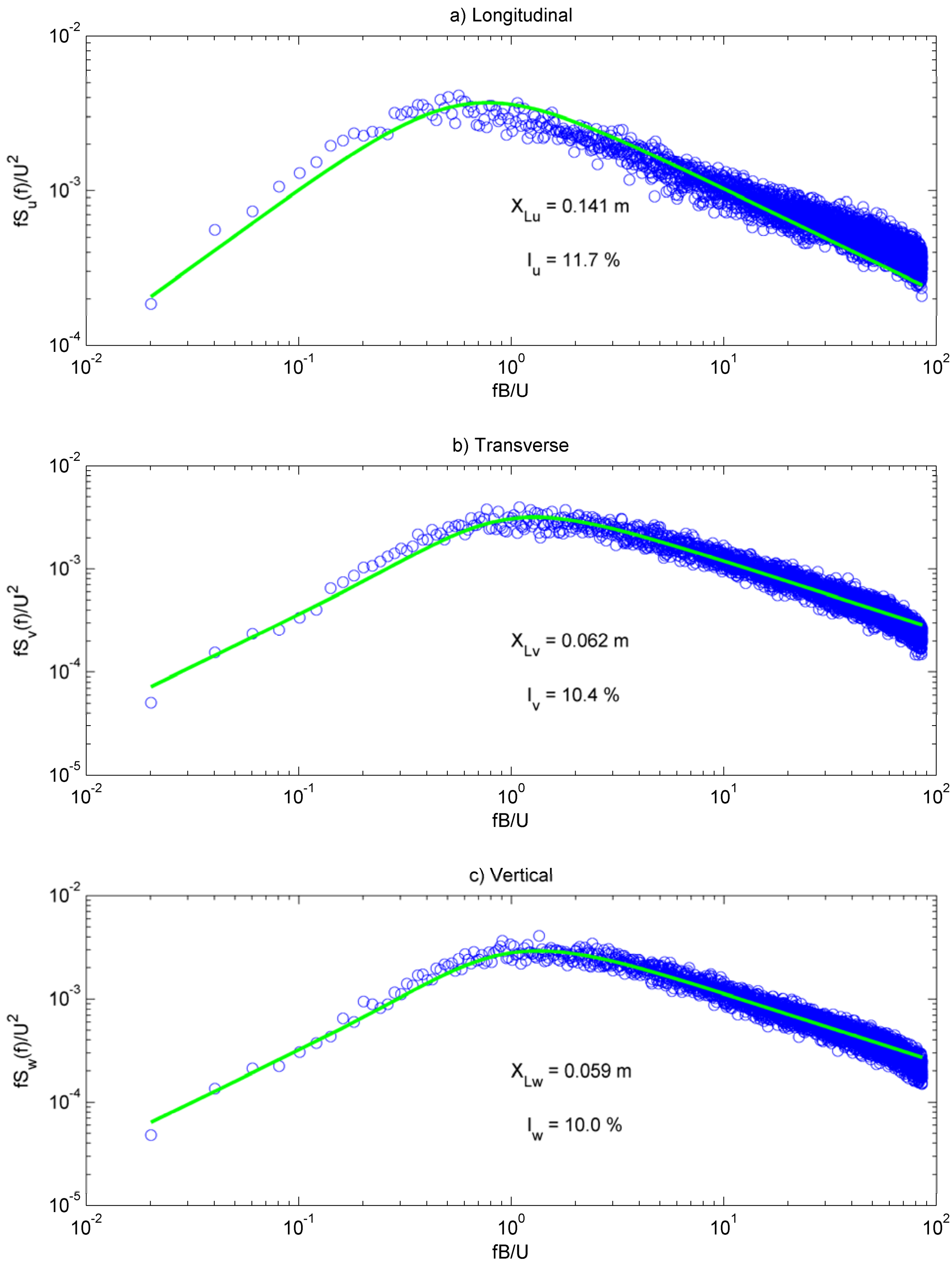

FIGURE 5.11 POWER SPECTRA OF GRID-GENERATED TURBULENCE

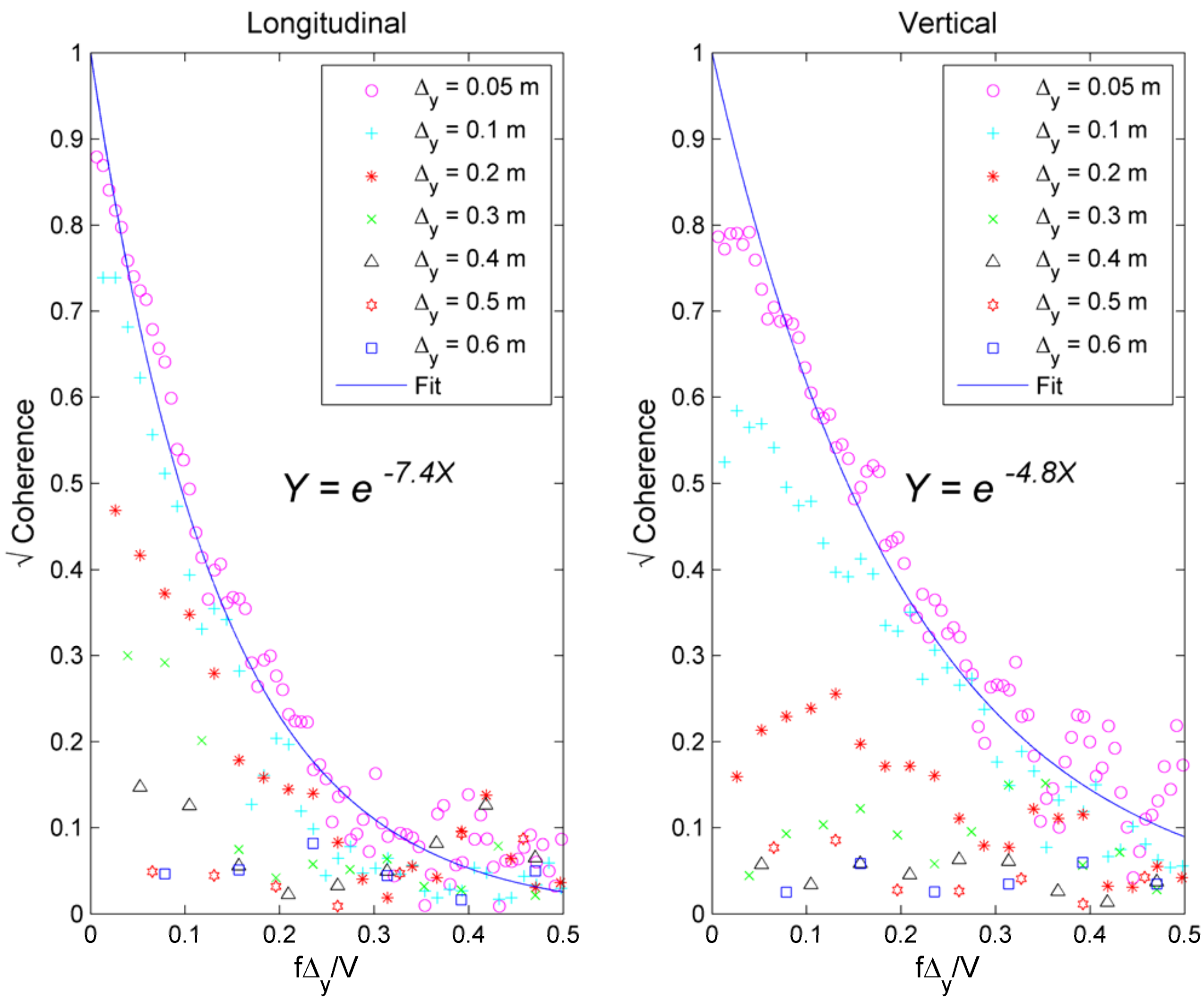

FIGURE 5.12 CORRELATION OF THE LONGITUDINAL AND VERTICAL COMPONENTS OF GRID-GENERATED TURBULENCE

APPENDIX A

THE SECTION MODEL APPROACH FOR THE STUDY OF WIND ACTION ON LONG SPAN BRIDGES

A1 DESIGN OF THE SECTION MODEL

The most elementary of the tools available to the wind engineer for the study of the aerodynamics of long span bridges is the section model. It is also, perhaps the most productive and economical of these tools [A1,A2].

The section model consists of a typical rigid section of the deck, geometrically and aerodynamically similar to the prototype, mounted in the wind tunnel in such a way as to measure the wind produced static and dynamic lift, drag and moment. The model is usually located within the parallel walls of the wind tunnel, or equipped with end plates in order to channel the wind over the deck in a two-dimensional manner.

In a fixed position, the section model can be instrumented to measure lift, drag and torsion either through the mounting of the model on a three component force balance, or on stiff springs to reduce the dynamic motions. The bridge deck is rotated with respect to the oncoming flow to measure the variation in the forces with angle of attack, usually between +15° and -15°. The force coefficients are typically specified as follows:

Lift force per unit length: $$L = \frac{1}{2}\rho V^2 B C_L \qquad \text{(A1)}$$

Drag force per unit length: $$D = \frac{1}{2}\rho V^2 B C_D \qquad \text{(A2)}$$

Torsional force per unit length: $$T = \frac{1}{2}\rho V^2 B^2 C_T \qquad \text{(A3)}$$

Where ρ is the air density, B is the model deck width and C_L, C_D, C_T are dimensionless lift, drag and torsional force coefficients, respectively.

As first used in early applications, the section model was conceived as a substitute for the prototype bridge. Since its dynamics and aerodynamics cannot fully duplicate those of the full scale bridge, interpretation of the results of any section model test is required. Research in recent years has better defined the limited but important role of the section model.

Mounted on springs, with scaled mass per unit length, mass moment of inertia per unit length, structural damping and natural frequencies, the section model is commonly used to investigate the following:

- the dynamic response to vortex shedding
- to ensure that the section is aerodynamically stable to an acceptably high wind speed, given the meteorology of the bridge site
- to determine the response to turbulence

Usually, the effect of turbulence is to reduce the response of the bridge deck to vortex shedding. Consequently, tests are conducted in flow conditions with low turbulence intensity (or, so-called “smooth flow”) in order to conservatively estimate the amplitudes of motion. Various edge treatments can be investigated to improve the response to vortex shedding. The model is also tested with the same low turbulence flow to provide conservative estimates of flutter behaviour of the section. The response is often investigated with several structural damping ratios.

A uniform grid or spires are used to provide simulations of the scaled atmospheric turbulence. Measured response to turbulent buffeting can be interpreted using an appropriate theory to provide estimates of the prototype wind loading that can be used in the design of the bridge.

The section model can also be used to measure the motion-related forces. Mounted on springs, or driven through sinusoidal motions, the section model experiences aerodynamic forces proportional to the bridge motion and the time derivatives of the motion. These so-called “flutter” forces can be measured and used in a dynamic theoretical model of the bridge in order to predict its performance and aerodynamic stability.

A2 DESIGN OF THE SECTION MODEL

Aeroelastic modeling of structures generally requires equality of the following non-dimensional quantities, in addition to an overall geometric similarity [A3, A4, A5]:

- Froude Number (ratio of the gravitational to the inertia forces);
- Cauchy Number (ratio of the elastic to inertia forces);
- Density Ratio (ratio of the inertia force of the structure to that of the flow);
- Damping Ratio
- Reynolds Number (based on the dimensions of the structure)

Froude Number scaling ($F_r = gL/V^2$) is not necessary in section model studies, since the stiffness is supplied by external springing and not due to gravitational effects. *L* is a characteristic dimension, *V* is the wind speed and *g* is the acceleration due to gravity. Cauchy Number is rewritten in terms of *V/(fB)* and provides the link in the wind speeds between model and prototype. *f* is a natural frequency and *B* is the bridge deck width. Density scaling (ρ_s/ρ_α) is important, where the subscripts *s* and *a* refer to the structure and air respectively. This ensures that the mass is scaled correctly, in relation to the added mass of air due to the moving bridge. Equal modal damping (ζ_s in a ratio to critical or δ_s in logarithmic decrement) between model and prototype is required, but exploratory tests are often performed with lower model damping in order to ensure that any instability can readily be identified.

Reynolds Number similarity ($R_e = VL/\nu$, where ν is the kinematic viscosity of the air) is not practical in most cases and section model tests are usually carried out at a Reynolds Number several orders of magnitude lower than that of full scale. For sharp edged bodies such as bridge decks, the effects of this relaxation of R_e scaling is not severe for overall wind induced forces and responses. In the case of the geometric modeling of circular objects such as the cables and handrails, however, R_e effects can be significant and an “equivalent force effect” approach should be taken.

The full scale data that is needed to design the model and springing system consists of:

- a constant mass ($m_v = \rho_s B^2$) per unit length of span, or a calculated value, giving the correct modal mass in the case of a non-uniform span-wise distribution

- a mass moment of inertia ($I_T = \rho_s B^4$) per unit length of span, or a calculated value, as for the mass, in the case of a non-uniform span-wise distribution, or a radius of gyration, *r*, of the mass, m_v

- target values of modal damping for the modes of vibration to be examined (nominally the fundamental vertical and torsional modes)

- natural frequencies of the modes to be examined

- location of the rotation centre of the deck cross section which determines the torsional mode

Most section model rigs have two dominant modes of vibration, namely, vertical and torsional motion. It is through the selection of the springs and the spring spacing that the above scaling is applied. Firstly, the geometric scale factor is selected, along with the model length. Typical geometric scales are in the order of 1:40 to 1:80, in order that deck details are well simulated. The length of the model should be of the order of 4-5 times the deck width in order that correlation effects of the wind on the structure are correct.

The target mass and mass moment of inertia are determined through the expressions above. Before selecting the model support stiffness a target value for the velocity scale factor, $V_{prototype}/V_{model} = (fB)_{prototype}/(fB)_{model}$, is set such that the range of wind speed available in the wind tunnel corresponds to a satisfactory range of wind speeds in the prototype.

It is important to include the model support mass as part of the moving mass of the model as well as providing sufficient model stiffness such that internal flexing or twisting of the model does not occur.

A typical arrangement of springs for the section model rig in use at the Boundary Layer Wind Tunnel Laboratory at the University of Western Ontario is as shown in Figure A1. The arrangement of the model mounting system incorporates radial bearings at the ends of the model at the K_3 support, which allow the locking of vertical or torsional motion to perform single degree of freedom tests.

The following spring stiffnesses are considered:

- k_1 is four main springs above the model, at a spacing *X*

- k_2 is four main springs below the model

- k_3 is four leaf springs in pairs on each end of the model which provide a drag restraint and allows only vertical motion (in other section model rigs, this spring system has often been modelled using a very long drag-wire fore and aft of the model)

- k_{lc} is four load cell transducers

The simplified equation for the natural frequencies of vertical and torsional modes of vibration is:

$$f_V = \frac{1}{2\pi}\sqrt{\frac{k_V}{m}} \qquad \text{(A4)}$$

and:

$$k_v \approx 4k_1 + 2k_3 + 4\frac{1}{\frac{1}{k_2}+\frac{1}{k_k}} \qquad \text{(A5)}$$

also: $f_T = f_v \left(\frac{X}{2r} \right)$ (where r is the radius of gyration and X is the spring spacing)

Dashpots are installed at appropriate locations on the main arms of the rig to provide the desired structural damping in the vertical and torsional modes of vibration. Although with this arrangement of spring supports it is not possible to prevent the model from undesirable rocking modes of vibration, by summing and differencing the load cell outputs, the electrical output from this type of mode can be eliminated.

The spring system is mounted on a frame structure which is independent of the wind tunnel and can accommodate virtually any length of model. The section model test set-up is shown in the wind tunnel in Figure A2 with the turbulence generating grid at the inlet to the test section. The frame structure is enclosed in an aerodynamic fairing system which minimizes the wall boundary layers and helps to ensure homogeneous flow conditions across the span of the model. The springing and dashpot system are shown in Figure A3. With this design, the model can be installed on the rig and calibrated outside of the wind tunnel, providing clear efficiencies in the test procedure. Both static and dynamic calibrations are performed on the model, ensuring that the modal mass and mass moment of inertia are as desired. A relationship between the dynamic deflection and the load cell output is obtained through this calibration, as well as a confirmation of the stiffness of the springing system.

A3 THE SECTION MODEL TEST AND ANALYSIS

The dynamic section model tests are usually comprised of a manual and automatic run. The manual run allows the wind tunnel operator to gradually increase the wind speed, while carefully noting any visual signs of instabilities and establishing a safe upper bound wind speed for the test. A set of wind speeds (~50) are selected and the test repeated under automatic control. Measurements include the time history of the vertical and torsional motions of the model as well as the wind speed. The time history is analyzed on-line and the instantaneous maximum, minimum, root-mean-square (RMS) and mean value is recorded. A Leiblein analysis of the peaks is also performed. This is repeated for each of the desired wind speeds. Additional wind speeds are set in the vicinity of any vortex shedding peaks in order to establish the response peak.

The presence of a vortex shedding peak or flutter instability is obvious from an examination of the response data. This type of instability is marked as a change in the response from a random motion to a sinusoidal motion. An examination of the “peak factor” (or the ratio of the peak to RMS value) clearly indicates this change. The peak factor for random motion is of the order of 3-4 while that for a pure sinusoid is $\sqrt{2}$.

The tests are performed both for uniform flow and for grid-generated turbulent flow conditions. The results in turbulent flow are often used in an analysis of Equivalent Static Loads, which effectively translate the results from the section model tests into effective loads which can be used for design [A6].

REFERENCES - APPENDIX A

A1. “Manual of Practice for Wind Tunnel Tests of Buildings and Structures”, American Society of Civil Engineers - Aerospace Division, New York, NY, June 1997.

A2. Hjorth-Hansen, E., "Section Model Tests", Proc. Aerodynamics of Large Bridges, Balkema, Rotterdam, 1992.

A3. Davenport, A.G. and Isyumov, N., "The Application of the Boundary Layer Wind Tunnel to the Prediction of Wind Loading", Proceedings of the Int. Res. Sem., N.R.C., Ottawa, Canada, September 1967, Vol. 1, Univ. of Toronto Press.

A4. Davenport, A.G. and King, J.P.C., "A Study of Wind Effects for the Sunshine Skyway Bridge, Tampa, Florida - Concrete Alternate", The University of Western Ontario, Faculty of Engineering Science Research Report, BLWT-SS24-1982, London, Ontario, Canada, 1982.

A5. Davenport, A.G. and King, J.P.C., "A Study of Wind Effects for the Sunshine Skyway Bridge, Tampa, Florida - Steel Alternate", The University of Western Ontario, Faculty of Engineering Science Research Report, BLWT-SS25-1982, The University of Western Ontario, London, Ontario, Canada, 1982.

A6. Davenport, A.G. and King, J.P.C., "Dynamic Wind Forces on Long Span Bridges", 12th IABSE Congress, Vancouver, Canada, September 1984.

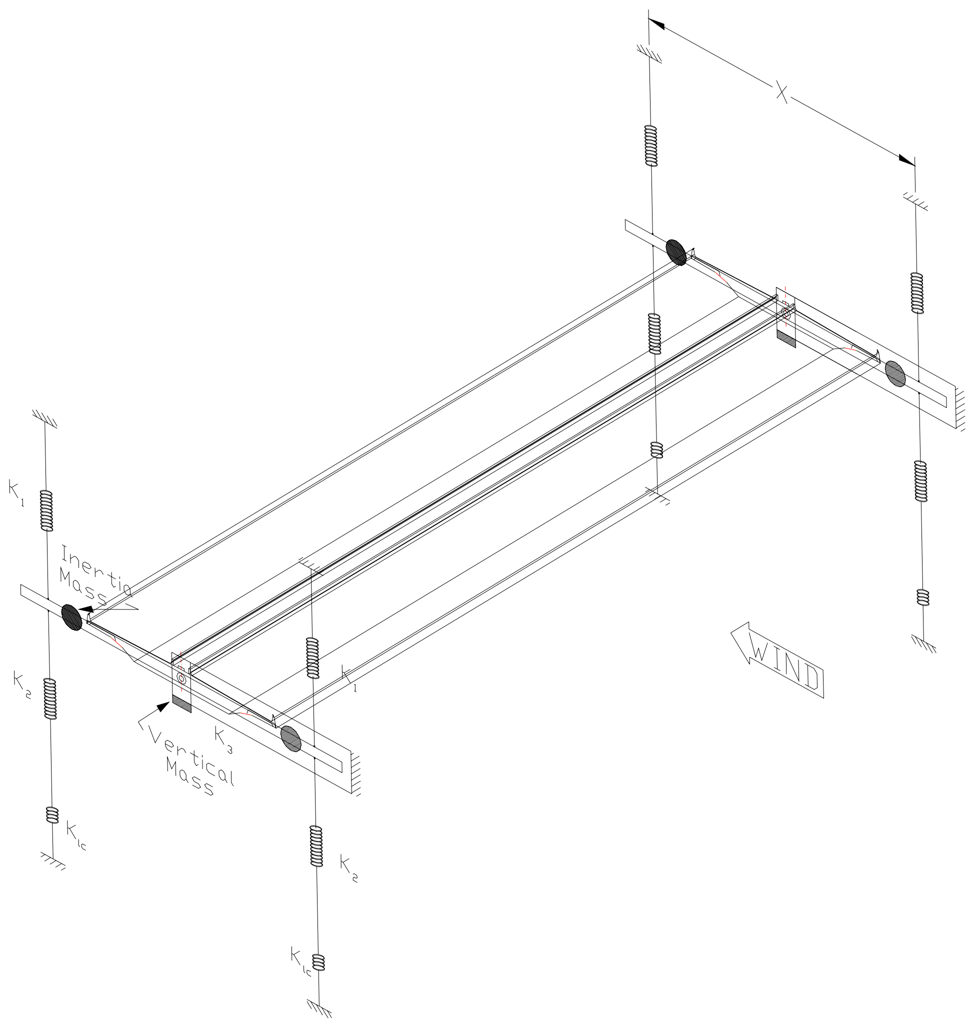

FIGURE A1 DYNAMIC SECTION MODEL RIG

FIGURE A2   2.7m LONG DYNAMIC SECTION MODEL

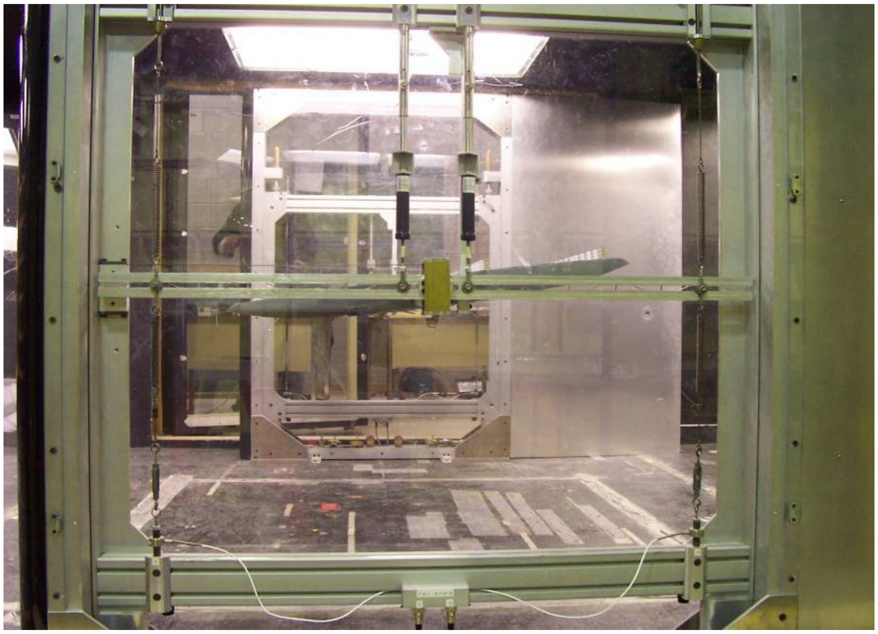

FIGURE A3 DETAILS OF DYNAMIC TEST RIG

APPENDIX B

FLUTTER INSTABILITY CRITERIA

The definition of “flutter” used in this report is related to the “peak factor”, which is defined as the ratio of the largest observed reading during the sample period to the Root Mean Square (RMS) of the sample. Each of the data points on the response plots result from the measurements of real, stable, limited amplitude motion as opposed to a negative total damping case where the amplitude continues to grow in magnitude for the same wind speed. The peak factor can be used to see whether the motion is in a “locked-in” state of sinusoidal motion or only a random type motion.

The onset of a “flutter instability” is defined as when the character of the response changes from a random type motion to that of a regular, sinusoidal motion, involving either pure torsional or a coupled vertical-torsional vibration. This can be clearly identified through an examination of the peak factor. A random signal has peak factors in the 3-4 range, while a sinusoid has a peak factor of $\sqrt{2}$ or 1.41. For the purposes of this investigation, a peak factor of less than 2 was selected as the governing criteria.

There are other definitions of flutter that have been used by this Laboratory and other researchers. One could determine a limiting amplitude beyond which the response is unacceptable. This criterion was used for the Tsing Ma Bridge [C1] and Ting Kau Bridge [C2] studies with a limiting RMS torsional amplitude of 0.5^o (or a peak amplitude of 3.5^o on the response plots).

Another method, has been also used, is based on the steepness of the response curves with wind speed to determine flutter instability. This has some logic associated with it since there is a very definite chance in the character of the response from a uniform, steady growth with wind speed to that which is becoming alarmingly violent. However, the steepness of the curves is highly dependent on the total damping of the structure (structure plus aerodynamic damping). In the low wind speed areas, the structural term dominates (or the aerodynamic term is positive). In the high wind speed range, the aerodynamic term dominates and is negative, but does not yet exceed the structural term in magnitude. Infinite amplitudes occur when the total damping becomes equal to zero or negative, since response is inversely proportional to the total damping.

REFERENCES - APPENDIX B

B1. King, J.P.C. and Davenport, A.G., "Lantau Fixed Crossing - Tsing Ma Bridge, Full Aeroelastic Model Tests of In-service", The University of Western Ontario, Faculty of Engineering Science Research Report, BLWT-SS11-1997, London, Ontario, Canada, 1997.

B2. King, J.P.C. and Davenport, A.G., "Ting Kau Bridge - Wind Tunnel Report", The University of Western Ontario, Faculty of Engineering Science Research Report, BLWT-SS29-1995, London, Ontario, Canada, 1995.

APPENDIX C

RESULTS OF STATIC SECTION MODEL TESTS

Notes:

C1. The static section model tests were performed for two bridge deck configurations: A) the in-service structure and B) the under construction stage with all deck furniture removed from the upper surface of the bridge deck (i.e. wind screens, inner and outer safety screens, crash barriers, light masts, catenary masts and rail platforms).

C2. A typical force coefficient is defined as follows:

$$C_{x,z,l,d} = \frac{F_{x,z,l,d}}{qB}$$

in which *C* is an aerodynamic coefficient, *F* is the mean aerodynamic force per unit length of the model, model length L (including triangular insert pieces), $q = \frac{1}{2}\rho V^2$ is the mean wind velocity pressure at deck level, ρ is the density of air (1.25 kg/m^3), *V* is the mean wind velocity at deck level in m/s, and *B* is the bridge deck width. The subscripts *x,z,l,d* refer to the X and Z body force components and lift and drag respectively. It is important to note that C_x, C_z and C_m are "Body-Force Coefficients", however are relative to the longitudinal axis of the wind tunnel and not aligned perpendicular to the axis of the model.

The torque coefficient is defined:

$$C_m = \frac{F_t}{qB^2}$$

TABLE C1 STATIC FORCE COEFFICIENTS, SMOOTH FLOW, UNDER CONSTRUCTION STAGE, SKEW=0°

Reynolds Number = 1.0 × 10^6					
Angle of Attack (degrees)	C_X	C_Z	C_m	C_D	C_L
-10	0.038	-0.536	-0.040	0.131	-0.522
-9.5	0.039	-0.517	-0.039	0.124	-0.504
-9	0.039	-0.497	-0.038	0.117	-0.485
-8.5	0.040	-0.477	-0.036	0.110	-0.466
-8	0.040	-0.455	-0.035	0.103	-0.445
-7.5	0.041	-0.434	-0.034	0.097	-0.424
-7	0.042	-0.413	-0.033	0.092	-0.404
-6.5	0.042	-0.392	-0.032	0.086	-0.384
-6	0.042	-0.372	-0.031	0.081	-0.366
-5.5	0.042	-0.352	-0.031	0.075	-0.347
-5	0.041	-0.331	-0.029	0.070	-0.326
-4.5	0.041	-0.306	-0.026	0.065	-0.302
-4	0.041	-0.279	-0.023	0.060	-0.276
-3.5	0.040	-0.251	-0.020	0.056	-0.248
-3	0.039	-0.224	-0.017	0.051	-0.222
-2.5	0.038	-0.199	-0.014	0.047	-0.197
-2	0.038	-0.175	-0.012	0.044	-0.174
-1.5	0.037	-0.152	-0.008	0.041	-0.151
-1	0.038	-0.131	-0.005	0.040	-0.130
-0.5	0.039	-0.110	-0.002	0.040	-0.110
0	0.041	-0.088	0.001	0.041	-0.088
0.5	0.042	-0.067	0.004	0.041	-0.067
1	0.043	-0.048	0.007	0.042	-0.048
1.5	0.045	-0.027	0.011	0.044	-0.029
2	0.047	-0.007	0.014	0.046	-0.009
2.5	0.049	0.010	0.017	0.049	0.008
3	0.052	0.025	0.019	0.053	0.022
3.5	0.055	0.036	0.020	0.057	0.033
4	0.059	0.046	0.020	0.062	0.042
4.5	0.062	0.056	0.021	0.066	0.051
5	0.065	0.067	0.021	0.071	0.061
5.5	0.068	0.078	0.022	0.076	0.071
6	0.072	0.089	0.023	0.080	0.081
6.5	0.075	0.099	0.023	0.085	0.090
7	0.078	0.109	0.023	0.090	0.099
7.5	0.080	0.119	0.023	0.095	0.107
8	0.083	0.129	0.024	0.100	0.116
8.5	0.085	0.142	0.025	0.105	0.128
9	0.087	0.156	0.027	0.110	0.140
9.5	0.089	0.168	0.028	0.115	0.151
10	0.090	0.179	0.029	0.120	0.161

TABLE C2 STATIC FORCE COEFFICIENTS, TURBULENT FLOW, UNDER CONSTRUCTION STAGE, SKEW=0°

Reynolds Number = 7.7 × 10^5					
Angle of Attack (degrees)	C_X	C_Z	C_m	C_D	C_L
-10	0.031	-0.444	-0.039	0.107	-0.432
-9.5	0.031	-0.423	-0.037	0.100	-0.412
-9	0.032	-0.408	-0.036	0.095	-0.398
-8.5	0.032	-0.393	-0.035	0.090	-0.384
-8	0.033	-0.373	-0.033	0.084	-0.365
-7.5	0.033	-0.353	-0.031	0.078	-0.345
-7	0.033	-0.337	-0.030	0.074	-0.331
-6.5	0.033	-0.316	-0.028	0.069	-0.311
-6	0.033	-0.301	-0.027	0.065	-0.296
-5.5	0.033	-0.283	-0.025	0.060	-0.279
-5	0.033	-0.262	-0.023	0.056	-0.258
-4.5	0.033	-0.243	-0.022	0.052	-0.240
-4	0.032	-0.223	-0.020	0.048	-0.220
-3.5	0.032	-0.202	-0.017	0.044	-0.200
-3	0.032	-0.181	-0.015	0.041	-0.179
-2.5	0.032	-0.162	-0.013	0.039	-0.160
-2	0.032	-0.143	-0.011	0.037	-0.142
-1.5	0.032	-0.126	-0.009	0.036	-0.125
-1	0.033	-0.108	-0.006	0.035	-0.108
-0.5	0.033	-0.093	-0.004	0.034	-0.092
0	0.034	-0.076	-0.002	0.034	-0.076
0.5	0.036	-0.061	0.000	0.035	-0.061
1	0.037	-0.046	0.002	0.036	-0.046
1.5	0.039	-0.031	0.004	0.038	-0.032
2	0.040	-0.017	0.006	0.040	-0.019
2.5	0.042	-0.004	0.008	0.042	-0.006
3	0.044	0.009	0.009	0.045	0.007
3.5	0.046	0.022	0.011	0.048	0.019
4	0.049	0.034	0.012	0.051	0.030
4.5	0.051	0.046	0.014	0.054	0.042
5	0.053	0.058	0.015	0.058	0.053
5.5	0.055	0.069	0.016	0.062	0.063
6	0.057	0.079	0.017	0.065	0.073
6.5	0.059	0.090	0.018	0.069	0.083
7	0.060	0.099	0.019	0.072	0.091
7.5	0.063	0.109	0.019	0.077	0.100
8	0.065	0.120	0.020	0.081	0.110
8.5	0.067	0.130	0.021	0.086	0.119
9	0.069	0.139	0.021	0.089	0.126
9.5	0.070	0.147	0.021	0.094	0.133
10	0.072	0.156	0.022	0.098	0.142

TABLE C3 STATIC FORCE COEFFICIENTS, SMOOTH FLOW, IN-SERVICE, NO TRAFFIC, SKEW=0^{O}

Reynolds Number = 9.0×10^5					
Angle of Attack (degrees)	C_X	C_Z	C_m	C_D	C_L
-10	0.162	-0.277	-0.017	0.208	-0.245
-9.5	0.158	-0.261	-0.016	0.199	-0.231
-9	0.154	-0.245	-0.016	0.190	-0.218
-8.5	0.150	-0.231	-0.015	0.182	-0.206
-8	0.145	-0.216	-0.014	0.174	-0.194
-7.5	0.141	-0.201	-0.013	0.166	-0.181
-7	0.136	-0.186	-0.013	0.158	-0.168
-6.5	0.131	-0.171	-0.013	0.150	-0.155
-6	0.127	-0.156	-0.013	0.142	-0.142
-5.5	0.122	-0.143	-0.013	0.135	-0.131
-5	0.117	-0.131	-0.013	0.128	-0.120
-4.5	0.112	-0.121	-0.013	0.121	-0.112
-4	0.108	-0.112	-0.013	0.115	-0.104
-3.5	0.103	-0.104	-0.013	0.110	-0.098
-3	0.099	-0.098	-0.013	0.104	-0.092
-2.5	0.096	-0.093	-0.012	0.100	-0.088
-2	0.092	-0.089	-0.011	0.095	-0.085
-1.5	0.089	-0.086	-0.010	0.092	-0.083
-1	0.087	-0.084	-0.009	0.089	-0.082
-0.5	0.086	-0.082	-0.008	0.087	-0.082
0	0.085	-0.082	-0.007	0.085	-0.082
0.5	0.086	-0.081	-0.005	0.085	-0.081
1	0.087	-0.080	-0.004	0.085	-0.081
1.5	0.089	-0.078	-0.003	0.087	-0.081
2	0.092	-0.076	-0.002	0.089	-0.080
2.5	0.096	-0.074	-0.002	0.093	-0.079
3	0.100	-0.072	-0.001	0.096	-0.077
3.5	0.104	-0.068	0.000	0.100	-0.074
4	0.109	-0.062	0.001	0.104	-0.070
4.5	0.114	-0.056	0.002	0.109	-0.064
5	0.119	-0.048	0.003	0.115	-0.059
5.5	0.125	-0.041	0.004	0.120	-0.053
6	0.130	-0.034	0.004	0.126	-0.047
6.5	0.136	-0.026	0.006	0.132	-0.041
7	0.141	-0.019	0.006	0.138	-0.036
7.5	0.147	-0.011	0.007	0.144	-0.031
8	0.153	-0.005	0.008	0.150	-0.026
8.5	0.159	0.001	0.008	0.157	-0.023
9	0.165	0.006	0.008	0.164	-0.020
9.5	0.171	0.014	0.008	0.171	-0.014
10	0.175	0.024	0.009	0.176	-0.007

TABLE C4 STATIC FORCE COEFFICIENTS, TURBULENT FLOW, IN-SERVICE, NO TRAFFIC, SKEW=0°

Reynolds Number = 5.9 × 10^5					
Angle of Attack (degrees)	C_X	C_Z	C_m	C_D	C_L
-10	0.139	-0.284	-0.021	0.186	-0.256
-9.5	0.136	-0.272	-0.020	0.179	-0.246
-9	0.132	-0.256	-0.019	0.171	-0.232
-8.5	0.128	-0.242	-0.019	0.163	-0.221
-8	0.124	-0.225	-0.018	0.154	-0.206
-7.5	0.120	-0.212	-0.017	0.147	-0.195
-7	0.117	-0.201	-0.017	0.141	-0.185
-6.5	0.114	-0.188	-0.016	0.134	-0.174
-6	0.109	-0.175	-0.016	0.127	-0.163
-5.5	0.105	-0.164	-0.015	0.121	-0.153
-5	0.102	-0.153	-0.015	0.115	-0.144
-4.5	0.099	-0.144	-0.014	0.110	-0.136
-4	0.097	-0.136	-0.014	0.106	-0.129
-3.5	0.094	-0.127	-0.013	0.102	-0.121
-3	0.092	-0.120	-0.012	0.098	-0.115
-2.5	0.090	-0.113	-0.011	0.095	-0.109
-2	0.088	-0.105	-0.010	0.092	-0.102
-1.5	0.087	-0.098	-0.009	0.090	-0.096
-1	0.087	-0.092	-0.008	0.088	-0.090
-0.5	0.086	-0.084	-0.007	0.087	-0.084
0	0.086	-0.077	-0.007	0.086	-0.077
0.5	0.087	-0.070	-0.006	0.086	-0.071
1	0.088	-0.064	-0.005	0.087	-0.065
1.5	0.090	-0.057	-0.004	0.088	-0.059
2	0.092	-0.050	-0.004	0.090	-0.053
2.5	0.094	-0.044	-0.003	0.092	-0.048
3	0.097	-0.037	-0.003	0.095	-0.042
3.5	0.100	-0.031	-0.002	0.098	-0.037
4	0.104	-0.025	-0.002	0.102	-0.032
4.5	0.107	-0.019	-0.001	0.105	-0.027
5	0.111	-0.013	0.000	0.109	-0.022
5.5	0.114	-0.007	0.000	0.113	-0.018
6	0.118	-0.001	0.001	0.117	-0.013
6.5	0.122	0.005	0.002	0.122	-0.009
7	0.126	0.010	0.003	0.126	-0.005
7.5	0.129	0.016	0.004	0.131	-0.001
8	0.133	0.023	0.005	0.135	0.004
8.5	0.137	0.029	0.006	0.140	0.009
9	0.140	0.036	0.007	0.144	0.014
9.5	0.144	0.043	0.008	0.149	0.019
10	0.147	0.050	0.009	0.154	0.024

TABLE C5 STATIC FORCE COEFFICIENTS, SMOOTH FLOW, IN-SERVICE, TRAFFIC CONDITION 1, SKEW=0^{O}

Reynolds Number = 6.4 × 10^5					
Angle of Attack (degree)	C_X	C_Z	C_m	C_D	C_L
-10	0.179	-0.203	-0.012	0.211	-0.169
-9.5	0.173	-0.185	-0.012	0.201	-0.154
-9	0.166	-0.166	-0.012	0.190	-0.137
-8.5	0.162	-0.154	-0.012	0.183	-0.128
-8	0.158	-0.143	-0.011	0.176	-0.120
-7.5	0.153	-0.132	-0.010	0.169	-0.111
-7	0.149	-0.122	-0.009	0.162	-0.103
-6.5	0.144	-0.111	-0.008	0.155	-0.094
-6	0.139	-0.101	-0.007	0.148	-0.086
-5.5	0.134	-0.091	-0.007	0.142	-0.078
-5	0.129	-0.082	-0.007	0.135	-0.071
-4.5	0.124	-0.074	-0.007	0.130	-0.064
-4	0.119	-0.068	-0.008	0.124	-0.059
-3.5	0.115	-0.062	-0.008	0.119	-0.055
-3	0.111	-0.058	-0.008	0.114	-0.053
-2.5	0.107	-0.056	-0.008	0.109	-0.051
-2	0.103	-0.054	-0.008	0.105	-0.051
-1.5	0.100	-0.053	-0.008	0.101	-0.051
-1	0.098	-0.053	-0.007	0.099	-0.052
-0.5	0.096	-0.054	-0.007	0.097	-0.053
0	0.095	-0.055	-0.006	0.095	-0.055
0.5	0.095	-0.056	-0.005	0.095	-0.057
1	0.096	-0.057	-0.004	0.095	-0.059
1.5	0.098	-0.058	-0.003	0.096	-0.060
2	0.100	-0.058	-0.003	0.098	-0.061
2.5	0.103	-0.057	-0.002	0.101	-0.062
3	0.107	-0.056	-0.002	0.104	-0.062
3.5	0.112	-0.055	-0.002	0.109	-0.062
4	0.117	-0.054	-0.002	0.113	-0.062
4.5	0.122	-0.050	-0.002	0.118	-0.059
5	0.128	-0.045	-0.002	0.124	-0.056
5.5	0.134	-0.040	-0.001	0.129	-0.052
6	0.139	-0.034	0.000	0.134	-0.048
6.5	0.144	-0.029	0.001	0.140	-0.045
7	0.149	-0.023	0.001	0.145	-0.041
7.5	0.154	-0.016	0.002	0.151	-0.036
8	0.160	-0.009	0.003	0.157	-0.031
8.5	0.164	0.001	0.005	0.163	-0.023
9	0.166	0.019	0.009	0.167	-0.007
9.5	0.168	0.037	0.013	0.172	0.009
10	0.170	0.055	0.017	0.177	0.024

TABLE C6 STATIC FORCE COEFFICIENTS, TURBULENT FLOW, IN-SERVICE, TRAFFIC CONDITION 1, SKEW=0^{O}

Reynolds Number = 5.6×10^5					
Angle of Attack (degree)	C_X	C_Z	C_m	C_D	C_L
-10	0.154	-0.216	-0.007	0.189	-0.186
-9.5	0.151	-0.204	-0.007	0.182	-0.176
-9	0.147	-0.190	-0.007	0.175	-0.165
-8.5	0.143	-0.178	-0.007	0.168	-0.154
-8	0.141	-0.168	-0.007	0.163	-0.146
-7.5	0.137	-0.157	-0.007	0.156	-0.138
-7	0.132	-0.145	-0.007	0.148	-0.128
-6.5	0.127	-0.134	-0.007	0.142	-0.118
-6	0.124	-0.126	-0.008	0.136	-0.112
-5.5	0.120	-0.117	-0.008	0.131	-0.105
-5	0.116	-0.109	-0.008	0.125	-0.098
-4.5	0.113	-0.102	-0.008	0.120	-0.093
-4	0.110	-0.096	-0.008	0.117	-0.088
-3.5	0.107	-0.090	-0.008	0.112	-0.083
-3	0.104	-0.084	-0.008	0.109	-0.078
-2.5	0.101	-0.079	-0.008	0.105	-0.074
-2	0.099	-0.074	-0.007	0.102	-0.070
-1.5	0.097	-0.069	-0.007	0.099	-0.066
-1	0.096	-0.064	-0.007	0.097	-0.063
-0.5	0.095	-0.060	-0.006	0.096	-0.059
0	0.096	-0.056	-0.006	0.096	-0.056
0.5	0.095	-0.051	-0.006	0.094	-0.051
1	0.097	-0.047	-0.005	0.096	-0.049
1.5	0.098	-0.042	-0.005	0.097	-0.045
2	0.100	-0.038	-0.004	0.098	-0.041
2.5	0.101	-0.033	-0.004	0.100	-0.038
3	0.104	-0.029	-0.004	0.102	-0.035
3.5	0.106	-0.024	-0.003	0.105	-0.031
4	0.112	-0.021	-0.003	0.110	-0.028
4.5	0.113	-0.016	-0.002	0.111	-0.025
5	0.116	-0.011	-0.002	0.115	-0.021
5.5	0.120	-0.006	-0.001	0.119	-0.017
6	0.125	-0.002	0.000	0.124	-0.015
6.5	0.127	0.003	0.001	0.127	-0.011
7	0.131	0.009	0.002	0.131	-0.007
7.5	0.134	0.015	0.003	0.135	-0.003
8	0.138	0.021	0.004	0.140	0.002
8.5	0.143	0.027	0.005	0.145	0.006
9	0.146	0.034	0.006	0.150	0.011
9.5	0.150	0.041	0.007	0.155	0.016
10	0.153	0.049	0.008	0.159	0.022

TABLE C7 STATIC FORCE COEFFICIENTS, SMOOTH FLOW, IN-SERVICE, TRAFFIC CONDITION 2, SKEW=0^{O}

Reynolds Number = 6.5 × 10^5					
Angle of Attack (degree)	C_X	C_Z	C_m	C_D	C_L
-10	0.167	-0.207	-0.027	0.200	-0.174
-9.5	0.162	-0.192	-0.026	0.191	-0.162
-9	0.156	-0.178	-0.025	0.182	-0.151
-8.5	0.153	-0.168	-0.024	0.176	-0.143
-8	0.149	-0.158	-0.022	0.169	-0.135
-7.5	0.145	-0.147	-0.021	0.163	-0.127
-7	0.141	-0.137	-0.019	0.157	-0.119
-6.5	0.137	-0.126	-0.017	0.151	-0.110
-6	0.133	-0.115	-0.016	0.144	-0.100
-5.5	0.129	-0.104	-0.014	0.138	-0.092
-5	0.124	-0.094	-0.013	0.132	-0.083
-4.5	0.120	-0.086	-0.012	0.127	-0.076
-4	0.116	-0.078	-0.011	0.121	-0.070
-3.5	0.111	-0.073	-0.011	0.115	-0.066
-3	0.107	-0.068	-0.011	0.110	-0.062
-2.5	0.103	-0.066	-0.011	0.105	-0.061
-2	0.099	-0.064	-0.010	0.101	-0.061
-1.5	0.095	-0.064	-0.010	0.097	-0.061
-1	0.093	-0.063	-0.009	0.094	-0.062
-0.5	0.091	-0.063	-0.008	0.092	-0.063
0	0.090	-0.064	-0.007	0.090	-0.064
0.5	0.089	-0.064	-0.006	0.089	-0.065
1	0.090	-0.065	-0.005	0.089	-0.067
1.5	0.091	-0.066	-0.004	0.090	-0.068
2	0.093	-0.067	-0.003	0.091	-0.070
2.5	0.097	-0.067	-0.003	0.094	-0.071
3	0.101	-0.066	-0.002	0.097	-0.071
3.5	0.105	-0.065	-0.002	0.101	-0.071
4	0.110	-0.063	-0.002	0.106	-0.071
4.5	0.116	-0.058	-0.001	0.111	-0.067
5	0.121	-0.051	-0.001	0.116	-0.062
5.5	0.127	-0.044	0.000	0.122	-0.056
6	0.132	-0.038	0.001	0.127	-0.052
6.5	0.137	-0.031	0.002	0.132	-0.047
7	0.142	-0.025	0.003	0.138	-0.042
7.5	0.147	-0.018	0.004	0.143	-0.037
8	0.150	-0.001	0.007	0.148	-0.022
8.5	0.148	0.028	0.015	0.151	0.005
9	0.151	0.043	0.018	0.156	0.019
9.5	0.154	0.055	0.020	0.161	0.029
10	0.157	0.067	0.022	0.166	0.039

TABLE C8 STATIC FORCE COEFFICIENTS, TURBULENT FLOW, IN-SERVICE, TRAFFIC CONDITION 2, SKEW=0°

Reynolds Number = 5.6×10^5					
Angle of Attack (degree)	C_X	C_Z	C_m	C_D	C_L
-10	0.156	-0.220	-0.019	0.192	-0.189
-9.5	0.152	-0.207	-0.018	0.184	-0.179
-9	0.147	-0.194	-0.018	0.176	-0.169
-8.5	0.143	-0.183	-0.017	0.169	-0.160
-8	0.139	-0.172	-0.017	0.162	-0.151
-7.5	0.135	-0.162	-0.016	0.155	-0.143
-7	0.132	-0.154	-0.016	0.149	-0.137
-6.5	0.127	-0.144	-0.015	0.143	-0.129
-6	0.123	-0.135	-0.015	0.136	-0.121
-5.5	0.119	-0.127	-0.014	0.130	-0.115
-5	0.115	-0.120	-0.014	0.125	-0.110
-4.5	0.111	-0.113	-0.014	0.120	-0.104
-4	0.108	-0.106	-0.013	0.115	-0.098
-3.5	0.104	-0.100	-0.013	0.110	-0.094
-3	0.101	-0.095	-0.012	0.106	-0.089
-2.5	0.098	-0.090	-0.011	0.102	-0.085
-2	0.097	-0.086	-0.011	0.100	-0.082
-1.5	0.094	-0.079	-0.010	0.096	-0.077
-1	0.092	-0.074	-0.009	0.093	-0.073
-0.5	0.093	-0.071	-0.009	0.093	-0.070
0	0.092	-0.065	-0.008	0.092	-0.065
0.5	0.093	-0.061	-0.007	0.092	-0.062
1	0.093	-0.056	-0.007	0.092	-0.057
1.5	0.095	-0.050	-0.006	0.093	-0.053
2	0.096	-0.045	-0.005	0.095	-0.049
2.5	0.097	-0.040	-0.005	0.096	-0.044
3	0.100	-0.035	-0.004	0.098	-0.040
3.5	0.104	-0.030	-0.004	0.102	-0.037
4	0.105	-0.025	-0.003	0.103	-0.032
4.5	0.110	-0.020	-0.002	0.108	-0.029
5	0.113	-0.015	-0.001	0.112	-0.025
5.5	0.116	-0.008	-0.001	0.114	-0.020
6	0.121	-0.004	0.000	0.120	-0.016
6.5	0.124	0.002	0.001	0.123	-0.012
7	0.129	0.008	0.002	0.129	-0.008
7.5	0.131	0.014	0.003	0.132	-0.003
8	0.135	0.021	0.005	0.137	0.002
8.5	0.137	0.028	0.006	0.140	0.007
9	0.141	0.035	0.007	0.145	0.013
9.5	0.145	0.043	0.008	0.150	0.018
10	0.150	0.051	0.010	0.157	0.024

TABLE C9 STATIC FORCE COEFFICIENTS, SMOOTH FLOW, IN-SERVICE, TRAFFIC CONDITION 3, SKEW=0^{O}

Reynolds Number = 6.5 × 10^{5}					
Angle of Attack (degree)	C_X	C_Z	C_m	C_D	C_L
-10	0.166	-0.209	-0.027	0.200	-0.177
-9.5	0.160	-0.190	-0.027	0.189	-0.161
-9	0.155	-0.176	-0.026	0.181	-0.150
-8.5	0.151	-0.166	-0.024	0.174	-0.142
-8	0.148	-0.156	-0.023	0.168	-0.134
-7.5	0.144	-0.145	-0.022	0.161	-0.125
-7	0.140	-0.135	-0.020	0.155	-0.117
-6.5	0.136	-0.123	-0.018	0.149	-0.107
-6	0.132	-0.112	-0.017	0.143	-0.098
-5.5	0.128	-0.102	-0.015	0.137	-0.089
-5	0.123	-0.091	-0.014	0.131	-0.080
-4.5	0.119	-0.082	-0.013	0.125	-0.072
-4	0.115	-0.074	-0.012	0.120	-0.066
-3.5	0.110	-0.068	-0.012	0.114	-0.062
-3	0.106	-0.064	-0.012	0.109	-0.058
-2.5	0.102	-0.061	-0.012	0.104	-0.057
-2	0.098	-0.060	-0.012	0.100	-0.057
-1.5	0.095	-0.060	-0.011	0.097	-0.057
-1	0.093	-0.060	-0.010	0.094	-0.058
-0.5	0.091	-0.060	-0.009	0.091	-0.060
0	0.090	-0.061	-0.007	0.090	-0.061
0.5	0.090	-0.062	-0.006	0.089	-0.063
1	0.090	-0.064	-0.005	0.089	-0.065
1.5	0.091	-0.065	-0.004	0.090	-0.067
2	0.093	-0.066	-0.003	0.091	-0.069
2.5	0.097	-0.066	-0.003	0.094	-0.070
3	0.101	-0.066	-0.002	0.097	-0.071
3.5	0.105	-0.065	-0.002	0.101	-0.071
4	0.110	-0.063	-0.002	0.105	-0.071
4.5	0.115	-0.058	-0.001	0.110	-0.067
5	0.121	-0.052	-0.001	0.116	-0.062
5.5	0.126	-0.045	0.000	0.121	-0.057
6	0.131	-0.039	0.001	0.126	-0.052
6.5	0.136	-0.032	0.002	0.132	-0.048
7	0.141	-0.026	0.003	0.137	-0.043
7.5	0.146	-0.019	0.004	0.143	-0.038
8	0.150	-0.003	0.007	0.148	-0.024
8.5	0.148	0.026	0.015	0.151	0.004
9	0.150	0.041	0.018	0.155	0.017
9.5	0.154	0.053	0.020	0.161	0.027
10	0.157	0.066	0.022	0.166	0.038

TABLE C10 STATIC FORCE COEFFICIENTS, TURBULENT FLOW, IN-SERVICE, TRAFFIC CONDITION 3, SKEW=0^{O}

Reynolds Number = 5.6 × 10^5					
Angle of Attack (degree)	C_X	C_Z	C_m	C_D	C_L
-10	0.151	-0.230	-0.016	0.189	-0.200
-9.5	0.151	-0.220	-0.016	0.185	-0.192
-9	0.146	-0.205	-0.016	0.176	-0.180
-8.5	0.140	-0.190	-0.015	0.166	-0.168
-8	0.138	-0.181	-0.015	0.162	-0.160
-7.5	0.133	-0.168	-0.015	0.153	-0.149
-7	0.130	-0.158	-0.015	0.148	-0.141
-6.5	0.125	-0.147	-0.015	0.141	-0.132
-6	0.121	-0.137	-0.014	0.134	-0.123
-5.5	0.119	-0.129	-0.014	0.130	-0.117
-5	0.114	-0.120	-0.014	0.124	-0.110
-4.5	0.111	-0.113	-0.014	0.119	-0.103
-4	0.107	-0.105	-0.014	0.114	-0.097
-3.5	0.105	-0.100	-0.013	0.111	-0.093
-3	0.102	-0.094	-0.013	0.107	-0.088
-2.5	0.099	-0.088	-0.012	0.102	-0.083
-2	0.097	-0.082	-0.011	0.099	-0.079
-1.5	0.095	-0.077	-0.011	0.097	-0.074
-1	0.093	-0.072	-0.010	0.095	-0.071
-0.5	0.092	-0.068	-0.009	0.093	-0.067
0	0.093	-0.062	-0.008	0.093	-0.062
0.5	0.093	-0.058	-0.008	0.092	-0.058
1	0.095	-0.054	-0.007	0.094	-0.055
1.5	0.095	-0.048	-0.006	0.094	-0.050
2	0.097	-0.044	-0.006	0.095	-0.047
2.5	0.100	-0.039	-0.005	0.098	-0.044
3	0.101	-0.034	-0.004	0.099	-0.039
3.5	0.104	-0.029	-0.004	0.102	-0.035
4	0.106	-0.024	-0.003	0.104	-0.031
4.5	0.110	-0.020	-0.002	0.108	-0.029
5	0.114	-0.014	-0.001	0.112	-0.024
5.5	0.118	-0.010	-0.001	0.116	-0.021
6	0.119	-0.004	0.000	0.118	-0.016
6.5	0.124	0.002	0.001	0.124	-0.012
7	0.128	0.007	0.002	0.128	-0.009
7.5	0.130	0.014	0.003	0.131	-0.003
8	0.135	0.020	0.005	0.136	0.001
8.5	0.138	0.027	0.006	0.140	0.006
9	0.142	0.034	0.007	0.145	0.012
9.5	0.145	0.042	0.008	0.150	0.017
10	0.149	0.050	0.010	0.156	0.023

TABLE C11 STATIC FORCE COEFFICIENTS, SMOOTH FLOW, IN-SERVICE, NO TRAFFIC, SKEW=10^o

Reynolds Number = 6.6 × 10^5					
Angle of Attack (degree)	C_X	C_Z	C_m	C_D	C_L
-10	0.152	-0.254	-0.014	0.194	-0.224
-9.5	0.148	-0.239	-0.013	0.185	-0.211
-9	0.145	-0.225	-0.012	0.178	-0.199
-8.5	0.141	-0.210	-0.012	0.170	-0.187
-8	0.137	-0.195	-0.011	0.163	-0.174
-7.5	0.133	-0.180	-0.010	0.155	-0.161
-7	0.129	-0.166	-0.010	0.148	-0.149
-6.5	0.125	-0.152	-0.010	0.141	-0.137
-6	0.121	-0.140	-0.010	0.135	-0.127
-5.5	0.116	-0.129	-0.010	0.128	-0.117
-5	0.112	-0.118	-0.010	0.121	-0.108
-4.5	0.107	-0.110	-0.011	0.116	-0.101
-4	0.103	-0.102	-0.011	0.110	-0.095
-3.5	0.099	-0.095	-0.011	0.105	-0.089
-3	0.095	-0.090	-0.010	0.100	-0.085
-2.5	0.092	-0.085	-0.010	0.096	-0.081
-2	0.089	-0.082	-0.009	0.092	-0.078
-1.5	0.087	-0.078	-0.008	0.089	-0.076
-1	0.085	-0.077	-0.008	0.086	-0.075
-0.5	0.083	-0.076	-0.007	0.084	-0.075
0	0.083	-0.073	-0.005	0.083	-0.073
0.5	0.084	-0.071	-0.004	0.083	-0.072
1	0.085	-0.069	-0.003	0.084	-0.071
1.5	0.088	-0.067	-0.003	0.086	-0.069
2	0.091	-0.064	-0.002	0.089	-0.067
2.5	0.094	-0.061	-0.002	0.092	-0.065
3	0.098	-0.058	-0.001	0.095	-0.063
3.5	0.103	-0.055	-0.001	0.099	-0.061
4	0.108	-0.050	-0.001	0.104	-0.058
4.5	0.113	-0.045	-0.001	0.109	-0.054
5	0.118	-0.038	0.000	0.114	-0.048
5.5	0.123	-0.031	0.000	0.119	-0.043
6	0.128	-0.025	0.001	0.125	-0.038
6.5	0.133	-0.018	0.002	0.130	-0.033
7	0.138	-0.012	0.002	0.136	-0.029
7.5	0.143	-0.006	0.003	0.141	-0.024
8	0.147	0.006	0.005	0.146	-0.015
8.5	0.149	0.019	0.008	0.151	-0.003
9	0.152	0.029	0.010	0.155	0.005
9.5	0.155	0.039	0.012	0.160	0.013
10	0.159	0.048	0.013	0.165	0.020

TABLE C12 STATIC FORCE COEFFICIENTS, TURBULENT FLOW, IN-SERVICE, NO TRAFFIC, SKEW=10^{O}

Reynolds Number = 8.3×10^5					
Angle of Attack (degree)	C_X	C_Z	C_m	C_D	C_L
-10	0.147	-0.296	-0.020	0.197	-0.266
-9.5	0.145	-0.286	-0.020	0.191	-0.258
-9	0.142	-0.274	-0.019	0.183	-0.248
-8.5	0.138	-0.261	-0.018	0.176	-0.238
-8	0.135	-0.249	-0.018	0.168	-0.228
-7.5	0.131	-0.235	-0.017	0.161	-0.216
-7	0.128	-0.225	-0.016	0.155	-0.208
-6.5	0.124	-0.211	-0.016	0.147	-0.196
-6	0.120	-0.198	-0.015	0.140	-0.185
-5.5	0.116	-0.187	-0.015	0.134	-0.175
-5	0.113	-0.176	-0.014	0.128	-0.165
-4.5	0.110	-0.166	-0.014	0.122	-0.157
-4	0.108	-0.157	-0.014	0.118	-0.149
-3.5	0.103	-0.146	-0.013	0.111	-0.139
-3	0.099	-0.136	-0.013	0.106	-0.130
-2.5	0.097	-0.128	-0.012	0.103	-0.124
-2	0.094	-0.119	-0.011	0.098	-0.116
-1.5	0.092	-0.111	-0.010	0.094	-0.108
-1	0.090	-0.103	-0.010	0.091	-0.102
-0.5	0.088	-0.096	-0.009	0.089	-0.095
0	0.087	-0.088	-0.008	0.087	-0.088
0.5	0.086	-0.081	-0.007	0.085	-0.082
1	0.086	-0.074	-0.006	0.084	-0.076
1.5	0.086	-0.066	-0.006	0.084	-0.069
2	0.087	-0.059	-0.005	0.085	-0.062
2.5	0.088	-0.052	-0.004	0.085	-0.056
3	0.089	-0.044	-0.003	0.087	-0.049
3.5	0.092	-0.036	-0.003	0.090	-0.042
4	0.094	-0.028	-0.002	0.092	-0.035
4.5	0.096	-0.022	-0.001	0.094	-0.029
5	0.101	-0.014	-0.001	0.100	-0.023
5.5	0.105	-0.007	0.000	0.104	-0.017
6	0.110	0.000	0.000	0.109	-0.012
6.5	0.115	0.007	0.001	0.115	-0.006
7	0.118	0.013	0.002	0.119	-0.001
7.5	0.124	0.020	0.003	0.125	0.003
8	0.126	0.020	0.003	0.128	0.002
8.5	0.130	0.031	0.004	0.133	0.012
9	0.136	0.038	0.005	0.140	0.016
9.5	0.139	0.044	0.006	0.145	0.020
10	0.141	0.051	0.007	0.148	0.025

TABLE C13 STATIC FORCE COEFFICIENTS, SMOOTH FLOW, IN-SERVICE, TRAFFIC CONDITION 1, SKEW=10°

Reynolds Number = 9.5×10^5					
Angle of Attack (degree)	C_X	C_Z	C_m	C_D	C_L
-10	0.166	-0.178	-0.010	0.195	-0.146
-9.5	0.161	-0.164	-0.009	0.186	-0.135
-9	0.158	-0.153	-0.008	0.180	-0.127
-8.5	0.154	-0.142	-0.007	0.174	-0.118
-8	0.151	-0.132	-0.005	0.168	-0.110
-7.5	0.147	-0.122	-0.004	0.162	-0.102
-7	0.143	-0.112	-0.003	0.155	-0.094
-6.5	0.138	-0.103	-0.002	0.149	-0.086
-6	0.134	-0.094	-0.002	0.143	-0.080
-5.5	0.129	-0.086	-0.003	0.136	-0.073
-5	0.124	-0.079	-0.004	0.130	-0.068
-4.5	0.119	-0.073	-0.005	0.125	-0.064
-4	0.115	-0.068	-0.005	0.119	-0.060
-3.5	0.110	-0.063	-0.006	0.114	-0.057
-3	0.106	-0.060	-0.007	0.109	-0.054
-2.5	0.102	-0.057	-0.007	0.105	-0.053
-2	0.099	-0.055	-0.007	0.101	-0.052
-1.5	0.096	-0.054	-0.007	0.097	-0.052
-1	0.094	-0.054	-0.006	0.095	-0.052
-0.5	0.093	-0.054	-0.006	0.093	-0.053
0	0.092	-0.055	-0.006	0.092	-0.055
0.5	0.092	-0.055	-0.005	0.092	-0.056
1	0.093	-0.055	-0.004	0.092	-0.056
1.5	0.094	-0.054	-0.004	0.093	-0.057
2	0.097	-0.053	-0.003	0.095	-0.057
2.5	0.100	-0.052	-0.003	0.097	-0.056
3	0.104	-0.049	-0.003	0.101	-0.055
3.5	0.107	-0.046	-0.002	0.104	-0.052
4	0.112	-0.042	-0.002	0.109	-0.049
4.5	0.116	-0.036	-0.001	0.113	-0.045
5	0.121	-0.030	0.000	0.118	-0.040
5.5	0.126	-0.023	0.001	0.123	-0.035
6	0.130	-0.017	0.002	0.128	-0.030
6.5	0.135	-0.010	0.003	0.133	-0.026
7	0.140	-0.004	0.004	0.138	-0.021
7.5	0.144	0.003	0.005	0.143	-0.015
8	0.149	0.010	0.006	0.149	-0.011
8.5	0.153	0.016	0.006	0.154	-0.007
9	0.158	0.021	0.006	0.160	-0.004
9.5	0.163	0.027	0.006	0.165	0.000
10	0.167	0.034	0.007	0.170	0.004

TABLE C14 STATIC FORCE COEFFICIENTS, TURBULENT FLOW, IN-SERVICE, TRAFFIC CONDITION 1, SKEW=10^{o}

Reynolds Number = 8.2 × 10^5					
Angle of Attack (degree)	C_X	C_Z	C_m	C_D	C_L
-10	0.156	-0.234	-0.005	0.194	-0.203
-9.5	0.152	-0.219	-0.005	0.186	-0.191
-9	0.149	-0.208	-0.005	0.180	-0.182
-8.5	0.147	-0.197	-0.004	0.175	-0.173
-8	0.142	-0.183	-0.004	0.166	-0.161
-7.5	0.139	-0.172	-0.004	0.160	-0.152
-7	0.134	-0.160	-0.004	0.153	-0.142
-6.5	0.132	-0.151	-0.005	0.149	-0.135
-6	0.128	-0.141	-0.005	0.142	-0.127
-5.5	0.124	-0.131	-0.005	0.136	-0.119
-5	0.121	-0.123	-0.005	0.131	-0.112
-4.5	0.118	-0.115	-0.005	0.127	-0.106
-4	0.113	-0.107	-0.005	0.121	-0.099
-3.5	0.110	-0.100	-0.005	0.116	-0.093
-3	0.107	-0.093	-0.006	0.112	-0.087
-2.5	0.104	-0.087	-0.006	0.107	-0.082
-2	0.101	-0.082	-0.006	0.104	-0.078
-1.5	0.099	-0.076	-0.006	0.101	-0.074
-1	0.097	-0.071	-0.005	0.098	-0.069
-0.5	0.095	-0.067	-0.005	0.096	-0.066
0	0.094	-0.062	-0.005	0.094	-0.062
0.5	0.093	-0.058	-0.005	0.093	-0.059
1	0.093	-0.053	-0.005	0.092	-0.055
1.5	0.093	-0.048	-0.005	0.092	-0.051
2	0.092	-0.043	-0.004	0.090	-0.047
2.5	0.093	-0.038	-0.004	0.091	-0.042
3	0.095	-0.034	-0.004	0.093	-0.039
3.5	0.097	-0.029	-0.003	0.095	-0.035
4	0.099	-0.024	-0.003	0.097	-0.031
4.5	0.101	-0.019	-0.003	0.099	-0.027
5	0.103	-0.014	-0.002	0.102	-0.023
5.5	0.107	-0.010	-0.002	0.106	-0.020
6	0.109	-0.005	-0.001	0.108	-0.016
6.5	0.111	0.000	-0.001	0.111	-0.013
7	0.116	0.006	0.000	0.115	-0.009
7.5	0.119	0.010	0.000	0.119	-0.005
8	0.123	0.015	0.001	0.124	-0.002
8.5	0.126	0.021	0.002	0.128	0.002
9	0.131	0.026	0.002	0.133	0.006
9.5	0.134	0.032	0.003	0.137	0.009
10	0.138	0.037	0.004	0.142	0.013

TABLE C15 STATIC FORCE COEFFICIENTS, SMOOTH FLOW, IN-SERVICE, TRAFFIC CONDITION 2, SKEW=10°

Reynolds Number = 9.5×10^5					
Angle of Attack (degree)	C_X	C_Z	C_m	C_D	C_L
-10	0.163	-0.195	-0.025	0.195	-0.164
-9.5	0.159	-0.183	-0.024	0.187	-0.155
-9	0.156	-0.173	-0.022	0.181	-0.146
-8.5	0.153	-0.163	-0.021	0.175	-0.138
-8	0.149	-0.152	-0.019	0.169	-0.130
-7.5	0.146	-0.143	-0.017	0.163	-0.122
-7	0.142	-0.133	-0.015	0.158	-0.115
-6.5	0.138	-0.123	-0.014	0.152	-0.107
-6	0.135	-0.115	-0.012	0.146	-0.100
-5.5	0.131	-0.107	-0.011	0.140	-0.094
-5	0.126	-0.099	-0.011	0.134	-0.088
-4.5	0.121	-0.092	-0.011	0.128	-0.082
-4	0.116	-0.086	-0.011	0.122	-0.077
-3.5	0.112	-0.080	-0.011	0.116	-0.073
-3	0.107	-0.075	-0.011	0.111	-0.069
-2.5	0.103	-0.071	-0.011	0.106	-0.066
-2	0.099	-0.068	-0.011	0.101	-0.065
-1.5	0.095	-0.066	-0.010	0.097	-0.064
-1	0.092	-0.065	-0.009	0.094	-0.064
-0.5	0.090	-0.065	-0.009	0.091	-0.064
0	0.088	-0.065	-0.008	0.088	-0.065
0.5	0.087	-0.065	-0.007	0.087	-0.066
1	0.088	-0.065	-0.006	0.086	-0.066
1.5	0.089	-0.064	-0.005	0.087	-0.067
2	0.091	-0.064	-0.004	0.088	-0.067
2.5	0.093	-0.062	-0.004	0.090	-0.066
3	0.096	-0.060	-0.003	0.093	-0.065
3.5	0.100	-0.057	-0.002	0.096	-0.063
4	0.104	-0.052	-0.002	0.100	-0.059
4.5	0.104	-0.052	-0.001	0.100	-0.060
5	0.114	-0.039	0.001	0.110	-0.049
5.5	0.119	-0.031	0.002	0.115	-0.042
6	0.124	-0.023	0.003	0.121	-0.036
6.5	0.129	-0.014	0.004	0.127	-0.029
7	0.135	-0.006	0.005	0.133	-0.022
7.5	0.141	0.001	0.006	0.140	-0.017
8	0.147	0.007	0.006	0.147	-0.013
8.5	0.153	0.013	0.006	0.153	-0.010
9	0.158	0.020	0.007	0.159	-0.005
9.5	0.161	0.028	0.008	0.164	0.001
10	0.165	0.036	0.008	0.169	0.007

TABLE C16 STATIC FORCE COEFFICIENTS, TURBULENT FLOW, IN-SERVICE, TRAFFIC CONDITION 2, SKEW=10^{o}

Reynolds Number = 8.3×10^5					
Angle of Attack (degree)	C_X	C_Z	C_m	C_D	C_L
-10	0.148	-0.214	-0.016	0.183	-0.185
-9.5	0.147	-0.206	-0.016	0.179	-0.179
-9	0.142	-0.194	-0.016	0.170	-0.170
-8.5	0.139	-0.184	-0.015	0.164	-0.161
-8	0.136	-0.175	-0.015	0.159	-0.155
-7.5	0.132	-0.165	-0.014	0.152	-0.146
-7	0.128	-0.156	-0.014	0.146	-0.139
-6.5	0.124	-0.146	-0.014	0.139	-0.131
-6	0.120	-0.138	-0.013	0.134	-0.125
-5.5	0.117	-0.130	-0.013	0.128	-0.118
-5	0.113	-0.122	-0.013	0.123	-0.112
-4.5	0.109	-0.115	-0.012	0.118	-0.106
-4	0.105	-0.108	-0.012	0.113	-0.100
-3.5	0.102	-0.102	-0.011	0.108	-0.095
-3	0.099	-0.096	-0.011	0.104	-0.091
-2.5	0.096	-0.090	-0.010	0.100	-0.086
-2	0.095	-0.086	-0.010	0.097	-0.082
-1.5	0.092	-0.080	-0.009	0.094	-0.078
-1	0.090	-0.074	-0.008	0.091	-0.073
-0.5	0.089	-0.070	-0.008	0.089	-0.069
0	0.088	-0.064	-0.007	0.088	-0.064
0.5	0.088	-0.059	-0.006	0.087	-0.060
1	0.088	-0.054	-0.006	0.087	-0.055
1.5	0.089	-0.048	-0.005	0.088	-0.050
2	0.091	-0.043	-0.005	0.089	-0.046
2.5	0.092	-0.037	-0.004	0.090	-0.041
3	0.095	-0.031	-0.003	0.093	-0.036
3.5	0.098	-0.025	-0.003	0.096	-0.031
4	0.100	-0.019	-0.002	0.099	-0.026
4.5	0.104	-0.013	-0.001	0.103	-0.021
5	0.108	-0.007	-0.001	0.107	-0.016
5.5	0.111	-0.001	0.000	0.110	-0.011
6	0.116	0.005	0.001	0.116	-0.007
6.5	0.120	0.011	0.002	0.120	-0.002
7	0.124	0.017	0.002	0.125	0.002
7.5	0.128	0.023	0.003	0.129	0.006
8	0.131	0.028	0.004	0.134	0.010
8.5	0.134	0.035	0.005	0.138	0.015
9	0.137	0.041	0.005	0.142	0.019
9.5	0.142	0.048	0.007	0.148	0.023
10	0.143	0.054	0.007	0.151	0.029

TABLE C17 STATIC FORCE COEFFICIENTS, SMOOTH FLOW, IN-SERVICE, TRAFFIC CONDITION 3, SKEW=10^{o}

Reynolds Number = 6.6 × 10^5					
Angle of Attack (degree)	C_X	C_Z	C_m	C_D	C_L
-10	0.159	-0.191	-0.023	0.190	-0.161
-9.5	0.155	-0.180	-0.022	0.183	-0.152
-9	0.152	-0.169	-0.021	0.177	-0.143
-8.5	0.149	-0.159	-0.019	0.171	-0.135
-8	0.147	-0.149	-0.017	0.166	-0.127
-7.5	0.143	-0.139	-0.015	0.160	-0.119
-7	0.140	-0.129	-0.014	0.154	-0.111
-6.5	0.136	-0.119	-0.012	0.149	-0.103
-6	0.132	-0.110	-0.011	0.143	-0.096
-5.5	0.128	-0.101	-0.011	0.137	-0.088
-5	0.123	-0.093	-0.010	0.131	-0.082
-4.5	0.118	-0.085	-0.011	0.125	-0.075
-4	0.114	-0.078	-0.011	0.119	-0.070
-3.5	0.109	-0.071	-0.011	0.113	-0.065
-3	0.104	-0.066	-0.012	0.108	-0.061
-2.5	0.100	-0.063	-0.012	0.103	-0.059
-2	0.097	-0.061	-0.011	0.099	-0.058
-1.5	0.094	-0.060	-0.010	0.095	-0.057
-1	0.091	-0.059	-0.010	0.092	-0.058
-0.5	0.090	-0.060	-0.009	0.090	-0.059
0	0.088	-0.061	-0.008	0.088	-0.061
0.5	0.088	-0.062	-0.007	0.087	-0.062
1	0.089	-0.062	-0.006	0.087	-0.063
1.5	0.090	-0.062	-0.004	0.088	-0.064
2	0.092	-0.061	-0.004	0.090	-0.064
2.5	0.095	-0.060	-0.003	0.092	-0.064
3	0.099	-0.059	-0.003	0.095	-0.064
3.5	0.103	-0.056	-0.002	0.099	-0.063
4	0.107	-0.053	-0.002	0.103	-0.061
4.5	0.112	-0.049	-0.002	0.108	-0.057
5	0.117	-0.042	-0.001	0.113	-0.052
5.5	0.122	-0.036	0.000	0.118	-0.047
6	0.127	-0.029	0.001	0.123	-0.042
6.5	0.132	-0.022	0.002	0.129	-0.037
7	0.137	-0.016	0.002	0.134	-0.032
7.5	0.142	-0.009	0.003	0.140	-0.028
8	0.146	0.001	0.004	0.145	-0.019
8.5	0.149	0.015	0.007	0.150	-0.007
9	0.152	0.026	0.010	0.154	0.002
9.5	0.155	0.036	0.012	0.159	0.010
10	0.158	0.046	0.013	0.164	0.018

TABLE C18 STATIC FORCE COEFFICIENTS, TURBULENT FLOW, IN-SERVICE, TRAFFIC CONDITION 3, SKEW=10^{o}

Reynolds Number = 8.2 × 10^{5}					
Angle of Attack (degree)	C_X	C_Z	C_m	C_D	C_L
-10	0.149	-0.237	-0.014	0.188	-0.208
-9.5	0.147	-0.227	-0.013	0.182	-0.200
-9	0.146	-0.218	-0.013	0.178	-0.193
-8.5	0.142	-0.206	-0.013	0.171	-0.183
-8	0.139	-0.195	-0.013	0.165	-0.174
-7.5	0.136	-0.184	-0.013	0.159	-0.165
-7	0.132	-0.173	-0.012	0.152	-0.156
-6.5	0.129	-0.163	-0.012	0.147	-0.147
-6	0.125	-0.152	-0.012	0.140	-0.138
-5.5	0.121	-0.143	-0.012	0.135	-0.131
-5	0.117	-0.134	-0.012	0.129	-0.123
-4.5	0.114	-0.125	-0.012	0.123	-0.115
-4	0.110	-0.117	-0.012	0.118	-0.109
-3.5	0.107	-0.109	-0.012	0.113	-0.103
-3	0.104	-0.102	-0.011	0.109	-0.097
-2.5	0.101	-0.097	-0.011	0.105	-0.092
-2	0.099	-0.090	-0.011	0.102	-0.087
-1.5	0.095	-0.084	-0.010	0.098	-0.082
-1	0.094	-0.079	-0.010	0.095	-0.077
-0.5	0.091	-0.073	-0.009	0.092	-0.073
0	0.090	-0.068	-0.009	0.090	-0.068
0.5	0.090	-0.064	-0.008	0.090	-0.064
1	0.089	-0.058	-0.007	0.088	-0.060
1.5	0.090	-0.053	-0.007	0.088	-0.055
2	0.090	-0.048	-0.006	0.088	-0.051
2.5	0.091	-0.042	-0.005	0.089	-0.046
3	0.092	-0.036	-0.005	0.090	-0.041
3.5	0.095	-0.032	-0.004	0.093	-0.037
4	0.097	-0.026	-0.003	0.095	-0.033
4.5	0.099	-0.021	-0.003	0.097	-0.029
5	0.102	-0.016	-0.002	0.100	-0.024
5.5	0.105	-0.010	-0.002	0.104	-0.020
6	0.109	-0.005	-0.001	0.108	-0.017
6.5	0.112	0.000	0.000	0.112	-0.013
7	0.116	0.006	0.001	0.116	-0.008
7.5	0.121	0.013	0.002	0.122	-0.003
8	0.125	0.020	0.003	0.127	0.002
8.5	0.130	0.027	0.004	0.132	0.007
9	0.134	0.033	0.005	0.138	0.012
9.5	0.140	0.041	0.006	0.145	0.018
10	0.141	0.048	0.007	0.148	0.022

TABLE C19 STATIC FORCE COEFFICIENTS, SMOOTH FLOW, IN-SERVICE, NO TRAFFIC, SKEW=20^{O}

Reynolds Number = 9.2×10^5					
Angle of Attack (degree)	C_X	C_Z	C_m	C_D	C_L
-10	0.152	-0.284	-0.020	0.199	-0.253
-9.5	0.149	-0.270	-0.019	0.191	-0.242
-9	0.145	-0.256	-0.018	0.183	-0.230
-8.5	0.141	-0.240	-0.017	0.175	-0.217
-8	0.137	-0.225	-0.017	0.167	-0.204
-7.5	0.133	-0.210	-0.016	0.160	-0.190
-7	0.129	-0.194	-0.015	0.152	-0.177
-6.5	0.125	-0.178	-0.015	0.144	-0.162
-6	0.120	-0.163	-0.014	0.137	-0.149
-5.5	0.116	-0.150	-0.014	0.130	-0.138
-5	0.112	-0.138	-0.014	0.123	-0.127
-4.5	0.107	-0.127	-0.014	0.117	-0.118
-4	0.104	-0.117	-0.013	0.112	-0.110
-3.5	0.100	-0.108	-0.013	0.106	-0.102
-3	0.097	-0.101	-0.012	0.102	-0.096
-2.5	0.094	-0.094	-0.011	0.098	-0.090
-2	0.091	-0.089	-0.010	0.094	-0.086
-1.5	0.089	-0.085	-0.010	0.091	-0.082
-1	0.088	-0.080	-0.009	0.089	-0.078
-0.5	0.087	-0.076	-0.008	0.088	-0.075
0	0.087	-0.071	-0.007	0.087	-0.071
0.5	0.089	-0.067	-0.006	0.088	-0.068
1	0.091	-0.063	-0.005	0.089	-0.065
1.5	0.094	-0.059	-0.004	0.092	-0.061
2	0.096	-0.055	-0.003	0.094	-0.058
2.5	0.100	-0.050	-0.003	0.097	-0.054
3	0.104	-0.044	-0.003	0.101	-0.050
3.5	0.107	-0.039	-0.002	0.105	-0.046
4	0.112	-0.032	-0.001	0.109	-0.040
4.5	0.117	-0.025	0.000	0.114	-0.034
5	0.122	-0.017	0.001	0.120	-0.027
5.5	0.127	-0.009	0.002	0.125	-0.021
6	0.131	-0.003	0.003	0.130	-0.017
6.5	0.136	0.004	0.004	0.135	-0.011
7	0.141	0.011	0.005	0.141	-0.006
7.5	0.145	0.018	0.006	0.146	-0.002
8	0.150	0.023	0.006	0.152	0.002
8.5	0.156	0.031	0.007	0.158	0.007
9	0.160	0.041	0.008	0.164	0.015
9.5	0.164	0.049	0.009	0.170	0.021
10	0.168	0.060	0.010	0.176	0.030

TABLE C20 STATIC FORCE COEFFICIENTS, TURBULENT FLOW, IN-SERVICE, NO TRAFFIC, SKEW=20^{o}

Reynolds Number = 6.1×10^5					
Angle of Attack (degree)	C_X	C_Z	C_m	C_D	C_L
-10	0.132	-0.278	-0.021	0.178	-0.251
-9.5	0.127	-0.261	-0.020	0.168	-0.236
-9	0.123	-0.246	-0.019	0.160	-0.224
-8.5	0.120	-0.232	-0.018	0.153	-0.212
-8	0.118	-0.221	-0.017	0.147	-0.203
-7.5	0.113	-0.205	-0.016	0.139	-0.188
-7	0.110	-0.192	-0.016	0.132	-0.177
-6.5	0.107	-0.180	-0.015	0.127	-0.167
-6	0.104	-0.169	-0.014	0.121	-0.157
-5.5	0.102	-0.159	-0.014	0.117	-0.149
-5	0.098	-0.146	-0.013	0.111	-0.137
-4.5	0.095	-0.135	-0.013	0.105	-0.128
-4	0.093	-0.126	-0.012	0.101	-0.119
-3.5	0.091	-0.118	-0.011	0.098	-0.112
-3	0.088	-0.108	-0.010	0.094	-0.103
-2.5	0.087	-0.100	-0.010	0.091	-0.096
-2	0.085	-0.092	-0.009	0.088	-0.089
-1.5	0.084	-0.084	-0.008	0.086	-0.081
-1	0.083	-0.076	-0.007	0.085	-0.075
-0.5	0.084	-0.071	-0.007	0.085	-0.070
0	0.085	-0.063	-0.006	0.085	-0.063
0.5	0.086	-0.056	-0.005	0.085	-0.056
1	0.086	-0.049	-0.005	0.086	-0.050
1.5	0.089	-0.042	-0.004	0.088	-0.045
2	0.090	-0.035	-0.004	0.089	-0.038
2.5	0.094	-0.029	-0.003	0.092	-0.033
3	0.096	-0.022	-0.003	0.095	-0.027
3.5	0.099	-0.016	-0.002	0.098	-0.022
4	0.101	-0.010	-0.002	0.100	-0.017
4.5	0.105	-0.004	-0.001	0.104	-0.012
5	0.108	0.002	-0.001	0.108	-0.008
5.5	0.112	0.008	0.000	0.113	-0.003
6	0.115	0.013	0.000	0.116	0.001
6.5	0.119	0.018	0.001	0.121	0.005
7	0.122	0.024	0.002	0.124	0.009
7.5	0.126	0.030	0.003	0.129	0.013
8	0.130	0.037	0.003	0.133	0.018
8.5	0.133	0.043	0.004	0.138	0.023
9	0.136	0.049	0.005	0.142	0.027
9.5	0.140	0.057	0.006	0.148	0.033
10	0.142	0.063	0.007	0.151	0.037

TABLE C21 STATIC FORCE COEFFICIENTS, SMOOTH FLOW, IN-SERVICE, TRAFFIC CONDITION 1, SKEW=20°

Reynolds Number = 9.3×10^5					
Angle of Attack (degree)	C_X	C_Z	C_m	C_D	C_L
-10	0.167	-0.210	-0.007	0.201	-0.178
-9.5	0.163	-0.197	-0.006	0.194	-0.168
-9	0.160	-0.186	-0.006	0.187	-0.159
-8.5	0.156	-0.175	-0.006	0.180	-0.150
-8	0.153	-0.163	-0.005	0.174	-0.140
-7.5	0.149	-0.150	-0.005	0.167	-0.129
-7	0.144	-0.138	-0.004	0.160	-0.119
-6.5	0.139	-0.125	-0.004	0.153	-0.109
-6	0.134	-0.114	-0.004	0.145	-0.099
-5.5	0.129	-0.104	-0.004	0.139	-0.091
-5	0.124	-0.095	-0.005	0.132	-0.084
-4.5	0.119	-0.087	-0.006	0.126	-0.077
-4	0.115	-0.079	-0.007	0.120	-0.071
-3.5	0.110	-0.073	-0.008	0.114	-0.066
-3	0.106	-0.068	-0.008	0.109	-0.062
-2.5	0.102	-0.063	-0.009	0.105	-0.059
-2	0.099	-0.060	-0.009	0.101	-0.056
-1.5	0.096	-0.057	-0.008	0.098	-0.055
-1	0.094	-0.056	-0.008	0.095	-0.054
-0.5	0.093	-0.054	-0.008	0.093	-0.054
0	0.092	-0.053	-0.007	0.092	-0.053
0.5	0.093	-0.052	-0.006	0.093	-0.053
1	0.095	-0.050	-0.006	0.094	-0.052
1.5	0.097	-0.048	-0.005	0.095	-0.051
2	0.100	-0.046	-0.005	0.098	-0.049
2.5	0.103	-0.043	-0.004	0.101	-0.047
3	0.106	-0.039	-0.004	0.104	-0.045
3.5	0.111	-0.034	-0.003	0.109	-0.041
4	0.116	-0.028	-0.003	0.113	-0.036
4.5	0.120	-0.023	-0.002	0.118	-0.032
5	0.125	-0.015	-0.001	0.124	-0.026
5.5	0.130	-0.008	0.000	0.128	-0.021
6	0.134	-0.001	0.001	0.133	-0.015
6.5	0.139	0.007	0.002	0.139	-0.008
7	0.143	0.016	0.004	0.144	-0.001
7.5	0.148	0.025	0.005	0.150	0.006
8	0.152	0.032	0.006	0.155	0.010
8.5	0.157	0.039	0.007	0.161	0.015
9	0.161	0.046	0.008	0.166	0.020
9.5	0.166	0.055	0.009	0.172	0.027
10	0.170	0.063	0.009	0.178	0.033

TABLE C22 STATIC FORCE COEFFICIENTS, TURBULENT FLOW, IN-SERVICE, TRAFFIC CONDITION 1, SKEW=20^{O}

Reynolds Number = 6.1×10^5					
Angle of Attack (degree)	C_X	C_Z	C_m	C_D	C_L
-10	0.141	-0.213	-0.005	0.176	-0.186
-9.5	0.140	-0.202	-0.004	0.171	-0.176
-9	0.138	-0.191	-0.004	0.166	-0.167
-8.5	0.132	-0.176	-0.004	0.156	-0.154
-8	0.130	-0.165	-0.004	0.151	-0.146
-7.5	0.127	-0.155	-0.004	0.146	-0.137
-7	0.122	-0.143	-0.004	0.139	-0.127
-6.5	0.119	-0.132	-0.004	0.133	-0.118
-6	0.115	-0.123	-0.004	0.128	-0.110
-5.5	0.113	-0.115	-0.005	0.123	-0.104
-5	0.110	-0.106	-0.005	0.118	-0.097
-4.5	0.105	-0.098	-0.005	0.112	-0.089
-4	0.104	-0.092	-0.005	0.110	-0.085
-3.5	0.100	-0.084	-0.005	0.105	-0.078
-3	0.096	-0.077	-0.005	0.100	-0.072
-2.5	0.094	-0.071	-0.005	0.097	-0.067
-2	0.094	-0.067	-0.005	0.096	-0.064
-1.5	0.092	-0.061	-0.005	0.094	-0.058
-1	0.090	-0.055	-0.005	0.091	-0.054
-0.5	0.090	-0.051	-0.005	0.090	-0.050
0	0.090	-0.046	-0.005	0.090	-0.046
0.5	0.091	-0.042	-0.005	0.091	-0.042
1	0.092	-0.037	-0.004	0.092	-0.039
1.5	0.093	-0.032	-0.004	0.092	-0.035
2	0.094	-0.028	-0.004	0.093	-0.031
2.5	0.097	-0.023	-0.004	0.096	-0.027
3	0.099	-0.018	-0.003	0.098	-0.023
3.5	0.101	-0.013	-0.003	0.100	-0.019
4	0.104	-0.008	-0.003	0.103	-0.015
4.5	0.106	-0.003	-0.002	0.106	-0.011
5	0.111	0.002	-0.002	0.111	-0.008
5.5	0.113	0.007	-0.001	0.113	-0.004
6	0.117	0.012	-0.001	0.117	-0.001
6.5	0.120	0.018	0.000	0.121	0.004
7	0.124	0.022	0.001	0.125	0.007
7.5	0.127	0.028	0.001	0.129	0.011
8	0.131	0.034	0.002	0.134	0.015
8.5	0.134	0.040	0.003	0.139	0.020
9	0.138	0.046	0.004	0.144	0.024
9.5	0.141	0.053	0.005	0.148	0.029
10	0.144	0.060	0.006	0.152	0.034

TABLE C23 STATIC FORCE COEFFICIENTS, SMOOTH FLOW, IN-SERVICE, TRAFFIC CONDITION 2, SKEW=20^{O}

Reynolds Number = 9.2×10^5					
Angle of Attack (degree)	C_X	C_Z	C_m	C_D	C_L
-10	0.165	-0.216	-0.023	0.200	-0.184
-9.5	0.161	-0.205	-0.022	0.192	-0.175
-9	0.157	-0.195	-0.021	0.186	-0.168
-8.5	0.153	-0.184	-0.020	0.179	-0.159
-8	0.150	-0.171	-0.019	0.173	-0.148
-7.5	0.147	-0.159	-0.017	0.166	-0.138
-7	0.143	-0.148	-0.016	0.160	-0.130
-6.5	0.138	-0.137	-0.015	0.153	-0.121
-6	0.133	-0.127	-0.014	0.146	-0.112
-5.5	0.129	-0.117	-0.013	0.139	-0.104
-5	0.124	-0.108	-0.013	0.133	-0.096
-4.5	0.119	-0.100	-0.012	0.126	-0.090
-4	0.114	-0.093	-0.012	0.120	-0.085
-3.5	0.109	-0.086	-0.012	0.114	-0.080
-3	0.105	-0.081	-0.012	0.109	-0.075
-2.5	0.101	-0.075	-0.012	0.104	-0.071
-2	0.097	-0.072	-0.011	0.099	-0.068
-1.5	0.094	-0.069	-0.010	0.096	-0.066
-1	0.092	-0.067	-0.010	0.093	-0.065
-0.5	0.090	-0.065	-0.009	0.091	-0.064
0	0.090	-0.062	-0.008	0.090	-0.062
0.5	0.090	-0.060	-0.007	0.090	-0.061
1	0.092	-0.059	-0.006	0.091	-0.060
1.5	0.094	-0.057	-0.005	0.092	-0.059
2	0.097	-0.054	-0.005	0.095	-0.057
2.5	0.100	-0.051	-0.004	0.097	-0.055
3	0.104	-0.046	-0.004	0.101	-0.052
3.5	0.107	-0.042	-0.003	0.104	-0.049
4	0.112	-0.034	-0.002	0.110	-0.042
4.5	0.117	-0.026	-0.001	0.115	-0.035
5	0.122	-0.018	0.000	0.120	-0.028
5.5	0.127	-0.009	0.001	0.126	-0.021
6	0.131	-0.003	0.002	0.130	-0.017
6.5	0.136	0.005	0.003	0.136	-0.010
7	0.141	0.014	0.005	0.142	-0.003
7.5	0.146	0.021	0.005	0.147	0.002
8	0.151	0.027	0.006	0.153	0.006
8.5	0.156	0.035	0.007	0.159	0.011
9	0.160	0.044	0.008	0.165	0.018
9.5	0.165	0.052	0.008	0.171	0.024
10	0.168	0.063	0.010	0.177	0.033

TABLE C24 STATIC FORCE COEFFICIENTS, TURBULENT FLOW, IN-SERVICE, TRAFFIC CONDITION 2, SKEW=20^{o}

Reynolds Number = 6.1 × 10^{5}					
Angle of Attack (degree)	C_X	C_Z	C_m	C_D	C_L
-10	0.142	-0.213	-0.017	0.177	-0.185
-9.5	0.138	-0.201	-0.016	0.170	-0.176
-9	0.135	-0.191	-0.016	0.164	-0.168
-8.5	0.132	-0.180	-0.015	0.157	-0.158
-8	0.129	-0.169	-0.015	0.151	-0.150
-7.5	0.125	-0.160	-0.014	0.145	-0.143
-7	0.122	-0.151	-0.014	0.139	-0.135
-6.5	0.118	-0.141	-0.013	0.134	-0.127
-6	0.113	-0.131	-0.013	0.126	-0.118
-5.5	0.111	-0.124	-0.012	0.123	-0.113
-5	0.108	-0.116	-0.012	0.117	-0.107
-4.5	0.105	-0.109	-0.012	0.113	-0.101
-4	0.102	-0.102	-0.011	0.108	-0.094
-3.5	0.097	-0.094	-0.010	0.103	-0.088
-3	0.095	-0.088	-0.010	0.100	-0.083
-2.5	0.092	-0.081	-0.009	0.096	-0.077
-2	0.092	-0.077	-0.009	0.094	-0.073
-1.5	0.089	-0.070	-0.008	0.091	-0.068
-1	0.088	-0.065	-0.008	0.089	-0.063
-0.5	0.087	-0.059	-0.007	0.088	-0.058
0	0.088	-0.054	-0.006	0.088	-0.054
0.5	0.089	-0.050	-0.006	0.089	-0.050
1	0.090	-0.044	-0.006	0.089	-0.046
1.5	0.091	-0.039	-0.005	0.090	-0.041
2	0.093	-0.033	-0.005	0.092	-0.037
2.5	0.095	-0.028	-0.004	0.093	-0.032
3	0.096	-0.022	-0.004	0.095	-0.027
3.5	0.099	-0.017	-0.003	0.098	-0.023
4	0.103	-0.011	-0.003	0.102	-0.018
4.5	0.105	-0.005	-0.002	0.105	-0.014
5	0.109	0.000	-0.002	0.108	-0.009
5.5	0.111	0.006	-0.001	0.111	-0.005
6	0.115	0.012	0.000	0.116	0.000
6.5	0.120	0.017	0.001	0.121	0.004
7	0.122	0.023	0.001	0.124	0.008
7.5	0.125	0.030	0.002	0.128	0.013
8	0.130	0.036	0.003	0.133	0.018
8.5	0.134	0.043	0.004	0.139	0.023
9	0.137	0.049	0.005	0.143	0.027
9.5	0.139	0.056	0.006	0.146	0.033
10	0.141	0.064	0.007	0.150	0.038

TABLE C25 STATIC FORCE COEFFICIENTS, SMOOTH FLOW, IN-SERVICE, TRAFFIC CONDITION 3, SKEW=20^{o}

Reynolds Number = 9.2×10^5					
Angle of Attack (degree)	C_X	C_Z	C_m	C_D	C_L
-10	0.163	-0.225	-0.022	0.199	-0.193
-9.5	0.159	-0.213	-0.021	0.192	-0.184
-9	0.156	-0.202	-0.021	0.186	-0.175
-8.5	0.153	-0.190	-0.019	0.179	-0.165
-8	0.150	-0.177	-0.018	0.173	-0.154
-7.5	0.146	-0.164	-0.017	0.166	-0.144
-7	0.142	-0.153	-0.015	0.160	-0.134
-6.5	0.138	-0.141	-0.014	0.153	-0.124
-6	0.133	-0.129	-0.014	0.146	-0.115
-5.5	0.129	-0.118	-0.013	0.139	-0.106
-5	0.124	-0.109	-0.013	0.133	-0.097
-4.5	0.119	-0.099	-0.013	0.126	-0.090
-4	0.114	-0.091	-0.013	0.120	-0.083
-3.5	0.109	-0.084	-0.013	0.114	-0.077
-3	0.105	-0.077	-0.013	0.108	-0.072
-2.5	0.101	-0.072	-0.013	0.104	-0.068
-2	0.097	-0.068	-0.013	0.100	-0.064
-1.5	0.094	-0.065	-0.012	0.096	-0.063
-1	0.092	-0.063	-0.011	0.093	-0.062
-0.5	0.091	-0.062	-0.010	0.091	-0.061
0	0.090	-0.060	-0.009	0.090	-0.060
0.5	0.091	-0.058	-0.008	0.090	-0.059
1	0.092	-0.057	-0.007	0.091	-0.059
1.5	0.094	-0.056	-0.006	0.092	-0.058
2	0.097	-0.053	-0.005	0.095	-0.056
2.5	0.100	-0.050	-0.005	0.098	-0.055
3	0.104	-0.046	-0.004	0.101	-0.051
3.5	0.107	-0.042	-0.004	0.104	-0.048
4	0.112	-0.035	-0.003	0.109	-0.043
4.5	0.117	-0.027	-0.001	0.114	-0.036
5	0.122	-0.019	0.000	0.120	-0.030
5.5	0.127	-0.011	0.001	0.125	-0.023
6	0.131	-0.005	0.002	0.130	-0.018
6.5	0.136	0.003	0.003	0.135	-0.012
7	0.141	0.012	0.005	0.141	-0.005
7.5	0.146	0.019	0.005	0.147	0.000
8	0.151	0.025	0.006	0.153	0.004
8.5	0.156	0.033	0.007	0.159	0.009
9	0.160	0.042	0.008	0.165	0.016
9.5	0.164	0.050	0.008	0.171	0.022
10	0.168	0.061	0.010	0.176	0.031

TABLE C26 STATIC FORCE COEFFICIENTS, TURBULENT FLOW, IN-SERVICE, TRAFFIC CONDITION 3, SKEW=20^{o}

Reynolds Number = 6.1 × 10^5					
Angle of Attack (degree)	C_X	C_Z	C_m	C_D	C_L
-10	0.139	-0.227	-0.014	0.176	-0.200
-9.5	0.136	-0.213	-0.013	0.169	-0.188
-9	0.133	-0.202	-0.013	0.163	-0.179
-8.5	0.130	-0.190	-0.013	0.156	-0.168
-8	0.127	-0.179	-0.012	0.151	-0.159
-7.5	0.124	-0.167	-0.012	0.145	-0.149
-7	0.120	-0.156	-0.012	0.138	-0.140
-6.5	0.116	-0.145	-0.012	0.132	-0.131
-6	0.113	-0.135	-0.012	0.126	-0.122
-5.5	0.110	-0.126	-0.011	0.121	-0.115
-5	0.106	-0.116	-0.011	0.115	-0.106
-4.5	0.104	-0.110	-0.011	0.113	-0.102
-4	0.102	-0.103	-0.011	0.109	-0.096
-3.5	0.097	-0.094	-0.011	0.103	-0.088
-3	0.095	-0.086	-0.010	0.099	-0.081
-2.5	0.093	-0.081	-0.010	0.097	-0.076
-2	0.091	-0.074	-0.009	0.094	-0.071
-1.5	0.089	-0.068	-0.009	0.091	-0.065
-1	0.089	-0.063	-0.008	0.090	-0.061
-0.5	0.088	-0.058	-0.008	0.089	-0.057
0	0.089	-0.053	-0.007	0.089	-0.053
0.5	0.088	-0.047	-0.007	0.088	-0.048
1	0.089	-0.042	-0.006	0.088	-0.044
1.5	0.093	-0.037	-0.006	0.092	-0.040
2	0.093	-0.032	-0.005	0.092	-0.035
2.5	0.094	-0.026	-0.005	0.093	-0.030
3	0.097	-0.021	-0.004	0.096	-0.026
3.5	0.100	-0.016	-0.004	0.099	-0.022
4	0.103	-0.011	-0.003	0.102	-0.018
4.5	0.105	-0.006	-0.002	0.104	-0.014
5	0.109	0.000	-0.002	0.108	-0.009
5.5	0.112	0.006	-0.001	0.112	-0.005
6	0.115	0.011	0.000	0.116	-0.001
6.5	0.119	0.016	0.000	0.120	0.003
7	0.122	0.022	0.001	0.124	0.007
7.5	0.125	0.028	0.002	0.127	0.011
8	0.129	0.034	0.003	0.133	0.016
8.5	0.132	0.041	0.004	0.137	0.021
9	0.135	0.047	0.005	0.140	0.026
9.5	0.139	0.054	0.006	0.146	0.031
10	0.141	0.061	0.007	0.150	0.036

TABLE C27 STATIC FORCE COEFFICIENTS, SMOOTH FLOW, IN-SERVICE, NO TRAFFIC, SKEW=30^{o}

Reynolds Number = 9.2 × 10^5					
Angle of Attack (degree)	C_X	C_Z	C_m	C_D	C_L
-10	0.135	-0.277	-0.021	0.181	-0.249
-9.5	0.133	-0.267	-0.020	0.175	-0.241
-9	0.130	-0.252	-0.019	0.168	-0.228
-8.5	0.127	-0.240	-0.018	0.161	-0.218
-8	0.124	-0.227	-0.017	0.155	-0.207
-7.5	0.121	-0.213	-0.016	0.148	-0.196
-7	0.118	-0.199	-0.015	0.141	-0.184
-6.5	0.114	-0.184	-0.014	0.134	-0.170
-6	0.110	-0.169	-0.013	0.127	-0.156
-5.5	0.106	-0.153	-0.012	0.120	-0.142
-5	0.102	-0.138	-0.011	0.114	-0.128
-4.5	0.098	-0.124	-0.011	0.108	-0.116
-4	0.095	-0.113	-0.010	0.102	-0.106
-3.5	0.091	-0.104	-0.010	0.097	-0.098
-3	0.088	-0.095	-0.009	0.093	-0.090
-2.5	0.086	-0.088	-0.009	0.090	-0.084
-2	0.084	-0.081	-0.008	0.086	-0.078
-1.5	0.082	-0.074	-0.007	0.084	-0.072
-1	0.081	-0.067	-0.006	0.082	-0.066
-0.5	0.081	-0.061	-0.005	0.081	-0.060
0	0.081	-0.055	-0.004	0.081	-0.055
0.5	0.083	-0.048	-0.003	0.082	-0.049
1	0.085	-0.043	-0.003	0.084	-0.044
1.5	0.088	-0.037	-0.002	0.087	-0.040
2	0.091	-0.032	-0.002	0.090	-0.035
2.5	0.095	-0.026	-0.002	0.094	-0.030
3	0.099	-0.019	-0.002	0.098	-0.025
3.5	0.104	-0.012	-0.001	0.103	-0.018
4	0.108	-0.005	0.000	0.107	-0.012
4.5	0.112	0.003	0.001	0.112	-0.006
5	0.115	0.011	0.002	0.116	0.001
5.5	0.119	0.019	0.004	0.120	0.007
6	0.122	0.026	0.005	0.124	0.013
6.5	0.125	0.033	0.006	0.128	0.019
7	0.129	0.040	0.008	0.133	0.024
7.5	0.132	0.047	0.009	0.137	0.029
8	0.136	0.053	0.010	0.142	0.034
8.5	0.139	0.060	0.011	0.146	0.038
9	0.142	0.066	0.012	0.151	0.043
9.5	0.145	0.074	0.013	0.155	0.049
10	0.148	0.082	0.014	0.160	0.056

TABLE C28 STATIC FORCE COEFFICIENTS, TURBULENT FLOW, IN-SERVICE, NO TRAFFIC, SKEW=30^{o}

Reynolds Number = 6.1 × 10^{5}					
Angle of Attack (degree)	C_X	C_Z	C_m	C_D	C_L
-10	0.110	-0.261	-0.023	0.154	-0.238
-9.5	0.108	-0.248	-0.022	0.147	-0.227
-9	0.105	-0.237	-0.021	0.141	-0.218
-8.5	0.102	-0.223	-0.020	0.134	-0.205
-8	0.101	-0.213	-0.019	0.130	-0.197
-7.5	0.097	-0.198	-0.018	0.122	-0.183
-7	0.094	-0.185	-0.017	0.116	-0.172
-6.5	0.093	-0.175	-0.016	0.112	-0.164
-6	0.089	-0.161	-0.015	0.106	-0.151
-5.5	0.087	-0.150	-0.014	0.101	-0.141
-5	0.085	-0.139	-0.014	0.096	-0.131
-4.5	0.082	-0.129	-0.013	0.092	-0.122
-4	0.081	-0.119	-0.012	0.089	-0.113
-3.5	0.078	-0.109	-0.011	0.084	-0.104
-3	0.077	-0.100	-0.010	0.082	-0.096
-2.5	0.075	-0.091	-0.009	0.079	-0.088
-2	0.074	-0.082	-0.008	0.077	-0.080
-1.5	0.074	-0.074	-0.007	0.075	-0.072
-1	0.073	-0.066	-0.006	0.074	-0.065
-0.5	0.073	-0.059	-0.005	0.074	-0.058
0	0.073	-0.050	-0.004	0.073	-0.050
0.5	0.075	-0.043	-0.004	0.075	-0.044
1	0.077	-0.036	-0.003	0.076	-0.037
1.5	0.078	-0.029	-0.003	0.077	-0.031
2	0.080	-0.022	-0.002	0.079	-0.025
2.5	0.082	-0.015	-0.002	0.081	-0.019
3	0.084	-0.008	-0.001	0.084	-0.013
3.5	0.086	-0.002	-0.001	0.086	-0.007
4	0.090	0.004	0.000	0.090	-0.002
4.5	0.092	0.011	0.001	0.092	0.004
5	0.096	0.017	0.001	0.097	0.009
5.5	0.097	0.023	0.002	0.099	0.014
6	0.100	0.029	0.003	0.103	0.018
6.5	0.104	0.035	0.004	0.107	0.023
7	0.106	0.041	0.005	0.110	0.028
7.5	0.108	0.046	0.006	0.113	0.032
8	0.111	0.052	0.007	0.117	0.036
8.5	0.112	0.058	0.008	0.120	0.041
9	0.118	0.066	0.009	0.126	0.047
9.5	0.118	0.071	0.010	0.128	0.051
10	0.121	0.077	0.011	0.132	0.055

TABLE C29 STATIC FORCE COEFFICIENTS, SMOOTH FLOW, IN-SERVICE, TRAFFIC CONDITION 1, SKEW=30^o

Reynolds Number = 9.2×10^5					
Angle of Attack (degree)	C_X	C_Z	C_m	C_D	C_L
-10	0.146	-0.207	-0.005	0.179	-0.178
-9.5	0.143	-0.194	-0.004	0.173	-0.168
-9	0.140	-0.183	-0.004	0.167	-0.159
-8.5	0.137	-0.172	-0.004	0.161	-0.149
-8	0.134	-0.160	-0.003	0.155	-0.140
-7.5	0.130	-0.149	-0.003	0.149	-0.131
-7	0.127	-0.139	-0.002	0.143	-0.122
-6.5	0.123	-0.127	-0.002	0.136	-0.112
-6	0.118	-0.115	-0.002	0.130	-0.102
-5.5	0.114	-0.104	-0.003	0.123	-0.093
-5	0.110	-0.093	-0.003	0.117	-0.083
-4.5	0.105	-0.084	-0.004	0.112	-0.075
-4	0.102	-0.076	-0.005	0.107	-0.068
-3.5	0.098	-0.068	-0.005	0.102	-0.062
-3	0.094	-0.063	-0.005	0.097	-0.058
-2.5	0.091	-0.058	-0.006	0.094	-0.054
-2	0.088	-0.054	-0.006	0.090	-0.050
-1.5	0.086	-0.050	-0.006	0.087	-0.048
-1	0.084	-0.047	-0.006	0.085	-0.045
-0.5	0.083	-0.044	-0.005	0.084	-0.043
0	0.083	-0.040	-0.005	0.083	-0.040
0.5	0.084	-0.037	-0.004	0.084	-0.038
1	0.086	-0.033	-0.004	0.085	-0.035
1.5	0.089	-0.029	-0.003	0.088	-0.031
2	0.092	-0.025	-0.003	0.091	-0.028
2.5	0.096	-0.021	-0.003	0.095	-0.025
3	0.100	-0.015	-0.003	0.099	-0.021
3.5	0.104	-0.009	-0.002	0.104	-0.015
4	0.109	-0.003	-0.002	0.108	-0.010
4.5	0.113	0.004	-0.001	0.113	-0.005
5	0.117	0.012	0.000	0.118	0.002
5.5	0.120	0.019	0.001	0.122	0.008
6	0.124	0.026	0.003	0.126	0.013
6.5	0.127	0.034	0.005	0.130	0.019
7	0.130	0.040	0.006	0.134	0.024
7.5	0.133	0.047	0.008	0.138	0.029
8	0.136	0.054	0.009	0.143	0.035
8.5	0.140	0.061	0.010	0.147	0.040
9	0.143	0.069	0.011	0.152	0.046
9.5	0.146	0.077	0.012	0.157	0.052
10	0.149	0.086	0.013	0.161	0.059

TABLE C30 STATIC FORCE COEFFICIENTS, TURBULENT FLOW, IN-SERVICE, TRAFFIC CONDITION 1, SKEW=30°

Reynolds Number = 6.1×10^5					
Angle of Attack (degree)	C_X	C_Z	C_m	C_D	C_L
-10	0.119	-0.207	-0.007	0.153	-0.183
-9.5	0.117	-0.197	-0.007	0.148	-0.175
-9	0.113	-0.183	-0.006	0.141	-0.163
-8.5	0.110	-0.170	-0.006	0.134	-0.152
-8	0.110	-0.163	-0.006	0.132	-0.146
-7.5	0.106	-0.151	-0.005	0.125	-0.136
-7	0.103	-0.139	-0.005	0.120	-0.126
-6.5	0.100	-0.129	-0.005	0.114	-0.117
-6	0.096	-0.118	-0.005	0.108	-0.108
-5.5	0.095	-0.111	-0.005	0.106	-0.102
-5	0.093	-0.103	-0.005	0.101	-0.094
-4.5	0.088	-0.092	-0.005	0.095	-0.085
-4	0.087	-0.087	-0.005	0.093	-0.081
-3.5	0.085	-0.080	-0.005	0.090	-0.074
-3	0.083	-0.073	-0.005	0.087	-0.069
-2.5	0.080	-0.066	-0.005	0.083	-0.062
-2	0.080	-0.060	-0.005	0.082	-0.057
-1.5	0.078	-0.054	-0.004	0.079	-0.052
-1	0.078	-0.048	-0.004	0.078	-0.047
-0.5	0.077	-0.042	-0.004	0.077	-0.042
0	0.077	-0.037	-0.004	0.077	-0.037
0.5	0.078	-0.031	-0.003	0.077	-0.031
1	0.079	-0.025	-0.003	0.078	-0.027
1.5	0.080	-0.020	-0.003	0.079	-0.022
2	0.081	-0.014	-0.002	0.080	-0.017
2.5	0.085	-0.009	-0.002	0.084	-0.013
3	0.086	-0.004	-0.002	0.085	-0.008
3.5	0.088	0.002	-0.001	0.088	-0.003
4	0.092	0.007	-0.001	0.092	0.001
4.5	0.094	0.013	0.000	0.095	0.006
5	0.096	0.018	0.000	0.097	0.010
5.5	0.099	0.024	0.001	0.100	0.014
6	0.101	0.029	0.002	0.104	0.019
6.5	0.104	0.035	0.003	0.107	0.023
7	0.107	0.041	0.004	0.111	0.028
7.5	0.110	0.047	0.005	0.115	0.032
8	0.112	0.053	0.006	0.118	0.037
8.5	0.115	0.060	0.007	0.123	0.042
9	0.116	0.065	0.008	0.125	0.046
9.5	0.121	0.073	0.009	0.131	0.052
10	0.123	0.080	0.010	0.135	0.057

TABLE C31 STATIC FORCE COEFFICIENTS, SMOOTH FLOW, IN-SERVICE, TRAFFIC CONDITION 2, SKEW=30^{O}

Reynolds Number = 9.2×10^5					
Angle of Attack (degree)	C_X	C_Z	C_m	C_D	C_L
-10	0.145	-0.206	-0.019	0.178	-0.178
-9.5	0.142	-0.196	-0.019	0.172	-0.170
-9	0.139	-0.188	-0.018	0.166	-0.164
-8.5	0.136	-0.178	-0.017	0.161	-0.156
-8	0.133	-0.168	-0.016	0.155	-0.148
-7.5	0.129	-0.158	-0.015	0.149	-0.140
-7	0.126	-0.148	-0.014	0.143	-0.132
-6.5	0.122	-0.138	-0.013	0.137	-0.123
-6	0.118	-0.128	-0.013	0.131	-0.115
-5.5	0.114	-0.117	-0.012	0.124	-0.106
-5	0.109	-0.107	-0.011	0.118	-0.097
-4.5	0.105	-0.097	-0.011	0.112	-0.088
-4	0.101	-0.088	-0.011	0.107	-0.080
-3.5	0.097	-0.080	-0.010	0.102	-0.074
-3	0.093	-0.074	-0.010	0.097	-0.069
-2.5	0.090	-0.068	-0.010	0.093	-0.064
-2	0.087	-0.063	-0.009	0.089	-0.060
-1.5	0.084	-0.059	-0.009	0.086	-0.057
-1	0.082	-0.055	-0.008	0.083	-0.054
-0.5	0.081	-0.051	-0.007	0.082	-0.051
0	0.081	-0.047	-0.006	0.081	-0.047
0.5	0.082	-0.043	-0.005	0.082	-0.044
1	0.085	-0.039	-0.004	0.084	-0.040
1.5	0.088	-0.035	-0.004	0.087	-0.037
2	0.091	-0.030	-0.003	0.090	-0.033
2.5	0.095	-0.024	-0.003	0.094	-0.029
3	0.099	-0.019	-0.003	0.098	-0.024
3.5	0.104	-0.013	-0.002	0.103	-0.019
4	0.108	-0.005	-0.001	0.108	-0.012
4.5	0.112	0.004	0.000	0.112	-0.005
5	0.116	0.013	0.002	0.117	0.003
5.5	0.119	0.021	0.003	0.121	0.010
6	0.122	0.029	0.004	0.125	0.016
6.5	0.126	0.037	0.006	0.129	0.022
7	0.129	0.044	0.007	0.133	0.028
7.5	0.132	0.051	0.008	0.138	0.033
8	0.136	0.058	0.009	0.142	0.038
8.5	0.139	0.065	0.010	0.147	0.044
9	0.141	0.073	0.012	0.151	0.050
9.5	0.144	0.081	0.013	0.156	0.056
10	0.147	0.090	0.015	0.161	0.063

TABLE C32 STATIC FORCE COEFFICIENTS, TURBULENT FLOW, IN-SERVICE, TRAFFIC CONDITION 2, SKEW=30^{o}

Reynolds Number = 6.1 × 10^5					
Angle of Attack (degree)	C_X	C_Z	C_m	C_D	C_L
-10	0.119	-0.205	-0.019	0.153	-0.181
-9.5	0.117	-0.195	-0.018	0.147	-0.173
-9	0.113	-0.182	-0.017	0.140	-0.162
-8.5	0.111	-0.172	-0.016	0.135	-0.154
-8	0.108	-0.163	-0.016	0.130	-0.146
-7.5	0.106	-0.153	-0.015	0.125	-0.138
-7	0.103	-0.145	-0.015	0.120	-0.131
-6.5	0.100	-0.134	-0.014	0.114	-0.122
-6	0.097	-0.125	-0.013	0.109	-0.114
-5.5	0.094	-0.117	-0.013	0.105	-0.108
-5	0.091	-0.109	-0.012	0.100	-0.101
-4.5	0.089	-0.102	-0.012	0.097	-0.094
-4	0.087	-0.095	-0.011	0.093	-0.088
-3.5	0.083	-0.086	-0.010	0.088	-0.081
-3	0.082	-0.080	-0.009	0.086	-0.076
-2.5	0.079	-0.073	-0.009	0.082	-0.069
-2	0.078	-0.067	-0.008	0.080	-0.064
-1.5	0.078	-0.061	-0.007	0.079	-0.059
-1	0.076	-0.054	-0.006	0.077	-0.053
-0.5	0.076	-0.049	-0.006	0.077	-0.048
0	0.076	-0.042	-0.005	0.076	-0.042
0.5	0.077	-0.036	-0.004	0.077	-0.037
1	0.078	-0.030	-0.004	0.078	-0.032
1.5	0.079	-0.024	-0.003	0.078	-0.026
2	0.081	-0.019	-0.003	0.080	-0.021
2.5	0.083	-0.012	-0.002	0.082	-0.016
3	0.086	-0.006	-0.002	0.085	-0.011
3.5	0.088	0.000	-0.001	0.088	-0.006
4	0.091	0.006	-0.001	0.091	-0.001
4.5	0.094	0.012	0.000	0.095	0.004
5	0.096	0.018	0.001	0.098	0.010
5.5	0.100	0.025	0.002	0.102	0.015
6	0.101	0.031	0.002	0.104	0.020
6.5	0.103	0.037	0.003	0.107	0.025
7	0.108	0.044	0.004	0.112	0.030
7.5	0.110	0.050	0.005	0.115	0.035
8	0.112	0.057	0.007	0.119	0.040
8.5	0.115	0.063	0.008	0.123	0.045
9	0.117	0.070	0.009	0.126	0.050
9.5	0.120	0.077	0.010	0.131	0.056
10	0.121	0.083	0.012	0.134	0.061

TABLE C33 STATIC FORCE COEFFICIENTS, SMOOTH FLOW, IN-SERVICE, TRAFFIC CONDITION 3, SKEW=30^{o}

Reynolds Number = 9.2×10^5					
Angle of Attack (degree)	C_X	C_Z	C_m	C_D	C_L
-10	0.143	-0.221	-0.016	0.179	-0.193
-9.5	0.140	-0.210	-0.016	0.173	-0.184
-9	0.137	-0.199	-0.015	0.167	-0.176
-8.5	0.135	-0.189	-0.015	0.161	-0.167
-8	0.132	-0.178	-0.014	0.155	-0.158
-7.5	0.129	-0.166	-0.013	0.149	-0.148
-7	0.125	-0.155	-0.012	0.143	-0.139
-6.5	0.122	-0.144	-0.012	0.137	-0.129
-6	0.118	-0.133	-0.011	0.131	-0.120
-5.5	0.113	-0.121	-0.011	0.124	-0.110
-5	0.109	-0.109	-0.011	0.118	-0.099
-4.5	0.105	-0.098	-0.011	0.112	-0.090
-4	0.101	-0.088	-0.011	0.107	-0.080
-3.5	0.097	-0.079	-0.010	0.101	-0.073
-3	0.093	-0.072	-0.010	0.097	-0.067
-2.5	0.090	-0.066	-0.010	0.092	-0.062
-2	0.087	-0.061	-0.010	0.089	-0.058
-1.5	0.084	-0.056	-0.010	0.085	-0.054
-1	0.082	-0.053	-0.009	0.083	-0.051
-0.5	0.081	-0.049	-0.008	0.082	-0.049
0	0.081	-0.045	-0.007	0.081	-0.045
0.5	0.082	-0.042	-0.006	0.082	-0.042
1	0.085	-0.037	-0.005	0.084	-0.039
1.5	0.088	-0.033	-0.004	0.087	-0.036
2	0.091	-0.029	-0.004	0.090	-0.032
2.5	0.095	-0.023	-0.003	0.094	-0.028
3	0.100	-0.018	-0.003	0.098	-0.023
3.5	0.104	-0.011	-0.002	0.103	-0.018
4	0.108	-0.004	-0.001	0.108	-0.011
4.5	0.113	0.004	0.000	0.113	-0.005
5	0.116	0.013	0.001	0.117	0.003
5.5	0.120	0.021	0.003	0.121	0.009
6	0.123	0.028	0.004	0.125	0.015
6.5	0.126	0.036	0.006	0.129	0.021
7	0.129	0.043	0.007	0.133	0.027
7.5	0.132	0.050	0.008	0.138	0.032
8	0.136	0.056	0.009	0.142	0.037
8.5	0.139	0.064	0.010	0.147	0.043
9	0.142	0.072	0.012	0.151	0.049
9.5	0.144	0.080	0.013	0.156	0.055
10	0.147	0.089	0.014	0.161	0.062

TABLE C34 STATIC FORCE COEFFICIENTS, TURBULENT FLOW, IN-SERVICE, TRAFFIC CONDITION 3, SKEW=30^{o}

Reynolds Number = 6.1 × 10^5					
Angle of Attack (degree)	C_X	C_Z	C_m	C_D	C_L
-10	0.116	-0.220	-0.015	0.152	-0.197
-9.5	0.114	-0.210	-0.014	0.147	-0.189
-9	0.112	-0.197	-0.014	0.141	-0.177
-8.5	0.109	-0.186	-0.013	0.136	-0.168
-8	0.106	-0.173	-0.013	0.129	-0.157
-7.5	0.104	-0.163	-0.013	0.125	-0.148
-7	0.100	-0.151	-0.012	0.118	-0.137
-6.5	0.097	-0.140	-0.012	0.112	-0.128
-6	0.096	-0.132	-0.012	0.109	-0.121
-5.5	0.092	-0.121	-0.011	0.104	-0.112
-5	0.090	-0.113	-0.011	0.100	-0.104
-4.5	0.088	-0.105	-0.011	0.096	-0.098
-4	0.084	-0.095	-0.010	0.091	-0.089
-3.5	0.084	-0.089	-0.010	0.089	-0.084
-3	0.081	-0.081	-0.009	0.085	-0.077
-2.5	0.079	-0.073	-0.009	0.082	-0.070
-2	0.078	-0.067	-0.008	0.080	-0.064
-1.5	0.077	-0.060	-0.008	0.078	-0.058
-1	0.075	-0.053	-0.007	0.076	-0.052
-0.5	0.075	-0.047	-0.006	0.075	-0.047
0	0.076	-0.041	-0.005	0.076	-0.041
0.5	0.076	-0.035	-0.005	0.075	-0.036
1	0.078	-0.029	-0.004	0.077	-0.031
1.5	0.078	-0.023	-0.004	0.078	-0.025
2	0.081	-0.017	-0.003	0.080	-0.020
2.5	0.082	-0.012	-0.003	0.082	-0.015
3	0.085	-0.006	-0.002	0.085	-0.011
3.5	0.086	0.000	-0.002	0.086	-0.005
4	0.091	0.006	-0.001	0.091	0.000
4.5	0.093	0.012	0.000	0.093	0.004
5	0.095	0.018	0.001	0.097	0.010
5.5	0.099	0.024	0.001	0.101	0.015
6	0.100	0.030	0.002	0.103	0.019
6.5	0.104	0.036	0.003	0.107	0.024
7	0.106	0.042	0.004	0.110	0.029
7.5	0.107	0.048	0.005	0.112	0.034
8	0.112	0.055	0.007	0.119	0.039
8.5	0.114	0.061	0.008	0.122	0.044
9	0.114	0.067	0.009	0.123	0.048
9.5	0.119	0.075	0.010	0.130	0.054
10	0.121	0.081	0.012	0.133	0.059

TABLE C35 STATIC FORCE COEFFICIENTS, SMOOTH FLOW, IN-SERVICE, NO TRAFFIC, SKEW=45^{O}

Reynolds Number = 8.8×10^5					
Angle of Attack (degree)	C_X	C_Z	C_m	C_D	C_L
-8	0.113	-0.230	-0.026	0.144	-0.212
-7.5	0.110	-0.216	-0.025	0.138	-0.200
-7	0.108	-0.203	-0.023	0.132	-0.188
-6.5	0.105	-0.190	-0.022	0.125	-0.176
-6	0.102	-0.176	-0.020	0.119	-0.165
-5.5	0.099	-0.163	-0.019	0.114	-0.153
-5	0.095	-0.149	-0.017	0.108	-0.141
-4.5	0.092	-0.137	-0.015	0.103	-0.129
-4	0.089	-0.124	-0.013	0.098	-0.118
-3.5	0.087	-0.113	-0.011	0.093	-0.107
-3	0.084	-0.101	-0.009	0.089	-0.097
-2.5	0.081	-0.091	-0.008	0.085	-0.087
-2	0.079	-0.080	-0.006	0.082	-0.077
-1.5	0.077	-0.070	-0.005	0.079	-0.068
-1	0.076	-0.060	-0.004	0.077	-0.059
-0.5	0.077	-0.051	-0.003	0.077	-0.051
0	0.078	-0.043	-0.003	0.078	-0.043
0.5	0.080	-0.036	-0.002	0.080	-0.036
1	0.083	-0.028	-0.002	0.083	-0.030
1.5	0.086	-0.020	-0.001	0.086	-0.023
2	0.090	-0.012	0.000	0.089	-0.015
2.5	0.094	-0.005	0.000	0.093	-0.009
3	0.097	0.003	0.001	0.097	-0.002
3.5	0.101	0.012	0.002	0.101	0.005
4	0.104	0.019	0.003	0.105	0.012
4.5	0.106	0.027	0.004	0.108	0.019
5	0.109	0.036	0.006	0.112	0.026
5.5	0.112	0.043	0.007	0.115	0.032
6	0.115	0.051	0.008	0.119	0.038
6.5	0.117	0.059	0.009	0.123	0.045
7	0.120	0.067	0.011	0.127	0.052
7.5	0.123	0.075	0.012	0.132	0.059
8	0.126	0.084	0.014	0.136	0.066

TABLE C36 STATIC FORCE COEFFICIENTS, TURBULENT FLOW, IN-SERVICE, NO TRAFFIC, SKEW=45^{o}

Reynolds Number = 5.8×10^5					
Angle of Attack (degree)	C_X	C_Z	C_m	C_D	C_L
-8	0.091	-0.212	-0.026	0.120	-0.197
-7.5	0.088	-0.197	-0.024	0.113	-0.184
-7	0.086	-0.186	-0.023	0.108	-0.175
-6.5	0.084	-0.175	-0.022	0.104	-0.164
-6	0.081	-0.160	-0.021	0.097	-0.151
-5.5	0.078	-0.148	-0.019	0.092	-0.140
-5	0.077	-0.139	-0.018	0.089	-0.132
-4.5	0.075	-0.127	-0.017	0.084	-0.121
-4	0.073	-0.118	-0.015	0.081	-0.113
-3.5	0.070	-0.105	-0.014	0.077	-0.101
-3	0.069	-0.095	-0.012	0.074	-0.092
-2.5	0.067	-0.085	-0.011	0.071	-0.082
-2	0.067	-0.076	-0.009	0.069	-0.074
-1.5	0.067	-0.067	-0.008	0.069	-0.066
-1	0.066	-0.058	-0.006	0.067	-0.057
-0.5	0.067	-0.049	-0.005	0.067	-0.049
0	0.068	-0.041	-0.004	0.068	-0.041
0.5	0.069	-0.033	-0.003	0.069	-0.033
1	0.071	-0.025	-0.002	0.070	-0.026
1.5	0.072	-0.016	-0.001	0.072	-0.018
2	0.074	-0.009	-0.001	0.073	-0.011
2.5	0.076	-0.001	0.000	0.075	-0.004
3	0.078	0.006	0.001	0.079	0.002
3.5	0.081	0.013	0.002	0.082	0.008
4	0.083	0.020	0.003	0.084	0.014
4.5	0.084	0.026	0.003	0.086	0.019
5	0.088	0.033	0.004	0.091	0.025
5.5	0.090	0.039	0.005	0.093	0.030
6	0.093	0.045	0.006	0.097	0.036
6.5	0.094	0.052	0.007	0.100	0.041
7	0.096	0.058	0.008	0.103	0.046
7.5	0.099	0.065	0.009	0.107	0.052
8	0.100	0.072	0.010	0.109	0.057

TABLE C37 STATIC FORCE COEFFICIENTS, SMOOTH FLOW, IN-SERVICE, TRAFFIC CONDITION 1, SKEW=45^{O}

Reynolds Number = 8.8×10^5					
Angle of Attack (degree)	C_X	C_Z	C_m	C_D	C_L
-8	0.118	-0.170	-0.008	0.141	-0.152
-7.5	0.115	-0.158	-0.007	0.135	-0.141
-7	0.112	-0.145	-0.007	0.129	-0.130
-6.5	0.108	-0.133	-0.006	0.123	-0.119
-6	0.105	-0.121	-0.006	0.117	-0.109
-5.5	0.102	-0.110	-0.006	0.112	-0.099
-5	0.098	-0.099	-0.006	0.106	-0.090
-4.5	0.094	-0.089	-0.005	0.101	-0.081
-4	0.091	-0.080	-0.005	0.097	-0.073
-3.5	0.088	-0.071	-0.005	0.092	-0.066
-3	0.085	-0.064	-0.004	0.088	-0.059
-2.5	0.082	-0.057	-0.004	0.085	-0.053
-2	0.080	-0.051	-0.004	0.082	-0.048
-1.5	0.078	-0.045	-0.003	0.079	-0.043
-1	0.078	-0.040	-0.003	0.078	-0.038
-0.5	0.078	-0.035	-0.002	0.079	-0.034
0	0.080	-0.030	-0.002	0.080	-0.030
0.5	0.081	-0.025	-0.002	0.081	-0.025
1	0.084	-0.020	-0.002	0.084	-0.021
1.5	0.087	-0.014	-0.001	0.087	-0.016
2	0.091	-0.008	-0.001	0.090	-0.011
2.5	0.094	-0.001	-0.001	0.094	-0.006
3	0.098	0.006	0.000	0.098	0.001
3.5	0.102	0.014	0.000	0.103	0.007
4	0.105	0.021	0.002	0.106	0.014
4.5	0.108	0.028	0.003	0.110	0.020
5	0.111	0.036	0.004	0.114	0.026
5.5	0.114	0.042	0.006	0.117	0.031
6	0.116	0.050	0.007	0.121	0.037
6.5	0.119	0.057	0.009	0.125	0.043
7	0.122	0.065	0.010	0.129	0.049
7.5	0.125	0.073	0.012	0.133	0.056
8	0.128	0.082	0.014	0.138	0.063

TABLE C38 STATIC FORCE COEFFICIENTS, TURBULENT FLOW, IN-SERVICE, TRAFFIC CONDITION 1, SKEW=45°

Reynolds Number = 5.8×10^5					
Angle of Attack (degree)	C_X	C_Z	C_m	C_D	C_L
-8	0.097	-0.163	-0.010	0.119	-0.148
-7.5	0.094	-0.152	-0.009	0.113	-0.138
-7	0.091	-0.139	-0.009	0.107	-0.127
-6.5	0.089	-0.130	-0.008	0.103	-0.119
-6	0.087	-0.121	-0.008	0.099	-0.111
-5.5	0.084	-0.111	-0.007	0.094	-0.102
-5	0.080	-0.100	-0.007	0.089	-0.092
-4.5	0.079	-0.093	-0.007	0.086	-0.087
-4	0.077	-0.084	-0.006	0.082	-0.078
-3.5	0.075	-0.076	-0.006	0.080	-0.072
-3	0.073	-0.069	-0.005	0.077	-0.065
-2.5	0.072	-0.061	-0.005	0.074	-0.058
-2	0.070	-0.055	-0.004	0.072	-0.052
-1.5	0.070	-0.048	-0.004	0.071	-0.046
-1	0.069	-0.041	-0.003	0.070	-0.040
-0.5	0.069	-0.035	-0.003	0.070	-0.034
0	0.069	-0.028	-0.003	0.069	-0.028
0.5	0.070	-0.022	-0.002	0.070	-0.022
1	0.071	-0.015	-0.002	0.071	-0.016
1.5	0.072	-0.009	-0.001	0.072	-0.011
2	0.074	-0.003	-0.001	0.074	-0.006
2.5	0.078	0.003	0.000	0.078	0.000
3	0.078	0.009	0.000	0.078	0.005
3.5	0.083	0.015	0.001	0.083	0.010
4	0.083	0.021	0.001	0.084	0.015
4.5	0.086	0.027	0.002	0.088	0.020
5	0.090	0.033	0.003	0.092	0.025
5.5	0.091	0.039	0.004	0.094	0.030
6	0.093	0.045	0.005	0.098	0.035
6.5	0.096	0.051	0.006	0.102	0.040
7	0.097	0.057	0.007	0.103	0.045
7.5	0.100	0.064	0.008	0.107	0.050
8	0.103	0.071	0.010	0.112	0.056

TABLE C39 STATIC FORCE COEFFICIENTS, SMOOTH FLOW, IN-SERVICE, TRAFFIC CONDITION 2, SKEW=45^{o}

Reynolds Number = 8.8×10^5					
Angle of Attack (degree)	C_X	C_Z	C_m	C_D	C_L
-8	0.119	-0.174	-0.021	0.142	-0.155
-7.5	0.116	-0.162	-0.020	0.136	-0.146
-7	0.113	-0.152	-0.019	0.130	-0.137
-6.5	0.109	-0.141	-0.018	0.124	-0.128
-6	0.106	-0.130	-0.017	0.119	-0.118
-5.5	0.102	-0.120	-0.016	0.113	-0.110
-5	0.098	-0.110	-0.014	0.108	-0.101
-4.5	0.095	-0.100	-0.013	0.102	-0.092
-4	0.091	-0.090	-0.012	0.097	-0.084
-3.5	0.088	-0.082	-0.010	0.093	-0.076
-3	0.084	-0.073	-0.009	0.088	-0.069
-2.5	0.081	-0.066	-0.008	0.084	-0.062
-2	0.078	-0.059	-0.007	0.080	-0.056
-1.5	0.076	-0.052	-0.006	0.078	-0.050
-1	0.075	-0.046	-0.005	0.076	-0.045
-0.5	0.076	-0.041	-0.004	0.077	-0.040
0	0.078	-0.035	-0.003	0.078	-0.035
0.5	0.081	-0.029	-0.003	0.080	-0.030
1	0.083	-0.023	-0.002	0.083	-0.024
1.5	0.086	-0.016	-0.002	0.086	-0.018
2	0.090	-0.008	-0.001	0.089	-0.011
2.5	0.093	-0.002	-0.001	0.093	-0.006
3	0.097	0.006	0.000	0.097	0.001
3.5	0.101	0.014	0.001	0.101	0.007
4	0.104	0.021	0.002	0.105	0.014
4.5	0.107	0.029	0.004	0.109	0.021
5	0.110	0.037	0.005	0.112	0.027
5.5	0.113	0.045	0.006	0.116	0.034
6	0.116	0.052	0.008	0.120	0.040
6.5	0.118	0.060	0.009	0.124	0.046
7	0.121	0.068	0.011	0.129	0.053
7.5	0.124	0.076	0.012	0.133	0.060
8	0.127	0.085	0.014	0.137	0.067

TABLE C40 STATIC FORCE COEFFICIENTS, TURBULENT FLOW, IN-SERVICE, TRAFFIC CONDITION 2, SKEW=45^{o}

Reynolds Number = 5.8 × 10^5					
Angle of Attack (degree)	C_X	C_Z	C_m	C_D	C_L
-8	0.097	-0.166	-0.021	0.119	-0.151
-7.5	0.093	-0.153	-0.019	0.112	-0.140
-7	0.090	-0.143	-0.018	0.107	-0.131
-6.5	0.089	-0.135	-0.018	0.103	-0.124
-6	0.087	-0.127	-0.017	0.100	-0.117
-5.5	0.083	-0.117	-0.016	0.094	-0.108
-5	0.081	-0.109	-0.015	0.090	-0.101
-4.5	0.078	-0.099	-0.013	0.085	-0.092
-4	0.076	-0.092	-0.013	0.082	-0.086
-3.5	0.074	-0.083	-0.011	0.079	-0.079
-3	0.072	-0.076	-0.011	0.076	-0.072
-2.5	0.070	-0.068	-0.009	0.073	-0.065
-2	0.069	-0.061	-0.008	0.071	-0.059
-1.5	0.069	-0.054	-0.007	0.070	-0.052
-1	0.068	-0.047	-0.006	0.069	-0.046
-0.5	0.067	-0.040	-0.005	0.068	-0.039
0	0.068	-0.033	-0.004	0.068	-0.033
0.5	0.070	-0.026	-0.003	0.069	-0.027
1	0.071	-0.019	-0.002	0.070	-0.020
1.5	0.072	-0.012	-0.002	0.072	-0.014
2	0.073	-0.005	-0.001	0.073	-0.008
2.5	0.075	0.002	0.000	0.075	-0.002
3	0.079	0.008	0.000	0.079	0.004
3.5	0.080	0.014	0.001	0.081	0.009
4	0.083	0.021	0.002	0.084	0.015
4.5	0.085	0.028	0.003	0.087	0.021
5	0.088	0.034	0.003	0.090	0.026
5.5	0.091	0.041	0.004	0.094	0.032
6	0.092	0.047	0.005	0.096	0.037
6.5	0.094	0.053	0.007	0.100	0.042
7	0.098	0.061	0.008	0.105	0.048
7.5	0.100	0.067	0.009	0.107	0.053
8	0.101	0.073	0.010	0.110	0.058

TABLE C41 STATIC FORCE COEFFICIENTS, SMOOTH FLOW, IN-SERVICE, TRAFFIC CONDITION 3, SKEW=45^{O}

Reynolds Number = 8.7 × 10^5					
Angle of Attack (degree)	C_X	C_Z	C_m	C_D	C_L
-8	0.116	-0.184	-0.018	0.140	-0.166
-7.5	0.113	-0.171	-0.017	0.134	-0.155
-7	0.110	-0.159	-0.016	0.129	-0.144
-6.5	0.107	-0.147	-0.016	0.123	-0.134
-6	0.104	-0.135	-0.015	0.117	-0.123
-5.5	0.100	-0.123	-0.014	0.112	-0.113
-5	0.097	-0.111	-0.013	0.106	-0.103
-4.5	0.093	-0.101	-0.013	0.101	-0.093
-4	0.090	-0.090	-0.011	0.096	-0.084
-3.5	0.087	-0.081	-0.010	0.091	-0.075
-3	0.083	-0.072	-0.009	0.087	-0.067
-2.5	0.080	-0.064	-0.009	0.083	-0.060
-2	0.078	-0.057	-0.008	0.079	-0.054
-1.5	0.076	-0.050	-0.007	0.077	-0.048
-1	0.075	-0.044	-0.006	0.076	-0.043
-0.5	0.076	-0.039	-0.005	0.076	-0.038
0	0.078	-0.033	-0.004	0.078	-0.033
0.5	0.080	-0.028	-0.003	0.080	-0.028
1	0.083	-0.022	-0.003	0.083	-0.023
1.5	0.086	-0.015	-0.002	0.086	-0.017
2	0.089	-0.008	-0.001	0.089	-0.011
2.5	0.093	-0.001	-0.001	0.093	-0.005
3	0.097	0.006	0.000	0.097	0.001
3.5	0.100	0.013	0.001	0.101	0.007
4	0.103	0.021	0.002	0.105	0.014
4.5	0.106	0.028	0.004	0.108	0.020
5	0.109	0.036	0.005	0.112	0.027
5.5	0.112	0.044	0.007	0.116	0.033
6	0.115	0.051	0.008	0.120	0.039
6.5	0.118	0.059	0.009	0.124	0.045
7	0.121	0.067	0.011	0.128	0.051
7.5	0.124	0.075	0.012	0.132	0.058
8	0.126	0.083	0.014	0.137	0.065

TABLE C42 STATIC FORCE COEFFICIENTS, TURBULENT FLOW, IN-SERVICE, TRAFFIC CONDITION 3, SKEW=45^{o}

Reynolds Number = 5.8 × 10^5					
Angle of Attack (degree)	C_X	C_Z	C_m	C_D	C_L
-8	0.095	-0.175	-0.017	0.118	-0.160
-7.5	0.092	-0.163	-0.017	0.113	-0.150
-7	0.090	-0.153	-0.016	0.108	-0.141
-6.5	0.087	-0.142	-0.016	0.103	-0.132
-6	0.085	-0.131	-0.015	0.098	-0.122
-5.5	0.083	-0.122	-0.014	0.094	-0.113
-5	0.079	-0.111	-0.013	0.089	-0.103
-4.5	0.077	-0.101	-0.013	0.085	-0.095
-4	0.075	-0.092	-0.012	0.081	-0.087
-3.5	0.073	-0.084	-0.011	0.078	-0.079
-3	0.072	-0.077	-0.010	0.076	-0.073
-2.5	0.070	-0.068	-0.009	0.072	-0.065
-2	0.069	-0.061	-0.008	0.071	-0.058
-1.5	0.068	-0.053	-0.008	0.070	-0.051
-1	0.068	-0.046	-0.006	0.069	-0.045
-0.5	0.068	-0.039	-0.006	0.068	-0.038
0	0.069	-0.032	-0.005	0.069	-0.032
0.5	0.069	-0.024	-0.004	0.069	-0.025
1	0.071	-0.018	-0.003	0.071	-0.019
1.5	0.072	-0.011	-0.002	0.072	-0.013
2	0.074	-0.004	-0.001	0.074	-0.007
2.5	0.076	0.002	-0.001	0.076	-0.001
3	0.079	0.009	0.000	0.080	0.004
3.5	0.081	0.015	0.001	0.082	0.010
4	0.083	0.021	0.001	0.085	0.015
4.5	0.087	0.027	0.002	0.089	0.020
5	0.088	0.033	0.003	0.091	0.025
5.5	0.090	0.040	0.004	0.093	0.031
6	0.092	0.045	0.005	0.096	0.036
6.5	0.094	0.051	0.006	0.099	0.040
7	0.097	0.059	0.008	0.104	0.046
7.5	0.100	0.065	0.009	0.108	0.052
8	0.101	0.072	0.010	0.110	0.057

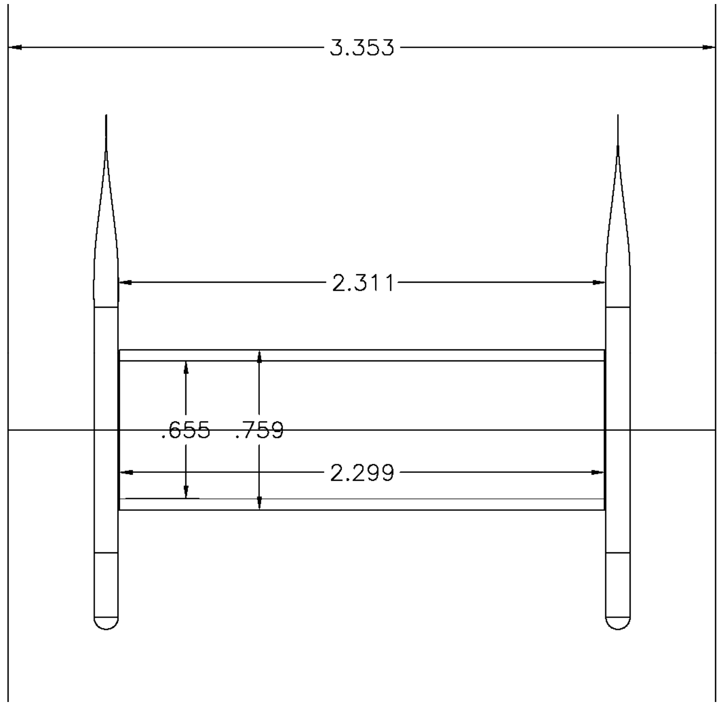

a) Model at Skew Wind Angle of 0°

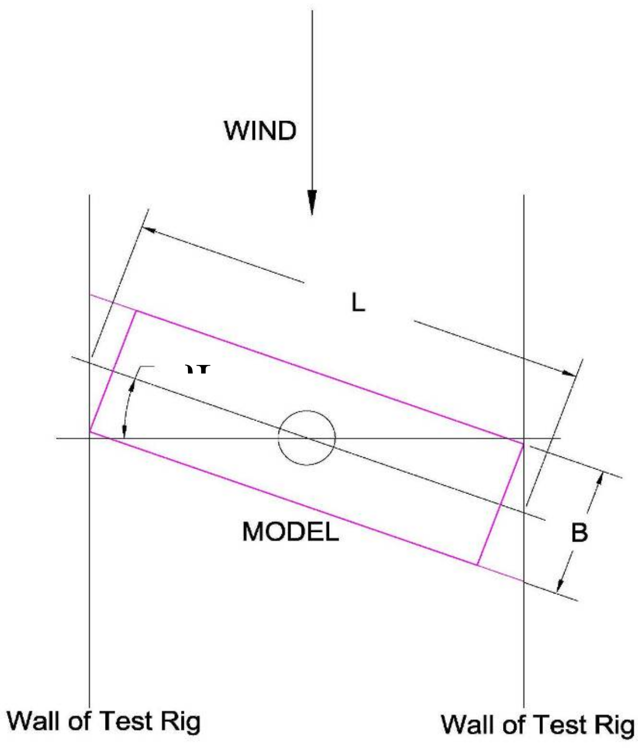

b) Model at Non-Zero Skew Wind Angle

FIGURE C1 DEFINITIONS OF SKEW ANGLE TESTS

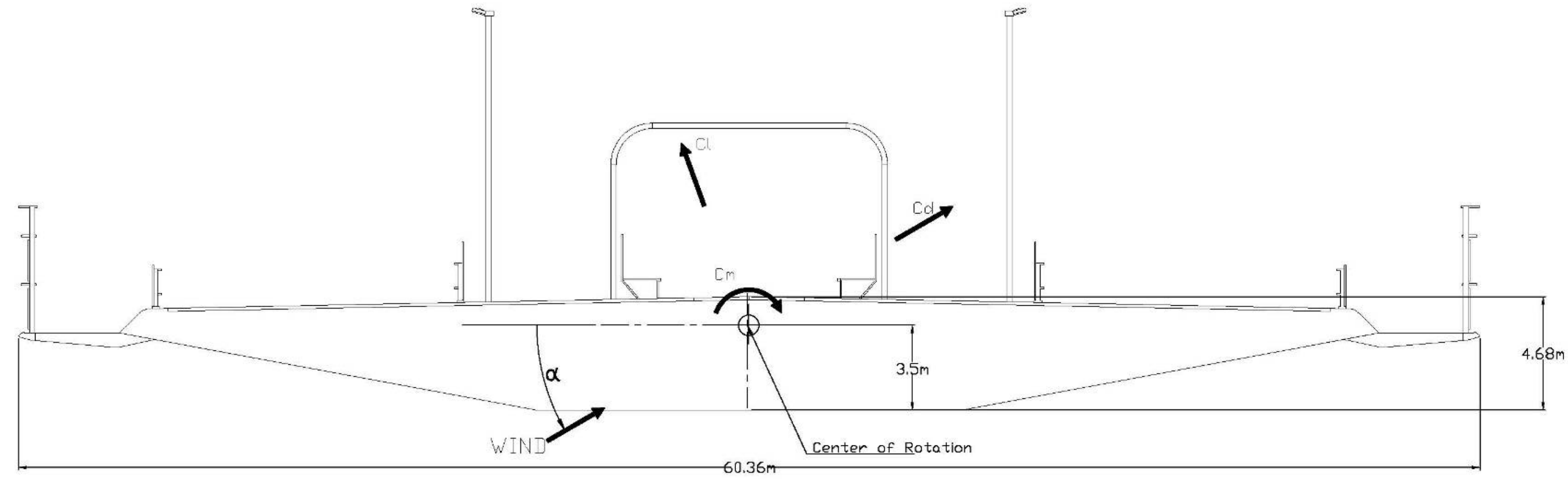

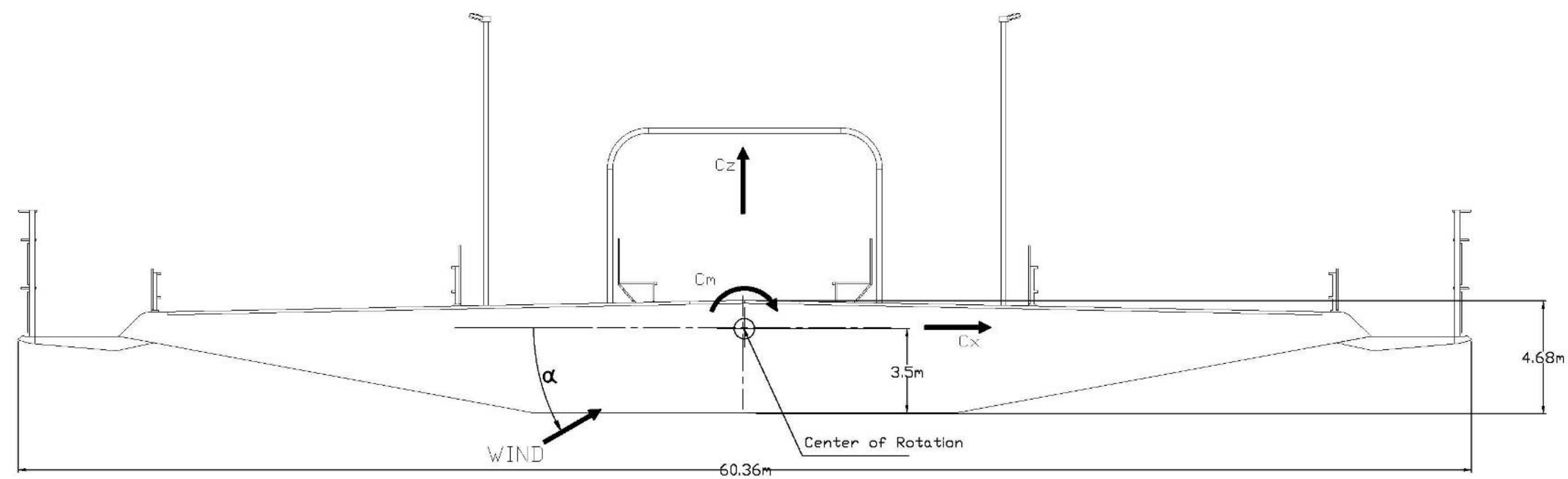

FIGURE C2 SIGN CONVENTION FOR STATIC TEST OF THE IN-SERVICE DECK SECTION

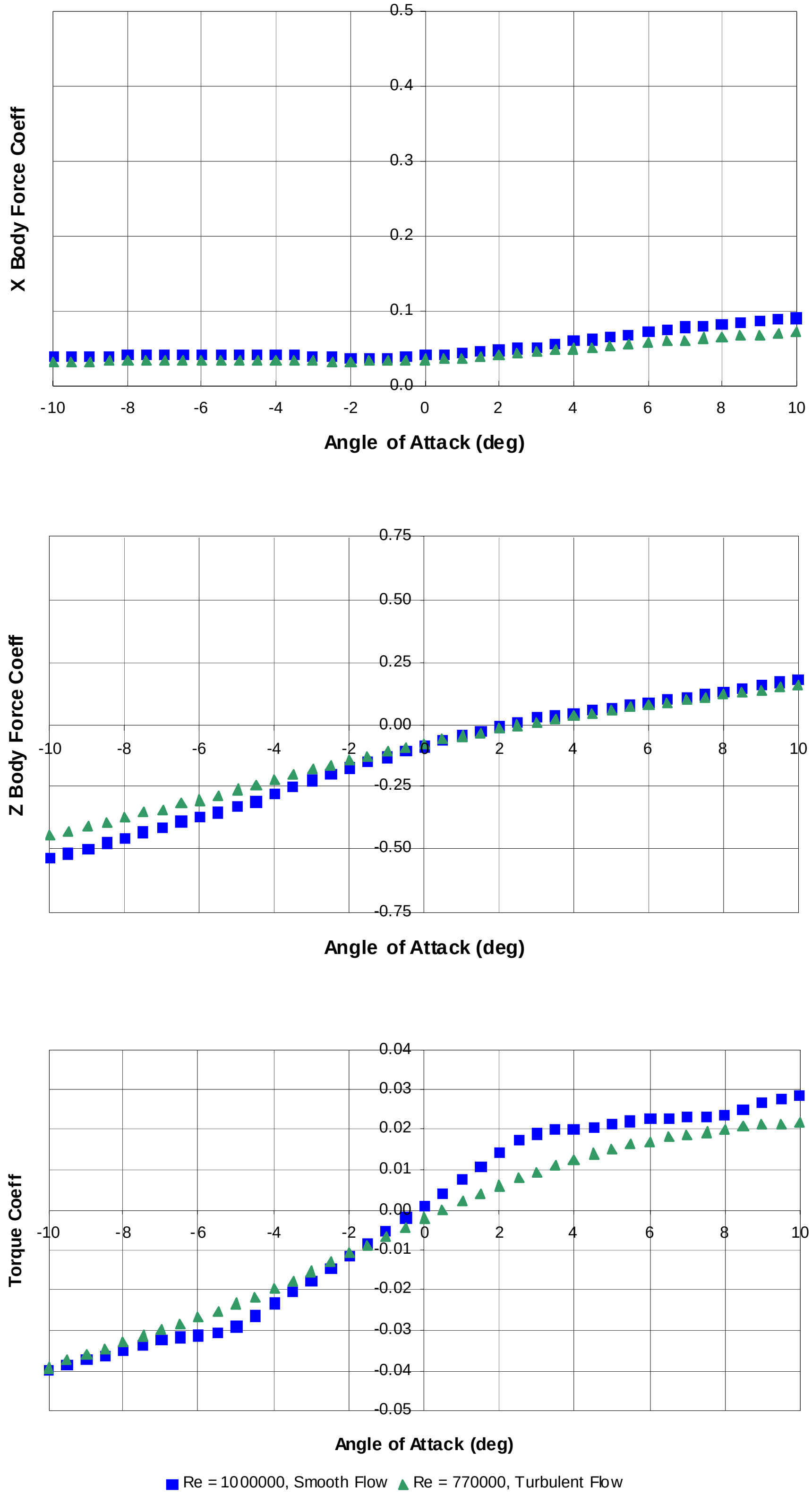

FIGURE C3 STATIC FORCE COEFFICIENTS (BODY FORCES), UNDER CONSTRUCTION, SKEW=0^{O}

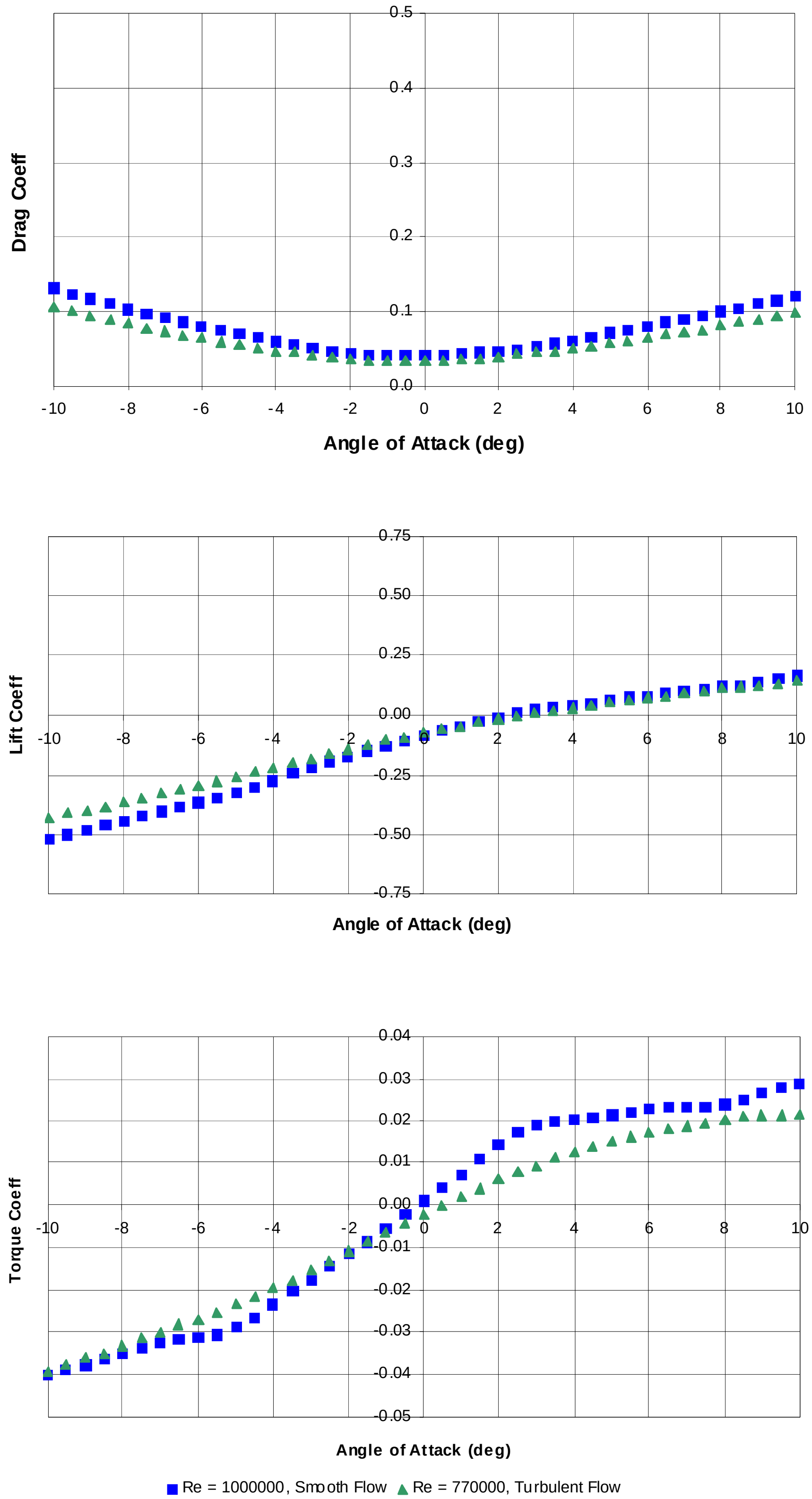

FIGURE C4 STATIC FORCE COEFFICIENTS (WIND AXIS FORCES), UNDER CONSTRUCTION, SKEW=0^{O}

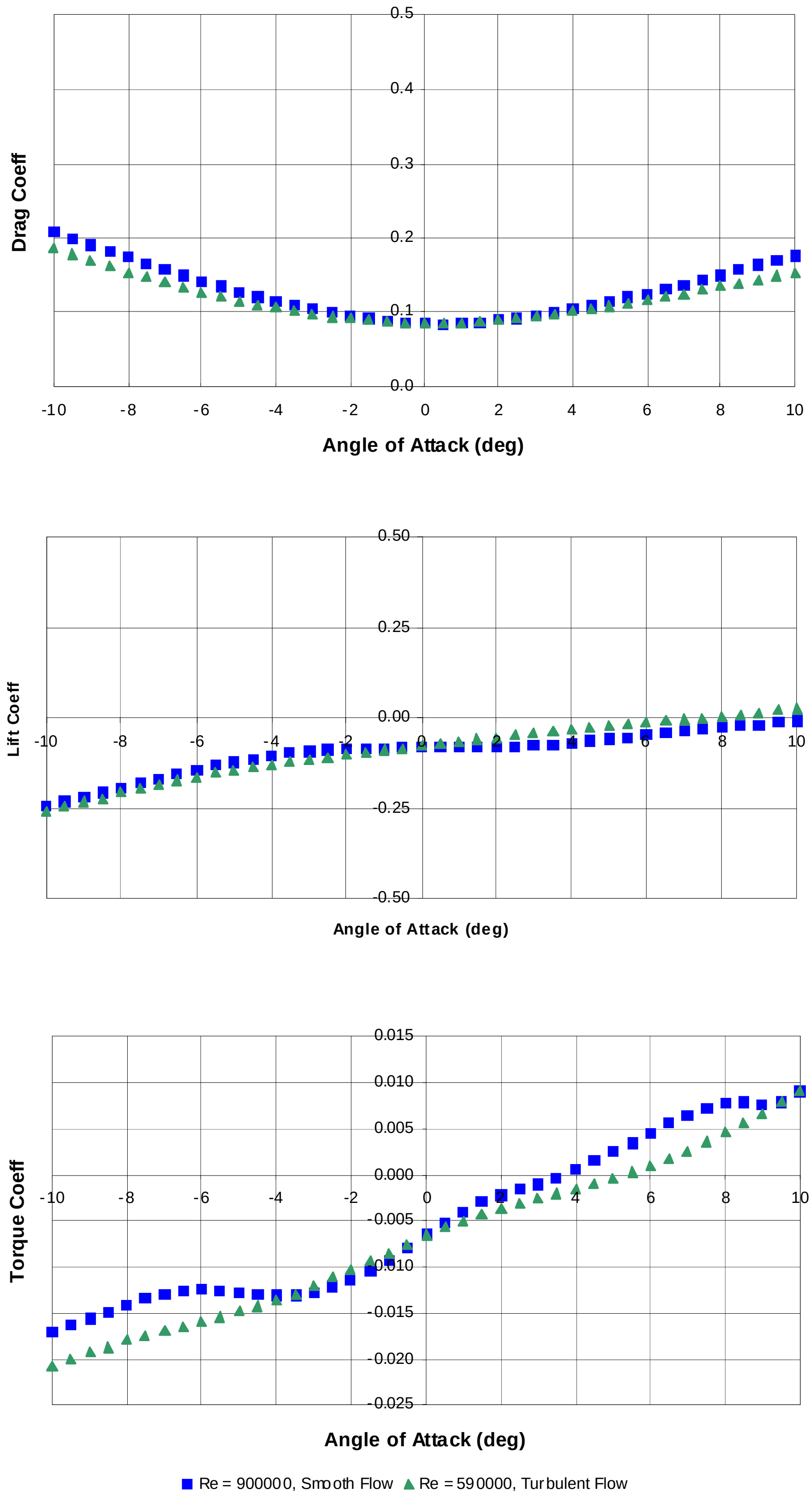

FIGURE C5 STATIC FORCE COEFFICIENTS (WIND AXIS FORCES), IN-SERVICE, NO TRAFFIC, SKEW=0^{O}

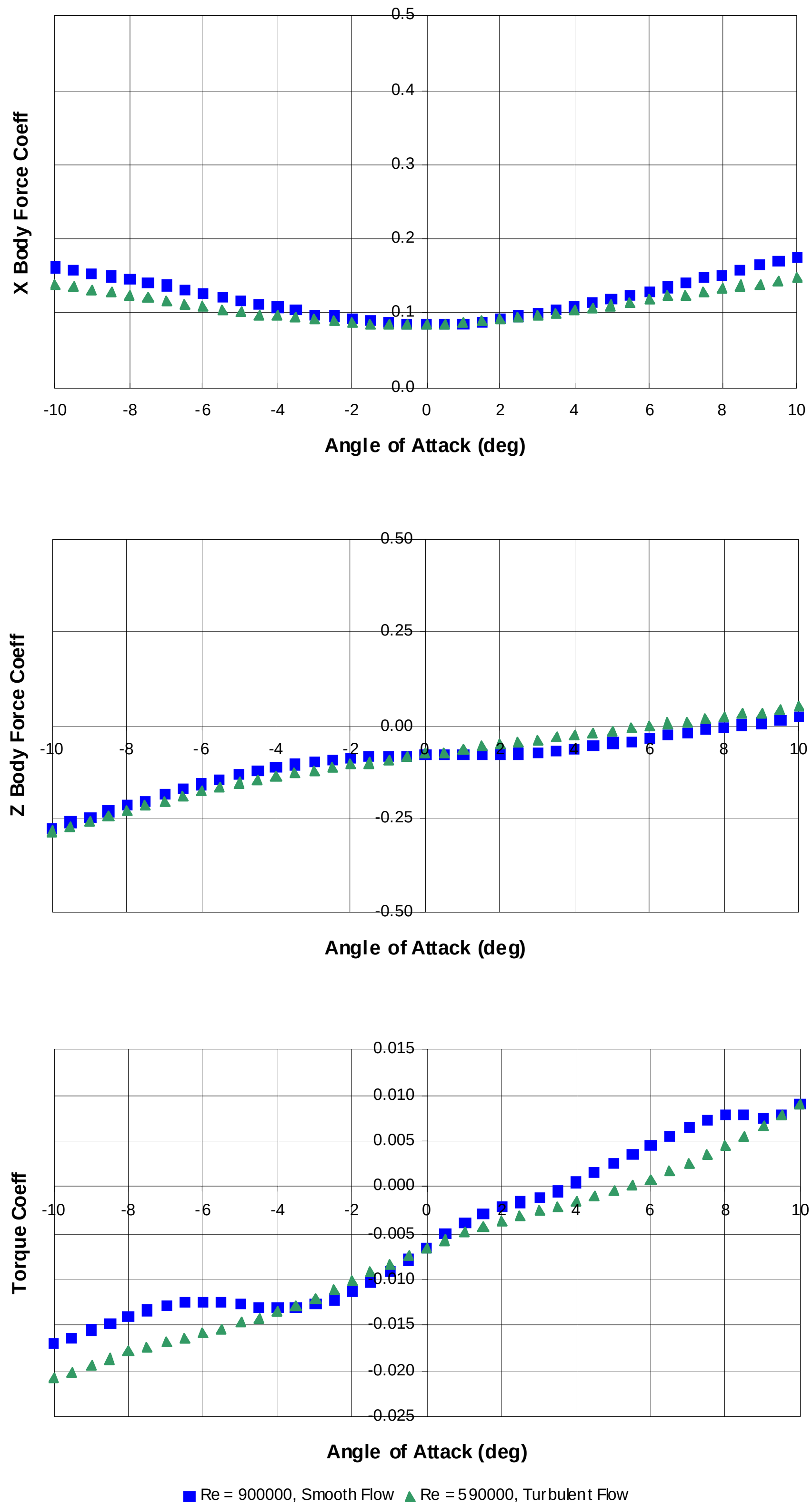

FIGURE C6 STATIC FORCE COEFFICIENTS (BODY FORCES), IN-SERVICE, NO TRAFFIC, SKEW=0^{O}

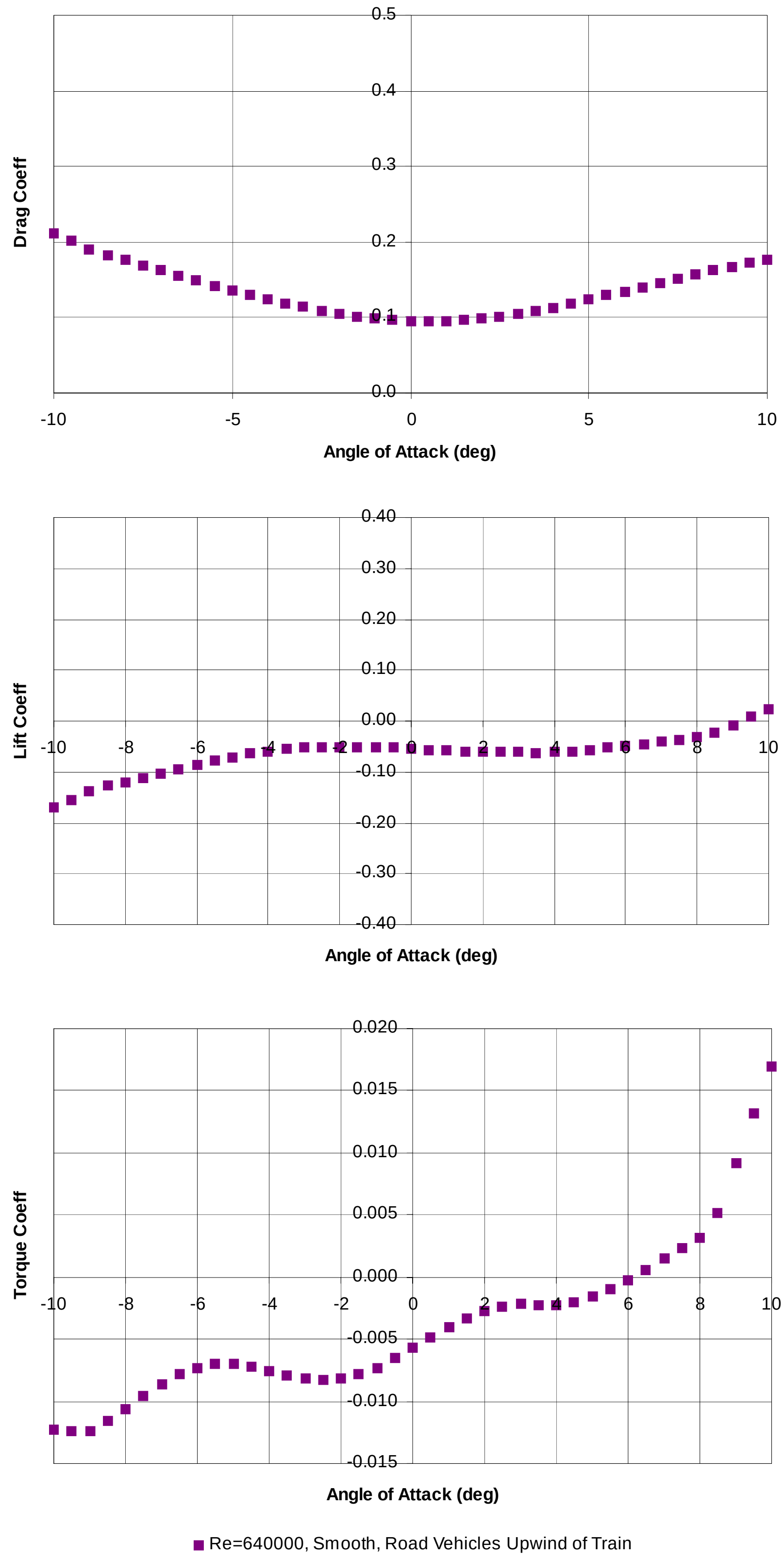

FIGURE C7 STATIC FORCE COEFFICIENTS (WIND AXIS FORCES), SMOOTH FLOW, IN-SERVICE, TRAFFIC CONDITION 1, SKEW=0^{O}

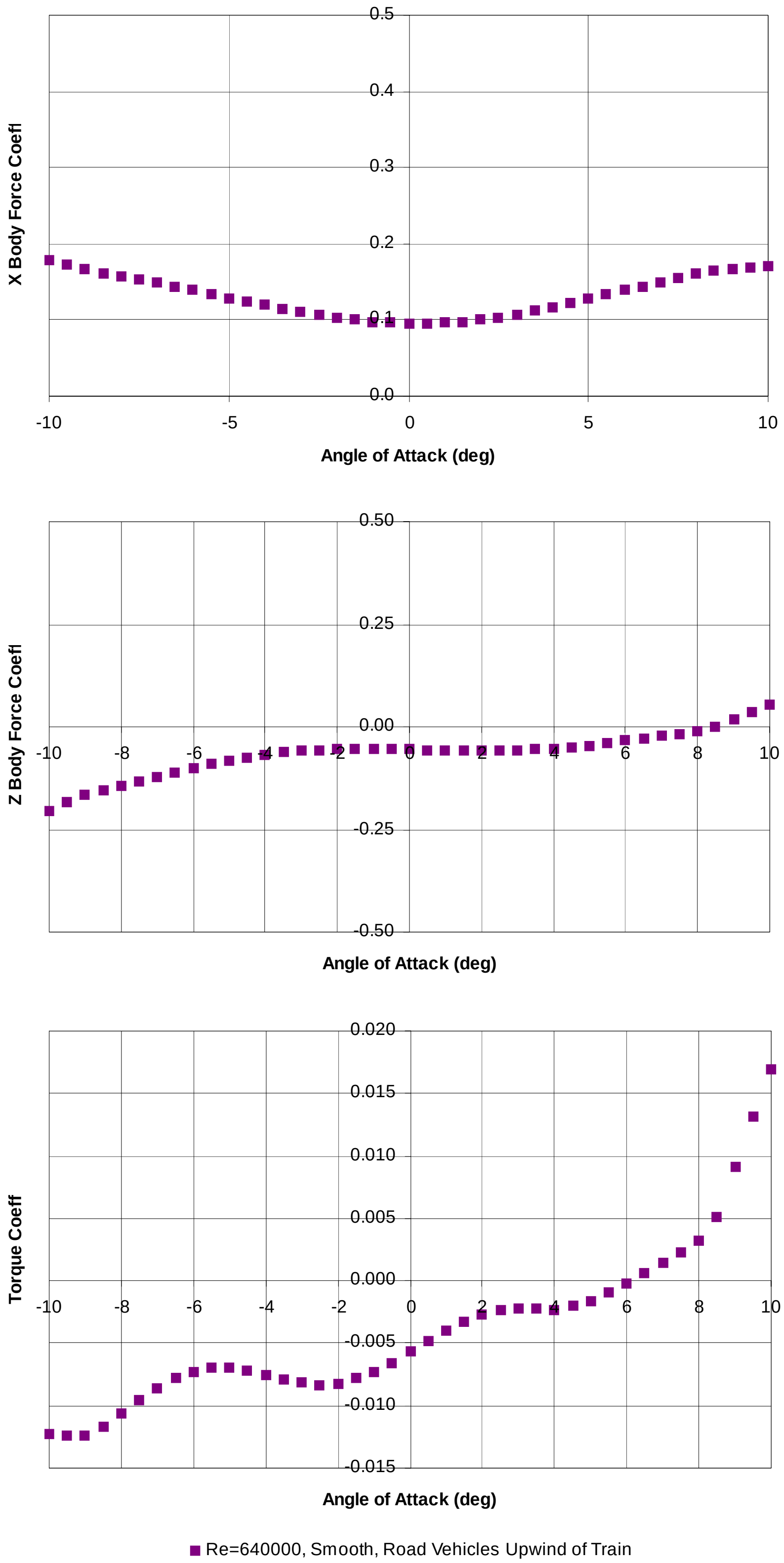

FIGURE C8 STATIC FORCE COEFFICIENTS (BODY FORCES), SMOOTH FLOW, IN-SERVICE, TRAFFIC CONDITION 1, SKEW=0^{O}

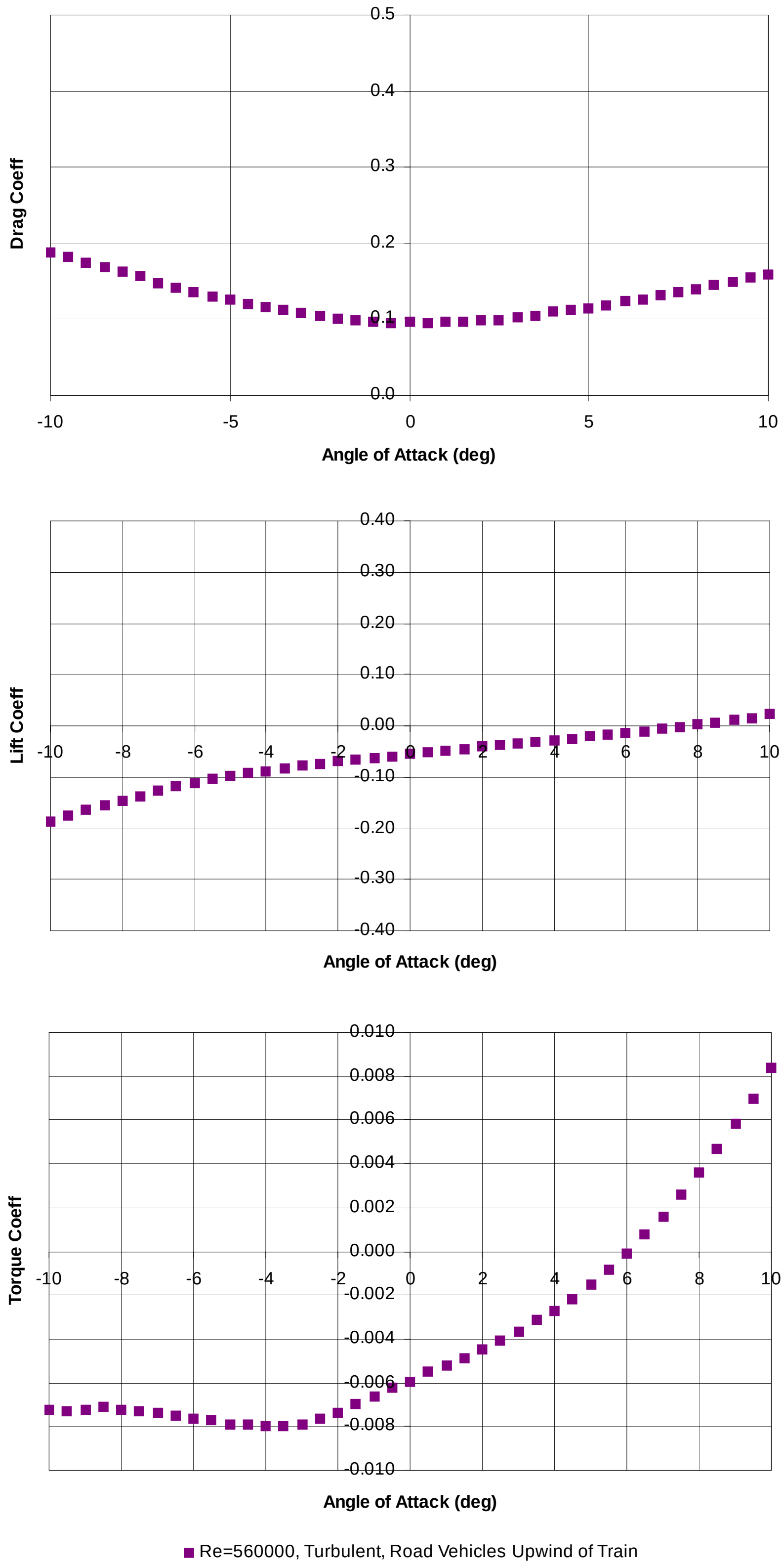

FIGURE C9 STATIC FORCE COEFFICIENTS (WIND AXIS FORCES), TURBULENT FLOW, IN-SERVICE, TRAFFIC CONDITION 1, SKEW=0^{O}

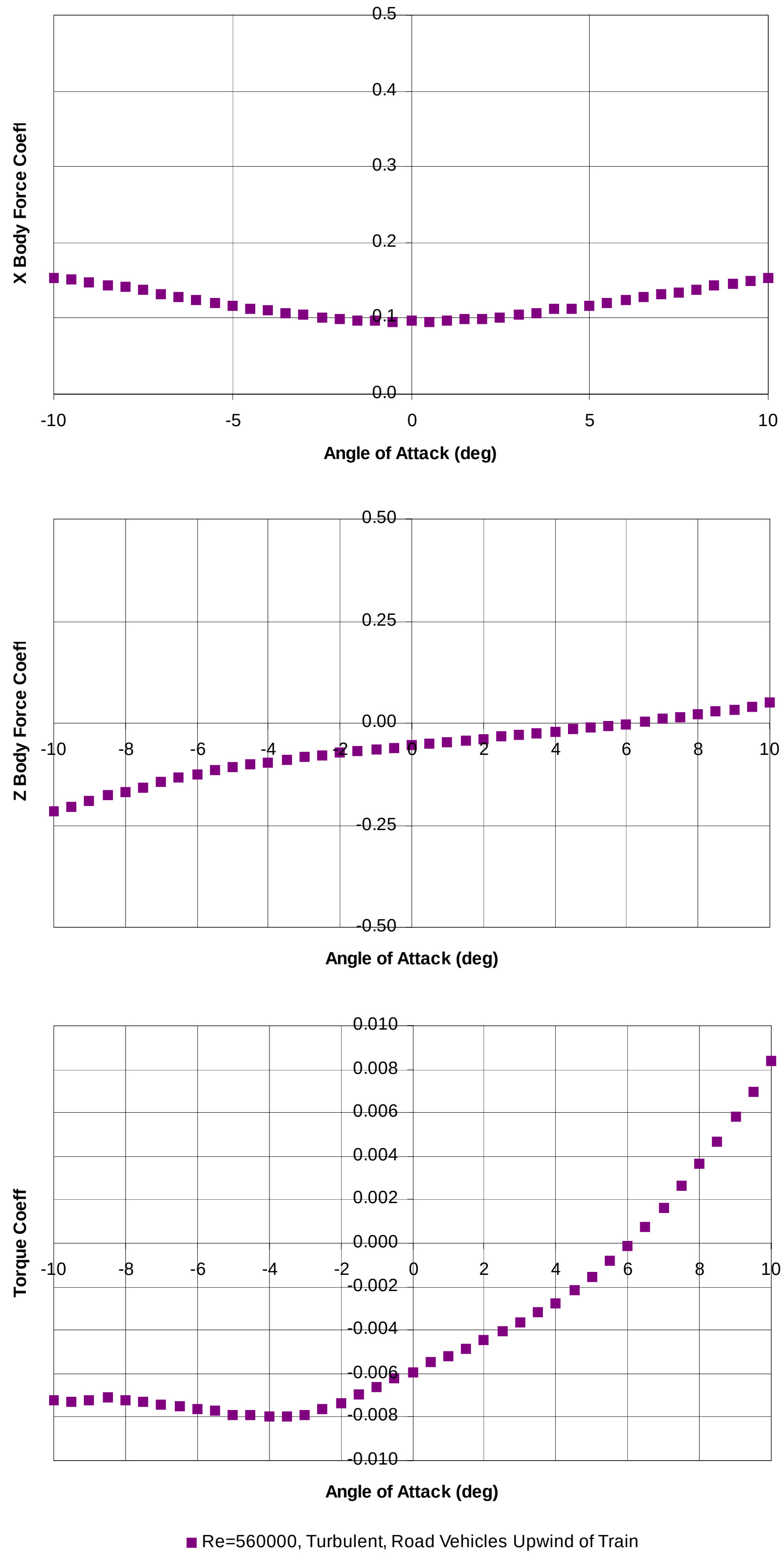

FIGURE C10 STATIC FORCE COEFFICIENTS (BODY FORCES), TURBULENT FLOW, IN-SERVICE, TRAFFIC CONDITION 1, SKEW=0^{O}

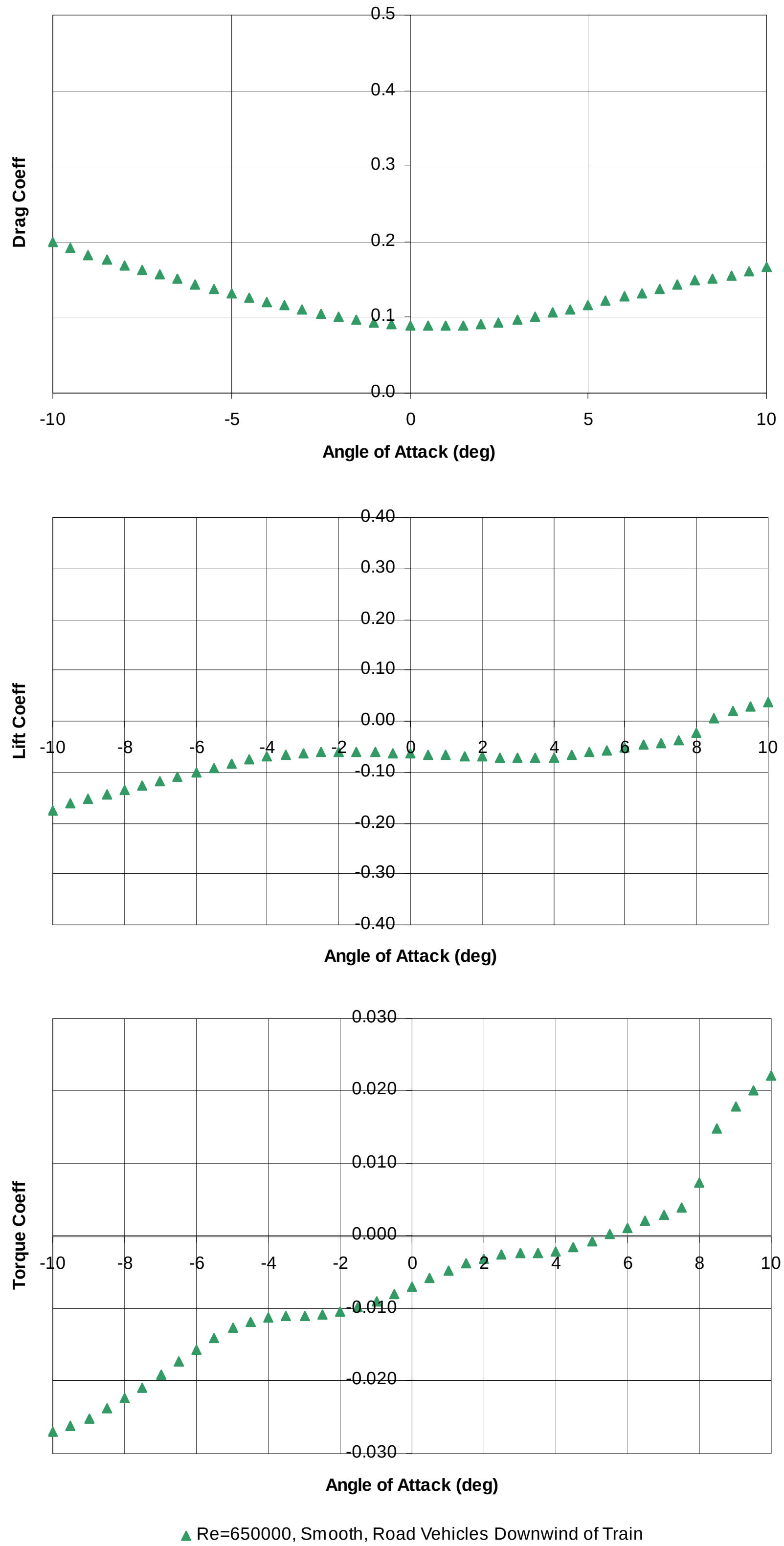

FIGURE C11 STATIC FORCE COEFFICIENTS (WIND AXIS FORCES), SMOOTH FLOW, IN-SERVICE, TRAFFIC CONDITION 2, SKEW=0^{O}

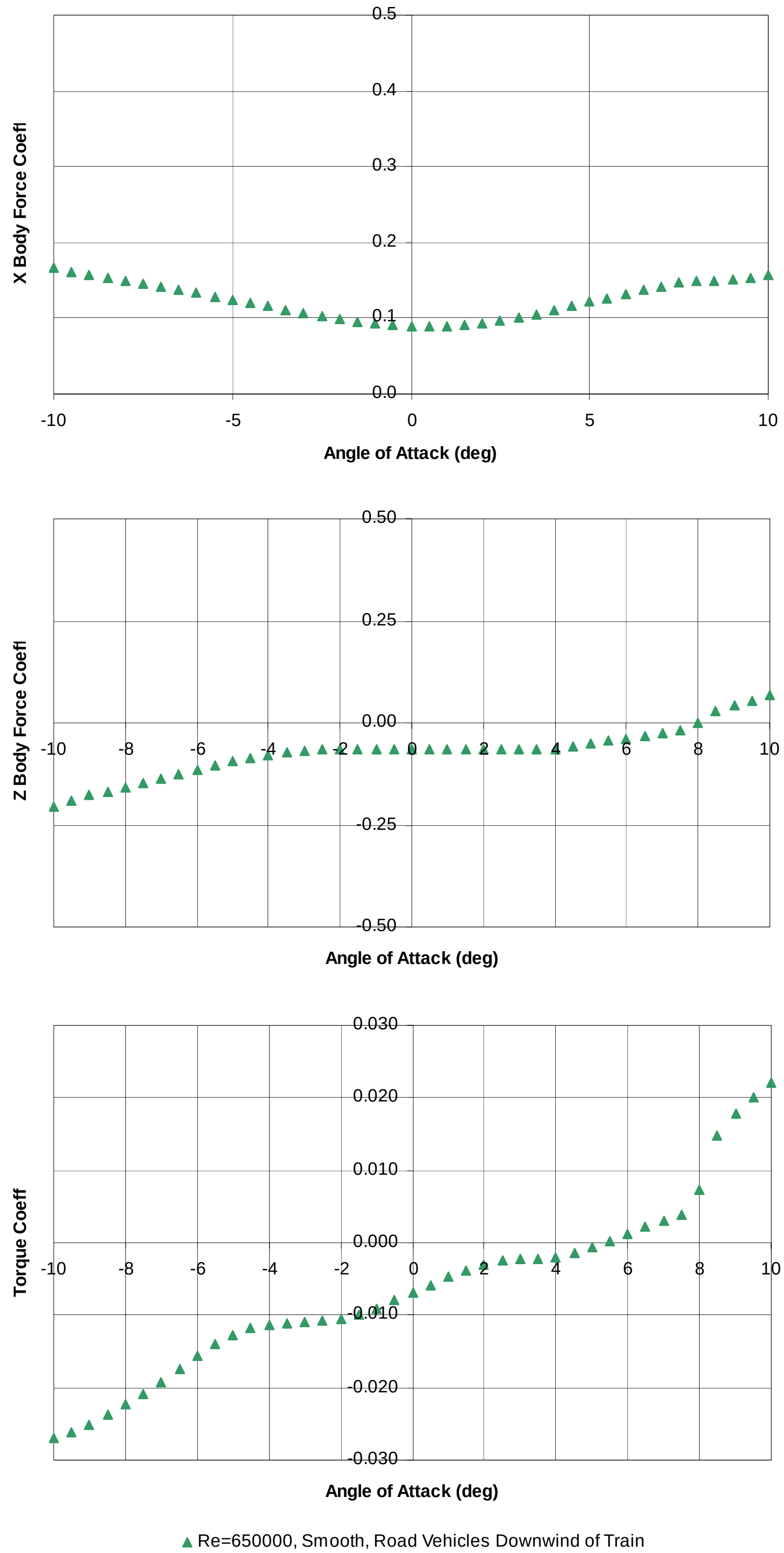

FIGURE C12 STATIC FORCE COEFFICIENTS (BODY FORCES), SMOOTH FLOW, IN-SERVICE, TRAFFIC CONDITION 2, SKEW=0^{O}

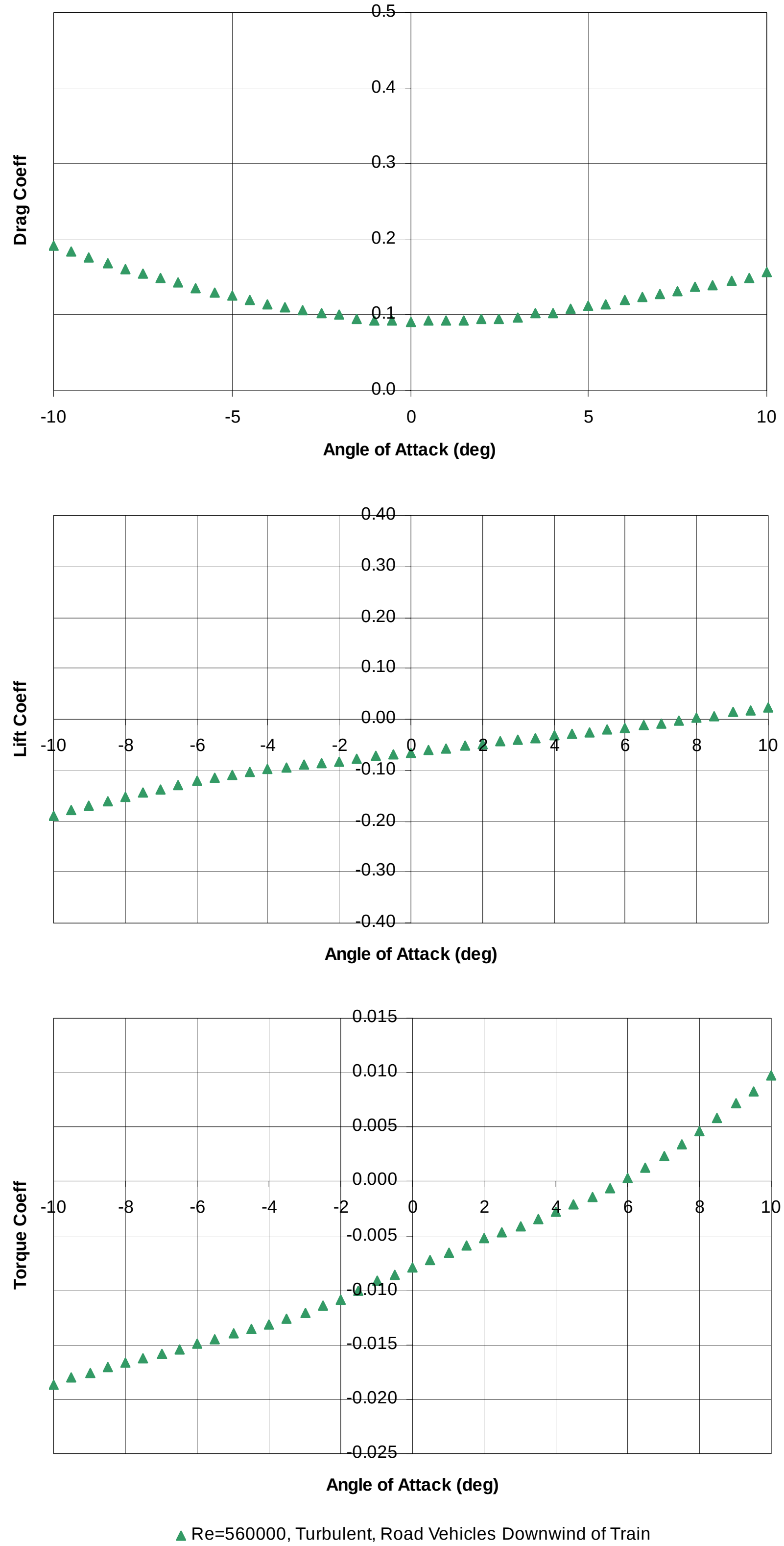

FIGURE C13 STATIC FORCE COEFFICIENTS (WIND AXIS FORCES), TURBULENT FLOW, IN-SERVICE, TRAFFIC CONDITION 2, SKEW=0^{O}

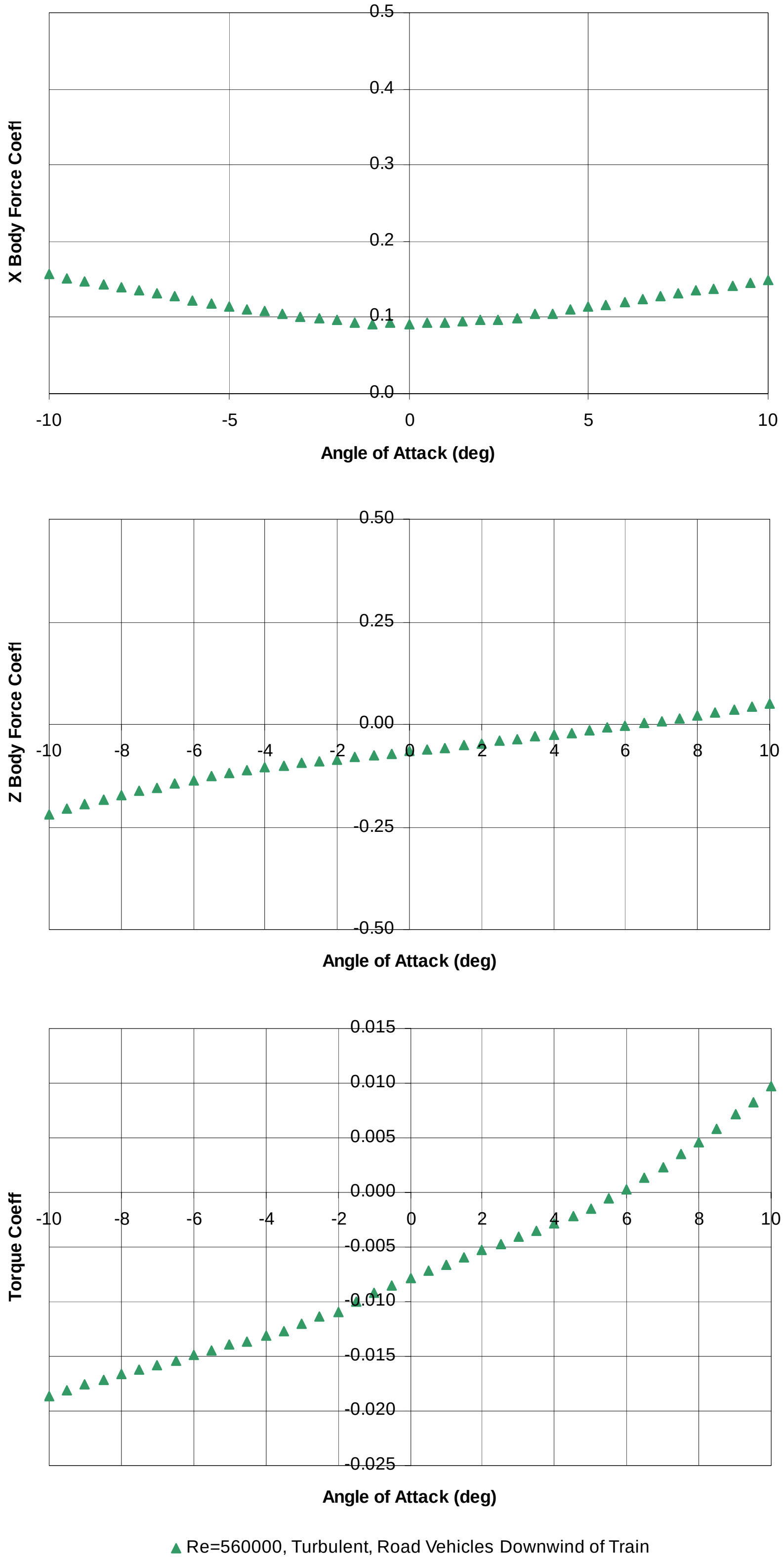

FIGURE C14 STATIC FORCE COEFFICIENTS (BODY FORCES), TURBULENT FLOW, IN-SERVICE, TRAFFIC CONDITION 2, SKEW=0^{O}

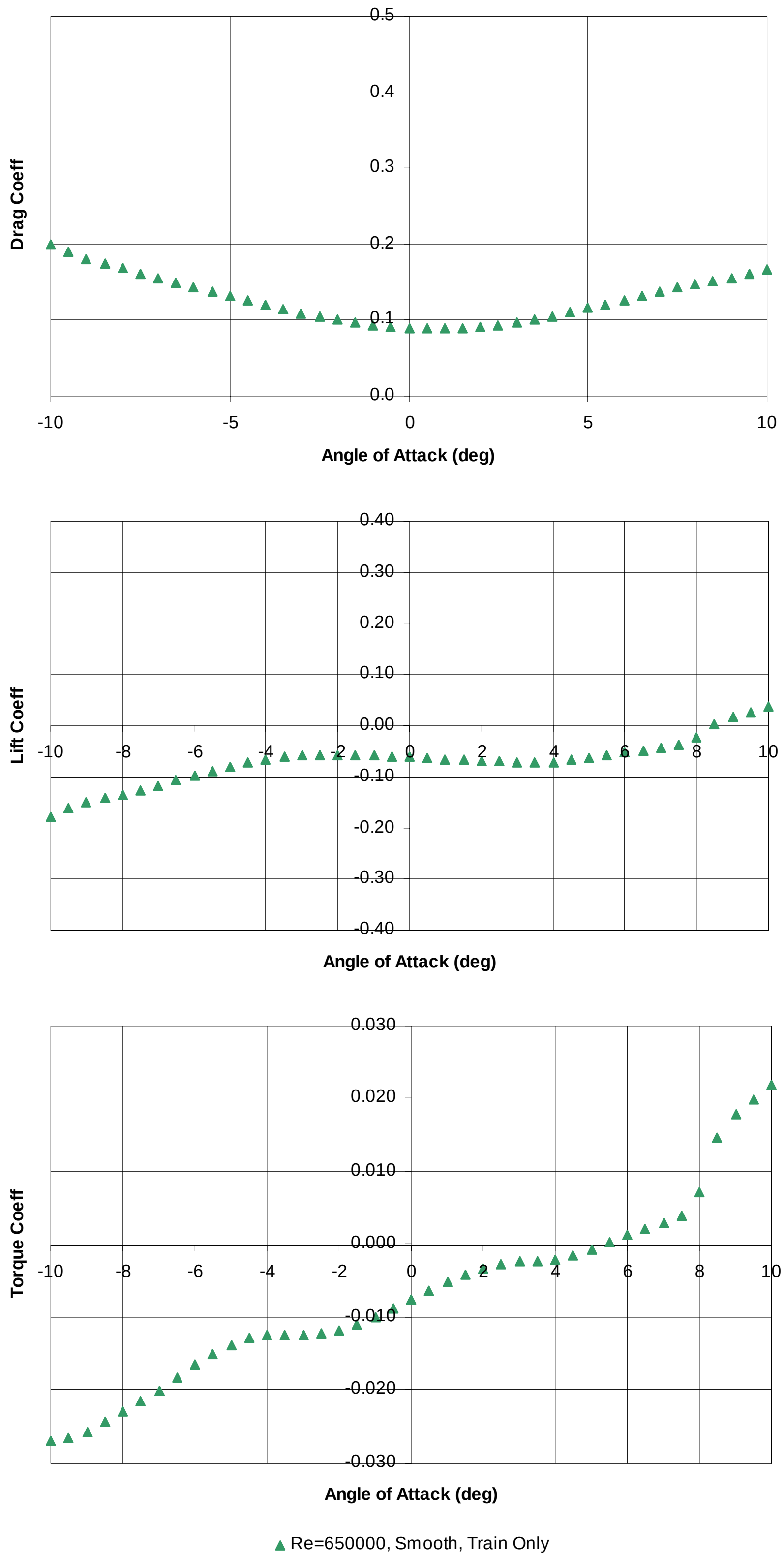

FIGURE C15 STATIC FORCE COEFFICIENTS (WIND AXIS FORCES), SMOOTH FLOW, IN-SERVICE, TRAFFIC CONDITION 3, SKEW=0^{O}

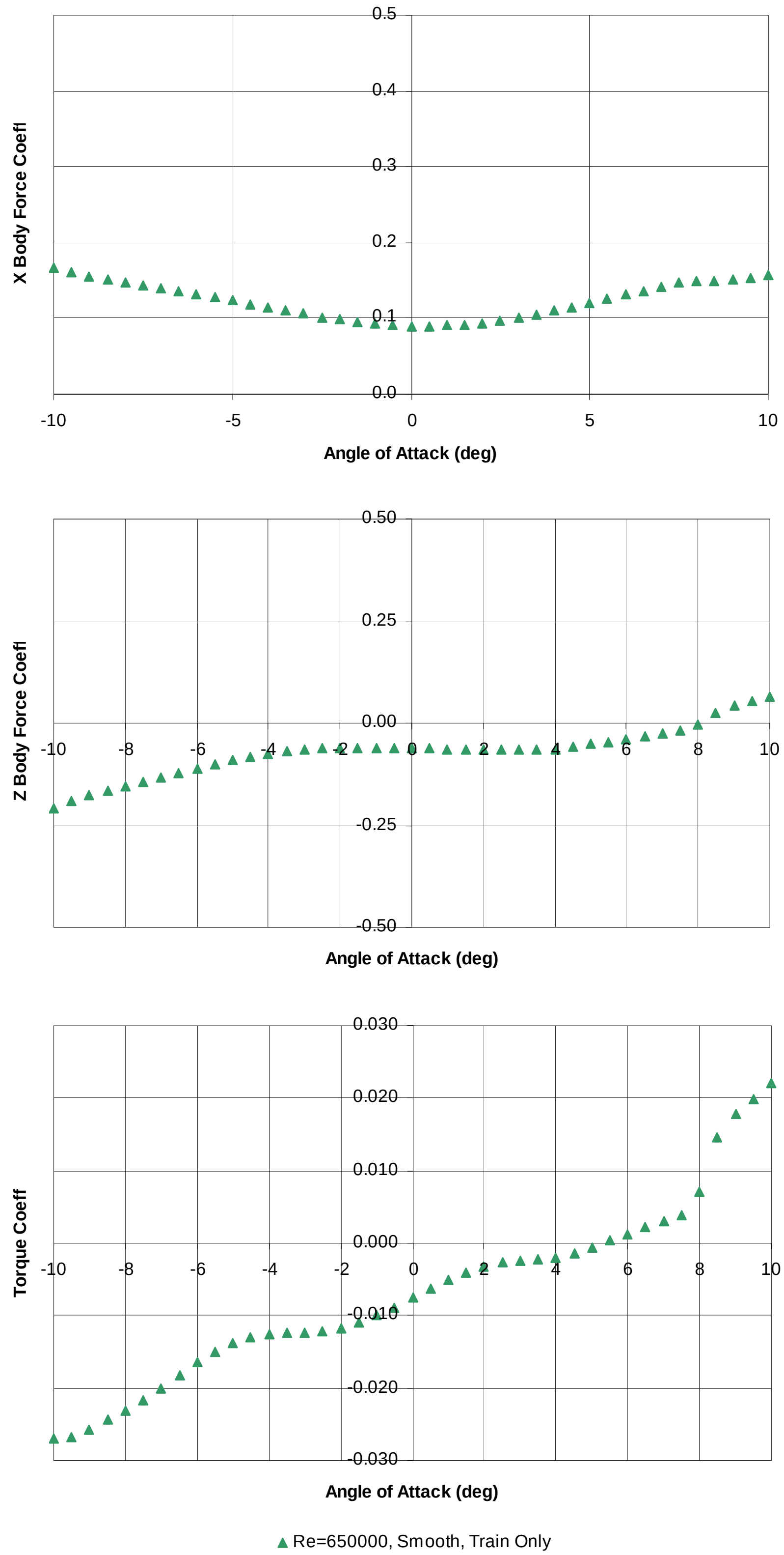

FIGURE C16 STATIC FORCE COEFFICIENTS (BODY FORCES), SMOOTH FLOW, IN-SERVICE, TRAFFIC CONDITION 3, SKEW=0^{O}

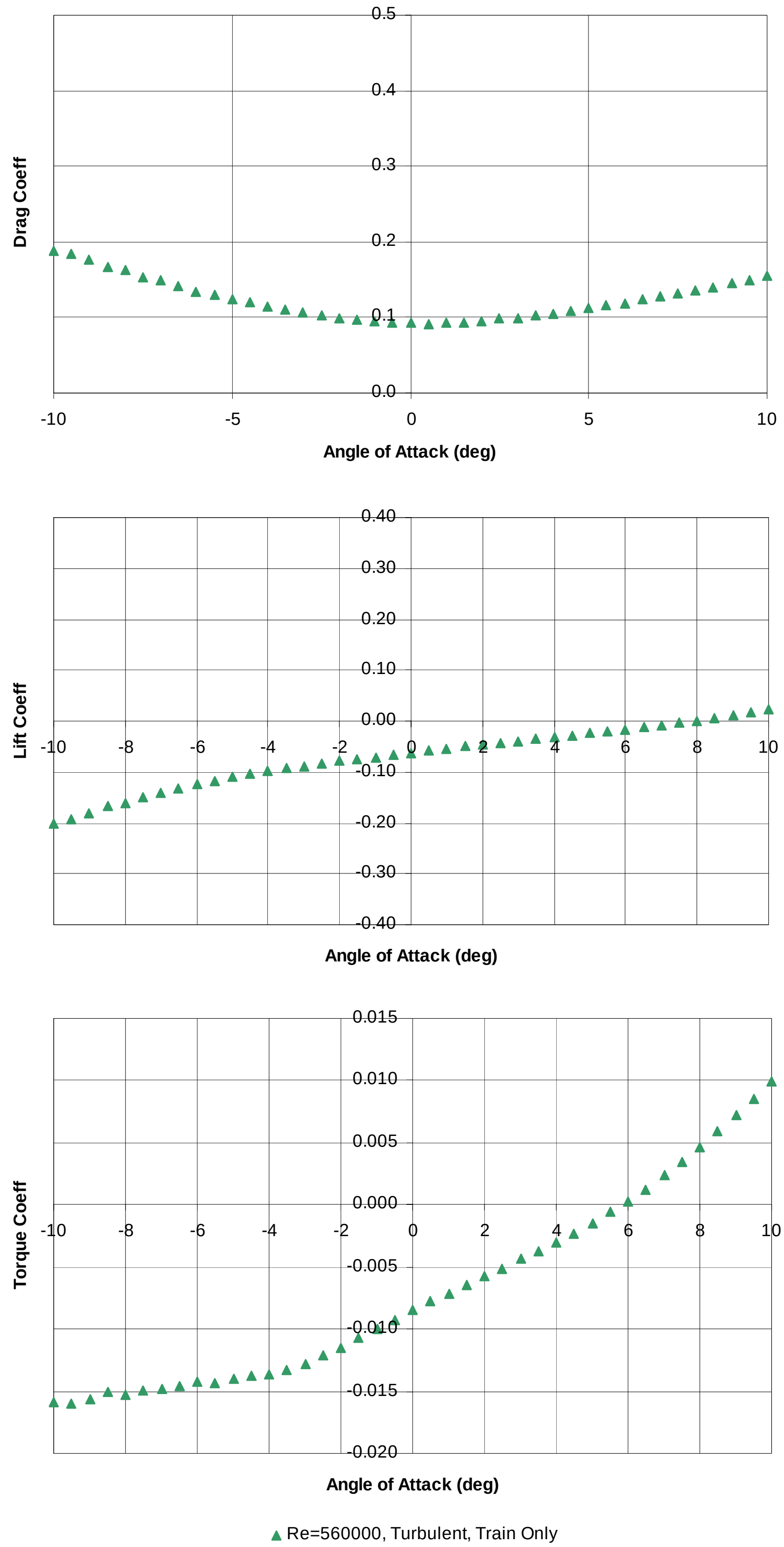

FIGURE C17 STATIC FORCE COEFFICIENTS (WIND AXIS FORCES), TURBULENT FLOW, IN-SERVICE, TRAFFIC CONDITION 3, SKEW=0^{O}

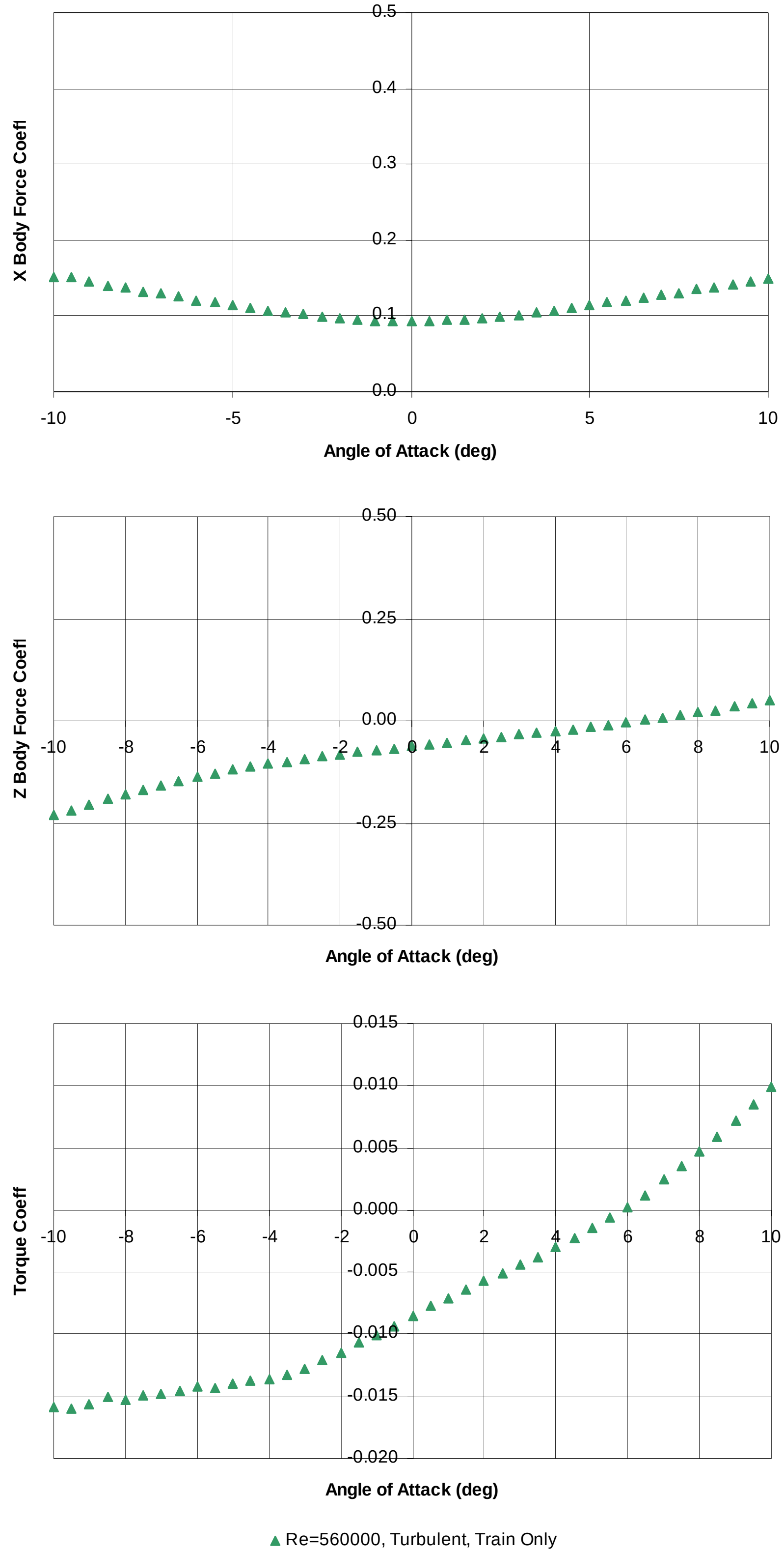

FIGURE C18 STATIC FORCE COEFFICIENTS (BODY FORCES), TURBULENT FLOW, IN-SERVICE, TRAFFIC CONDITION 3, SKEW=0^{O}

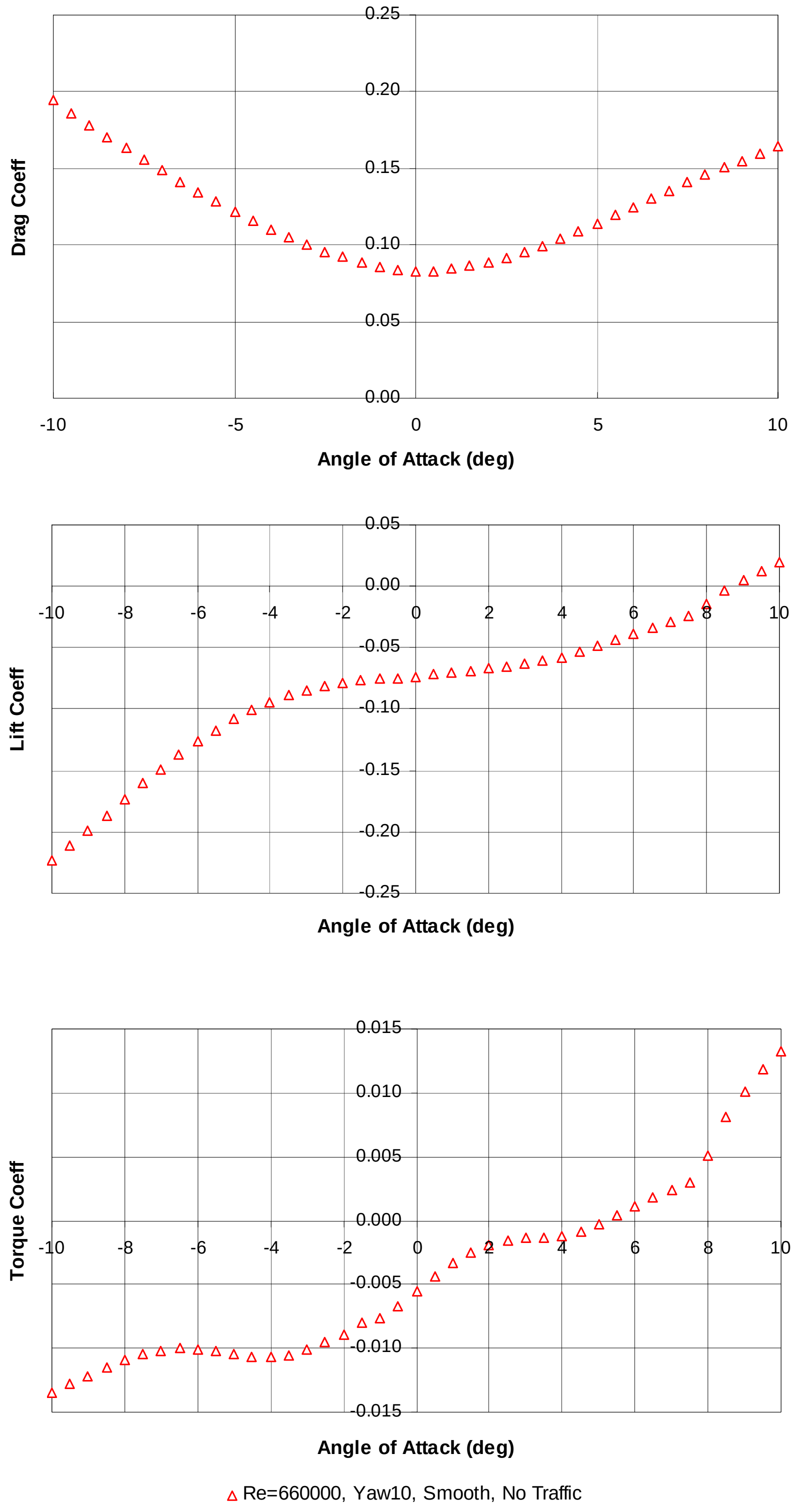

FIGURE C19 STATIC FORCE COEFFICIENTS (WIND AXIS FORCES), SMOOTH FLOW, IN-SERVICE, NO TRAFFIC, SKEW=10^{O}

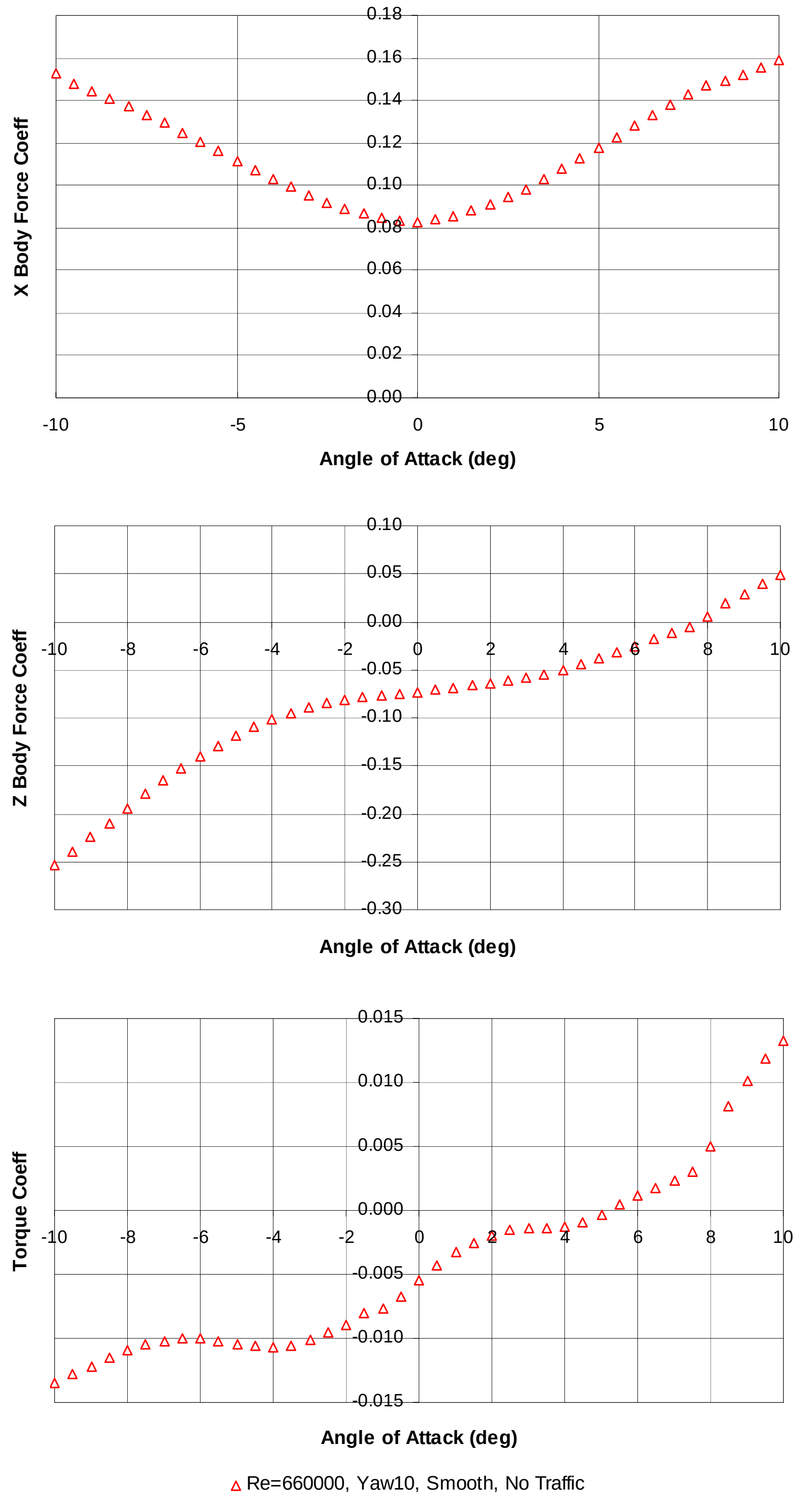

FIGURE C20 STATIC FORCE COEFFICIENTS (BODY FORCES), SMOOTH FLOW, IN-SERVICE, NO TRAFFIC, SKEW=10^{O}

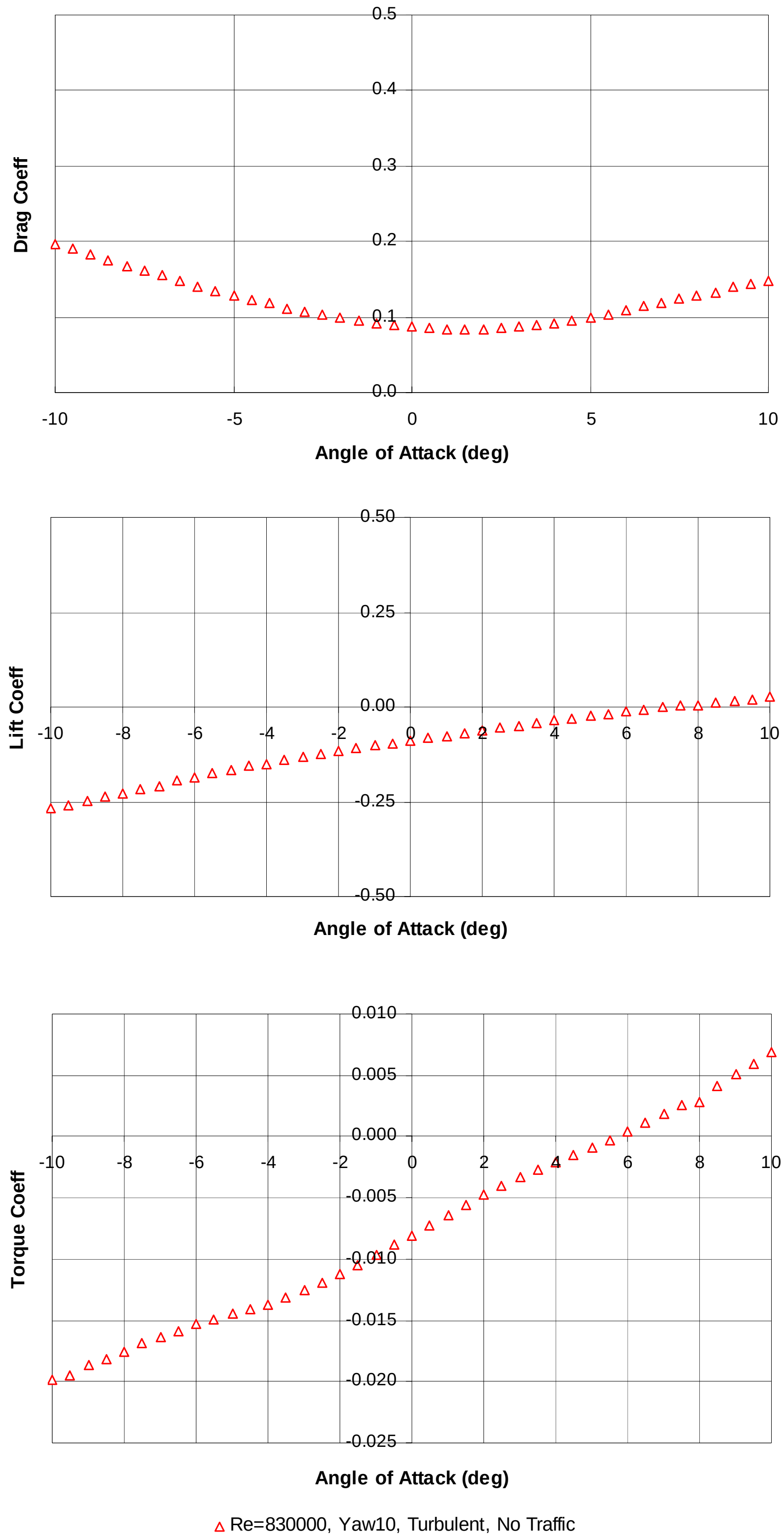

FIGURE C21 STATIC FORCE COEFFICIENTS (WIND AXIS FORCES), TURBULENT FLOW, IN-SERVICE, NO TRAFFIC, SKEW=10^{O}

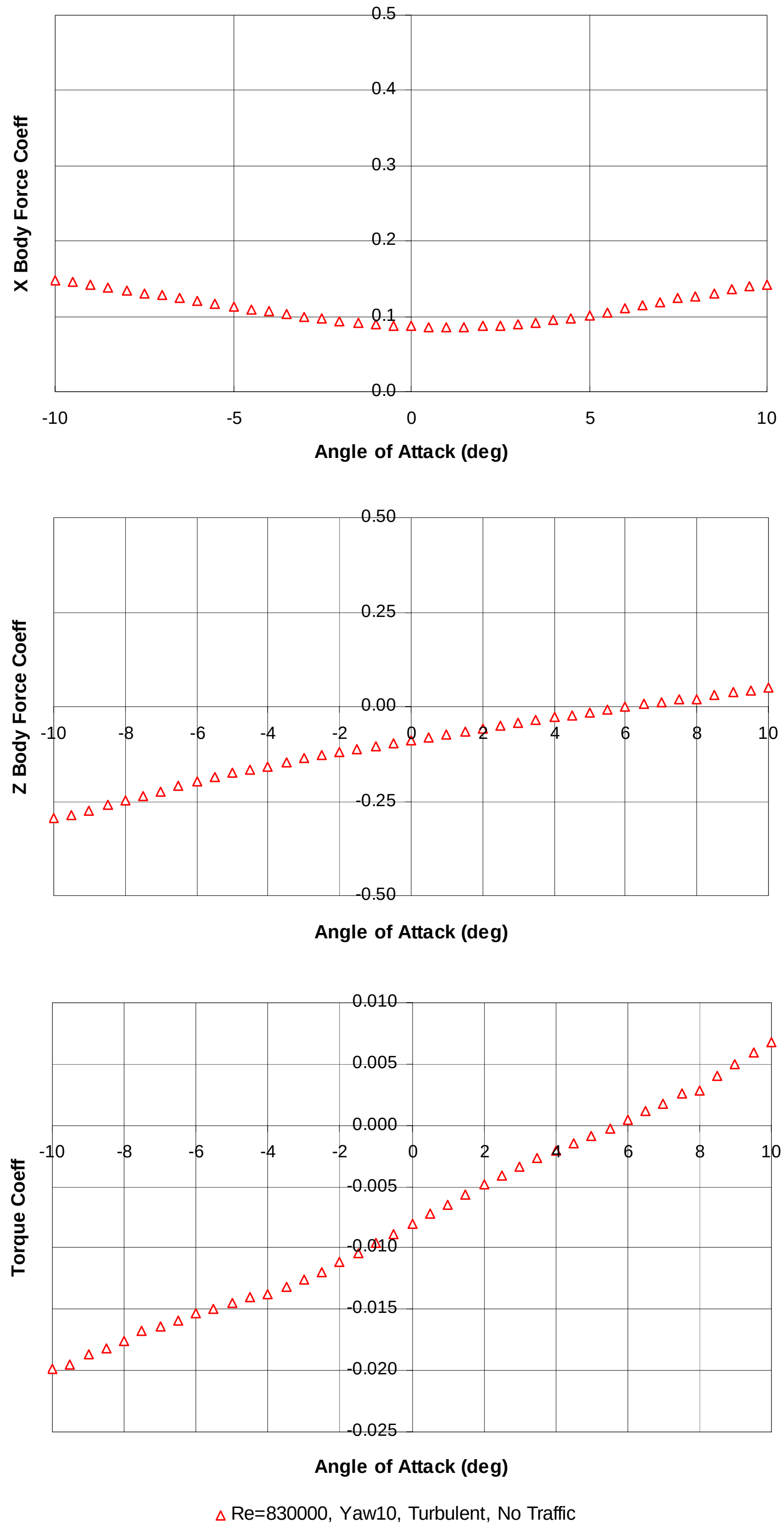

FIGURE C22 STATIC FORCE COEFFICIENTS (BODY FORCES), TURBULENT FLOW, IN-SERVICE, NO TRAFFIC, SKEW=10^{O}

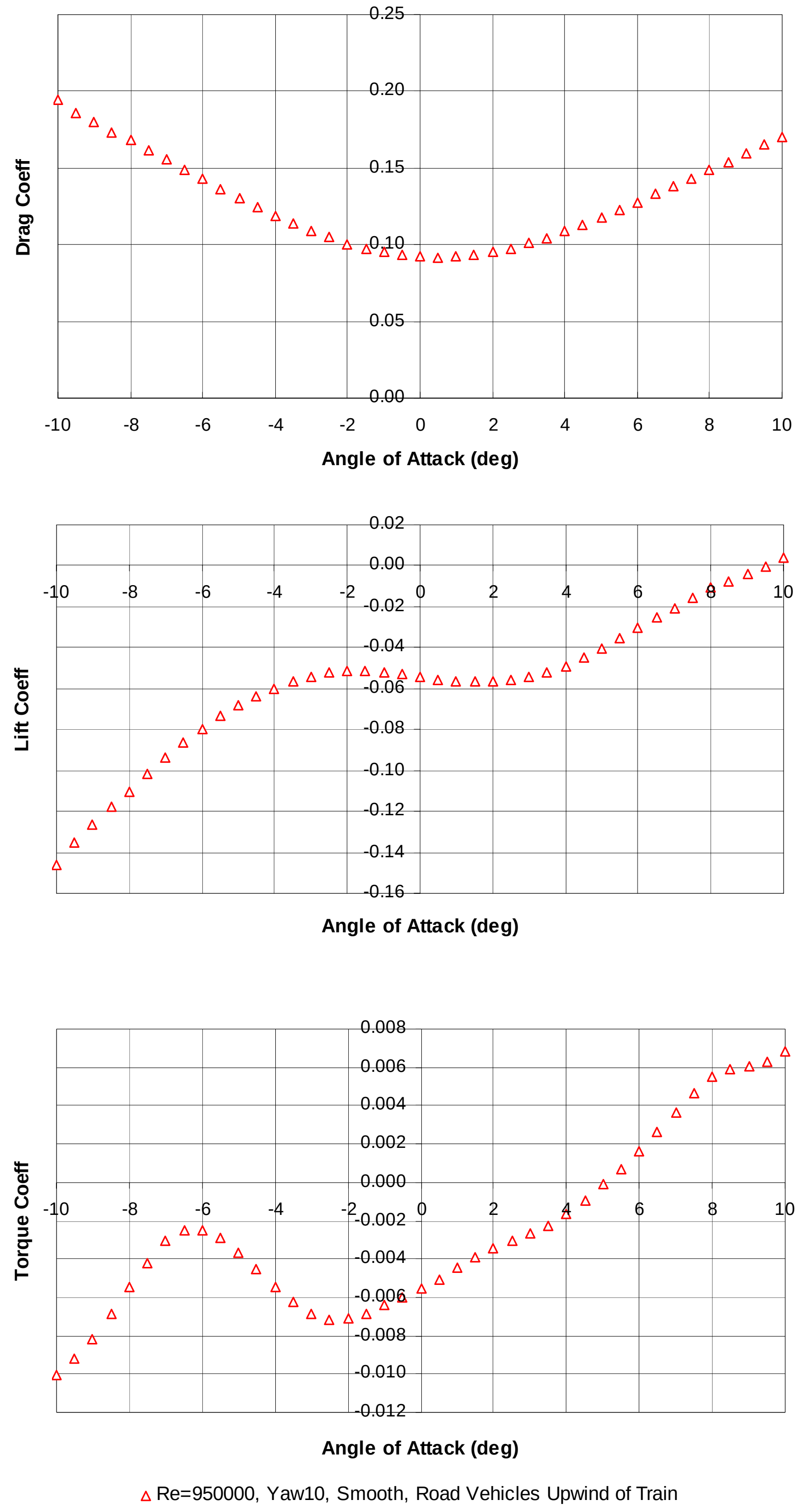

FIGURE C23 STATIC FORCE COEFFICIENTS (WIND AXIS FORCES), SMOOTH FLOW, IN-SERVICE, TRAFFIC CONDITION 1, SKEW=10^{O}

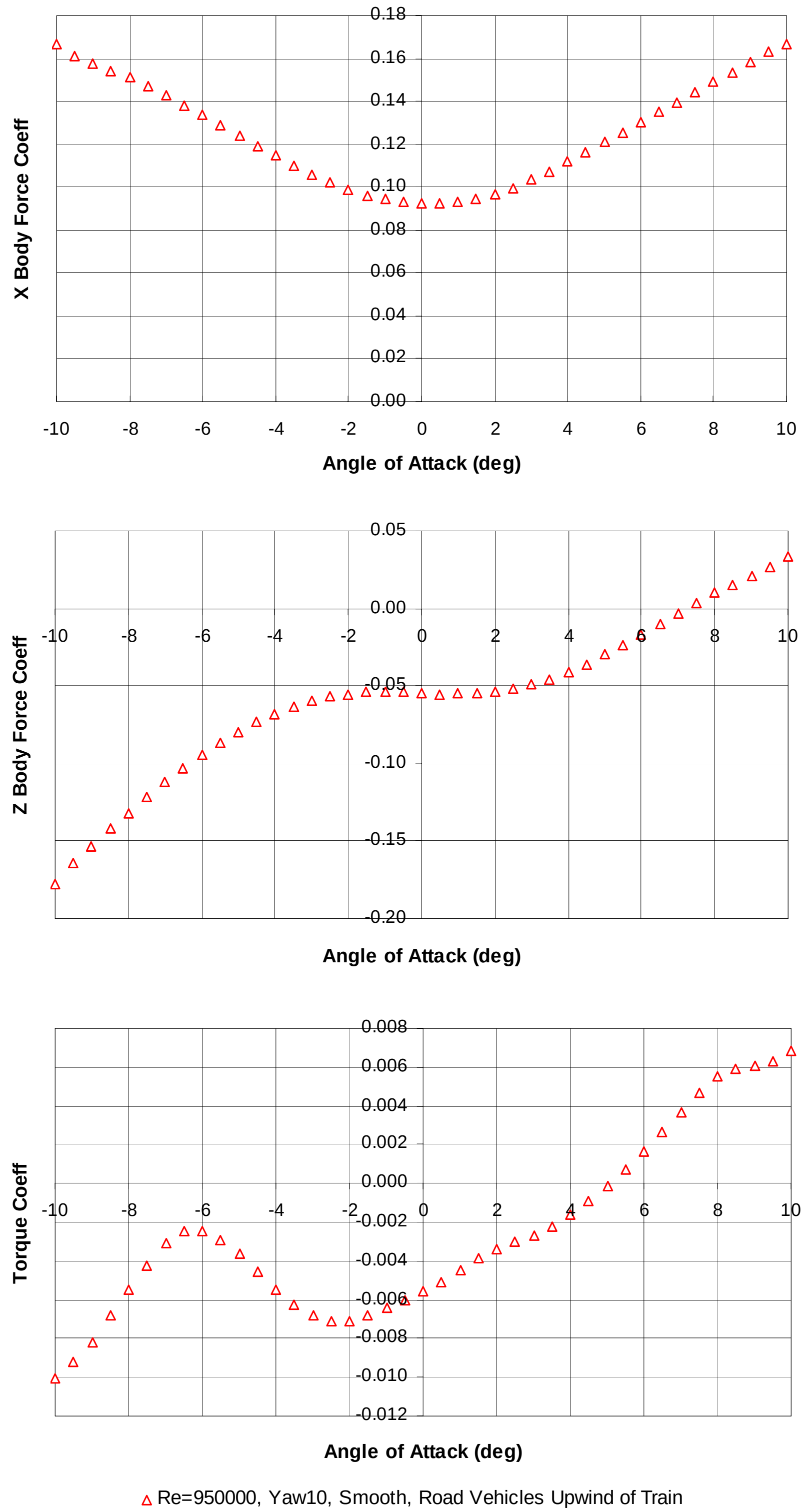

FIGURE C24 STATIC FORCE COEFFICIENTS (BODY FORCES), SMOOTH FLOW, IN-SERVICE, TRAFFIC CONDITION 1, SKEW=10^{O}

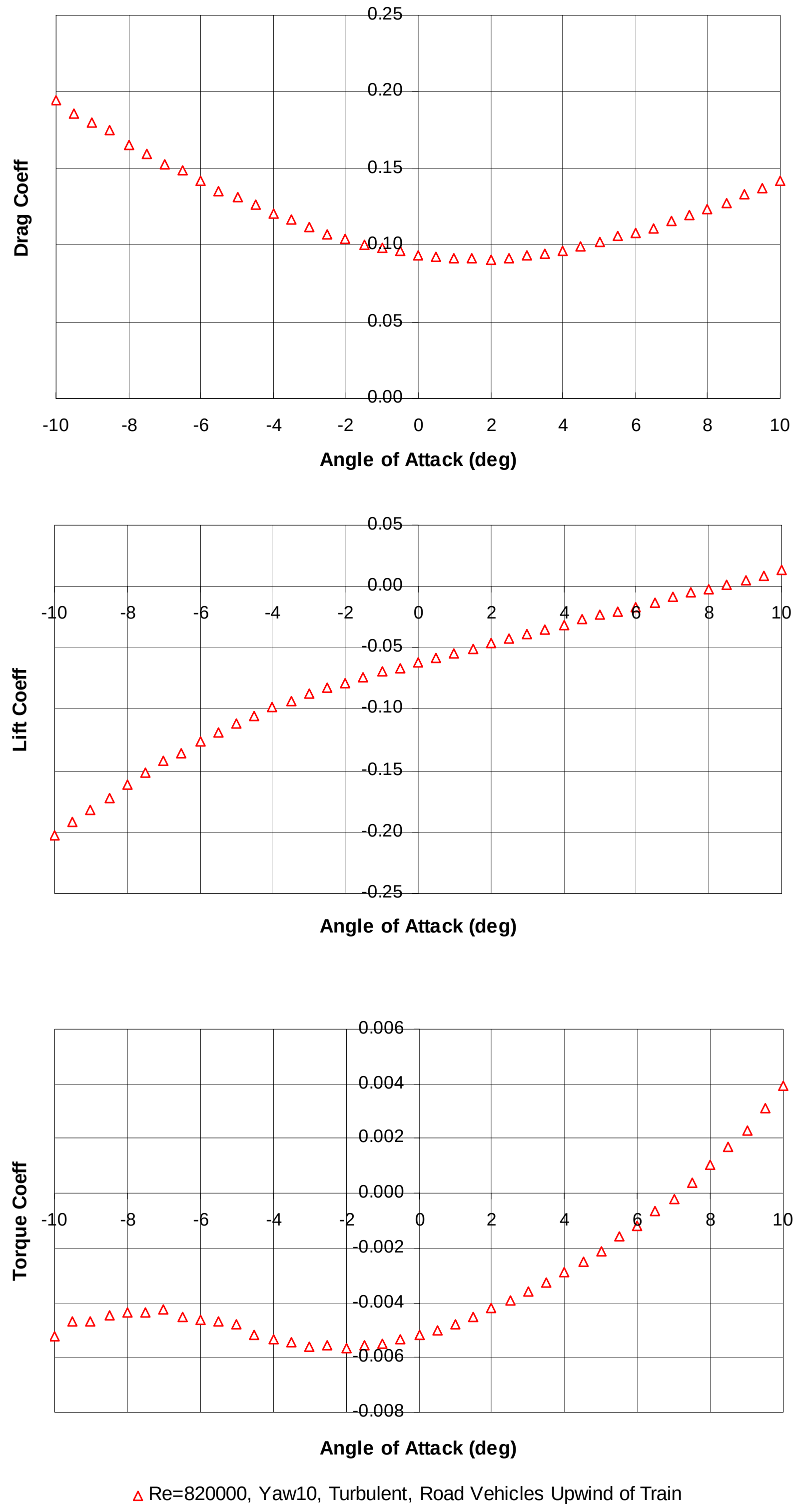

FIGURE C25 STATIC FORCE COEFFICIENTS (WIND AXIS FORCES), TURBULENT FLOW, IN-SERVICE, TRAFFIC CONDITION 1, SKEW=10^{O}

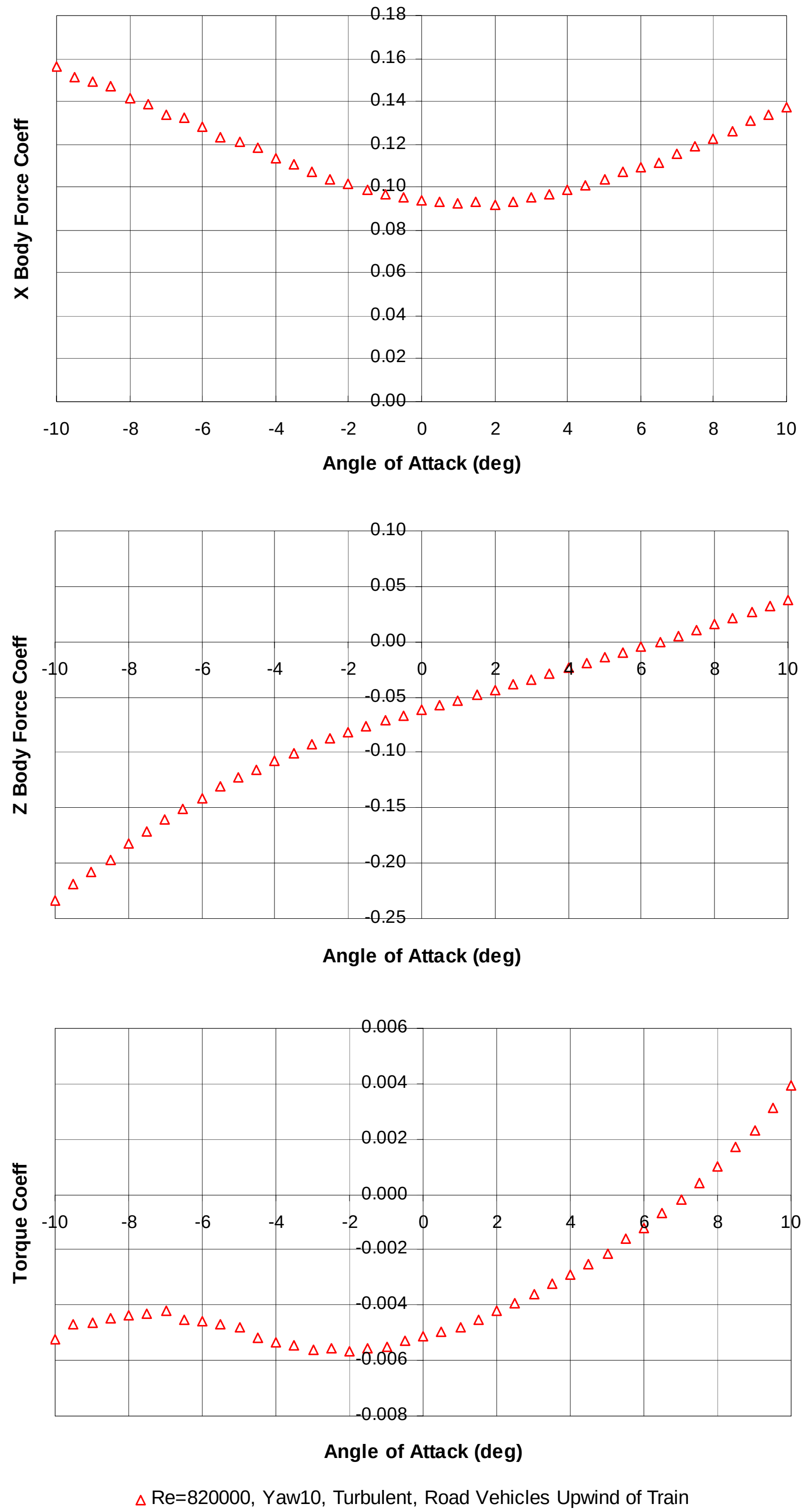

FIGURE C26 STATIC FORCE COEFFICIENTS (BODY FORCES), TURBULENT FLOW, IN-SERVICE, TRAFFIC CONDITION 1, SKEW=10^{O}

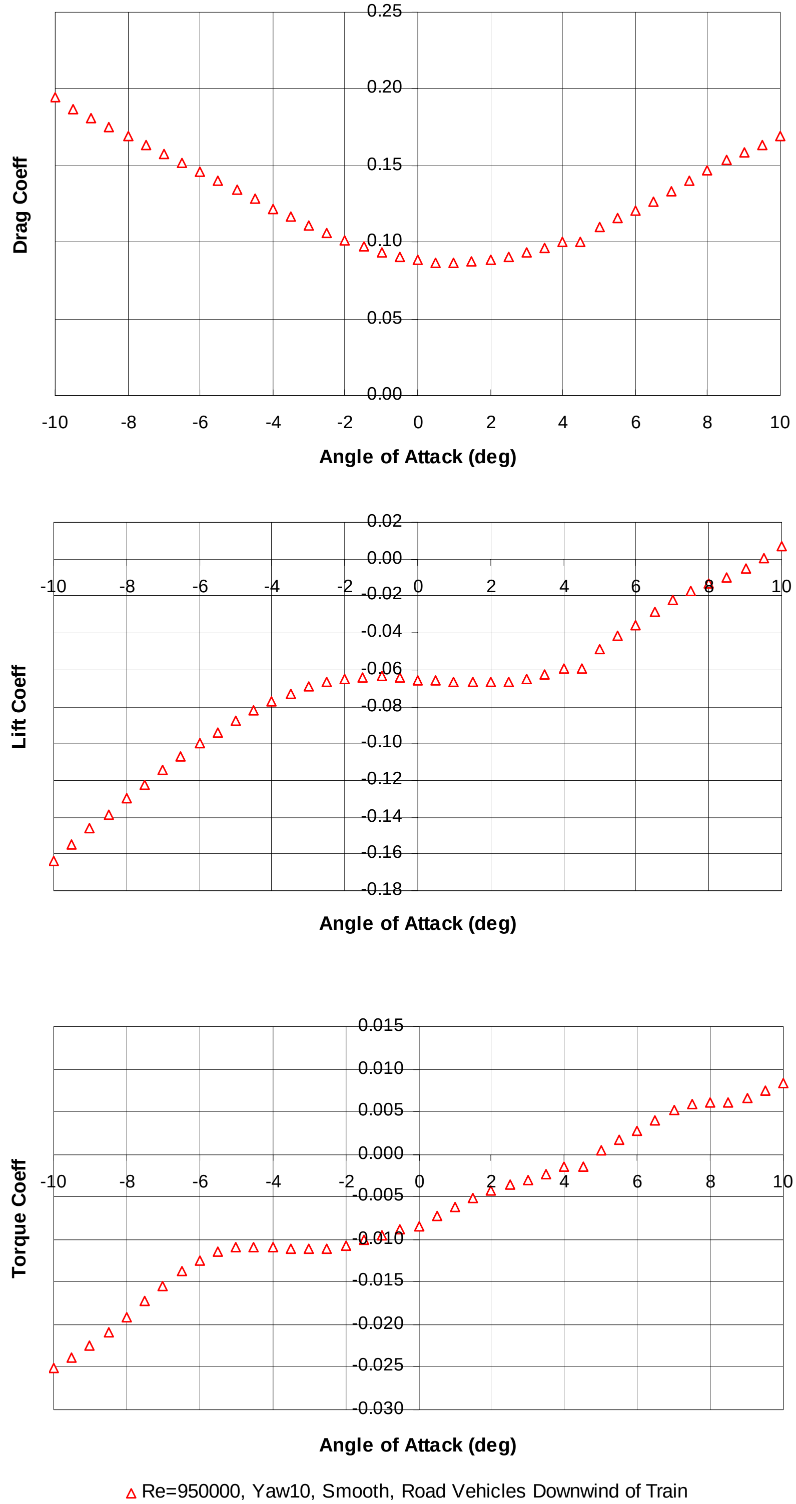

FIGURE C27 STATIC FORCE COEFFICIENTS (WIND AXIS FORCES), SMOOTH FLOW, IN-SERVICE, TRAFFIC CONDITION 2, SKEW=10^{O}

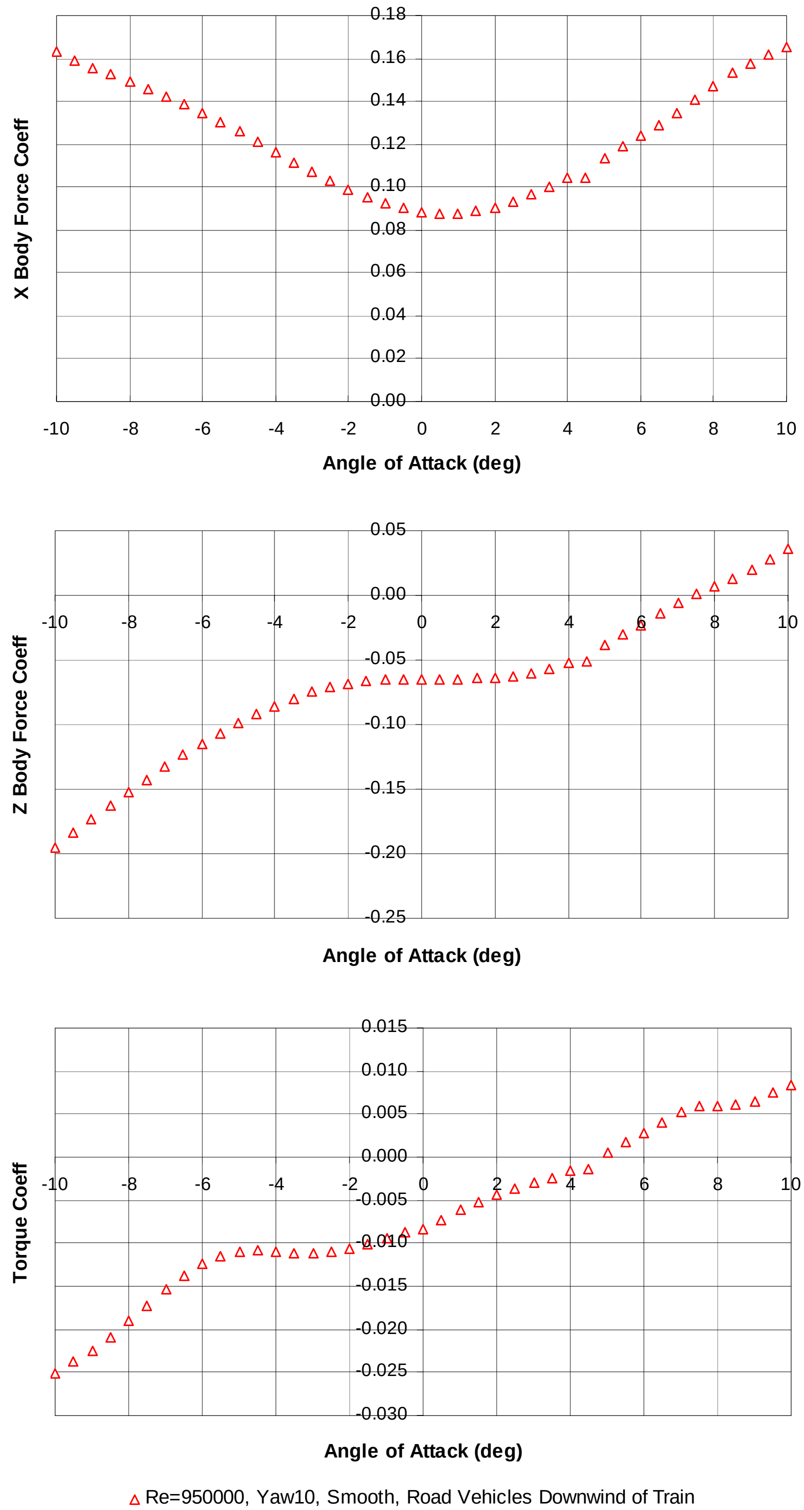

FIGURE C28 STATIC FORCE COEFFICIENTS (BODY FORCES), SMOOTH FLOW, IN-SERVICE, TRAFFIC CONDITION 2, SKEW=10^{O}

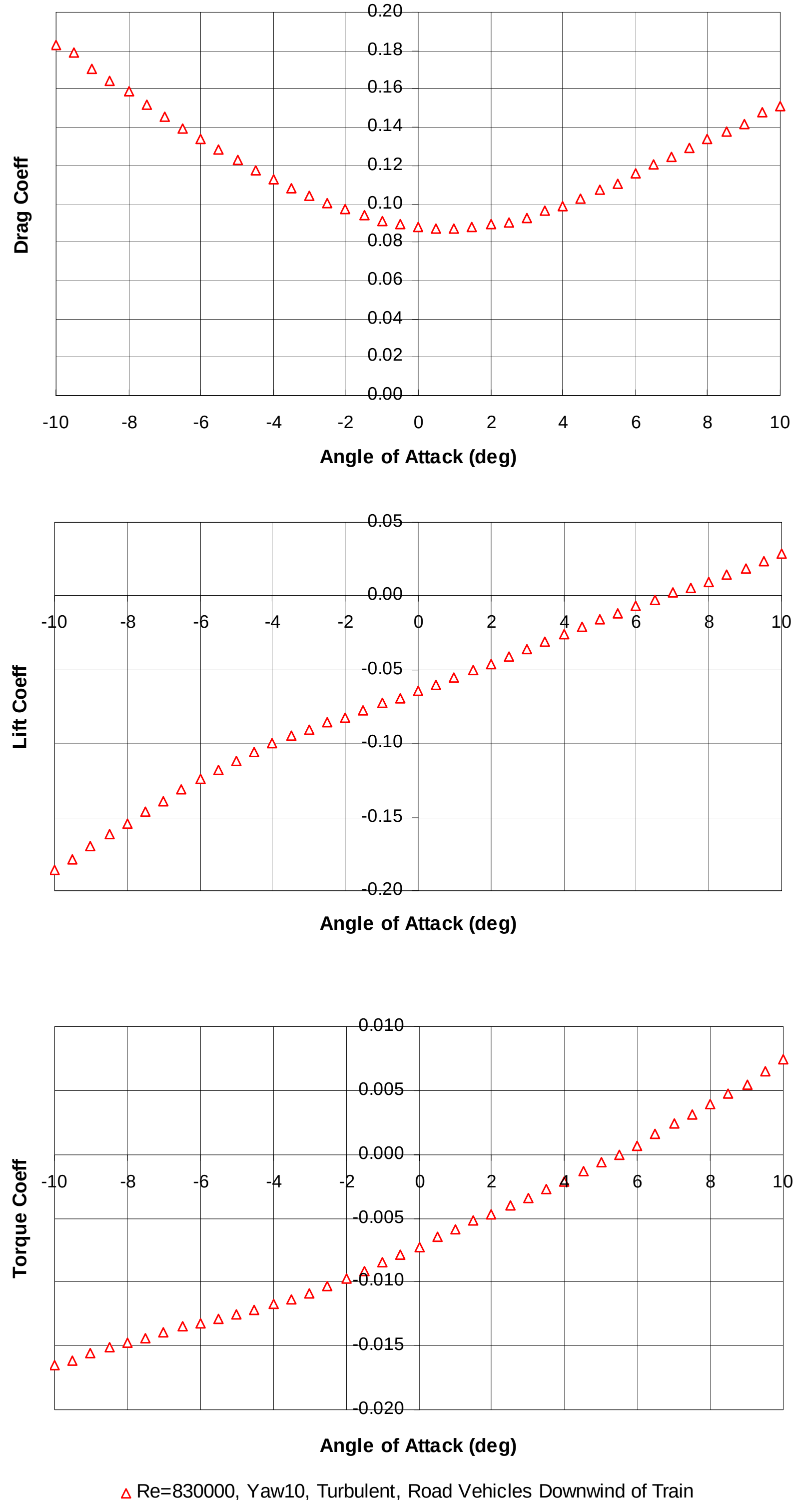

FIGURE C29 STATIC FORCE COEFFICIENTS (WIND AXIS FORCES), TURBULENT FLOW, IN-SERVICE, TRAFFIC CONDITION 2, SKEW=10^{O}

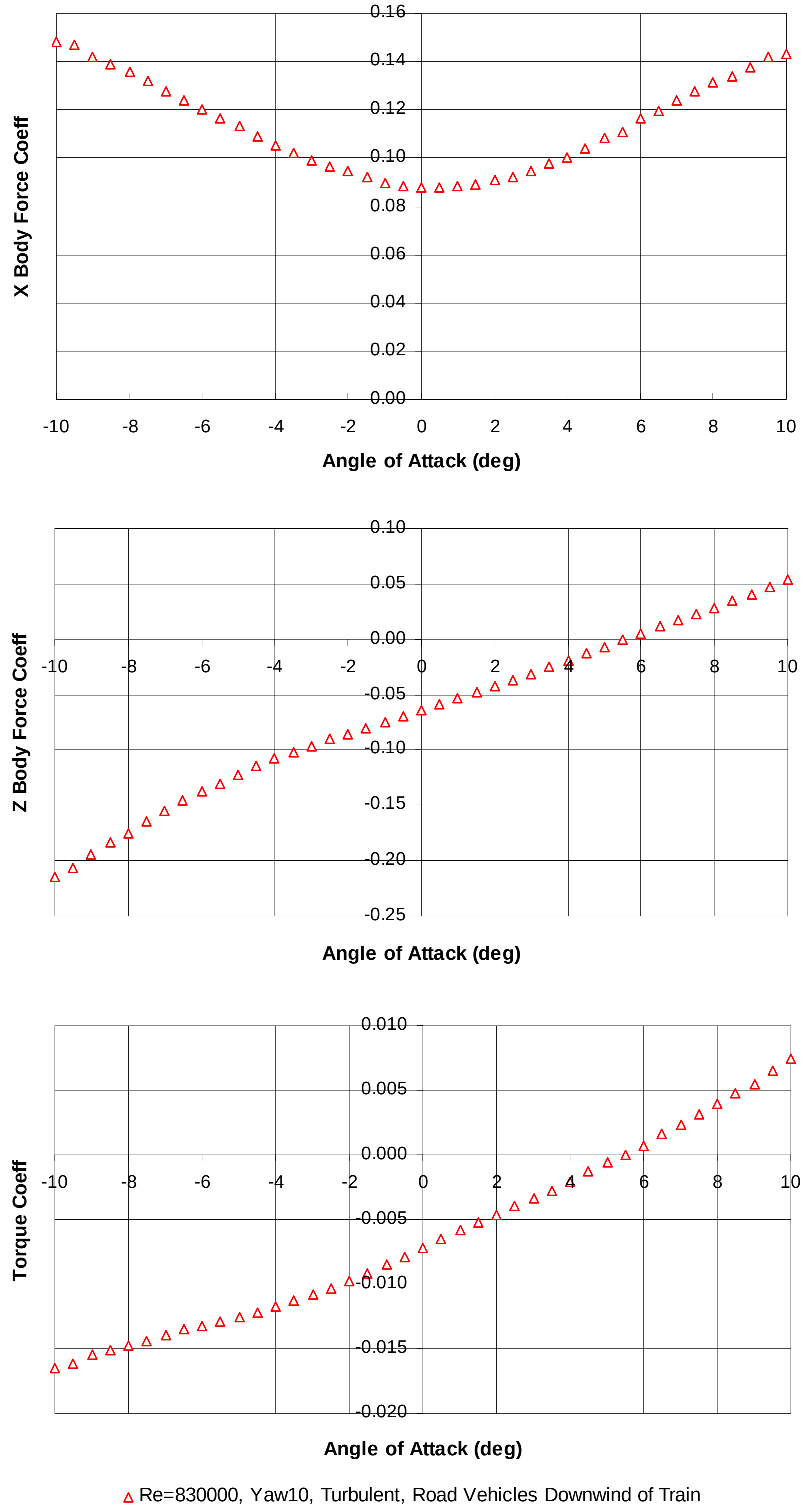

FIGURE C30 STATIC FORCE COEFFICIENTS (BODY FORCES), TURBULENT FLOW, IN-SERVICE, TRAFFIC CONDITION 2, SKEW=10^{O}

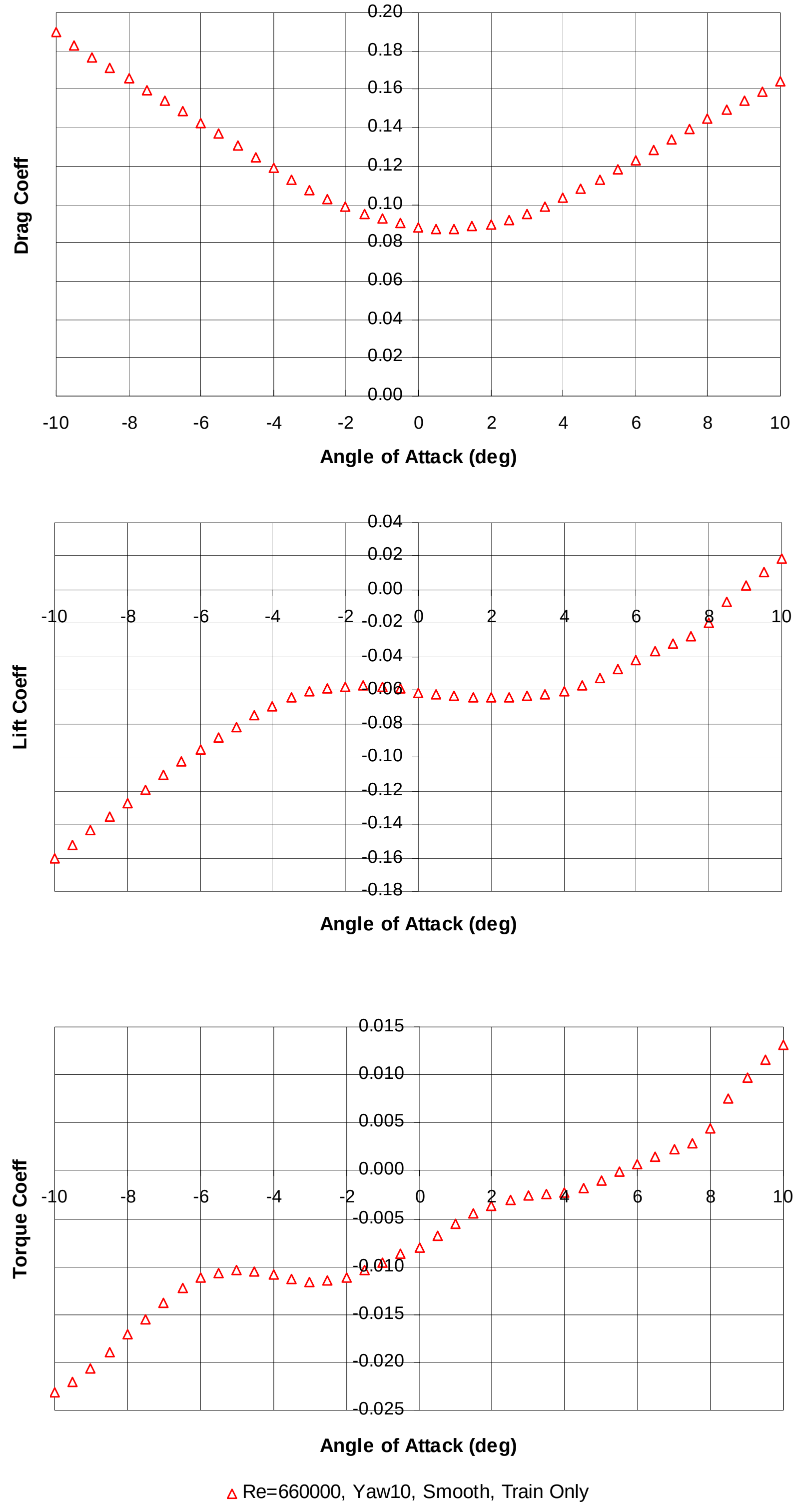

FIGURE C31 STATIC FORCE COEFFICIENTS (WIND AXIS FORCES), SMOOTH FLOW, IN-SERVICE, TRAFFIC CONDITION 3, SKEW=10^{O}

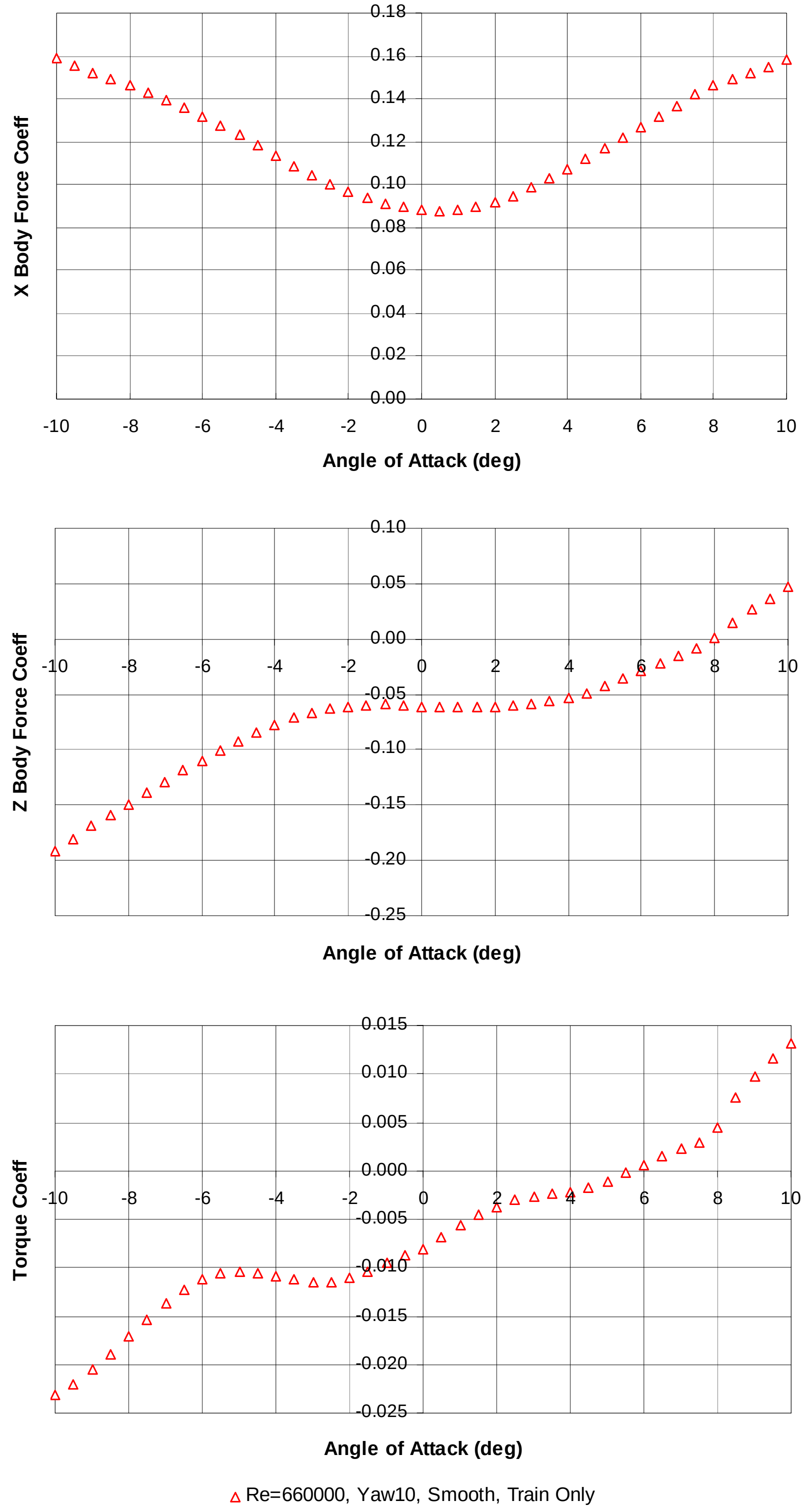

FIGURE C32 STATIC FORCE COEFFICIENTS (BODY FORCES), SMOOTH FLOW, IN-SERVICE, TRAFFIC CONDITION 3, SKEW=10^{O}

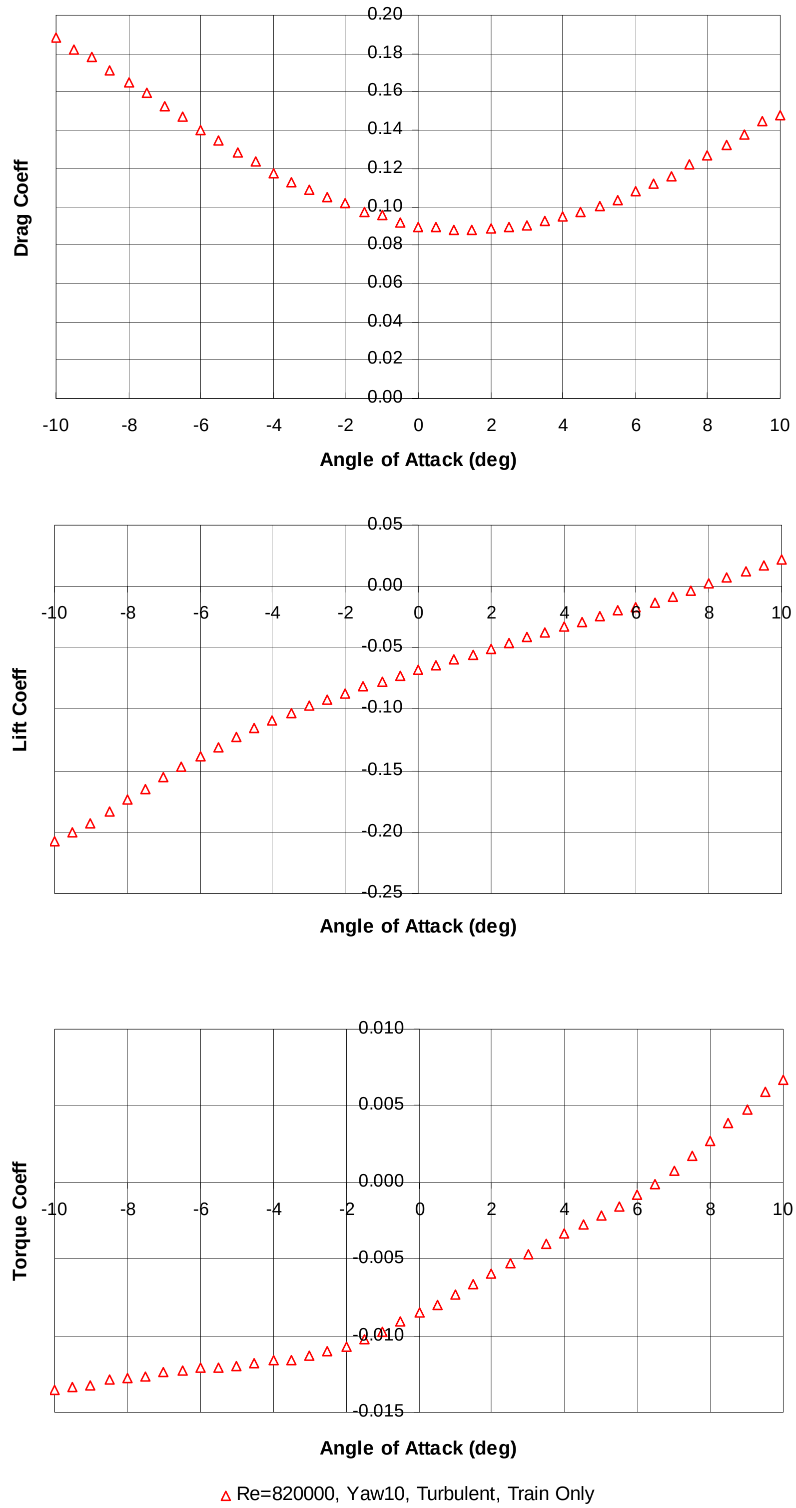

FIGURE C33 STATIC FORCE COEFFICIENTS (WIND AXIS FORCES), TURBULENT FLOW, IN-SERVICE, TRAFFIC CONDITION 3, SKEW=10^{O}

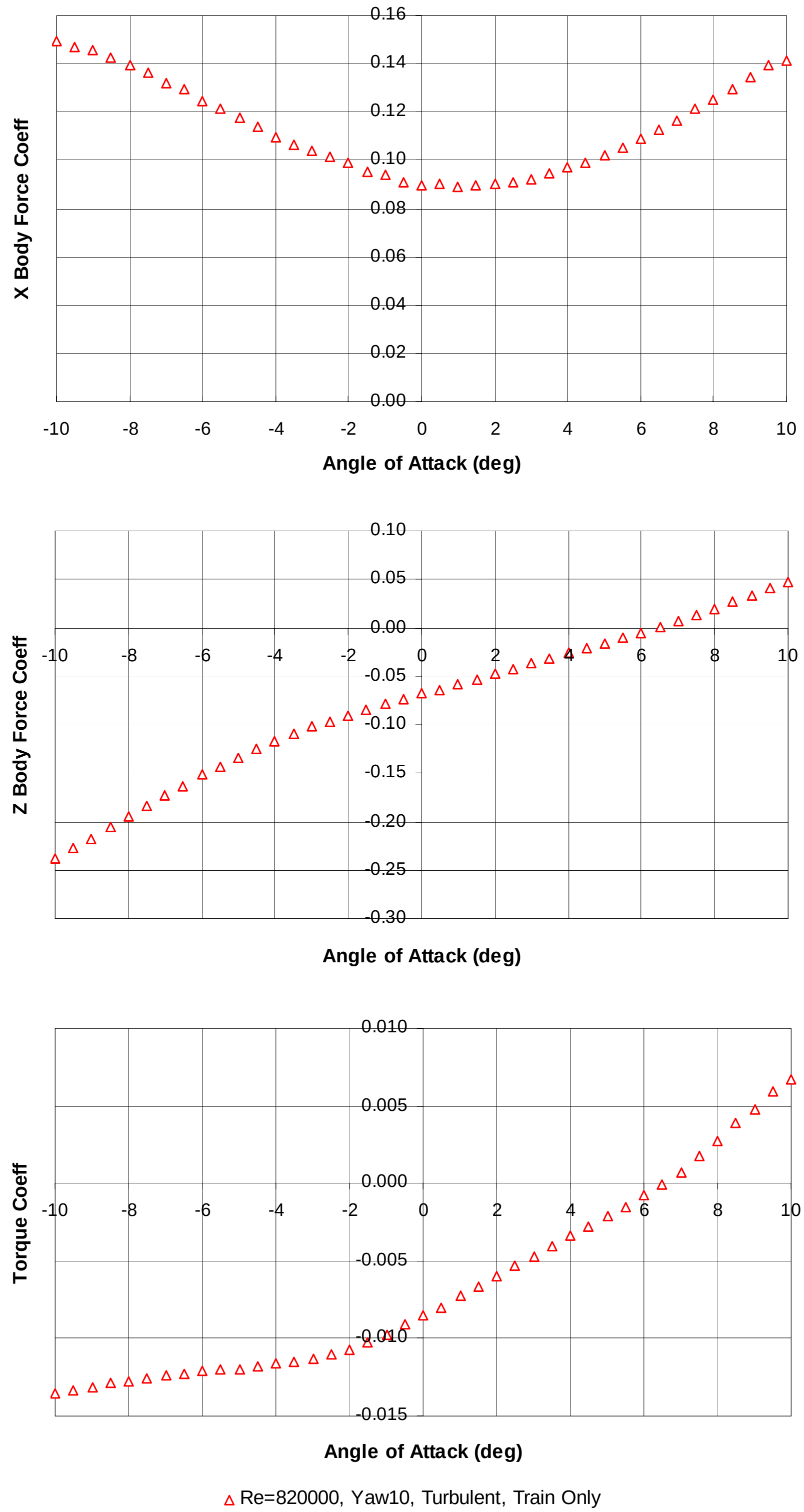

FIGURE C34 STATIC FORCE COEFFICIENTS (BODY FORCES), TURBULENT FLOW, IN-SERVICE, TRAFFIC CONDITION 3, SKEW=10^{O}

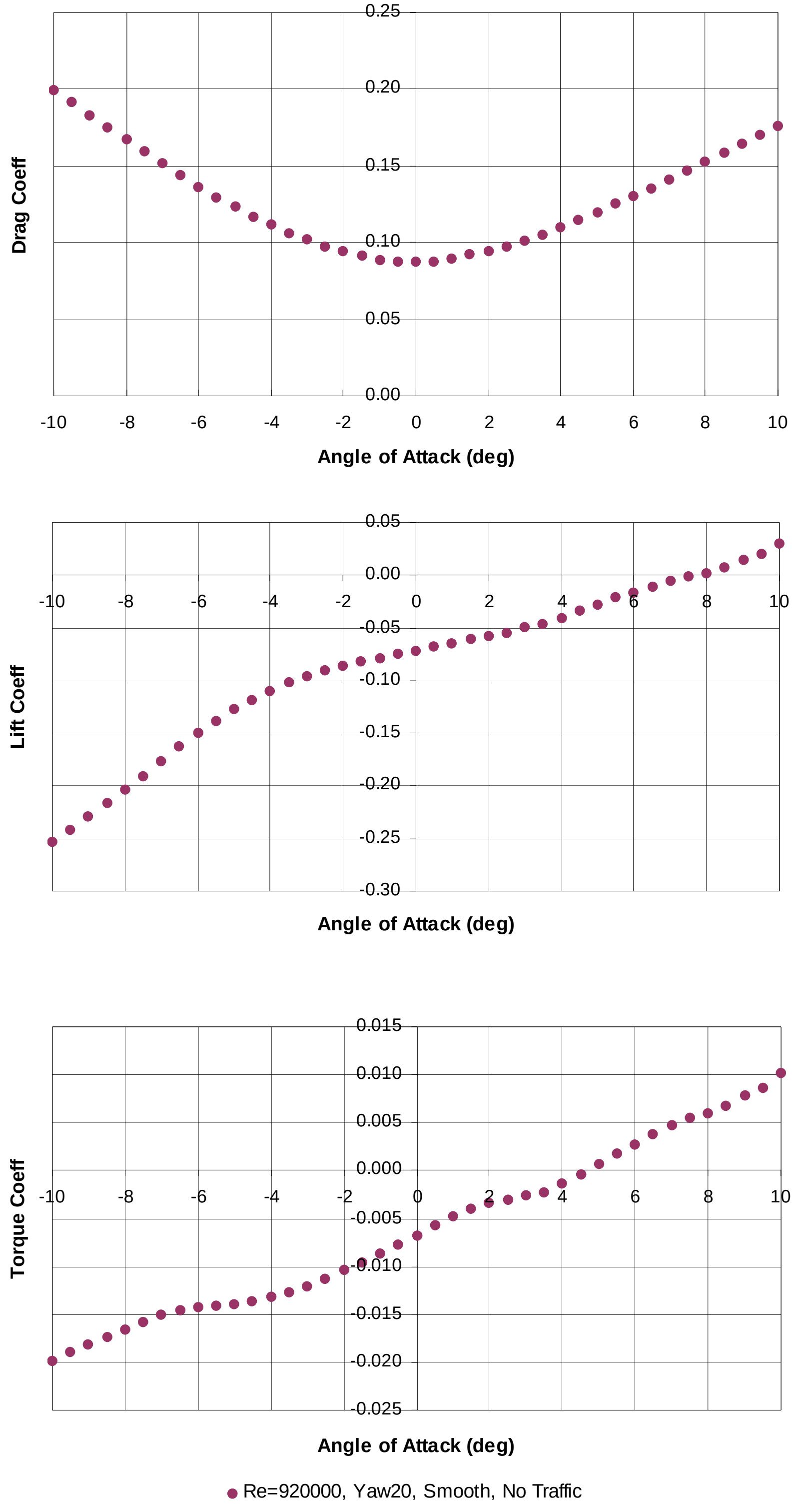

FIGURE C35 STATIC FORCE COEFFICIENTS (WIND AXIS FORCES), SMOOTH FLOW, IN-SERVICE, NO TRAFFIC, SKEW=20^{O}

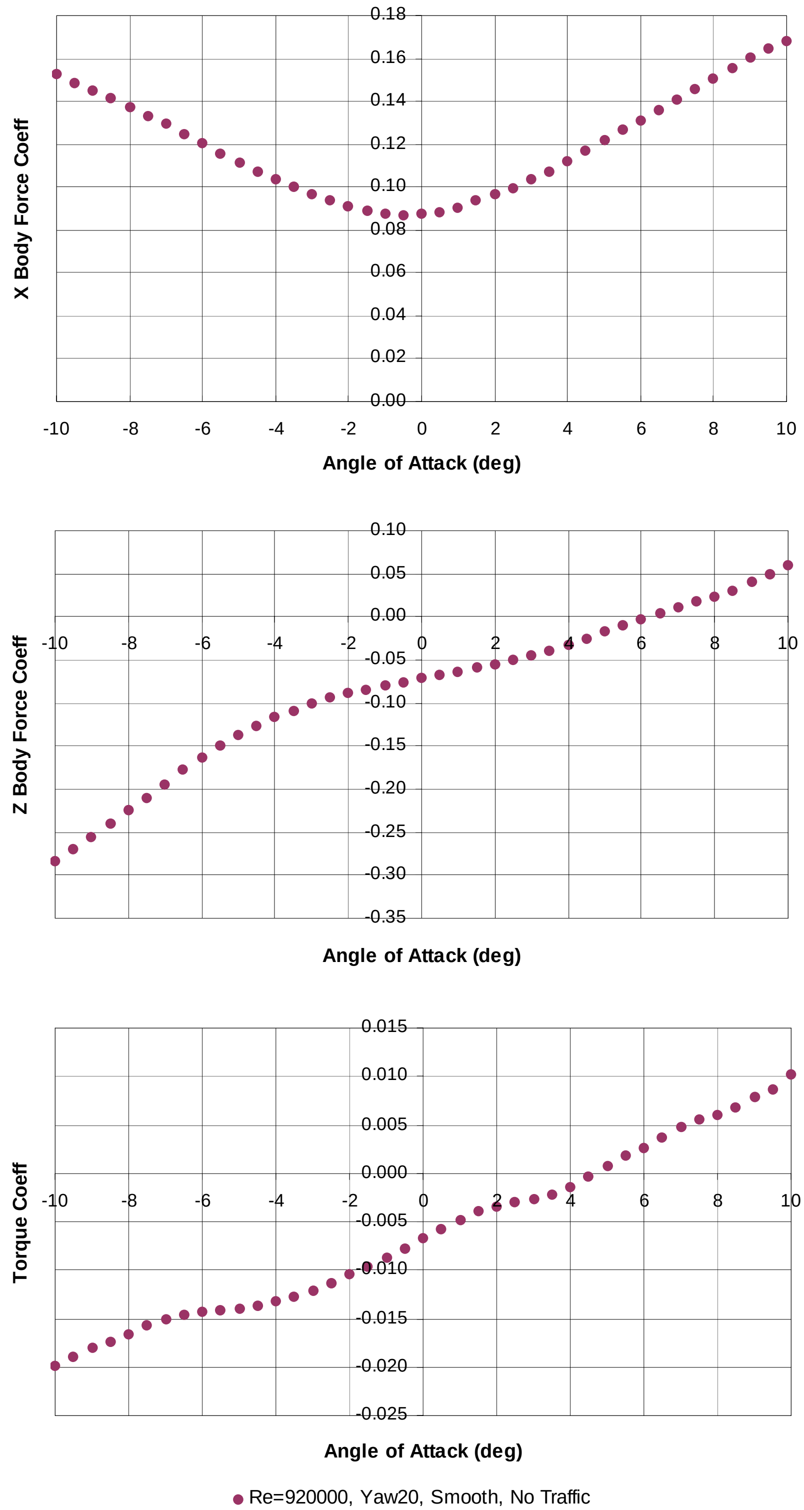

FIGURE C36 STATIC FORCE COEFFICIENTS (BODY FORCES), SMOOTH FLOW, IN-SERVICE, NO TRAFFIC, SKEW=20^{O}

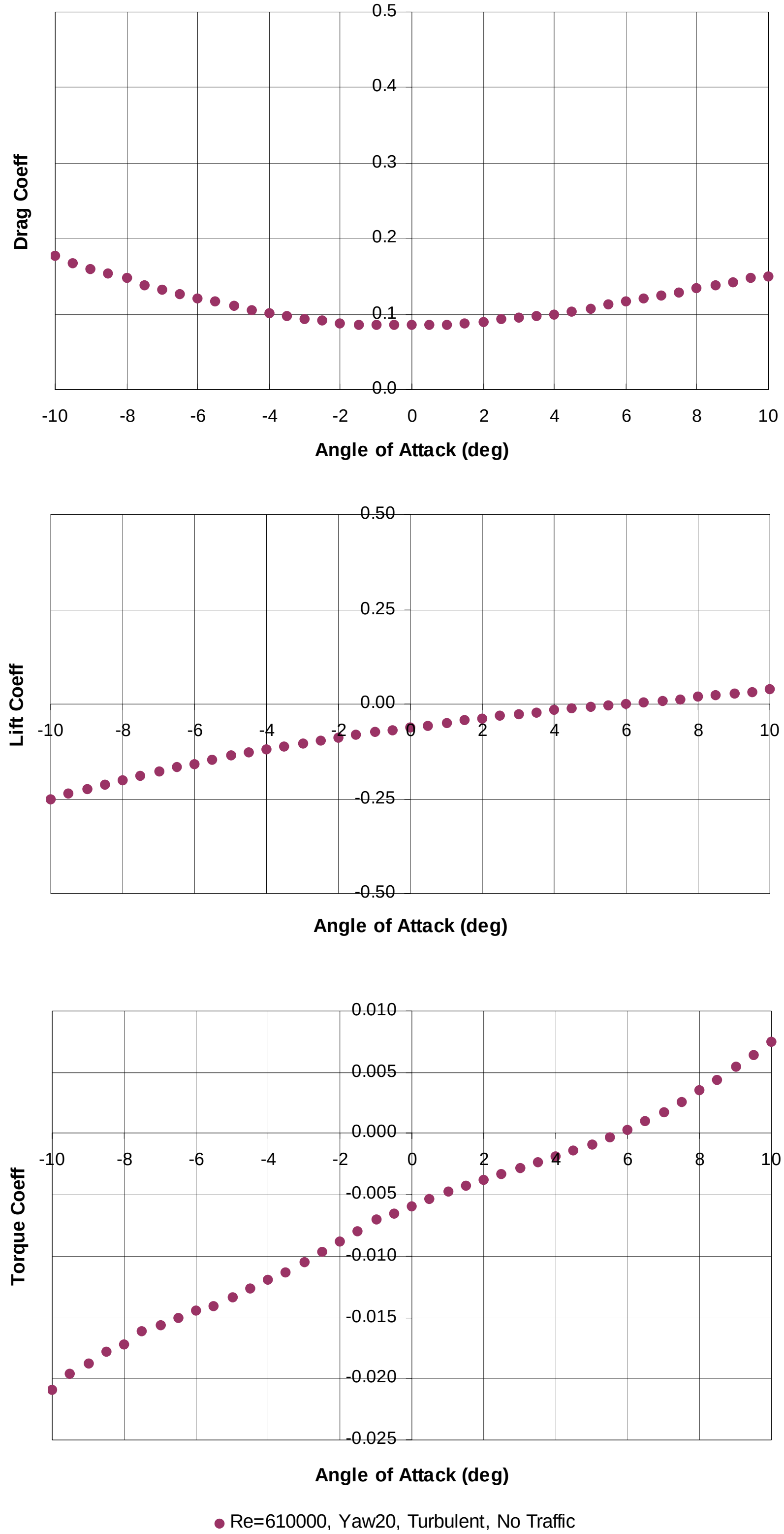

FIGURE C37 STATIC FORCE COEFFICIENTS (WIND AXIS FORCES), TURBULENT FLOW, IN-SERVICE, NO TRAFFIC, SKEW=20^{O}

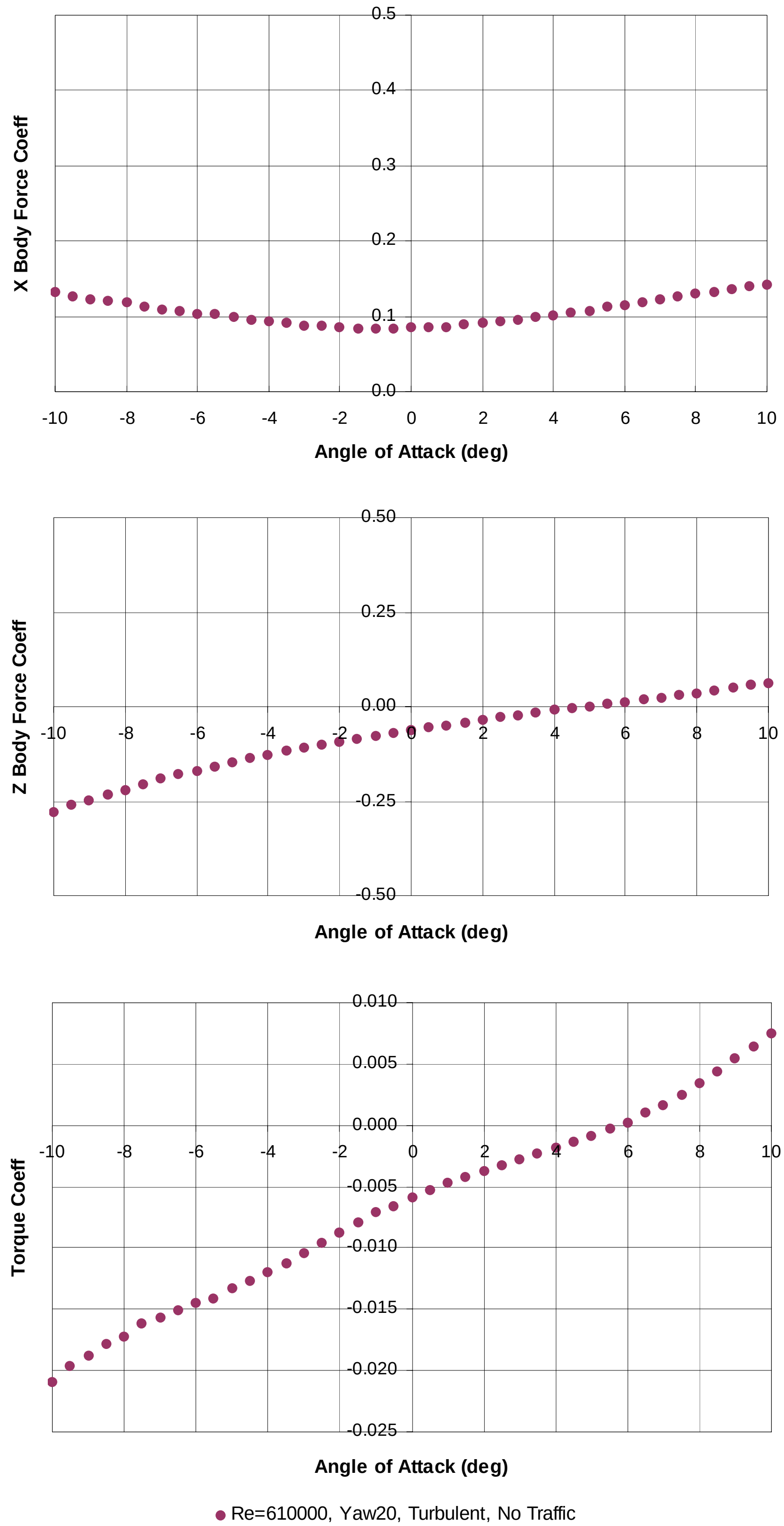

FIGURE C38 STATIC FORCE COEFFICIENTS (BODY FORCES), TURBULENT FLOW, IN-SERVICE, NO TRAFFIC, SKEW=20^{O}

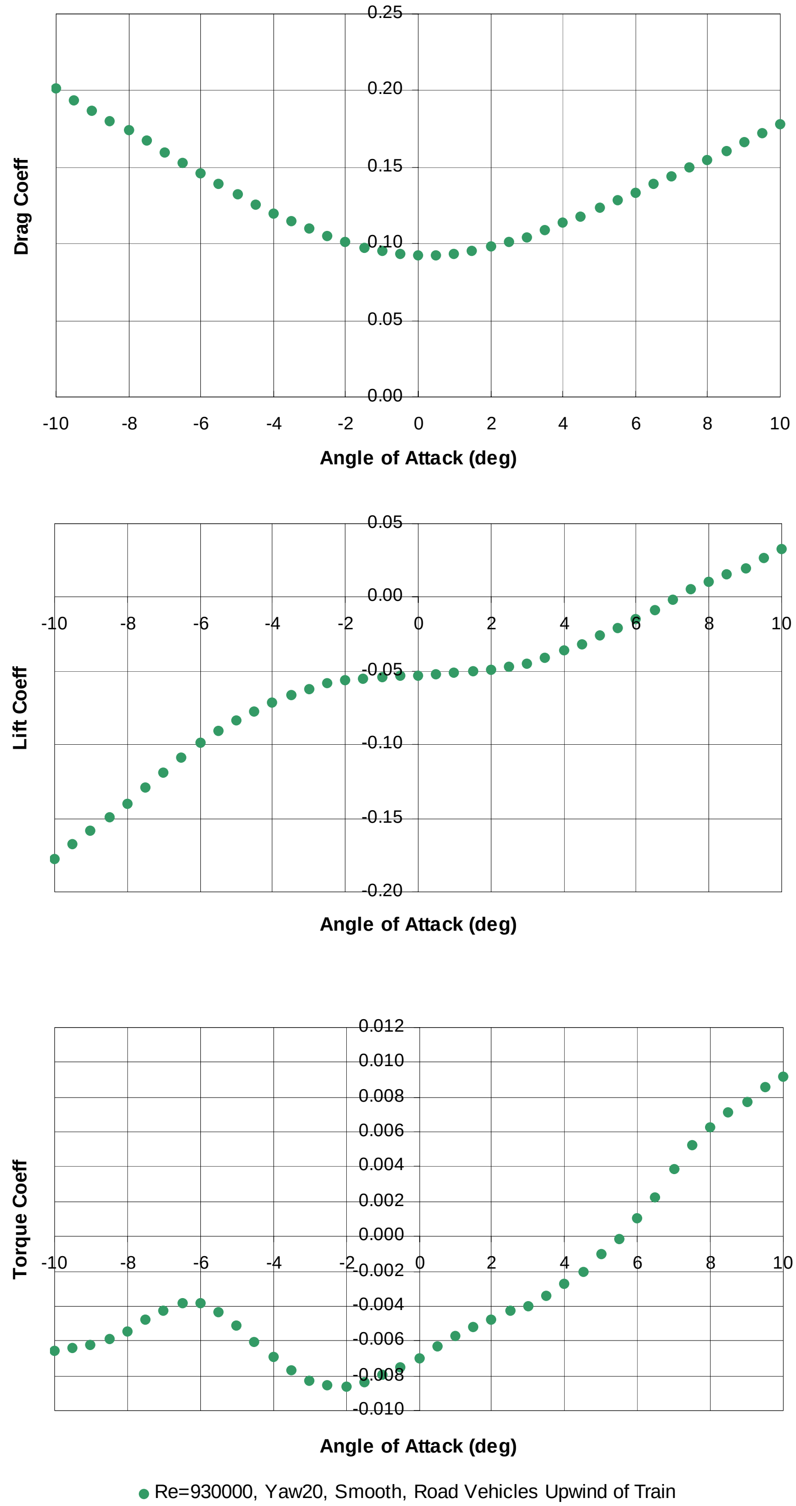

FIGURE C39 STATIC FORCE COEFFICIENTS (WIND AXIS FORCES), SMOOTH FLOW, IN-SERVICE, TRAFFIC CONDITION 1, SKEW=20^{O}

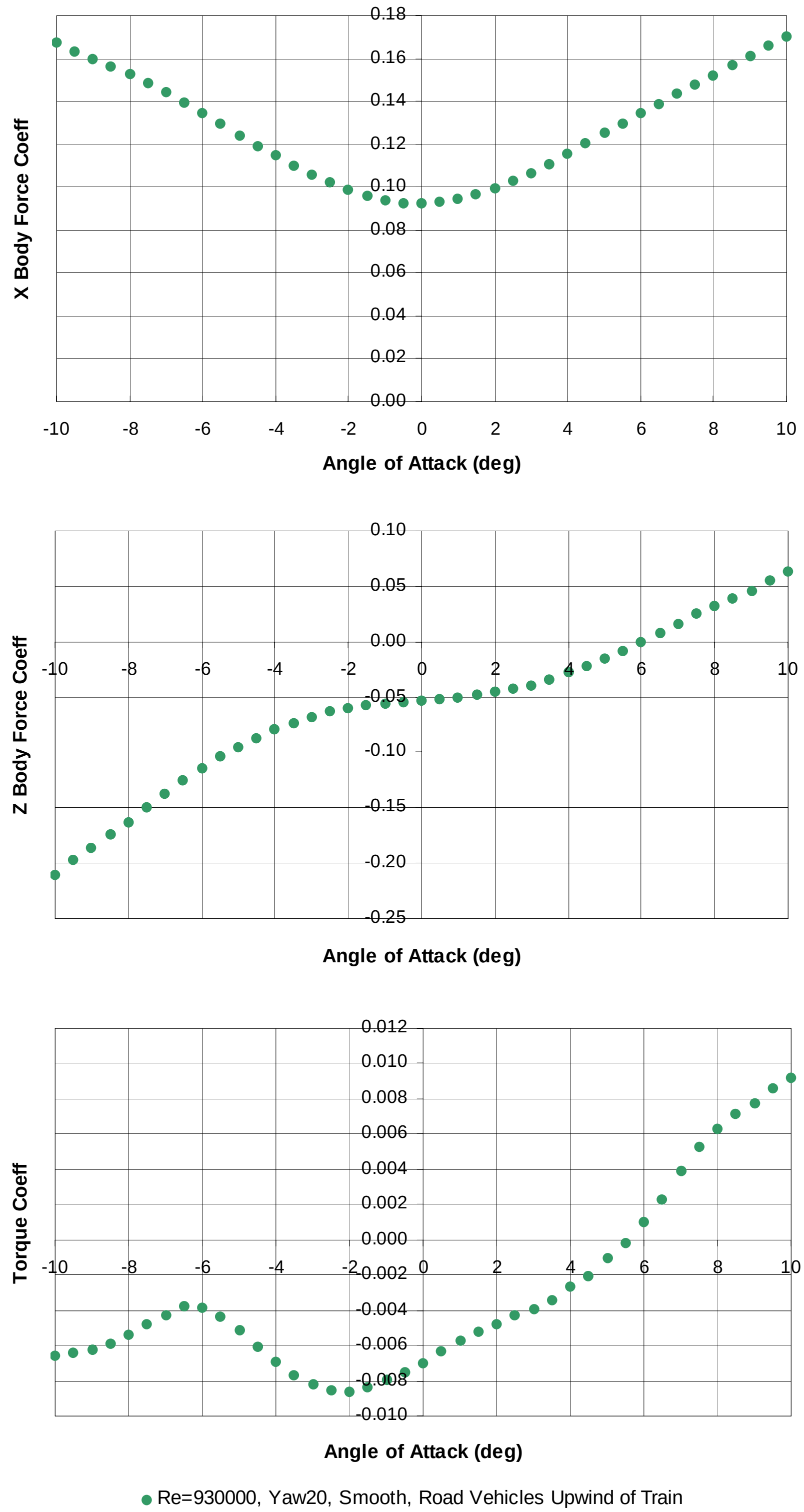

FIGURE C40 STATIC FORCE COEFFICIENTS (BODY FORCES), SMOOTH FLOW, IN-SERVICE, TRAFFIC CONDITION 1, SKEW=20^{O}

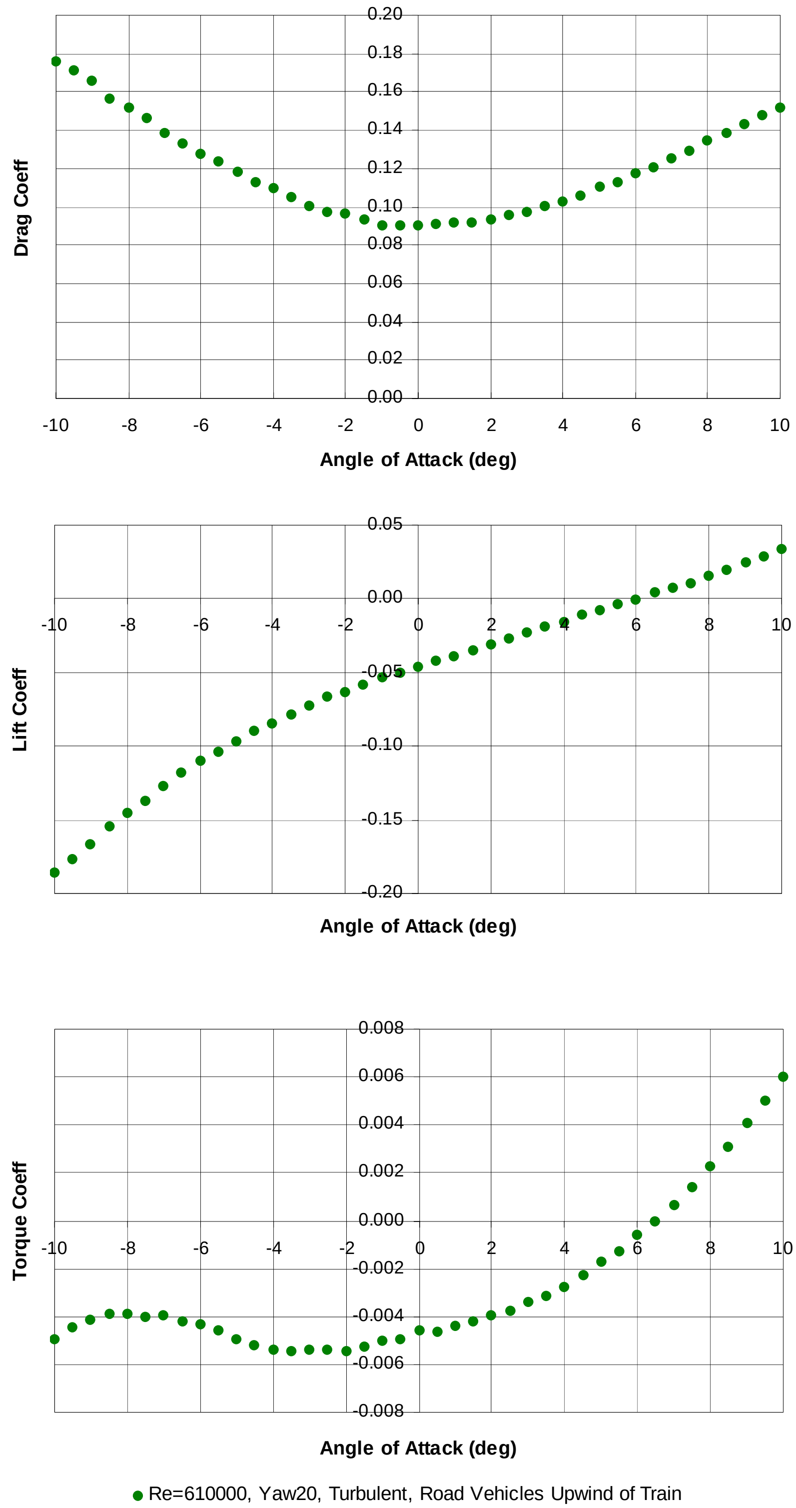

FIGURE C41 STATIC FORCE COEFFICIENTS (WIND AXIS FORCES), TURBULENT FLOW, IN-SERVICE, TRAFFIC CONDITION 1, SKEW=20^{O}

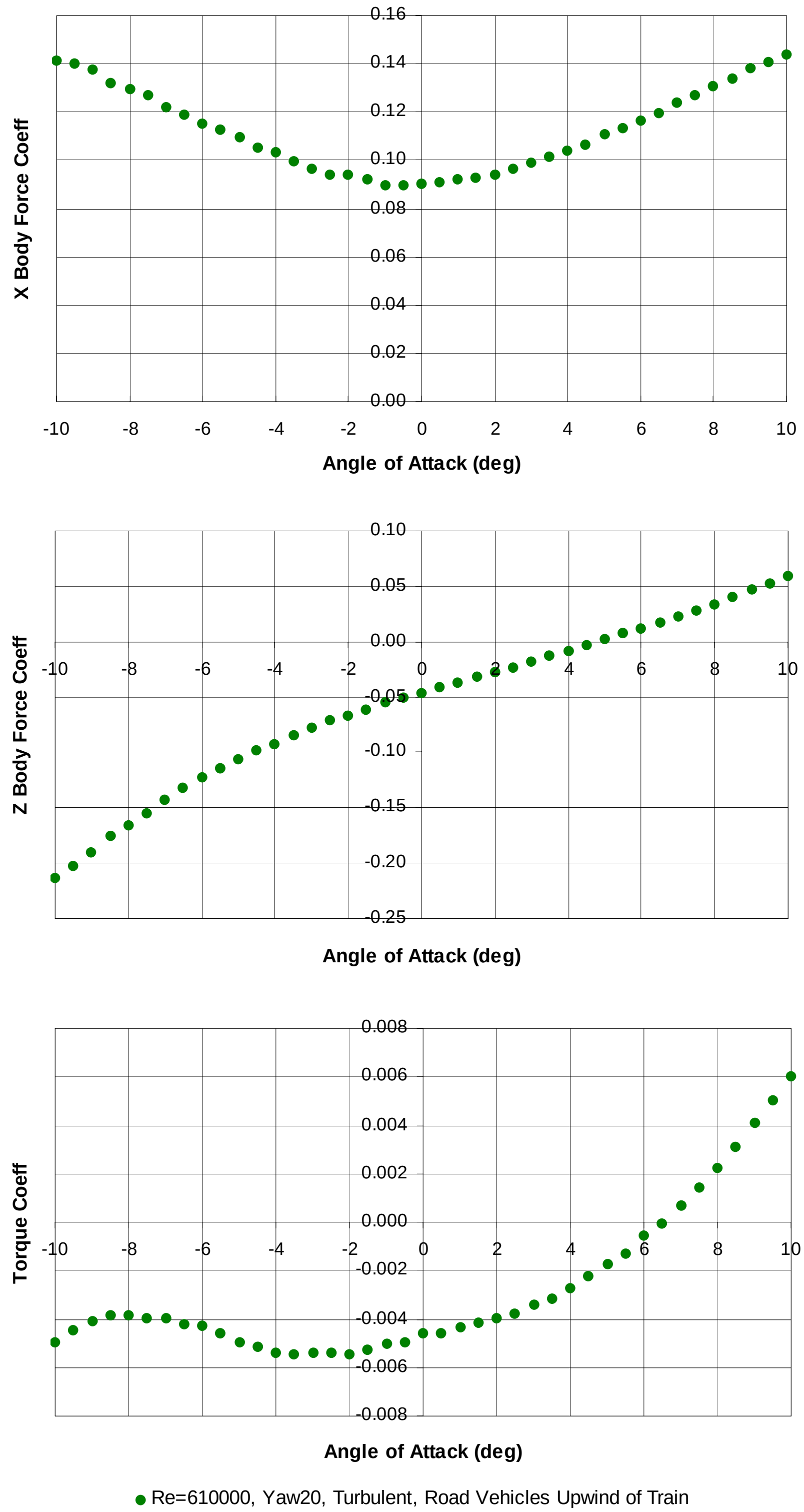

FIGURE C42 STATIC FORCE COEFFICIENTS (BODY FORCES), TURBULENT FLOW, IN-SERVICE, TRAFFIC CONDITION 1, SKEW=20^{O}

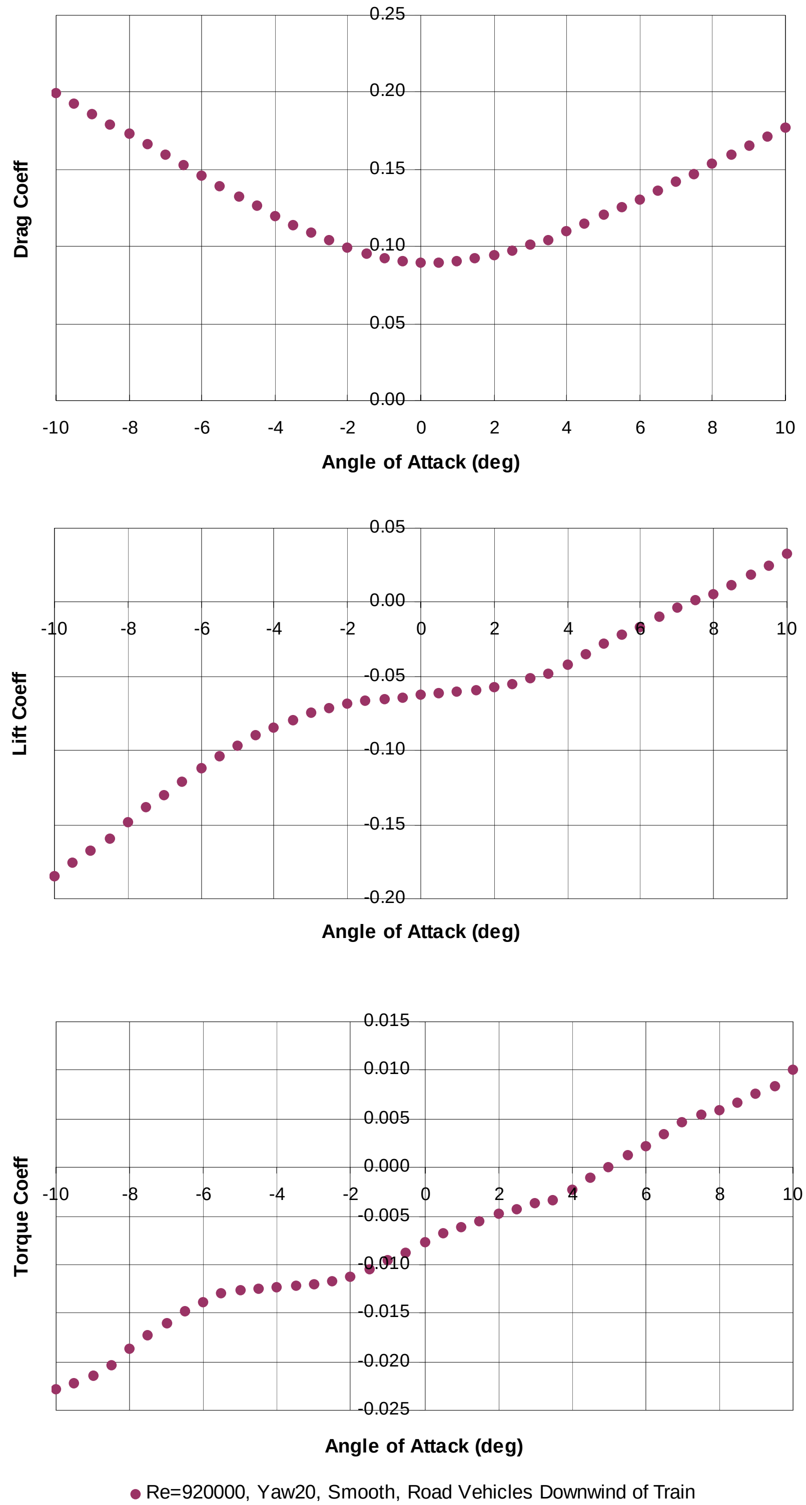

FIGURE C43 STATIC FORCE COEFFICIENTS (WIND AXIS FORCES), SMOOTH FLOW, IN-SERVICE, TRAFFIC CONDITION 2, SKEW=20^{O}

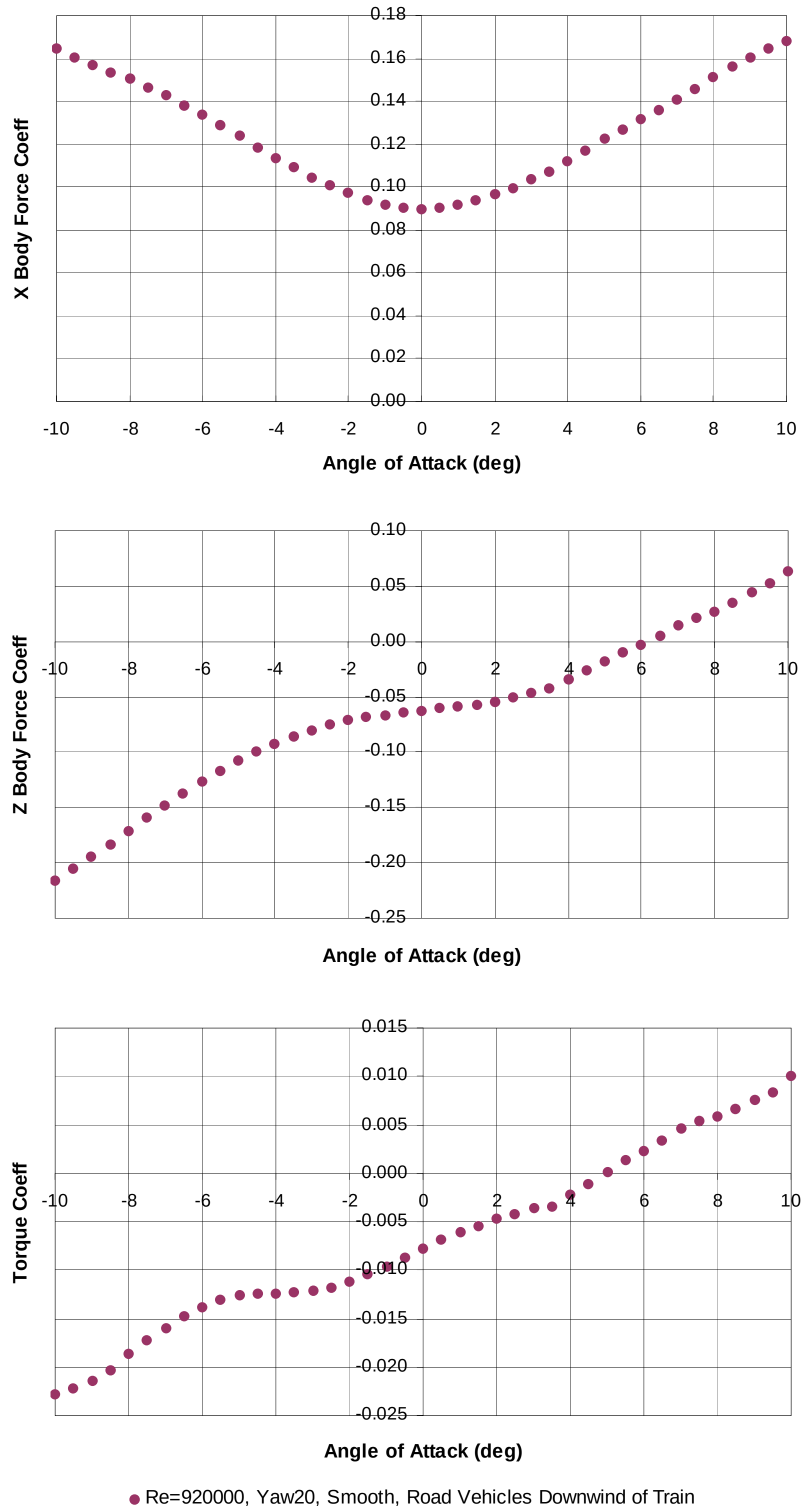

FIGURE C44 STATIC FORCE COEFFICIENTS (BODY FORCES), SMOOTH FLOW, IN-SERVICE, TRAFFIC CONDITION 2, SKEW=20^{O}

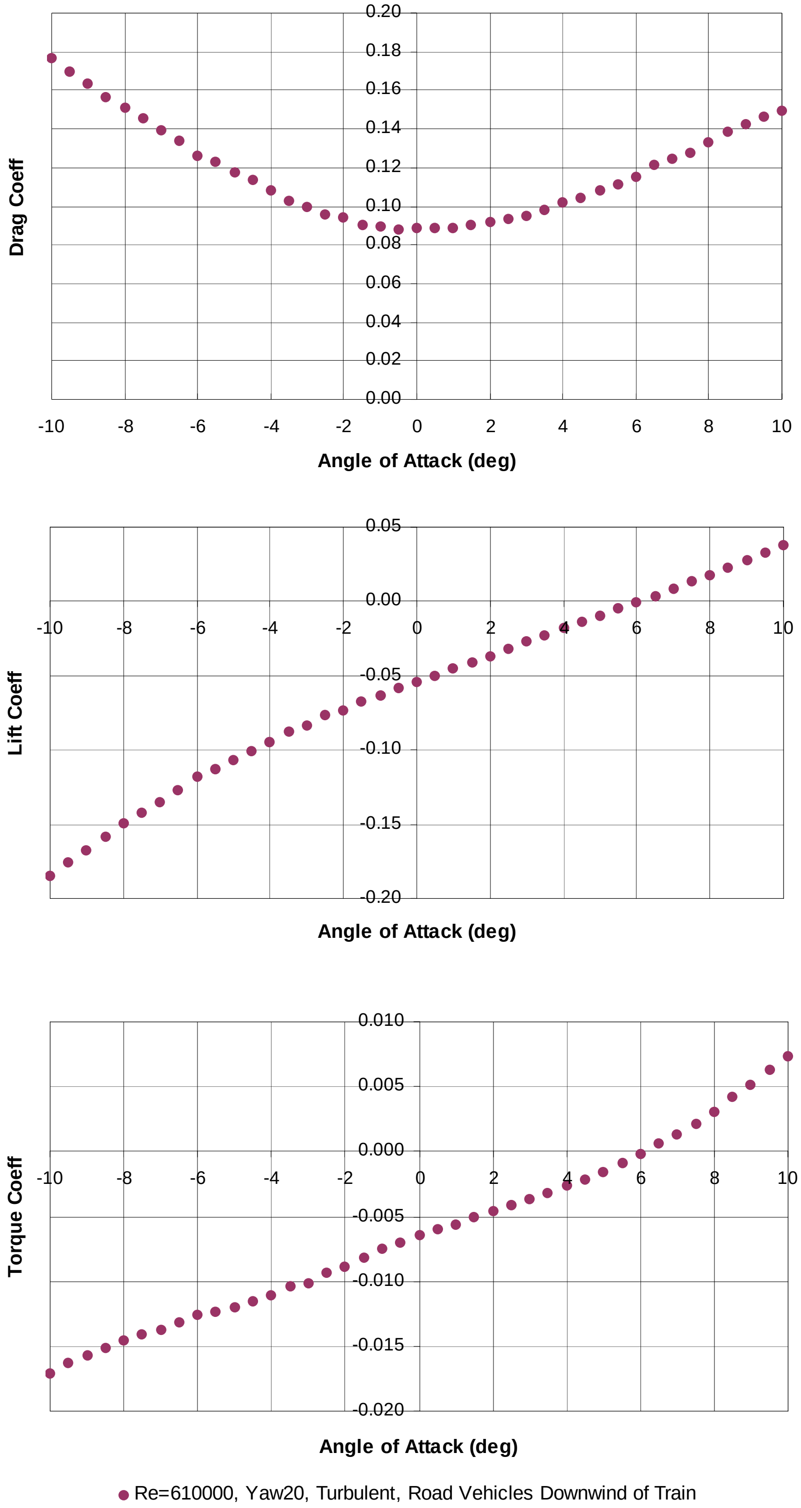

FIGURE C45 STATIC FORCE COEFFICIENTS (WIND AXIS FORCES), TURBULENT FLOW, IN-SERVICE, TRAFFIC CONDITION 2, SKEW=20^{O}

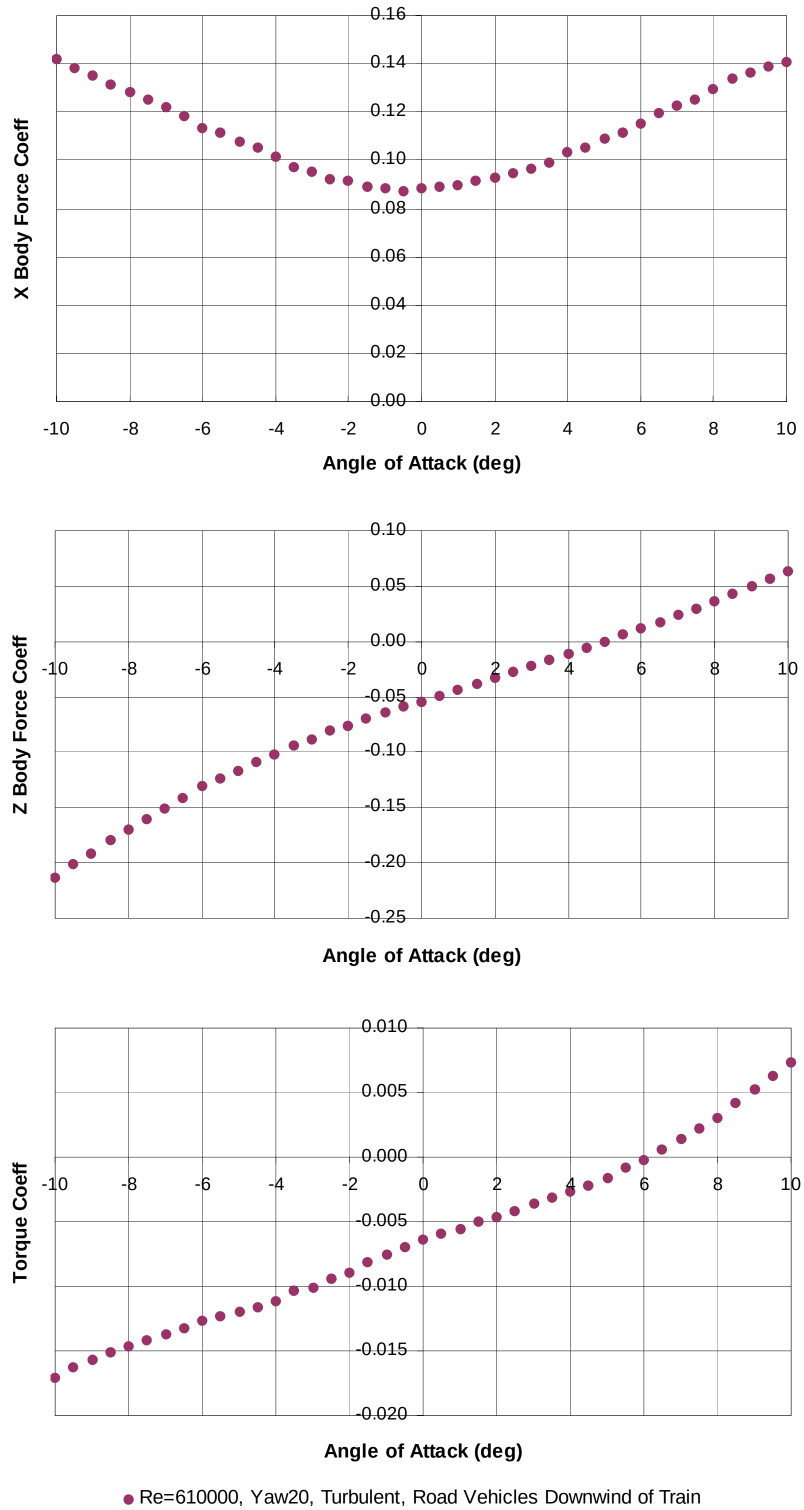

FIGURE C46 STATIC FORCE COEFFICIENTS (BODY FORCES), TURBULENT FLOW, IN-SERVICE, TRAFFIC CONDITION 2, SKEW=20^{O}

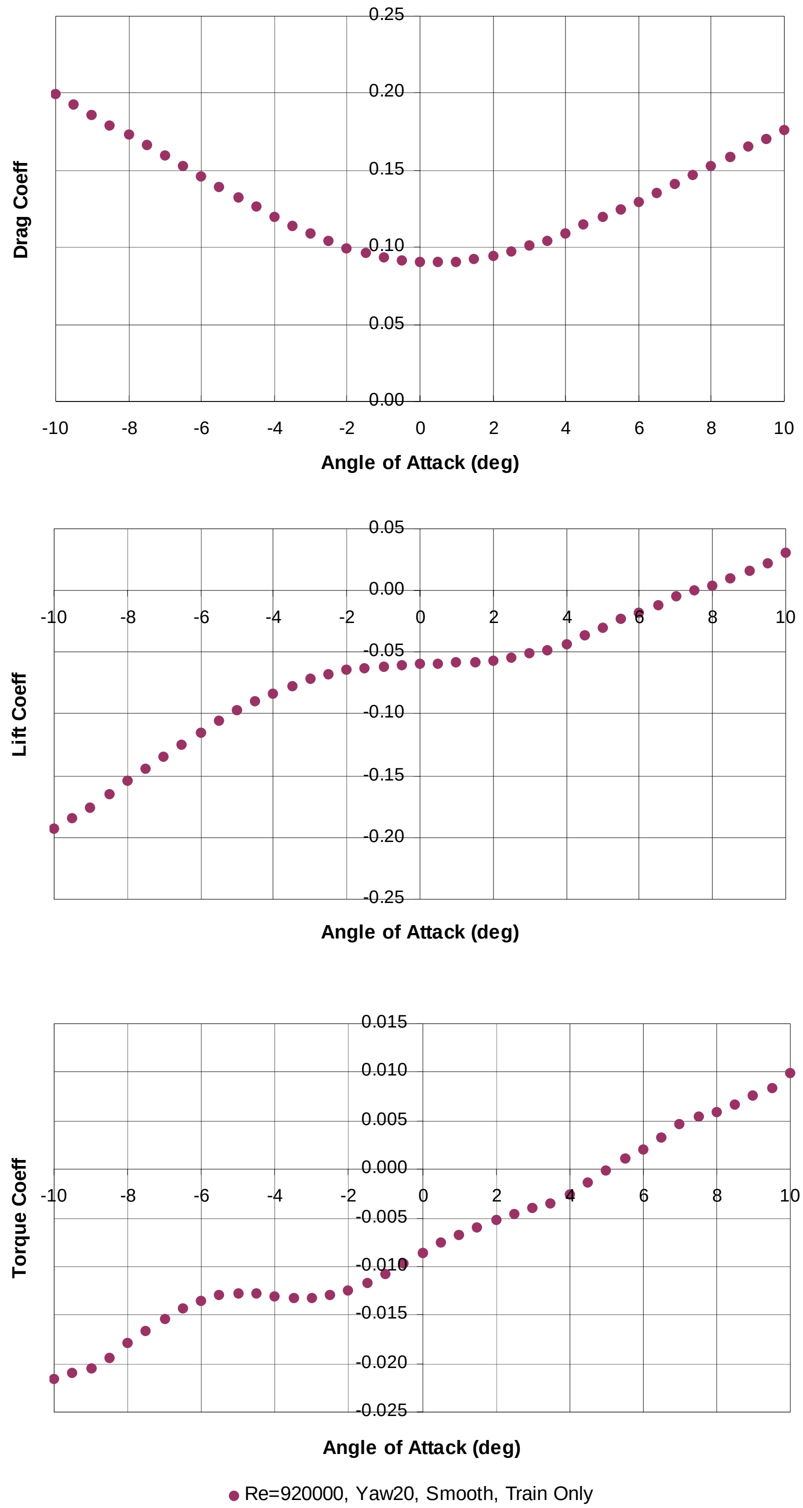

FIGURE C47 STATIC FORCE COEFFICIENTS (WIND AXIS FORCES), SMOOTH FLOW, IN-SERVICE, TRAFFIC CONDITION 3, SKEW=20^{O}

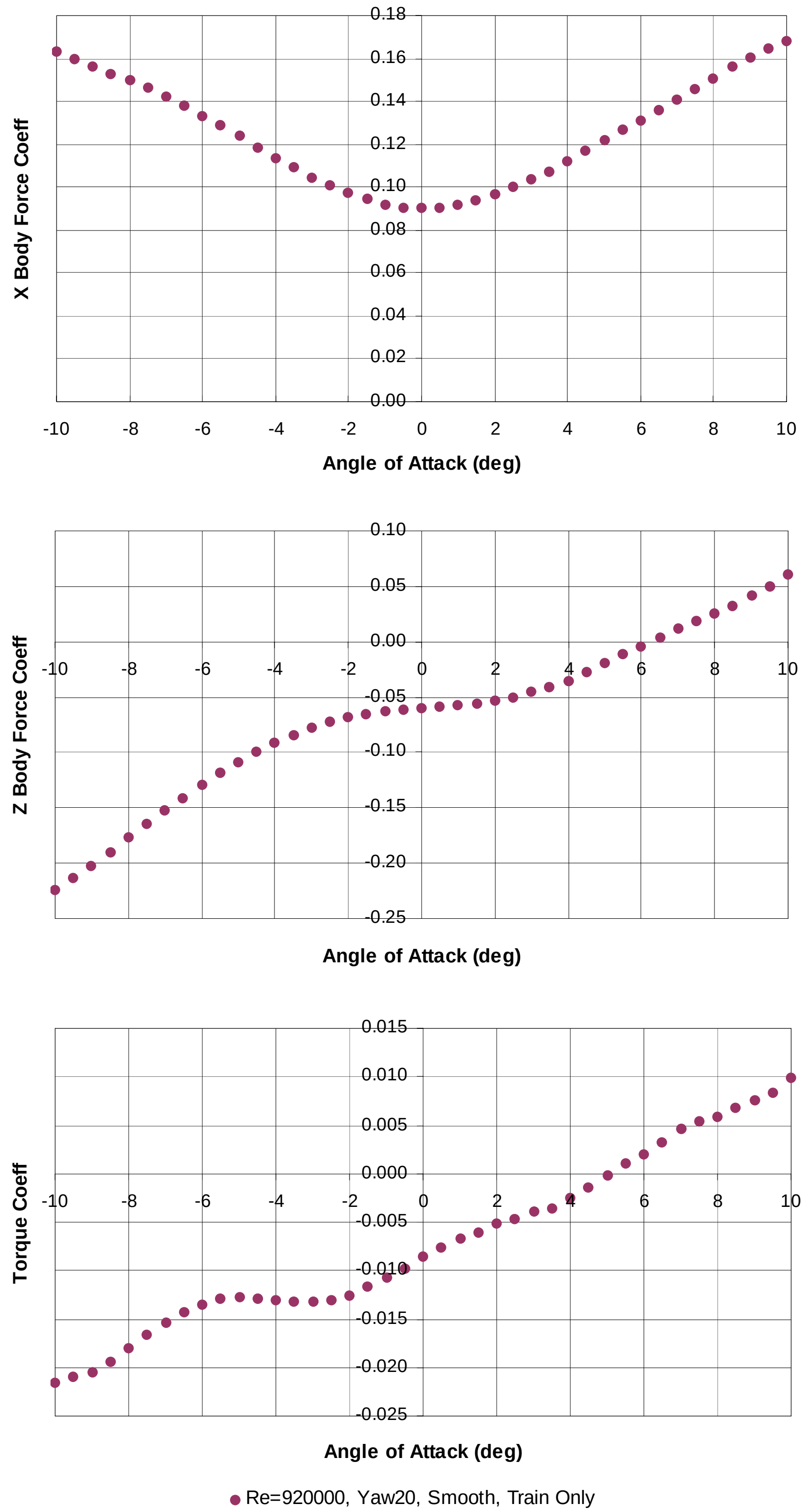

FIGURE C48 STATIC FORCE COEFFICIENTS (BODY FORCES), SMOOTH FLOW, IN-SERVICE, TRAFFIC CONDITION 3, SKEW=20^{O}

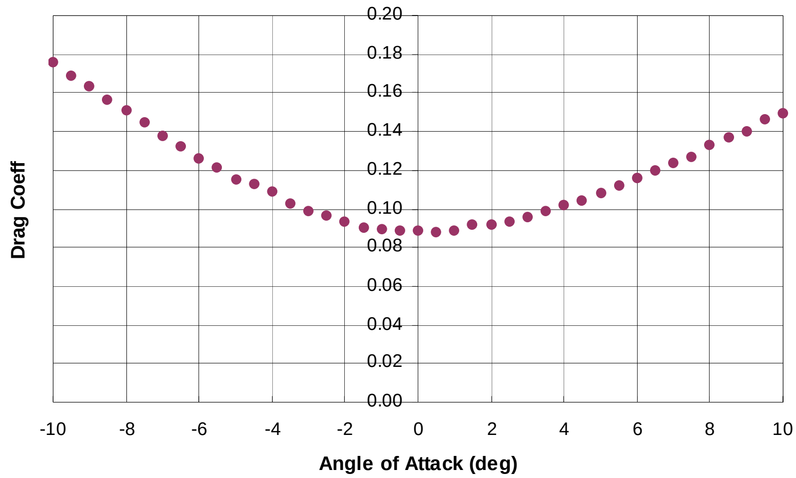

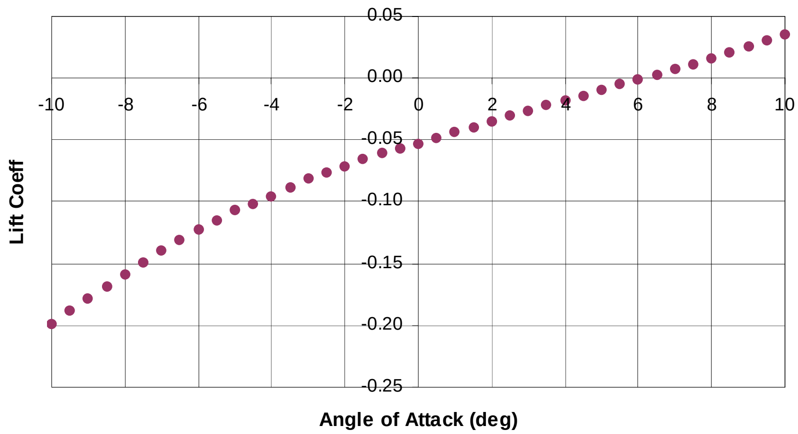

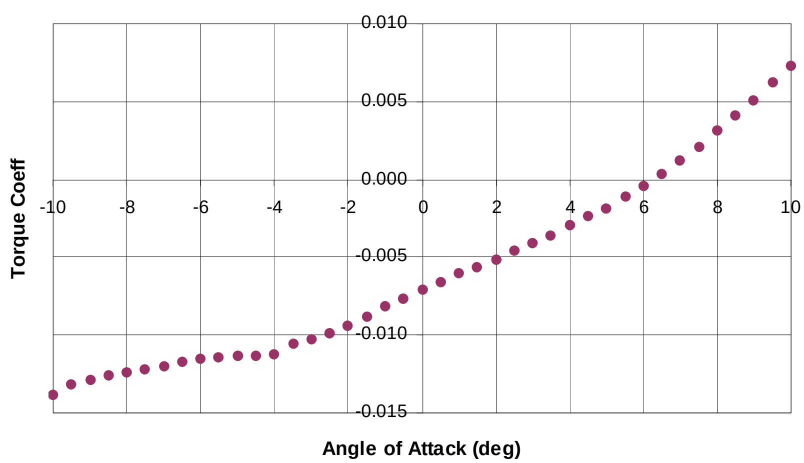

FIGURE C49 STATIC FORCE COEFFICIENTS (WIND AXIS FORCES), TURBULENT FLOW, IN-SERVICE, TRAFFIC CONDITION 3, SKEW=20^{O}

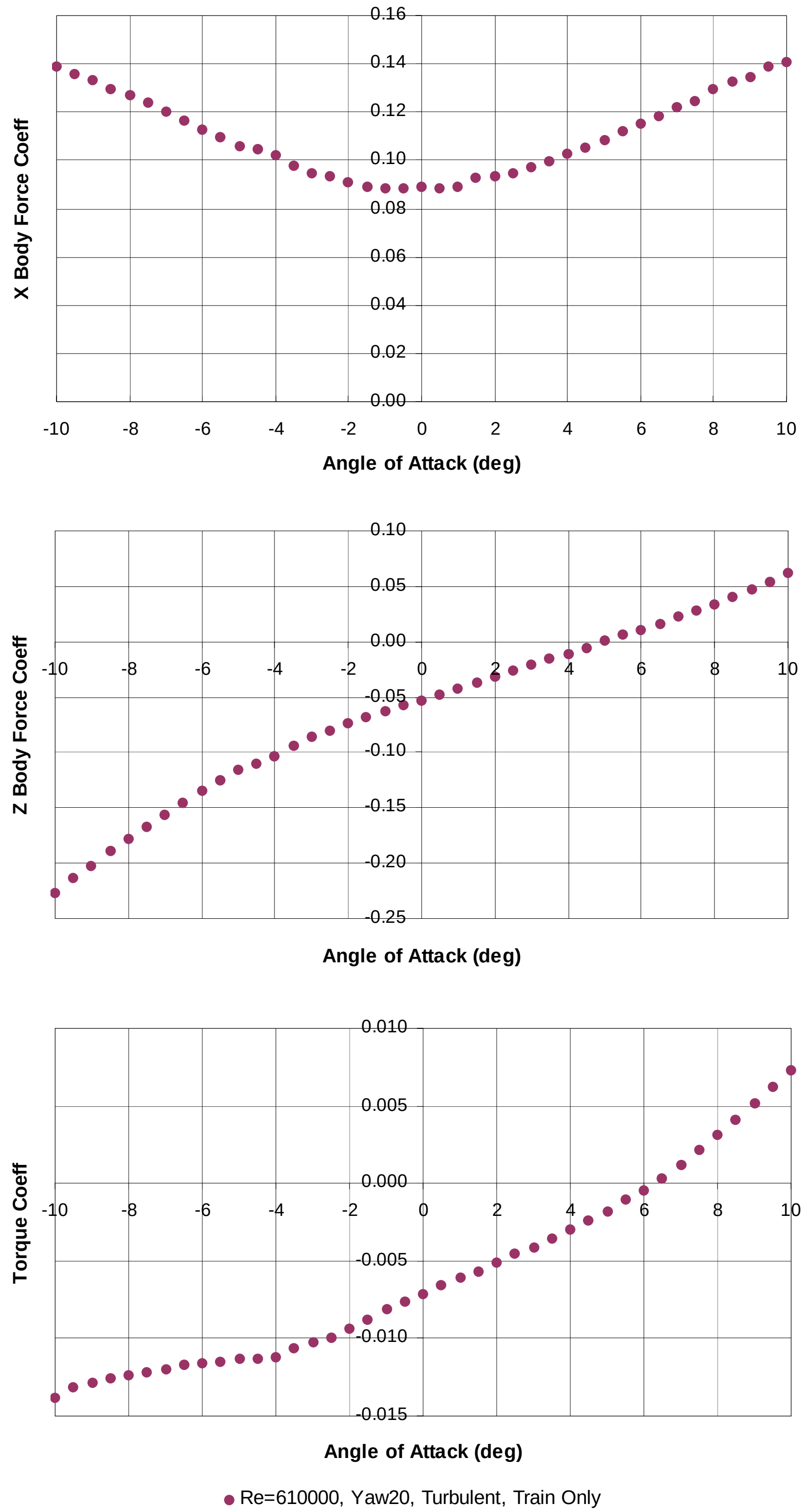

FIGURE C50 STATIC FORCE COEFFICIENTS (BODY FORCES), TURBULENT FLOW, IN-SERVICE, TRAFFIC CONDITION 3, SKEW=20^{O}

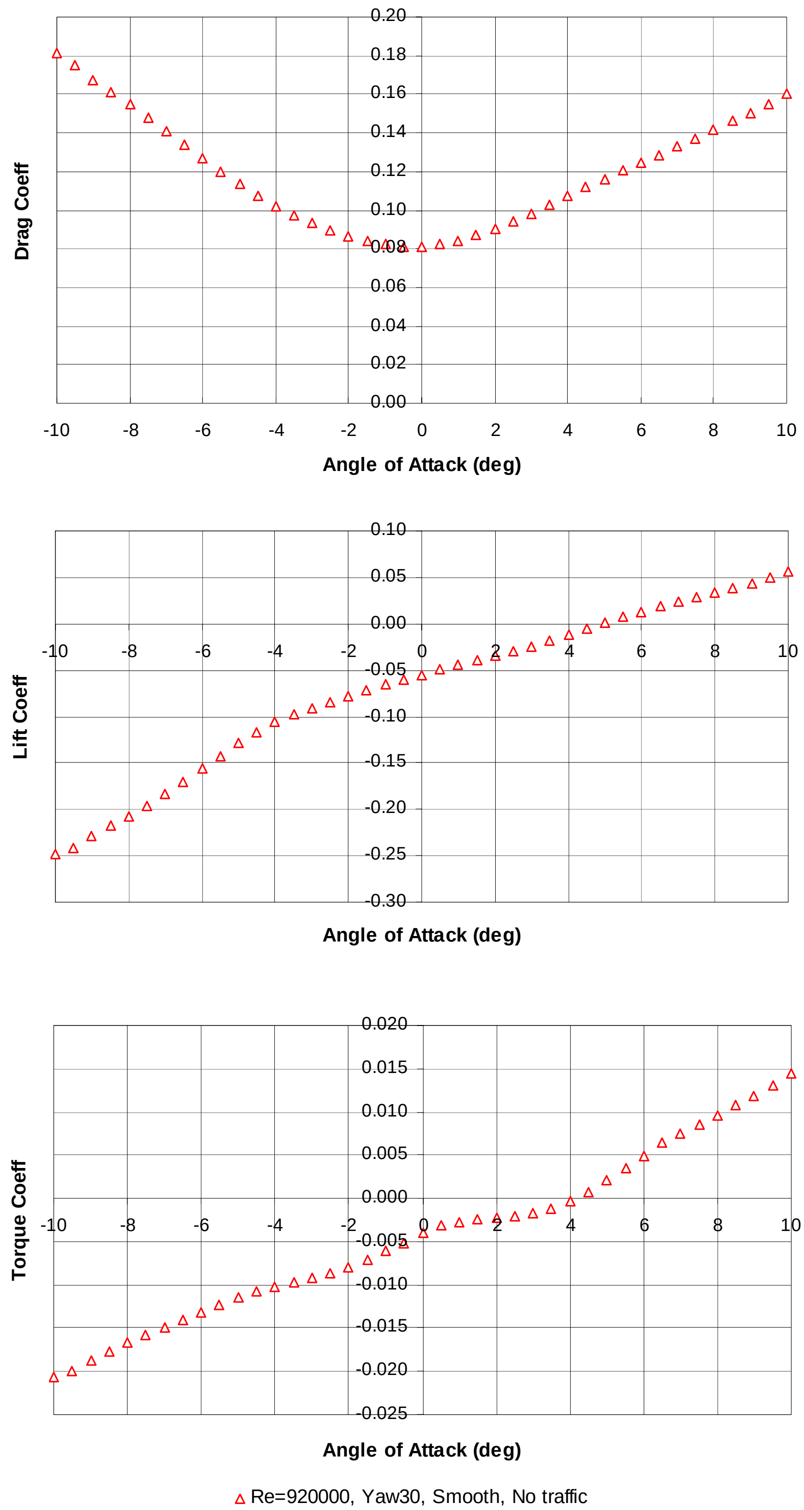

FIGURE C51 STATIC FORCE COEFFICIENTS (WIND AXIS FORCES), SMOOTH FLOW, IN-SERVICE, NO TRAFFIC, SKEW=30^{O}

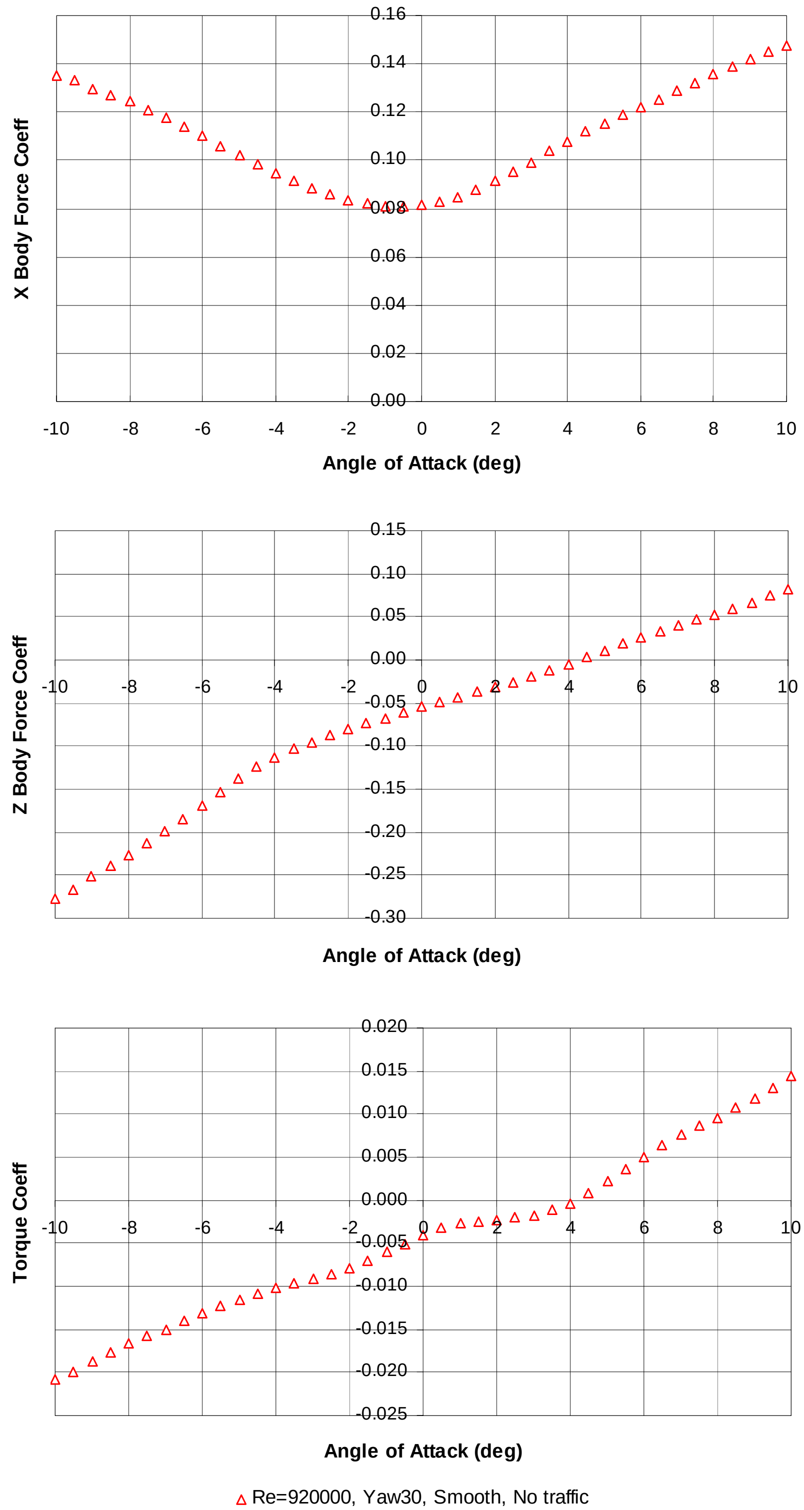

FIGURE C52 STATIC FORCE COEFFICIENTS (BODY FORCES), SMOOTH FLOW, IN-SERVICE, NO TRAFFIC, SKEW=30^{O}

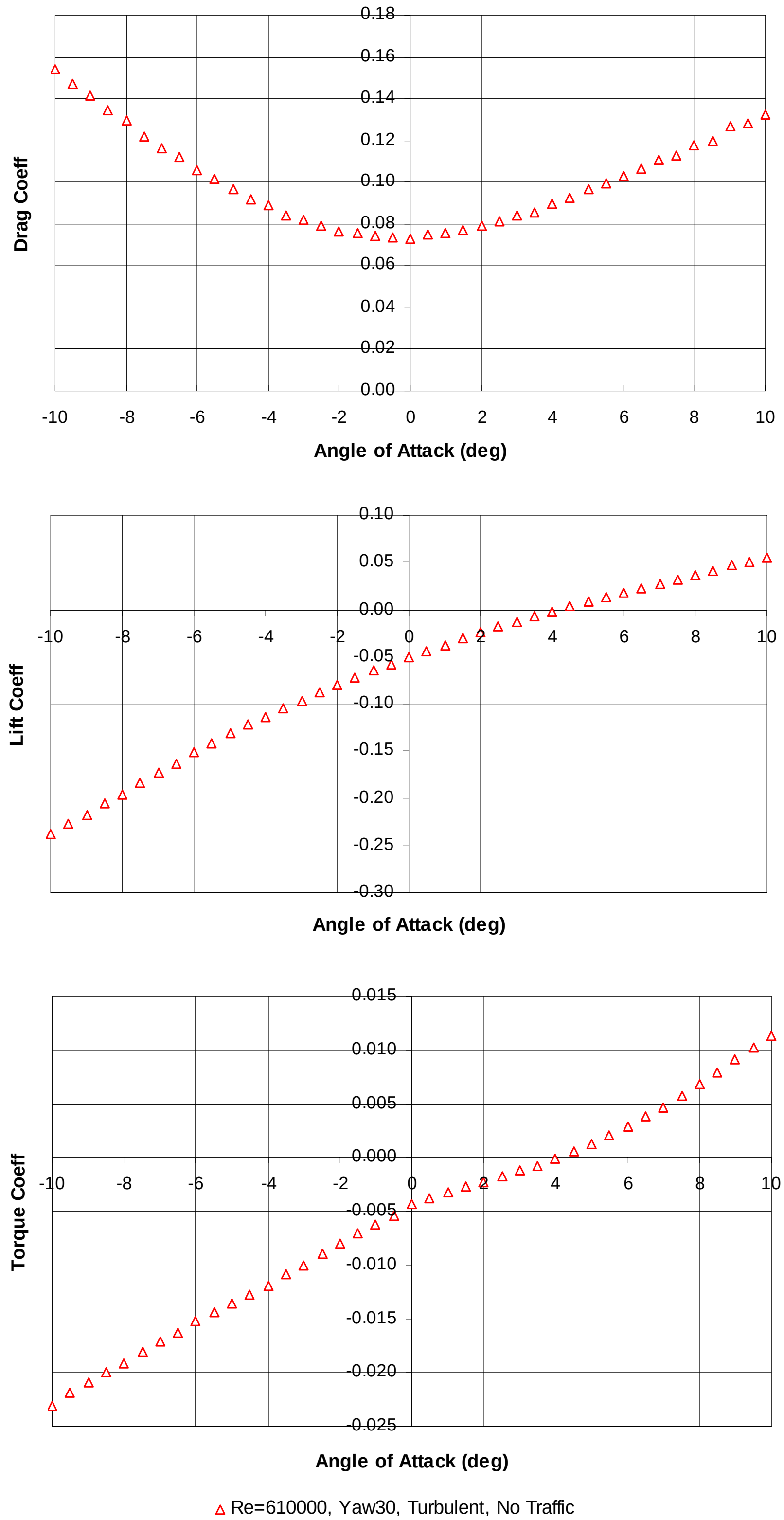

FIGURE C53 STATIC FORCE COEFFICIENTS (WIND AXIS FORCES), TURBULENT FLOW, IN-SERVICE, NO TRAFFIC, SKEW=30°

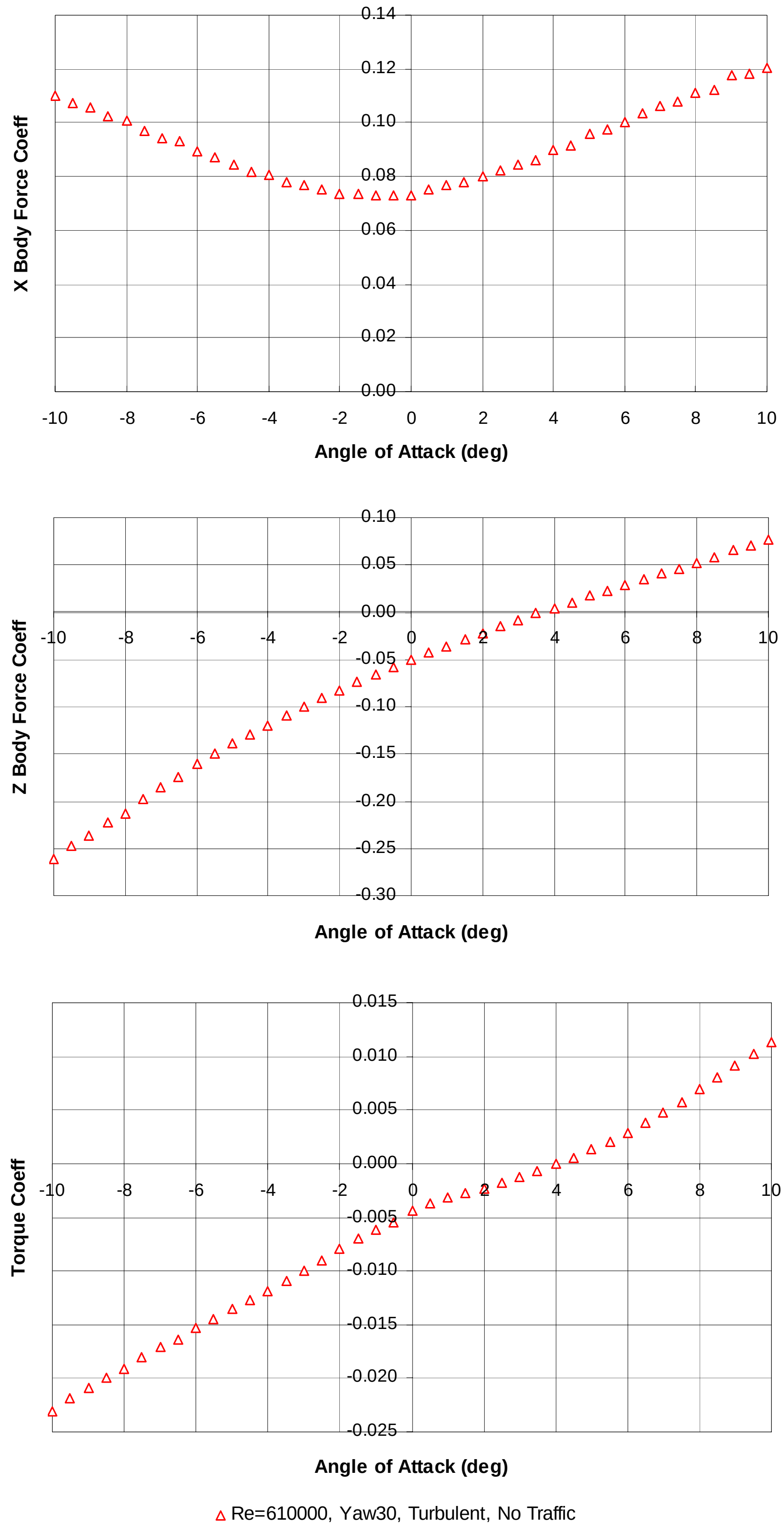

FIGURE C54 STATIC FORCE COEFFICIENTS (BODY FORCES), TURBULENT FLOW, IN-SERVICE, NO TRAFFIC, SKEW=30^{O}

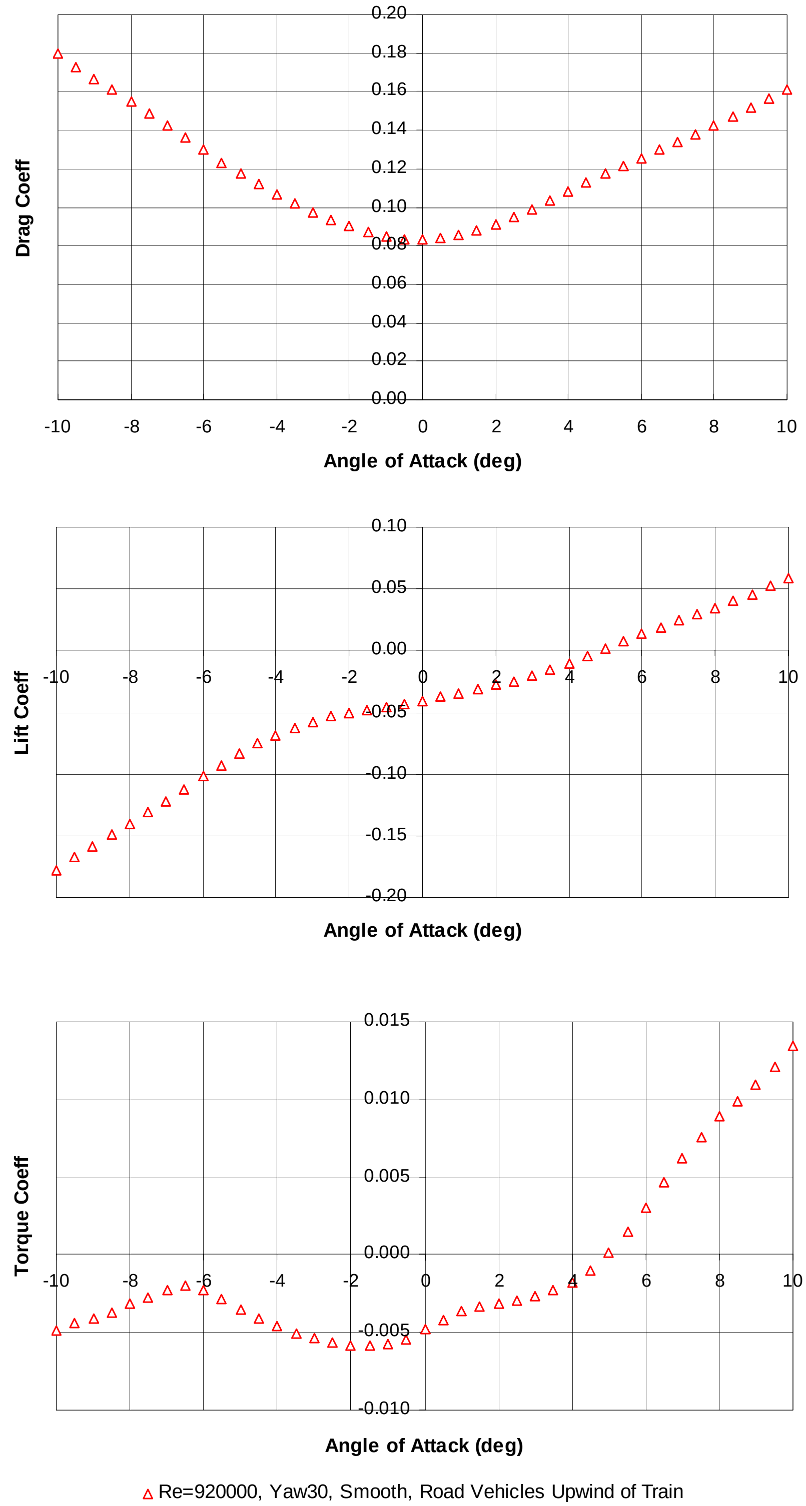

FIGURE C55 STATIC FORCE COEFFICIENTS (WIND AXIS FORCES), SMOOTH FLOW, IN-SERVICE, TRAFFIC CONDITION 1, SKEW=30^{O}

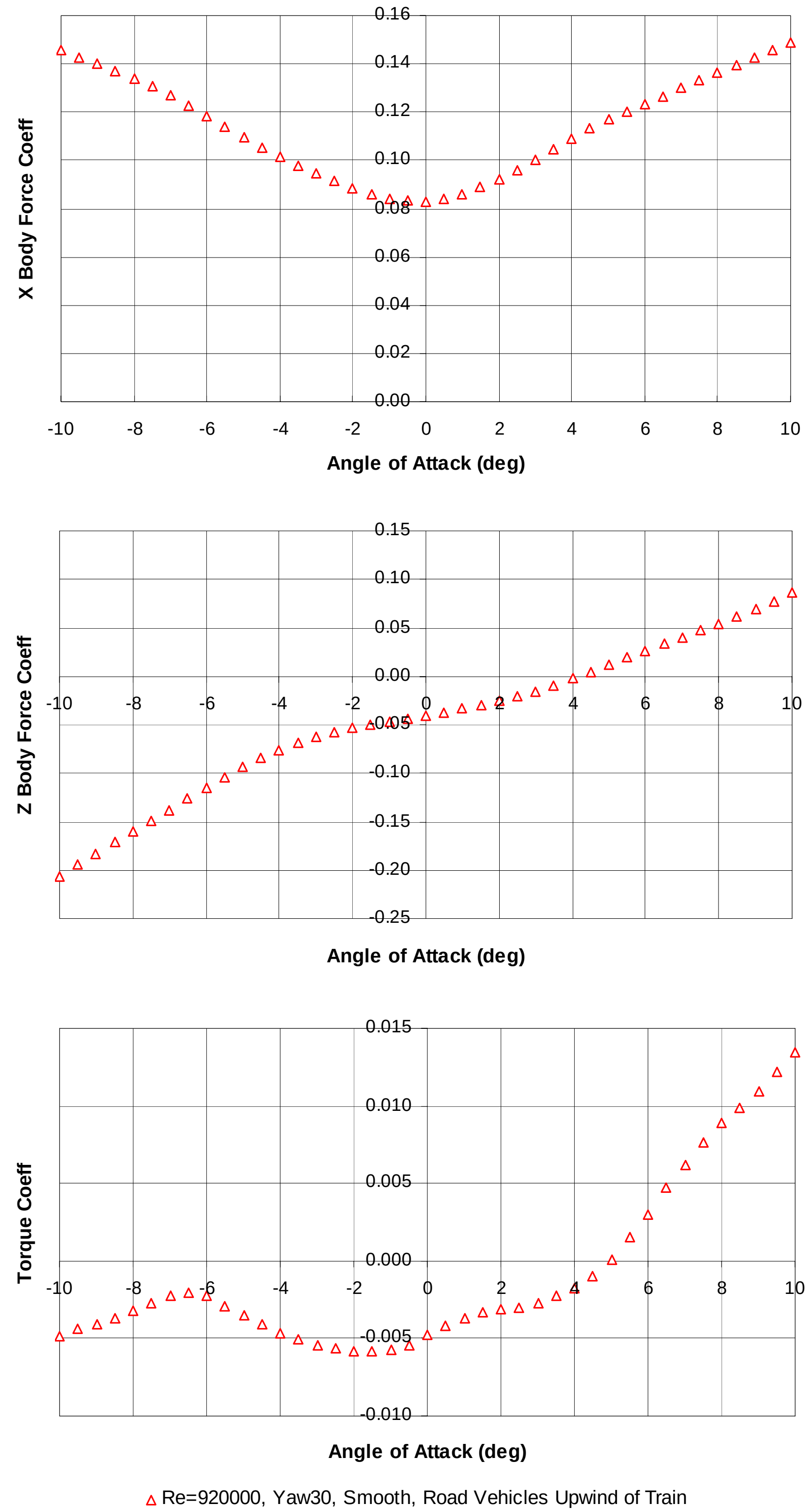

FIGURE C56 STATIC FORCE COEFFICIENTS (BODY FORCES), SMOOTH FLOW, IN-SERVICE, TRAFFIC CONDITION 1, SKEW=30^{O}

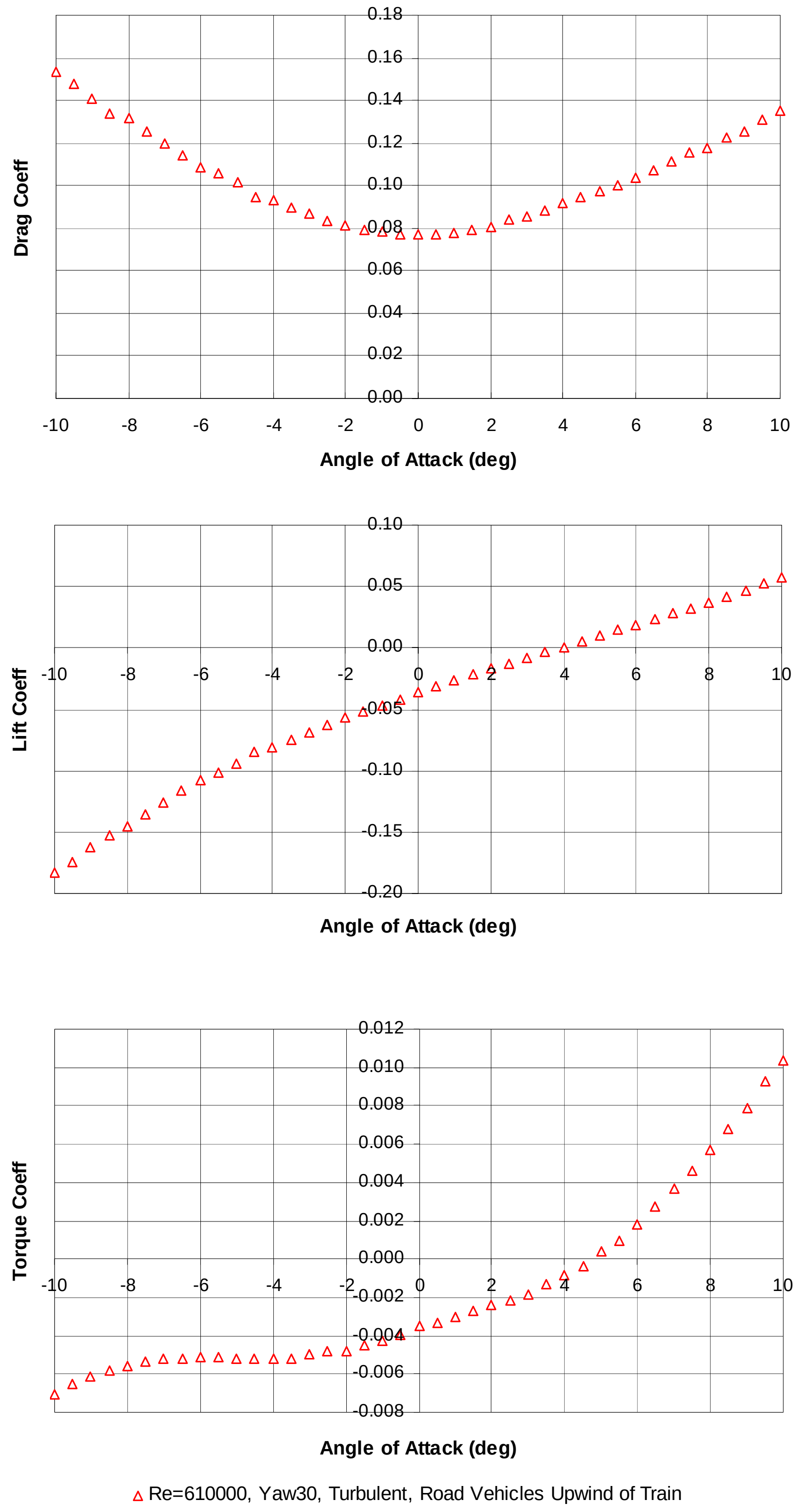

FIGURE C57 STATIC FORCE COEFFICIENTS (WIND AXIS FORCES), TURBULENT FLOW, IN-SERVICE, TRAFFIC CONDITION 1, SKEW=30^O

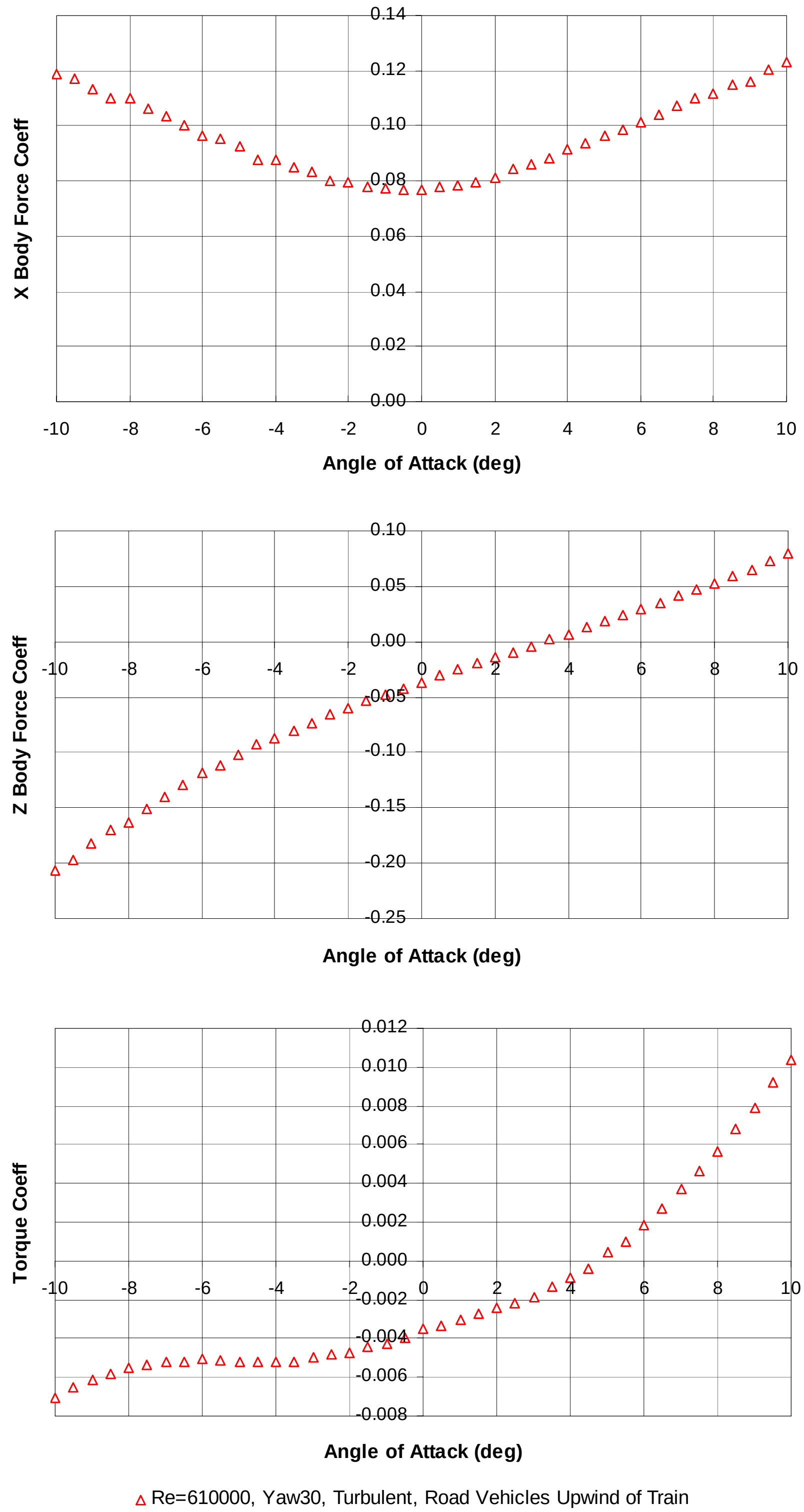

FIGURE C58 STATIC FORCE COEFFICIENTS (BODY FORCES), TURBULENT FLOW, IN-SERVICE, TRAFFIC CONDITION 1, SKEW=30^{O}

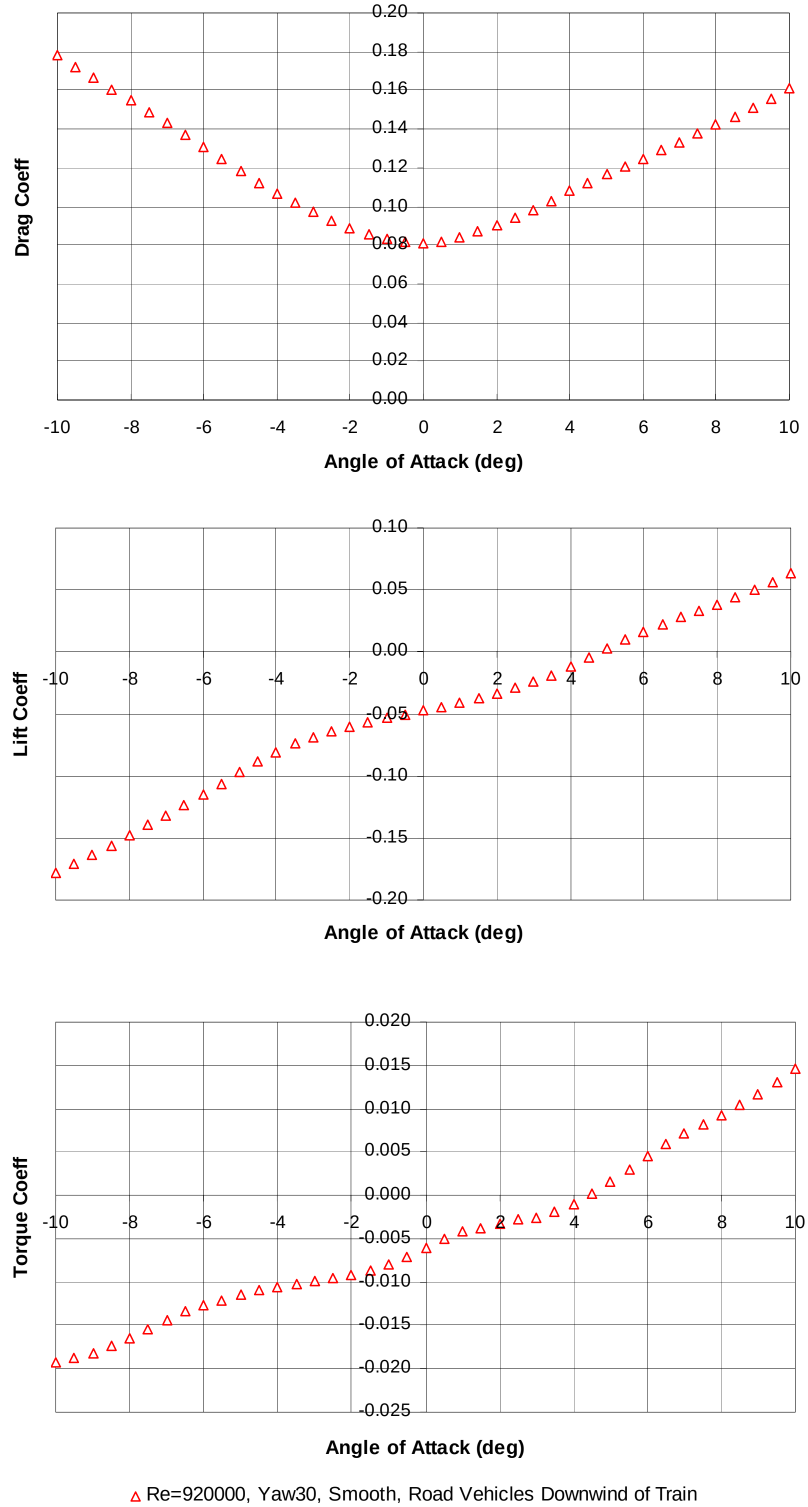

FIGURE C59 STATIC FORCE COEFFICIENTS (WIND AXIS FORCES), SMOOTH FLOW, IN-SERVICE, TRAFFIC CONDITION 2, SKEW=30^{O}

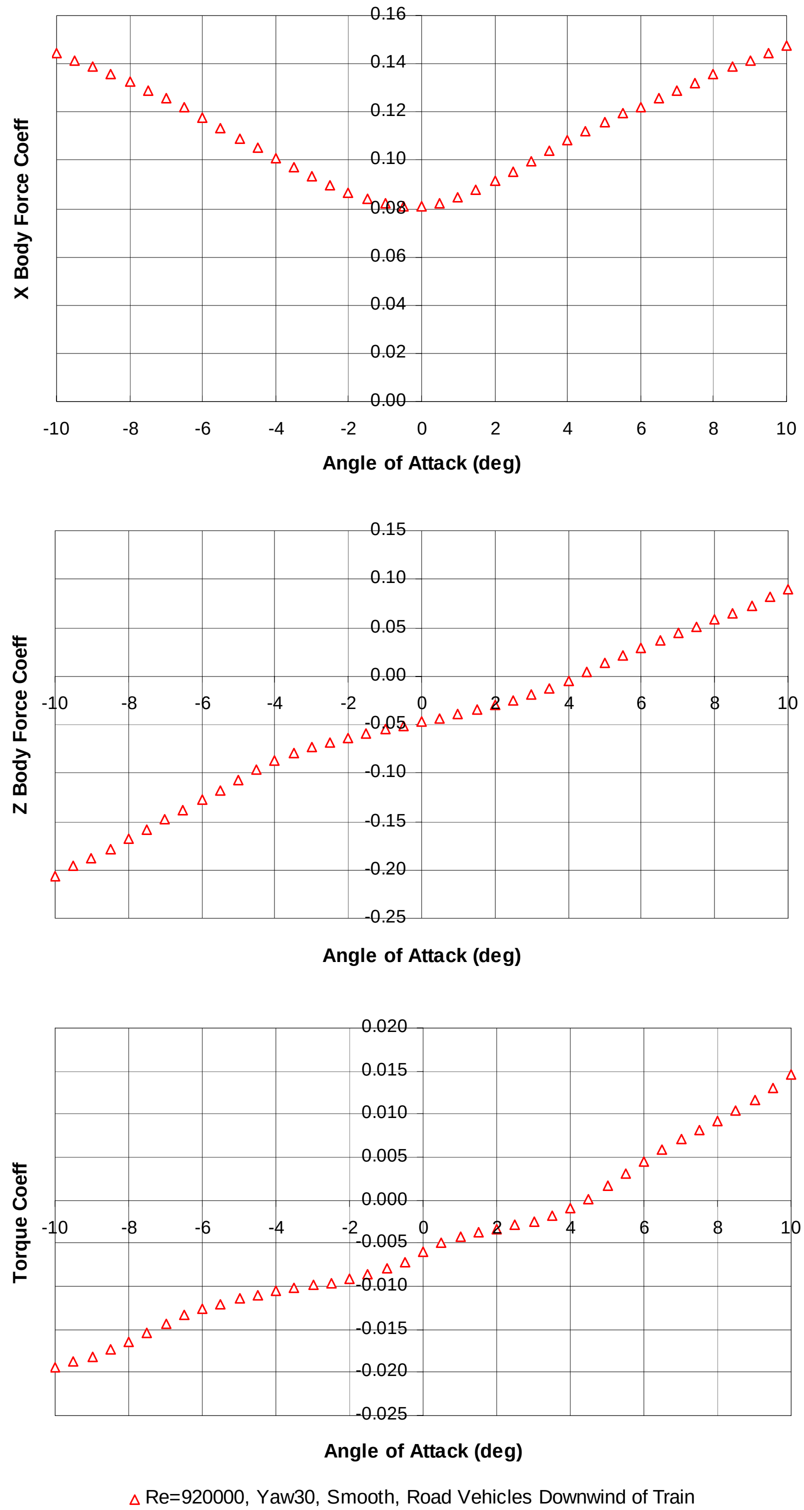

FIGURE C60 STATIC FORCE COEFFICIENTS (BODY FORCES), SMOOTH FLOW, IN-SERVICE, TRAFFIC CONDITION 2, SKEW=30^{O}

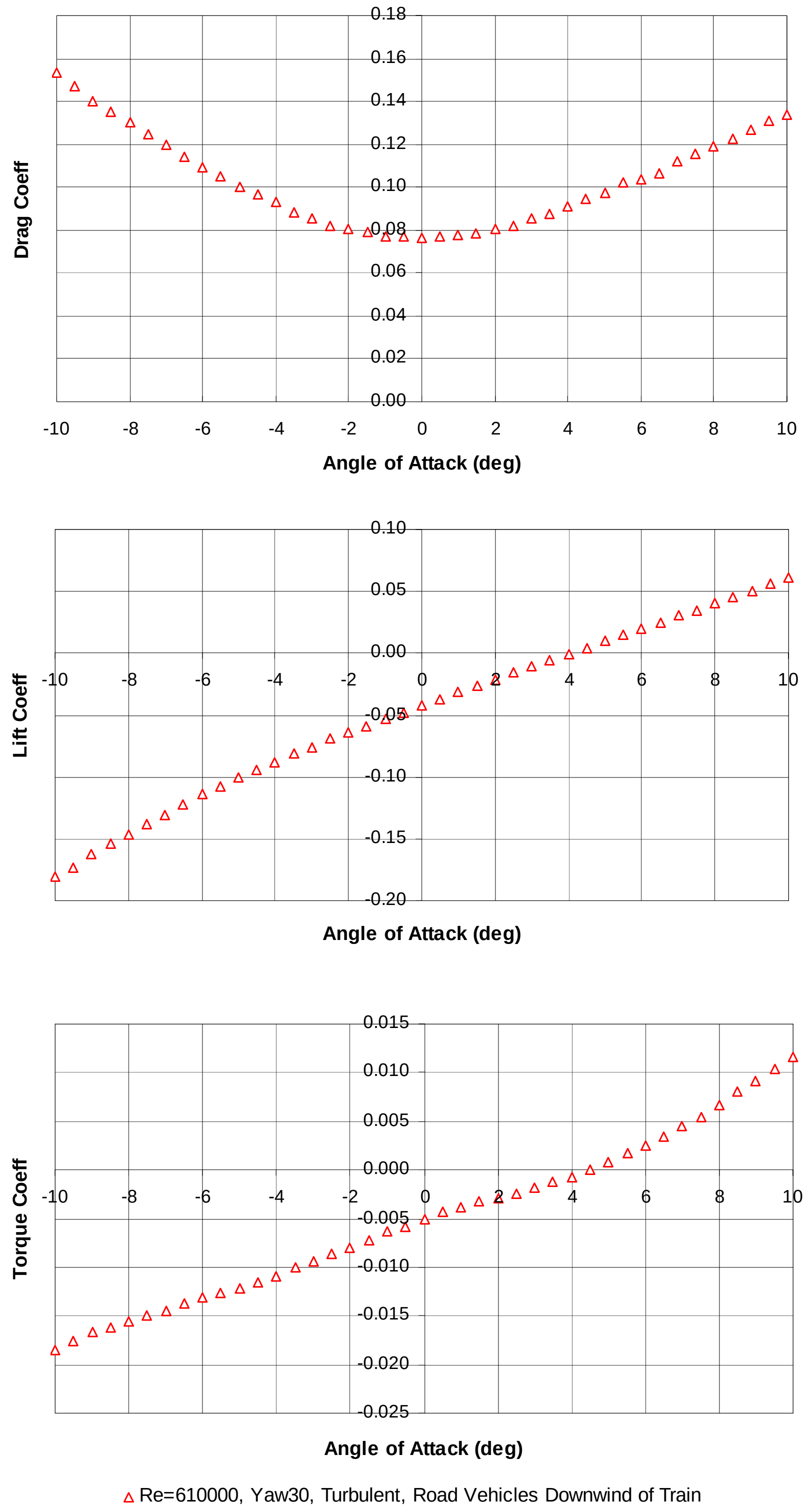

FIGURE C61 STATIC FORCE COEFFICIENTS (WIND AXIS FORCES), TURBULENT FLOW, IN-SERVICE, TRAFFIC CONDITION 2, SKEW=30^{O}

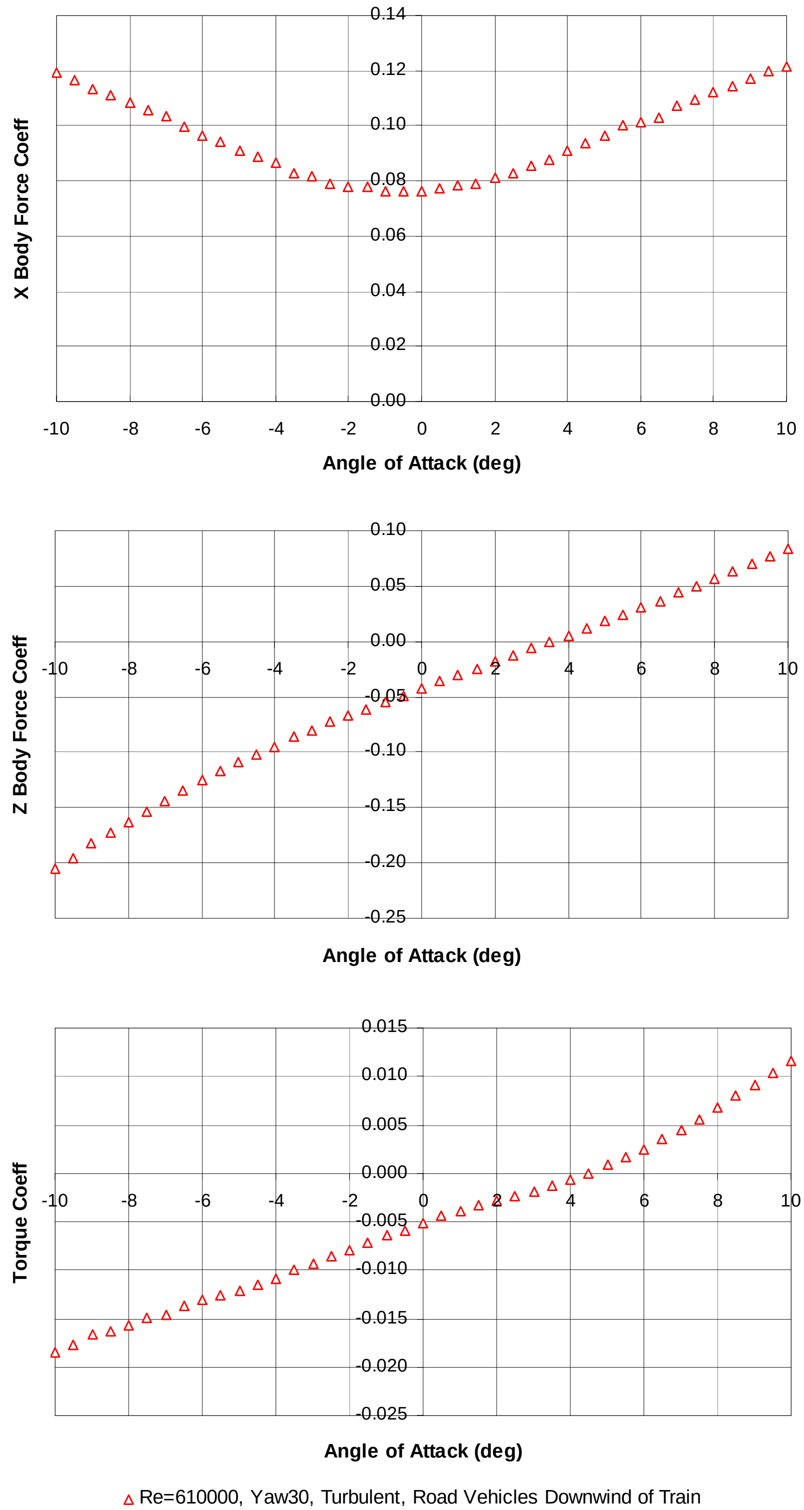

FIGURE C62 STATIC FORCE COEFFICIENTS (BODY FORCES), TURBULENT FLOW, IN-SERVICE, TRAFFIC CONDITION 2, SKEW=30^{O}

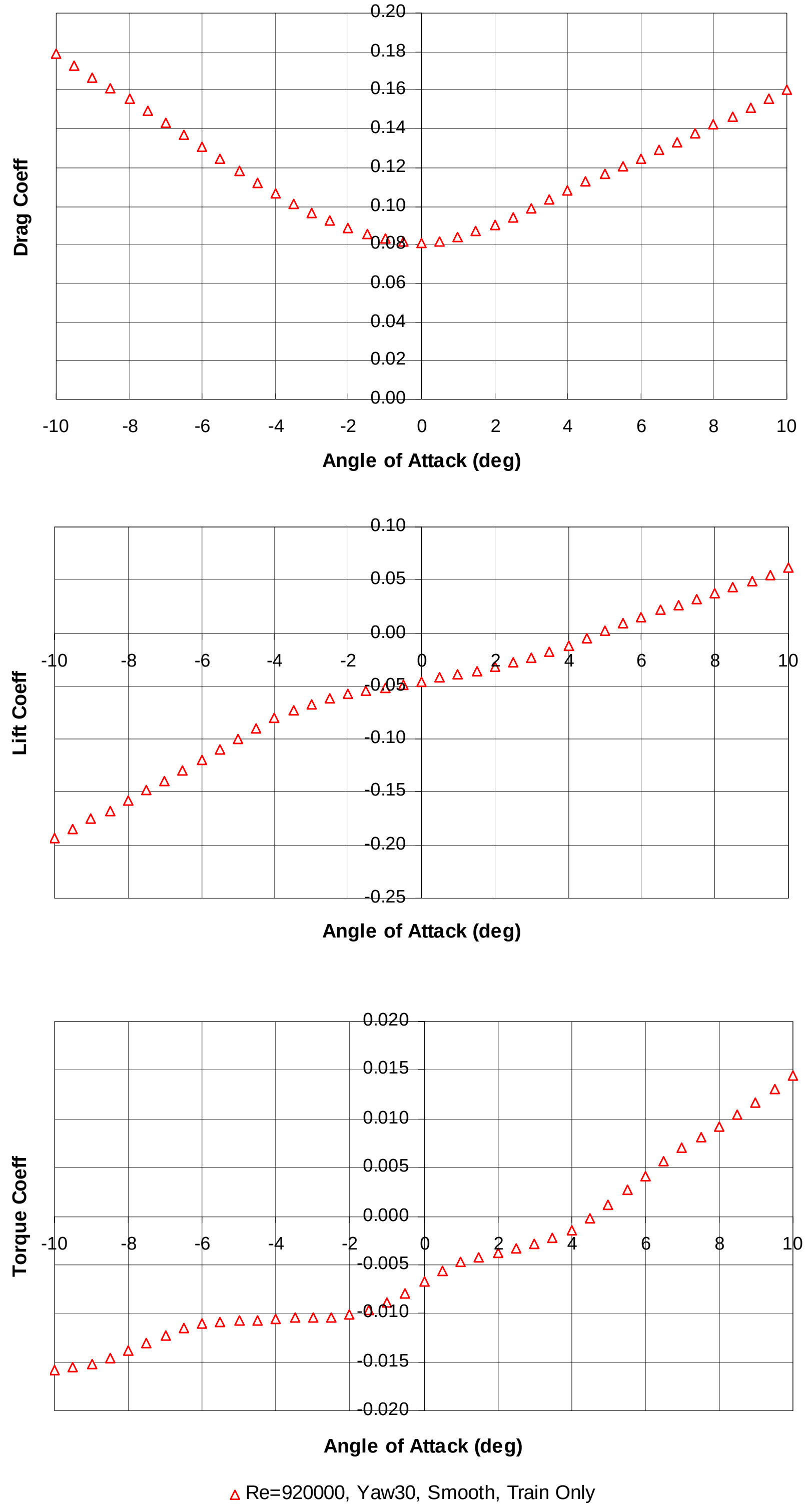

FIGURE C63 STATIC FORCE COEFFICIENTS (WIND AXIS FORCES), SMOOTH FLOW, IN-SERVICE, TRAFFIC CONDITION 3, SKEW=30^{O}

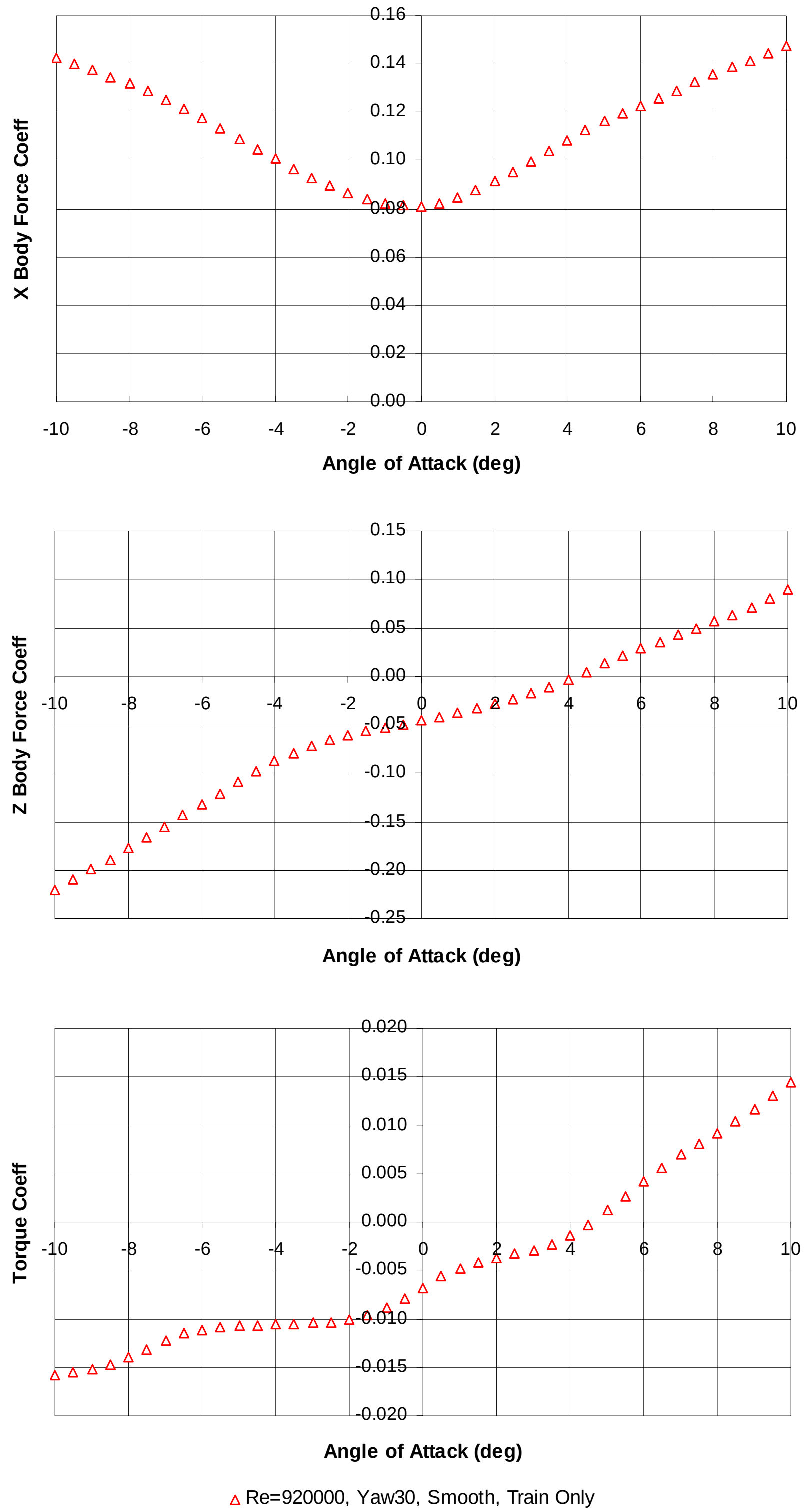

FIGURE C64 STATIC FORCE COEFFICIENTS (BODY FORCES), SMOOTH FLOW, IN-SERVICE, TRAFFIC CONDITION 3, SKEW=30^{O}

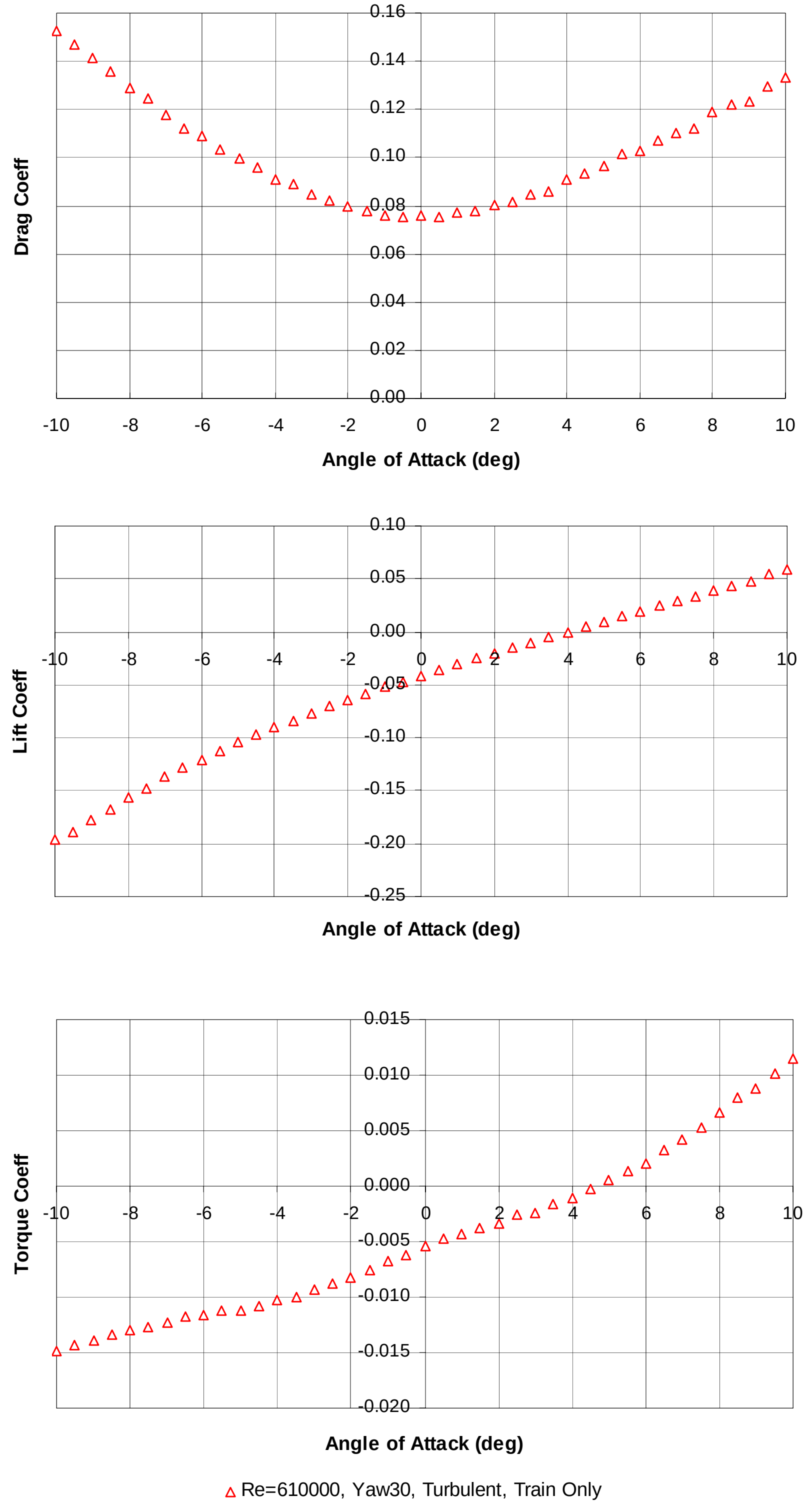

FIGURE C65 STATIC FORCE COEFFICIENTS (WIND AXIS FORCES), TURBULENT FLOW, IN-SERVICE, TRAFFIC CONDITION 3, SKEW=30^{O}

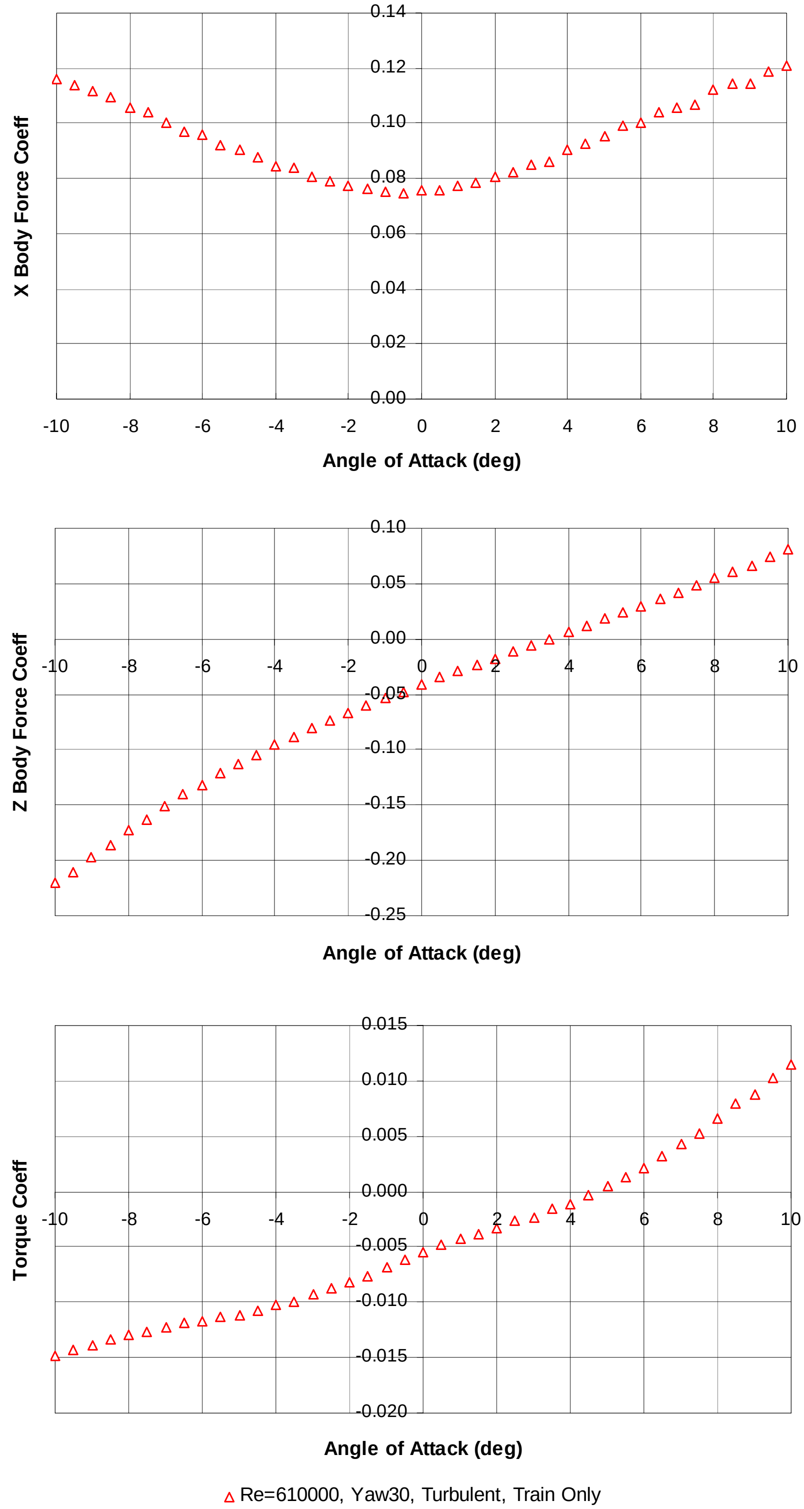

FIGURE C66 STATIC FORCE COEFFICIENTS (BODY FORCES), TURBULENT FLOW, IN-SERVICE, TRAFFIC CONDITION 3, SKEW=30^{O}

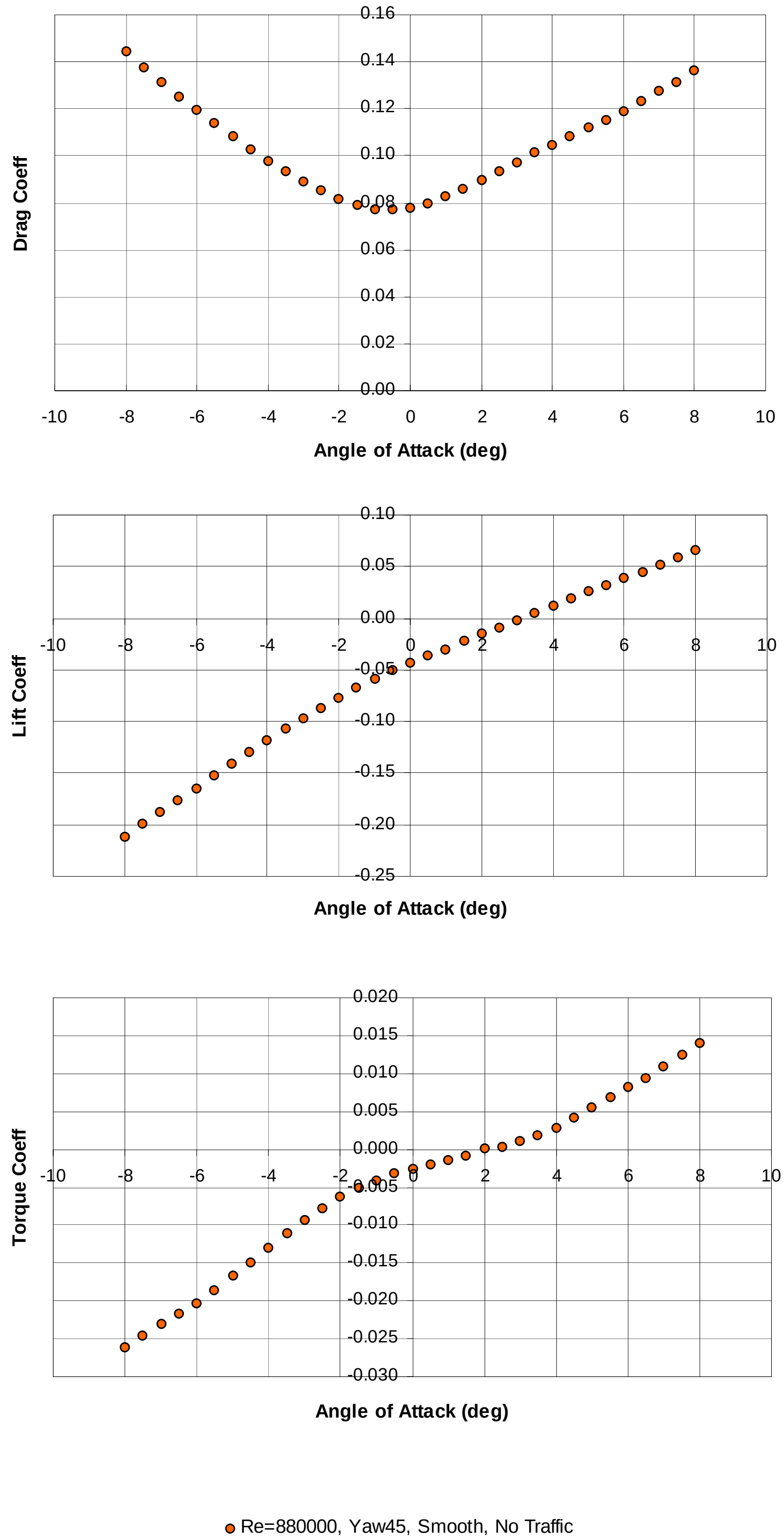

FIGURE C67 STATIC FORCE COEFFICIENTS (WIND AXIS FORCES), SMOOTH FLOW, IN-SERVICE, NO TRAFFIC, SKEW=45^{O}

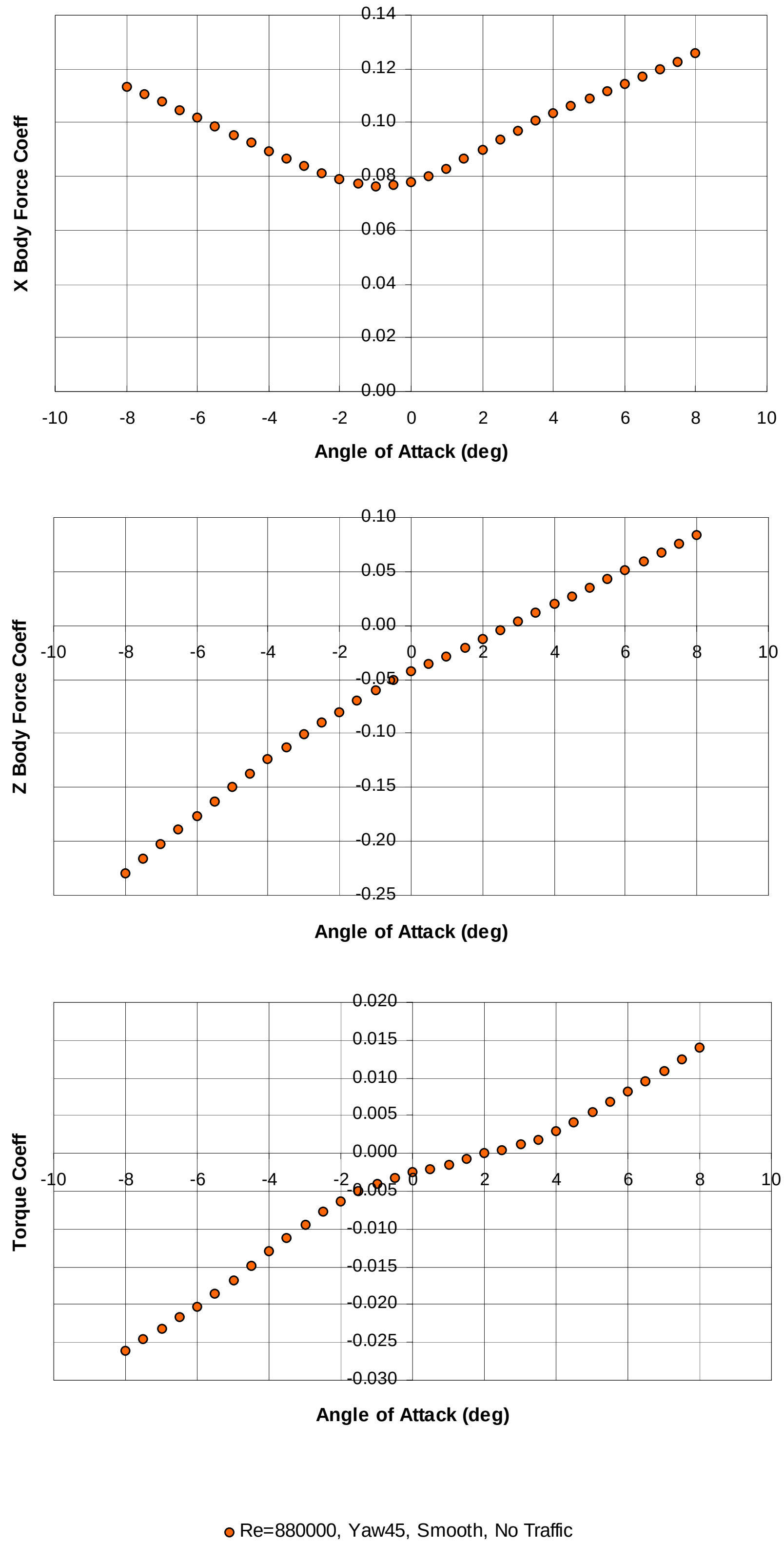

FIGURE C68 STATIC FORCE COEFFICIENTS (BODY FORCES), SMOOTH FLOW, IN-SERVICE, NO TRAFFIC, SKEW=45^{O}

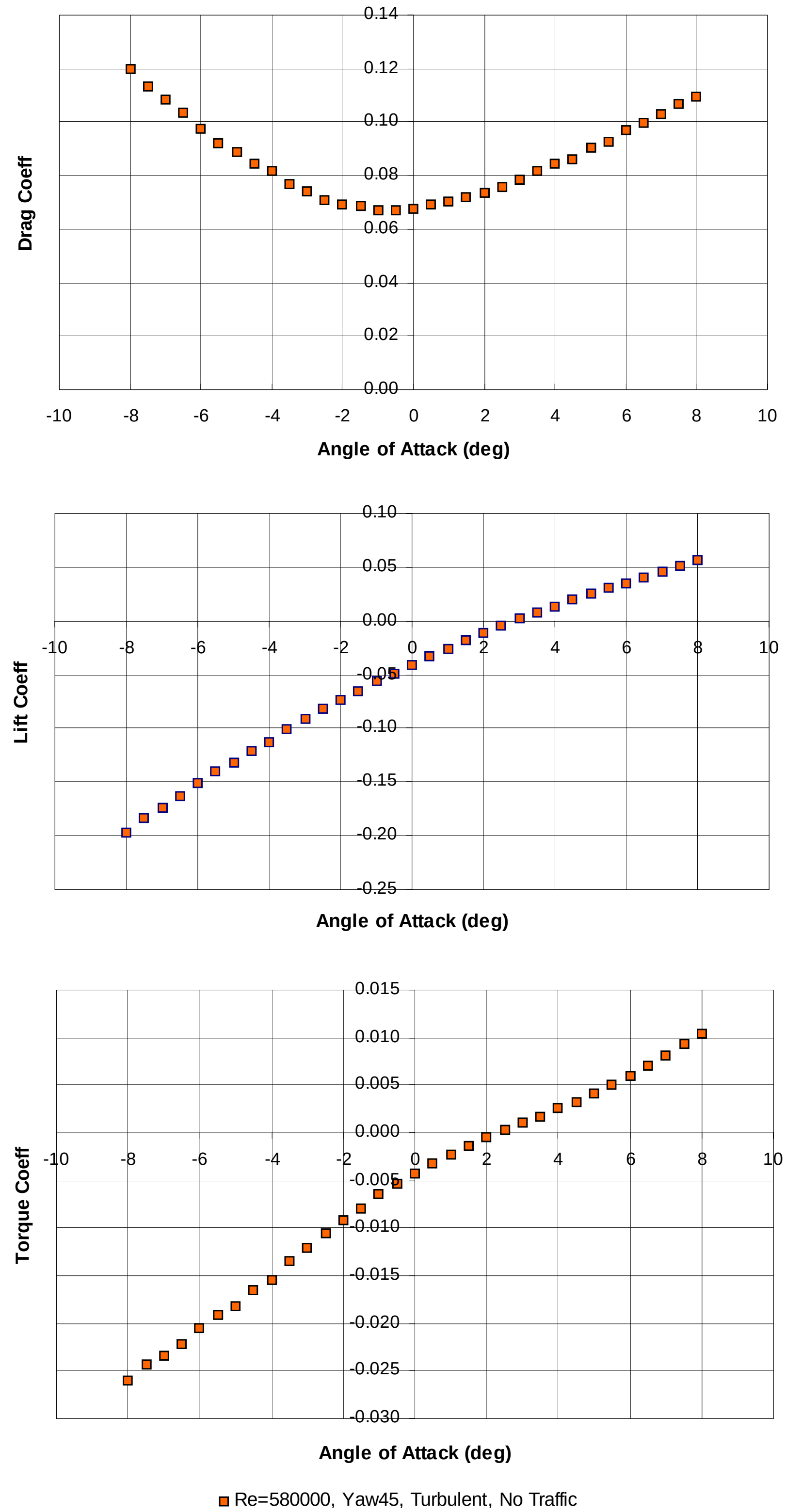

FIGURE C69 STATIC FORCE COEFFICIENTS (WIND AXIS FORCES), TURBULENT FLOW, IN-SERVICE, NO TRAFFIC, SKEW=45^{O}

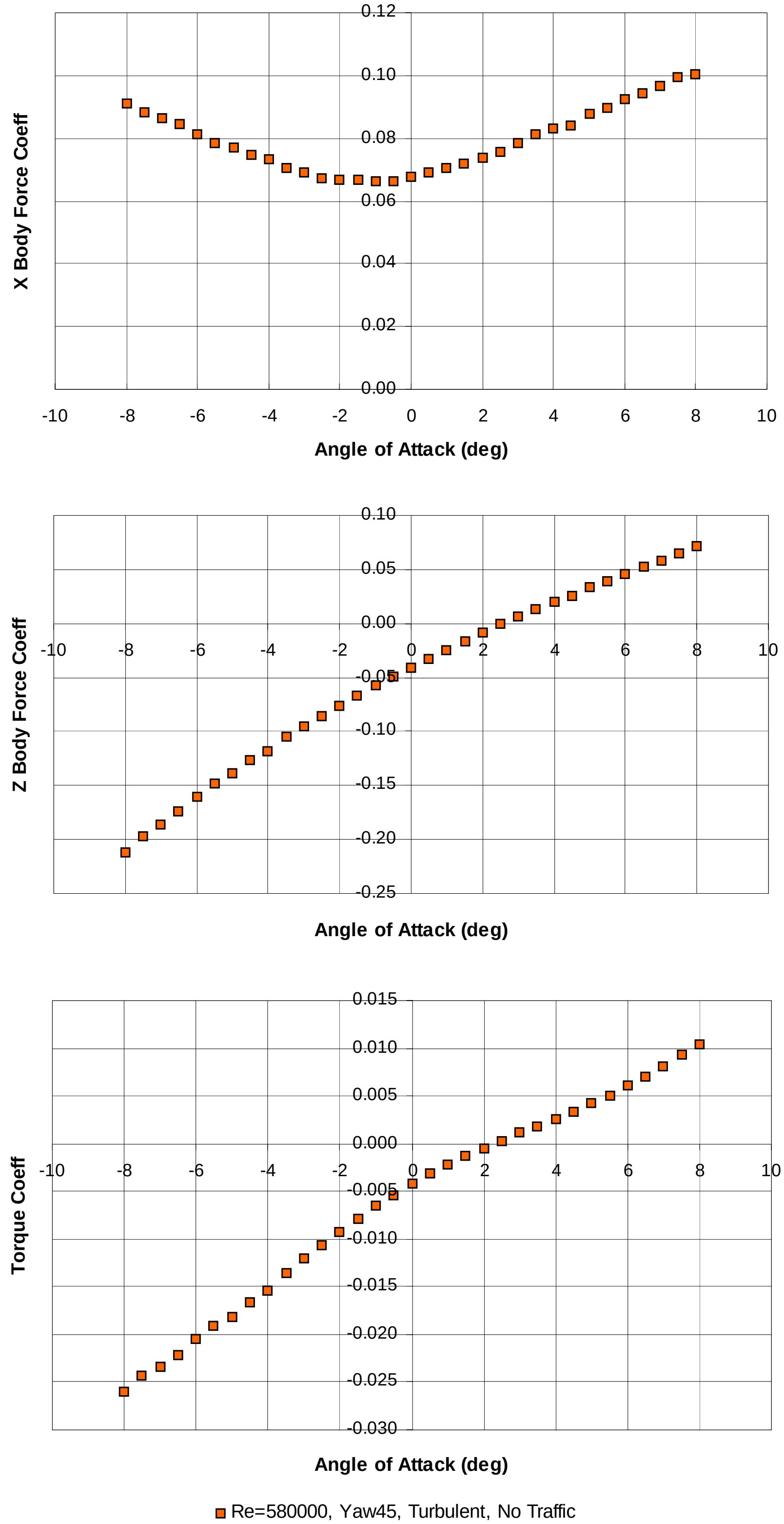

FIGURE C70 STATIC FORCE COEFFICIENTS (BODY FORCES), TURBULENT FLOW, IN-SERVICE, NO TRAFFIC, SKEW=45^{O}

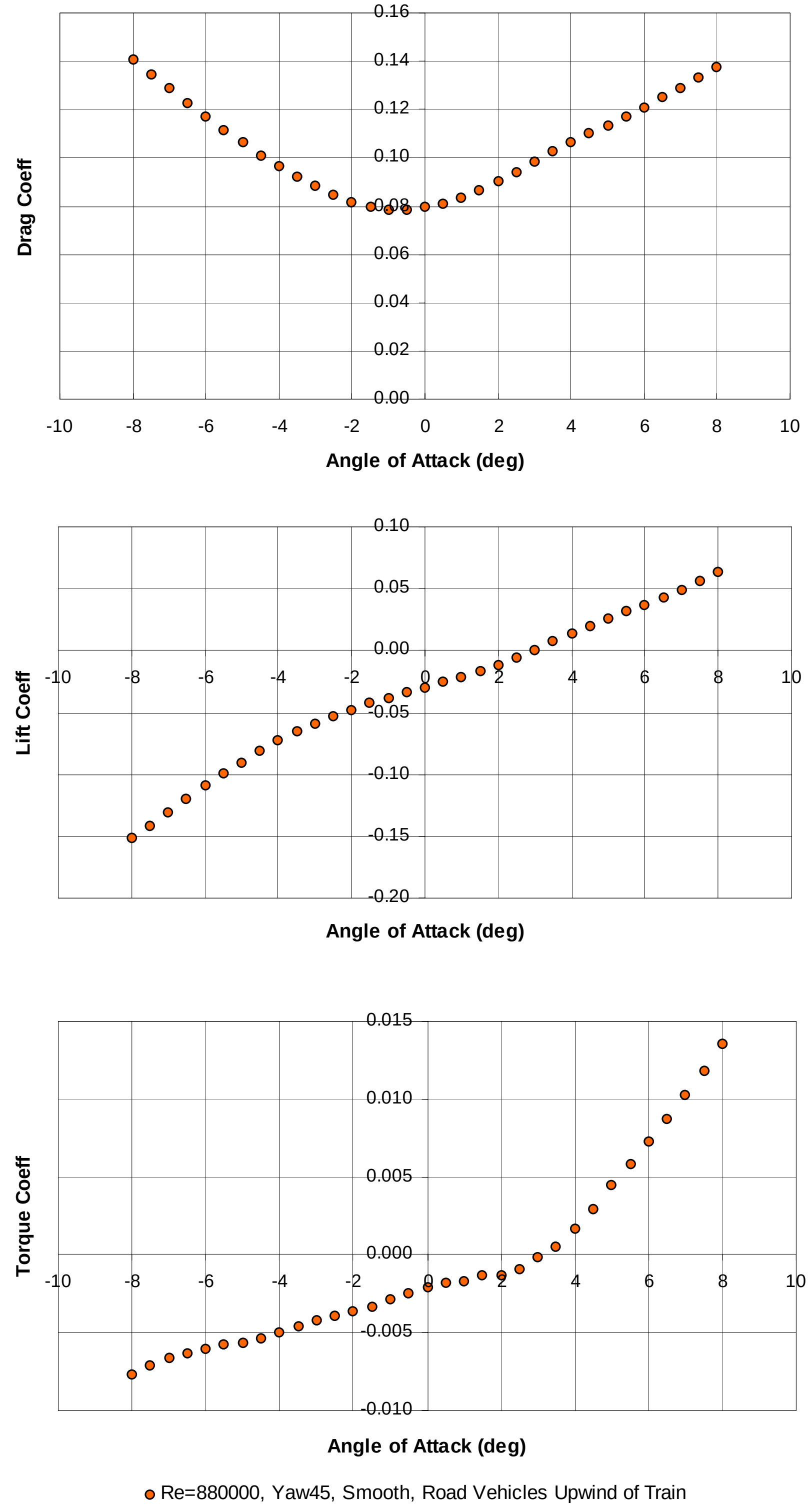

FIGURE C71 STATIC FORCE COEFFICIENTS (WIND AXIS FORCES), SMOOTH FLOW, IN-SERVICE, TRAFFIC CONDITION 1, SKEW=45^{O}

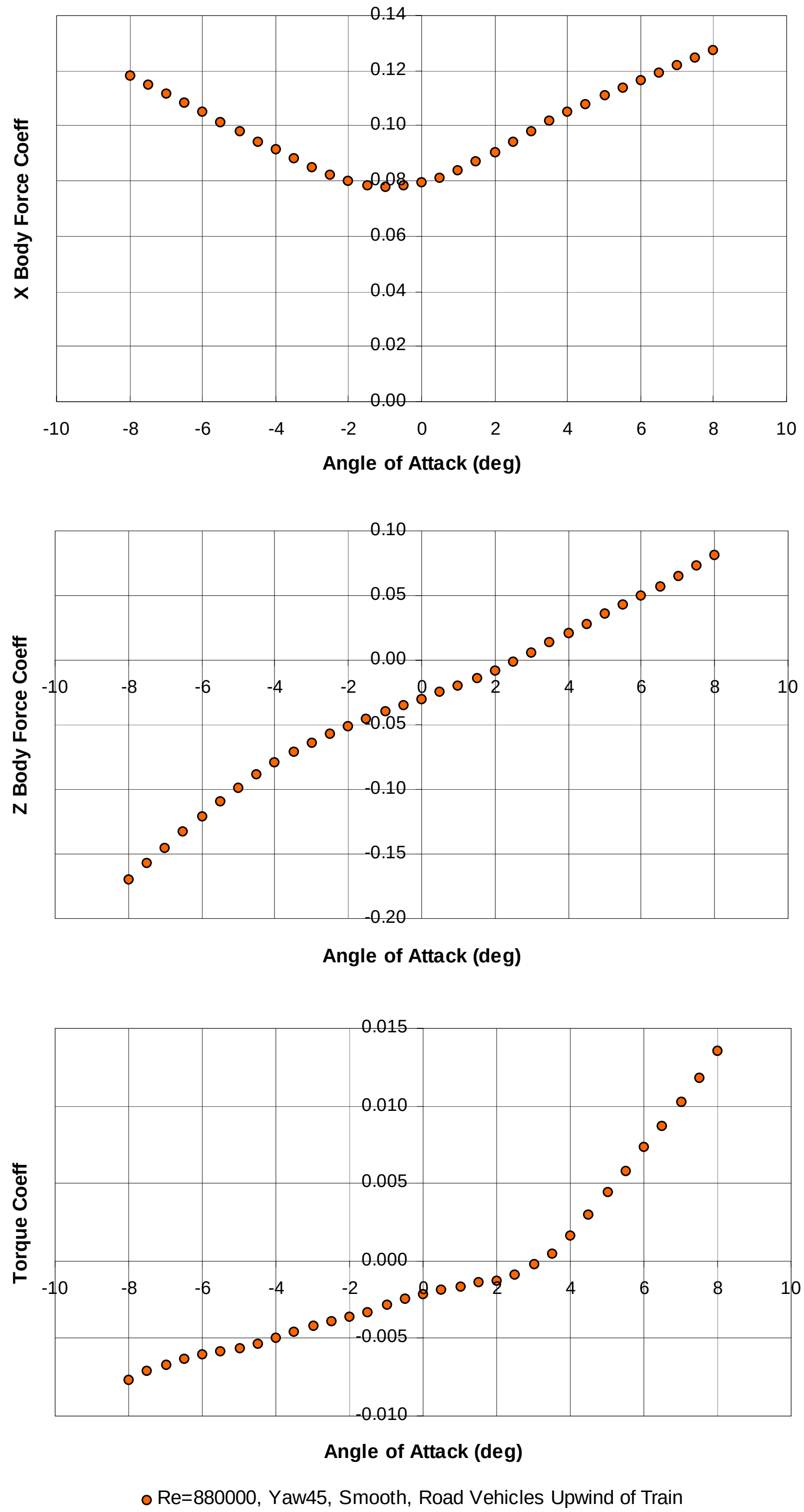

FIGURE C72 STATIC FORCE COEFFICIENTS (BODY FORCES), SMOOTH FLOW, IN-SERVICE, TRAFFIC CONDITION 1, SKEW=45^{O}

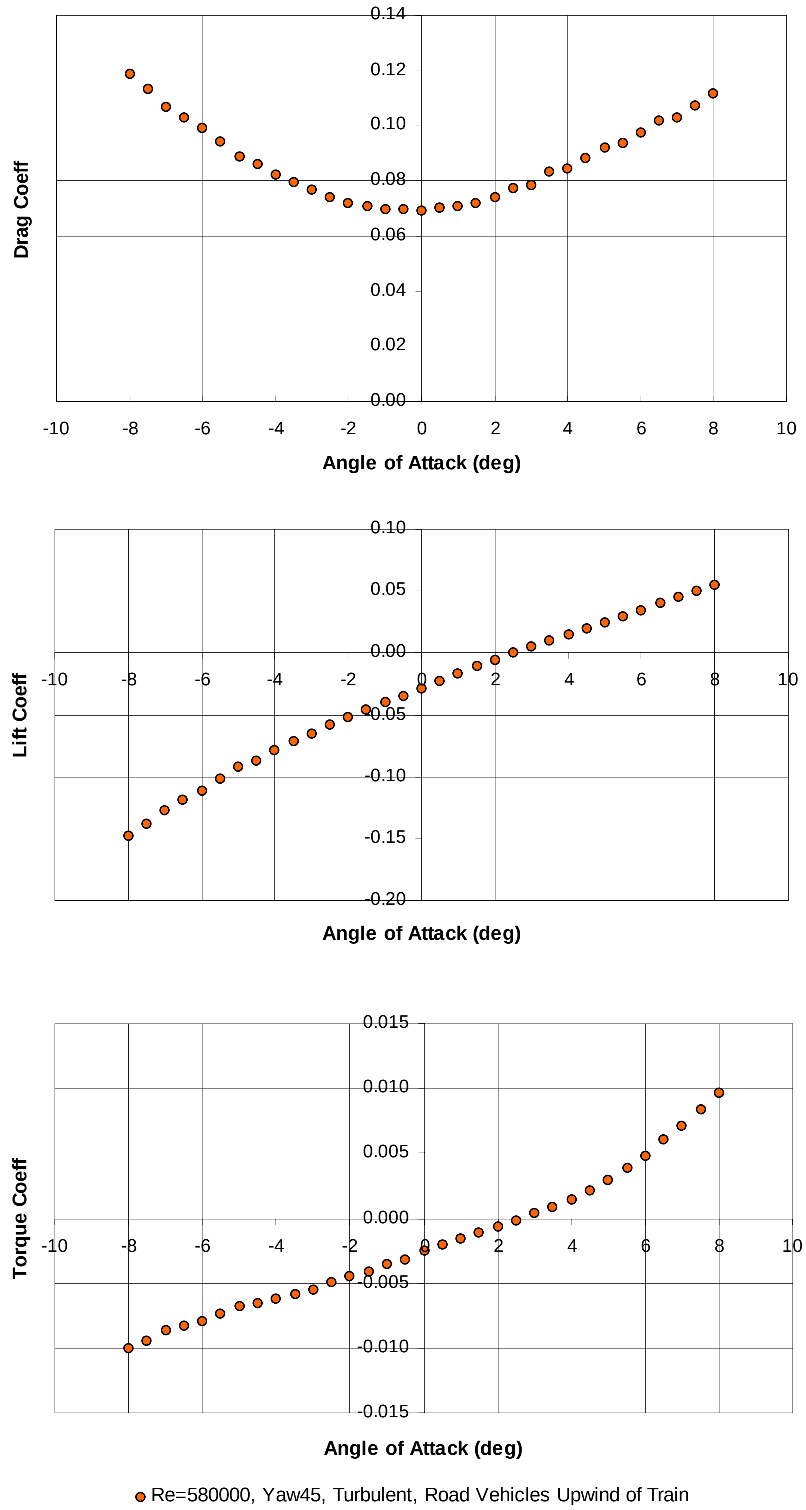

FIGURE C73 STATIC FORCE COEFFICIENTS (WIND AXIS FORCES), TURBULENT FLOW, IN-SERVICE, TRAFFIC CONDITION 1, SKEW=45^{O}

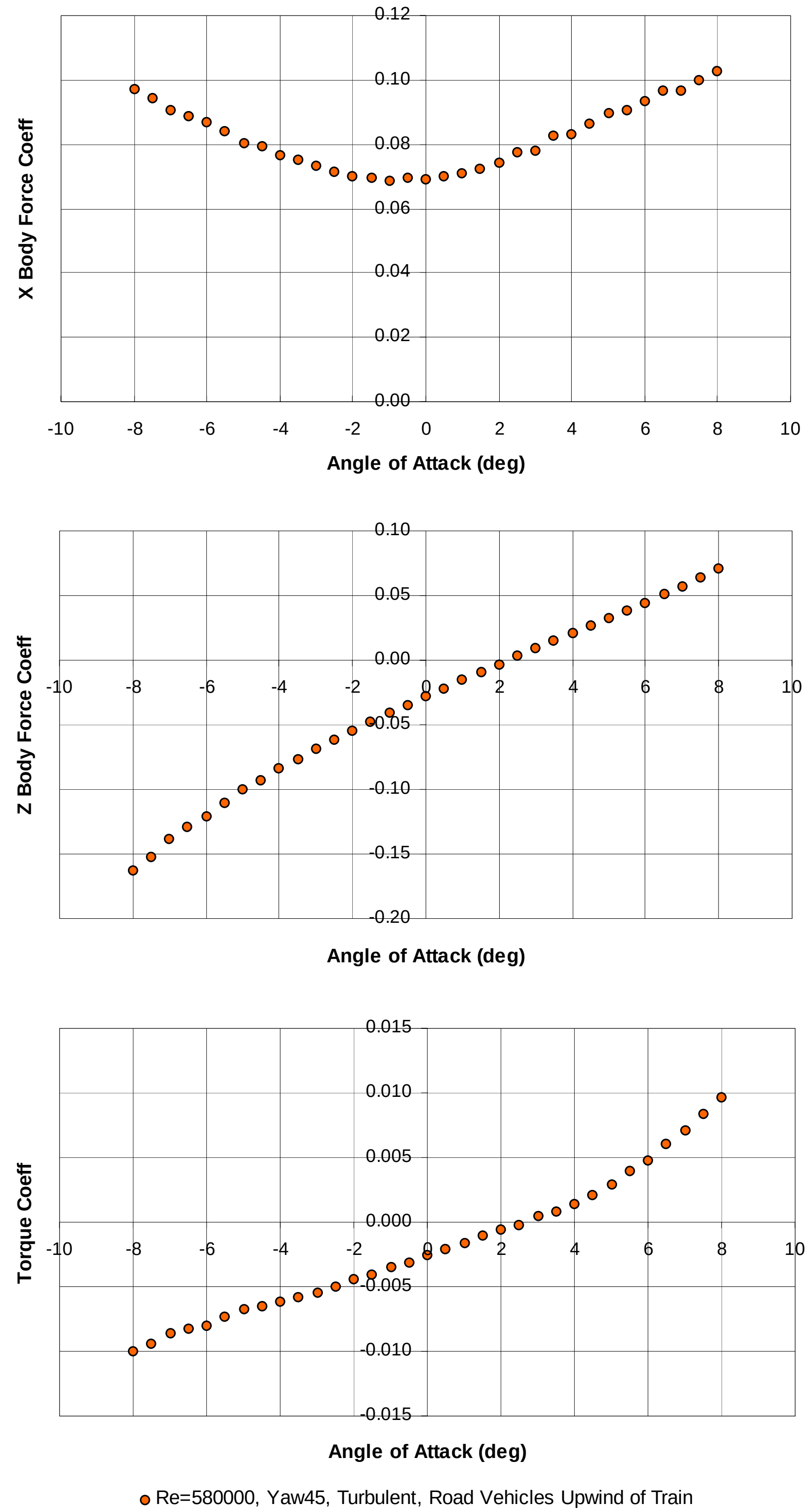

FIGURE C74 STATIC FORCE COEFFICIENTS (BODY FORCES), TURBULENT FLOW, IN-SERVICE, TRAFFIC CONDITION 1, SKEW=45^{O}

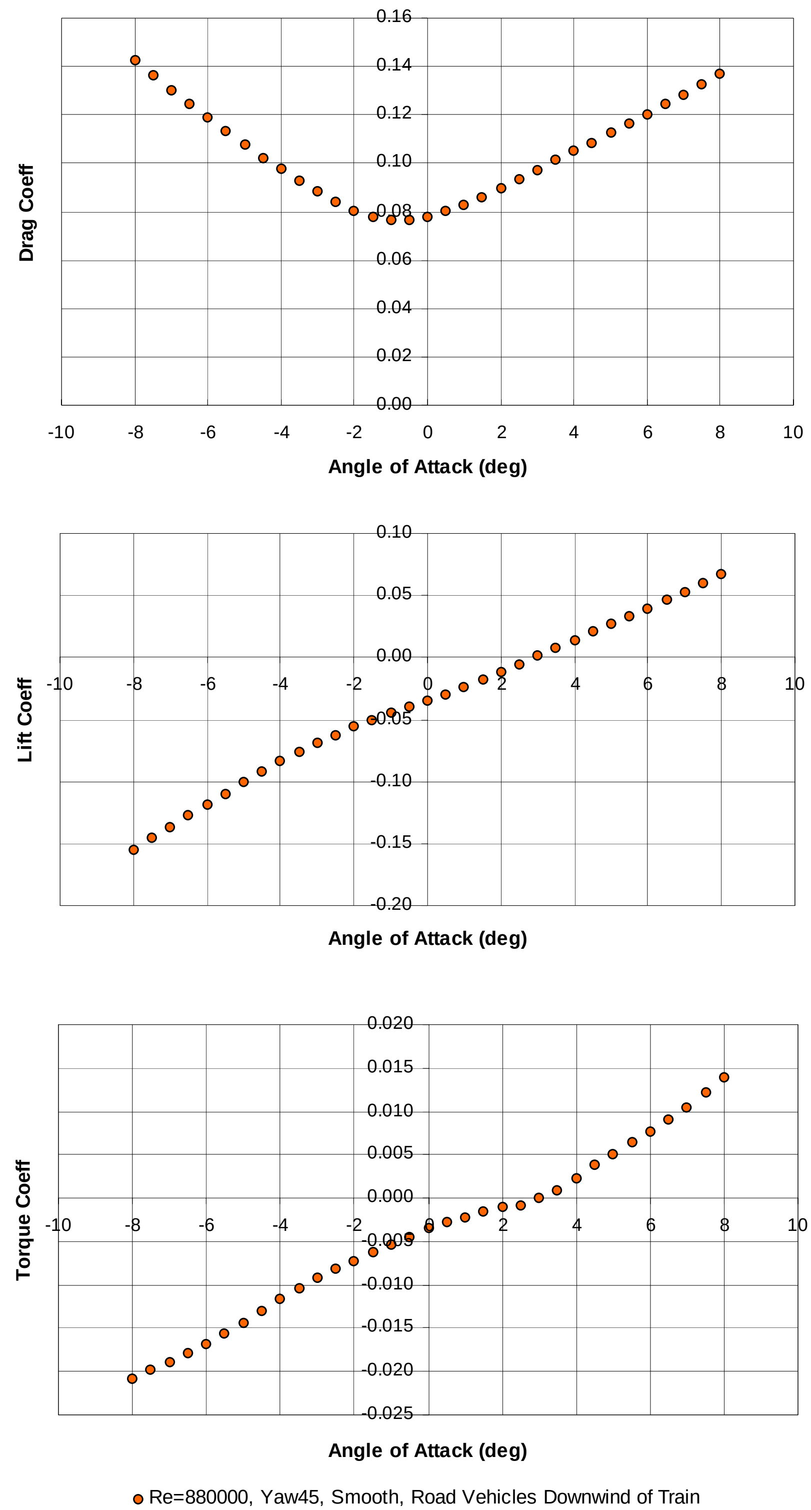

FIGURE C75 STATIC FORCE COEFFICIENTS (WIND AXIS FORCES), SMOOTH FLOW, IN-SERVICE, TRAFFIC CONDITION 2, SKEW=45^{O}

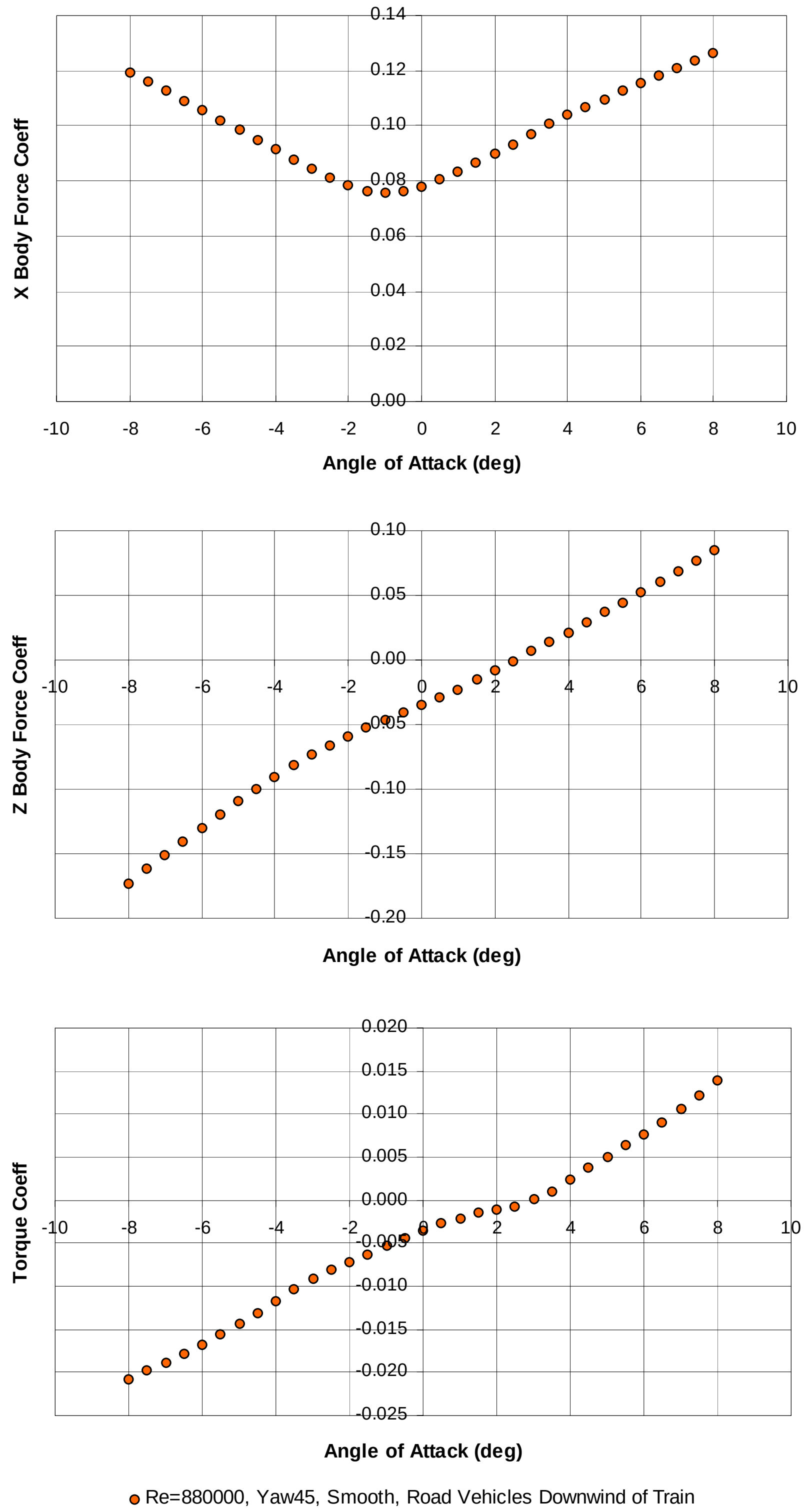

FIGURE C76 STATIC FORCE COEFFICIENTS (BODY FORCES), SMOOTH FLOW, IN-SERVICE, TRAFFIC CONDITION 2, SKEW=45^{O}

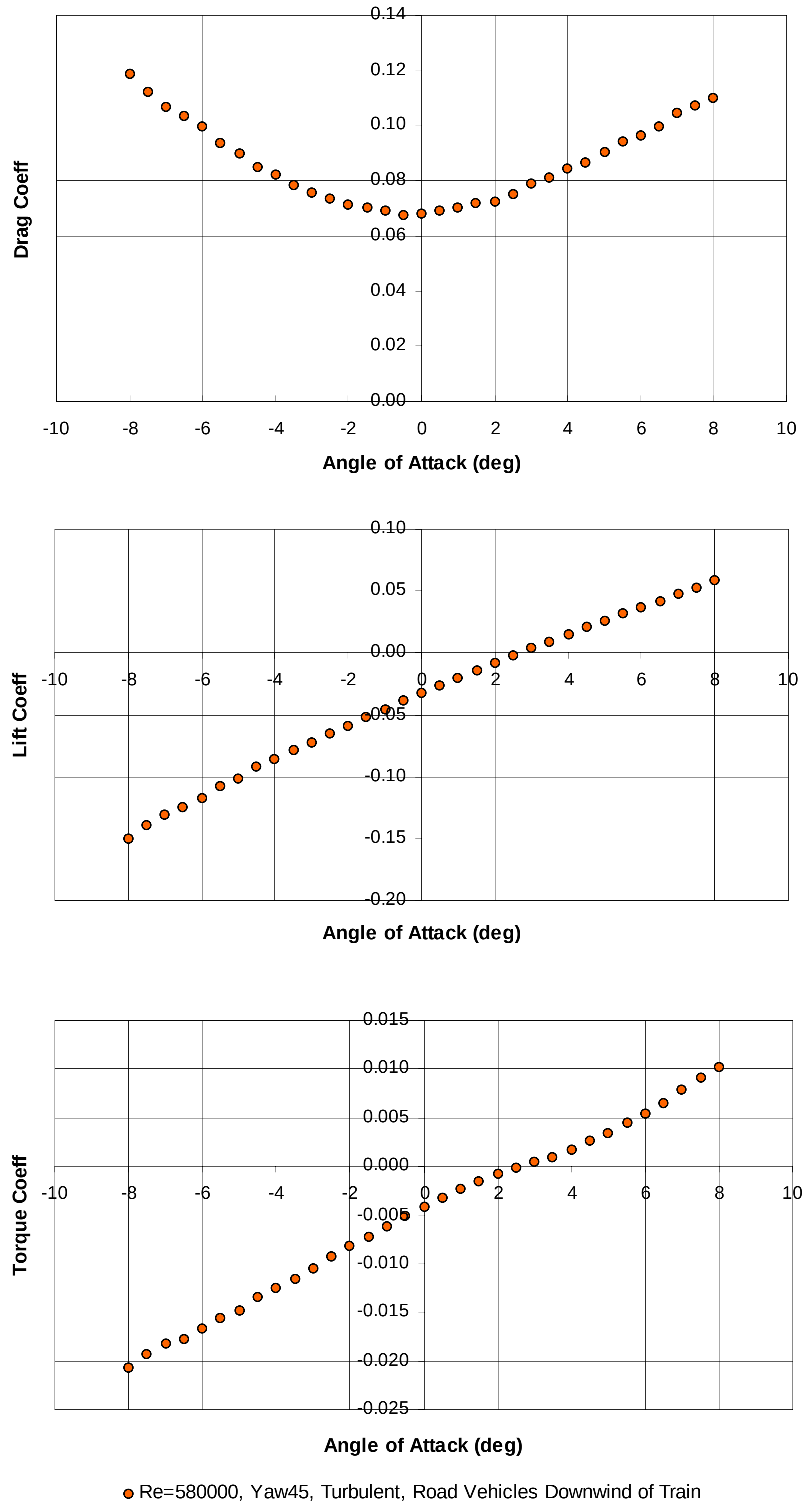

FIGURE C77 STATIC FORCE COEFFICIENTS (WIND AXIS FORCES), TURBULENT FLOW, IN-SERVICE, TRAFFIC CONDITION 2, SKEW=45^{O}

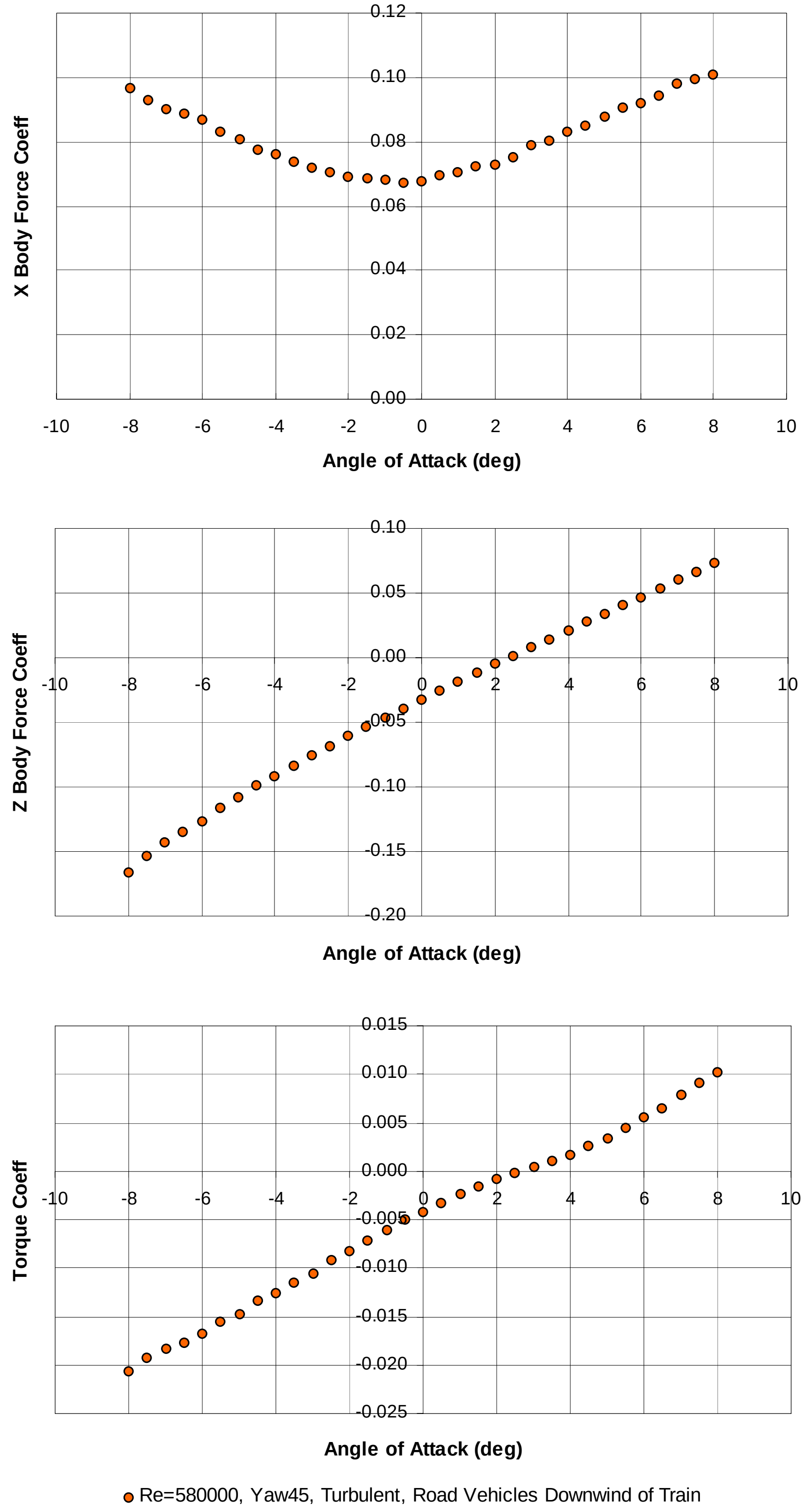

FIGURE C78 STATIC FORCE COEFFICIENTS (BODY FORCES), TURBULENT FLOW, IN-SERVICE, TRAFFIC CONDITION 2, SKEW=45^{O}

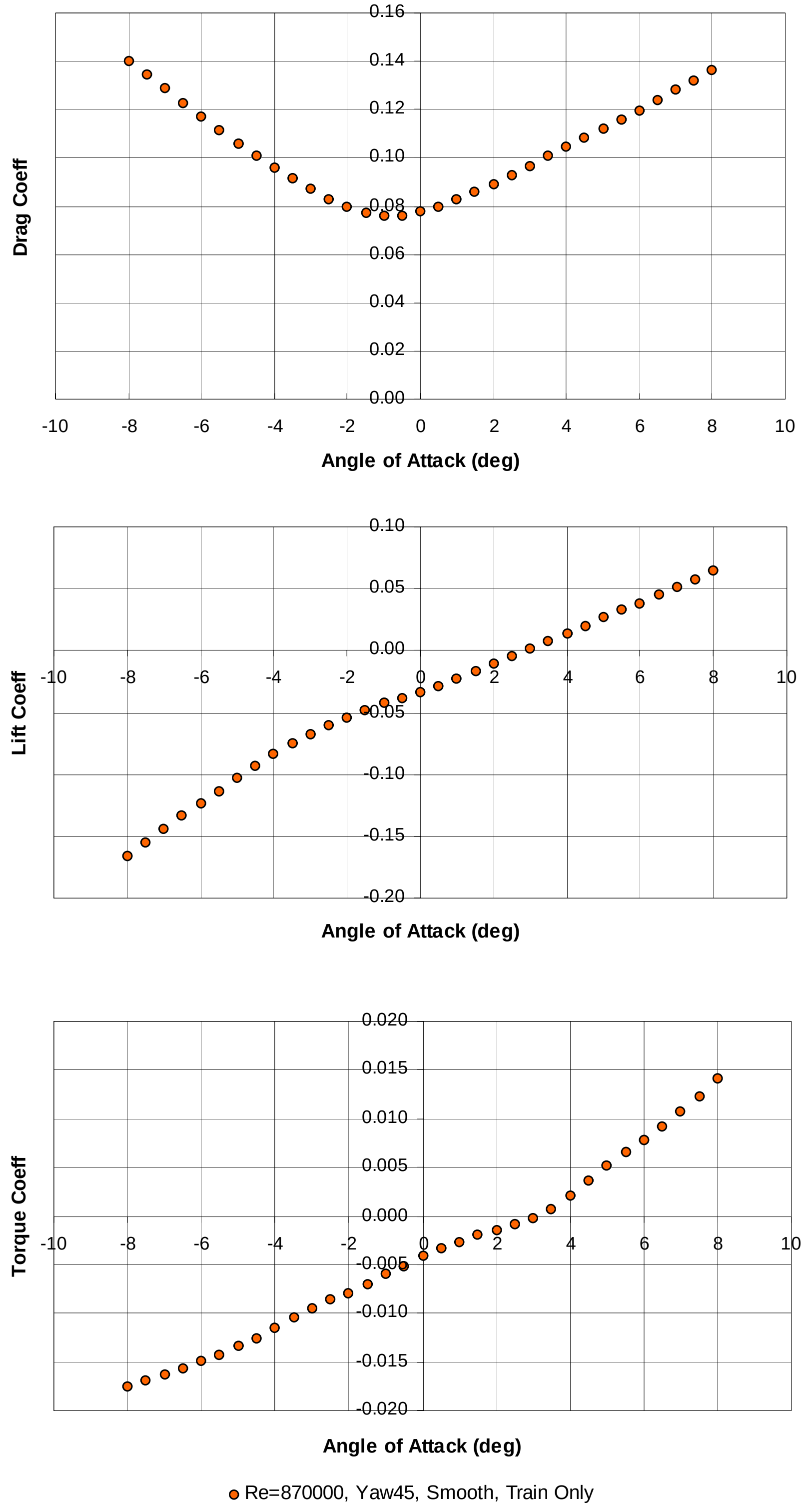

FIGURE C79 STATIC FORCE COEFFICIENTS (WIND AXIS FORCES), SMOOTH FLOW, IN-SERVICE, TRAFFIC CONDITION 3, SKEW=45^{O}

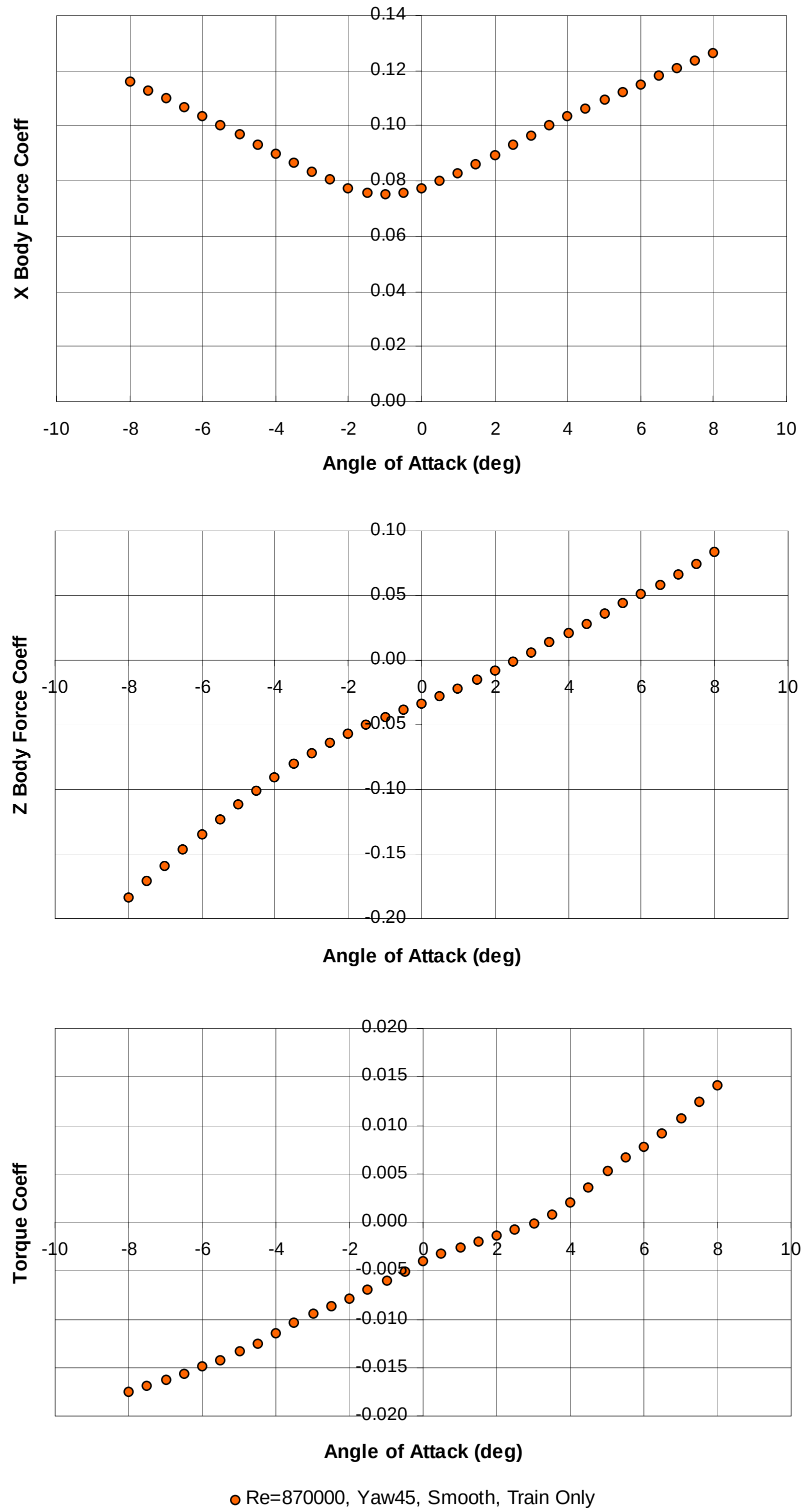

FIGURE C80 STATIC FORCE COEFFICIENTS (BODY FORCES), SMOOTH FLOW, IN-SERVICE, TRAFFIC CONDITION 3, SKEW=45^{O}

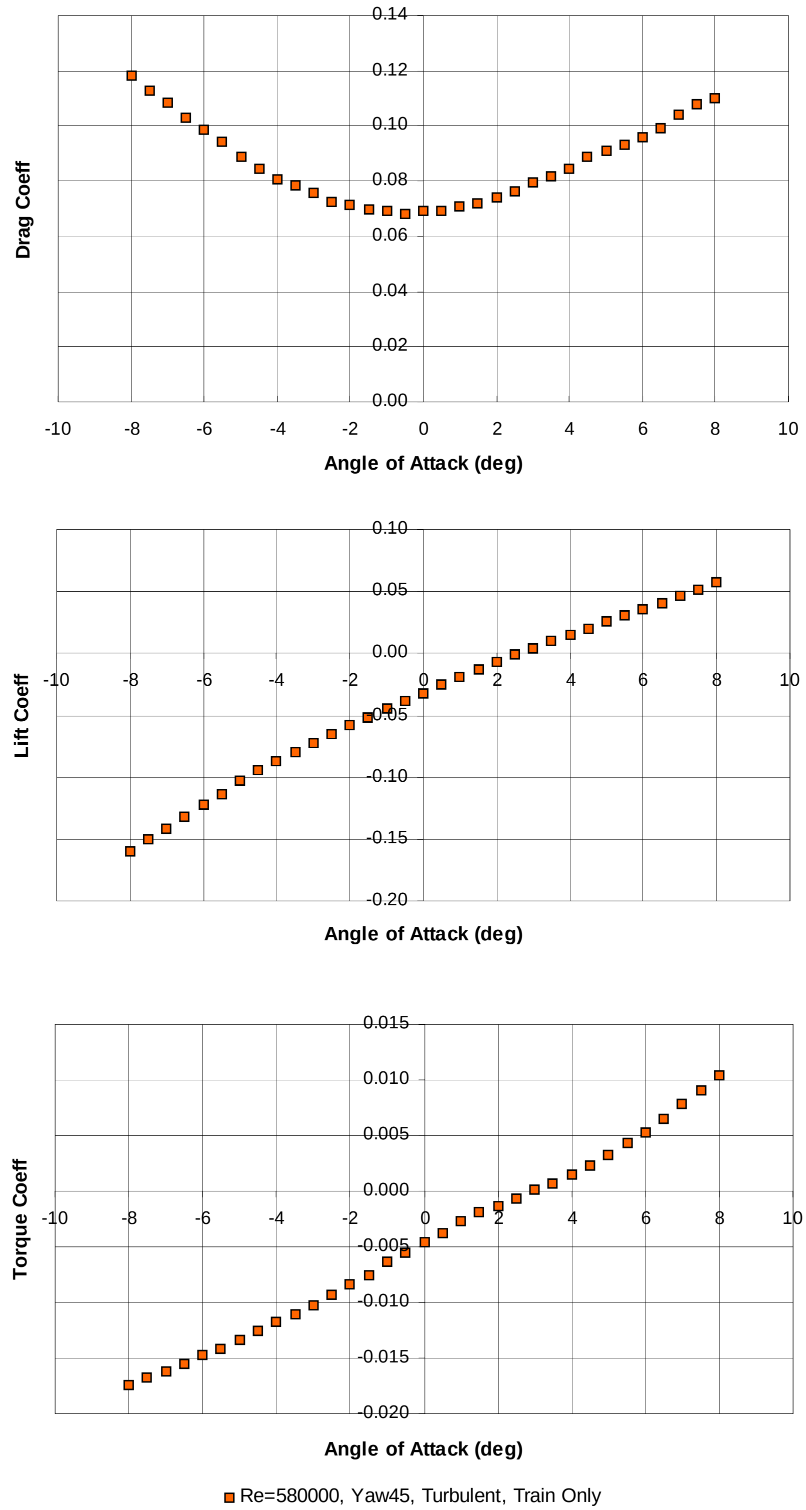

FIGURE C81 STATIC FORCE COEFFICIENTS (WIND AXIS FORCES), TURBULENT FLOW, IN-SERVICE, TRAFFIC CONDITION 3, SKEW=45^{O}

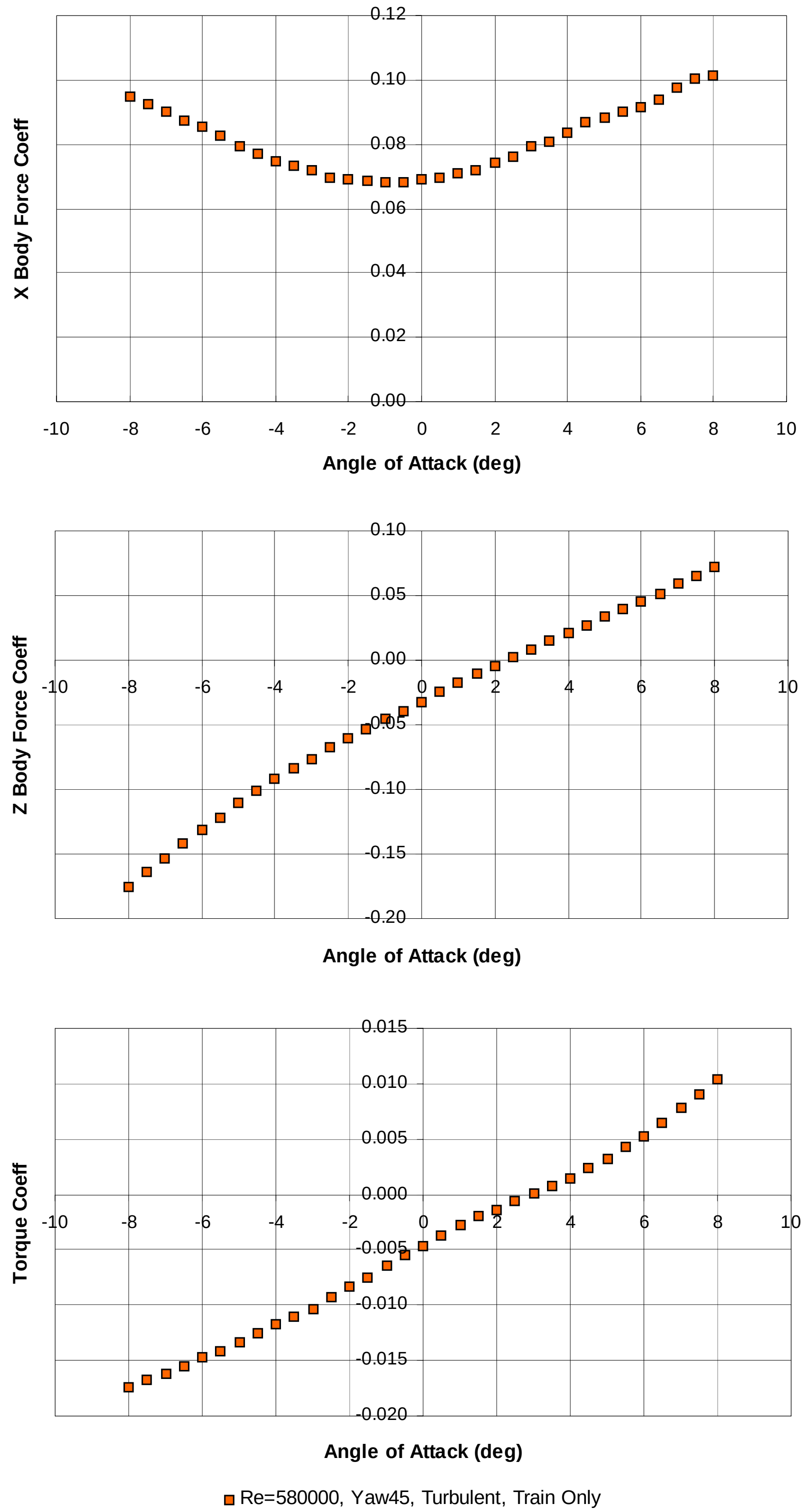

FIGURE C82 STATIC FORCE COEFFICIENTS (BODY FORCES), TURBULENT FLOW, IN-SERVICE, TRAFFIC CONDITION 3, SKEW=45^{O}

APPENDIX D

FORMULATION OF AERODYNAMIC DERIVATIVES FROM FREE OSCILLATION TESTS

Aerodynamic derivatives are defined as functions of reduced frequency by considering sinusoidal motion. They can be evaluated using the unsteady aerodynamic forces expressed as follows (King et al. 2000),

$$L = \frac{1}{2}\rho U^2 B\left(KH_1^*\dot{h}/U + KH_2^*B\dot{\alpha}/U + K^2H_3^*\alpha + K^2H_4^*h/B + KH_5^*\dot{p}/U + K^2H_6^*p/B\right) \quad \text{(D-1a)}$$

$$M = \frac{1}{2}\rho U^2 B^2\left(KA_1^*\dot{h}/U + KA_2^*B\dot{\alpha}/U + K^2A_3^*\alpha + K^2A_4^*h/B + KA_5^*\dot{p}/U + K^2A_6^*p/B\right) \quad \text{(D-1b)}$$

$$D = \frac{1}{2}\rho U^2 B\left(KP_1^*\dot{p}/U + KP_2^*B\dot{\alpha}/U + K^2P_3^*\alpha + K^2P_4^*p/B + KP_5^*\dot{h}/U + K^2P_6^*h/B\right) \quad \text{(D-1c)}$$

where h, α and p denote the lift, torsion and drag responses, L, M and D are the lift, moment and drag forces produced by the moving deck, ρ is the air density, B is the characteristic width of the bridge deck, K is a reduced frequency which equals $B\omega/U$, U is the wind speed at deck height and ω is the circular natural frequency and, H_i^*, A_i^* and P_i^*, $i = 1,\cdots,6,$ are the lift, torsion and drag aerodynamic derivatives.

By neglecting the buffeting effect, the equations of motion are:

$$m_h\left(\ddot{h} + 2\zeta_h\omega_h\dot{h} + \omega_h^2 h\right) = L \quad \text{(D-2a)}$$

$$m_\alpha\left(\ddot{\alpha} + 2\zeta_\alpha\omega_\alpha\dot{\alpha} + \omega_\alpha^2\alpha\right) = M \quad \text{(D-2b)}$$

$$m_p\left(\ddot{p} + 2\zeta_p\omega_p\dot{p} + \omega_p^2 p\right) = D \quad \text{(D-2c)}$$

where: m, ζ and ω with a sub-index (h, α or p) represent the mass, damping ratio, and the frequency of vibration of that subindex. When only the lift and torsion are considered, p and $\dot{p}$ in Equations (D-2a) and (D-2b) are set equal to zero and Equation (D-2c) is ignored.

The objective of the analysis is to use the equations of motion to identify the aerodynamic derivatives for a particular structure, given the measured oscillation (responses) from wind tunnel experiment under constant mean wind speed. This is a system identification problem and can be solved using methods such as the “Prediction-Error Identification Method” (PEM), and the “Autoregressive Model with Exogenous Input” (ARX). These methods are implemented in MATLAB and the mathematical details of these methods are given in (Söderström and Stoica. 1989, Ljung 1999). In simple terms, these methods estimate the values of the unknown parameters of the system by minimizing the differences between predicted and observed system behaviour. For example, the aerodynamic derivatives can be obtained by using the PEM that minimizes the error defined as a scale that is a function of the differences between the measured and predicted displacements of the model.

When the PEM and ARX methods are implemented in MATLAB, the equations of motion or the “system” may be described using, for example, the state-space model, the “grey” model, and the ARX model.

The state-space model requires that the equations of motion to be re-written as a system of first order differential equations. The “grey” model considers that some of the system parameters that are to be identified depend on a common set of parameters. The ARX model (Autoregressive Model with Exogenous Input) is a general time series model with external perturbation.

The implementation of state-space model and the ARX model in MATLAB for the evaluation of the aerodynamic derivatives was considered for both two- and three-degree-of freedom problem (i.e., considering only two of the equations shown in Equation (D-2) or the three equations shown in Equation (D-2)). Only the implementation for the two-degree-of-freedom problem (i.e., lift and torsion) is described in detail in the following, for simplicity of explanation and without loss of generality.

We re-write Equations (D-2a) and (D-2b) as following for the state-space model,

$$\frac{d}{dt}\mathbf{X} = \mathbf{AX} \tag{D-3}$$

where

$$\mathbf{A} = \begin{bmatrix} 0 & 0 & 1 & 0 \\ 0 & 0 & 0 & 1 \\ C_1K^2H_4^*/(Bm_h) - \omega_h^2 & C_1K^2H_3^*/m_h & C_1KH_1^*/(Um_h) - 2\zeta_h\omega_h & C_1KH_2^*B/(Um_h) \\ C_2K^2A_4^*/(Bm_\alpha) & C_2K^2A_3^*/m_\alpha - \omega_\alpha^2 & C_2KA_1^*/(Um_\alpha) & C_2KA_2^*B/(Um_\alpha) - 2\zeta_\alpha\omega_\alpha \end{bmatrix}$$

$C_1 = \frac{1}{2}\rho U^2 B$, $C_2 = \frac{1}{2}\rho U^2 B^2$, and $\mathbf{X} = [h \quad \alpha \quad \dot{h} \quad \dot{\alpha}]^T$.

The observed response will be represented by the vector $\mathbf{Y}$,

$$\mathbf{Y} = \mathbf{CX} + \mathbf{e} \tag{D-4}$$

where: $\mathbf{C} = \begin{bmatrix} 1 & 0 & 0 & 0 \\ 0 & 1 & 0 & 0 \end{bmatrix}$, $\mathbf{Y} = [y_1 \quad y_2]^T$, $y_1 = h$ represents the observed lift response, and $y_2 = \alpha$ represents the observed torsional response, and **e** is a 2x1 vector denoting the noise in the measured responses.

The use of the PEM requires the unknowns of the dynamic system to be defined. In this case the unknowns are the twelve aerodynamic derivatives H_i^* and A_i^* $i = 1,\cdots,6$. This model is implemented in MATLAB. The initial condition of the response (i.e., **X** evaluated at time equal to zero) is also considered to be unknown and to be identified.

The implemented model is tested using a set of experimental results recorded with a time interval of 0.01 seconds. First, it was considered that the elements a_{ij} of matrix **A** for i = 3, 4 and j = 1,2,3,4, are unknown, and an evaluation of the values of these elements was carried out. Comparison of the experimental results and the predicted responses obtained from Equation (D3) with the parameters a_{ij} identified previously is depicted in Figure A1. This figure shows that the fit is excellent.

The aerodynamic derivatives H_i^* and A_i^* $i = 1,\cdots,4$, can then be evaluated using the identified values of a_{ij} for i = 3, 4 and j = 1,2,3,4, given the structural characteristics of the model (frequencies and damping ratios) and the mean wind speed.

It should be noted that for the evaluation of the aerodynamic derivatives a non-zero measurement noise **e** vector must be employed. For the results shown in Figure A1, **e** is considered to be two independent identically distributed normal sequences with means of zero and standard deviations of 0.001. Numerical analysis by varying this standard deviation was carried out and the obtained results are almost identical.

The ARX model was also implemented and considered for estimating the aerodynamic derivatives to investigate whether the PEM is the best method that can be employed to identify the aerodynamic derivatives.

Equation (D-3) is re-written as an autoregressive model to implement the ARX model. This is done by noting that for a given time increment Δt, the response **X** at time i+1, $\mathbf{X}_{i+1}$, can be expressed as:

$$\mathbf{X}_{i+1} = \exp(\Delta t \times \mathbf{A})\mathbf{X}_i \quad \text{(D-5)}$$

It can be shown that this and Equation (D-4) leads to the following autoregressive model (Shinozuka et al. 1982):

$$\mathbf{Y}_i - \mathbf{F}_1\mathbf{Y}_{i-1} - \mathbf{F}_2\mathbf{Y}_{i-2} = \mathbf{e} \quad \text{(D-6)}$$

where $\mathbf{F}_1$ and $\mathbf{F}_2$ are two matrices that depend on the elements in **A**. $\mathbf{F}_1$ is defined by rows 3 and 4, and columns 1 to 2 of $\begin{bmatrix}\mathbf{C}\\\mathbf{CA}\end{bmatrix}\mathbf{A}\begin{bmatrix}\mathbf{C}\\\mathbf{CA}\end{bmatrix}^{-1}$, while $\mathbf{F}_2$ is defined by rows 3 and 4, and columns 3 to 4 of $\begin{bmatrix}\mathbf{C}\\\mathbf{CA}\end{bmatrix}\mathbf{A}\begin{bmatrix}\mathbf{C}\\\mathbf{CA}\end{bmatrix}^{-1}$.

The system identification procedure is carried out once again, using the ARX model and the identical set of experimental results used in the PEM analysis. Using the identified parameters, the predicted response is calculated and compared with the experimental results in Figure A2. Comparison of the results shown in Figure A1 and Figure A2 suggest that the fit obtained by using the system parameters identified from PEM is somewhat superior to that from the ARX model.

REFERENCES

D1. King, J. P. C., Kong, L. Z., Hirai, S. and Isyumov, N., “A Study of Wind Effects for the Bronx-Whitestone Bridge, Investigation of Aerodynamic Derivatives”, Report BLWT-SS33-2000, The University of Western Ontario, 2000.

D2. Ljung L., “System Identification - Theory for the User”, Prentice Hall, Upper Saddle River, N.J. 2nd edition, 1999.

D3. Söderström T. and P. Stoica., “System Identification”, Prentice Hall International, London. 1989.

D4. Shinozuka, M., Yun, C. and Imai, H., “Identification of Linear Structural Dynamic Theory”, Journal of Structural Engineering, ASCE, Vol. 108, No. 6, 1982.

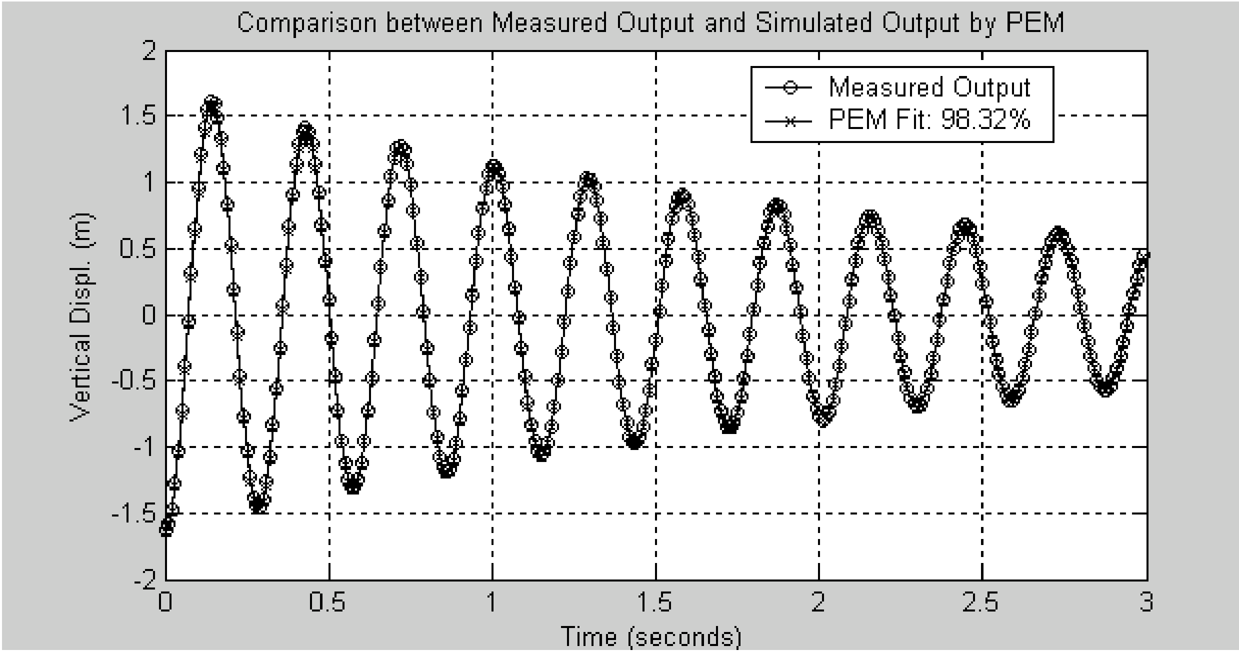

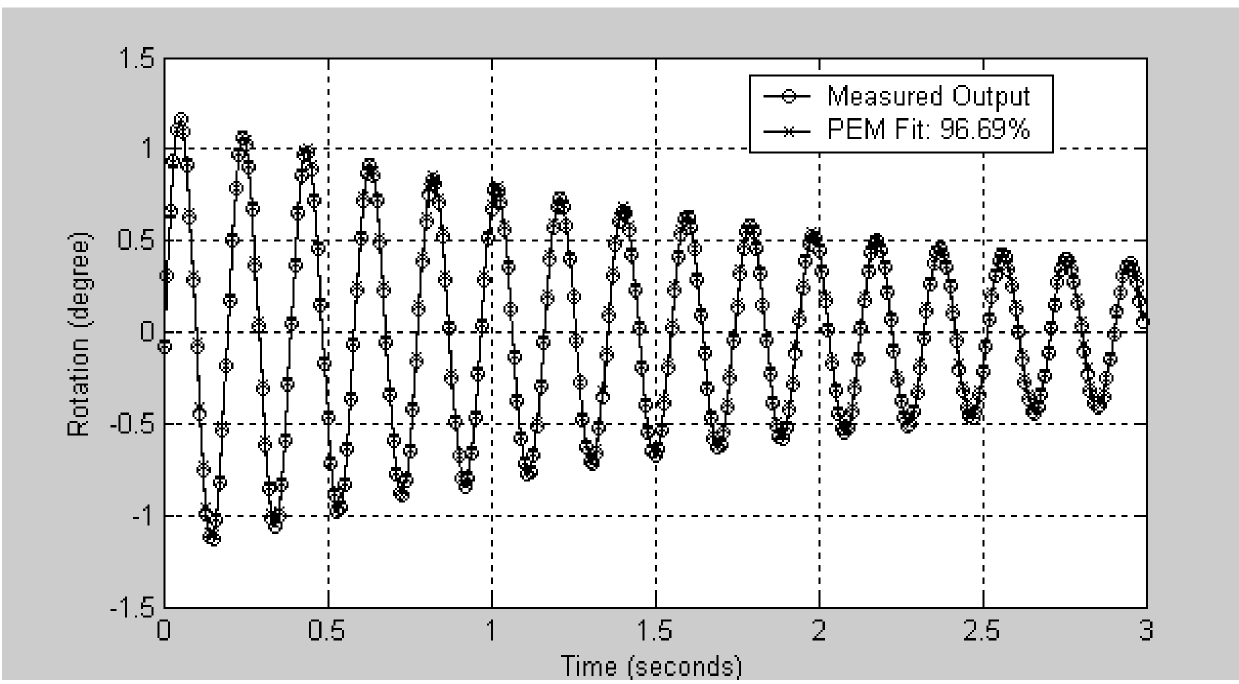

FIGURE D1 MEASURED AND SIMULATED OUTPUT USING THE PREDICTION-ERROR IDENTIFICATION METHOD (PEM)

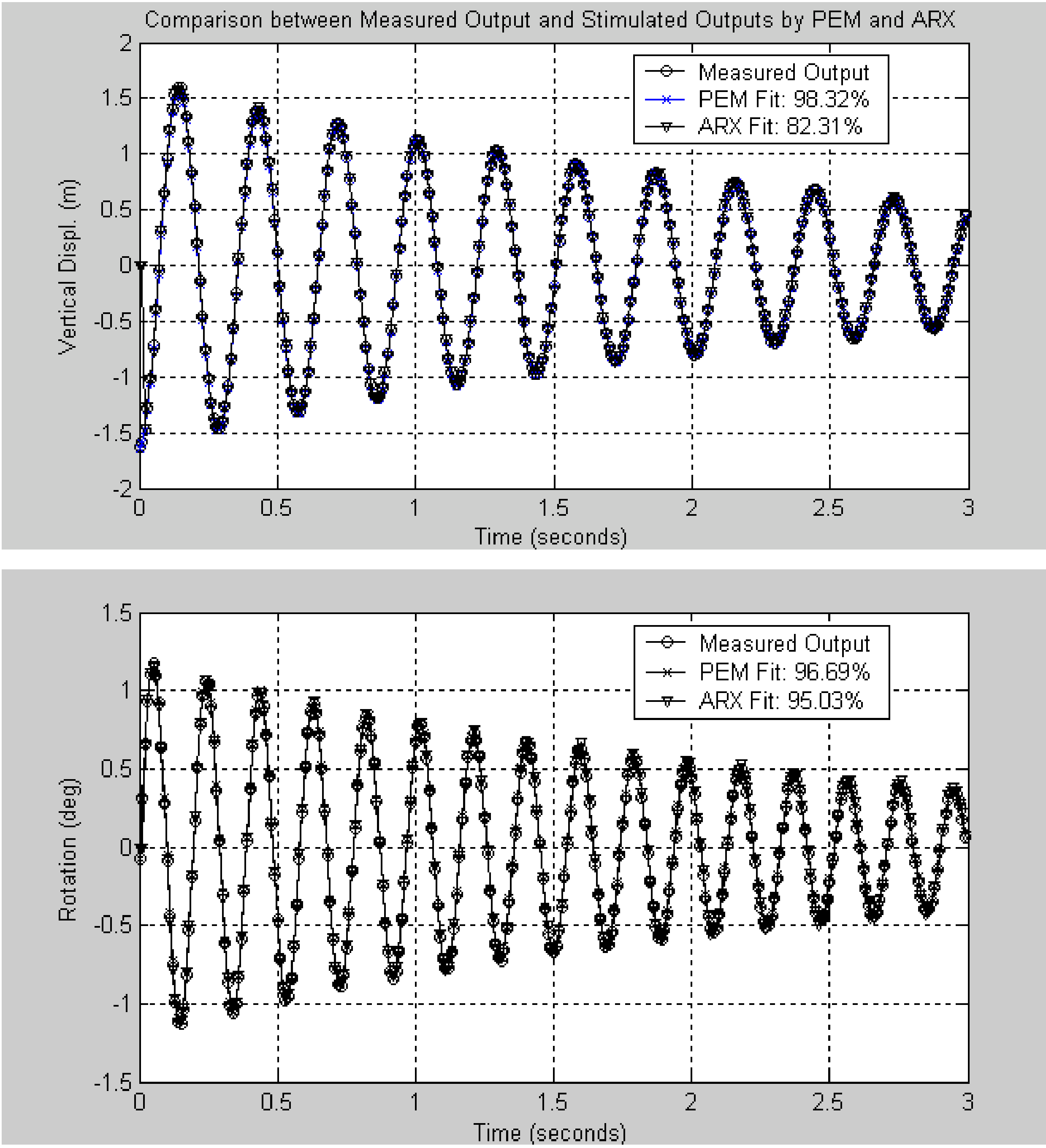

FIGURE D2 COMPARISON BETWEEN MEASURED AND SIMULATED OUTPUT USING THE PREDICTION-ERROR IDENTIFICATION METHOD (PEM) AND THE AUTO-REGRESSIVE WITH EXOGENEOUS INPUT (ARX) METHOD

APPENDIX E

AERODYNAMIC DERIVATIVES IN SdM NOTATION

TABLE E1 SUMMARY OF AERODYNAMIC DERIVATIVE TESTS

TEST GROUP	CONFIGURATION	FLOW CONDITION	ANGLE OF ATTACK	NO. OF SPEEDS	FILENAME	OTHER TEST CONDITIONS
A)	In-Service	Smooth	-6	10	A1	Yaw angle: 0 degrees; Initial Amplitude: Vertical & Lateral: 2.5 to 7.5mm Rotation: 0.5 to 1.5 deg.
			-4		A2	
			-2		A3	
			0		A4	
			2		A5	
			4		A6	
			6		A7	
B)	Construction Stage		-6		B1	
			-4		B2	
			-2		B3	
			0		B4	
			2		B5	
			4		B6	
			6		B7	

TABLE E2 AERODYNAMIC DERIVATIVES, 0 DEGREES, SMOOTH FLOW, SdM FORMAT, IN-SERVICE

	Vrh	Vra	Vrp	a1*	a2*	a3*	a4*	a5*	a6*
M072a4E01R008P002a.wttd	1.51	1.25	1.12	-0.06459	0.11132	-0.91423	-0.05580	0.11825	-0.07393
M072a4E01R008P003a.wttd	4.62	3.76	3.37	0.03636	0.10100	-0.02869	-0.09060	0.02589	-0.08210
M072a4E01R008P004a.wttd	7.79	6.36	5.65	0.09884	0.13907	0.04816	-0.10066	0.01386	-0.08839
M072a4E01R008P005a.wttd	10.93	9.10	7.93	0.10539	0.13150	0.07931	-0.08601	0.00981	-0.09220
M072a4E01R008P006a.wttd	14.08	12.07	10.18	0.10925	0.12339	0.08545	-0.07500	0.00257	-0.08869
M072a4E01R008P007a.wttd	17.14	15.14	12.48	0.11130	0.11632	0.08912	-0.06553	-0.00135	-0.08273
M072a4E01R008P008a.wttd	20.46	18.46	14.74	0.11442	0.12093	0.08417	-0.05959	-0.00529	-0.08307
M072a4E01R008P009a.wttd	23.62	22.47	16.98	0.10527	0.11019	0.07422	-0.05318	-0.01013	-0.08321
M072a4E01R008P010a.wttd	26.71	25.58	19.23	0.08988	0.11700	0.05911	-0.06276	-0.01066	-0.09161
M072a4E01R008P011a.wttd	29.47	27.86	21.49	0.06192	0.10921	0.04153	-0.08056	-0.01158	-0.10986
	Vrh	Vra	Vrp	h1*	h2*	h3*	h4*	h5*	h6*
M072a4E01R008P002a.wttd	1.51	1.25	1.12	1.86518	-0.09856	3.95708	-0.01062	-0.18555	0.02440
M072a4E01R008P003a.wttd	4.62	3.76	3.37	0.94146	-0.83003	1.81870	0.55184	0.02328	0.04469
M072a4E01R008P004a.wttd	7.79	6.36	5.65	0.28318	-1.39855	0.63958	0.63738	-0.05265	0.05832
M072a4E01R008P005a.wttd	10.93	9.10	7.93	0.15344	-1.46269	0.29499	0.68615	-0.01816	0.04648
M072a4E01R008P006a.wttd	14.08	12.07	10.18	0.11150	-1.48222	0.19280	0.72104	-0.05199	0.02355
M072a4E01R008P007a.wttd	17.14	15.14	12.48	0.12659	-1.44652	0.15115	0.76114	-0.04893	-0.01113
M072a4E01R008P008a.wttd	20.46	18.46	14.74	0.16200	-1.41291	0.14494	0.86307	-0.05393	-0.06075
M072a4E01R008P009a.wttd	23.62	22.47	16.98	0.21479	-1.38519	0.15508	0.95283	-0.04574	-0.08957
M072a4E01R008P010a.wttd	26.71	25.58	19.23	0.30294	-1.46507	0.20852	1.06029	-0.04200	-0.13028
M072a4E01R008P011a.wttd	29.47	27.86	21.49	0.51449	-1.31730	0.16761	0.53463	-0.18426	-0.36691
	Vrh	Vra	Vrp	p1*	p2*	p3*	p4*	p5*	p6*
M072a4E01R008P002a.wttd	1.51	1.25	1.12	0.23173	0.21768	-11.24009	0.05699	0.14563	0.05999
M072a4E01R008P003a.wttd	4.62	3.76	3.37	0.06784	-0.05143	-1.26721	0.12405	0.21774	0.12128
M072a4E01R008P004a.wttd	7.79	6.36	5.65	-0.04834	-0.22479	-0.57825	0.11354	0.17314	0.13282
M072a4E01R008P005a.wttd	10.93	9.10	7.93	-0.07974	-0.23982	-0.43518	0.10798	0.19433	0.14566
M072a4E01R008P006a.wttd	14.08	12.07	10.18	-0.10262	-0.22226	-0.36951	0.06795	0.18017	0.15025
M072a4E01R008P007a.wttd	17.14	15.14	12.48	-0.15681	-0.18585	-0.38109	0.03159	0.20497	0.21498
M072a4E01R008P008a.wttd	20.46	18.46	14.74	-0.22040	-0.13954	-0.41168	-0.00058	0.19654	0.30194
M072a4E01R008P009a.wttd	23.62	22.47	16.98	-0.32497	0.00461	-0.48177	-0.14878	0.21737	0.30064
M072a4E01R008P010a.wttd	26.71	25.58	19.23	-0.43693	0.20684	-0.58934	-0.33291	0.20936	0.44843
M072a4E01R008P011a.wttd	29.47	27.86	21.49	-0.60533	0.66710	-0.76071	-0.66871	0.23545	0.55600

Notes: $V_{rh}=V/(f_vB)$, $V_{ra}=V/(f_aB)$ and $V_{rp}=V/(f_pB)$,
B – deck width of 60.36m,
V – deck height wind speed,
f_v, f_a and f_p – vertical, torsional and lateral frequencies respectively

TABLE E3 AERODYNAMIC DERIVATIVES, -2 DEGREES, SMOOTH FLOW, SDM FORMAT, IN-SERVICE

	Vrh	Vra	Vrp	a1*	a2*	a3*	a4*	a5*	a6*
M072a3E01R001P002a.wttd	1.51	1.24	1.11	0.02909	0.12747	-1.11180	-0.05202	0.12534	-0.12895
M072a3E01R001P003a.wttd	3.62	2.97	2.65	-0.01235	0.12139	0.10555	-0.08360	-0.05380	-0.13079
M072a3E01R001P004a.wttd	5.71	4.66	4.15	0.01513	0.09819	-0.02607	-0.07757	0.01275	-0.13698
M072a3E01R001P005a.wttd	7.91	6.41	5.71	0.04364	0.13260	-0.00032	-0.08662	0.00475	-0.13607
M072a3E01R001P006a.wttd	10.02	8.15	7.23	0.05154	0.14785	0.00991	-0.07942	-0.00347	-0.14725
M072a3E01R001P007a.wttd	12.13	9.94	8.74	0.07127	0.15653	0.03024	-0.07790	-0.00714	-0.14658
M072a3E01R001P008a.wttd	14.28	11.81	10.25	0.06593	0.14692	0.04158	-0.06564	-0.00740	-0.14176
M072a3E01R001P009a.wttd	16.50	13.62	11.79	0.07467	0.15464	0.04399	-0.06300	-0.01175	-0.14359
M072a3E01R001P010a.wttd	18.61	15.58	13.33	0.06841	0.15594	0.04202	-0.07879	-0.00889	-0.13751
M072a3E01R001P011a.wttd	20.79	17.15	14.87	0.06082	0.15852	0.03856	-0.07601	-0.01299	-0.14143
M072a3E01R001P012a.wttd	22.74	19.20	16.37	0.04015	0.14121	0.02765	-0.07517	-0.01036	-0.13831
M072a3E01R001P013a.wttd	24.56	20.30	17.83	0.01699	0.13133	0.01122	-0.06490	-0.00591	-0.14109
	Vrh	Vra	Vrp	h1*	h2*	h3*	h4*	h5*	h6*
M072a3E01R001P002a.wttd	1.51	1.24	1.11	2.09713	0.11245	5.05569	0.04712	-0.32268	0.05018
M072a3E01R001P003a.wttd	3.62	2.97	2.65	1.55901	-0.50731	1.75681	0.41559	0.11696	0.02212
M072a3E01R001P004a.wttd	5.71	4.66	4.15	1.08250	-0.99671	1.65317	0.59481	-0.13427	0.04090
M072a3E01R001P005a.wttd	7.91	6.41	5.71	0.64038	-1.41918	1.11389	0.72466	-0.11921	0.05823
M072a3E01R001P006a.wttd	10.02	8.15	7.23	0.49810	-1.62071	0.82011	0.87879	-0.08174	0.02637
M072a3E01R001P007a.wttd	12.13	9.94	8.74	0.40265	-1.73991	0.63295	0.87573	-0.07421	0.04290
M072a3E01R001P008a.wttd	14.28	11.81	10.25	0.40603	-1.73387	0.51669	0.87994	-0.08763	0.00769
M072a3E01R001P009a.wttd	16.50	13.62	11.79	0.38509	-1.79422	0.49790	0.99574	-0.05938	-0.00971
M072a3E01R001P010a.wttd	18.61	15.58	13.33	0.40458	-1.80615	0.48063	1.08665	-0.06214	-0.05274
M072a3E01R001P011a.wttd	20.79	17.15	14.87	0.46915	-1.84964	0.51622	1.18335	-0.06745	-0.13666
M072a3E01R001P012a.wttd	22.74	19.20	16.37	0.56795	-1.82684	0.54494	1.23224	-0.10461	-0.17910
M072a3E01R001P013a.wttd	24.56	20.30	17.83	0.61048	-2.03681	0.56697	0.55107	-0.00717	0.02351
	Vrh	Vra	Vrp	p1*	p2*	p3*	p4*	p5*	p6*
M072a3E01R001P002a.wttd	1.51	1.24	1.11	-0.01589	0.11319	-7.31308	0.04968	0.05171	0.15120
M072a3E01R001P003a.wttd	3.62	2.97	2.65	-0.21351	0.05128	-1.52611	0.03614	0.03968	0.19618
M072a3E01R001P004a.wttd	5.71	4.66	4.15	-0.28958	-0.12515	-1.00212	0.07541	0.18521	0.16633
M072a3E01R001P005a.wttd	7.91	6.41	5.71	-0.31598	-0.11591	-0.83411	0.05681	0.16352	0.16500
M072a3E01R001P006a.wttd	10.02	8.15	7.23	-0.36366	-0.08954	-0.75806	0.02781	0.16904	0.17077
M072a3E01R001P007a.wttd	12.13	9.94	8.74	-0.35208	-0.05358	-0.71449	-0.00640	0.18372	0.18719
M072a3E01R001P008a.wttd	14.28	11.81	10.25	-0.36094	-0.01843	-0.66527	-0.01583	0.18903	0.20208
M072a3E01R001P009a.wttd	16.50	13.62	11.79	-0.37300	0.01601	-0.66967	-0.05142	0.18296	0.21381
M072a3E01R001P010a.wttd	18.61	15.58	13.33	-0.39631	0.05183	-0.65929	-0.08288	0.20680	0.28782
M072a3E01R001P011a.wttd	20.79	17.15	14.87	-0.42294	0.09870	-0.69660	-0.11184	0.22830	0.35108
M072a3E01R001P012a.wttd	22.74	19.20	16.37	-0.47866	0.10096	-0.71195	-0.15010	0.26531	0.37410
M072a3E01R001P013a.wttd	24.56	20.30	17.83	-0.54167	0.16921	-0.87171	-0.40595	0.29854	0.51626

Notes: $V_{rh}=V/(f_vB)$, $V_{ra}=V/(f_aB)$ and $V_{rp}=V/(f_pB)$,
B – deck width of 60.36m,
V – deck height wind speed,
f_v, f_a and f_p – vertical, torsional and lateral frequencies respectively

TABLE E4 AERODYNAMIC DERIVATIVES, -4 DEGREES, SMOOTH FLOW, SDM FORMAT, IN-SERVICE

	Vrh	Vra	Vrp	a1*	a2*	a3*	a4*	a5*	a6*
M072a2E01R001P002a.wttd	1.84	1.52	1.36	0.35544	0.41305	-1.24118	-0.07235	0.09883	-0.14027
M072a2E01R001P003a.wttd	3.93	3.26	2.89	-0.03018	0.07201	0.11256	-0.00633	-0.05100	-0.13922
M072a2E01R001P004a.wttd	6.06	4.98	4.43	-0.07956	0.01296	0.01881	-0.01258	0.00372	-0.14420
M072a2E01R001P005a.wttd	8.20	6.61	5.94	-0.05420	0.04601	-0.03933	-0.04192	0.00087	-0.14349
M072a2E01R001P006a.wttd	10.31	8.26	7.42	-0.03867	0.08317	-0.05202	-0.05159	-0.00577	-0.14973
M072a2E01R001P007a.wttd	12.43	9.99	8.98	-0.03366	0.08357	-0.04508	-0.05051	-0.00986	-0.14435
M072a2E01R001P008a.wttd	14.53	11.56	10.48	-0.02857	0.09031	-0.04452	-0.04841	-0.00905	-0.14218
M072a2E01R001P009a.wttd	16.88	13.24	12.06	-0.03265	0.08779	-0.04646	-0.05635	-0.00888	-0.14172
M072a2E01R001P010a.wttd	18.81	14.78	13.53	-0.03493	0.08794	-0.04724	-0.04658	-0.01002	-0.14186
M072a2E01R001P011a.wttd	20.78	16.19	15.12	-0.03292	0.08850	-0.04312	-0.03435	-0.00399	-0.14582
	Vrh	Vra	Vrp	h1*	h2*	h3*	h4*	h5*	h6*
M072a2E01R001P002a.wttd	1.84	1.52	1.36	1.47654	-0.62364	4.59884	0.09500	-0.58594	0.02469
M072a2E01R001P003a.wttd	3.93	3.26	2.89	1.83897	-0.29131	1.99518	0.15322	-0.12128	0.06825
M072a2E01R001P004a.wttd	6.06	4.98	4.43	1.82808	-0.62165	2.12425	0.47762	-0.20786	0.03869
M072a2E01R001P005a.wttd	8.20	6.61	5.94	1.56245	-1.04862	1.90421	0.65018	-0.18177	0.00980
M072a2E01R001P006a.wttd	10.31	8.26	7.42	1.31316	-1.45655	1.68052	0.85950	-0.13996	0.00455
M072a2E01R001P007a.wttd	12.43	9.99	8.98	1.21234	-1.64072	1.47895	0.97403	-0.13856	-0.04121
M072a2E01R001P008a.wttd	14.53	11.56	10.48	1.13219	-1.82100	1.40426	1.02496	-0.14666	-0.04199
M072a2E01R001P009a.wttd	16.88	13.24	12.06	1.15496	-1.90542	1.37264	1.21486	-0.14494	-0.07011
M072a2E01R001P010a.wttd	18.81	14.78	13.53	1.17442	-2.01257	1.35690	1.27088	-0.12442	-0.10586
M072a2E01R001P011a.wttd	20.78	16.19	15.12	1.24628	-1.91416	1.32496	0.66170	-0.02932	-0.09602
	Vrh	Vra	Vrp	p1*	p2*	p3*	p4*	p5*	p6*
M072a2E01R001P002a.wttd	1.84	1.52	1.36	-0.33701	0.07732	-6.89433	0.01044	0.32217	0.05949
M072a2E01R001P003a.wttd	3.93	3.26	2.89	-0.57713	-0.04580	-1.75358	0.07732	0.18620	0.11395
M072a2E01R001P004a.wttd	6.06	4.98	4.43	-0.75276	-0.18018	-1.44351	0.04261	0.27350	0.09143
M072a2E01R001P005a.wttd	8.20	6.61	5.94	-0.70209	-0.09506	-1.37516	0.00646	0.27327	0.09258
M072a2E01R001P006a.wttd	10.31	8.26	7.42	-0.69705	0.04097	-1.32129	-0.05354	0.27566	0.08708
M072a2E01R001P007a.wttd	12.43	9.99	8.98	-0.68875	0.11385	-1.24562	-0.10684	0.27127	0.13098
M072a2E01R001P008a.wttd	14.53	11.56	10.48	-0.66218	0.20062	-1.23150	-0.14829	0.28402	0.15295
M072a2E01R001P009a.wttd	16.88	13.24	12.06	-0.68964	0.20296	-1.21276	-0.18769	0.29790	0.24288
M072a2E01R001P010a.wttd	18.81	14.78	13.53	-0.69933	0.26869	-1.22475	-0.23786	0.29825	0.31643
M072a2E01R001P011a.wttd	20.78	16.19	15.12	-0.68281	0.37166	-1.23727	-0.37606	0.36007	0.43473

Notes: $V_{rh}=V/(f_vB)$, $V_{ra}=V/(f_aB)$ and $V_{rp}=V/(f_pB)$,
B – deck width of 60.36m,
V – deck height wind speed,
f_v, f_a and f_p – vertical, torsional and lateral frequencies respectively

TABLE E5 AERODYNAMIC DERIVATIVES, -6 DEGREES, SMOOTH FLOW, SDM FORMAT, IN-SERVICE

	Vrh	Vra	Vrp	a1*	a2*	a3*	a4*	a5*	a6*
M072a1E01R001P002a.wttd	1.71	1.37	1.26	-0.16397	0.19251	-1.56757	-0.12280	0.26131	-0.12093
M072a1E01R001P003a.wttd	3.55	2.91	2.62	0.00818	0.11029	0.27427	0.02672	-0.05418	-0.14276
M072a1E01R001P004a.wttd	5.38	4.47	4.00	-0.11512	-0.01098	0.09592	0.04544	-0.00003	-0.15761
M072a1E01R001P005a.wttd	7.37	5.98	5.39	-0.08998	-0.00482	-0.01029	0.01424	0.02447	-0.15017
M072a1E01R001P006a.wttd	9.47	7.45	6.80	-0.06441	0.03388	-0.02443	-0.02172	0.02276	-0.14603
M072a1E01R001P007a.wttd	11.31	8.98	8.17	-0.03205	0.08578	-0.02240	-0.04525	0.01299	-0.14985
M072a1E01R001P008a.wttd	13.26	10.52	9.55	-0.01460	0.09400	-0.01153	-0.05493	0.01424	-0.14512
M072a1E01R001P009a.wttd	15.21	12.38	10.96	-0.00529	0.09238	0.00282	-0.04280	0.00703	-0.14739
M072a1E01R001P010a.wttd	17.35	13.94	12.35	0.00971	0.10586	0.01575	-0.05482	0.00020	-0.14350
M072a1E01R001P011a.wttd	18.68	15.45	13.86	0.01938	0.09742	0.02655	-0.04749	-0.00230	-0.13938
	Vrh	Vra	Vrp	h1*	h2*	h3*	h4*	h5*	h6*
M072a1E01R001P002a.wttd	1.71	1.37	1.26	2.27972	0.03086	5.90521	0.23067	-0.87632	0.02237
M072a1E01R001P003a.wttd	3.55	2.91	2.62	2.06210	-0.13704	1.84540	-0.08641	-0.03235	0.05732
M072a1E01R001P004a.wttd	5.38	4.47	4.00	2.53842	-0.10139	2.51408	0.12081	-0.34866	0.10798
M072a1E01R001P005a.wttd	7.37	5.98	5.39	2.35424	-0.58993	2.72733	0.44165	-0.38281	0.01674
M072a1E01R001P006a.wttd	9.47	7.45	6.80	2.00509	-1.06585	2.49632	0.68825	-0.31239	-0.04100
M072a1E01R001P007a.wttd	11.31	8.98	8.17	1.92495	-1.48454	2.21535	0.91718	-0.34150	-0.06225
M072a1E01R001P008a.wttd	13.26	10.52	9.55	1.77448	-1.63083	2.06524	1.01191	-0.30581	-0.07173
M072a1E01R001P009a.wttd	15.21	12.38	10.96	1.66967	-1.74299	1.76504	1.07200	-0.30278	-0.11711
M072a1E01R001P010a.wttd	17.35	13.94	12.35	1.61487	-1.96064	1.70638	1.19124	-0.29892	-0.12319
M072a1E01R001P011a.wttd	18.68	15.45	13.86	1.55890	-1.92502	1.49736	0.59085	-0.23038	0.02519
	Vrh	Vra	Vrp	p1*	p2*	p3*	p4*	p5*	p6*
M072a1E01R001P002a.wttd	1.71	1.37	1.26	-0.89912	0.02498	-7.50746	0.03167	0.05117	0.10043
M072a1E01R001P003a.wttd	3.55	2.91	2.62	-0.58436	0.13642	-2.27860	0.09155	-0.00575	0.15029
M072a1E01R001P004a.wttd	5.38	4.47	4.00	-0.97003	-0.23000	-1.72982	0.12789	0.18342	0.06571
M072a1E01R001P005a.wttd	7.37	5.98	5.39	-0.97009	-0.15189	-1.80611	0.04974	0.28549	0.09458
M072a1E01R001P006a.wttd	9.47	7.45	6.80	-0.87140	0.03368	-1.71498	-0.04130	0.31206	0.13486
M072a1E01R001P007a.wttd	11.31	8.98	8.17	-0.86502	0.27758	-1.63035	-0.12606	0.33146	0.10226
M072a1E01R001P008a.wttd	13.26	10.52	9.55	-0.80451	0.35215	-1.52835	-0.18197	0.34708	0.16732
M072a1E01R001P009a.wttd	15.21	12.38	10.96	-0.77211	0.43380	-1.35641	-0.22222	0.35640	0.23473
M072a1E01R001P010a.wttd	17.35	13.94	12.35	-0.75509	0.58797	-1.34716	-0.31188	0.36967	0.29587
M072a1E01R001P011a.wttd	18.68	15.45	13.86	-0.77059	0.72441	-1.34213	-0.48834	0.45781	0.49970

Notes: $V_{rh}=V/(f_v B)$, $V_{ra}=V/(f_a B)$ and $V_{rp}=V/(f_p B)$,
B – deck width of 60.36m,
V – deck height wind speed,
f_v, f_a and f_p – vertical, torsional and lateral frequencies respectively

TABLE E6 AERODYNAMIC DERIVATIVES, +2 DEGREES, SMOOTH FLOW, SDM FORMAT, IN-SERVICE

	Vrh	Vra	Vrp	a1*	a2*	a3*	a4*	a5*	a6*
M072a5E01R001P002a.wttd	2.74	2.24	2.02	-0.17223	0.17825	-0.54567	-0.08315	0.12933	-0.12189
M072a5E01R001P003a.wttd	5.68	4.57	4.14	0.02813	0.18594	-0.12379	-0.09130	0.07155	-0.12347
M072a5E01R001P004a.wttd	8.72	7.05	6.31	0.06422	0.16611	-0.01212	-0.09115	0.05639	-0.12655
M072a5E01R001P005a.wttd	11.69	9.60	8.48	0.07796	0.15146	0.04148	-0.08703	0.04336	-0.12470
M072a5E01R001P006a.wttd	14.59	12.30	10.60	0.09050	0.15037	0.06317	-0.08538	0.02308	-0.12340
M072a5E01R001P007a.wttd	17.66	15.12	12.77	0.09318	0.14003	0.07299	-0.07765	0.00787	-0.12402
M072a5E01R001P008a.wttd	20.67	18.73	14.85	0.10176	0.12224	0.07519	-0.06781	0.00723	-0.10886
M072a5E01R001P009a.wttd	23.59	22.63	17.10	0.11609	0.12239	0.07846	-0.05041	-0.00265	-0.10291
M072a5E01R001P010a.wttd	26.15	28.91	19.12	0.13163	0.10341	0.07110	-0.02702	-0.01759	-0.11886
M072a5E01R001P011a.wttd	29.08	35.43	21.25	0.12842	0.09455	0.05718	-0.03753	-0.01152	-0.14562
	Vrh	Vra	Vrp	h1*	h2*	h3*	h4*	h5*	h6*
M072a5E01R001P002a.wttd	2.74	2.24	2.02	1.77638	-0.14046	2.66560	0.21724	-0.09015	0.08199
M072a5E01R001P003a.wttd	5.68	4.57	4.14	0.55609	-1.18576	1.37971	0.60123	-0.01918	0.09808
M072a5E01R001P004a.wttd	8.72	7.05	6.31	0.17491	-1.47195	0.54309	0.66024	-0.03884	0.10756
M072a5E01R001P005a.wttd	11.69	9.60	8.48	0.11934	-1.45410	0.31449	0.65782	-0.11305	0.05900
M072a5E01R001P006a.wttd	14.59	12.30	10.60	0.10393	-1.43340	0.20178	0.64330	-0.11116	0.03681
M072a5E01R001P007a.wttd	17.66	15.12	12.77	0.09674	-1.40499	0.14147	0.67004	-0.07914	0.02089
M072a5E01R001P008a.wttd	20.67	18.73	14.85	0.10040	-1.30124	0.10046	0.69907	-0.10848	0.04733
M072a5E01R001P009a.wttd	23.59	22.63	17.10	0.11080	-1.22098	0.08117	0.72581	-0.09687	-0.03051
M072a5E01R001P010a.wttd	26.15	28.91	19.12	0.14332	-1.03323	0.06281	0.73880	-0.07734	-0.09738
M072a5E01R001P011a.wttd	29.08	35.43	21.25	0.19255	-0.94390	0.05869	0.76388	-0.08673	-0.19274
	Vrh	Vra	Vrp	p1*	p2*	p3*	p4*	p5*	p6*
M072a5E01R001P002a.wttd	2.74	2.24	2.02	0.37403	0.14749	-2.25343	0.04892	0.35050	0.11907
M072a5E01R001P003a.wttd	5.68	4.57	4.14	0.32816	-0.03510	-0.16477	0.10487	0.30379	0.15266
M072a5E01R001P004a.wttd	8.72	7.05	6.31	0.26871	-0.17833	0.07553	0.11390	0.27153	0.15367
M072a5E01R001P005a.wttd	11.69	9.60	8.48	0.23422	-0.19516	0.12648	0.10925	0.21219	0.15364
M072a5E01R001P006a.wttd	14.59	12.30	10.60	0.22407	-0.22369	0.15464	0.10302	0.20775	0.13132
M072a5E01R001P007a.wttd	17.66	15.12	12.77	0.19385	-0.23740	0.12972	0.10681	0.19881	0.08138
M072a5E01R001P008a.wttd	20.67	18.73	14.85	0.15411	-0.21973	0.06779	0.08873	0.21709	0.17257
M072a5E01R001P009a.wttd	23.59	22.63	17.10	0.10098	-0.18603	0.00343	0.04797	0.21674	0.27458
M072a5E01R001P010a.wttd	26.15	28.91	19.12	0.01111	-0.11983	-0.06629	-0.07386	0.20663	0.19554
M072a5E01R001P011a.wttd	29.08	35.43	21.25	-0.07657	-0.08785	-0.10082	-0.14982	0.19184	0.49258

Notes: $V_{rh}=V/(f_vB)$, $V_{ra}=V/(f_aB)$ and $V_{rp}=V/(f_pB)$,
B – deck width of 60.36m,
V – deck height wind speed,
f_v, f_a and f_p – vertical, torsional and lateral frequencies respectively

TABLE E7 AERODYNAMIC DERIVATIVES, +4 DEGREES, SMOOTH FLOW, SDM FORMAT, IN-SERVICE

	Vrh	Vra	Vrp	a1*	a2*	a3*	a4*	a5*	a6*
M072a6E01R001P002a.wttd	2.74	2.27	2.03	-0.01434	0.13990	-0.31159	-0.08345	0.12894	-0.10601
M072a6E01R001P003a.wttd	5.67	4.68	4.20	0.20062	0.44906	-0.07298	-0.22433	0.10687	-0.07200
M072a6E01R001P004a.wttd	8.75	7.13	6.37	0.05950	0.17979	-0.02802	-0.05005	0.08222	-0.09004
M072a6E01R001P005a.wttd	11.74	9.57	8.55	0.00603	0.19220	-0.02454	-0.08813	-0.12137	-0.05586
M072a6E01R001P006a.wttd	14.73	12.16	10.73	0.03348	0.16454	-0.00056	-0.08822	-0.01565	-0.11678
M072a6E01R001P007a.wttd	17.77	14.95	12.91	0.05437	0.16399	0.02776	-0.10274	0.00852	-0.11892
M072a6E01R001P008a.wttd	20.71	18.36	14.99	0.07509	0.16742	0.05621	-0.07851	0.00864	-0.11529
M072a6E01R001P009a.wttd	23.72	22.10	17.28	0.09255	0.16289	0.06505	-0.06182	0.00977	-0.11703
M072a6E01R001P010a.wttd	26.15	28.06	19.24	0.11548	0.16265	0.06145	-0.05671	0.00839	-0.12263
M072a6E01R001P011a.wttd	29.53	28.91	21.33	0.12654	0.19637	0.07639	-0.05115	0.00966	-0.11384
	Vrh	Vra	Vrp	h1*	h2*	h3*	h4*	h5*	h6*
M072a6E01R001P002a.wttd	2.74	2.27	2.03	1.64475	-0.01544	2.41414	0.05466	0.01156	0.13062
M072a6E01R001P003a.wttd	5.67	4.68	4.20	1.06522	-0.39945	1.08722	0.03434	0.22940	0.06699
M072a6E01R001P004a.wttd	8.75	7.13	6.37	0.65041	-1.15528	0.67051	0.48628	0.27178	-0.07848
M072a6E01R001P005a.wttd	11.74	9.57	8.55	0.35858	-1.52173	0.54592	0.65871	0.08895	0.09676
M072a6E01R001P006a.wttd	14.73	12.16	10.73	0.33443	-1.49906	0.46712	0.71047	-0.03683	0.12802
M072a6E01R001P007a.wttd	17.77	14.95	12.91	0.42600	-1.35946	0.45222	0.69627	-0.05216	0.11424
M072a6E01R001P008a.wttd	20.71	18.36	14.99	0.48907	-1.21894	0.41865	0.58885	-0.05343	0.05195
M072a6E01R001P009a.wttd	23.72	22.10	17.28	0.55560	-1.02114	0.40613	0.46892	-0.09979	0.05219
M072a6E01R001P010a.wttd	26.15	28.06	19.24	0.59341	-0.83898	0.33410	0.43819	-0.10594	0.01672
M072a6E01R001P011a.wttd	29.53	28.91	21.33	0.59779	-0.87325	0.41176	0.40001	-0.11225	-0.03444
	Vrh	Vra	Vrp	p1*	p2*	p3*	p4*	p5*	p6*
M072a6E01R001P002a.wttd	2.74	2.27	2.03	0.84372	0.12188	-0.88743	0.06874	0.46777	0.13446
M072a6E01R001P003a.wttd	5.67	4.68	4.20	0.67148	-0.35347	0.60279	0.18093	0.40924	0.10695
M072a6E01R001P004a.wttd	8.75	7.13	6.37	0.70695	-0.37976	0.78646	0.17189	0.28892	0.06592
M072a6E01R001P005a.wttd	11.74	9.57	8.55	0.74916	-0.40822	0.89206	0.22489	0.30324	0.16133
M072a6E01R001P006a.wttd	14.73	12.16	10.73	0.70428	-0.45280	0.83817	0.27058	0.27526	0.26573
M072a6E01R001P007a.wttd	17.77	14.95	12.91	0.66162	-0.54675	0.74983	0.27060	0.29357	0.27531
M072a6E01R001P008a.wttd	20.71	18.36	14.99	0.62538	-0.55495	0.63876	0.24583	0.28057	0.34393
M072a6E01R001P009a.wttd	23.72	22.10	17.28	0.61607	-0.53784	0.57138	0.22353	0.24670	0.36086
M072a6E01R001P010a.wttd	26.15	28.06	19.24	0.63440	-0.52423	0.46894	0.25377	0.22749	0.35930
M072a6E01R001P011a.wttd	29.53	28.91	21.33	0.61370	-0.61640	0.56176	0.24377	0.25424	0.43556

Notes: $V_{rh}=V/(f_v B)$, $V_{ra}=V/(f_a B)$ and $V_{rp}=V/(f_p B)$,
B – deck width of 60.36m,
V – deck height wind speed,
f_v, f_a and f_p – vertical, torsional and lateral frequencies respectively

TABLE E8 AERODYNAMIC DERIVATIVES, +6 DEGREES, SMOOTH FLOW, SDM FORMAT, IN-SERVICE

	Vrh	Vra	Vrp	a1*	a2*	a3*	a4*	a5*	a6*
M072a7E01R001P002a.wttd	2.76	2.30	2.05	0.06826	0.10675	-0.11968	-0.04076	0.22689	-0.13708
M072a7E01R001P003a.wttd	5.72	4.75	4.20	0.15625	0.22023	0.04070	-0.06816	0.13852	-0.09954
M072a7E01R001P004a.wttd	8.66	7.38	6.42	0.27487	0.37263	0.16307	-0.08660	0.11007	-0.06217
M072a7E01R001P005a.wttd	11.62	9.64	8.58	0.16030	0.19442	0.06056	-0.00959	0.10782	-0.23981
M072a7E01R001P006a.wttd	14.70	12.32	10.73	0.06803	0.17616	0.04932	-0.07825	0.00307	-0.12093
M072a7E01R001P007a.wttd	17.78	15.39	12.96	0.08081	0.18130	0.05867	-0.09095	0.01444	-0.11604
M072a7E01R001P008a.wttd	20.76	18.76	15.12	0.10624	0.19779	0.07512	-0.08683	0.01789	-0.11647
M072a7E01R001P009a.wttd	23.63	23.20	17.31	0.11684	0.17405	0.07787	-0.05754	0.02002	-0.11254
M072a7E01R001P010a.wttd	26.11	25.64	19.31	0.10806	0.05081	0.03918	0.04702	0.03683	-0.07916
M072a7E01R001P011a.wttd	Malfunction Instrumentation								
	Vrh	Vra	Vrp	h1*	h2*	h3*	h4*	h5*	h6*
M072a7E01R001P002a.wttd	2.76	2.30	2.05	1.41170	-0.05417	2.12103	0.03780	0.01365	0.14678
M072a7E01R001P003a.wttd	5.72	4.75	4.20	1.25046	-0.54608	1.53972	0.23097	0.35248	0.08254
M072a7E01R001P004a.wttd	8.66	7.38	6.42	1.37456	-0.38033	1.22016	0.17973	0.34397	0.21760
M072a7E01R001P005a.wttd	11.62	9.64	8.58	0.93022	-0.57528	0.39418	-0.03996	0.50700	-0.10188
M072a7E01R001P006a.wttd	14.70	12.32	10.73	0.58505	-1.08690	0.55177	0.47221	-0.02956	0.15455
M072a7E01R001P007a.wttd	17.78	15.39	12.96	0.57953	-1.11254	0.49883	0.55791	-0.01064	0.11075
M072a7E01R001P008a.wttd	20.76	18.76	15.12	0.56807	-1.16240	0.45007	0.61312	0.00081	0.07385
M072a7E01R001P009a.wttd	23.63	23.20	17.31	0.55069	-1.07978	0.35726	0.58216	-0.01713	0.05488
M072a7E01R001P010a.wttd	26.11	25.64	19.31	0.09772	-1.27305	0.39236	0.39483	0.04936	-0.00036
M072a7E01R001P011a.wttd	Malfunction Instrumentation								
	Vrh	Vra	Vrp	p1*	p2*	p3*	p4*	p5*	p6*
M072a7E01R001P002a.wttd	2.76	2.30	2.05	0.97779	0.09670	-0.71012	0.08439	0.31370	0.19426
M072a7E01R001P003a.wttd	5.72	4.75	4.20	0.83319	-0.24199	0.85413	0.16794	0.37759	0.13207
M072a7E01R001P004a.wttd	8.66	7.38	6.42	0.65707	-0.57666	0.77675	0.21723	0.41617	0.11881
M072a7E01R001P005a.wttd	11.62	9.64	8.58	0.58481	-0.63599	0.64749	0.10940	0.55812	0.11234
M072a7E01R001P006a.wttd	14.70	12.32	10.73	0.78139	-0.65015	0.90251	0.26601	0.41365	0.19555
M072a7E01R001P007a.wttd	17.78	15.39	12.96	0.76190	-0.64105	0.81468	0.27349	0.34864	0.32207
M072a7E01R001P008a.wttd	20.76	18.76	15.12	0.72451	-0.70142	0.72793	0.27715	0.35125	0.38183
M072a7E01R001P009a.wttd	23.63	23.20	17.31	0.67240	-0.71723	0.58682	0.20218	0.32505	0.43544
M072a7E01R001P010a.wttd	26.11	25.64	19.31	0.39394	-0.99311	0.56408	-0.84804	0.34083	0.56307
M072a7E01R001P011a.wttd	Malfunction Instrumentation								

Notes: $V_{rh}=V/(f_v B)$, $V_{ra}=V/(f_a B)$ and $V_{rp}=V/(f_p B)$,
B – deck width of 60.36m,
V – deck height wind speed,
f_v, f_a and f_p – vertical, torsional and lateral frequencies respectively

TABLE E9 AERODYNAMIC DERIVATIVES, 0 DEGREES, SMOOTH FLOW, SDM FORMAT, CONSTRUCTION STAGE

	Vrh	Vra	Vrp	a1*	a2*	a3*	a4*	a5*	a6*
M072b4E01R001P002a.wttd	1.30	1.09	0.96	-0.02466	0.11493	-0.32907	-0.03204	0.11797	-0.13334
M072b4E01R001P003a.wttd	2.76	2.32	2.05	0.24077	0.27107	0.01334	-0.07599	0.15140	-0.14404
M072b4E01R001P004a.wttd	4.23	3.58	3.12	0.34215	0.29275	0.21068	-0.08308	0.07977	-0.14571
M072b4E01R001P005a.wttd	5.64	4.83	4.18	0.30828	0.25192	0.22785	-0.07655	0.02975	-0.15344
M072b4E01R001P006a.wttd	7.19	6.21	5.28	0.29843	0.23001	0.24847	-0.06309	0.02433	-0.14852
M072b4E01R001P007a.wttd	8.59	7.60	6.37	0.27466	0.18789	0.24846	-0.04916	0.02705	-0.13350
M072b4E01R001P008a.wttd	9.92	9.13	7.45	0.28853	0.17101	0.24328	-0.03673	0.00820	-0.13406
M072b4E01R001P009a.wttd	11.41	10.76	8.54	0.23826	0.12713	0.21724	-0.02881	0.00220	-0.17778
M072b4E01R001P010a.wttd	Malfunction Instrumentation								
M072b4E01R002P002a.wttd	14.24	13.89	10.49	0.28197	0.16753	0.20791	-0.04176	0.00569	-0.13414
	Vrh	Vra	Vrp	h1*	h2*	h3*	h4*	h5*	h6*
M072b4E01R001P002a.wttd	1.30	1.09	0.96	2.48713	-0.04769	3.58177	0.00504	-0.04487	0.08098
M072b4E01R001P003a.wttd	2.76	2.32	2.05	2.00251	-0.37551	2.63663	0.05722	-0.02026	0.08173
M072b4E01R001P004a.wttd	4.23	3.58	3.12	1.95239	-0.46952	2.15598	0.05013	-0.06545	0.07915
M072b4E01R001P005a.wttd	5.64	4.83	4.18	1.86458	-0.50138	1.91510	0.00731	-0.06300	0.02987
M072b4E01R001P006a.wttd	7.19	6.21	5.28	1.86740	-0.49865	1.83368	0.00352	-0.07877	0.02357
M072b4E01R001P007a.wttd	8.59	7.60	6.37	1.86175	-0.52995	1.76840	0.02402	-0.01058	0.07590
M072b4E01R001P008a.wttd	9.92	9.13	7.45	1.82865	-0.57402	1.65350	0.07246	-0.07949	0.03967
M072b4E01R001P009a.wttd	11.41	10.76	8.54	1.61815	-0.70496	1.52078	0.14792	-0.32660	-0.14612
M072b4E01R001P010a.wttd	Malfunction Instrumentation								
M072b4E01R002P002a.wttd	14.24	13.89	10.49	1.99975	-0.45392	1.49549	-0.00485	-0.13495	0.02969
	Vrh	Vra	Vrp	p1*	p2*	p3*	p4*	p5*	p6*
M072b4E01R001P002a.wttd	1.30	1.09	0.96	-0.01444	0.05565	-12.13907	0.06789	0.01289	0.09943
M072b4E01R001P003a.wttd	2.76	2.32	2.05	0.01455	0.00880	-2.63260	0.07317	0.09050	0.09386
M072b4E01R001P004a.wttd	4.23	3.58	3.12	0.05533	0.03784	-1.11057	0.05315	0.06096	0.09470
M072b4E01R001P005a.wttd	5.64	4.83	4.18	0.11461	0.07029	-0.56936	0.03590	0.07450	0.09124
M072b4E01R001P006a.wttd	7.19	6.21	5.28	0.11217	0.04990	-0.30533	0.03905	0.08977	0.08389
M072b4E01R001P007a.wttd	8.59	7.60	6.37	0.15754	0.05806	-0.15694	0.03866	0.11093	0.09703
M072b4E01R001P008a.wttd	9.92	9.13	7.45	0.18571	0.09028	-0.08250	0.01671	0.10800	0.09703
M072b4E01R001P009a.wttd	11.41	10.76	8.54	0.17506	0.06276	-0.02796	0.03155	0.08792	0.08153
M072b4E01R001P010a.wttd	Malfunction Instrumentation								
M072b4E01R002P002a.wttd	14.24	13.89	10.49	0.12879	0.16953	-0.06031	-0.03892	0.09174	0.14027

Notes: $V_{rh}=V/(f_vB)$, $V_{ra}=V/(f_aB)$ and $V_{rp}=V/(f_pB)$,
B – deck width of 60.36m,
V – deck height wind speed,
f_v, f_a and f_p – vertical, torsional and lateral frequencies respectively

TABLE E10 AERODYNAMIC DERIVATIVES, -2 DEGREES, SMOOTH FLOW, SDM FORMAT, CONSTRUCTION STAGE

	Vrh	Vra	Vrp	a1*	a2*	a3*	a4*	a5*	a6*
M072b3E01R001P002a.wttd	1.25	1.04	0.92	0.00941	0.10654	-0.67494	-0.04896	0.19446	-0.14258
M072b3E01R001P003a.wttd	2.72	2.29	2.02	0.17067	0.18682	-0.01086	-0.05132	0.12760	-0.14842
M072b3E01R001P004a.wttd	4.13	3.50	3.06	0.21526	0.22619	0.13199	-0.06682	0.09447	-0.14820
M072b3E01R001P005a.wttd	5.62	4.79	4.14	0.23688	0.22173	0.19335	-0.07222	0.04610	-0.14768
M072b3E01R001P006a.wttd	7.05	6.13	5.24	0.23380	0.19910	0.20394	-0.06265	0.01370	-0.14319
M072b3E01R001P007a.wttd	8.53	7.51	6.32	0.23415	0.17862	0.21415	-0.03319	0.02846	-0.14267
M072b3E01R001P008a.wttd	10.04	8.95	7.40	0.24661	0.17282	0.20910	-0.04048	0.02041	-0.14245
M072b3E01R001P009a.wttd	11.43	10.47	8.48	0.25231	0.16471	0.20242	-0.04517	-0.01869	-0.15626
M072b3E01R002P002a.wttd	12.74	11.65	9.44	0.22032	0.05547	0.20158	0.01668	-0.02358	-0.15117
M072b3E01R003P002a.wttd	12.80	11.70	9.48	0.25789	0.17558	0.20786	-0.04701	-0.01038	-0.13631
	Vrh	Vra	Vrp	h1*	h2*	h3*	h4*	h5*	h6*
M072b3E01R001P002a.wttd	1.25	1.04	0.92	2.30118	-0.06702	3.34950	-0.00233	-0.25812	0.06290
M072b3E01R001P003a.wttd	2.72	2.29	2.02	1.95863	-0.25373	2.52640	-0.02746	-0.15131	0.07399
M072b3E01R001P004a.wttd	4.13	3.50	3.06	2.11119	-0.25956	2.44992	-0.06353	-0.15904	0.09062
M072b3E01R001P005a.wttd	5.62	4.79	4.14	2.10081	-0.31736	2.34422	-0.07537	-0.19279	0.09338
M072b3E01R001P006a.wttd	7.05	6.13	5.24	2.15880	-0.38394	2.24496	-0.03648	-0.14883	0.07482
M072b3E01R001P007a.wttd	8.53	7.51	6.32	2.15194	-0.38642	2.10916	-0.11575	-0.14111	0.05932
M072b3E01R001P008a.wttd	10.04	8.95	7.40	2.11651	-0.44313	2.01017	-0.07364	-0.07689	0.03570
M072b3E01R001P009a.wttd	11.43	10.47	8.48	2.16877	-0.56520	1.99066	0.13743	-0.23517	-0.02025
M072b3E01R002P002a.wttd	12.74	11.65	9.44	2.18584	-0.86268	2.10757	0.24079	-0.30371	-0.10743
M072b3E01R003P002a.wttd	12.80	11.70	9.48	2.08934	-0.61869	1.89710	0.10265	-0.15101	0.02633
	Vrh	Vra	Vrp	p1*	p2*	p3*	p4*	p5*	p6*
M072b3E01R001P002a.wttd	1.25	1.04	0.92	-0.11067	0.03732	-13.38708	0.05717	0.06413	0.10077
M072b3E01R001P003a.wttd	2.72	2.29	2.02	-0.18391	0.00796	-3.02276	0.07053	0.09063	0.10055
M072b3E01R001P004a.wttd	4.13	3.50	3.06	-0.13443	0.02122	-1.48286	0.06074	0.09114	0.09482
M072b3E01R001P005a.wttd	5.62	4.79	4.14	-0.08030	0.02984	-0.90236	0.05815	0.09179	0.10865
M072b3E01R001P006a.wttd	7.05	6.13	5.24	-0.08242	0.04707	-0.67004	0.04186	0.09500	0.10712
M072b3E01R001P007a.wttd	8.53	7.51	6.32	-0.09510	0.01308	-0.52187	0.07054	0.09626	0.10615
M072b3E01R001P008a.wttd	10.04	8.95	7.40	-0.07149	0.07357	-0.46259	0.01158	0.08729	0.12746
M072b3E01R001P009a.wttd	11.43	10.47	8.48	-0.08030	0.10553	-0.42816	-0.02254	0.08464	0.14964
M072b3E01R002P002a.wttd	12.74	11.65	9.44	-0.15961	0.11650	-0.64580	-0.07850	0.06891	0.25848
M072b3E01R003P002a.wttd	12.80	11.70	9.48	-0.08240	0.09123	-0.39916	-0.00558	0.10990	0.18998

Notes: $V_{rh}=V/(f_vB)$, $V_{ra}=V/(f_aB)$ and $V_{rp}=V/(f_pB)$,
B – deck width of 60.36m,
V – deck height wind speed,
f_v, f_a and f_p – vertical, torsional and lateral frequencies respectively

TABLE E11 AERODYNAMIC DERIVATIVES, -4 DEGREES, SMOOTH FLOW, SDM FORMAT, CONSTRUCTION STAGE

	Vrh	Vra	Vrp	a1*	a2*	a3*	a4*	a5*	a6*
M072b2E01R001P002a.wttd	1.11	0.94	0.83	-0.04256	0.07504	-0.58286	-0.01975	0.15750	-0.12479
M072b2E01R001P003a.wttd	2.37	2.00	1.76	0.22188	0.17436	0.02752	-0.05240	0.08025	-0.13443
M072b2E01R001P004a.wttd	3.62	3.07	2.68	0.28157	0.18018	0.17672	-0.05555	0.04390	-0.13596
M072b2E01R001P005a.wttd	4.88	4.19	3.63	0.27245	0.16150	0.21704	-0.03601	0.02271	-0.14660
M072b2E01R001P006a.wttd	6.17	5.34	4.60	0.24274	0.13543	0.22224	-0.01391	0.00460	-0.14897
M072b2E01R001P007a.wttd	7.47	6.56	5.56	0.22904	0.12001	0.23642	0.03796	0.06014	-0.14383
M072b2E01R001P008a.wttd	8.78	7.82	6.52	0.25661	0.13590	0.22063	-0.01989	-0.00329	-0.14479
M072b2E01R001P009a.wttd	10.11	9.08	7.47	0.25323	0.12789	0.20870	-0.02672	-0.02976	-0.14998
M072b2E01R001P010a.wttd	Malfunction Instrumentation								
M072b2E01R002P002a.wttd	12.93	11.44	9.90	0.09698	0.01585	0.13147	-0.01130	-0.02043	-0.13934
	Vrh	Vra	Vrp	h1*	h2*	h3*	h4*	h5*	h6*
M072b2E01R001P002a.wttd	1.11	0.94	0.83	1.80364	-0.00813	2.70798	-0.07100	-0.58126	0.05775
M072b2E01R001P003a.wttd	2.37	2.00	1.76	1.86860	-0.20684	2.75320	-0.08218	-0.30478	0.03909
M072b2E01R001P004a.wttd	3.62	3.07	2.68	2.06560	-0.21562	2.67286	-0.15434	-0.28898	0.03763
M072b2E01R001P005a.wttd	4.88	4.19	3.63	2.26801	-0.21420	2.69285	-0.16769	-0.31498	0.02022
M072b2E01R001P006a.wttd	6.17	5.34	4.60	2.30804	-0.26130	2.64760	-0.18452	-0.30592	0.01220
M072b2E01R001P007a.wttd	7.47	6.56	5.56	2.39294	-0.22076	2.50457	-0.27282	-0.11031	0.03607
M072b2E01R001P008a.wttd	8.78	7.82	6.52	2.41901	-0.35375	2.47770	-0.12317	-0.27360	-0.01996
M072b2E01R001P009a.wttd	10.11	9.08	7.47	2.33479	-0.49142	2.38850	-0.00134	-0.30771	0.00807
M072b2E01R001P010a.wttd	Malfunction Instrumentation								
M072b2E01R002P002a.wttd	12.93	11.44	9.90	2.12444	-0.89821	2.29725	0.07167	-0.30557	-0.06558
	Vrh	Vra	Vrp	p1*	p2*	p3*	p4*	p5*	p6*
M072b2E01R001P002a.wttd	1.11	0.94	0.83	-0.26428	-0.03036	-16.17268	0.08714	0.09558	0.15973
M072b2E01R001P003a.wttd	2.37	2.00	1.76	-0.19162	0.00673	-4.16293	0.04361	0.10533	0.13317
M072b2E01R001P004a.wttd	3.62	3.07	2.68	-0.16605	0.02600	-2.12693	0.02407	0.14402	0.11586
M072b2E01R001P005a.wttd	4.88	4.19	3.63	-0.21023	0.00232	-1.42475	0.02718	0.14116	0.12403
M072b2E01R001P006a.wttd	6.17	5.34	4.60	-0.22533	-0.02365	-1.09306	0.04659	0.12950	0.13888
M072b2E01R001P007a.wttd	7.47	6.56	5.56	-0.26607	-0.13141	-0.83727	0.14927	0.09943	0.15317
M072b2E01R001P008a.wttd	8.78	7.82	6.52	-0.21907	-0.00857	-0.81374	0.02858	0.14485	0.18783
M072b2E01R001P009a.wttd	10.11	9.08	7.47	-0.16977	0.10245	-0.77000	-0.05162	0.13517	0.21205
M072b2E01R001P010a.wttd	Malfunction Instrumentation								
M072b2E01R002P002a.wttd	12.93	11.44	9.90	-0.23658	0.16034	-0.82672	-0.13112	0.13951	0.32920

Notes: $V_{rh}=V/(f_vB)$, $V_{ra}=V/(f_aB)$ and $V_{rp}=V/(f_pB)$,
B – deck width of 60.36m,
V – deck height wind speed,
f_v, f_a and f_p – vertical, torsional and lateral frequencies respectively

TABLE E12 AERODYNAMIC DERIVATIVES, -6 DEGREES, SMOOTH FLOW, SDM FORMAT, CONSTRUCTION STAGE

	Vrh	Vra	Vrp	a1*	a2*	a3*	a4*	a5*	a6*
M072b1E01R001P002a.wttd	0.92	0.78	0.68	-0.06807	0.06832	-0.73186	-0.04486	0.19018	-0.13330
M072b1E01R001P003a.wttd	2.03	1.71	1.50	0.24540	0.16503	0.06458	-0.06720	0.09696	-0.13025
M072b1E01R001P004a.wttd	3.16	2.67	2.34	0.29186	0.17235	0.27333	-0.01540	0.04466	-0.13141
M072b1E01R001P005a.wttd	4.23	3.61	3.14	0.25724	0.11115	0.27925	-0.01579	0.00017	-0.13668
M072b1E01R001P006a.wttd	5.34	4.59	3.97	0.20694	0.07131	0.25033	0.01976	0.00096	-0.13521
M072b1E01R001P007a.wttd	6.48	5.61	4.81	0.20013	0.04981	0.21843	0.02194	-0.03207	-0.13660
M072b1E01R001P008a.wttd	7.70	6.59	5.64	0.18061	0.01804	0.19432	0.03999	-0.03501	-0.14044
M072b1E01R001P009a.wttd	8.95	7.57	6.47	0.15986	-0.00890	0.17182	0.05380	-0.04254	-0.13888
M072b1E01R001P010a.wttd	Malfunction Instrumentation								
M072b1E01R002P002a.wttd	11.53	9.94	8.43	0.14511	-0.04266	0.12066	0.06729	-0.03458	-0.13265
	Vrh	Vra	Vrp	h1*	h2*	h3*	h4*	h5*	h6*
M072b1E01R001P002a.wttd	0.92	0.78	0.68	2.43557	0.17414	1.50303	-0.05285	-0.56532	0.06814
M072b1E01R001P003a.wttd	2.03	1.71	1.50	2.15797	-0.22229	2.83149	0.00138	-0.49396	0.03590
M072b1E01R001P004a.wttd	3.16	2.67	2.34	2.18978	-0.25718	2.59155	-0.02325	-0.47308	0.03585
M072b1E01R001P005a.wttd	4.23	3.61	3.14	2.29817	-0.26913	2.63793	-0.03044	-0.44246	0.02668
M072b1E01R001P006a.wttd	5.34	4.59	3.97	2.36948	-0.30092	2.62793	0.01955	-0.37888	0.02395
M072b1E01R001P007a.wttd	6.48	5.61	4.81	2.39867	-0.36288	2.58341	0.05926	-0.44428	0.05697
M072b1E01R001P008a.wttd	7.70	6.59	5.64	2.32295	-0.47973	2.53408	0.12028	-0.48869	0.02039
M072b1E01R001P009a.wttd	8.95	7.57	6.47	2.20392	-0.84791	2.30496	0.35195	-0.53710	-0.02992
M072b1E01R001P010a.wttd	Malfunction Instrumentation								
M072b1E01R002P002a.wttd	11.53	9.94	8.43	2.23876	-0.88268	2.49790	0.35195	-0.53955	-0.02992
	Vrh	Vra	Vrp	p1*	p2*	p3*	p4*	p5*	p6*
M072b1E01R001P002a.wttd	0.92	0.78	0.68	-0.27811	0.03883	-24.01325	0.06247	-0.21039	0.08811
M072b1E01R001P003a.wttd	2.03	1.71	1.50	-0.16774	0.06441	-5.75009	0.02581	0.07684	0.08144
M072b1E01R001P004a.wttd	3.16	2.67	2.34	-0.26636	-0.00523	-2.71407	0.06236	0.10699	0.08664
M072b1E01R001P005a.wttd	4.23	3.61	3.14	-0.25986	0.01476	-1.90133	0.00529	0.11608	0.08527
M072b1E01R001P006a.wttd	5.34	4.59	3.97	-0.27940	-0.00424	-1.46459	0.02312	0.10864	0.11152
M072b1E01R001P007a.wttd	6.48	5.61	4.81	-0.26669	0.02308	-1.24199	-0.00634	0.11183	0.09852
M072b1E01R001P008a.wttd	7.70	6.59	5.64	-0.26074	0.03640	-1.10940	-0.01466	0.14709	0.11463
M072b1E01R001P009a.wttd	8.95	7.57	6.47	-0.25305	0.05010	-1.03103	-0.02197	0.15544	0.15629
M072b1E01R001P010a.wttd	Malfunction Instrumentation								
M072b1E01R002P002a.wttd	11.53	9.94	8.43	-0.25051	0.10303	-0.97496	-0.08597	0.22117	0.38142

Notes: $V_{rh}=V/(f_vB)$, $V_{ra}=V/(f_aB)$ and $V_{rp}=V/(f_pB)$,
B – deck width of 60.36m,
V – deck height wind speed,
f_v, f_a and f_p – vertical, torsional and lateral frequencies respectively

TABLE E13 AERODYNAMIC DERIVATIVES, +2 DEGREES, SMOOTH FLOW, SDM FORMAT, CONSTRUCTION STAGE

	Vrh	Vra	Vrp	a1*	a2*	a3*	a4*	a5*	a6*
M072b5E01R001P002a.wttd	1.62	1.36	1.20	0.04379	-0.07322	0.04603	-0.04960	0.19305	-0.13251
M072b5E01R001P003a.wttd	3.44	2.89	2.54	0.24797	0.18264	0.16526	-0.10127	0.21072	-0.13229
M072b5E01R001P004a.wttd	5.22	4.48	3.87	0.38450	0.32527	0.28984	-0.16378	0.13060	-0.12554
M072b5E01R001P005a.wttd	7.05	6.24	5.21	0.49622	0.40312	0.36394	-0.17605	0.07633	-0.13086
M072b5E01R001P006a.wttd	8.87	8.02	6.58	0.59498	0.48771	0.40236	-0.16755	0.07189	-0.14850
M072b5E01R001P007a.wttd	9.96	8.44	7.95	0.83231	0.90895	0.61649	-0.33359	-0.00485	-0.10616
M072b5E01R001P008a.wttd	13.39	12.10	9.30	0.33708	0.34363	0.34044	-0.13955	-0.06023	-0.12930
M072b5E01R001P009a.wttd	14.39	13.29	10.61	0.31228	0.37998	0.18008	-0.26958	-0.01647	-0.13295
M072b5E01R001P010a.wttd	16.57	14.82	11.99	0.15428	0.18168	0.11242	-0.12744	0.08233	-0.13977
M072b5E01R001P011a.wttd	18.69	17.10	13.35	0.13217	0.17865	0.09894	-0.08337	0.02618	-0.16521
	Vrh	Vra	Vrp	h1*	h2*	h3*	h4*	h5*	h6*
M072b5E01R001P002a.wttd	1.62	1.36	1.20	2.37342	-0.18997	3.66018	0.04538	0.09801	0.09036
M072b5E01R001P003a.wttd	3.44	2.89	2.54	1.87592	-0.53653	2.33154	0.12579	-0.04636	0.10486
M072b5E01R001P004a.wttd	5.22	4.48	3.87	1.77062	-0.45046	1.79099	0.04245	0.07943	0.09596
M072b5E01R001P005a.wttd	7.05	6.24	5.21	1.90682	-0.21150	1.61863	-0.11612	-0.00599	0.12109
M072b5E01R001P006a.wttd	8.87	8.02	6.58	2.20638	0.12745	1.62454	-0.29533	0.06626	0.12038
M072b5E01R001P007a.wttd	9.96	8.44	7.95	3.19744	1.11811	2.52323	-0.73810	-0.19761	0.30549
M072b5E01R001P008a.wttd	13.39	12.10	9.30	1.13037	-0.29278	1.06136	-0.41289	-0.05971	-0.13311
M072b5E01R001P009a.wttd	14.39	13.29	10.61	1.56907	-0.35067	1.15268	-0.17735	-0.05951	0.07109
M072b5E01R001P010a.wttd	16.57	14.82	11.99	1.26899	-0.84234	1.03584	0.20231	0.17601	0.07215
M072b5E01R001P011a.wttd	18.69	17.10	13.35	0.83623	-0.92721	0.66548	-0.49593	0.05801	0.26466
	Vrh	Vra	Vrp	p1*	p2*	p3*	p4*	p5*	p6*
M072b5E01R001P002a.wttd	1.62	1.36	1.20	0.33578	0.04078	-7.10444	0.05386	-0.08808	0.05796
M072b5E01R001P003a.wttd	3.44	2.89	2.54	0.31946	-0.02784	-1.10611	0.06932	0.07932	0.06145
M072b5E01R001P004a.wttd	5.22	4.48	3.87	0.26404	-0.11978	-0.24100	0.10041	0.14441	0.07409
M072b5E01R001P005a.wttd	7.05	6.24	5.21	0.21999	-0.16454	0.03116	0.11920	0.09838	0.07716
M072b5E01R001P006a.wttd	8.87	8.02	6.58	0.24013	-0.18747	0.16759	0.12999	0.13074	0.05271
M072b5E01R001P007a.wttd	9.96	8.44	7.95	0.30948	-0.31690	0.39532	0.17442	0.10612	0.04987
M072b5E01R001P008a.wttd	13.39	12.10	9.30	-0.17762	0.36145	-0.16323	-0.13100	-0.00766	0.13978
M072b5E01R001P009a.wttd	14.39	13.29	10.61	0.35418	-0.08635	0.32780	0.01051	0.04835	0.02384
M072b5E01R001P010a.wttd	16.57	14.82	11.99	0.45121	-0.11834	0.48511	0.10775	0.11012	-0.28705
M072b5E01R001P011a.wttd	18.69	17.10	13.35	0.52808	-0.11513	0.54898	0.22552	0.12957	-0.27077

Notes: $V_{rh}=V/(f_vB)$, $V_{ra}=V/(f_aB)$ and $V_{rp}=V/(f_pB)$,
B – deck width of 60.36m,
V – deck height wind speed,
f_v, f_a and f_p – vertical, torsional and lateral frequencies respectively

TABLE E14 AERODYNAMIC DERIVATIVES, +4 DEGREES, SMOOTH FLOW, SDM FORMAT, CONSTRUCTION STAGE

	Vrh	Vra	Vrp	a1*	a2*	a3*	a4*	a5*	a6*
M072b6E01R001P002a.wttd	1.10	0.92	0.81	-0.15515	0.03157	-0.79542	0.01753	0.27543	-0.13324
M072b6E01R001P003a.wttd	2.47	2.06	1.82	0.07842	0.17493	-0.12821	-0.00473	0.20768	-0.13412
M072b6E01R001P004a.wttd	3.78	3.19	2.80	0.14820	0.22174	0.08766	-0.02984	0.20501	-0.12754
M072b6E01R001P005a.wttd	5.14	4.29	3.75	0.24817	0.28026	0.15440	-0.02661	0.22736	-0.12019
M072b6E01R001P006a.wttd	6.39	5.45	4.75	0.18863	0.26728	0.16023	0.00749	0.15610	-0.13188
M072b6E01R001P007a.wttd	7.75	6.66	5.75	0.25605	0.29954	0.20903	-0.01935	0.16385	-0.12860
M072b6E01R001P008a.wttd	8.31	7.59	6.74	-0.00952	0.22126	0.08028	-0.22047	0.10173	-0.13545
M072b6E01R001P009a.wttd	10.71	9.39	7.74	0.33524	0.30956	0.23836	0.00297	0.13785	-0.06432
M072b6E01R001P010a.wttd	12.21	10.55	8.81	0.20850	0.22112	0.18082	0.00347	0.10129	-0.10022
M072b6E01R001P011a.wttd	13.06	11.86	9.65	0.20940	0.23990	0.16759	-0.01279	0.01053	0.00154
M072b6E01R002P002a.wttd	19.80	17.30	14.30	-0.30263	-0.15079	-0.13055	-0.23794	0.01438	-0.02771
	Vrh	Vra	Vrp	h1*	h2*	h3*	h4*	h5*	h6*
M072b6E01R001P002a.wttd	1.10	0.92	0.81	2.29204	-0.07532	4.34853	-0.02776	-0.06161	0.10847
M072b6E01R001P003a.wttd	2.47	2.06	1.82	1.93399	-0.49943	3.04647	0.07918	0.13171	0.12054
M072b6E01R001P004a.wttd	3.78	3.19	2.80	1.86261	-0.61157	2.32339	0.11434	0.13361	0.11904
M072b6E01R001P005a.wttd	5.14	4.29	3.75	1.54740	-0.76388	2.05667	0.20218	0.00892	0.14136
M072b6E01R001P006a.wttd	6.39	5.45	4.75	1.94008	-0.80133	2.02064	0.46260	0.02871	0.11519
M072b6E01R001P007a.wttd	7.75	6.66	5.75	1.23241	-0.97111	1.69073	0.19880	0.13120	0.10110
M072b6E01R001P008a.wttd	8.31	7.59	6.74	1.34507	-1.10021	1.55649	0.10479	0.24782	0.15719
M072b6E01R001P009a.wttd	10.71	9.39	7.74	1.34419	-1.15634	1.41130	0.42934	-0.04114	-0.05654
M072b6E01R001P010a.wttd	12.21	10.55	8.81	1.52478	-1.19598	1.50410	0.63885	0.00423	-0.17049
M072b6E01R001P011a.wttd	13.06	11.86	9.65	1.25225	-1.04118	1.00907	-0.20902	0.70822	-0.37215
M072b6E01R002P002a.wttd	19.80	17.30	14.30	0.46696	-3.36224	1.83251	3.77242	0.53788	0.01803
	Vrh	Vra	Vrp	p1*	p2*	p3*	p4*	p5*	p6*
M072b6E01R001P002a.wttd	1.10	0.92	0.81	0.98306	0.09031	-15.68876	0.16620	-0.10960	0.06104
M072b6E01R001P003a.wttd	2.47	2.06	1.82	0.53949	-0.01908	-2.34534	0.12377	0.15079	0.08330
M072b6E01R001P004a.wttd	3.78	3.19	2.80	0.42480	-0.07303	-0.53515	0.11278	0.22110	0.08282
M072b6E01R001P005a.wttd	5.14	4.29	3.75	0.37044	-0.17493	0.03667	0.18129	0.29402	0.08167
M072b6E01R001P006a.wttd	6.39	5.45	4.75	0.44038	-0.23044	0.30921	0.18301	0.18088	0.07469
M072b6E01R001P007a.wttd	7.75	6.66	5.75	0.36004	-0.24507	0.40744	0.17776	0.28398	0.05391
M072b6E01R001P008a.wttd	8.31	7.59	6.74	0.35019	-0.31482	0.43507	0.07343	0.16579	0.05138
M072b6E01R001P009a.wttd	10.71	9.39	7.74	0.60018	-0.24504	0.63652	0.23264	0.28509	0.11618
M072b6E01R001P010a.wttd	12.21	10.55	8.81	0.45355	-0.34397	0.61069	0.17799	0.20590	-0.11893
M072b6E01R001P011a.wttd	13.06	11.86	9.65	0.48787	-0.43181	0.67691	0.29575	0.55517	-0.56941
M072b6E01R002P002a.wttd	19.80	17.30	14.30	1.15271	0.01379	1.33366	0.67036	0.43772	-0.61026

Notes: $V_{rh}=V/(f_vB)$, $V_{ra}=V/(f_aB)$ and $V_{rp}=V/(f_pB)$,
B – deck width of 60.36m,
V – deck height wind speed,
f_v, f_a and f_p – vertical, torsional and lateral frequencies respectively

TABLE E15 AERODYNAMIC DERIVATIVES, +6 DEGREES, SMOOTH FLOW, SDM FORMAT, CONSTRUCTION STAGE

	Vrh	Vra	Vrp	a1*	a2*	a3*	a4*	a5*	a6*
M072b7E01R001P002a.wttd	1.29	1.08	0.95	-0.05013	0.05047	-0.57804	0.00549	0.32853	-0.13025
M072b7E01R001P003a.wttd	2.74	2.30	2.02	0.09987	0.15958	0.00603	0.04611	0.26278	-0.13133
M072b7E01R001P004a.wttd	4.23	3.57	3.12	-0.00675	0.10100	0.06226	0.07685	0.20599	-0.13253
M072b7E01R001P005a.wttd	5.74	4.80	4.22	-0.02481	0.09109	0.01877	0.05790	0.17070	-0.13096
M072b7E01R001P006a.wttd	7.26	6.00	5.31	0.06967	0.11394	0.01583	0.07611	0.20359	-0.12848
M072b7E01R001P007a.wttd	8.79	7.37	6.43	0.25765	0.24379	-0.00944	-0.11657	0.19500	-0.12531
M072b7E01R001P008a.wttd	10.34	8.43	7.59	0.12459	0.23569	0.02459	0.03460	0.08226	-0.01543
M072b7E01R001P009a.wttd	12.38	9.60	8.60	0.08918	0.22181	0.06144	0.07177	-0.00526	-0.11259
M072b7E01R001P010a.wttd	13.08	11.15	9.71	0.12224	0.15412	0.06443	0.10671	0.02741	-0.10761
M072b7E01R002P002a.wttd	14.24	12.57	10.75	-0.35413	-0.30236	-0.05983	-0.07377	0.11350	-0.02715
	Vrh	Vra	Vrp	h1*	h2*	h3*	h4*	h5*	h6*
M072b7E01R001P002a.wttd	1.29	1.08	0.95	1.91908	-0.10988	4.18410	0.00808	-0.00175	0.10392
M072b7E01R001P003a.wttd	2.74	2.30	2.02	1.92996	-0.45274	2.69074	0.00861	0.07763	0.11307
M072b7E01R001P004a.wttd	4.23	3.57	3.12	2.26929	-0.43006	2.47858	0.13332	0.10287	0.13223
M072b7E01R001P005a.wttd	5.74	4.80	4.22	1.79206	-0.72460	2.44550	0.42293	0.11644	0.17530
M072b7E01R001P006a.wttd	7.26	6.00	5.31	1.69491	-1.09389	2.35269	0.59844	0.10691	0.12266
M072b7E01R001P007a.wttd	8.79	7.37	6.43	1.12801	-1.62049	2.09399	1.17756	0.02472	0.03689
M072b7E01R001P008a.wttd	10.34	8.43	7.59	1.24842	-1.72204	1.92160	0.59358	0.19985	-0.13876
M072b7E01R001P009a.wttd	12.38	9.60	8.60	1.30153	-1.79185	1.82866	0.48981	0.60802	-0.14718
M072b7E01R001P010a.wttd	13.08	11.15	9.71	1.21738	-1.51635	1.34460	-0.82404	0.27877	0.09754
M072b7E01R002P002a.wttd	14.24	12.57	10.75	1.35103	-1.45336	1.96978	2.36415	0.56281	-0.02897
	Vrh	Vra	Vrp	p1*	p2*	p3*	p4*	p5*	p6*
M072b7E01R001P002a.wttd	1.29	1.08	0.95	0.79289	0.05808	-10.56388	0.14020	0.35793	0.04945
M072b7E01R001P003a.wttd	2.74	2.30	2.02	0.67823	-0.08483	-1.41448	0.14591	0.36573	0.06660
M072b7E01R001P004a.wttd	4.23	3.57	3.12	0.72547	-0.03122	0.04585	0.13698	0.34500	0.04462
M072b7E01R001P005a.wttd	5.74	4.80	4.22	0.57958	-0.10967	0.60837	0.22063	0.34462	0.02524
M072b7E01R001P006a.wttd	7.26	6.00	5.31	0.74221	-0.12176	0.88314	0.17651	0.41512	0.03268
M072b7E01R001P007a.wttd	8.79	7.37	6.43	0.83459	-0.15431	0.98724	0.10223	0.35716	0.04555
M072b7E01R001P008a.wttd	10.34	8.43	7.59	0.78063	-0.22095	1.13034	0.17086	0.18382	0.23157
M072b7E01R001P009a.wttd	12.38	9.60	8.60	0.56869	-0.28586	1.10139	0.11911	0.17662	-0.10368
M072b7E01R001P010a.wttd	13.08	11.15	9.71	0.43682	-0.28463	0.90991	0.27270	0.23968	-0.00375
M072b7E01R002P002a.wttd	14.24	12.57	10.75	1.03619	-0.28168	1.50610	1.10683	0.64003	-0.31031

Notes: $V_{rh}=V/(f_vB)$, $V_{ra}=V/(f_aB)$ and $V_{rp}=V/(f_pB)$,
B – deck width of 60.36m,
V – deck height wind speed,
f_v, f_a and f_p – vertical, torsional and lateral frequencies respectively

APPENDIX F

WIND PROFILES IN TRAFFIC LANES

Notes:

F1. Wind Profiles were measured at the centreline of each traffic lane for four conditions of the deck:

a. No Traffic,

b. Traffic Condition 1 - road traffic on outward upwind lane plus train on upwind track;

c. Traffic Condition 2 - road traffic on outward downwind lane plus train on upwind track;

d. Traffic Condition 3 - train on upwind track only.

F2. No measurements were made for the lane in which traffic was present

F3. Profile measurements included Mean Horizontal Wind Speed (i.e. $\overline{U}$), and RMS of the u , v and w component wind speeds. Mean wind speed data have been normalised to the mean free-stream wind speed and local turbulence intensities computed from the mean and RMS data $I_u(z) = \sigma_u(z)/\overline{U}(z)$, $I_v(z) = \sigma_v(z)/\overline{U}(z)$ and $I_w(z) = \sigma_w(z)/\overline{U}(z)$, where u , v and w are the horizontal, lateral and vertical components of the wind speed and z is the distance above the bridge deck.

F4. Data presented in the appendix include the measured data in tabular form, a key to the measurements and plots of the data.

Bare Bridge Deck Profiles

z (m)	Outer Downwind Vehicle Lane, U_{max}/U_{ref} = 0.968				Middle Downwind Vehicle Lane, U_{max}/U_{ref} = 0.972				Inner Downwind Vehicle Lane, U_{max}/U_{ref} = 0.967			
	$U(z)/U_{max}$	I_u	I_v	I_w	$U(z)/U_{max}$	I_u	I_v	I_w	$U(z)/U_{max}$	I_u	I_v	I_w
0.8	0.153	1.146	0.712	0.531	0.110	1.393	0.829	0.841	0.038	1.724	1.051	1.071
1.6	0.243	0.882	0.538	0.415	0.231	0.931	0.535	0.490	0.152	1.109	0.640	0.769
2.4	0.332	0.726	0.426	0.323	0.360	0.676	0.396	0.313	0.366	0.700	0.342	0.329
3.2	0.448	0.561	0.324	0.235	0.468	0.546	0.305	0.233	0.531	0.503	0.251	0.220
4	0.547	0.461	0.261	0.188	0.586	0.427	0.236	0.179	0.655	0.381	0.203	0.174
4.8	0.645	0.373	0.213	0.150	0.670	0.362	0.202	0.148	0.750	0.302	0.166	0.139
5.6	0.723	0.312	0.183	0.128	0.753	0.292	0.166	0.119	0.819	0.248	0.147	0.114
6.4	0.802	0.254	0.152	0.106	0.826	0.231	0.144	0.102	0.887	0.198	0.126	0.092
8	0.902	0.168	0.118	0.081	0.923	0.151	0.110	0.074	0.971	0.124	0.097	0.067
16	1.000	0.079	0.075	0.064	1.000	0.075	0.075	0.064	1.006	0.076	0.075	0.065
24	1.000	0.077	0.074	0.067	1.000	0.077	0.073	0.069	1.000	0.080	0.077	0.069

z (m)	Leeward Train Lane, U_{max}/U_{ref} = 0.978				Windward Train Lane, U_{max}/U_{ref} = 0.975			
	$U(z)/U_{max}$	I_u	I_v	I_w	$U(z)/U_{max}$	I_u	I_v	I_w
0.8	0.028	1.766	1.047	1.222	0.019	1.686	1.045	1.044
1.6	0.096	1.372	0.799	0.997	0.020	2.180	1.371	1.315
2.4	0.308	0.713	0.393	0.374	0.171	0.860	0.493	0.583
3.2	0.535	0.473	0.234	0.171	0.556	0.437	0.196	0.127
4	0.692	0.341	0.174	0.112	0.734	0.278	0.151	0.088
4.8	0.794	0.257	0.141	0.086	0.837	0.205	0.131	0.074
5.6	0.876	0.186	0.121	0.072	0.910	0.161	0.112	0.064
6.4	0.938	0.146	0.107	0.065	0.954	0.128	0.101	0.060
8	0.998	0.099	0.091	0.058	1.005	0.094	0.086	0.060
16	1.005	0.074	0.078	0.068	1.010	0.077	0.077	0.069
24	1.000	0.080	0.078	0.072	1.000	0.084	0.079	0.072

z (m)	Inner Upwind Vehicle Lane, U_{max}/U_{ref} = 0.949				Middle Upwind Vehicle Lane, U_{max}/U_{ref} = 0.946				Outer Upwind Vehicle Lane, U_{max}/U_{ref} = 0.935			
	$U(z)/U_{max}$	I_u	I_v	I_w	$U(z)/U_{max}$	I_u	I_v	I_w	$U(z)/U_{max}$	I_u	I_v	I_w
0.8	0.125	0.885	0.545	0.473	0.155	0.561	0.441	0.364	0.143	0.628	0.509	0.370
1.6	0.274	0.571	0.353	0.289	0.276	0.516	0.332	0.293	0.263	0.389	0.322	0.263
2.4	0.462	0.383	0.225	0.156	0.489	0.352	0.204	0.132	0.592	0.234	0.146	0.062
3.2	0.641	0.269	0.163	0.093	0.691	0.217	0.140	0.074	0.762	0.156	0.119	0.071
4	0.771	0.184	0.130	0.069	0.809	0.156	0.114	0.062	0.860	0.139	0.103	0.058
4.8	0.861	0.140	0.113	0.064	0.871	0.130	0.103	0.061	0.906	0.115	0.092	0.065
5.6	0.913	0.118	0.102	0.061	0.927	0.113	0.097	0.061	0.953	0.102	0.089	0.067
6.4	0.953	0.104	0.094	0.062	0.961	0.100	0.090	0.062	0.977	0.091	0.088	0.069
8	0.991	0.083	0.085	0.067	0.985	0.085	0.085	0.069	0.987	0.083	0.084	0.075
16	1.002	0.079	0.081	0.073	0.991	0.085	0.084	0.073	0.991	0.083	0.085	0.077
24	1.000	0.084	0.081	0.077	1.000	0.086	0.081	0.076	1.000	0.084	0.083	0.077

Figure Number:

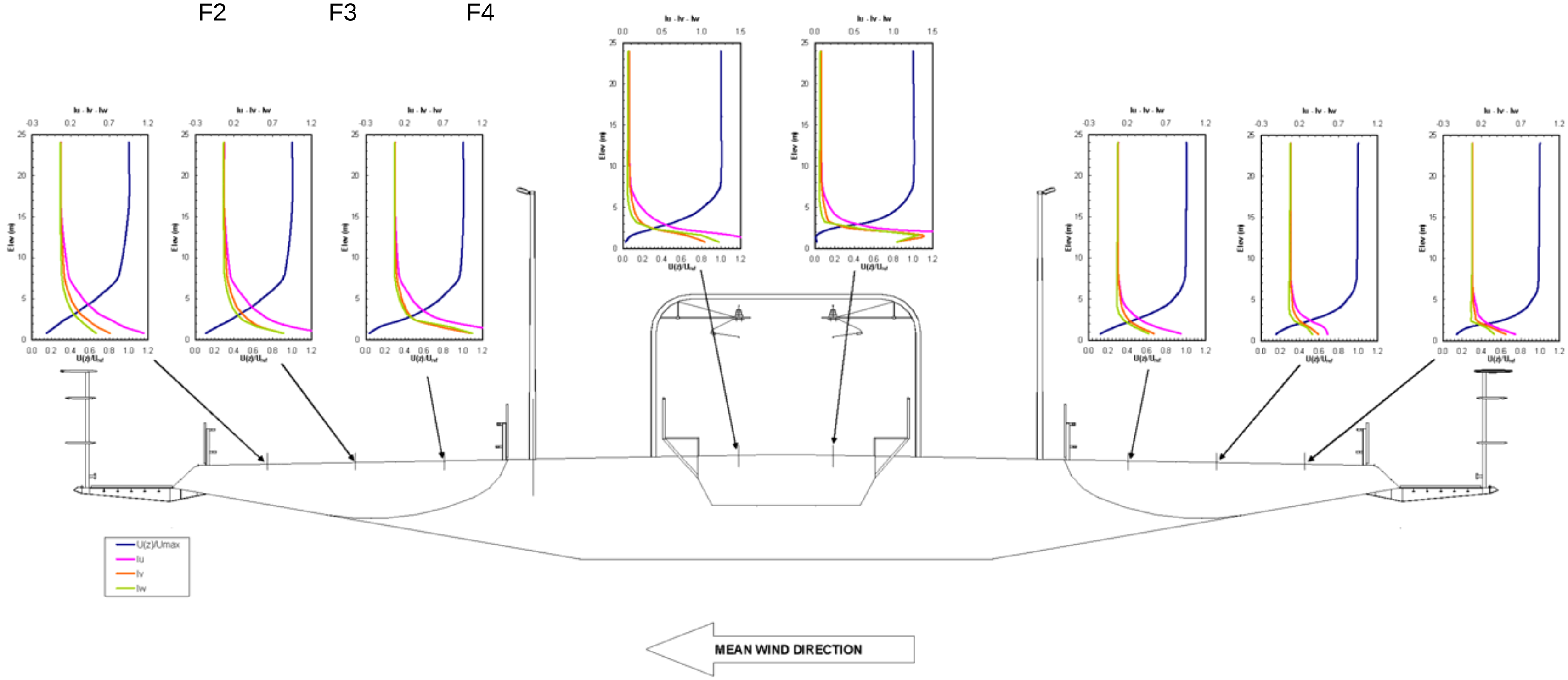

FIGURE F1 VELOCITY PROFILE FOR TRAFFIC LANES OVER BARE DECK – KEY TO MEASUREMENTS

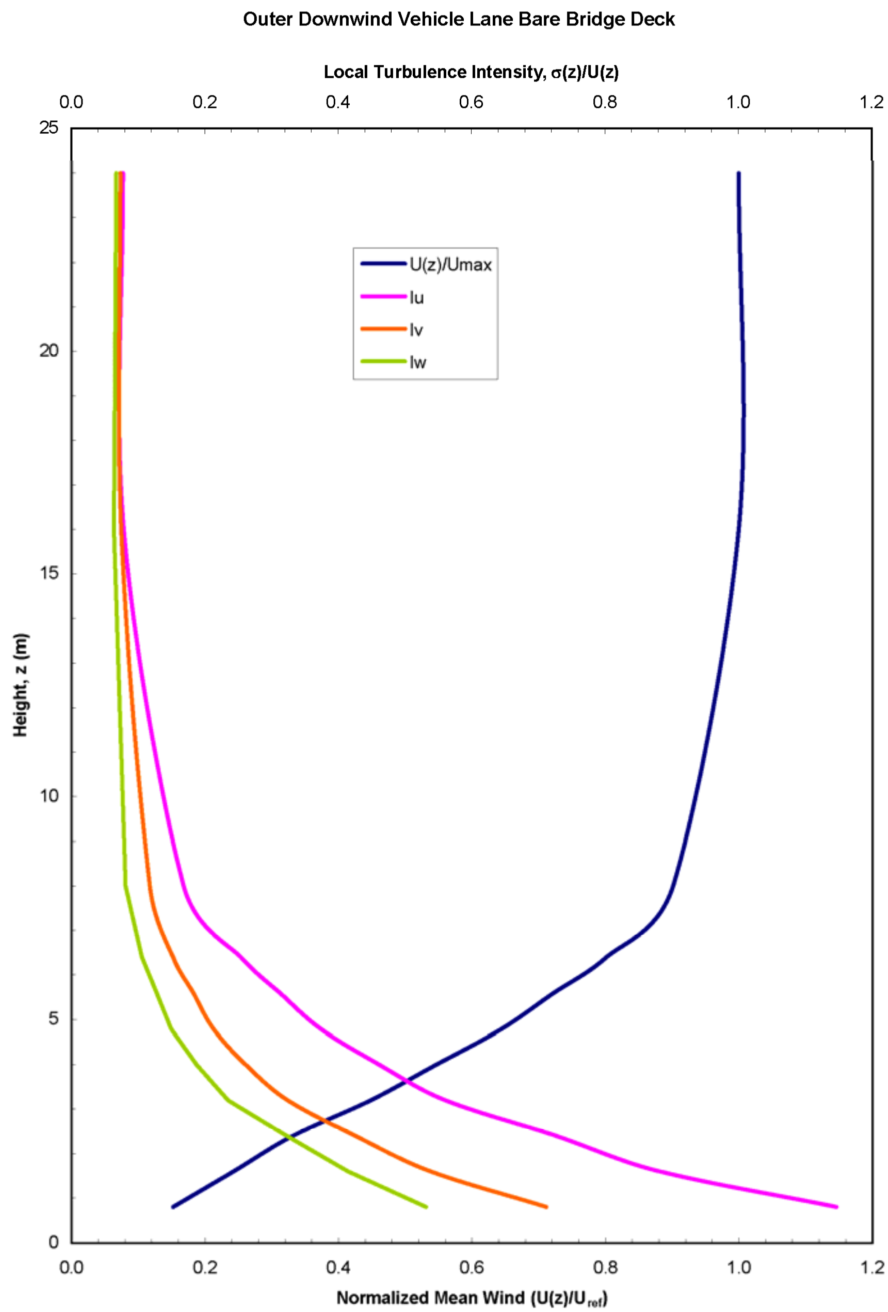

FIGURE F2 VELOCITY PROFILE IN OUTER (SLOW) LANE ON DOWNWIND GIRDER NO TRAFFIC

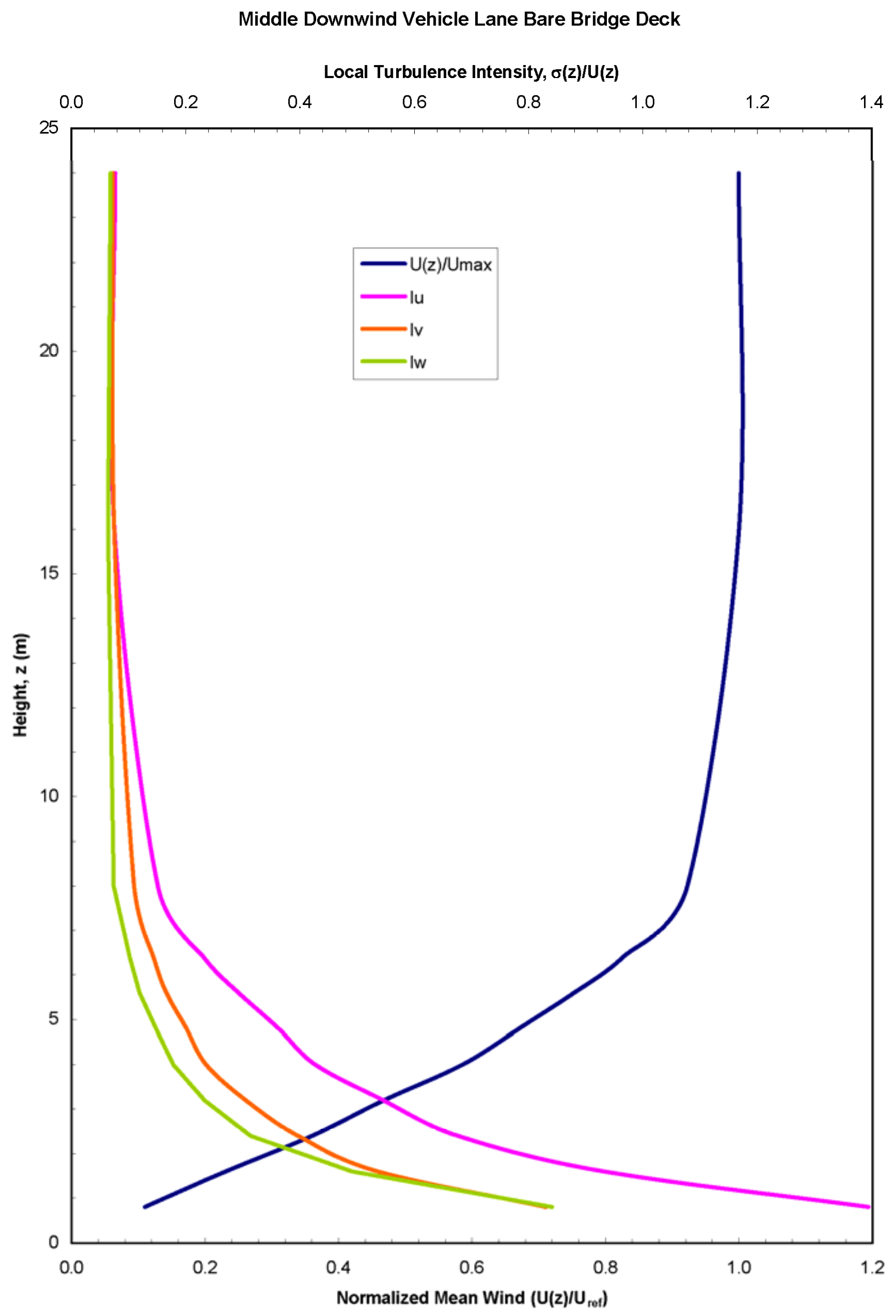

FIGURE F3 VELOCITY PROFILE IN MIDDLE LANE ON DOWNWIND GIRDER NO TRAFFIC

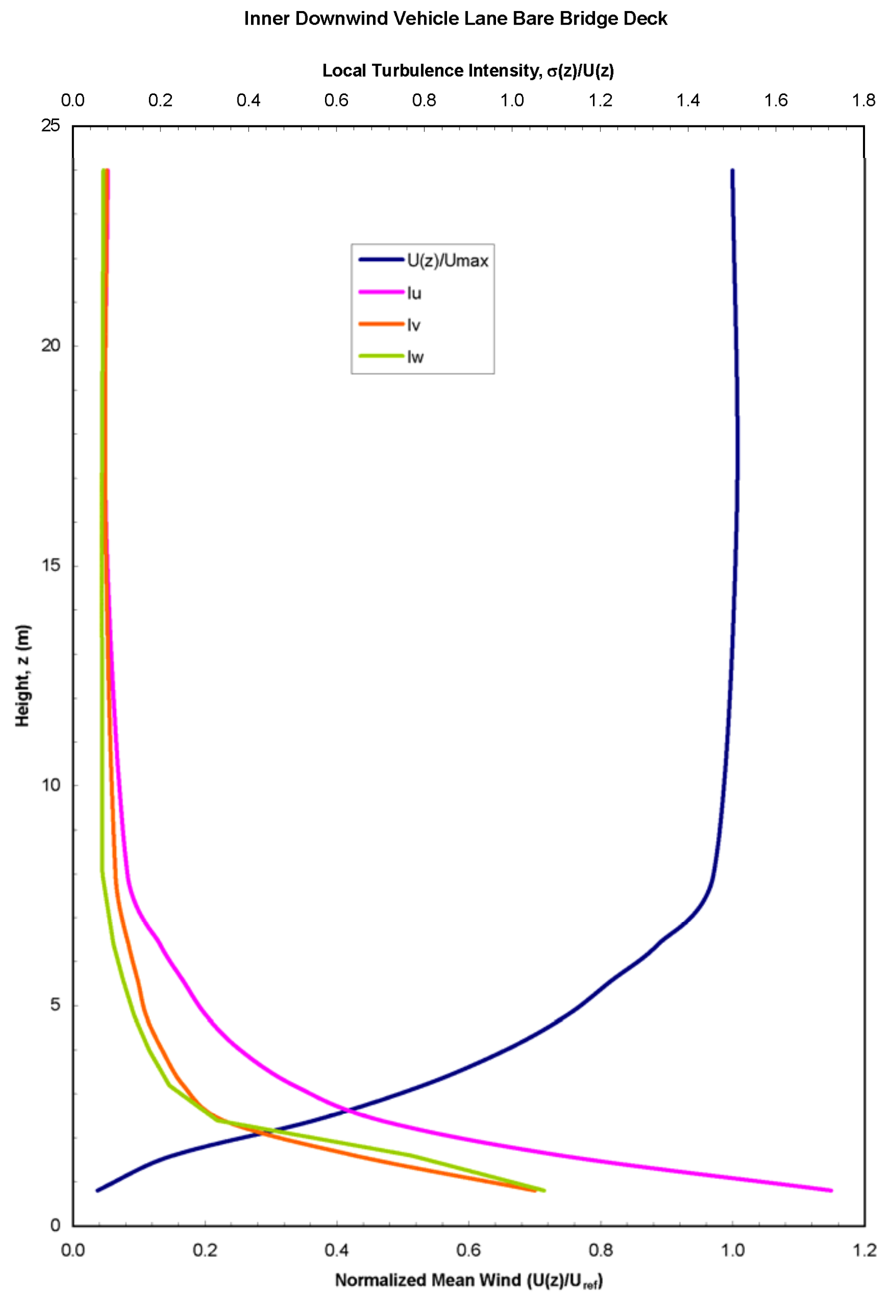

FIGURE F4 VELOCITY PROFILE IN INNER (FAST) LANE ON DOWNWIND GIRDER NO TRAFFIC

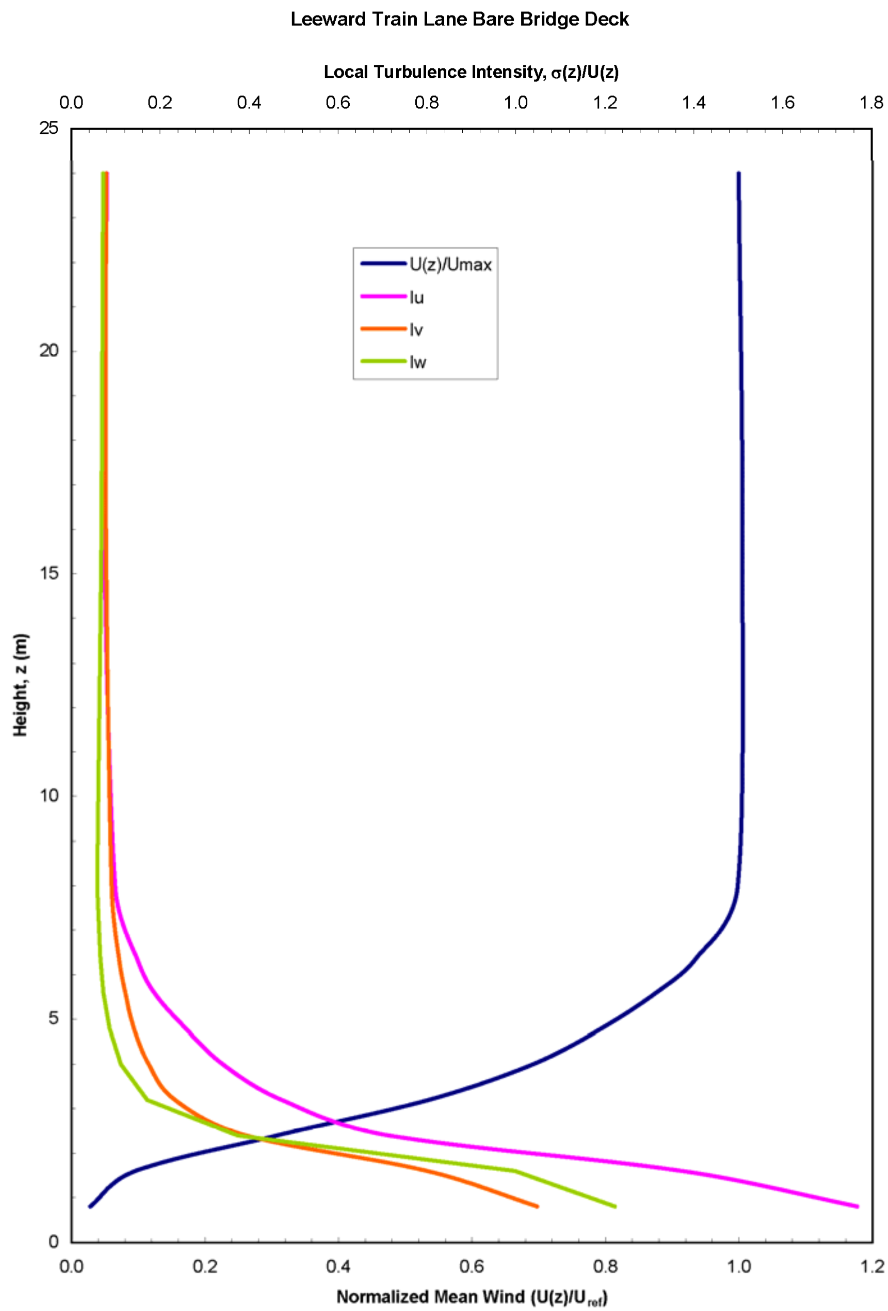

FIGURE F5 VELOCITY PROFILE IN DOWNWIND RAIL LINE - NO TRAFFIC

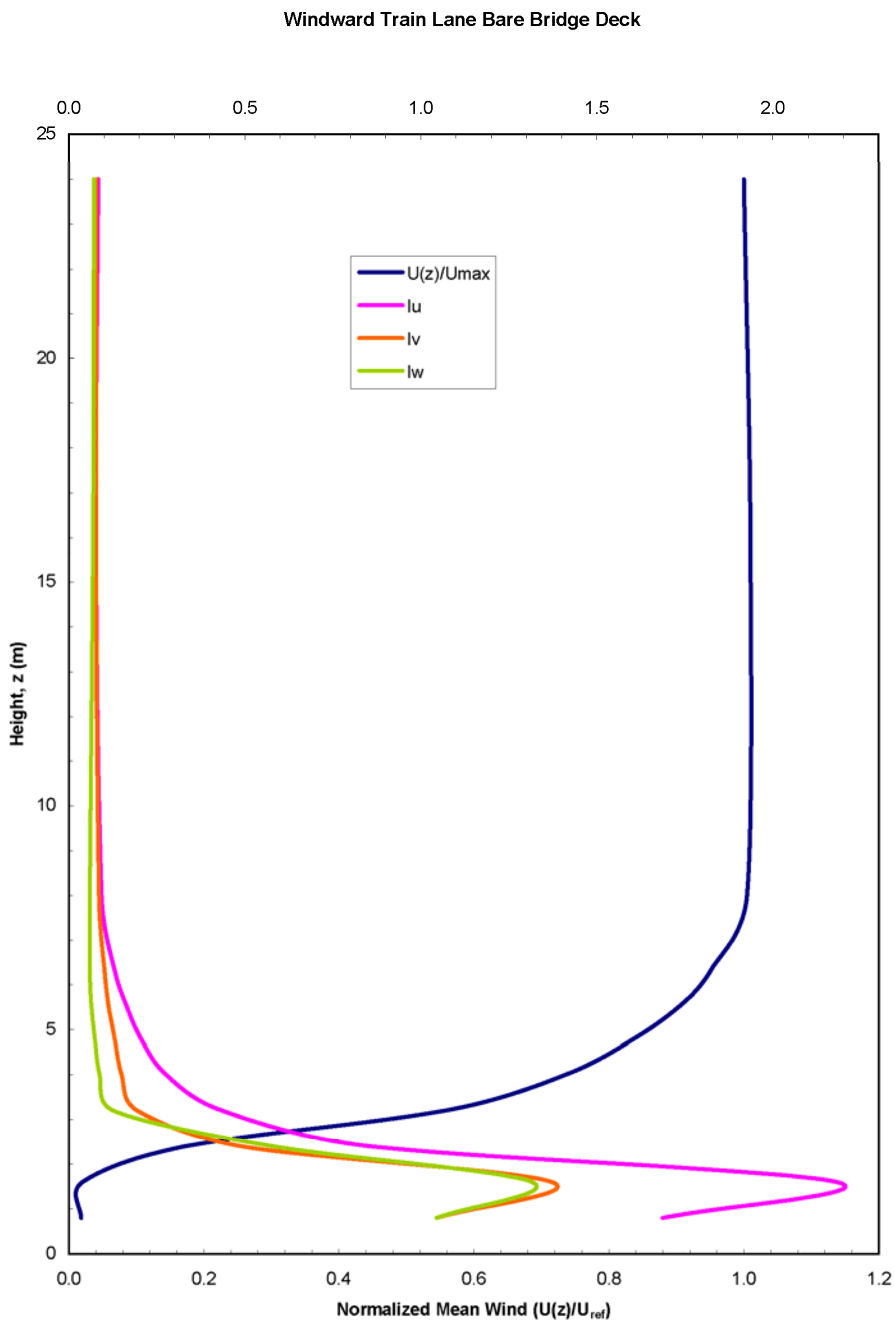

FIGURE F6 VELOCITY PROFILE IN WINDWARD RAIL LINE - NO TRAFFIC

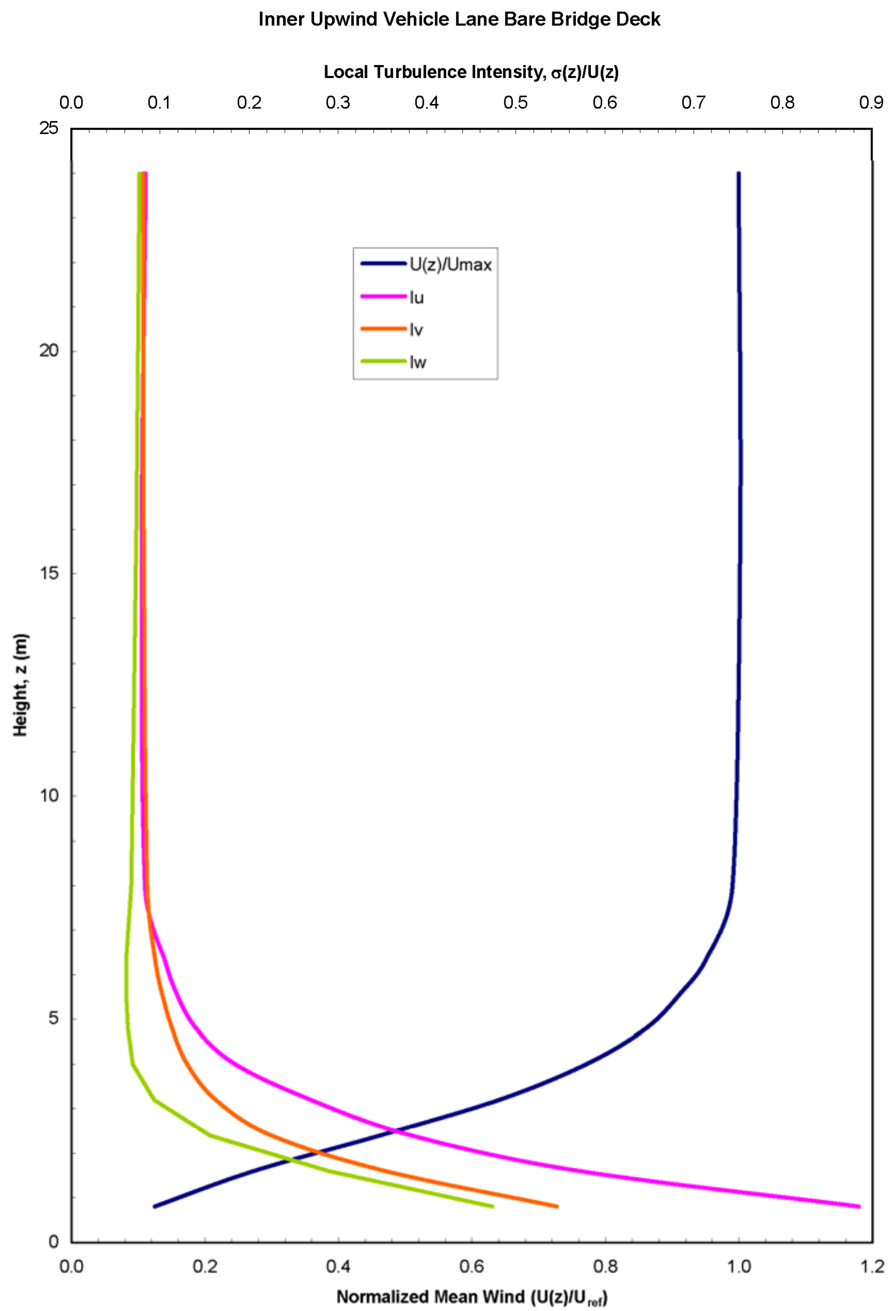

FIGURE F7 VELOCITY PROFILE IN INNER (FAST) LANE ON UPWIND GIRDER NO TRAFFIC

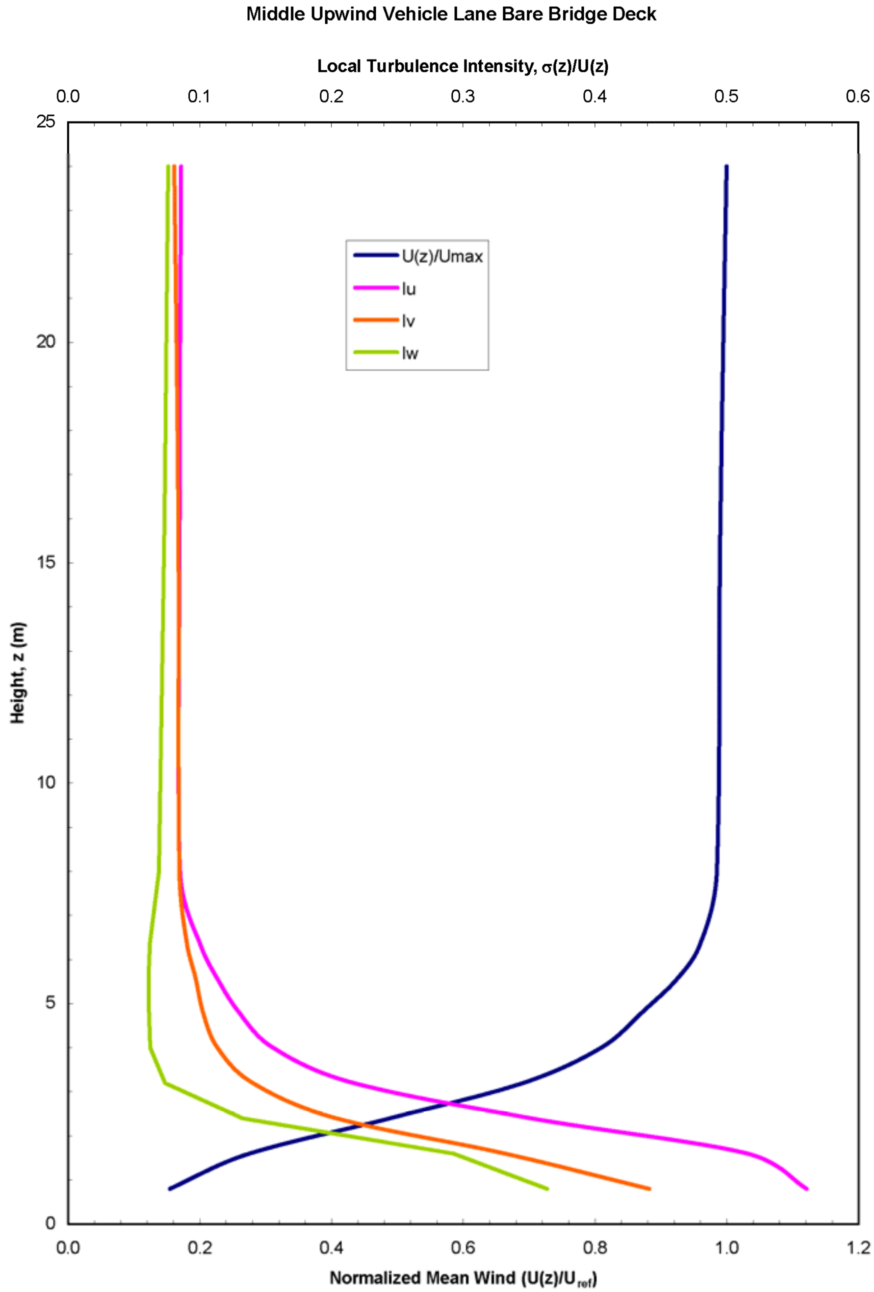

FIGURE F8 VELOCITY PROFILE IN MIDDLE LANE ON UPWIND GIRDER NO TRAFFIC

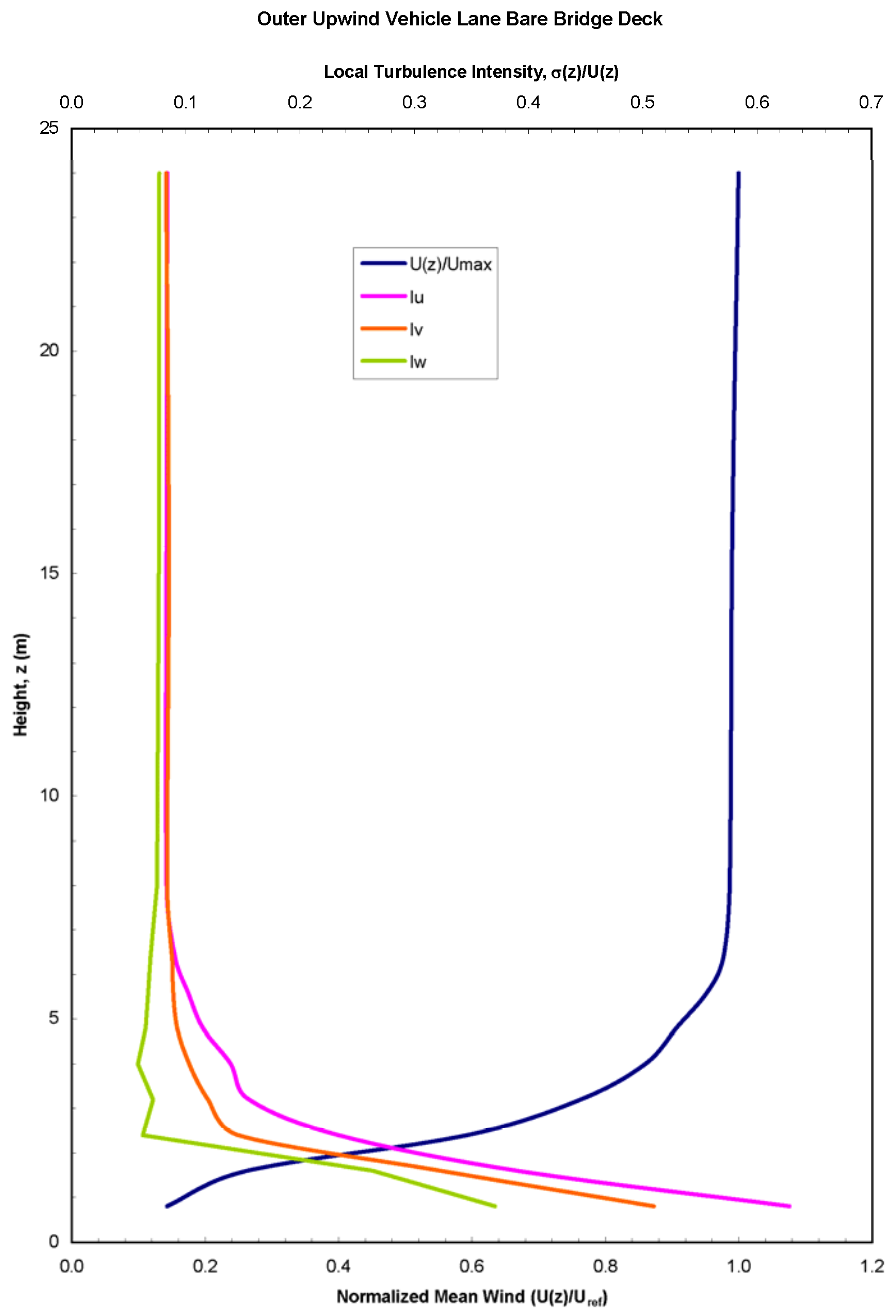

FIGURE F9 VELOCITY PROFILE IN OUTER (SLOW) LANE ON UPWIND GIRDER NO TRAFFIC

Figure Number:

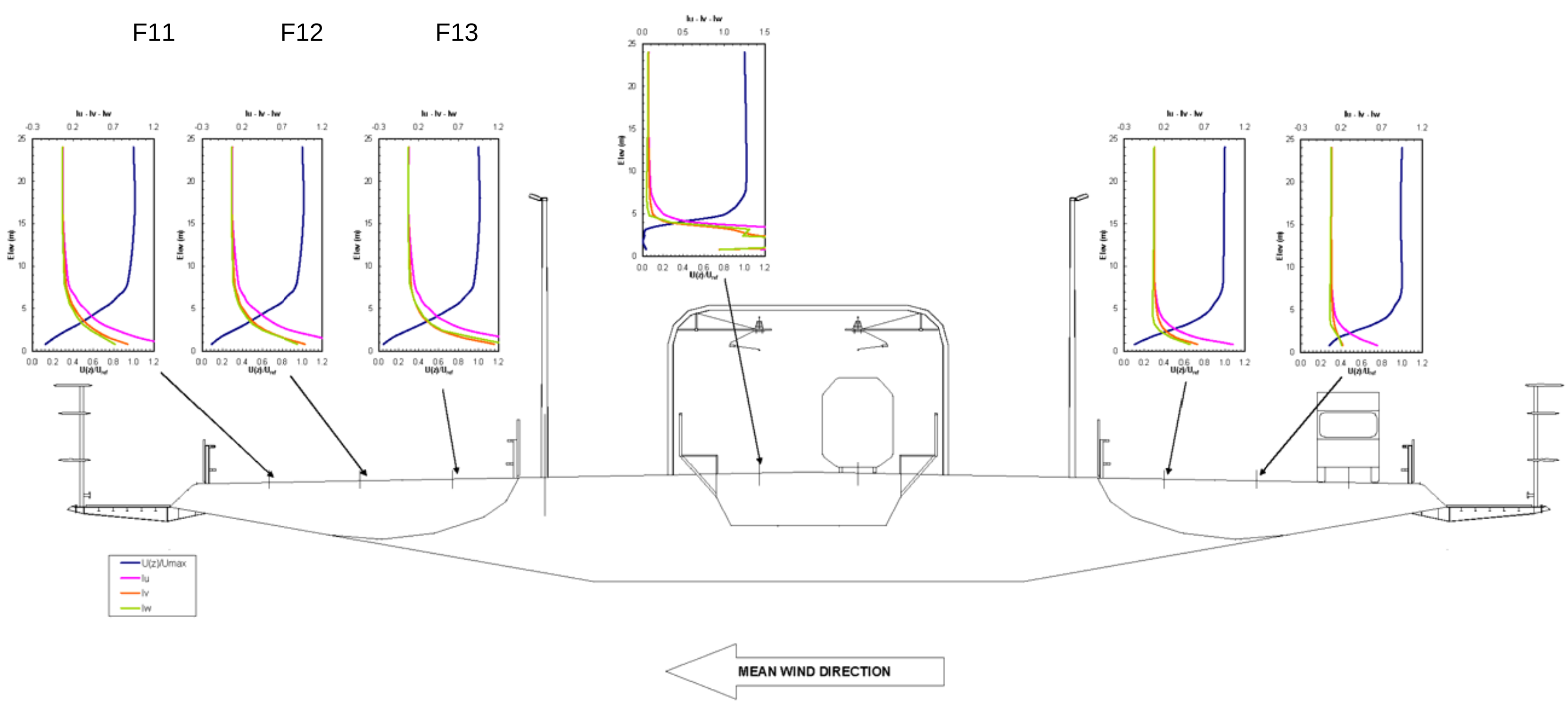

FIGURE F10 VELOCITY PROFILE FOR TRAFFIC LANES FOR TRAFFIC CONDITION 1 – KEY TO MEASUREMENTS

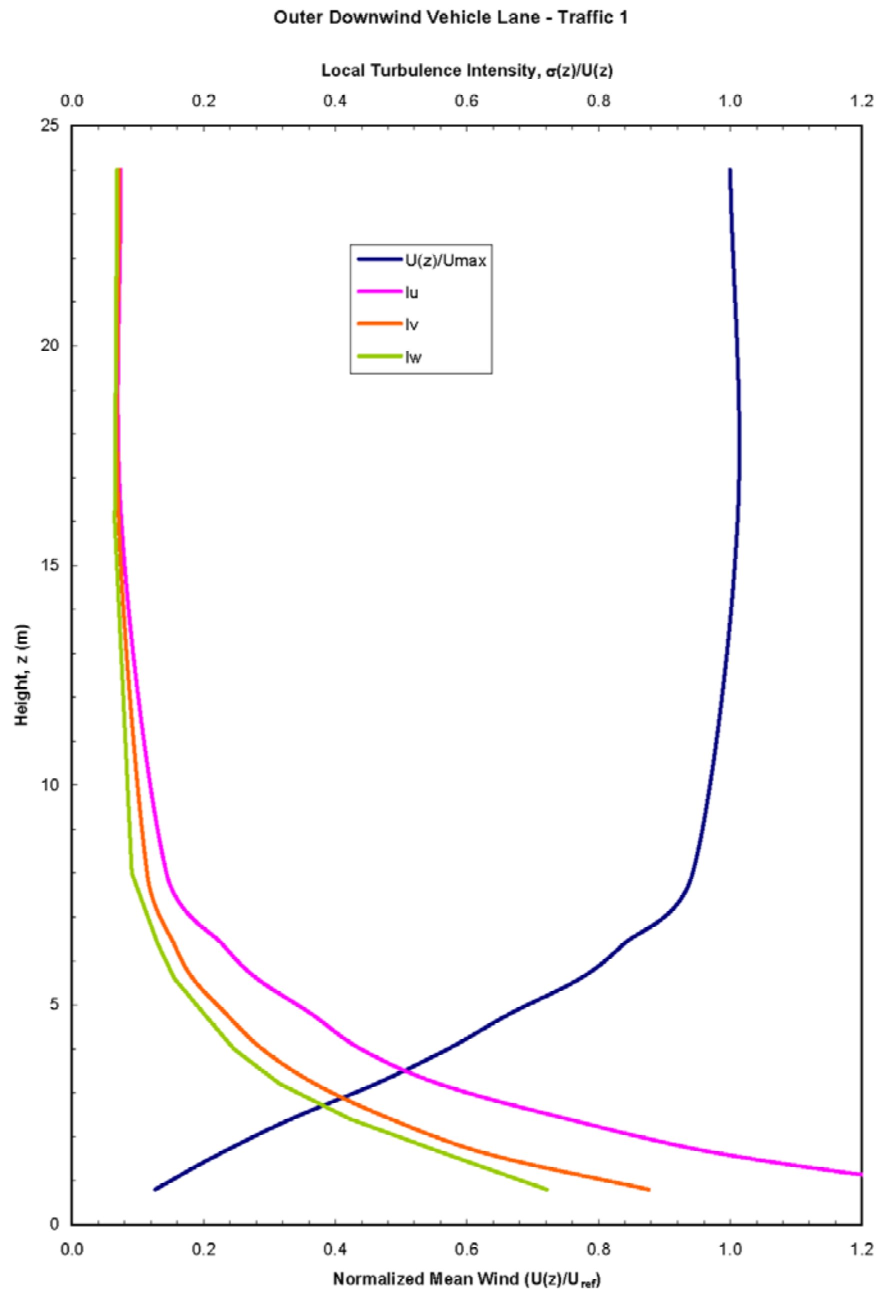

FIGURE F11 VELOCITY PROFILE IN OUTER (SLOW) LANE ON DOWNWIND GIRDER TRAFFIC CONDITION 1

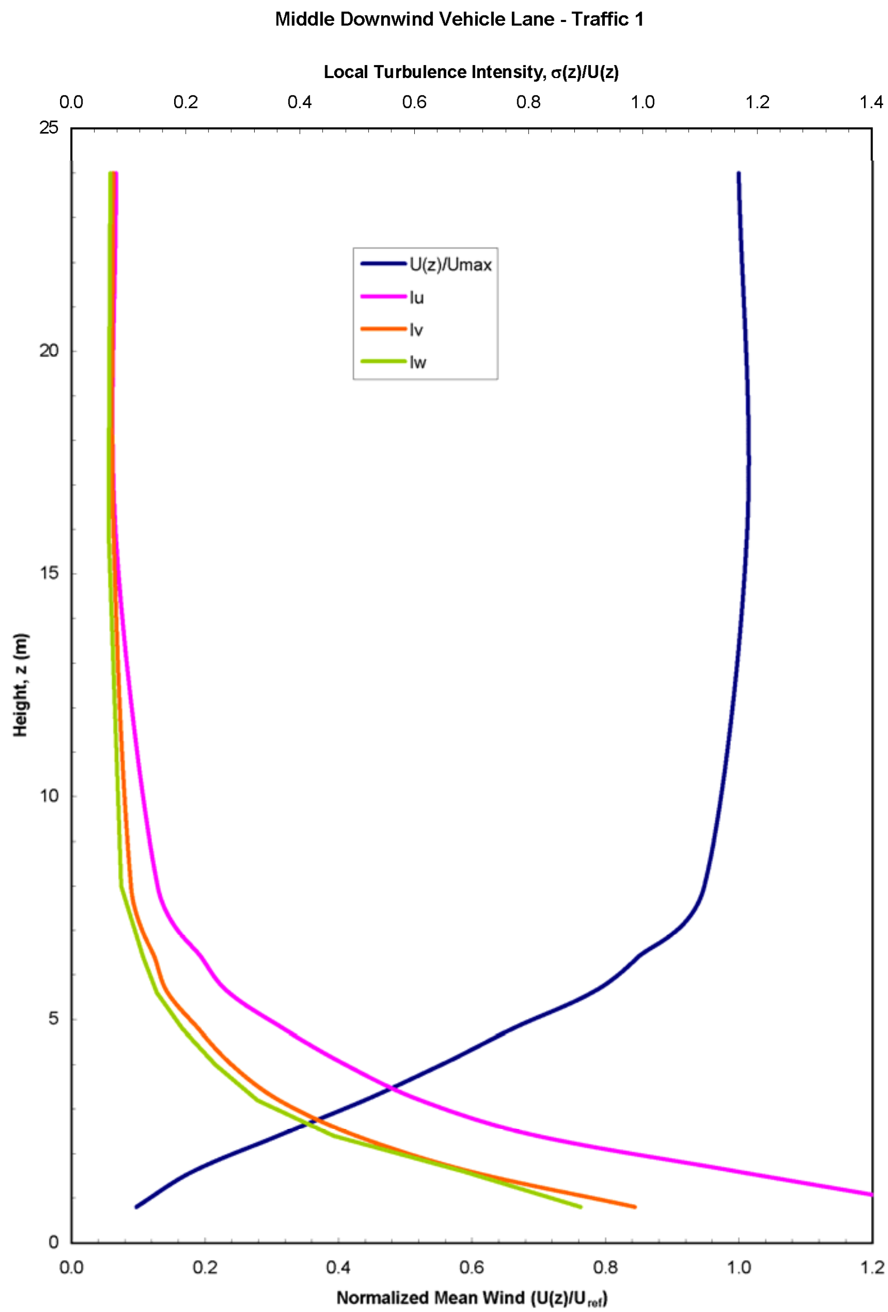

FIGURE F12 VELOCITY PROFILE IN MIDDLE LANE ON DOWNWIND GIRDER TRAFFIC CONDITION 1

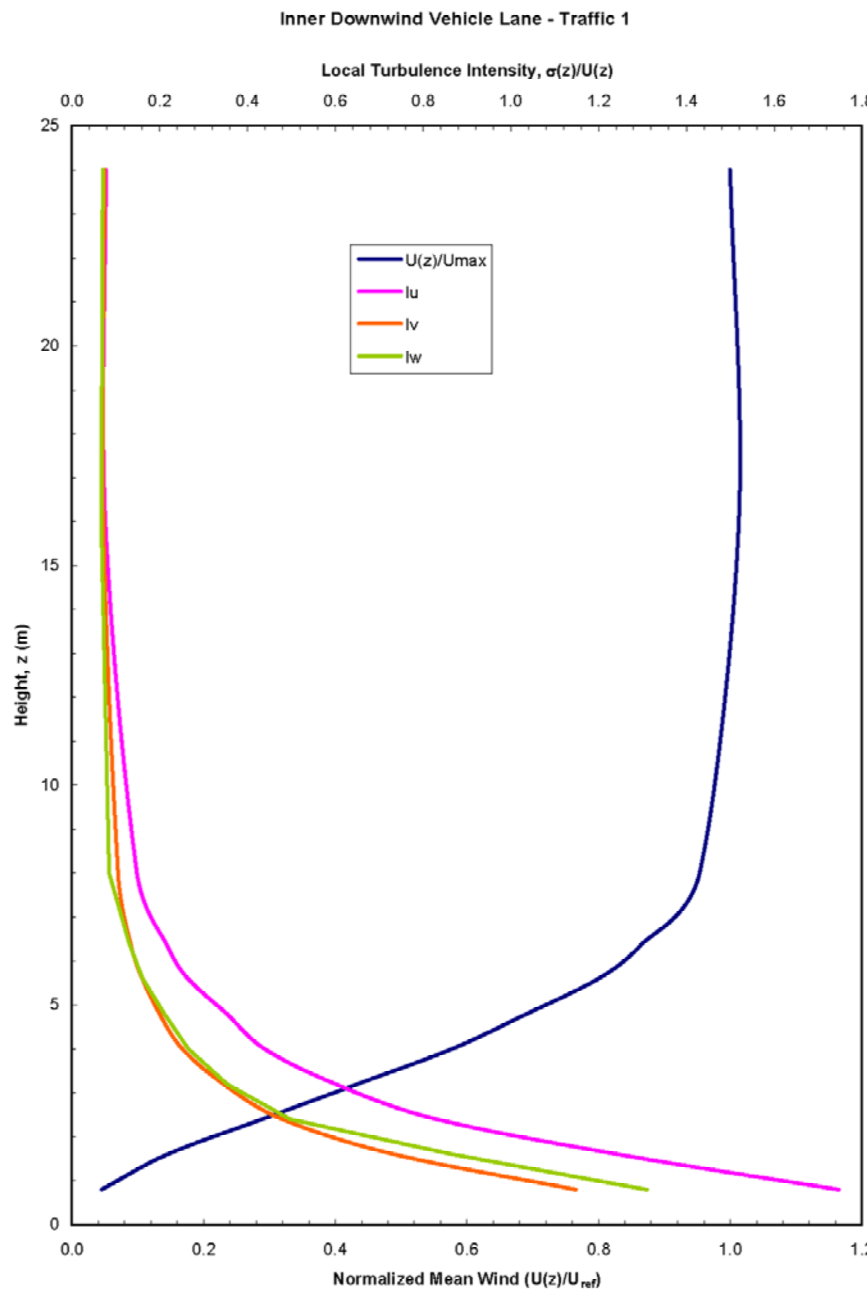

FIGURE F13 VELOCITY PROFILE IN INNER (FAST) LANE ON DOWNWIND GIRDER TRAFFIC CONDITION 1

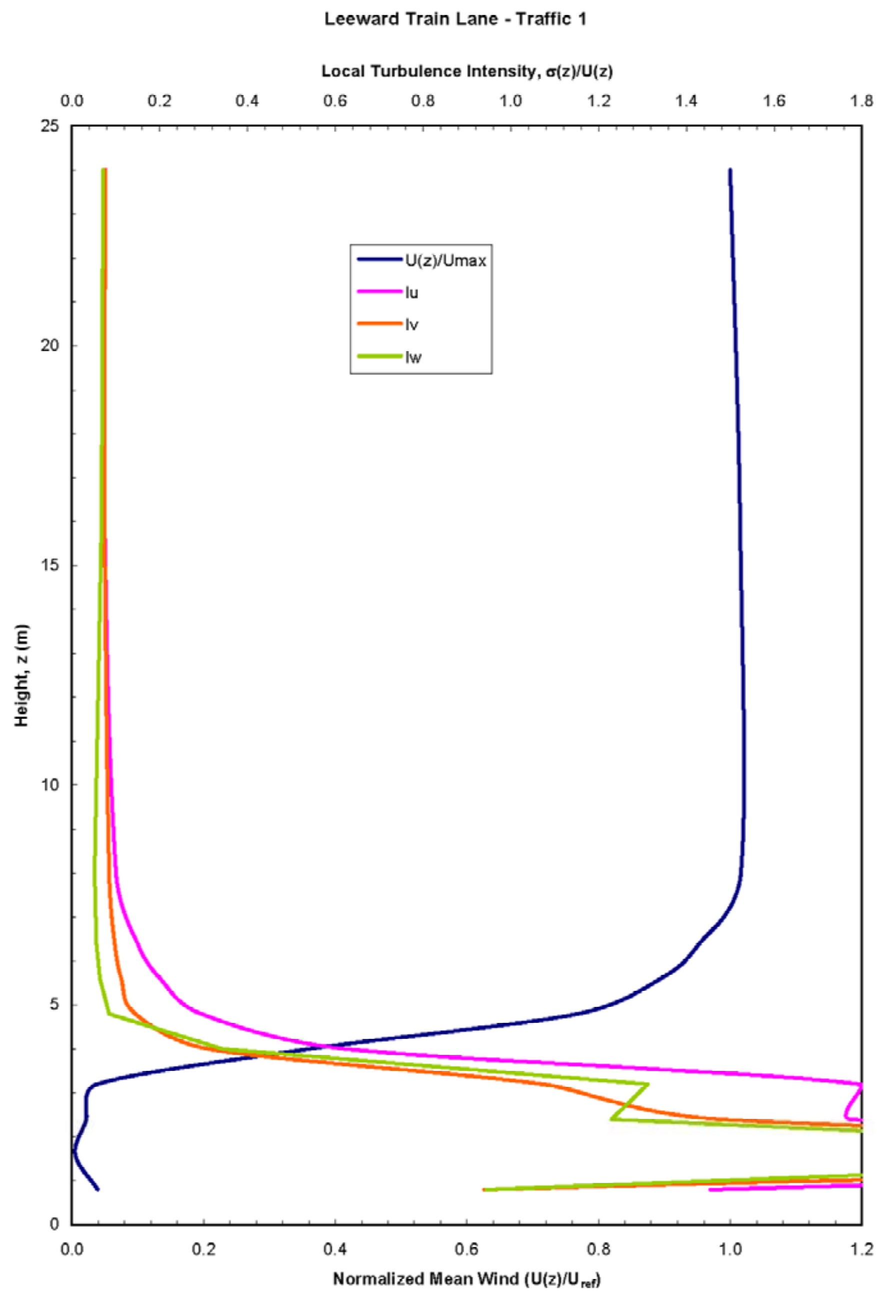

FIGURE F14 VELOCITY PROFILE IN LEEWARD TRACK ON RAIL GIRDER TRAFFIC CONDITION 1

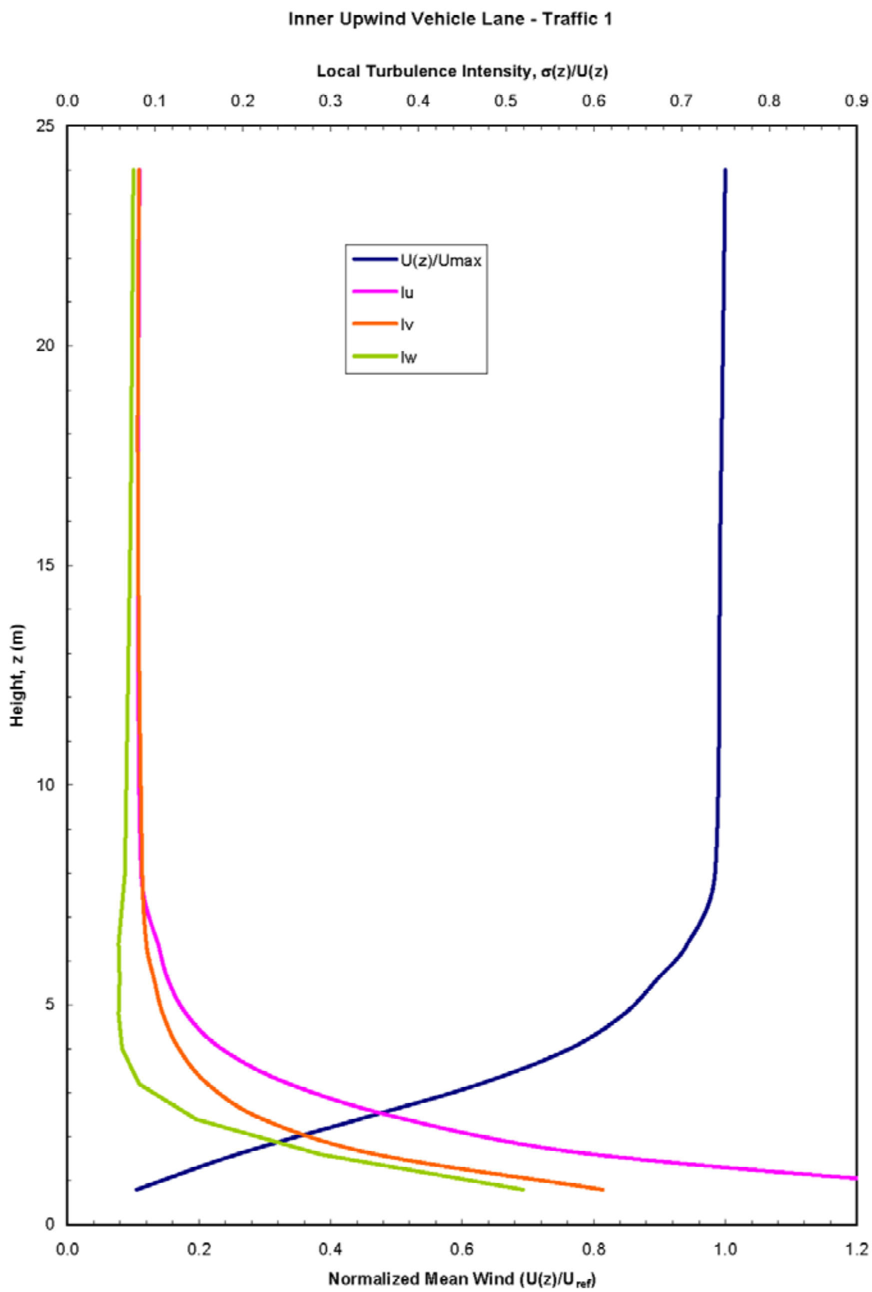

FIGURE F15 VELOCITY PROFILE IN INNER (FAST) LANE ON WINDWARD GIRDER TRAFFIC CONDITION 1

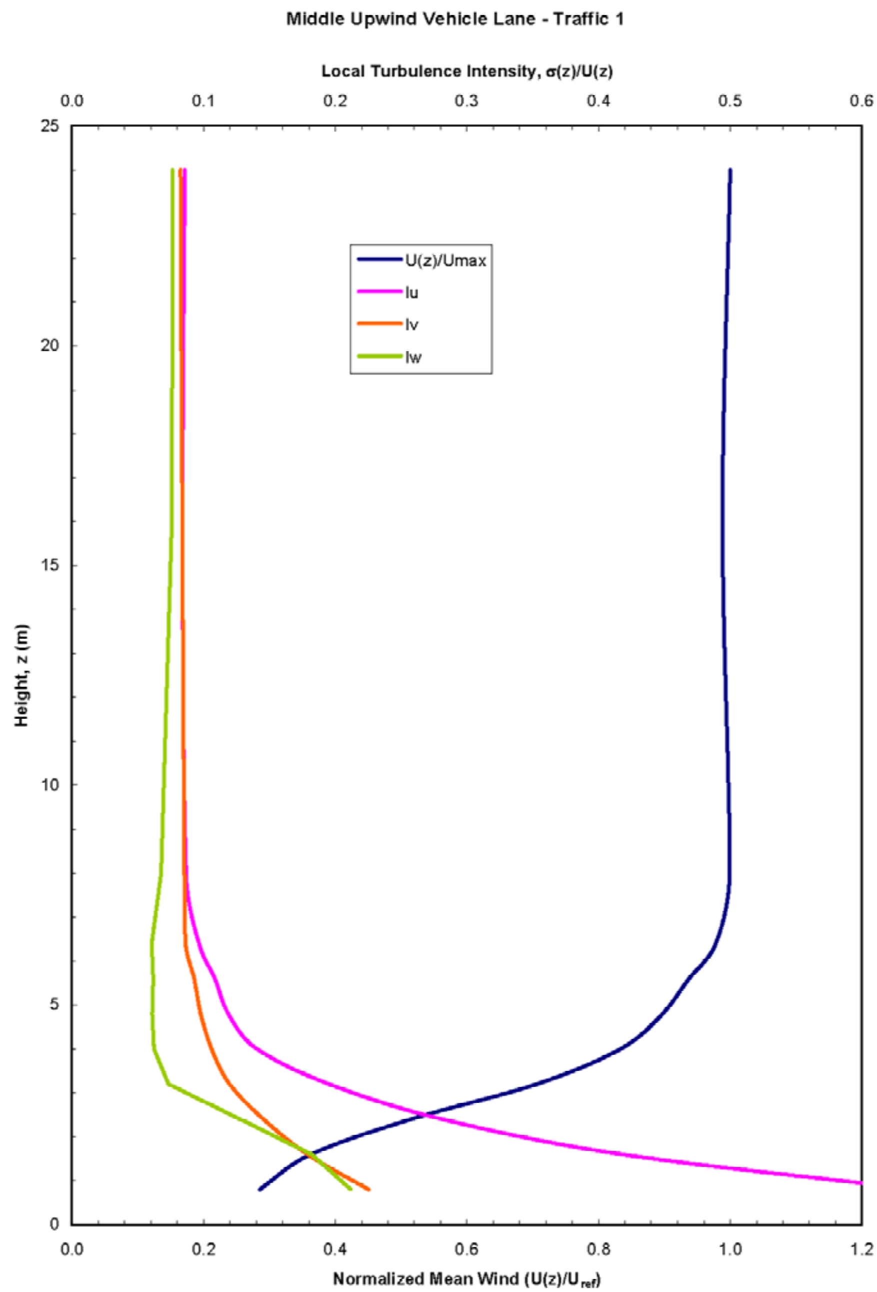

FIGURE F16 VELOCITY PROFILE IN MIDDLE LANE ON WINDWARD GIRDER TRAFFIC CONDITION 1

Traffic 2 - Bridge Deck Profiles

z (m)	Outer Downwind Vehicle Lane, U_{max}/U_{ref} = 0.968				Middle Downwind Vehicle Lane, U_{max}/U_{ref} = 0.972				Inner Downwind Vehicle Lane, U_{max}/U_{ref} = 0.967			
	$U(z)/U_{max}$	I_u	I_v	I_w	$U(z)/U_{max}$	I_u	I_v	I_w	$U(z)/U_{max}$	I_u	I_v	I_w
0.8					0.079	1.685	1.068	1.025	0.036	1.938	1.289	1.417
1.6					0.155	1.239	0.766	0.748	0.121	1.379	0.839	1.013
2.4					0.275	0.896	0.538	0.488	0.252	0.894	0.542	0.590
3.2					0.414	0.623	0.378	0.323	0.408	0.622	0.377	0.402
4					0.534	0.482	0.285	0.244	0.541	0.471	0.279	0.300
4.8					0.661	0.369	0.218	0.183	0.670	0.361	0.210	0.227
5.6					0.765	0.284	0.174	0.144	0.779	0.278	0.165	0.172
6.4					0.844	0.222	0.147	0.115	0.856	0.225	0.139	0.131
8					0.949	0.137	0.108	0.078	0.955	0.142	0.104	0.082
16					1.012	0.076	0.071	0.065	1.015	0.076	0.073	0.067
24					1.000	0.075	0.073	0.070	1.000	0.078	0.075	0.069

z (m)	Leeward Train Lane, U_{max}/U_{ref} = 0.978				Windward Train Lane, U_{max}/U_{ref} = 0.975			
	$U(z)/U_{max}$	I_u	I_v	I_w	$U(z)/U_{max}$	I_u	I_v	I_w
0.8	0.026	1.798	1.130	1.185				
1.6	0.008	2.979	2.471	2.224				
2.4	0.021	1.747	1.348	1.218				
3.2	0.044	1.790	1.001	1.320				
4	0.382	0.618	0.303	0.312				
4.8	0.764	0.295	0.150	0.086				
5.6	0.889	0.201	0.118	0.064				
6.4	0.947	0.154	0.106	0.058				
8	1.015	0.101	0.086	0.052				
16	1.009	0.076	0.074	0.068				
24	1.000	0.080	0.076	0.072				

z (m)	Inner Upwind Vehicle Lane, U_{max}/U_{ref} = 0.949				Middle Upwind Vehicle Lane, U_{max}/U_{ref} = 0.946				Outer Upwind Vehicle Lane, U_{max}/U_{ref} = 0.935			
	$U(z)/U_{max}$	I_u	I_v	I_w	$U(z)/U_{max}$	I_u	I_v	I_w	$U(z)/U_{max}$	I_u	I_v	I_w
0.8	0.107	0.941	0.574	0.466	0.137	0.617	0.478	0.370	0.137	0.611	0.526	0.367
1.6	0.228	0.643	0.380	0.317	0.245	0.558	0.365	0.332	0.269	0.425	0.322	0.274
2.4	0.409	0.432	0.250	0.176	0.468	0.362	0.212	0.143	0.583	0.233	0.154	0.070
3.2	0.581	0.300	0.178	0.103	0.669	0.226	0.148	0.079	0.751	0.161	0.122	0.075
4	0.729	0.204	0.140	0.071	0.787	0.164	0.120	0.067	0.850	0.142	0.105	0.061
4.8	0.820	0.149	0.117	0.063	0.864	0.132	0.106	0.065	0.898	0.116	0.096	0.066
5.6	0.883	0.125	0.103	0.062	0.914	0.117	0.098	0.064	0.943	0.108	0.091	0.066
6.4	0.926	0.104	0.095	0.061	0.947	0.104	0.091	0.063	0.971	0.096	0.089	0.068
8	0.968	0.085	0.087	0.066	0.978	0.088	0.087	0.071	0.977	0.087	0.087	0.074
16	0.988	0.081	0.081	0.072	0.989	0.086	0.084	0.076	0.986	0.089	0.086	0.076
24	1.000	0.082	0.082	0.075	1.000	0.087	0.084	0.075	1.000	0.090	0.085	0.077

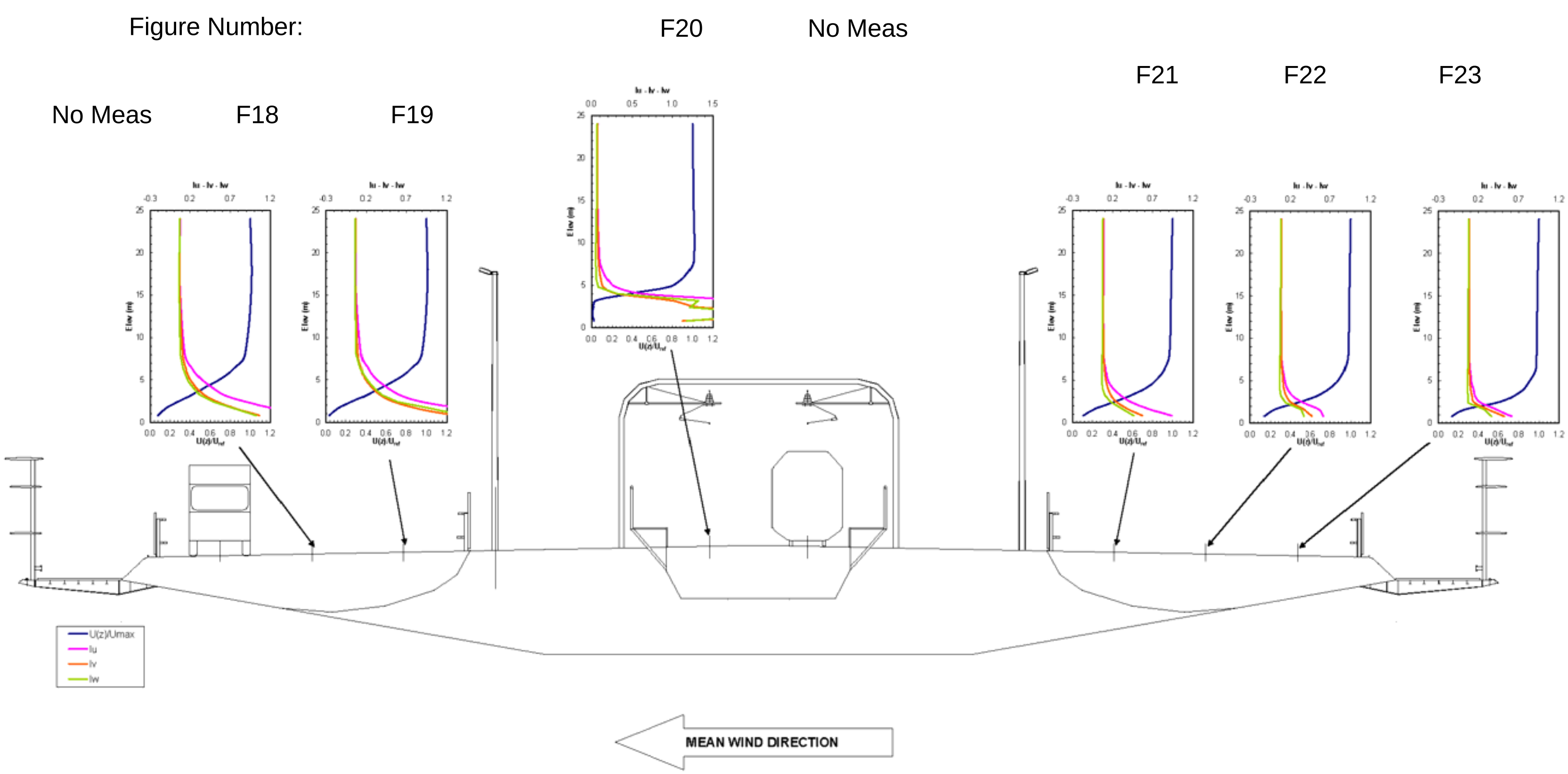

FIGURE F17 VELOCITY PROFILE FOR TRAFFIC LANES FOR TRAFFIC CONDITION 2 – KEY TO MEASUREMENTS

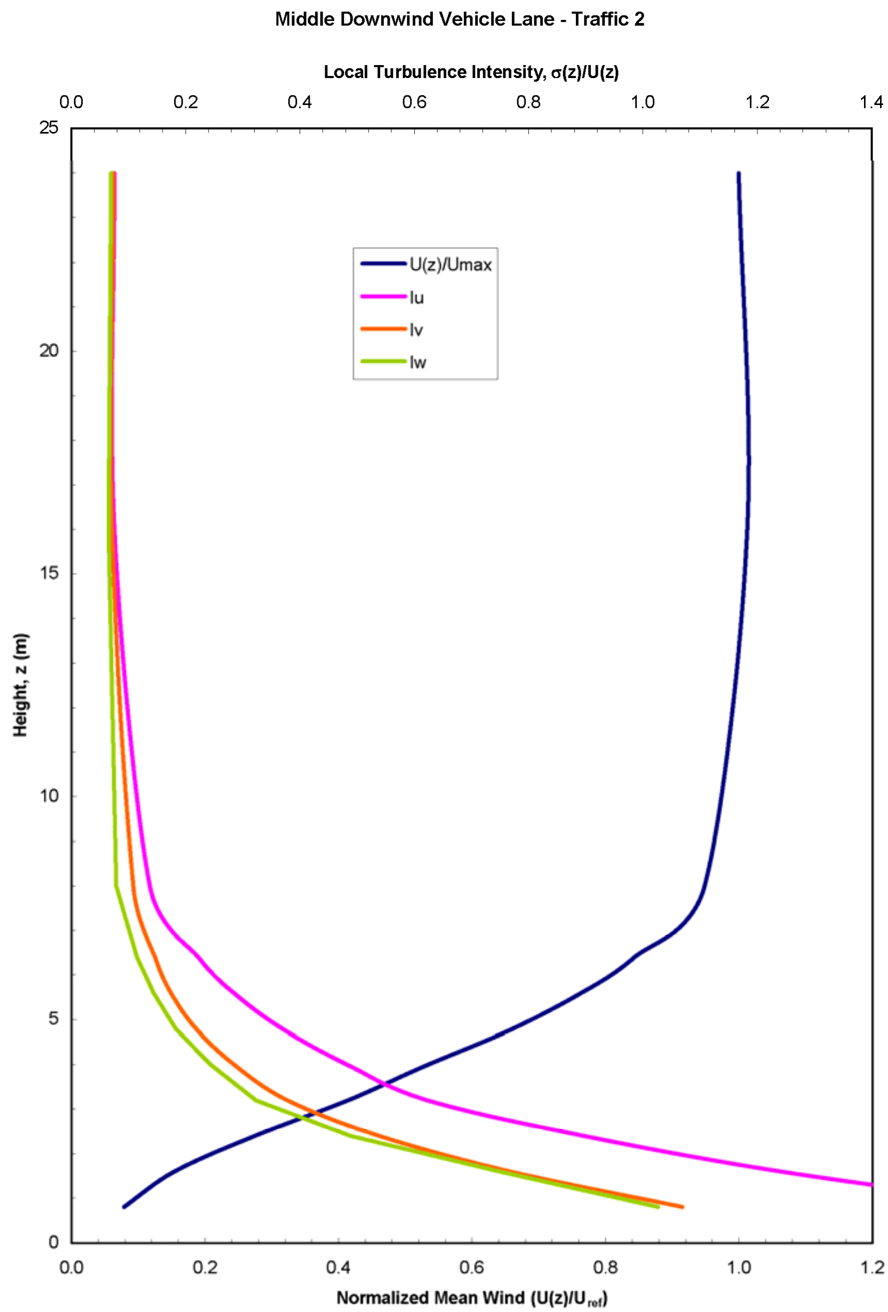

FIGURE F18 VELOCITY PROFILE IN MIDDLE LANE ON DOWNWIND GIRDER TRAFFIC CONDITION 2

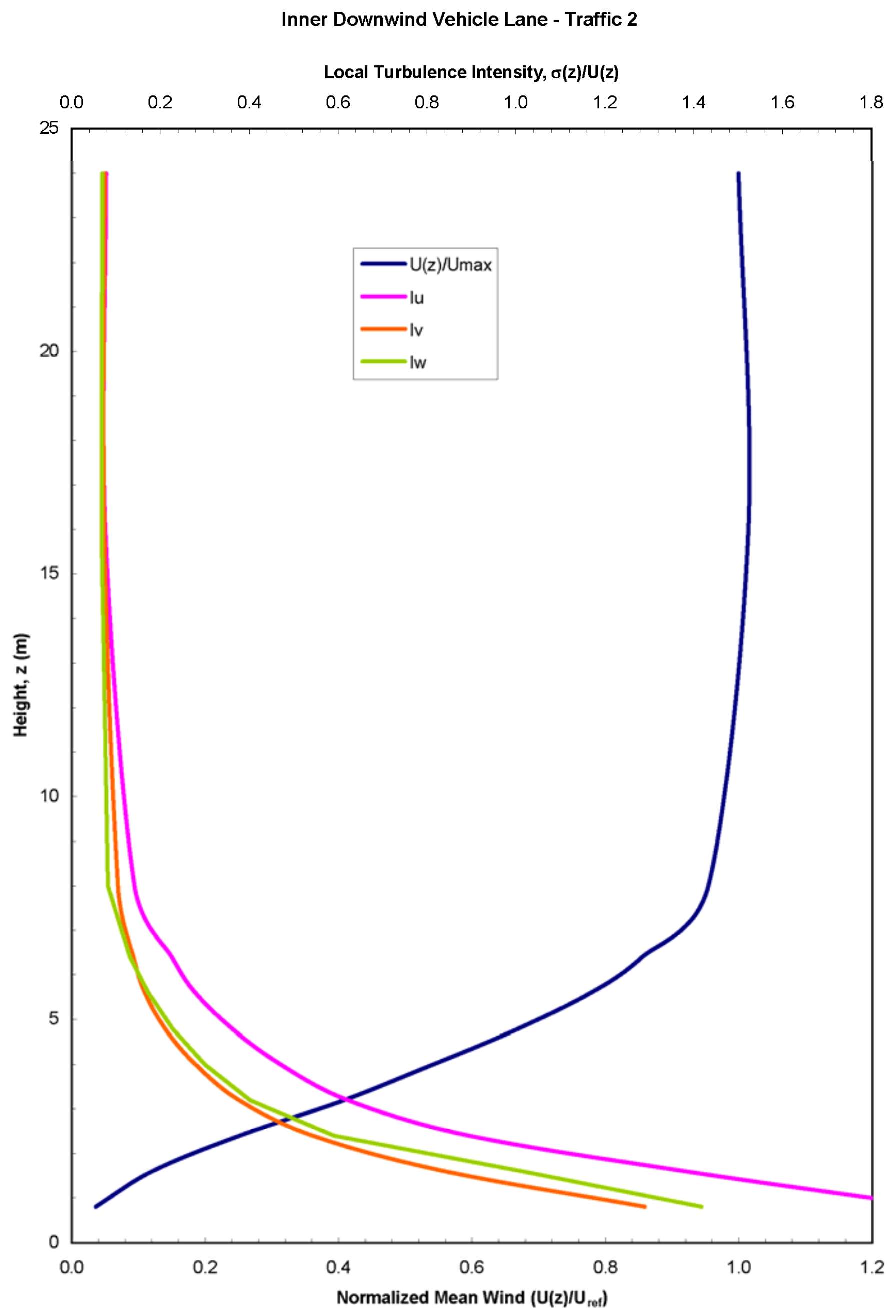

FIGURE F19 VELOCITY PROFILE IN INNER (FAST) LANE ON DOWNWIND GIRDER TRAFFIC CONDITION 2

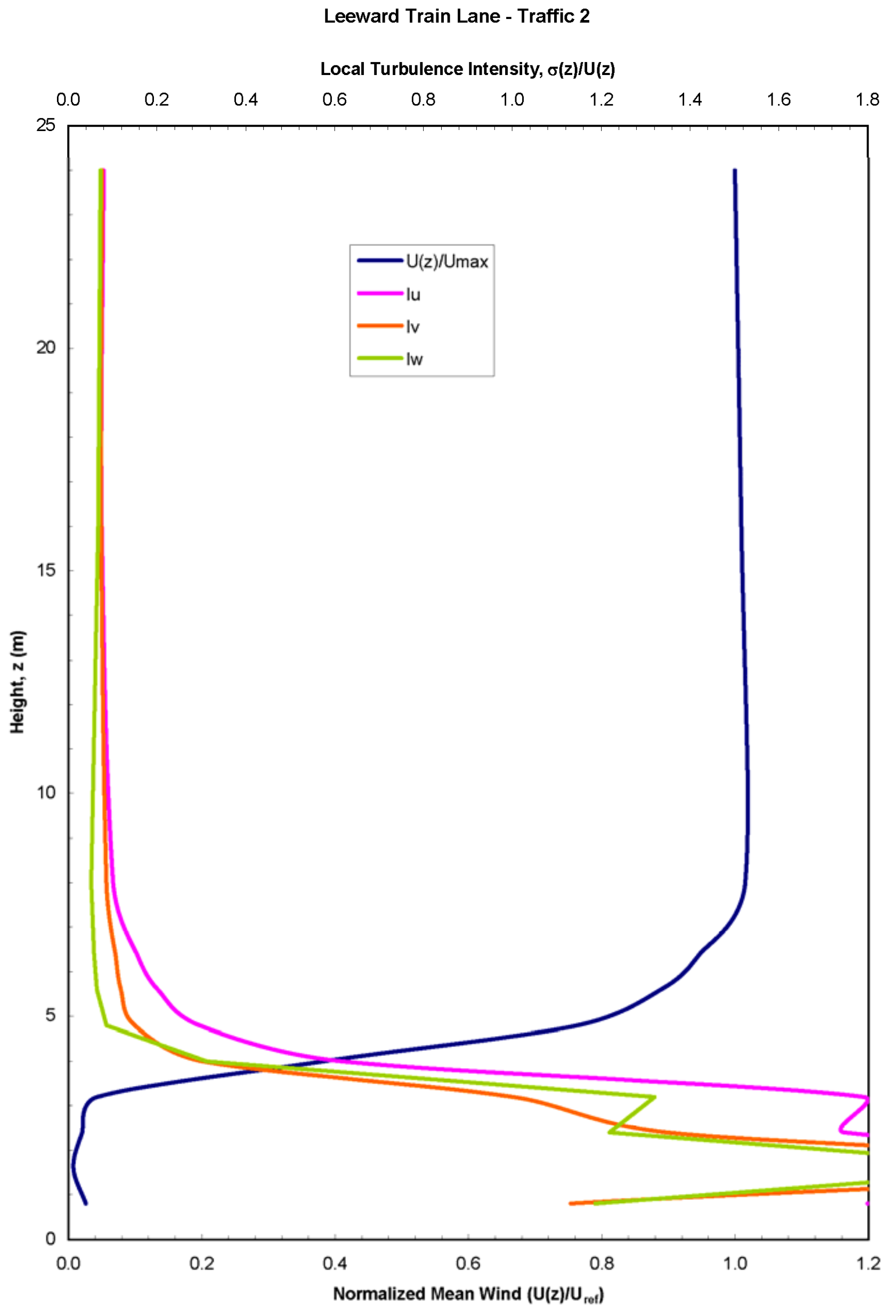

FIGURE F20 VELOCITY PROFILE IN LEEWARD TRACK ON RAIL GIRDER TRAFFIC CONDITION 2

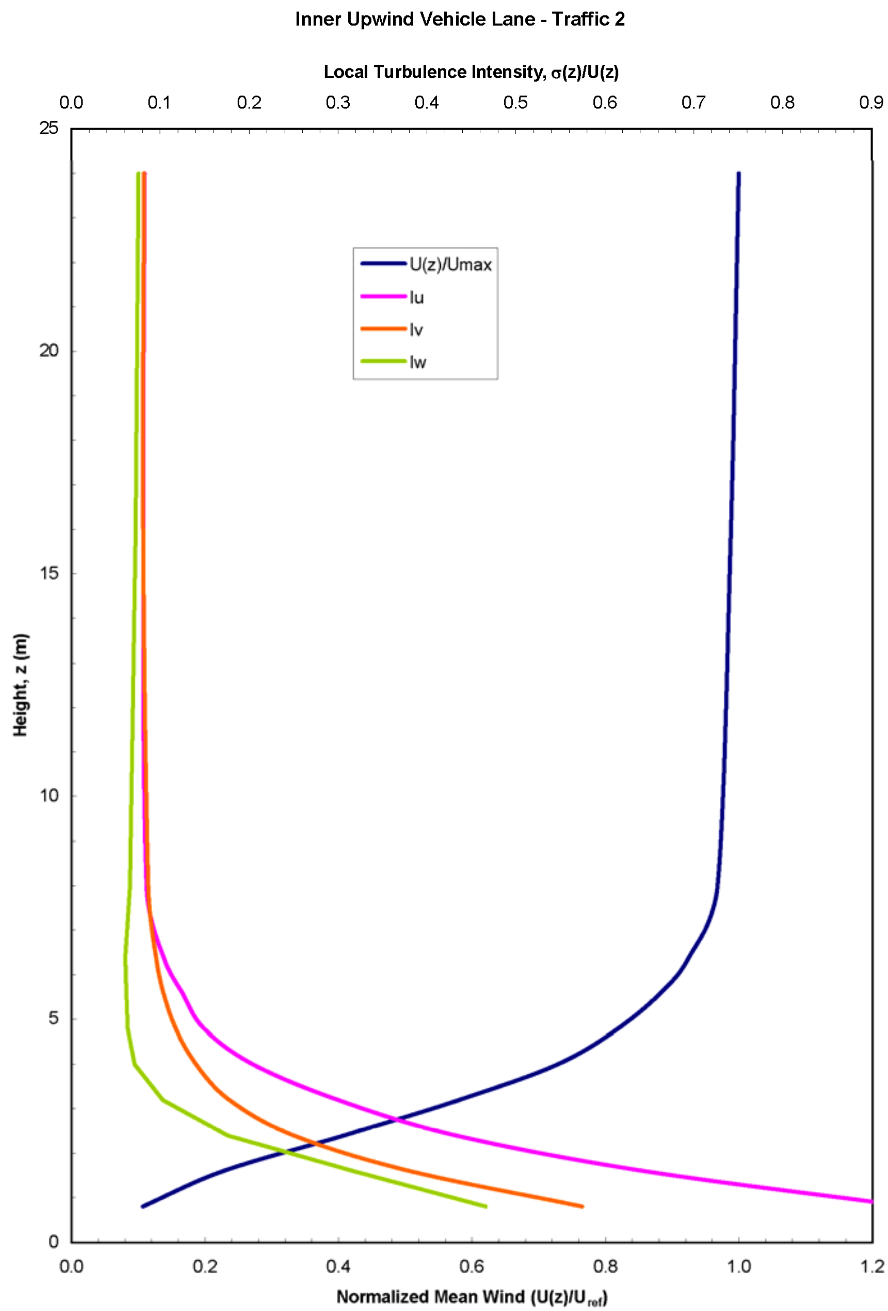

FIGURE F21 VELOCITY PROFILE IN INNER (FAST) LANE ON UPWIND GIRDER TRAFFIC CONDITION 2

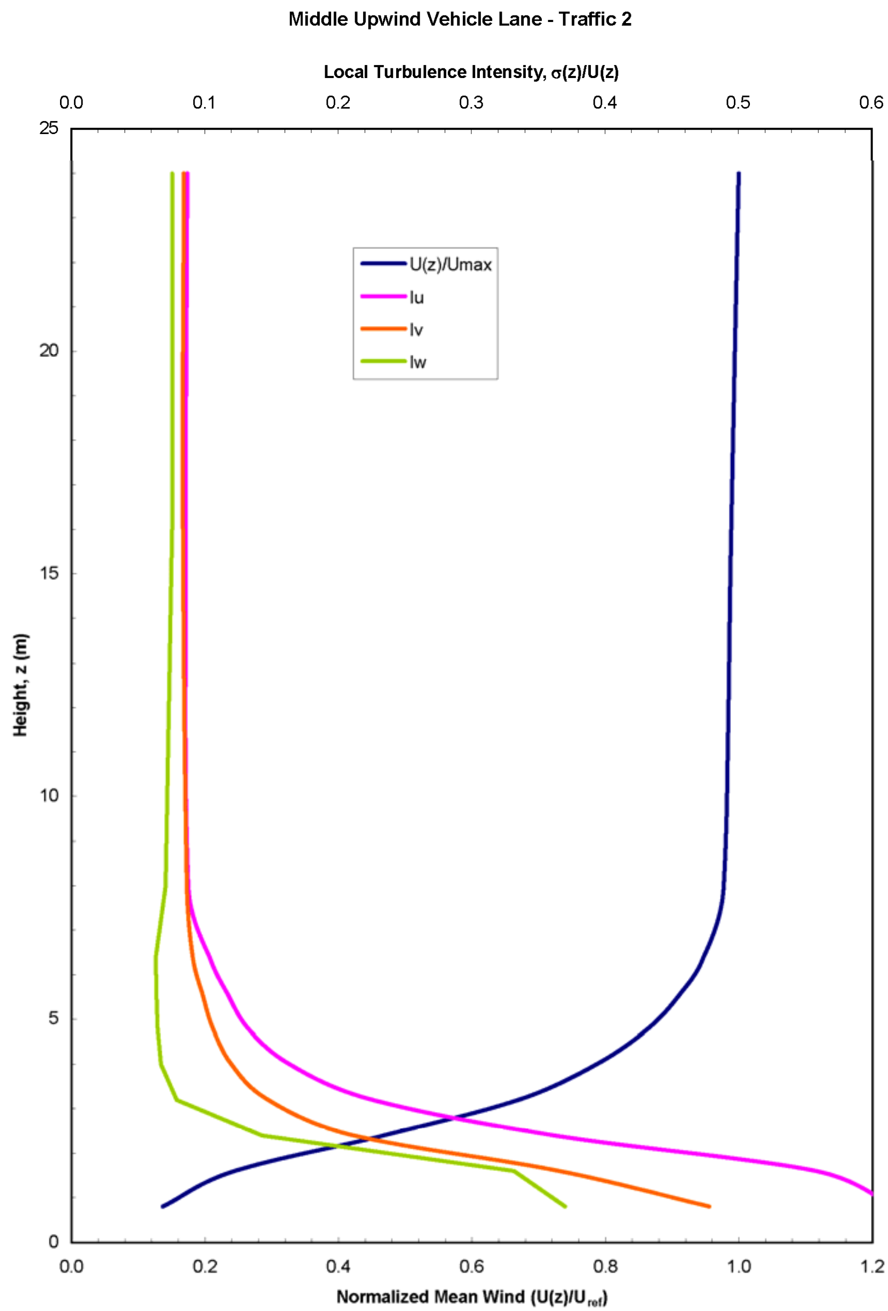

FIGURE F22 VELOCITY PROFILE IN MIDDLE LANE ON UPWIND GIRDER TRAFFIC CONDITION 2

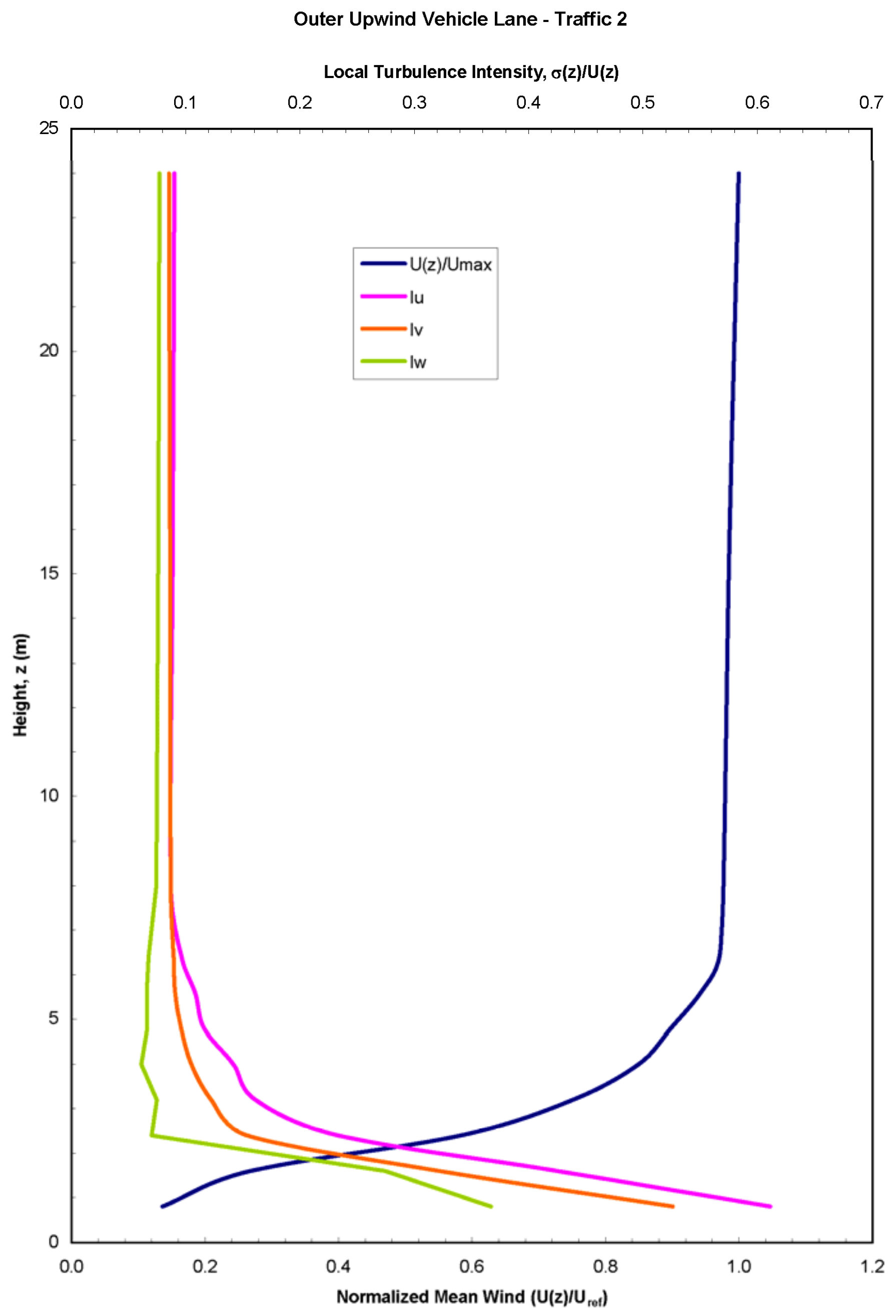

FIGURE F23 VELOCITY PROFILE IN OUTER (SLOW) LANE ON UPWIND GIRDER TRAFFIC CONDITION 2

Traffic 3 - Bridge Deck Profiles

z (m)	Outer Downwind Vehicle Lane, U_{max}/U_{ref} = 0.968				Middle Downwind Vehicle Lane, U_{max}/U_{ref} = 0.972				Inner Downwind Vehicle Lane, U_{max}/U_{ref} = 0.967			
	$U(z)/U_{max}$	I_u	I_v	I_w	$U(z)/U_{max}$	I_u	I_v	I_w	$U(z)/U_{max}$	I_u	I_v	I_w
0.8	0.122	1.423	0.910	0.723	0.084	1.625	1.047	0.994	0.036	1.834	1.187	1.348
1.6	0.218	1.019	0.650	0.580	0.169	1.191	0.732	0.727	0.112	1.395	0.846	0.973
2.4	0.331	0.743	0.476	0.424	0.292	0.840	0.524	0.488	0.241	0.911	0.527	0.554
3.2	0.462	0.539	0.351	0.303	0.420	0.622	0.376	0.347	0.394	0.629	0.355	0.373
4	0.580	0.429	0.278	0.238	0.555	0.466	0.283	0.254	0.537	0.465	0.271	0.279
4.8	0.682	0.342	0.221	0.189	0.681	0.362	0.212	0.189	0.663	0.360	0.209	0.215
5.6	0.768	0.280	0.181	0.154	0.776	0.286	0.173	0.148	0.768	0.287	0.170	0.166
6.4	0.839	0.227	0.152	0.126	0.856	0.230	0.143	0.117	0.848	0.233	0.140	0.122
8	0.936	0.151	0.113	0.090	0.951	0.152	0.111	0.085	0.950	0.153	0.109	0.077
16	1.012	0.076	0.074	0.064	1.016	0.076	0.074	0.066	1.008	0.074	0.074	0.067
24	1.000	0.075	0.076	0.070	1.000	0.079	0.076	0.071	1.000	0.076	0.073	0.070

z (m)	Leeward Train Lane, U_{max}/U_{ref} = 0.978				Windward Train Lane, U_{max}/U_{ref} = 0.975			
	$U(z)/U_{max}$	I_u	I_v	I_w	$U(z)/U_{max}$	I_u	I_v	I_w
0.8	0.047	1.182	0.782	0.853				
1.6	0.003	5.371	5.086	2.384				
2.4	0.007	3.700	3.406	1.802				
3.2	0.030	2.202	1.372	1.496				
4	0.357	0.635	0.335	0.359				
4.8	0.765	0.294	0.155	0.091				
5.6	0.896	0.192	0.114	0.063				
6.4	0.957	0.155	0.100	0.056				
8	1.018	0.099	0.083	0.052				
16	1.010	0.076	0.074	0.067				
24	1.000	0.080	0.075	0.071				

z (m)	Inner Upwind Vehicle Lane, U_{max}/U_{ref} = 0.949				Middle Upwind Vehicle Lane, U_{max}/U_{ref} = 0.946				Outer Upwind Vehicle Lane, U_{max}/U_{ref} = 0.935			
	$U(z)/U_{max}$	I_u	I_v	I_w	$U(z)/U_{max}$	I_u	I_v	I_w	$U(z)/U_{max}$	I_u	I_v	I_w
0.8	0.110	0.953	0.570	0.507	0.144	0.590	0.453	0.359	0.141	0.620	0.509	0.362
1.6	0.251	0.611	0.370	0.310	0.247	0.556	0.364	0.325	0.256	0.400	0.322	0.268
2.4	0.422	0.425	0.239	0.169	0.448	0.376	0.217	0.149	0.569	0.244	0.156	0.065
3.2	0.606	0.285	0.171	0.100	0.651	0.240	0.148	0.079	0.741	0.159	0.127	0.075
4	0.737	0.203	0.139	0.075	0.780	0.162	0.118	0.064	0.838	0.143	0.106	0.059
4.8	0.834	0.147	0.114	0.065	0.850	0.132	0.107	0.063	0.894	0.113	0.094	0.066
5.6	0.893	0.119	0.102	0.062	0.900	0.118	0.096	0.062	0.934	0.102	0.089	0.067
6.4	0.939	0.105	0.093	0.063	0.937	0.106	0.091	0.063	0.963	0.091	0.087	0.070
8	0.974	0.083	0.084	0.067	0.973	0.085	0.083	0.070	0.976	0.082	0.085	0.075
16	0.990	0.079	0.082	0.073	0.979	0.086	0.083	0.075	0.981	0.086	0.084	0.077
24	1.000	0.083	0.081	0.075	1.000	0.085	0.082	0.075	1.000	0.085	0.083	0.077

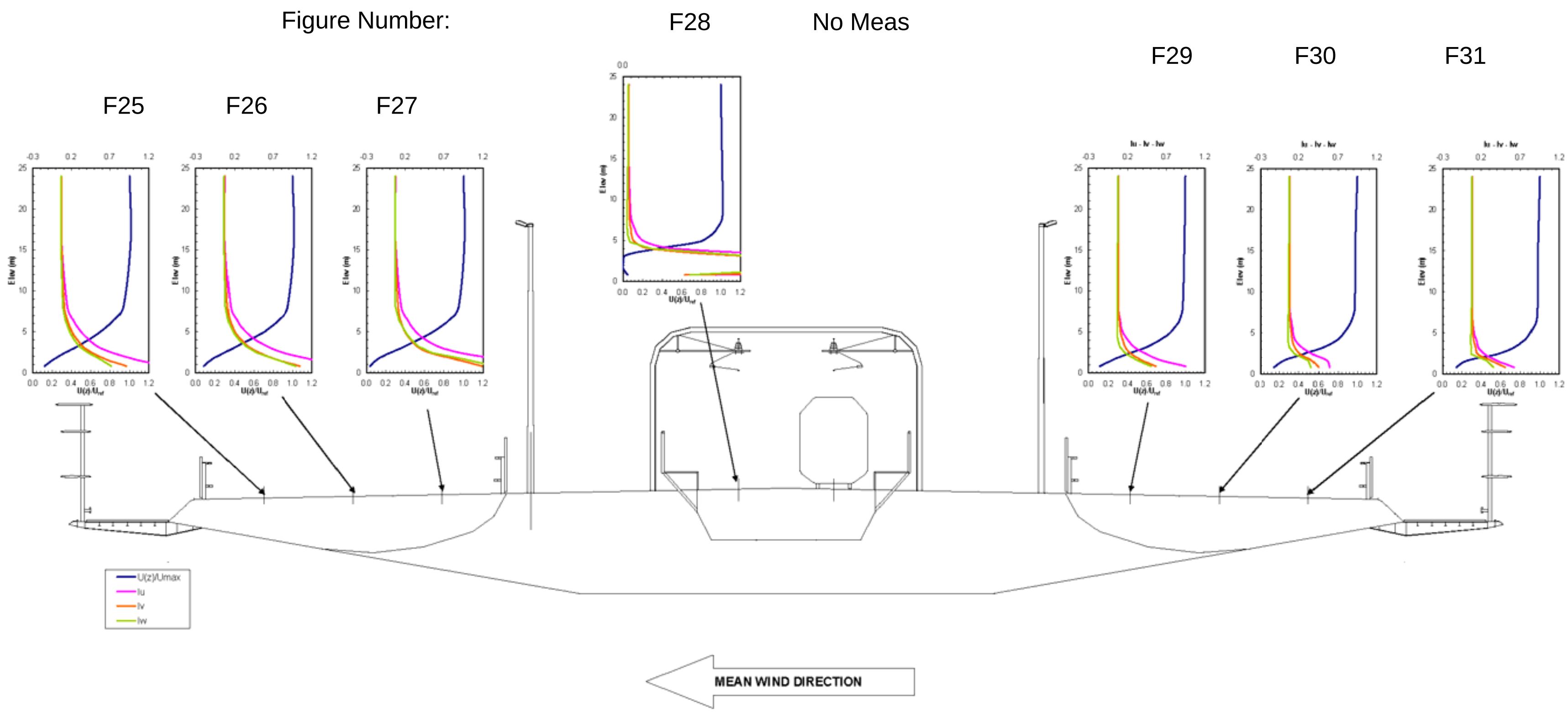

FIGURE F24 VELOCITY PROFILE FOR TRAFFIC LANES FOR TRAFFIC CONDITION 3 – KEY TO MEASUREMENTS

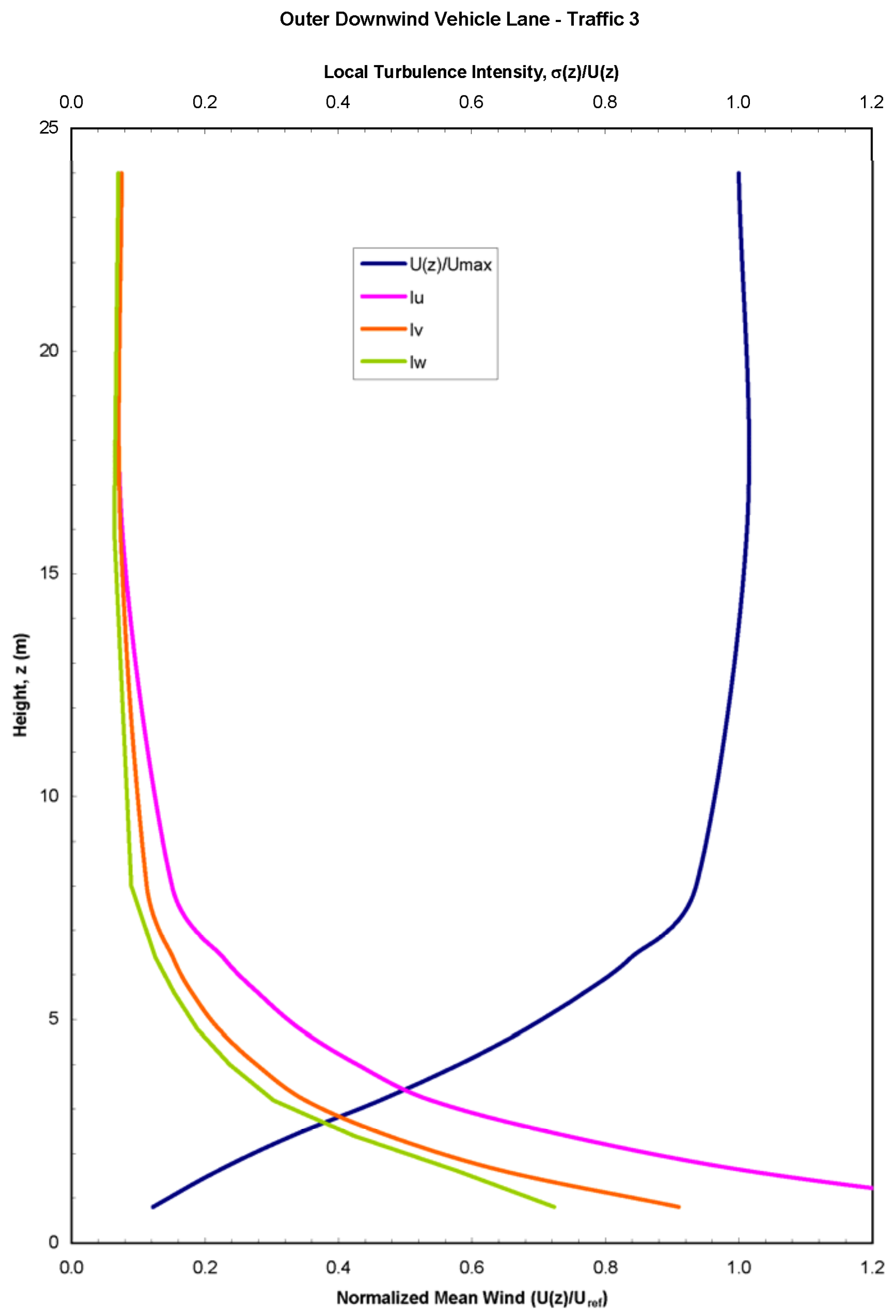

FIGURE F25 VELOCITY PROFILE IN OUTER (SLOW) LANE ON DOWNWIND GIRDER TRAFFIC CONDITION 3

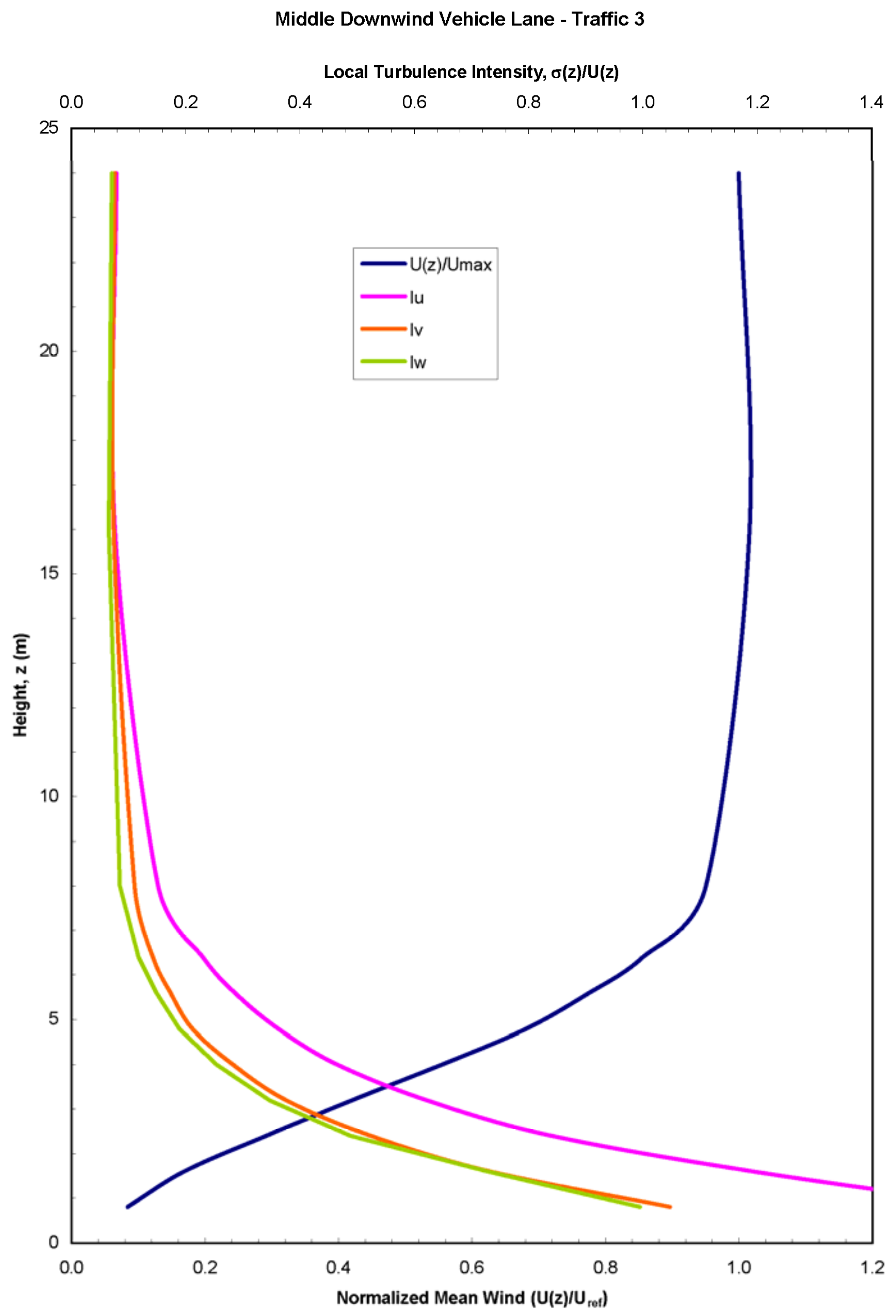

FIGURE F26 VELOCITY PROFILE IN MIDDLE LANE ON DOWNWIND GIRDER TRAFFIC CONDITION 3

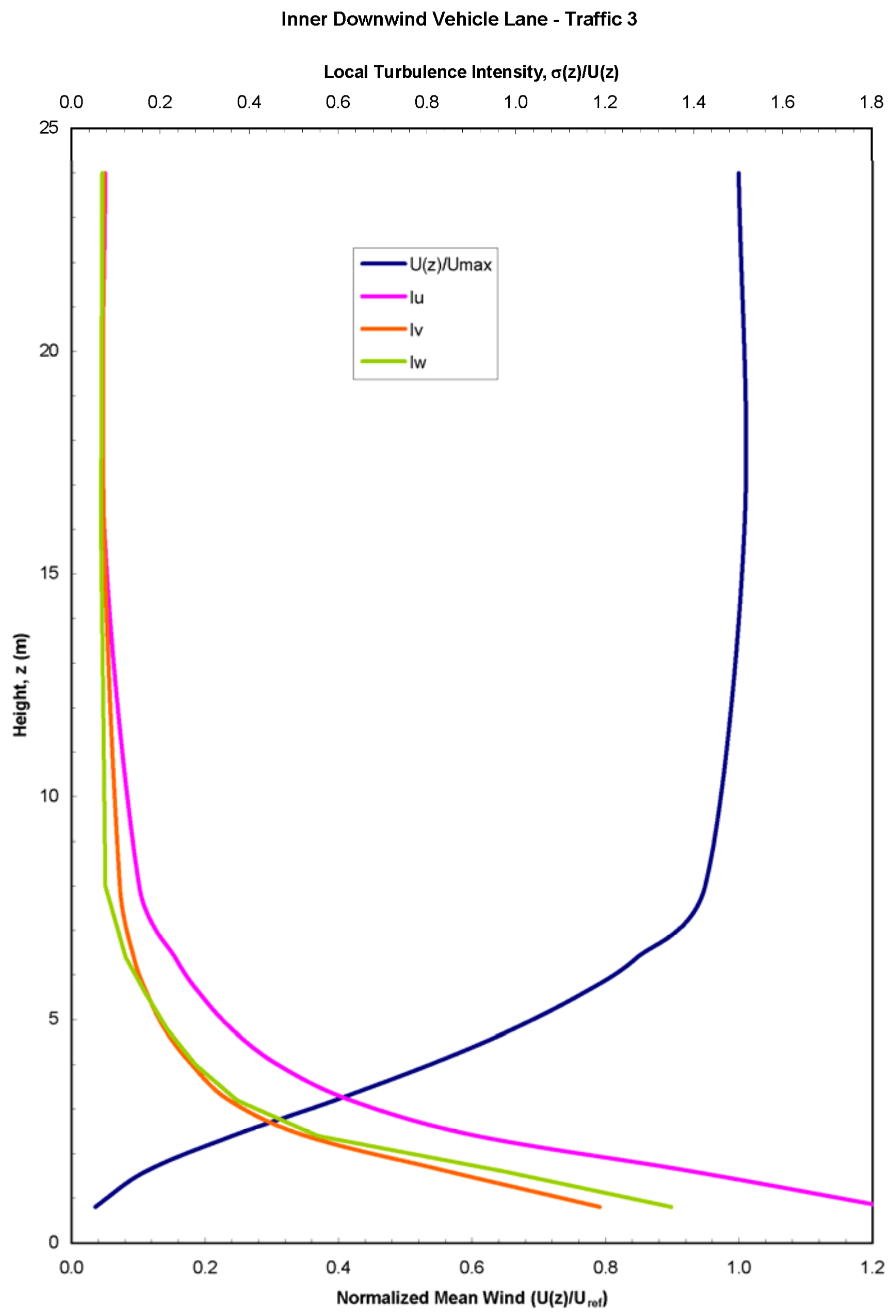

FIGURE F27 VELOCITY PROFILE IN INNER (FAST) LANE ON DOWNWIND GIRDER TRAFFIC CONDITION 3

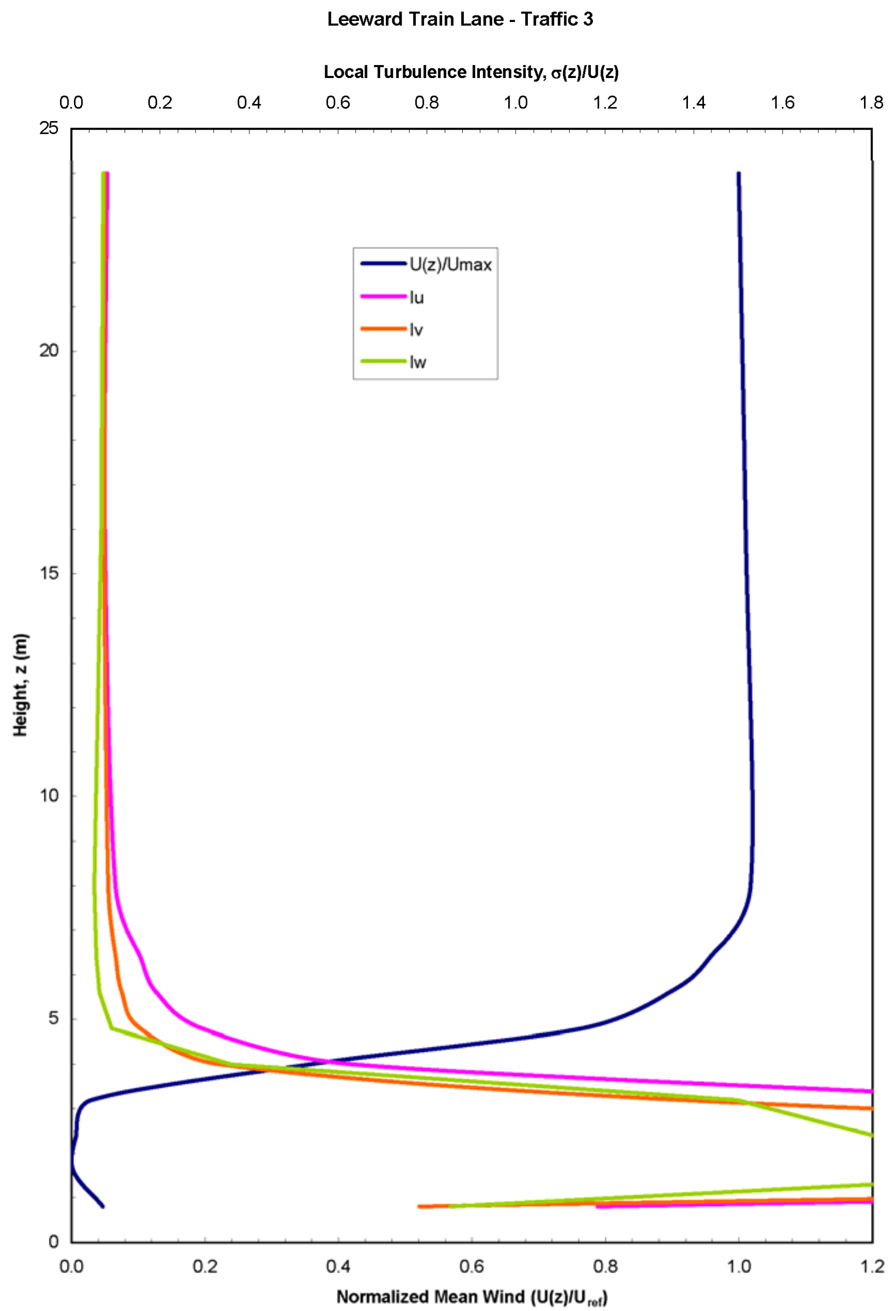

FIGURE F28 VELOCITY PROFILE IN LEEWARD TRACK ON RAIL GIRDER TRAFFIC CONDITION 3

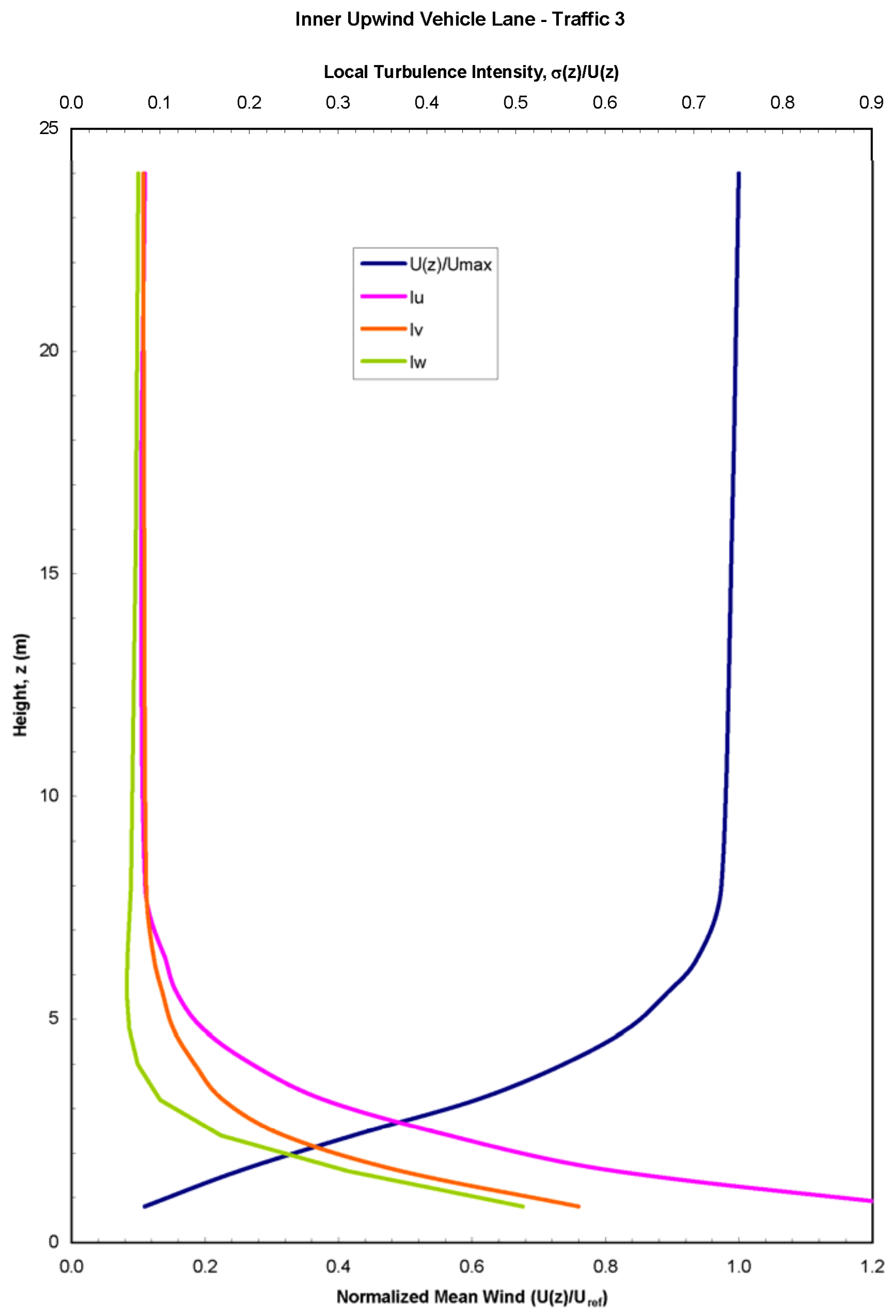

FIGURE F29 VELOCITY PROFILE IN INNER (FAST) LANE ON UPWIND GIRDER TRAFFIC CONDITION 3

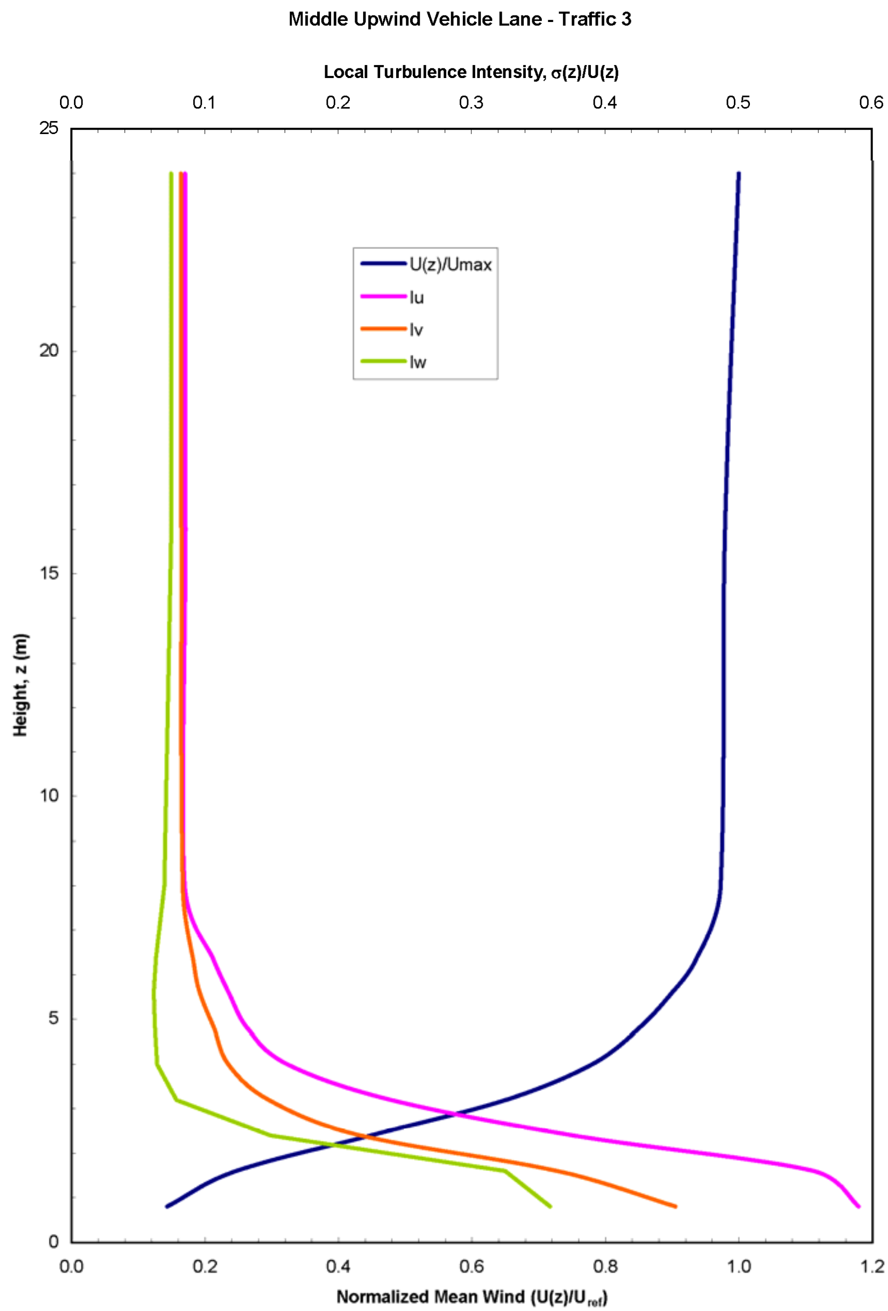

FIGURE F30 VELOCITY PROFILE IN MIDDLE LANE ON UPWIND GIRDER TRAFFIC CONDITION 3

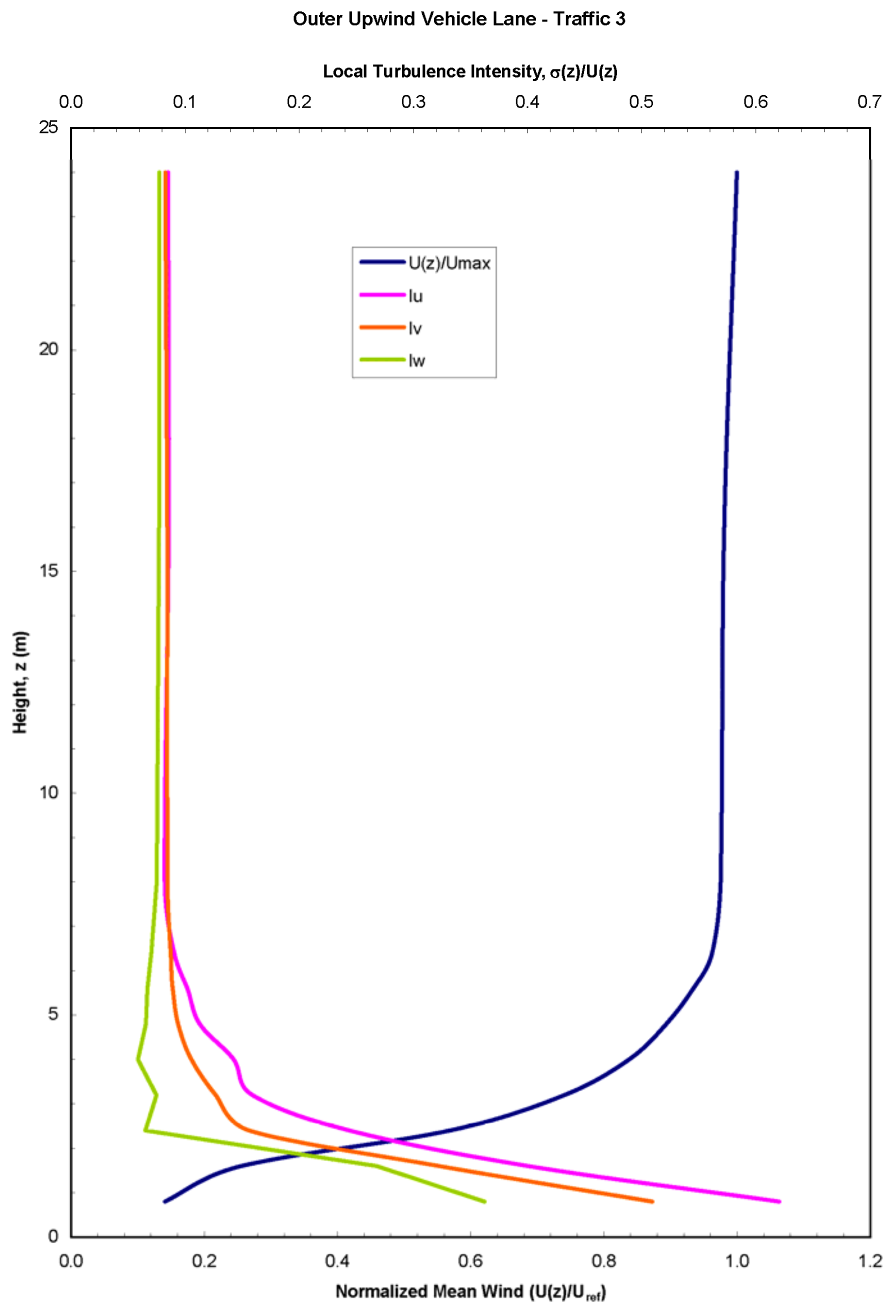

FIGURE F31 VELOCITY PROFILE IN OUTER (SLOW) LANE ON UPWIND GIRDER TRAFFIC CONDITION 3

APPENDIX G

RESULTS OF DYNAMIC SECTION MODEL TESTS, IN-SERVICE

Notes:

G1. The dynamic section model tests were performed for the in-service structure.

G2. The wind speed indicated is the mean hourly wind speed at the deck height in m/s. The bridge vertical and horizontal responses are presented as full scale responses (meters), while torsional response is given as deck rotation in degrees.

G3. Traffic Condition 2 was mistakenly performed as the “Road traffic in outward (slow) lane on windward girder” and omitted the train traffic in the dynamic section model tests. The tests for this condition are therefore referred to as Traffic Condition 2*.

G4. Tests were performed for the following conditions of the deck:

a. No Traffic,
b. Traffic Condition 1 - road traffic on outward (slow) lane upwind girder <u>plus</u> train on upwind track;
c. Traffic Condition 2* - road traffic on outward (slow) lane of upwind girder;
d. Traffic Condition 3 - train on upwind track only

TABLE G1 DYNAMIC SECTION MODEL TESTS OF THE COMPLETED DECK (DRAG)

Horizontal Responses							
NO.	**Config.**	**Test**	**Flow**	**Maximum Wind Speeds**	**Angle of Attack**	**Still-air Damping**	**Figure No.**
				m/s	degrees	% of critical	
1	No Traffic	M072m1E01R001	Smooth	94	0	0.15%	FIGURE G1
2	TC-2* Road Vehicles	M072m2E01R001	Smooth	79	0	0.15%	FIGURE G2
3	TC-3 Train	M072m3E01R001	Smooth	83	0	0.15%	FIGURE G3
4	TC-1 Train & Road Vehicles	M072m4E01R001	Smooth	54	0	0.15%	FIGURE G4
5	No Traffic	M072l1E01R001	Smooth	90	-4	0.15%	FIGURE G5
6	TC-2* Road Vehicles	M072l2E01R001	Smooth	79	-4	0.15%	FIGURE G6
7	TC-3 Train	M072l3E01R001	Smooth	82	-4	0.15%	FIGURE G7
8	TC-1 Train & Road Vehicles	M072l4E01R001	Smooth	78	-4	0.15%	FIGURE G8
9	No Traffic	M072n1E01R001	Smooth	65	+4	0.15%	FIGURE G9
10	TC-2* Road Vehicles	M072n2E01R001	Smooth	74	+4	0.15%	FIGURE G10
11	TC-3 Train	M072n3E01R001	Smooth	64	+4	0.15%	FIGURE G11
12	TC-1 Train & Road Vehicles	M072n4E01R001	Smooth	73	+4	0.15%	FIGURE G12
13	No Traffic	M072o1E02R001	Turbulent	78	0	0.15%	FIGURE G13
14	TC-2* Road Vehicles	M072o2E02R001	Turbulent	78	0	0.15%	FIGURE G14
15	TC-3 Train	M072o3E02R001	Turbulent	76	0	0.15%	FIGURE G15
16	TC-1 Train & Road Vehicles	M072o4E02R001	Turbulent	78	0	0.15%	FIGURE G16

TABLE G2 DYNAMIC SECTION MODEL TESTS OF THE COMPLETED DECK (LIFT)

Vertical Responses								
NO.	Config.	Test	Flow	Maximum Wind Speeds	Angle of Attack	Damping	Figure No.	Instability
				m/s	degrees	% of critical		
1	No Traffic	M072m1E01R001	Smooth	120	0	0.34%	FIGURE G1	Not Observed
2	TC-2* Road Vehicles	M072m2E01R001	Smooth	101	0	0.34%	FIGURE G2	Not Observed
3	TC-3 Train	M072m3E01R001	Smooth	105	0	0.34%	FIGURE G3	Not Observed
4	TC-1 Train & Road Vehicles	M072m4E01R001	Smooth	69	0	0.34%	FIGURE G4	Limited Amplitude Oscillation at about 50m/s
5	No Traffic	M072l1E01R001	Smooth	114	-4	0.34%	FIGURE G5	Not Observed
6	TC-2* Road Vehicles	M072l2E01R001	Smooth	100	-4	0.34%	FIGURE G6	Not Observed
7	TC-3 Train	M072l3E01R001	Smooth	105	-4	0.34%	FIGURE G7	Not Observed
8	TC-1 Train & Road Vehicles	M072l4E01R001	Smooth	100	-4	0.34%	FIGURE G8	Not Observed
9	No Traffic	M072n1E01R001	Smooth	83	+4	0.34%	FIGURE G9	at about 84m/s
10	TC-2* Road Vehicles	M072n2E01R001	Smooth	94	+4	0.34%	FIGURE G10	at about 94m/s
11	TC-3 Train	M072n3E01R001	Smooth	81	+4	0.34%	FIGURE G11	at about 83m/s
12	TC-1 Train & Road Vehicles	M072n4E01R001	Smooth	93	+4	0.34%	FIGURE G12	at about 93m/s
13	No Traffic	M072o1E02R001	Turbulent	99	0	0.34%	FIGURE G13	Not Observed
14	TC-2* Road Vehicles	M072o2E02R001	Turbulent	99	0	0.34%	FIGURE G14	Not Observed
15	TC-3 Train	M072o3E02R001	Turbulent	97	0	0.34%	FIGURE G15	Not Observed
16	TC-1 Train & Road Vehicles	M072o4E02R001	Turbulent	100	0	0.34%	FIGURE G16	Not Observed

TABLE G3 DYNAMIC SECTION MODEL TESTS OF THE COMPLETED DECK (TORQUE)

Torsional Responses								
NO.	**Config.**	**Test**	**Flow**	**Maximum Wind Speeds**	**Angle of Attack**	**Damping**	**Figure No.**	**Instability**
				m/s	degrees	% of critical		
1	No Traffic	M072m1E01R001	Smooth	124	0	0.49%	FIGURE G1	Not Observed
2	TC-2* Road Vehicles	M072m2E01R001	Smooth	105	0	0.49%	FIGURE G2	Not Observed
3	TC-3 Train	M072m3E01R001	Smooth	109	0	0.49%	FIGURE G3	Not Observed
4	TC-1 Train & Road Vehicles	M072m4E01R001	Smooth	71	0	0.49%	FIGURE G4	Limited Amplitude Oscillation at about 50m/s
5	No Traffic	M072l1E01R001	Smooth	118	-4	0.49%	FIGURE G5	Not Observed
6	TC-2* Road Vehicles	M072l2E01R001	Smooth	104	-4	0.49%	FIGURE G6	Not Observed
7	TC-3 Train	M072l3E01R001	Smooth	109	-4	0.49%	FIGURE G7	Not Observed
8	TC-1 Train & Road Vehicles	M072l4E01R001	Smooth	104	-4	0.49%	FIGURE G8	Not Observed
9	No Traffic	M072n1E01R001	Smooth	86	+4	0.49%	FIGURE G9	at about 84m/s
10	TC-2* Road Vehicles	M072n2E01R001	Smooth	97	+4	0.49%	FIGURE G10	at about 94m/s
11	TC-3 Train	M072n3E01R001	Smooth	84	+4	0.49%	FIGURE G11	at about 83m/s
12	TC-1 Train & Road Vehicles	M072n4E01R001	Smooth	96	+4	0.49%	FIGURE G12	at about 93m/s
13	No Traffic	M072o1E02R001	Turbulent	103	0	0.49%	FIGURE G13	Not Observed
14	TC-2* Road Vehicles	M072o2E02R001	Turbulent	103	0	0.49%	FIGURE G14	Not Observed
15	TC-3 Train	M072o3E02R001	Turbulent	101	0	0.49%	FIGURE G15	Not Observed
16	TC-1 Train & Road Vehicles	M072o4E02R001	Turbulent	103	0	0.49%	FIGURE G16	Not Observed

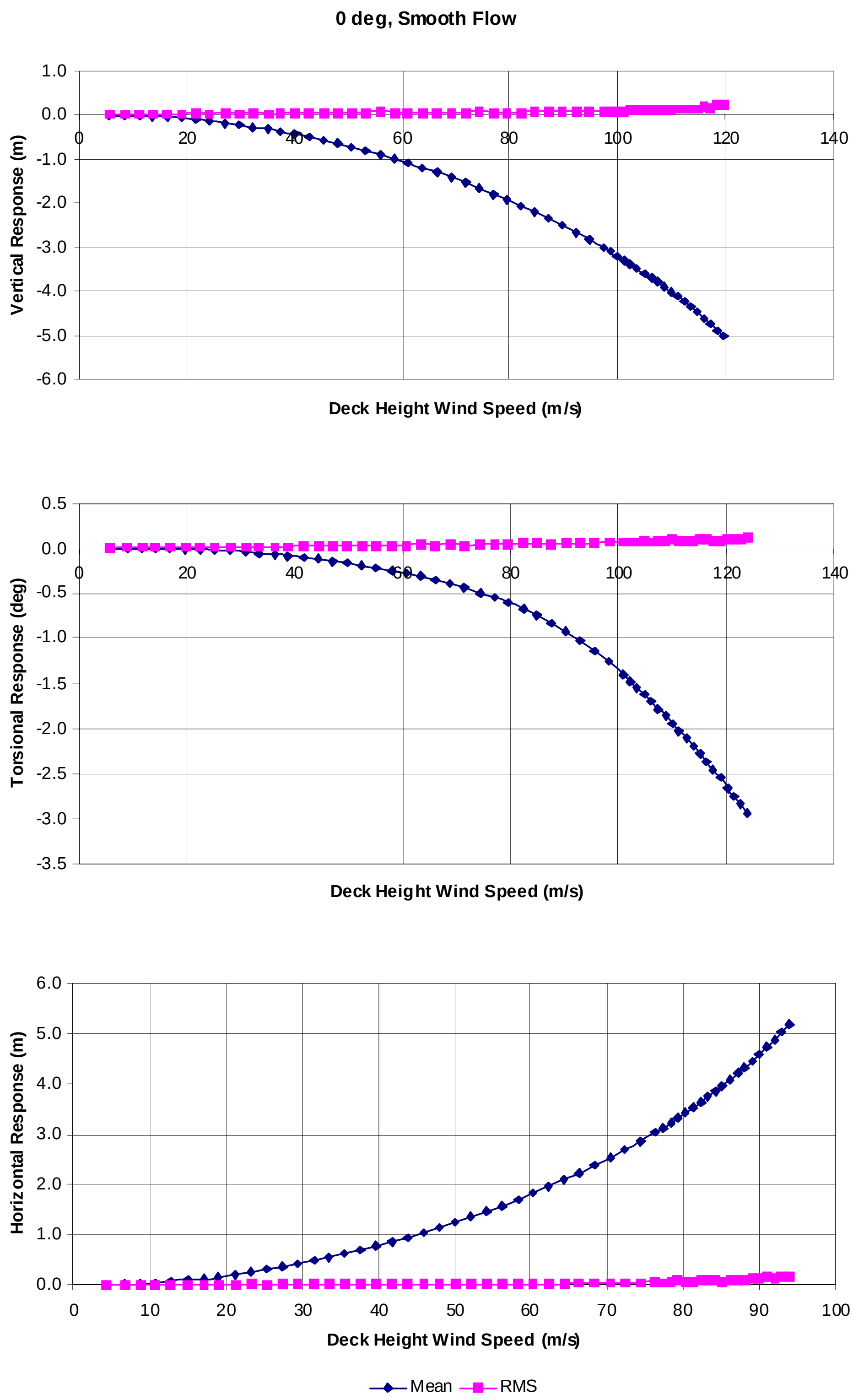

FIGURE G1 DYNAMIC SECTION MODEL TEST, ZERO DEGREES, SMOOTH FLOW, NO TRAFFIC

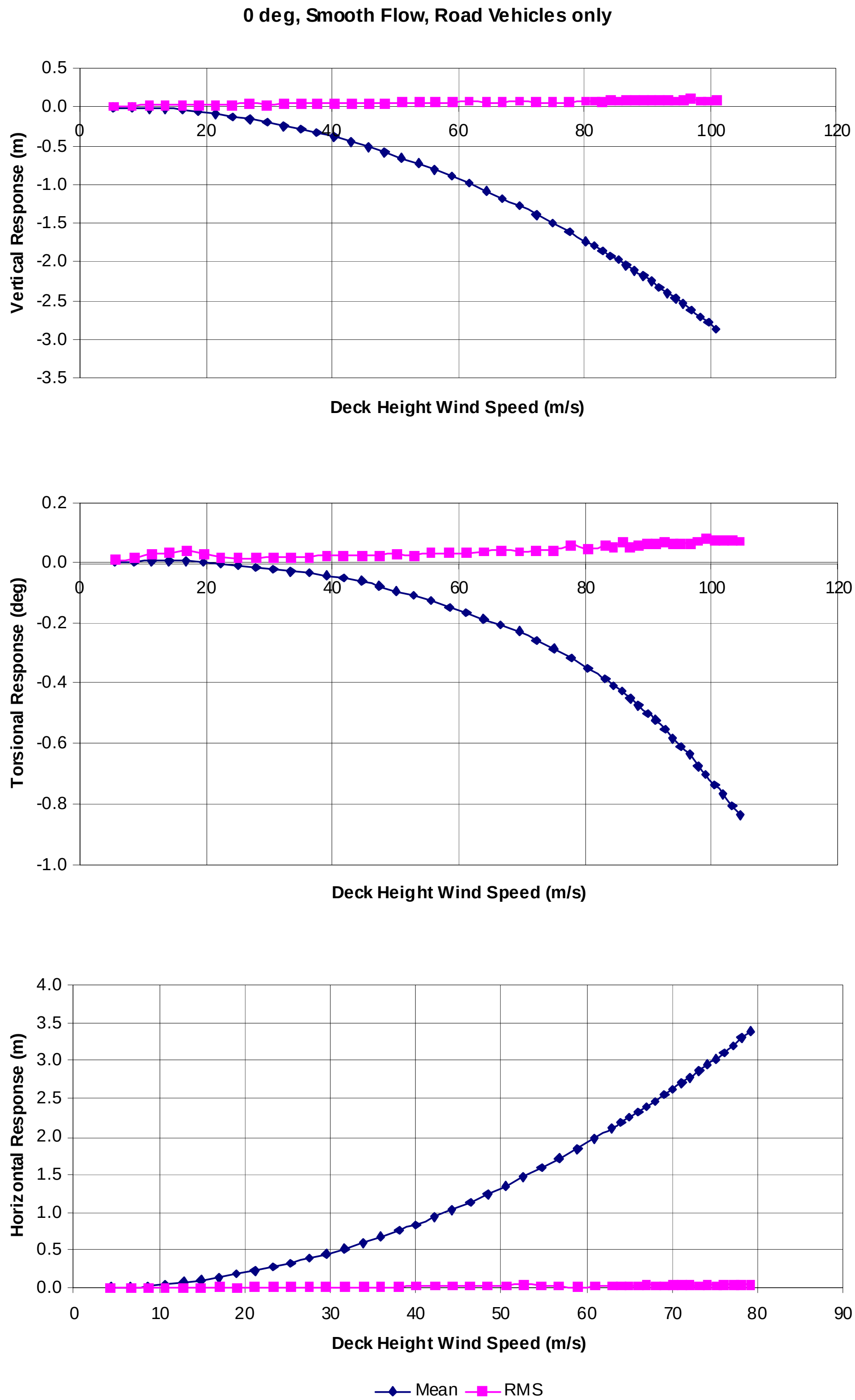

FIGURE G2 DYNAMIC SECTION MODEL TEST, ZERO DEGREES, SMOOTH FLOW TRAFFIC TC-2*: ROAD VEHICLES ONLY

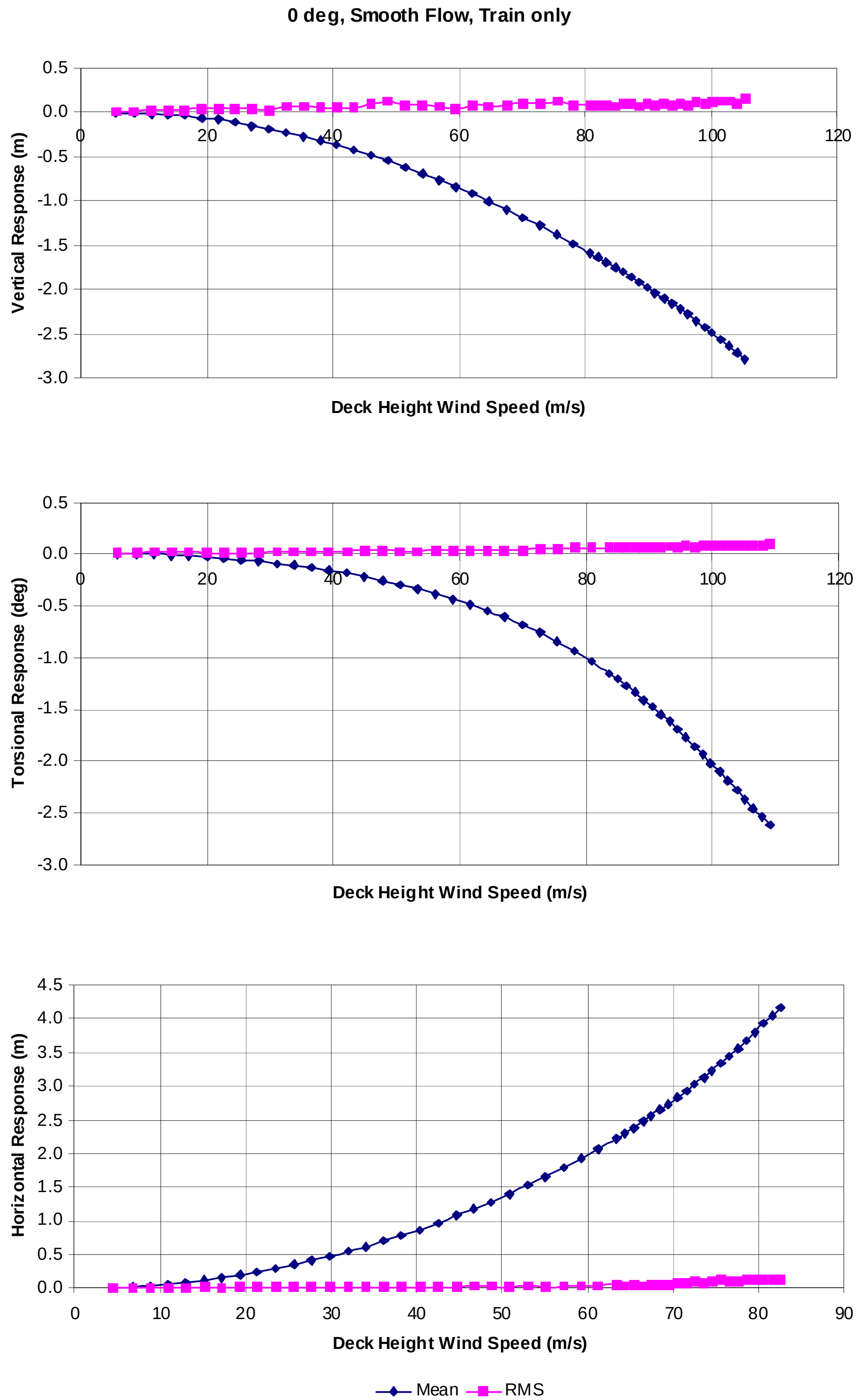

FIGURE G3 DYNAMIC SECTION MODEL TEST, ZERO DEGREES, SMOOTH FLOW TRAFFIC TC-3: TRAIN ONLY

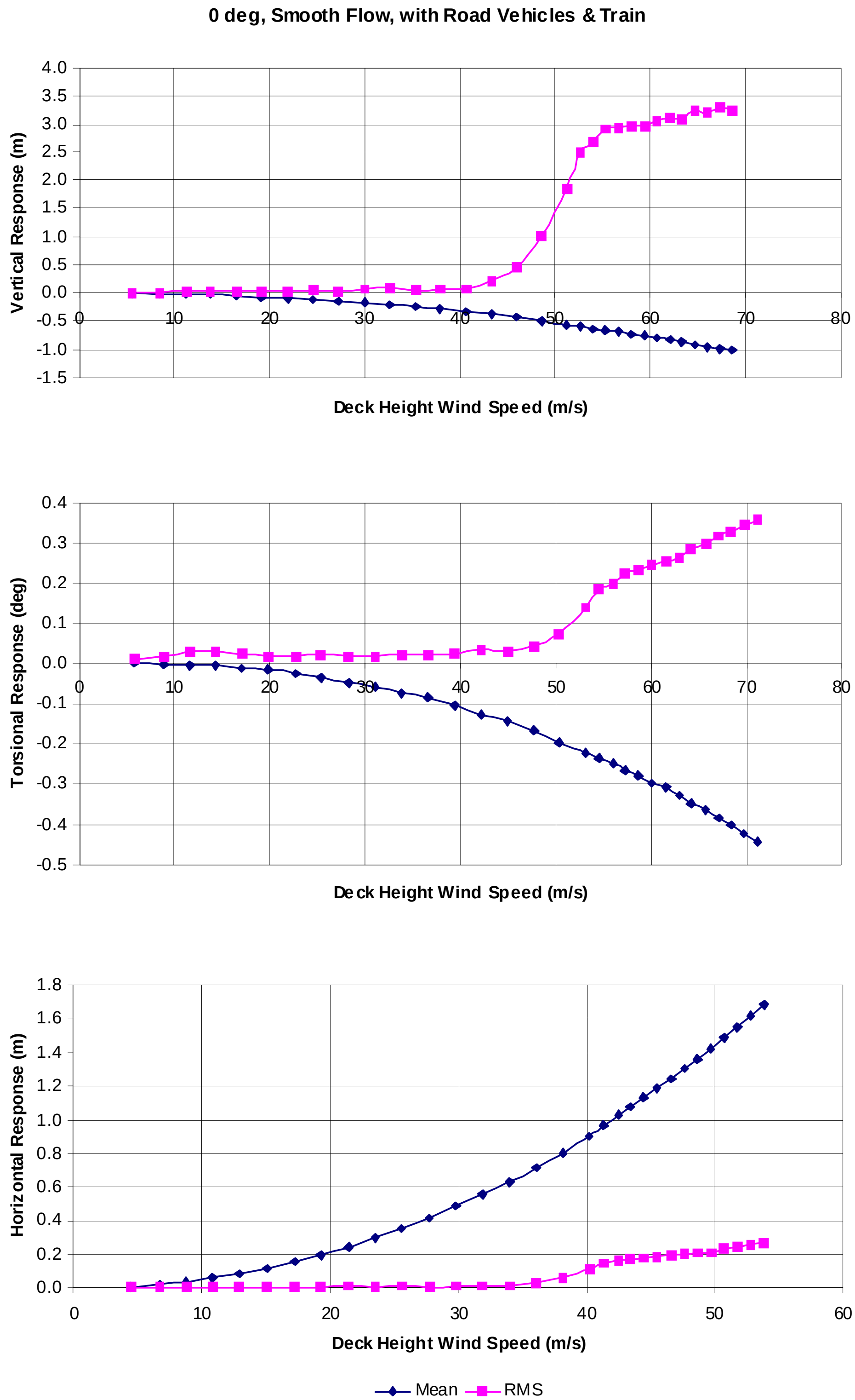

FIGURE G4 DYNAMIC SECTION MODEL TEST, ZERO DEGREES, SMOOTH FLOW, TRAFFIC TC-1: ROAD VEHICLES & TRAIN

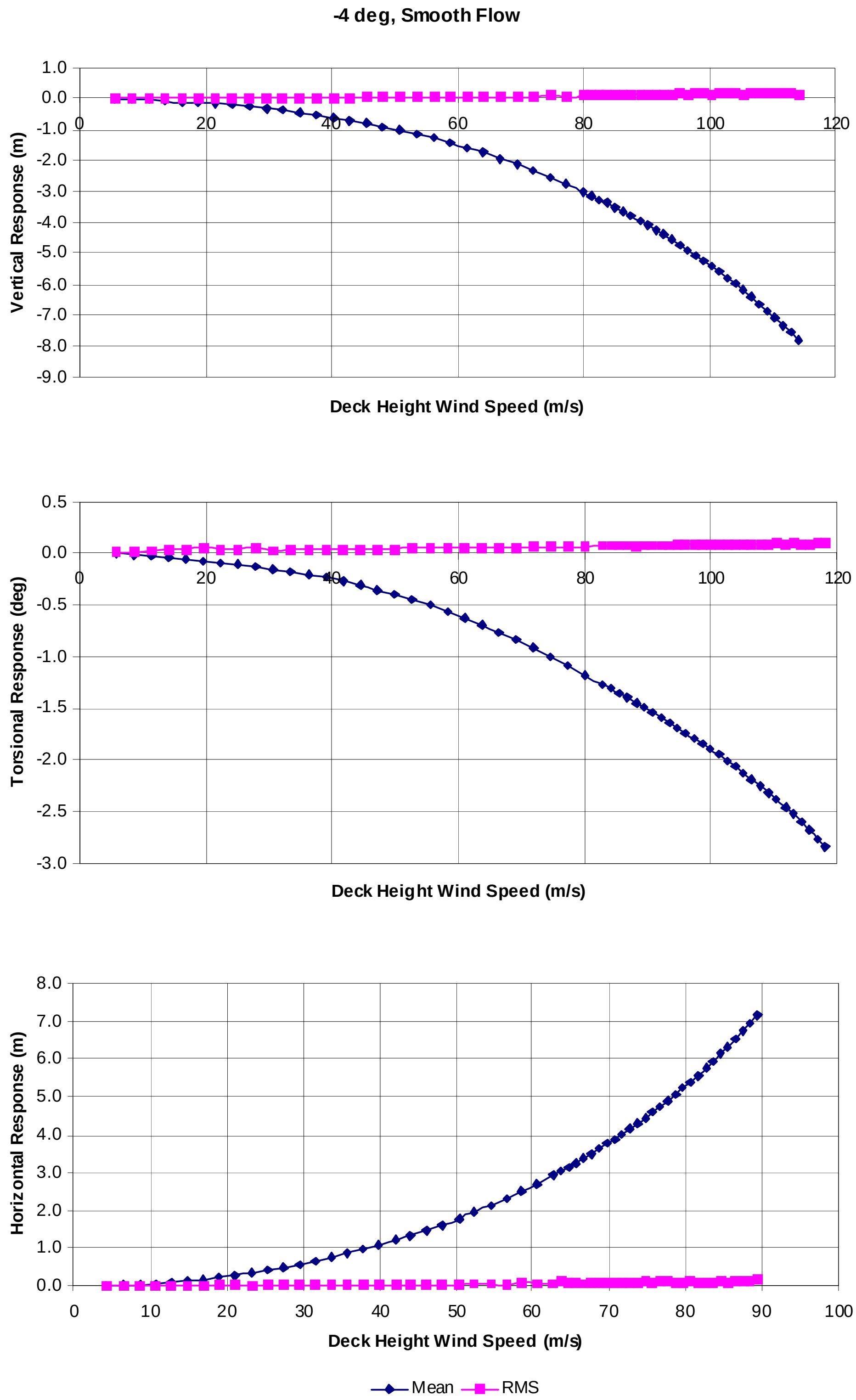

FIGURE G5 DYNAMIC SECTION MODEL TEST, -4 DEGREES, SMOOTH FLOW, NO TRAFFIC

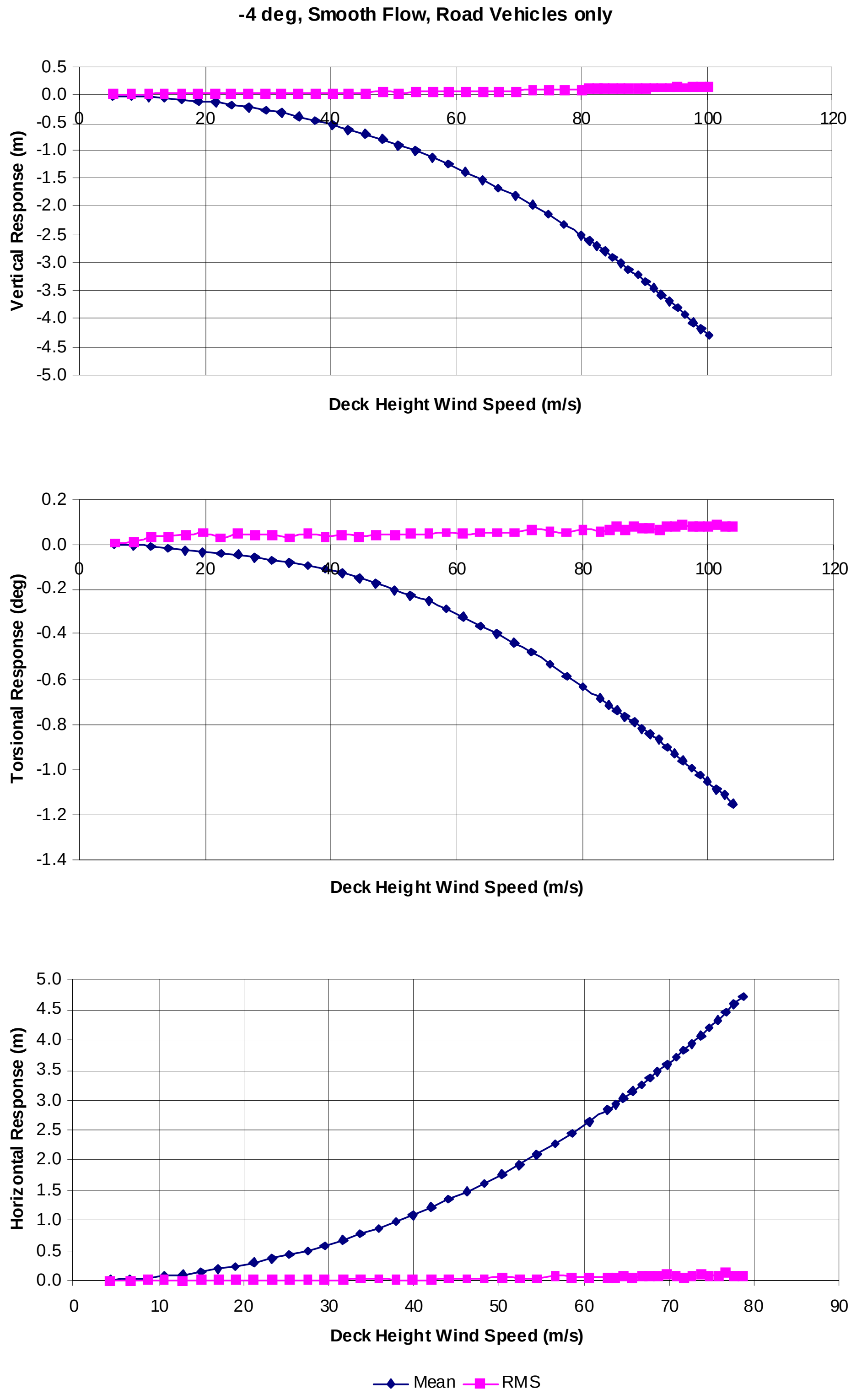

FIGURE G6 DYNAMIC SECTION MODEL TEST, -4 DEGREES, SMOOTH FLOW TRAFFIC TC-2*: ROAD VEHICLES ONLY

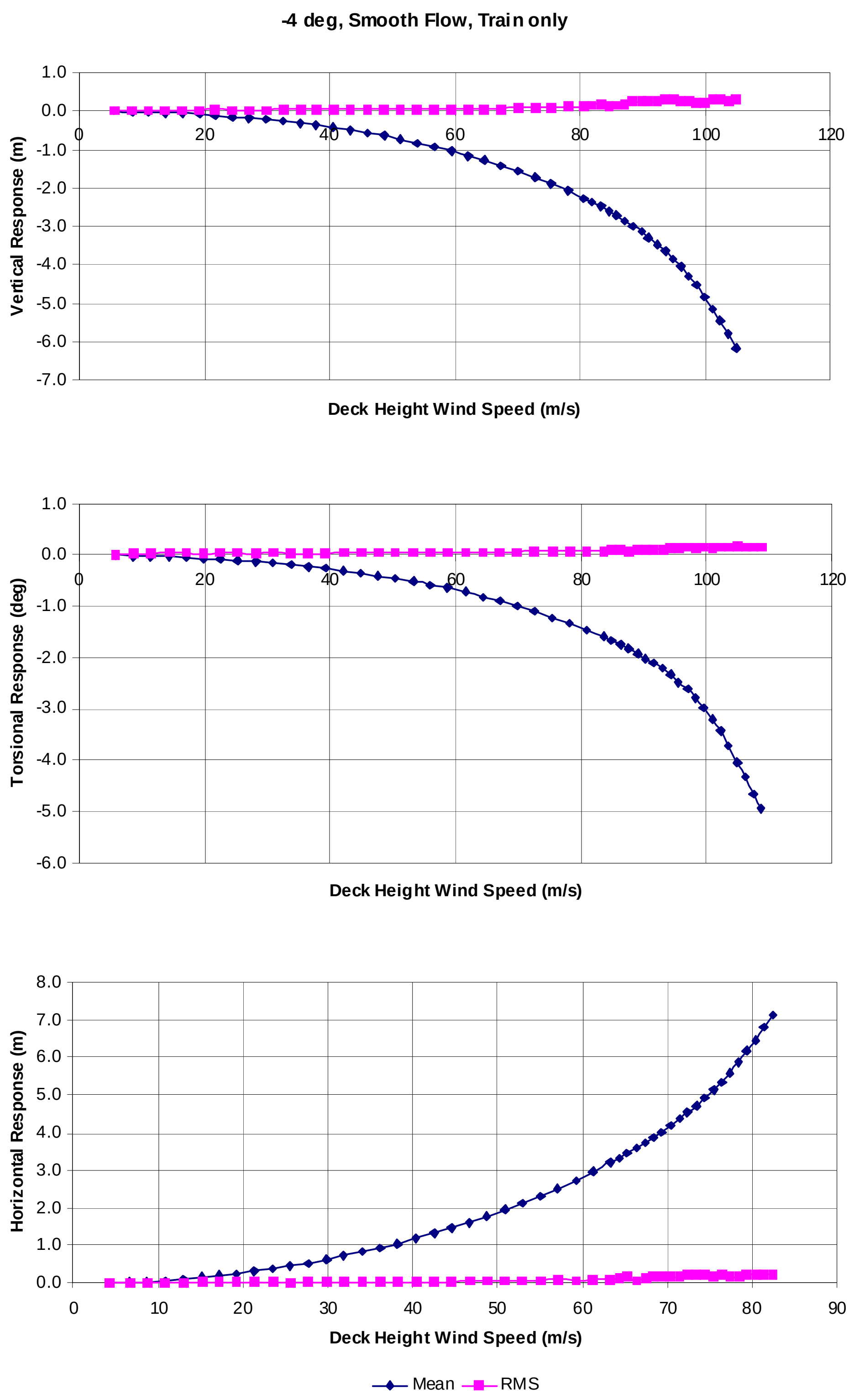

FIGURE G7 DYNAMIC SECTION MODEL TEST, -4 DEGREES, SMOOTH FLOW TRAFFIC TC-3: TRAIN ONLY

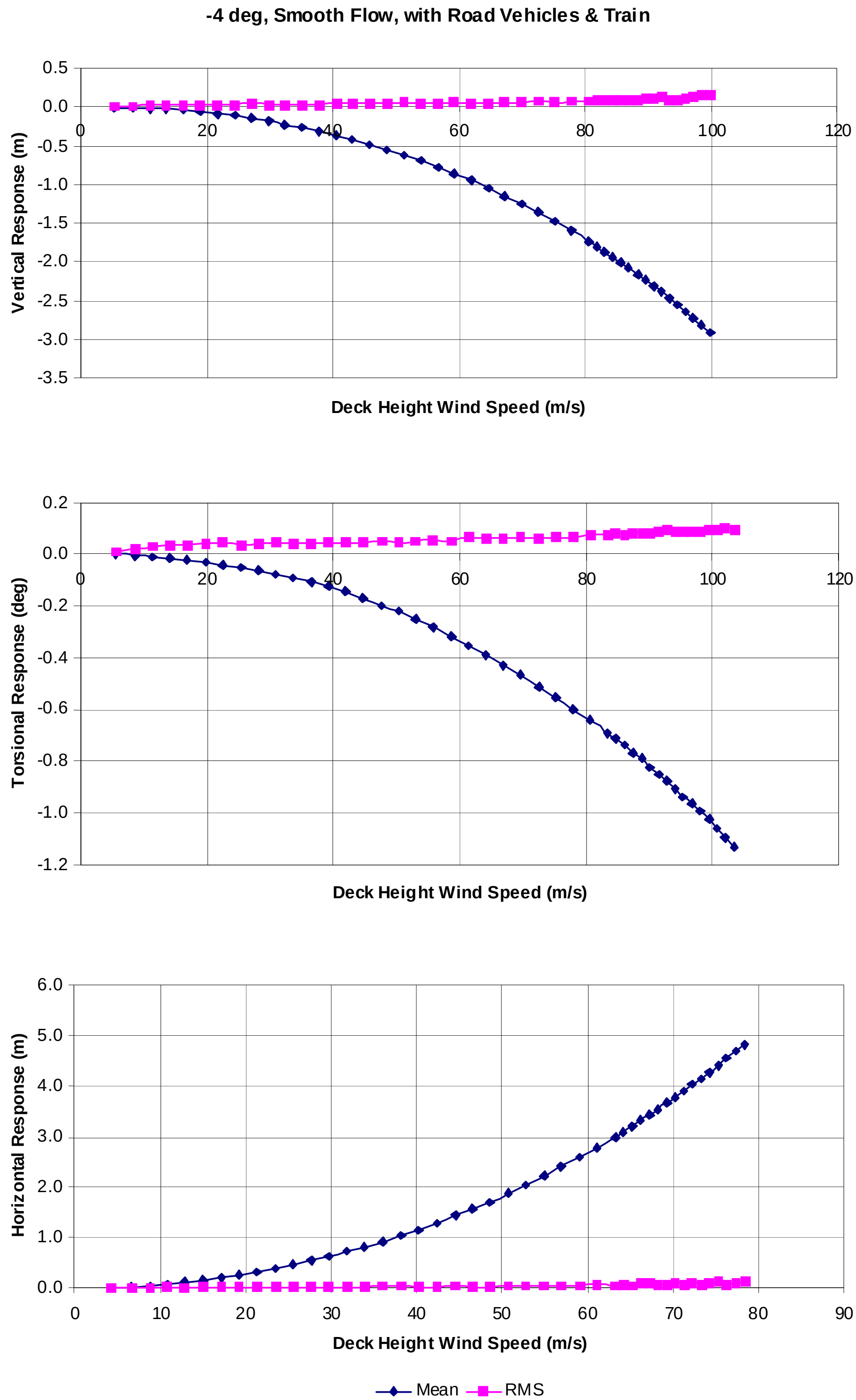

FIGURE G8 DYNAMIC SECTION MODEL TEST, -4 DEGREES, SMOOTH FLOW TRAFFIC TC-1: ROAD VEHICLES & TRAIN

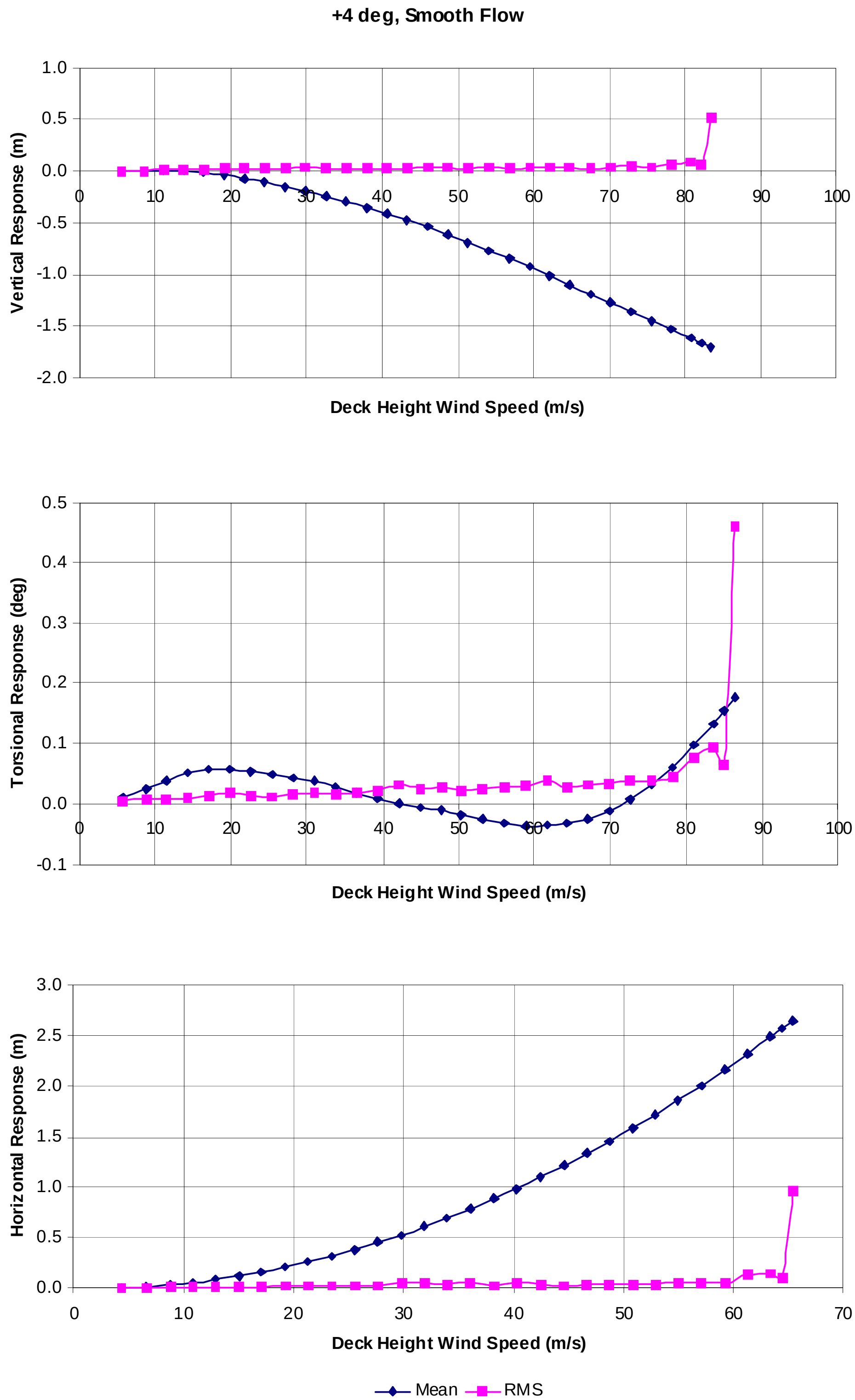

FIGURE G9 DYNAMIC SECTION MODEL TEST, +4 DEGREES, SMOOTH FLOW, NO TRAFFIC

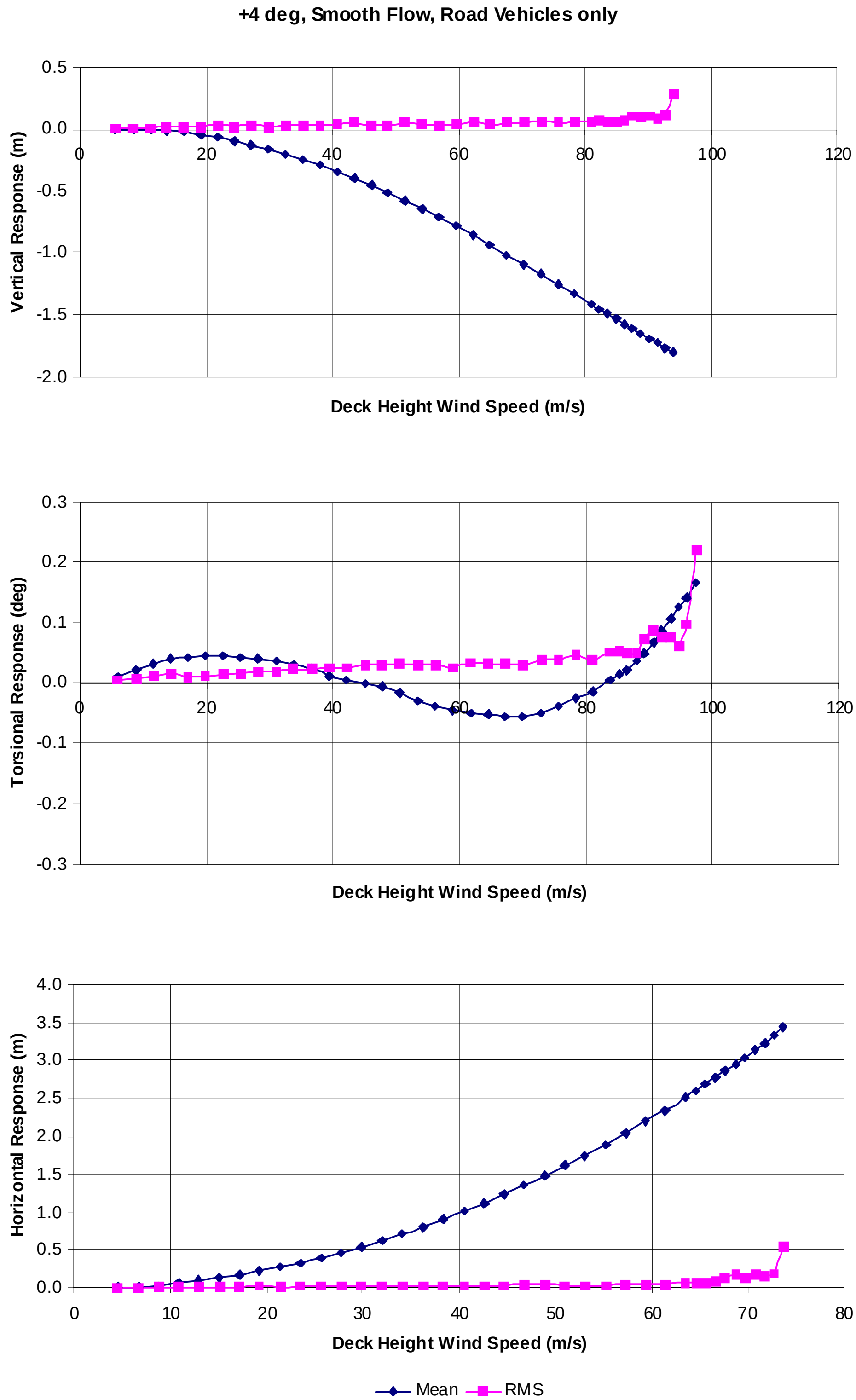

FIGURE G10 DYNAMIC SECTION MODEL TEST, +4 DEGREES, SMOOTH FLOW TRAFFIC TC-2*: ROAD VEHICLES ONLY

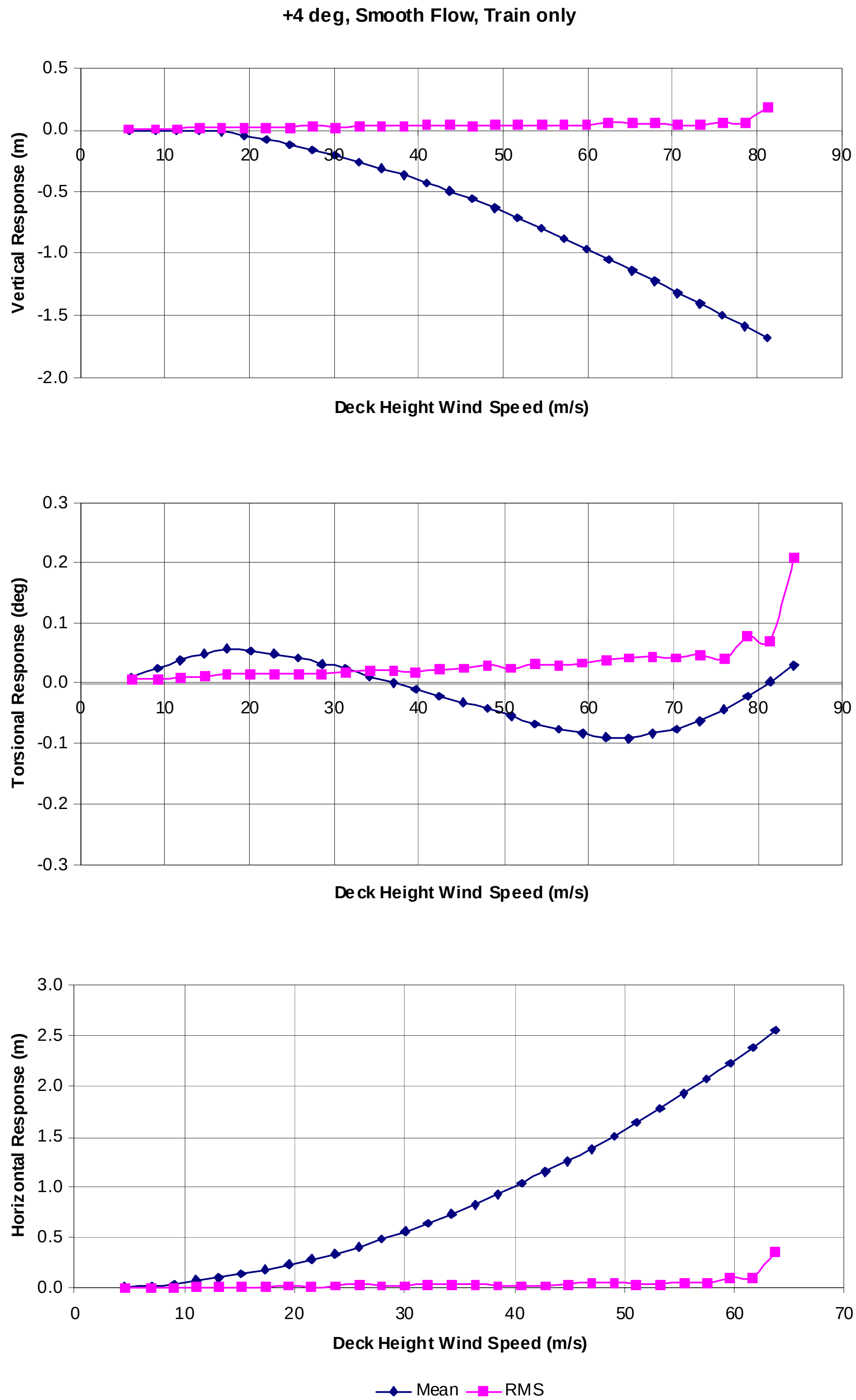

FIGURE G11 DYNAMIC SECTION MODEL TEST, +4 DEGREES, SMOOTH FLOW TRAFFIC TC-3: TRAIN ONLY

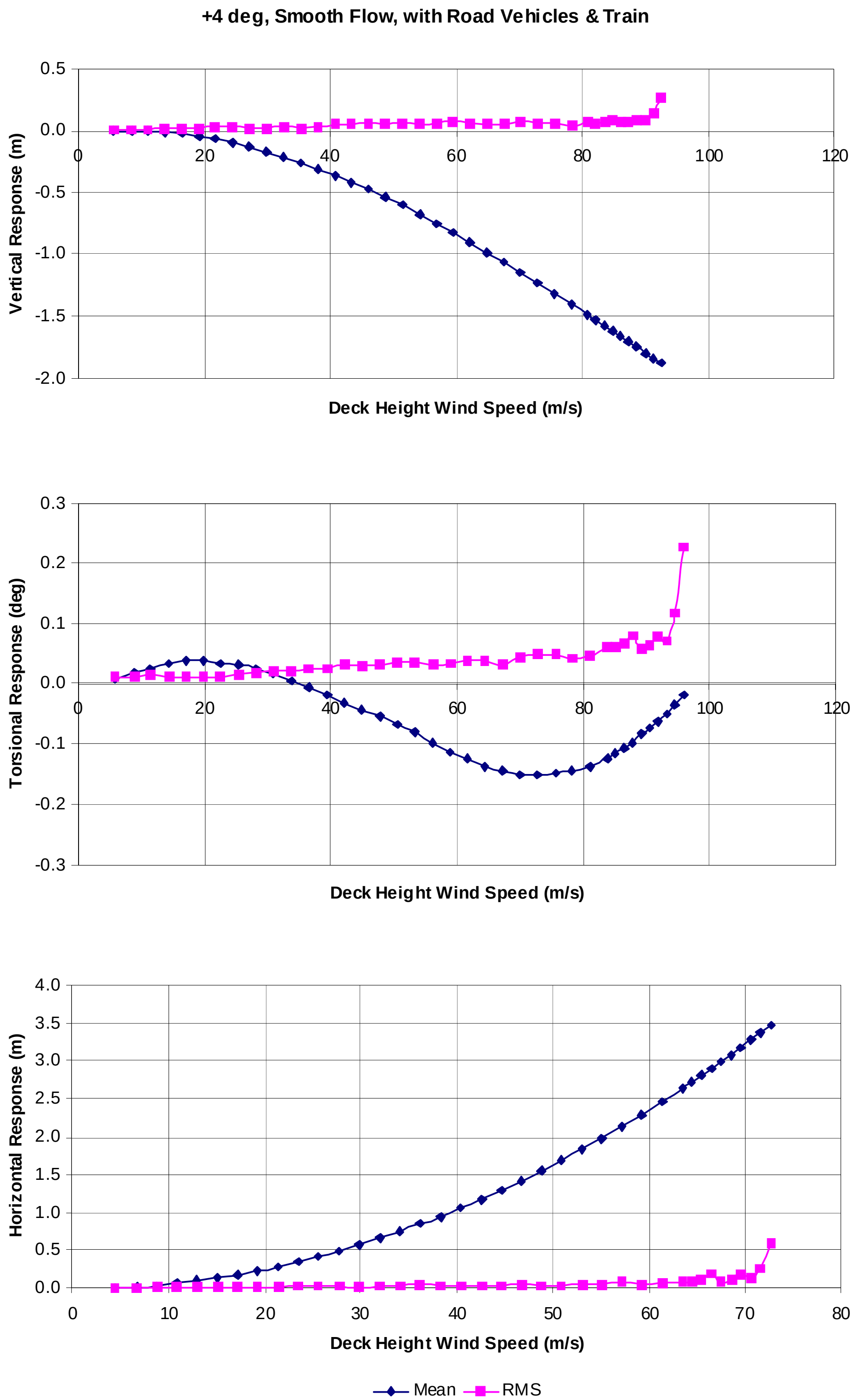

FIGURE G12 DYNAMIC SECTION MODEL TEST, +4 DEGREES, SMOOTH FLOW TRAFFIC TC-1: BOTH ROAD VEHICLES & TRAIN

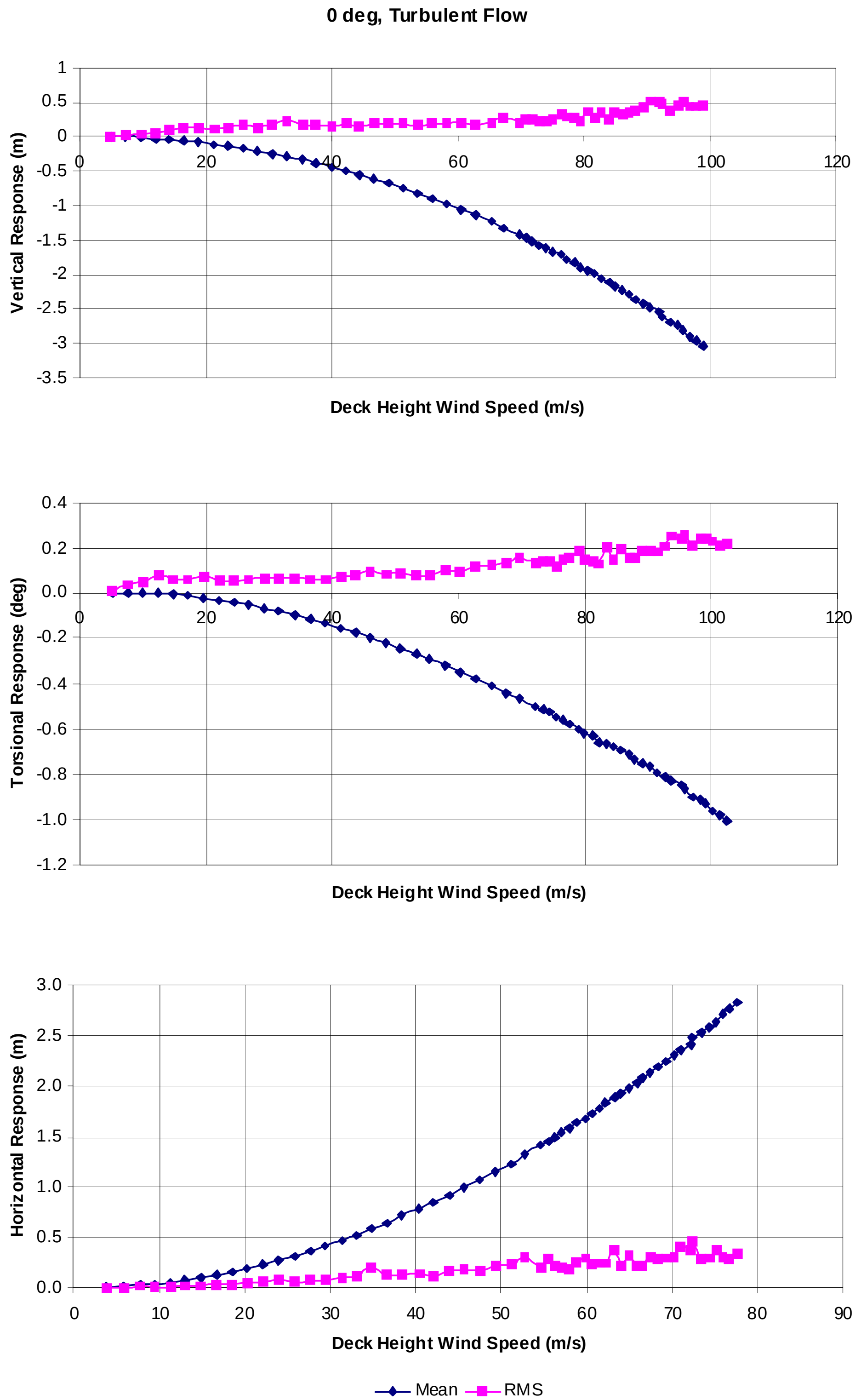

FIGURE G13 DYNAMIC SECTION MODEL TEST, ZERO DEGREES, TURBULENT FLOW, NO TRAFFIC

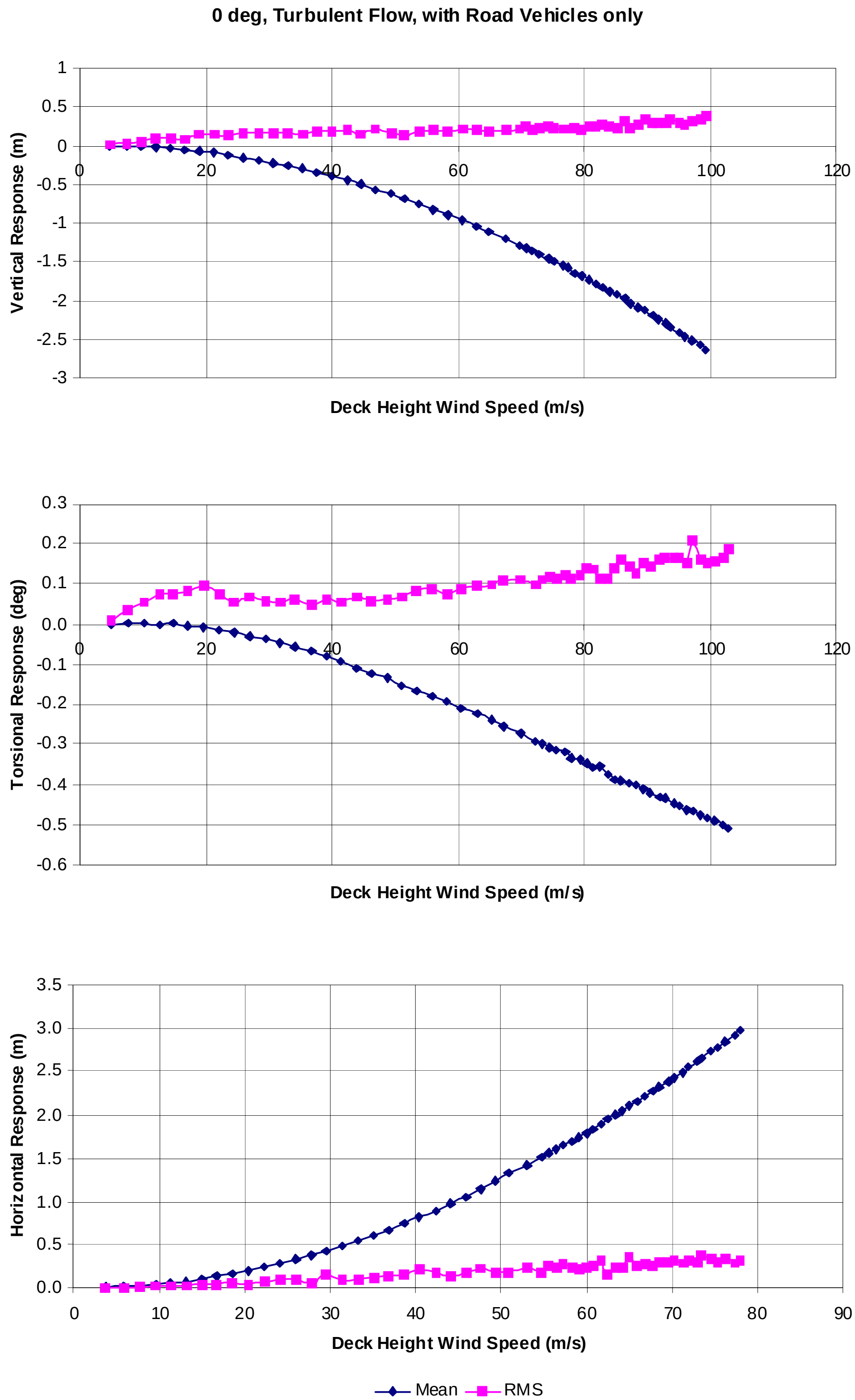

FIGURE G14 DYNAMIC SECTION MODEL TEST, ZERO DEGREES, TURBULENT FLOW TRAFFIC TC-2*: ROAD VEHICLES ONLY

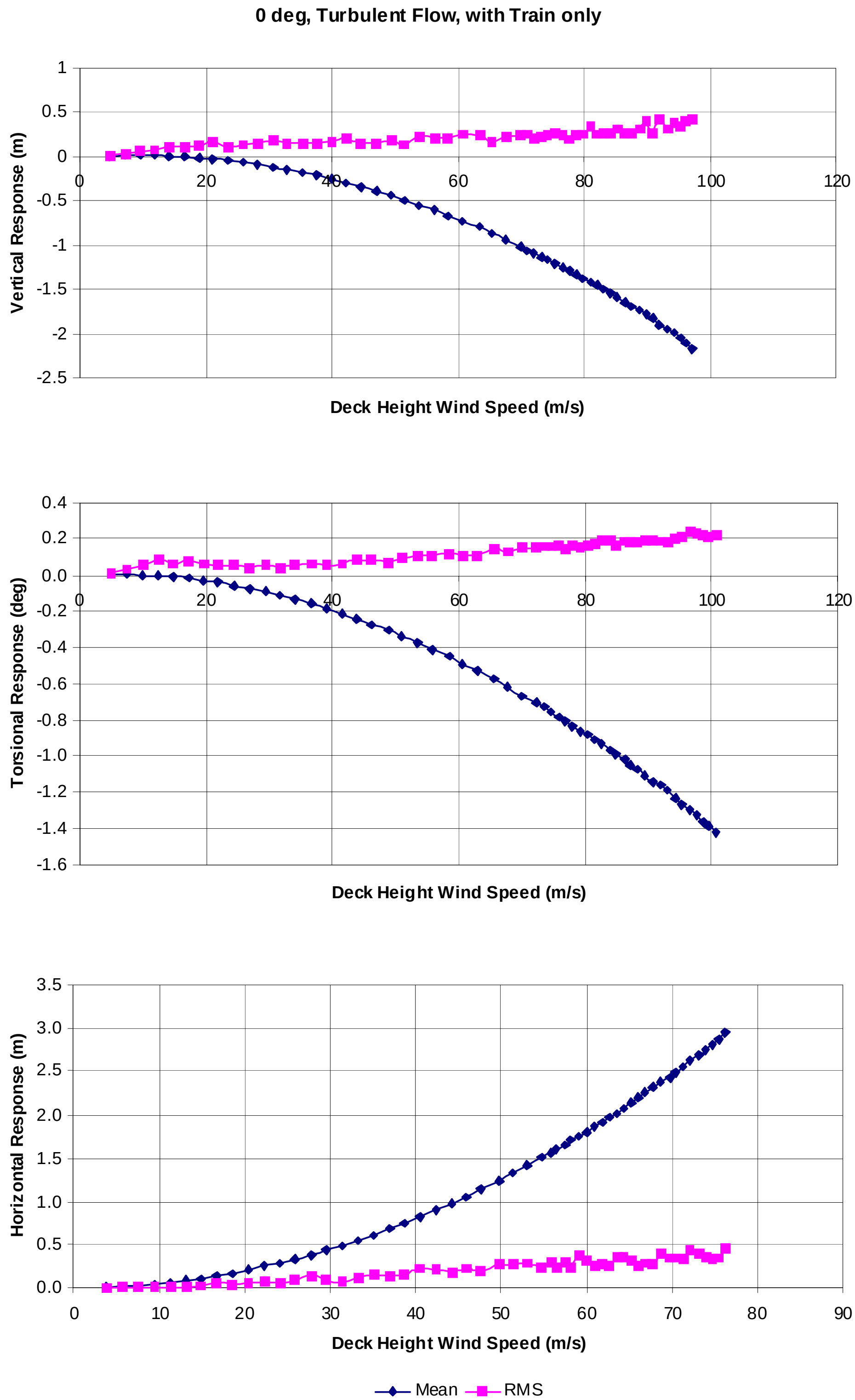

FIGURE G15 DYNAMIC SECTION MODEL TEST, ZERO DEGREES, TURBULENT FLOW TRAFFIC TC-3: TRAIN ONLY

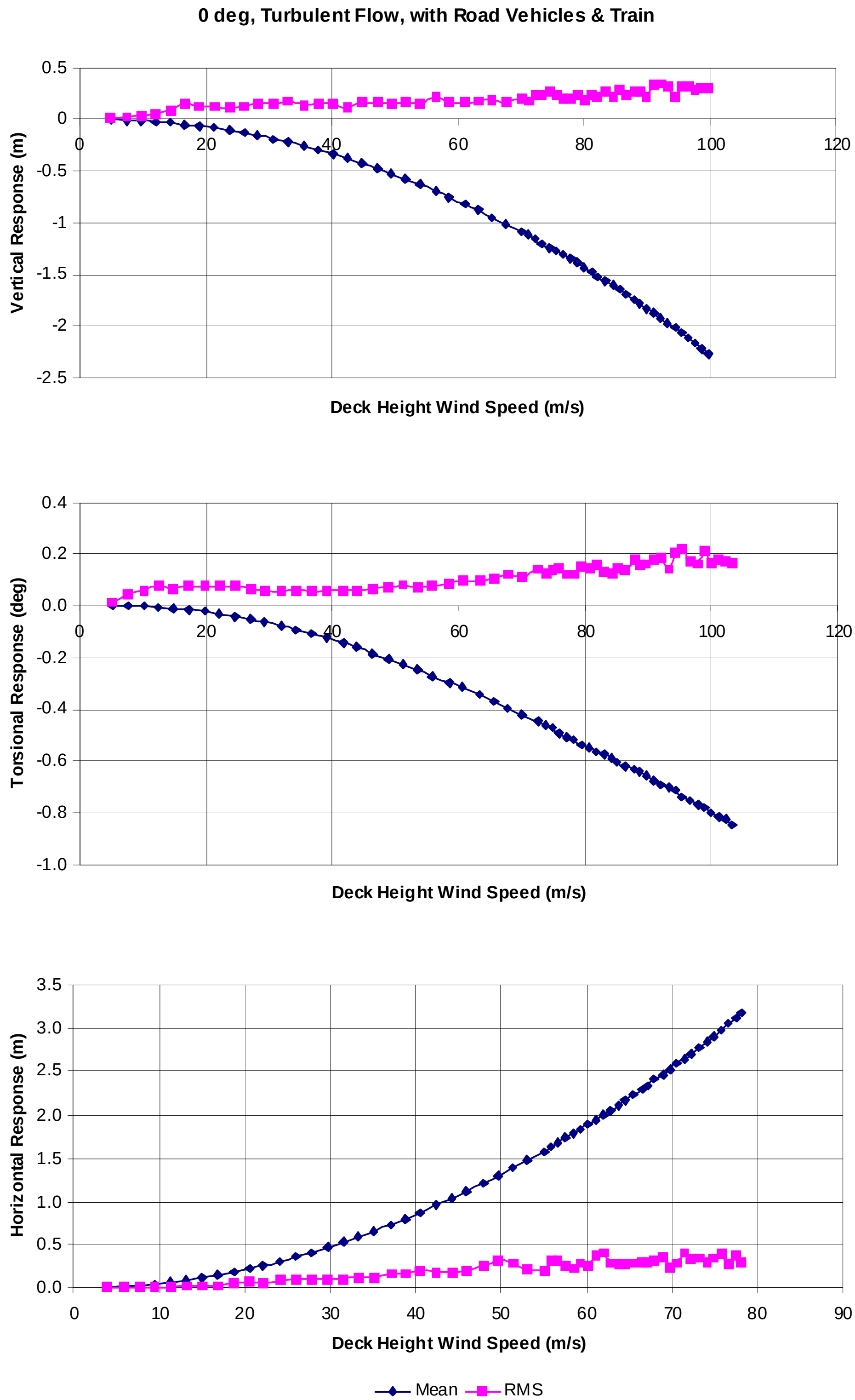

FIGURE G16 DYNAMIC SECTION MODEL TEST, ZERO DEGREES, TURBULENT FLOW TRAFFIC TC-1: BOTH ROAD VEHICLES & TRAIN